UNIVERSITY OF CALIFORNIA, SAN DIEGO

Ruthenium-Mediated Cycloaromatization of Tri-Pi Systems

A dissertation submitted in partial satisfaction of the requirements for the degree of

Doctor of Philosophy

in

Chemistry

by

Stephen Kyle Cope

Committee in charge:

Professor Joseph M. O'Connor, Chair
Professor William Fenical
Professor Thomas Herrman
Professor Joseph Noel
Professor Charles Perrin

2015

The dissertation of Stephen Kyle Cope is approved, and it is acceptable in quality and form for publication on microfilm and electronically:

Chair

University of California, San Diego

2015

DEDICATION

I dedicate this thesis and all work therein to my wife Amber and my children.

Without you, none of this would be possible.

.

EPIGRAPH

As beautiful and useful as chemistry is, nothing chemical is likely to be simple, this reaction is no exception.

Roald Hoffmann

TABLE OF CONTENTS

LIST OF FIGURES

LIST OF SCHEMES

LIST OF TABLES

LIST OF ABBREVIATIONS

Alphabetical within Category

Chemical Abbreviations

(- indicates covalent substituent)

B: general base

1,4-CHD: 1,4-cyclohexadiene

-^{n}Bu: *n*-butyl, -$CH_2(CH_2)_2CH_3$

-^{t}Bu: *t*-butyl, -$C(CH_3)_3$

Cp: cyclopentadienyl

Cp*: pentamethylcyclopentadienyl

Cp‡: 1,2,3,4-tetramethyl-5-trifluoromethylcyclopentadienyl

D/ -d: deuterium

DCM: dichloromethane

DMF: N,N-dimethylformamide

-Et: ethyl, -CH_2CH_3

IPA: isopropyl alcohol

L: metal ligand (e.g. AuL)

-Me: methyl, -CH_3

MeCN: acetonitrile

NBS: N-bromosuccimide

-OAc: acetate, -$OC(O)CH_3$

-OTf: triflate, -$OS(O)_2CF_3$

-Ph: phenyl, -C_6H_5

-^{n}Pr: *n*-propyl, -$CH_2CH_2CH_3$

THF: tetrahydrofuran

-TMS: trimethylsilyl

Experimental/ Spectroscopic

ΔG^0_{rxn}: standard reaction energy

δ: chemical shift

η^x: x atoms π bound to metal

λ: wavelength

σ_{meta}: subsituent constant *meta*

A: conformational energy

APCI: atmospheric pressure chemical ionization

COSY: correlation spectroscopy

d: doublet

DR: diastereomeric ratio

ESI: electrospray ionization

FT-IR: fourier transform infrared spectroscopy

hν: ultraviolent radiation

HMBC: heteronuclear multiple-bond correlation spectroscopy

HMQC: heteronuclear multiple-quantum correlation spectroscopy

HRMS: high resolution mass spectrometry

J: coupling constant

KIE: kinetic isotope effect

m: multiplet

NMR: nuclear magnetic resonance spectroscopy

p: pentet

q: quartet

RDS: rate determining step

rt: room temperature

s: singlet

t: triplet

TLC: thin layer chromatography

TOF: time of flight

UV: ultraviolet radiation

Parameter Units

(*Conventional SI prefixes were used)*

Å: Angstrom

°C: degree Celsius

h: hour

Hz: Hertz

Cal: calorie

cm^{-1}: wavenumber

eV: electron volt

K: Kelvin

L: liter

M: molar

m: meter

min: minute

mol: mole

ppm: parts per million

s: second

Torr: millimeter of mercury

ACKNOWLEDGEMENTS

I would like to thank my advisor, Joseph M. O'Connor, for his guidance and being a wonderful person to work for. I would also like to thank my committee and Professor Charles Perrin for insightful discussions and suggestions throughout my studies here at UCSD. I would be remiss if I do not thank my wife Amber and my family, without their love and support, none of this would be possible.

Curtis E. Moore and Professor Arnold L. Rheingold are acknowledged for acquisition of data for X-ray structures. Yongxuan Su is acknowledged for acquisition of HRMS data. Anthony Mrse is acknowledged for assistance with acquisition of NMR data and for always being open to a stimulating conversation.

The material in Chapter 2, in part, is currently being prepared for submission for publication with the following authors: Cope, S.K.; O'Connor, J.M. The dissertation author was the primary investigator and author of this material.

The material in Chapter 3, in part, is currently being prepared for submission for publication with the following authors: Cope, S.K.; O'Connor, J.M. The dissertation author was the primary investigator and author of this material.

The material in Chapter 4, in part, is currently being prepared for submission for publication with the following authors: Cope, S.K.; O'Connor, J.M. The dissertation author was the primary investigator and author of this material.

The material in Chapter 5, in part, is currently being prepared for submission for publication with the following authors: Cope, S.K.; O'Connor, J.M.; Hitt, D.M.;

Raub, A. G. The dissertation author was the primary investigator and author of this material.

VITA

Education

2009-2015 University of California, San Diego
Doctor of Philosophy, Chemistry
Advisor: Professor Joseph M. O'Connor
Thesis Title: "Ruthenium-Mediated Cycloaromatization of Tri-Pi Systems."

2008-2009 University of North Carolina, Charlotte
Master of Science, Chemistry
Advisor: Professor Craig A. Ogle
Thesis Title: "Investigations into the Reactions of Organocuprates with Allylic Substrates and the Addition to α,β-unsaturated Enones and Enals"

2002-2008 University of North Carolina, Charlotte
Bachelor of Science, Chemistry

Research Experience

August 2009-August 2015
Ph.D. Student: UC San Diego, Advisor: Joseph M. O'Connor
Investigated transition metal interactions with polyunsaturated (enediyne, dienyne, and triene) organic substrates and the influence of the transition metal on the reactivity pattern of the organic substrates. The main areas of study were the interrogation of the initial η^6-metal complexation of unsaturated systems and the mechanism for the formation of the products formed via the interaction. In addition, the observed reactions with transition metal complexes were compared with reaction patterns observed for the substrates in the absence of transition metals.

July 2008-July 2009
M.Sc. Student, UNC Charlotte, Advisor: Craig A. Ogle
Investigated the interaction of lithium dialkyl cuprates with a variety of organic substrates and products formed from these interactions with a novel NMR technique called Rapid Injection NMR (RI-NMR). These investigations allowed the preparations of reaction intermediates proposed for these reactions and characterization of the intermediates by NMR spectroscopy at low temperature.

July 2008-July 2009
Research Assistant, RACheL Laboratory, Director: Craig A. Ogle
Employed as a research assistant in the Regional Analytical Chemistry Laboratory (RACheL) operated through the chemistry department at UNC Charlotte.

Responsibilities included sample preparation for a variety of analytical tests, laboratory equipment maintenance, and working as a mentor to undergraduate student assistants.

September 2004-June 2008
Undergraduate Research Assistant, UNC Charlotte, Advisor: Craig A. Ogle
Investigated the interaction of lithium dialkyl cuprates with a variety of organic substrates and products formed from these interactions with a novel NMR technique called Rapid Injection NMR (RI-NMR). These investigations allowed the preparations of reaction intermediates proposed for these reactions and characterization of the intermediates by NMR spectroscopy at low temperature. In addition, enantioselective syntheses with chiral n-silylamido cuprates was investigated.

Laboratory Technical Expertise

Synthetic organic chemistry in the construction of small organic molecules, synthetic organometallic chemistry in the construction of organometallic reagents, Air free techniques (both Schlenk line technique and glove box manipulations) for handling oxygen and water sensitive solids and mixtures, NMR, IR, UV-Vis, and Mass spectroscopy, chromatographic techniques(LC, HPLC, GC), instrumentation upkeep and machining parts for experimental setups.

Awards

2006 McKernan Scholarship from the Carolina Chemistry Club
2006 1st place, Undergraduate Research Conference, UNC Charlotte
2007 1st place, Undergraduate Research Conference, UNC Charlotte

Teaching Experience

August 2009-March 2015
Teaching Assistant: Organic Chemistry I & II, UC San Diego
Served as a discussion section leader for 90-120 students enrolled in 200-400 student organic chemistry classes. Primary responsibility was to hold weekly problem-solving sessions designed for open discussions of material covered in lecture and problems encountered in working problems assigned in the text. Secondary responsibility included midterm/final exam proctoring, quiz writing and grading.

September 2009-June 2011
Teaching Assistant: Organic Chemistry Laboratory I, UC San Diego
Employed as in-lab instructor for one class per quarter ranging from 16-24 students. Primary responsibilities included teaching students in introductory organic

laboratory techniques, skills and instrumentation in addition to writing quizzes and grading laboratory reports and quizzes.

August 2006-December 2007
Undergraduate Teaching Assistant: Physical Chemistry Laboratory I & II, UNC Charlotte
Employed as in-lab assistant for two classes per semester ranging from 8-12 students. Primary responsibilities was assisting students with the setup of laboratory instruments and equipment and collection of data.

August 2004-May 2006
Undergraduate Teaching Assistant: Organic Chemistry Laboratory I & II, UNC Charlotte
Employed as in-lab instructor for one class per quarter ranging from 24-32 students. Primary responsibilities included teaching students in introductory organic laboratory techniques, skills and instrumentation.

Publications

Hitt, D.M.; **Cope, S.K**.; Raub, A.W.; Baldridge, K.K.; O'Connor, J.M.; "Non-aryne Cycloaromatization of Enediynes with Halogen Incorporation from Haloforms: Routes to Aryl Halides" *JACS*, in preparation

Holland, R.L.; O'Connor, J.M.; Bunker, K.D.; Qin, P.; **Cope, S.K.**; Baldridge, K.K.; Siegel, J.S.; "Stererospecific Oxidative Demetallation of Highly Functionalized CpCo(1,3-Diene) Compexes: An Experimental and Computational Study" *Synlett*, published online 24.08.2015

Bertz, S.H.; **Cope, S.K.**; Hardin, R.A.; Murphy, M.D.; Ogle, C.A.; Smith, D.T.; Thomas, A.A.; Whaley, T.N.; "Complexes of the Gilman Reagent with Double Bonds across the π-σ Continuum" *Organometallics* **2012** *21*(22), 789-27-7838

O'Connor, J.M.; Closson, A.P.; Holland, R.L.; **Cope, S.K.**; Velez, C.L.; Moore, C.E.; Rheingold, A.L.; "Synthesis and Solid-state Structures of (Triphos)iridacyclopentadiene Complexes as Models for Vinylidene Intermediates in the [2+2+1] Cyclotrimerization of Alkynes" *Inorg. Chim. Acta.* **2010**, *364*(1), 220-225

Bartholomew, E.R.; Bertz, S.H.; **Cope, S.K.**; Murphy, M.D.; Ogle, C.A.; Thomas, A.A.; "Serendipity Strikes Again-Efficient Preparation of Lithium Tetramethylcuprate (III) via Rapid Injection NMR" *Chemical Communications* **2010**, *46*(8), 1253-1254

Bartholomew, E.R.; Bertz, S.H.; **Cope, S.K.**; Murphy, M.D.; Ogle, C.A.; "Preparation of σ and π-allyl Copper Intermediates in S_N2 and S_N2' Reactions of Organocuprate(I) Reagents with Allylic Substrates" *J. Am. Chem. Soc.* **2008**, *130*(34), 11244-11245

Bartholomew, E.R.; Bertz, S.H.; **Cope, S.K.**; Dorton, D.C.; Murphy, M.D.; Ogle, C.A.; "Neutral Organocopper(III) Complexes" *Chemical Communications* **2008**, *10*, 1176-1177

Bertz, S.H.; **Cope, S.K.**; Dorton, D.H.; Murphy, M.D.; Ogle, C.A.; "Organocuprate Cross-Coupling: The Central Role of the Copper(III) Intermediate and the Importance of the Copper(I) Precursor" *Angewandte Chemie, International Edition* **2007** *46*(37), 7082-7085

Bertz, S.H.; **Cope, S.K.**; Murphy, M.D.; Ogle, C.A.; Taylor, B.T.; "Rapid Injection NMR in Mechanistic Organocopper Chemistry. Preparation of the Elusive Copper(III) Intermediate" *J. Am. Chem. Soc.* **2007** *129*(23), 7208-7209

Watson, A.J.; **Cope, S.K.**; Jones, D.S.; Ogle, C.A.; "*Cis*-2,2-Dimethyl-1,3-diphenyl-2,3-dihydro-1*H*-benzo[C]silole" *Acta Crystallographica, Section E: Structure Reports Online* **2007**, *63*(7), 3346

Doung, L.C.; **Cope, S.K.**; Jones, D.S.; Ogle, C.A.; "*cis*-1,2,2,3-Tetraphenyl-2,3-dihydro-1*H*-2-benzosilole" *Acta Crystallographica, Section E: Structure Reports Online* **2006** *62*(8), 3574-3576

Invited Talks

University of California San Diego, Inorganic Seminar Series, April 25, 2014

Presentations

Cope, S.K.; Ogle, C.A.; Bertz, S.H.; Murphy, M.D.; Bartholomew, E.R.; "Rapid Injection NMR: Insights into the Reactions of Dimethyl Cuprates with Dihalides" *Abstracts*, 237th ACS National Meeting, Salt Lake City, UT, March 22-26, **2009**, ORGN-467

Cope, S.K.; Ogle, C.A.; Bertz, S.H.; Murphy, M.D.; Dorton, D.H.; Bartholomew, E.R.; "Neutral Organocopper(III) Complexes" *Abstracts*, 235th ACS National Meeting, New Orleans, LA, April 6-10, **2008**, INOR-939

Cope, S.K.; Ogle, C.A.; Bertz, S.H.; Murphy, M.D.; "Rapid Injection NMR: Observation and Characterization of Cu(III) Intermediates in the Reaction of

Lithium Dimethylcuprate with Alkyl Iodides" *Abstracts*, 233rd ACS National Meeting, Chicago, IL, March 25-29, **2007**, INOR-680

Cope, S.K.; Ogle, C.A.; Bertz, S.H; "An Investigation of Silyl groups on Asymmetic Induction in a Conjugate Addition Reactions with Chiral N-silylamidocuprates" *Abstracts*, 230th ACS National Meeting, Washington DC, August 28-September 1, **2005**, CHED-215

ABSTRACT OF THE DISSERTATION

Ruthenium-Mediated Cycloaromatization of Tri-Pi Systems

by

Stephen Kyle Cope

Doctor of Philosophy in Chemistry

University of California, San Diego, 2015

Professor Joseph M. O'Connor, Chair

This work describes mechanistic studies into a ruthenium-mediated cycloaromatization of dienynes. The results of deuterium labeling experiments are consistent with a mechanism that proceeds via a 6π-electrocyclization to form an η^4-*iso*benzene adduct followed by a metal-mediated [1,5]-hydride shift. The cycloaromatization of dienynes with substituents in the *E*-position of the distal alkene is proposed to give arene product via a process involving two sequential [1,2]-hydride

shifts. Dienynes bearing phenyl substituents in either the *E* or *Z*-position of the distal alkene or acetylenic position were shown to cycloaromatize.

The ruthenium-mediated cycloaromatization of acyclic trienes was accomplished in excellent yields. Observation and characterization of an η^6-triene ruthenium complex were accomplished. Deuterium labeling experiments led to a mechanistic proposal involving η^6-complexation of ruthenium to the triene followed by disrotatory electrocyclic ring closure. The deprotonation of the η^4-1,3-cyclohexadiene intermediate is proposed to generate a cyclohexadienyl ligand, which aromatizes via a ruthenium-assisted protolytic cleavage of a C-H or C-C bond.

In continuation of catalytic metal-triggered cyclization of enediynes under photolytic conditions, the effects of sterics and electronics in Cp-ligated iron and ruthenium were investigated with the 1,2,3,4-tetramethyl-5-trifluoromethylcyclopentadienyl (Cp‡) ligand. A series of Cp‡-ligated iron and ruthenium complexes were prepared. Attempts to generate [Cp‡Fe(η^6-benzene)]PF_6 led to activation of all three C-F bonds and the formation of a new (diphenylmethyl)tetramethylcyclopentadienyl ligand. The cyclization of an enediyne bearing a propargylic stereocenter was shown to have similar stereoselectivity for Cp- and Cp‡-ligated ruthenium (1:1), as compared to Cp* (8:2). The photochemical release of naphthalene from ruthenium in the presence of enediynes or dienynes was observed to give cycloaromatized products in excellent yields.

Finally, a recently discovered thermal cyclization of enediynes was extended to include incorporation of chloride or bromide from chloroform or bromoform,

respectively. The haloform was demonstrated to react with 1,4-cyclohexadiene to generate hydrogen halide *in situ*, which then added across an alkyne to produce a *cis*, *cis*-dienyne. The chloro and bromo dienyne intermediates were independently prepared and shown to undergo the cyclization. The cyclization is proposed to involve a cascade of pericyclic reactions initiated by either a [1,7]-hydride shift or 6π-electrocyclization leading to arene products with different substitution patterns. When iodoform was used, the iodo dienyne was observed at lower temperatures, but the product of a formal Bergman cyclization was the only product observed at higher temperatures. Fluoroform was observed to have no effect on the rate or product of the enediyne cyclization, presumably due to high bond strengths in fluoroform.

Chapter 1 Introduction

1-1 Tri-π Systems

Interest in the reactions of polyunsaturated organic systems has been on an upward swing since the late 1980s, catalyzed in part by the so-called Bergman cyclization. The reactions of these substrates have a rich synthetic and mechanistic history starting in the mid-20th century. One major limitation that has been observed for the reactions of polyunsaturated systems, especially the tri-π systems covered herein, is the high activation barrier for the reactions. The high temperatures needed for the reactions to occur and the competitive formation of byproducts has limited the usefulness of these reactions. The major goal of the current work is the activation of tri-π substrates to cycloaromatize at room temperature by interaction with transition metal complexes. The systems of interests in this work are enediynes (**1**), dienynes (**2**), and trienes (**3**); as shown in Figure 1-1.

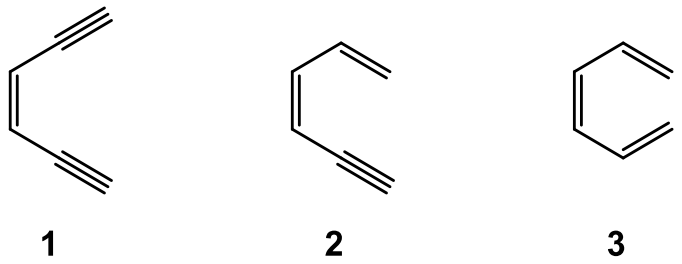

Figure 1-1. Conjugated tri-π systems are a focus of this thesis.

This thesis is split into four parts; (i) the reactions of dienynes (**2**) with transition metals, (ii) the reactions of trienes (**3**) with transition metals, (iii) attempts

at the development of new chemistry with Cp-ligated iron and ruthenium complexes and (iv) novel thermal reactions involving enediynes (**1**).

1-2 Chemistry of Enediynes

In the early 1970s Bergman demonstrated that the deuterium-enriched *cis*-enediyne **4** isomerized upon heating to > 200 °C to give the *cis*-enediyne isomer **5**, without formation of an isomer that contained deuterium at both a vinyl and terminal acetylenic position.[1]

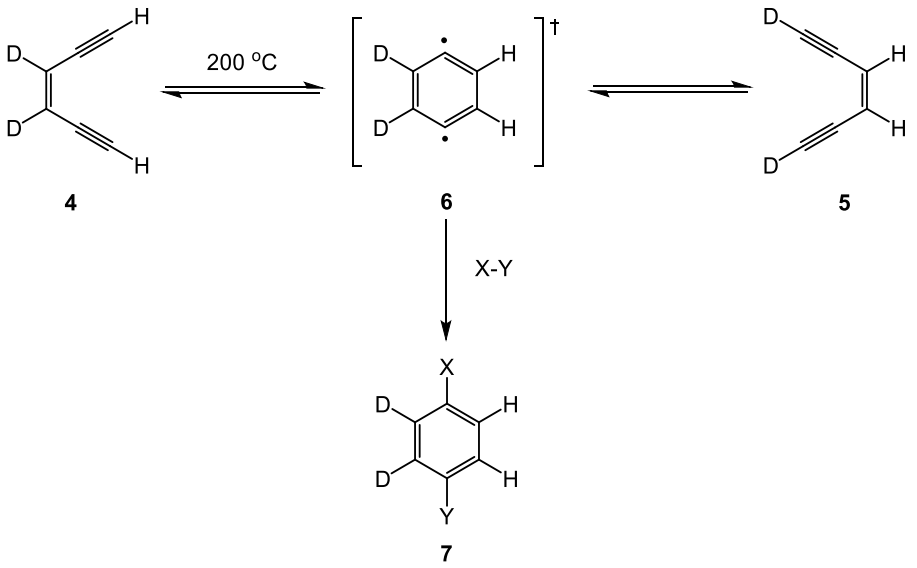

Figure 1-2. Bergman's initial observations with enediynes.[1] Note X-Y does not imply a diatomic molecule.

It was observed that when **4** was heated in the presence of a suitable radical source, such as toluene, 1,4-CHD or CCl_4, the group would add across an arene to generate

complexes of type **7**. This led Bergman to propose a highly symmetric *para*-benzyne intermediate (**6**) for the interconversion of **4** and **5**. The high cycloaromatization activation barrier, ~25 kcal/mol, necessitated high reaction temperatures which limited the reaction to an academic curiosity for many years. Interest in enediyne cycloaromatizations was renewed when the enediyne natural product Calicheamicin-γ^1 was discovered in caliche pits in Texas (Figure 1-3).[2]

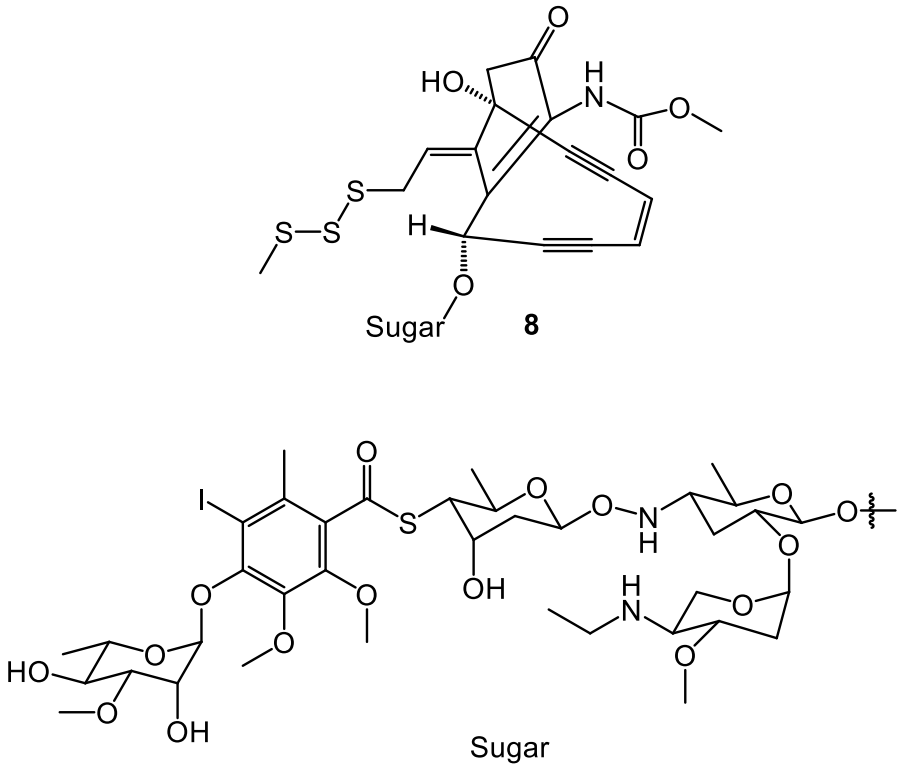

Figure 1-3. Calicheamicin-γ^1.[2]

Calicheamicin was demonstrated to have antitumor and antibiotic properties. The mechanism of action is proposed to involve calicheamicin binding to the minor

grove of DNA, followed by a chemical reaction that triggers the formation of a highly reactive *p*-aryne intermediate. The *p*-benzyne then abstracts a hydrogen atom from both strands of DNA, ultimately leading to cell death. This mechanism of action rekindled interest in the chemistry of enediynes, from both a synthetic and mechanistic standpoint.

Around this time several enedyine natural products were isolated and demonstrated to have remarkable biological activity as anticancer compounds and antibiotics.[3] These compounds overcame the inherent high activation barrier of acyclic enediynes by incorporating the enediyne framework into a marcocycle. This activation pathway for enediynes was demonstrated very elegantly by Nicolaou, who made a series of molecules in which the enediyne was incorporated into 9-membered to 13-membered rings (Figure 1-4).[4] The distance between the distal acetylenic carbons, the so-called *c-d* distance, was measured from computational data and the temperature required for cyclization was correlated with the *c-d* distance.

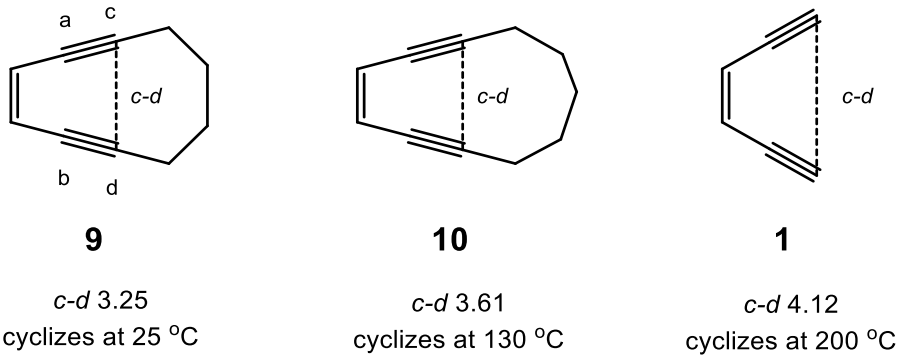

Figure 1-4. Nicolaou's work with cyclic enediynes.[4]

It was concluded that *c-d* distances of 3.0 to 3.2 Å should lead to cyclization at room temperature. It was later pointed out that the increase in the rate of cyclization observed for smaller rings is more directly related to the increase in the ground state energies of the enediyne than the *c-d* distance.[5] In essence, the transition state energy remains approximately the same for all Bergman cyclizations, but by incorporating the enediyne into a ring the ground state energy is raised. Thus the effective activation barrier of cyclic enediynes is lowered relative to that for acyclic enediynes.

The O'Connor group demonstrated that Cp^*Ru^+ triggers the cycloaromatization of enediynes in the presence of hydrogen-atom donors such as THF and 1,4-CHD.[6] These cyclization proceeded in moderate to excellent yield at rt.

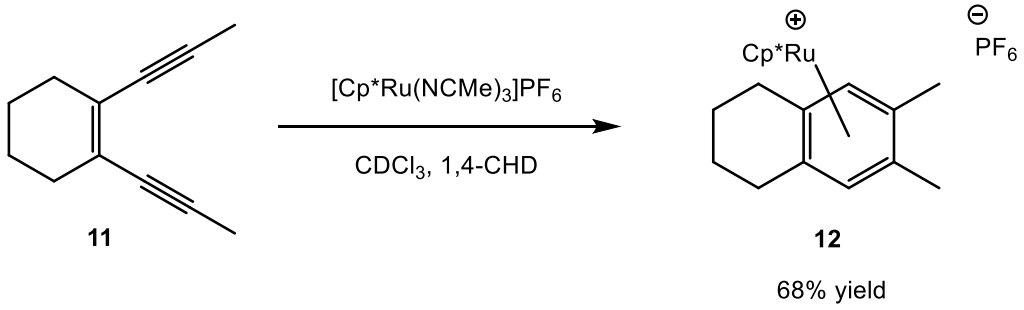

Scheme 1-1. Bergman cyclization mediated by Cp^*Ru^+.[6]

Through a combination of experimental and computational studies, the mechanism of this reaction was suggested to proceed as shown in Scheme 1-2.[6,7]

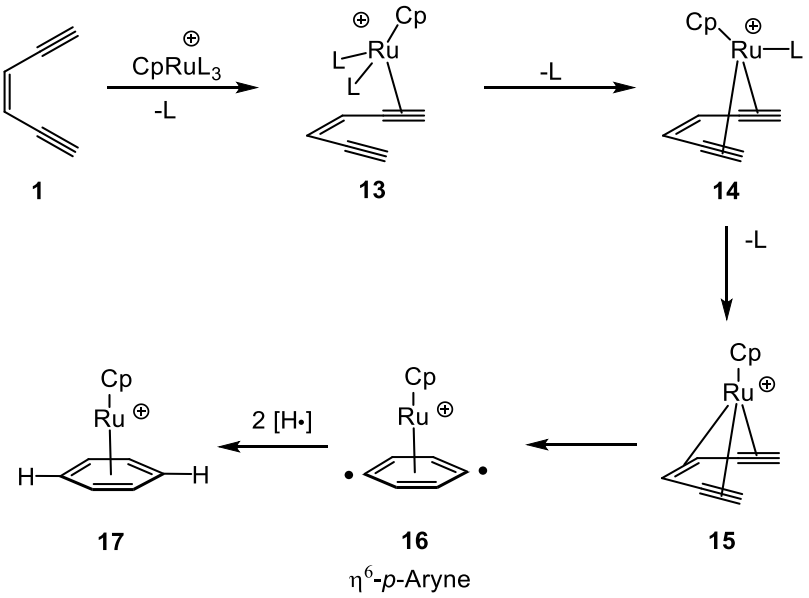

Scheme 1-2. A proposed mechanism for ruthenium-mediated enediyne cycloaromatization.[6,7]

The loss of one MeCN ligand and coordination to an alkyne was shown to be more favorable than alkene coordination (Δ = 16.5 kcal mol^{-1}).[7] In a similar fashion, loss of a second MeCN ligand and coordination of ruthenium to a second alkyne is favored over enyne coordination (Δ = 16.6 kcal mol^{-1}). Finally, loss of the third MeCN leads to coordination to the alkene, thereby generating an η^6-enediyne intermediate. η^6-Coordination of ruthenium to the enediyne leads to spontaneous cyclization to an η^6-bound *p*-benzyne, which quickly abstracts hydrogens from a hydrogen-atom source. The computed structure of the η^6-enediyne is shown in Figure 1-5. The *c*-*d* distance for the structure is 2.98 Å, well under the Nicolaou critical distance of 3.2 to 3.31 Å.

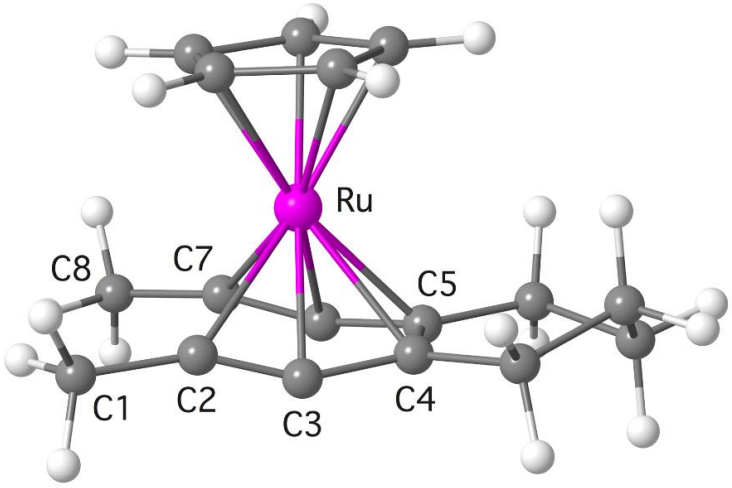

Figure 1-5. Calculated structure of CpRu(η^6-enediyne)$^+$.[7]

1-3 Chemistry of Dienynes

It was discovered in 1969 by Höpf that 184.9 nm irradiation of benzene resulted in the formation of *cis*-1,3-hexadien-5-yne (**19**), which subsequently isomerized to the *trans* isomer, *trans*-1,3-hexadien-5-yne (**20**). [8]

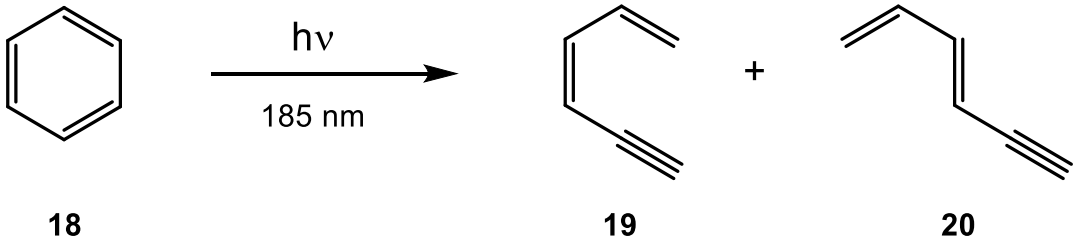

Scheme 1-3. Höpf's original work with dienynes.[8]

Höpf reasoned that unsaturated hydrocarbons could be excited either photochemically or thermally, which led to the study of dienyne thermolysis chemistry. Thus, it was

demonstrated that when a sample of **19** was heated at 274 °C for 90 min, a mixture of **19** : **20** : **18** was formed in a 64 : 11 : 25 ratio. When a sample of **20** was subjected to the same conditions; a ratio of **19** : **20** : **18** of 9 : 55 : 36, respectively, was obtained. Through experimental and computational studies, Höpf and others proposed the mechanism for dienyne cycloaromatization shown in Scheme 1-4.[9]

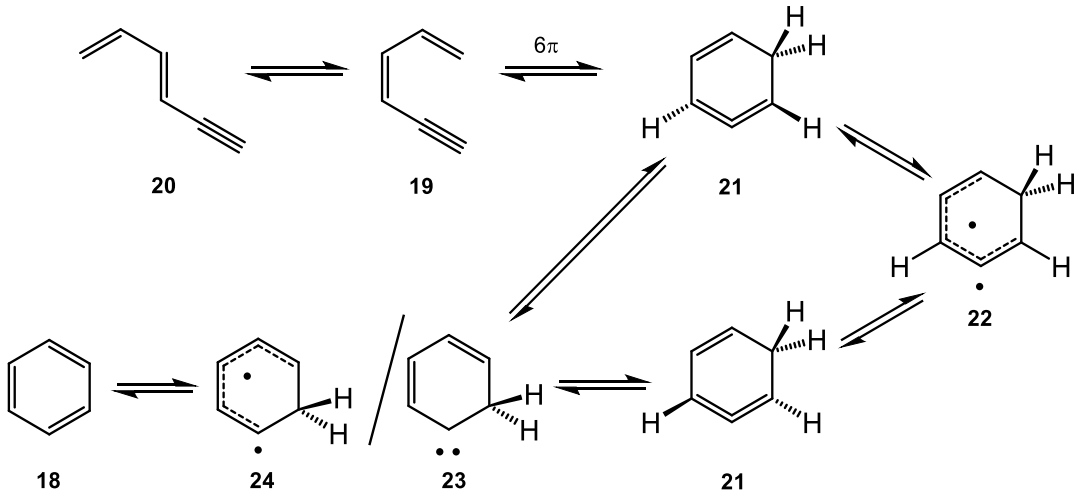

Scheme 1-4. Proposed mechanism for cycloaromatization of dienynes.[9]

In this mechanism *trans*-1,3-hexadien-5-yne isomerizes at 274 °C to *cis*-1,3-hexadien-5-yne, which then undergoes a 6π-electrocyclization to *iso*benzene intermediate **21**. The 6π-electrocyclization is proposed to proceed through a disrotatory ring closure in either direction to form a pair of enantiomers, which interconvert via planar diradical species **22**. Then **21** undergoes a [1,2]-hydride shift to give singlet/triplet carbene structures **23** and **24**, with a calculated singlet/triplet gap of 1 kcal mol^{-1}. This intermediate is then convert to benzene via a second [1,2]-hydride shift.

The high temperature necessary for cycloaromatization to proceed has generally limited the thermal reaction to the synthesis of polyaromatic hydrocarbons. For example, the key step in a synthesis of corannulene (**26**) was the flash vacuum pyrolysis of benzannulated diyne **25** (Scheme 1-5).[10]

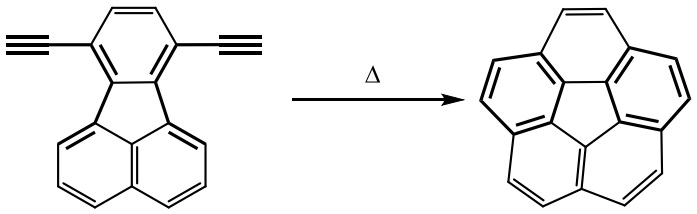

25 **26**

Scheme 1-5. Synthesis of corannulene (**26**) by flash vacuum pyrolysis.[10]

There are a number of examples of lowering the temperature at which the onset of reaction occurs.[11] One of the first examples came from the lab of Sondheimer, who was studying the isomerization of non-conjugated diynes with KO^{t}Bu.[12] When 1,6-heptadiyne was heated in the presence of KO^{t}Bu in ^{t}BuOH at 80 °C for 6 h, the formation of toluene and *trans*-1,3-heptadien-5-yne was observed in approximately 30% yield each.

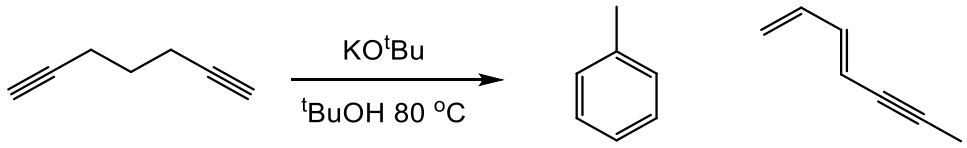

27 **28** **29**

Scheme 1-6. Sondheimer's reaction of 1,6-heptadiyne with KO^{t}Bu.[12]

It was shown that a non-conjugated diyne could rearrange to both *cis* and *trans* dienynes, but no explanation was given for the formation of toluene. Höpf in a subsequent paper showed that heating an authentic sample of *cis*-1,3-heptadien-5-yne in the presence of KO^{t}Bu in ^{t}BuOH at 80 °C resulted in the formation of toluene.[13] This led to a proposal that *cis*-1,3-heptadien-5-yne was generated as an intermediate under the conditions of Sondheimer and then this species cyclized to toluene. Höpf attributed the increase in the rate of cyclization to a symmetry-forbidden [1,3]-hydride shift in the slow step, which under the conditions could proceed through a deprotonation/protonation pathway.

Another approach toward lowering the activation barrier for dienyne cycloaromatization was the incorporation of the dienyne into a macrocycle, by analogy to the lowering of activation barriers for strained-ring enediynes. The first example was the formation of the 8-membered ring dienyne **31**, generated by the thermal decomposition of selenadiazol **30**.[14]

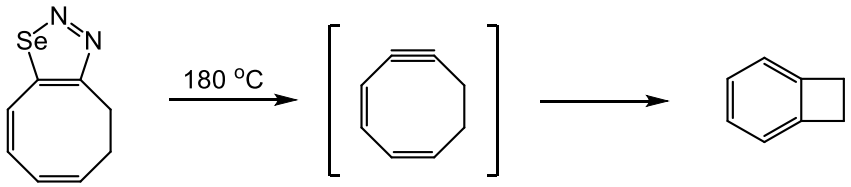

30 **31** **32**

Scheme 1-7. First example of a strained-ring dienyne.[14]

Highly strained **31** was observed as only a trace product in the reaction mixture, but the formation of **31** could be inferred by the isomerization to benzocyclobutene, **32**.

In subsequent years both Höpf and Zimmermann prepared strained-ring dienynes in the range of 10-membered to 14-membered ring sizes.[15] It was shown through this work that incorporation of a dienyne into a macrocycle could lower the temperature for the onset of cycloaromatization.

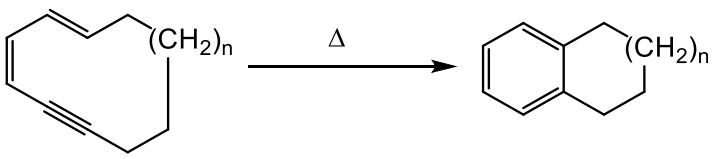

33 a-e 34 a-e

34	n	$T_{cycl.}$, °C
a	1	25
b	2	100
c	3	150
d	4	210
e	5	>210

Scheme 1-8: Strained-ring dienynes and corresponding temperatures for onset of cyclization.[15]

When the dienynes were incorporated into a 10-membered ring, the cycloaromatization was observed to occur at room temperature. As the ring became larger, the strain on the dienyne decreased and the temperature for onset of cyclization increased.

The next pathway taken to lower the activation barrier is the interaction of dienynes with metals, which can be divided into two basic mechanisms. The first involves coordination of a transition or main-group metal to the alkyne which activates it toward Umpolung attack by the alkene, and subsequent isomerization to product. Shibata showed that cationic gold complexes catalyzed the cyclization of benzannulated dienynes (**35**) at room temperature to give substituted naphthalenes (**36**).[16]

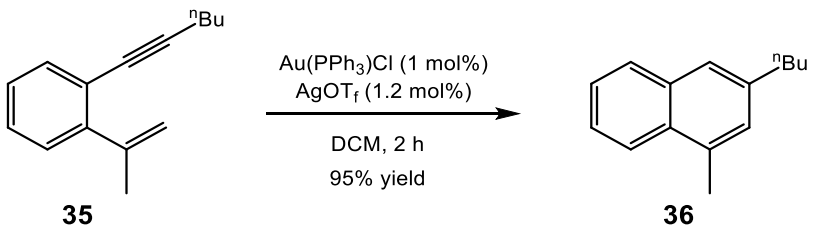

Scheme 1-9. Gold-catalyzed cyclizations.[16]

The cyclizations of a number of dienynes proceed cleanly at room temperature, with two main limitations. The first is there must be a substituent at the 2-position, as the mechanism involves the formation of a carbocation at the 2-position. The second limitation is the nature and position of substituents on the unsaturated systems. When terminal alkynes were subjected to the conditions, the formation of naphthalenes was accompanied by the formation of 1-methylene-1*H*-indene derivatives.

The second metal-based pathway for activation of dienynes involves the formation of transition metal vinylidene intermediates, which subsequently isomerize to arene products. An example is found in Merlic's 1996 report on the reaction of terminal alkyne **37** with $RuCl_2(C_6H_6)PPh_3$ in DCM (Scheme 1-10).[17]

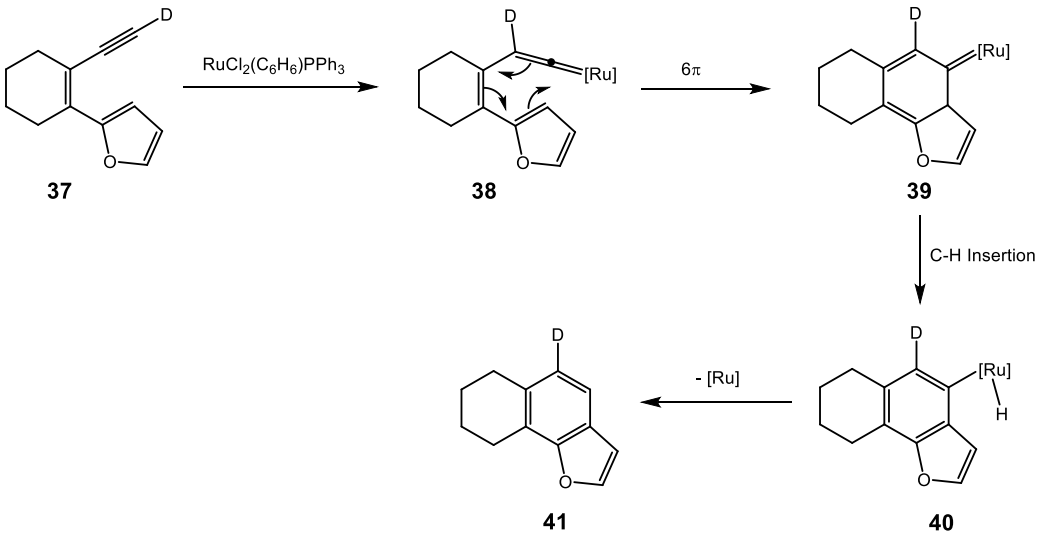

Scheme 1-10. Merlic's vinylidene-based cyclization of dienynes.[17]

Coordination of ruthenium to the alkyne leads to migration of the terminal deutride to the internal carbon of the alkyne and formation of vinylidene **38**. Intermediate **38** then undergoes a 6π-electrocyclization to give carbene **39**, which then proceeds to ruthenium-hydride **40**, restoring aromaticity. Then reductive elimination from **40** leads to product **41** and regeneration of the ruthenium catalyst. The formation of a transition metal vinylidene drastically lowers the temperature for the onset of cycloaromatization, with the one major limitation that the dienyne must possess a terminal alkyne.

The O'Connor group, as an extension of their work on the cycloaromatizations of enediynes, showed that dienynes could be cycloaromatized by $[CpRu(NCMe)_3]PF_6$ in $CDCl_3$ at room temperature.[6,18]

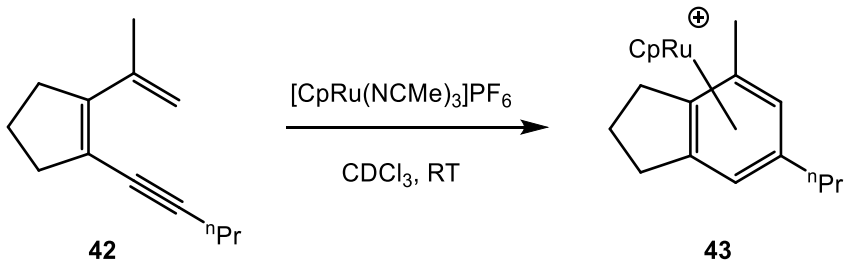

42 43

Scheme 1-11. Cycloaromatization mediated by $CpRu^{+}$.[6,18]

There were a number of key observations during these studies about the pathway of the cyclization. The current work is focused on the mechanism of this reaction.

1-4 Chemistry of Trienes

Of the linear tri-π conjugated systems **1-3**, trienes are the ones with the longest reaction history. One of the earliest examples was the thermal conversion of vitamin D (**42)** to a mixture of pyro- (**44**) and isopyro- (**45**) calciferols at 188 °C.[19] The reaction is initiated by a [1,7]-hydride shift to give precalciferol (**43)**, which then undergoes a 6π-electrocyclization to give **44** and **45**.

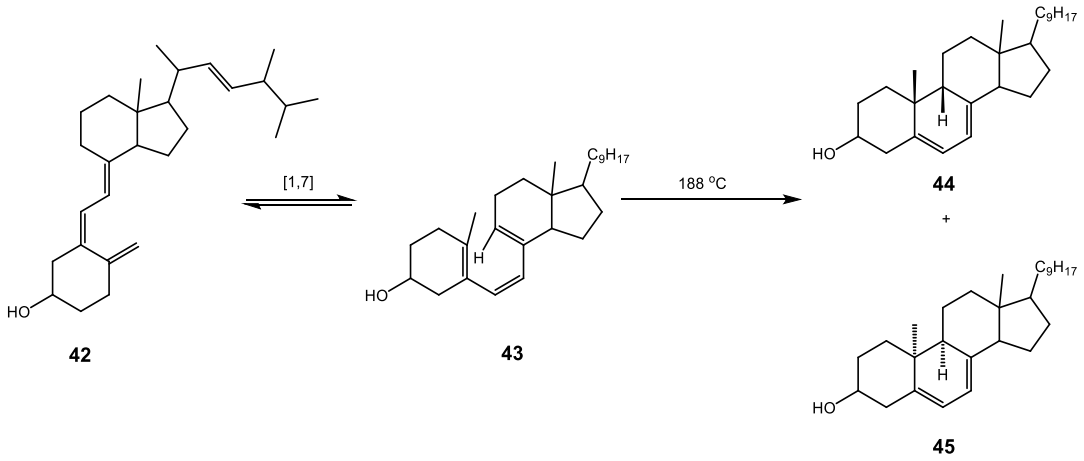

Scheme 1-12. Electrocyclization of a vitamin D derivative.[19]

The stereochemistry of the product was not fully established until 1959 and the mechanism leading to the observed stereochemistry in **44** and **45** was not understood.[20] It was not until 1964 that the thermal cyclization of the parent linear triene, 1,3,5-hexatriene (**46**), was reported by Lewis & Steiner.[21]

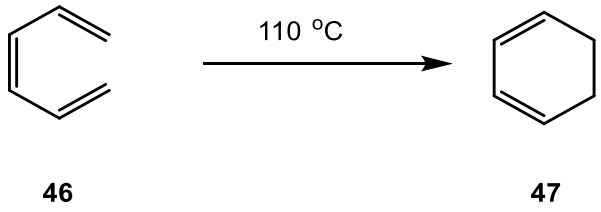

Scheme 1-13. Electrocyclization of *cis*-1,3,5-hexatriene.[21]

It was shown that when *cis*-1,3,5-hexatriene (**46**) was heated at 110 °C, the formation of 1,3-cyclohexadiene (**47**) was observed after 2 h. When the reaction was carried out on the *trans* isomer, no reaction was observed up to 192 °C (2 h). The

authors proposed a cyclic transition state for this reaction, but gave no hint as to the stereochemical outcome of the reaction.

It was not until the seminal publication by Woodward and Hoffmann on the conservation of orbital symmetries, that the mechanism of electrocyclization and stereochemical outcome thereof gain a theoretical underpinning.[22] The authors used molecular orbital diagrams to show the phase relationship of reacting groups and proposed that conjugated systems react via a cyclic transition state. The theory goes on to state that energetically favorable transition states for particular moieties can be achieved only under certain rotational operations. These energetically favorable rotational operations give rise to the stereochemistry observed in products. The theory predicts that conjugated substrates with 4n π-electrons will proceed through a rotational operation where the reacting termini rotate in the same direction, coining the term conrotatory (e.g. **48** to **49**). A 4n+2 π-electron system will proceed through a rotational operation where the reacting termini rotate in opposite directions, coining the term disrotatory (e.g. **50** to **51**).

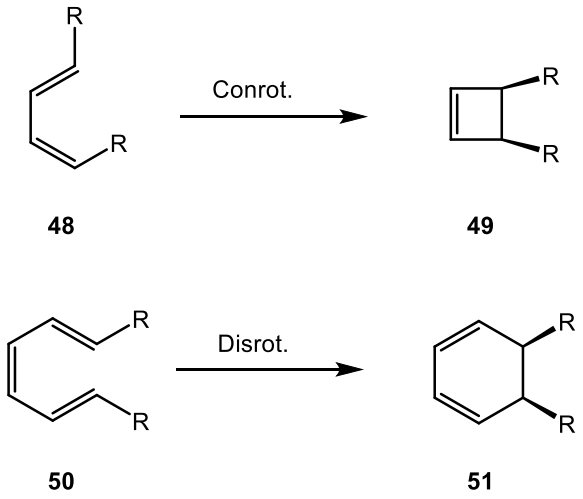

Figure 1-6. Stereochemical outcomes from electrocyclization as predicted by conservation of orbital symmetry.[22]

With these rules, the stereochemical outcome of a reaction can be easily predicted from the stereochemistry of the starting material and whether the unsaturated system is 4n or 4n+2. The expected stereochemical outcome was observed in the formation of **44** and **45** from **43**, wherein the hydrogen and methyl groups were *syn* in the newly formed cyclohexadiene ring.

While electrocyclizations of trienes proceed under milder conditions, 100 to 140 °C, as compared to the > 200 °C conditions required for the enediyne or dienyne systems discussed above, the lowering of the activation barrier for triene electrocyclizations is also desired. The first efforts in this area were made by Bergman and Trauner.[23] They reasoned that since electrocyclizations had been shown to be more facile when an electron-withdrawing group was present at the 2-position, coordination of a Lewis acid to a Lewis basic electron-withdrawing substituent at the

2-position would facilitate the reaction.[24] They computationally assessing the proposed system. This was accomplished by calculating the reaction energies of a simple triene ester with the ester in the 1-position (both *E* and *Z*), the 2-position and the 3-position. Indeed it was shown that the system with the ester in the 2-position resulted in the most facile cyclization. They then performed the same calculations with a proton bound to the carbonyl oxygen. The protonated ester in the 2-position was calculated to have an activation barrier of only 14 kcal mol^{-1}, a full 10 kcal mol^{-1} lower than the unprotonated analogy, 24 kcal mol^{-1}.

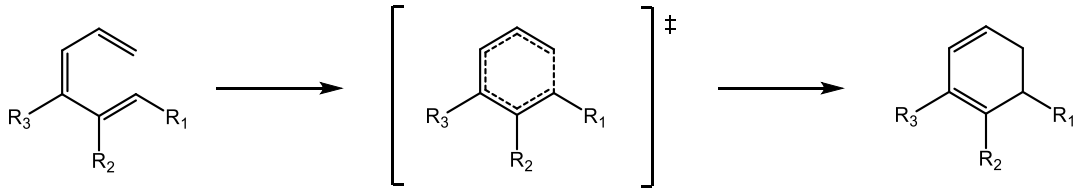

Scheme 1-14. Trienes studied computationally by Bergman and Trauner.[23]

Table 1-1. Relative Electronic Energies of the Thermal (Protonated Carbonyl) Electrocyclization.[a,b]

	TS (**53**)	Product (**54**)	$\Delta\Delta E^{‡}$
R_1=CO_2Me, R_2=R_3=H	+31 (+35)	-6 (+9)	+4
R_2=CO_2Me, R_1=R_3=H	+24 (+14)	-20 (-29)	-10
R_3=CO_2Me, R_1=R_2=H	+26 (+24)	-5 (-17)	-2

[a] In kcal mol^{-1}. [b] Computed at the B3LYP/6-31G** level of theory with the reference point for each isomer as **52**.[23]

To test the calculated predictions, the triene ester **55** was synthesized. In C_6D_6, **55** was shown to cleanly cyclize to **56** at 50 °C with a half-life of 4 hours.

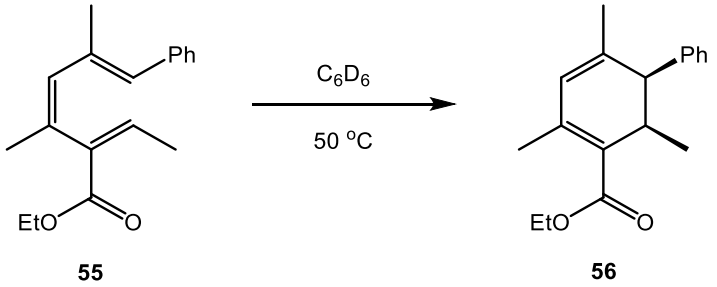

55 **56**

Scheme 1-15. Triene ester used in the studies of Bergman and Trauner.[23]

When one equivalent of Me_2AlCl was added to a solution of **55** in C_6D_6 and heated to 50 °C, the clean formation of **56** was again observed, with a half-life of 21 minutes. This showed the potential to activate a triene toward electrocyclization by coordination of a Lewis acid to a Lewis basic substituent. These results point toward the development of better Lewis acid catalysts and the development of chiral Lewis acid catalyst to afford enantioselective electrocyclizations.

New methodologies in the electrocyclizations of trienes could allow the further lowering of the temperature necessary for electrocyclization. In addition, new methodology directed toward the development of enantioselective electrocyclizations would be beneficial.

1-5 Pericyclic Reactions and Transition Metal Coordination

After publication of the Woodward-Hoffmann rules, there was considerable effort directed toward the conversion of forbidden reactions to allowed reactions by the coordination of metals. Mango published a set of selection rules for when this forbidden-to-allowed transformation can occur and the stereochemical outcome of the transformation.[25] The basic idea put forward by Mango was that transformations which allowed for continuous metal coordination to the substrate throughout the reaction coordinate would be allowed. In the example of ring-opening of cyclobutene to butadiene, a conrotatory ring-opening would not be allowed upon coordination to a metal, as the metal must lose coordination to the olefins due to symmetry constraints. The disrotatory ring-opening of cyclobutene on a metal would be allowed as the metal maintains continuous coordination to the substrate throughout the reaction coordinate.

The ring-opening of cyclobutene by $Fe(CO)_3$ is one of the most well studied metal-catalyzed electrocyclic reactions.[26,27,28] While the ring-opening of cyclobutene on $Fe(CO)_3$ has proven to be problematic to study experimentally,[26] the ring-opening of strained cyclobutene coordinated to $Fe(CO)_4$ have been demonstrated to proceed in a disrotatory fashion (Scheme 1-16).[27]

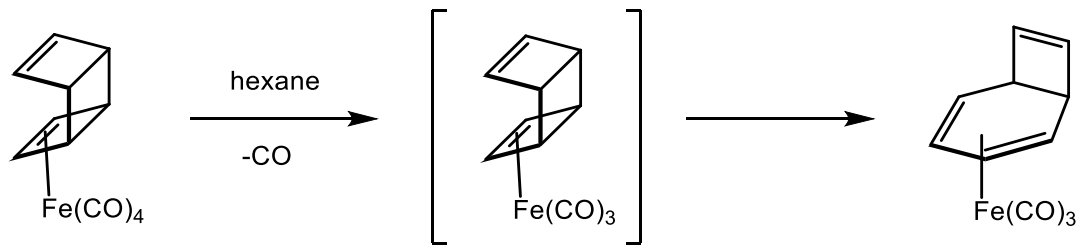

57 **58** **59**

Scheme 1-16. $Fe(CO)_3$-mediated ring-opening of cyclobutenes.[27]

The reaction is proposed to proceed by initial loss of a CO ligand to generate unsaturated 16-electron intermediate **58** which then undergoes a disrotatory ring-opening to give **59**. It is unlikely that the cyclobutene in **57** could open through a conrotatory pathway due to the geometric constraints imposed by the second cyclobutene ring.

This and other examples are proposed to proceed through a pericyclic ring-opening, the nature of this pericyclic ring-opening was investigated computationally by Hoffmann and Tantillo.[28] They chose to study the ring-opening of the parent cyclobutene on $Fe(CO)_4$ as no substrate enforced geometric constraints would be present to favor the disrotatory ring-opening. They proposed two pathways for this transformation. The first starts with loss of CO from **60**, with an activation barrier of 31.5 kcal mol^{-1}, to form **62**. Complex **62** exists as a pair of rotomers that interconvert with an activation barrier of 1.5 kcal mol^{-1}. Complex **62** then undergoes a disrotatory electrocyclic ring-opening to **61** with an activation barrier of 30 kcal mol^{-1} over **62**.

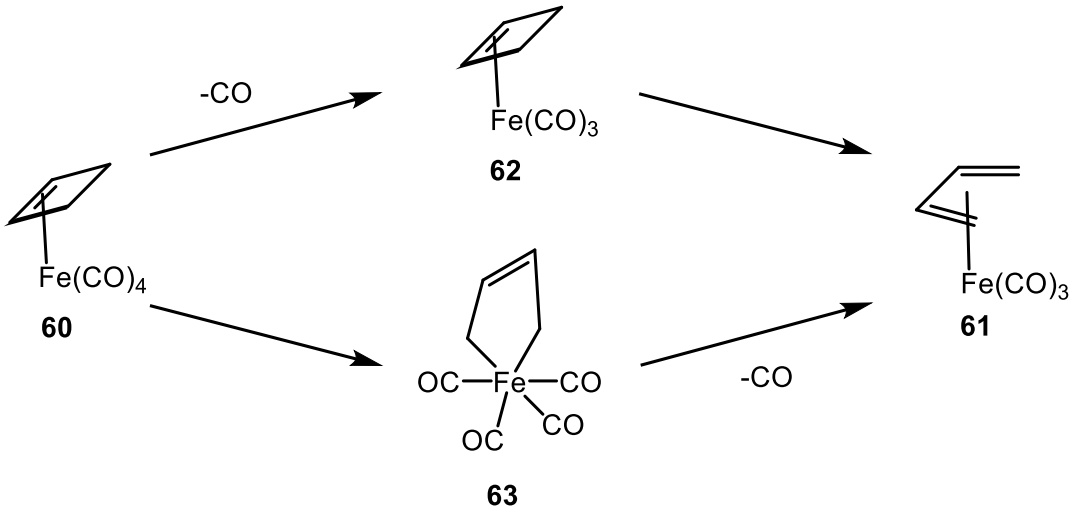

Scheme 1-17. Proposed pathways for the ring-opening of cyclobutene on $Fe(CO)_3$.[28]

From **62** they were unable to locate a transition state for the conrotatory ring-opening. The second pathway was the oxidative addition to the sigma bond opposite the olefin to give **63** with an activation barrier of 46.8 kcal mol^{-1}. Complex **63** then loses a CO ligand with an activation barrier of 28 kcal mol^{-1}, to generate an unsaturated 16-electron iron complex from which reductive elimination (10 kcal mol^{-1} activation barrier) gives **61**. From these studies, it appears that an oxidative addition/reductive elimination pathway is the lower energy pathway, but the small difference in energy may mean the two pathways compete. In the ring-opening of **57**, the oxidative addition to the sigma-bond is less likely due to steric clashing in the transition state between the iron center and bicyclic structure of the substrate.

There are numerous examples of metal-catalyzed cycloaddition reactions proposed to proceed through a pericyclic mechanism,[26] but to the best of our knowledge there are no examples of 6π-electrocyclization reactions occurring on

transition metals. One aim of the current research is to demonstrate the η^6-coordination of a tri-π system to a transition metal center and the subsequent 6π-electrocyclization induced by coordination of the unsaturated system to the transition metal.

1-6 References

1. Bergman, R.G. *Acc. Chem. Res.* **1973**, *6*, 25.

2. (a) Lee, M.D.; Dunne, T.S.; Siegel, M.M.; Chang, C.C.; Morton, G.O.; Borders, D.B. *J. Am. Chem. Soc.* **1987**, *109*, 3464. (b) Lee, M.D.; Dunne, T.S.; Chang, C.C.; Ellestad, G.A.; Siegel, M.M.; Morton, G.O.; McGahren, W.J.; Borders, D.B. *J. Am. Chem. Soc.* **1987**, *109*, 3466.

3. Nicolaou, K.C.; Smith, A.L.; Yue, E.W. *Proc. Natl. Acad. Sci. U.S.A.* **1993**, *90*, 5881.

4. (a) Nicolaou, K.C.; Zuccarello, G.; Ogawa, Y.; Schweiger, E.J.; Kumazawa, T. *J. Am. Chem. Soc.* **1988**, *110*, 4866. (b)Nicolaou, K.C.; Zuccarello, G.; Riemer, C.; Estevez, V.A.; Dai, W.M. *J. Am. Chem. Soc.* **1992**, *114*, 7360.

5. (a) Snyder, J.P. *J. Am. Chem. Soc.* **1989**, *111*, 7630. (b) Magnus, P.; Carter, P.; Elliott, J.; Lewis, R.; Harling, J.; Pitterna, T.; Bauta, W.E.; Fortt, S. *J. Am. Chem. Soc.* **1992**, *114*, 2544.

6. (a) O'Connor, J.M.; Friese, S.J.; Rodgers, B.L. *J. Am. Chem. Soc.* **2005**, *127*, 16342. (b) O'Connor, J.M.; Friese, S.J. *Organomet.* **2008**, *27*, 4280. (c) O'Connor, J.M.; Friese, S.J.; Tichenor, M. *J. Am. Chem. Soc.* **2002**, *124*, 3506.

7. Calculations performed by Kim Baldridge using BP86 density functional, Def2-TZVPP basis set, GAMESS Program.

8. Höpf, H.; Musso, H. *Angew. Chem. Int. Ed. Engl.* **1969**, *8*, 680.

9. (a) Prall, M.; Kruger, A.; Schreiner, P.R.; Höpf, H. *Chem. Eur. J.* **2001**, *7*, 4386. (b) Litovitz, A.E.; Carpenter, B.K.; Höpf, H. *Org. Lett.* **2005**, *7*, 507.

10. Scott, L.T.; Cheng, P.C.; Hashemi, M.M.; Bratcher, M.S.; Meyer, D.T.; Warren, H.B. *J. Am. Chem. Soc.* **1997**, *119*, 10963.

11. Hitt, D.M.; O'Connor, J.M. *Chem. Rev.* **2011**, *111*, 7904.

12. Ben-Efraim, D.A.; Sondheimer, F. *Tetrahedron* **1969**, *25*, 2837.

13. Höpf, H. *Tet. Lett.* **1970**, 1107.

14. (a) Hanold, N.; Meier, H. *Chem. Ber.* **1985**, *118*, 198. (b) Meier, H.; Hanold, N.; Kolshorn, H. *Angew. Chem.* **1982**, *94*, 67; *Angew. Chem. Int. Ed. Engl.* **1982**, *21*, 66.

15. (a) Schreiner, P.R. *Chem. Comm.* **1998**, *4*, 483. (b) Schreiner, P.R. *J. Am. Chem. Soc.* **1998**, *120*, 4184.

16. Shibata, T.; Ueno, Y.; Kanda, K. *Synlett* **2006**, 411.

17. Merlic, C.A.; Pauly, M.E. *J. Am. Chem. Soc.* **1996**, *118*, 11319.

18. O'Connor, J.M.; Friese, S.J.; Rodgers, B.L.; Rheingold, A.L.; Zakharov, L. *J. Am. Chem. Soc.* **2005**, *127*, 9346.

19. Busse, P. *Z. Physiol*. **1933**, *214*, 211.

20. Castello, J.; Jones, E.R.H.; Meakins, G.D.; Williams, R.W.J. *J. Chem. Soc.* **1959**, 1159.

21. Lewis, K.E.; Steiner, H. *J. Chem. Soc.* **1964**, 3080.

22. Woodward, R.B.; Hoffmann, R. "Conservation of Orbital Symmetry," Verlag Chemie, Weinhiem, **1970**.

23. Bishop, L.M.; Barbarow, J.E.; Bergman, R.G.; Trauner, D. *Angew. Chem. Int. Ed. Engl.* **2008**, *47*, 8100.

24. Prinzbach, H.M.; Druckery, E. *Tet. Lett.* **1965**, 2959.

25. (a) Mango, F.D. *Advan. Catalysis* **1969**, *20*, 291. (b) Mango, F.D. *Tet. Lett.* **1973**, *17*, 1509.

26. Pinhas, A.R. PhD. Thesis, Cornell University, **1980**.

27. Knolker, H.J. *Chem. Rev.* **2000**, *100*, 2941.

28. (a) Tantillo, D.J.; Hoffmann, R. *J. Am. Chem. Soc.* **2001**, *123*, 9855. (b) Tantillo, D.J.; Hoffmann, R. *Helv. Chim. Acta* **2001**, *84*, 1396.

29. Mango, F.D. *Coord. Chem. Rev.* **1975**, *15*, 109.

Chapter 2 Ruthenium-Mediated Cycloaromatization of Dienynes

2-1 Introduction

The cycloaromatization of dienynes, **1**, commonly called a Höpf cyclization, has garnered attention for its relation to the Bergman cyclization and the ability to generate a highly substituted aromatic system in a single step from easily constructed starting materials.[1]

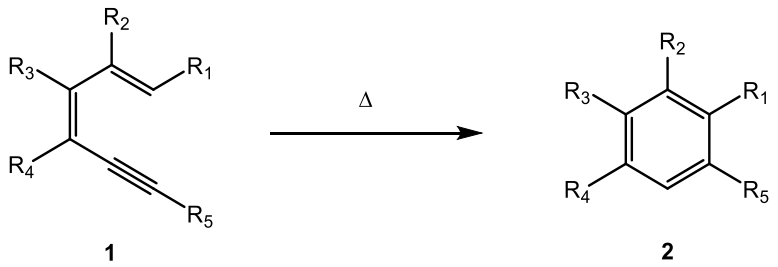

1 **2**

Figure 2-1. Höpf cycloaromatization.[1]

One of the major limitations for the Höpf cyclization is the high temperatures necessary for reaction to occur. As mentioned in Chapter 1, attempts have been made to lower the activation barrier for the reaction but limitations were uncovered with respect to the substitution pattern that can be tolerated.[2]

As an extension of their work on the cycloaromatization of enediynes by ruthenium, the O'Connor group demonstrated the Cp^*Ru^+ (**5**) mediated cycloaromatization of dienynes in $CDCl_3$ at room temperature (Scheme 2-1).[3]

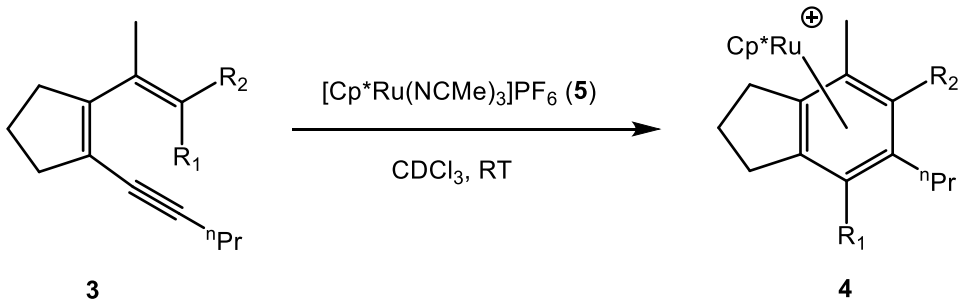

3 4

Scheme 2-1. Cyclization of dienynes by $[Cp^*Ru]^+$.[3]

There were a number of substituents (R_1, R_2 = alkyl, ester, chloro) tolerated at positions R_1 and R_2, with the caveat that either R_1 or R_2 has to be a hydrogen, which is to be expected for a Höpf cyclization. During low-temperature (-60 °C) NMR studies on the reaction of **5** with terminal dienyne **6** the appearance of new resonances hinted at the presence of a possible π-bound intermediate. These new resonances at δ 0.11 and 3.27 were ascribed to the terminal hydrogens of an η^6-bound dienyne, **7** (Scheme 2-2).[4]

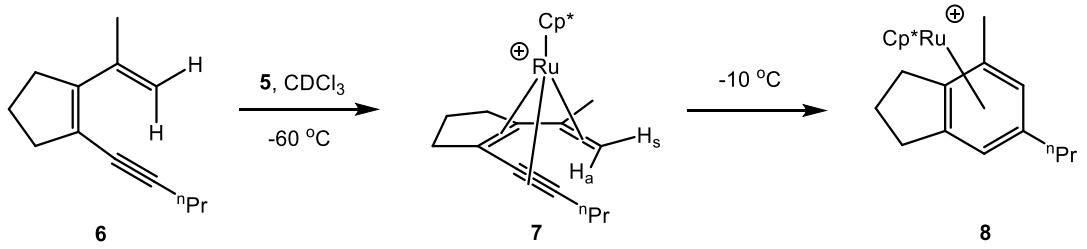

6 7 8

Scheme 2-2. Low-temperature NMR studies support the formation of an η^6-dienyne complex.[4]

When this solution was allowed to warm to -10 °C, the formation of the expected arene product, **8**, was observed. This pointed to **7** being a possible intermediate on the path to **8**. The experiment was setup again and the formation of **7** was observed by NMR spectroscopy. Then the NMR tube was removed from the spectrometer. The solution was kept cold and Et_2O was cannula transferred into the tube. After 18 h at -60 °C, the formation of single crystals was observed. Through a single crystal X-ray diffraction study, the structure of **7** was confirmed as [Cp*Ru(η^6-dienyne)]PF_6. The key features of this structure are the η^6-binding of the dienyne to ruthenium, the pronounced bending of the alkyne from linearity, and the proximity of the terminal alkene hydrogens to the ruthenium center. This was the first example of an η^6-bound linear polyunsaturated metal complex. This binding forced the alkyne from linearity, with angles at both sp-carbons of approximately 150°. The hydrogen that is *syn* to the methyl group, H_s, was 2.87(5) Å from the metal center, while the hydrogen *anti* to the methyl group, H_a, was 2.19(4) Å. The close proximity of H_a led the assignment of the ^{1}H NMR resonance at δ 0.11 to this hydrogen.

As a means to check for intramolecular hydrogen transfer, **6-d** (85% deuterium incorporation), was prepared and reacted with **5** in $CDCl_3$ (Scheme 2-3).[5] The product **8-d** showed 85% deuterium incorporation in both arene positions, indicative of selective deuterium migration to the internal alkyne position. When the experiment was repeated in the presence of a small amount of H_2O, **8-d** now showed 85% deuterium incorporation at the 2-position, but only 45% deuterium incorporation

at the 4-position. This hinted at the presence of transition metal hydride during the course of the reaction.

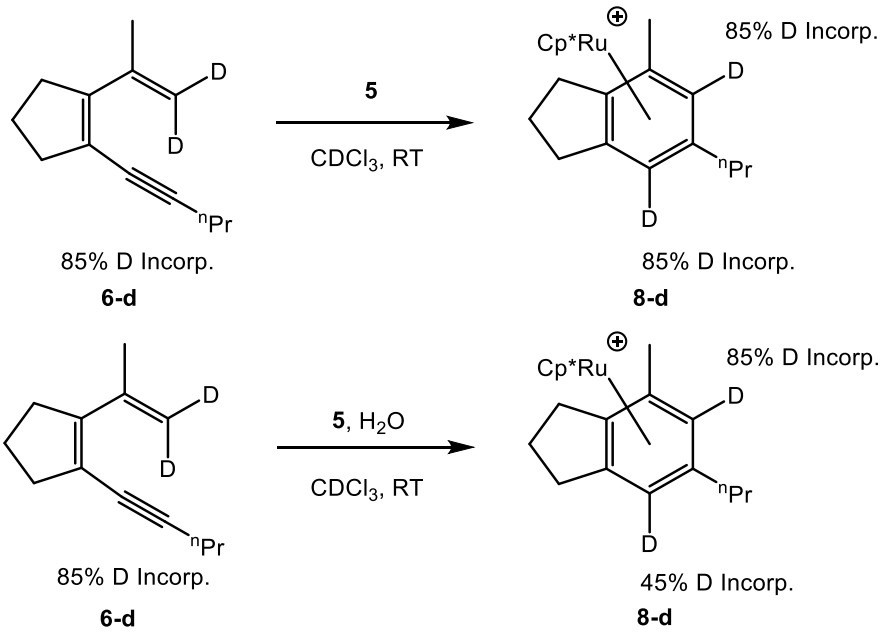

Scheme 2-3. Deuterium labeling studies.[5]

With these results, two primary mechanistic pathways were proposed at that time.[5] The reaction starts with loss of three MeCN ligands from **5** and coordination of dienyne **9** to form the η^6-intermediate **10**, as was seen by NMR spectroscopy and a solid-state X-ray structure of related complex **7** (Scheme 2-4). From **10** there are two different mechanistic pathways that could be taken. The ruthenium center could insert into the C-D bond, (which was shown to be closer to the metal center in the X-ray structure of **7**) to form Ru(IV)-deuteride **11**. A *trans*-migratory insertion of the alkyne would then generate a ruthenacycloheptatriene (**12**) and reductive elimination would generate the observed arene product **13**. The presence of **11** could explain the

exchange of D for H in the reaction of **6-d** with **5** in the presence of H_2O. In addition, this pathway is supported by the proposed intermediacy of ruthenacycloheptatriene **12**, which is related to intermediates that have been proposed in other ruthenium-catalyzed arene formations.[6]

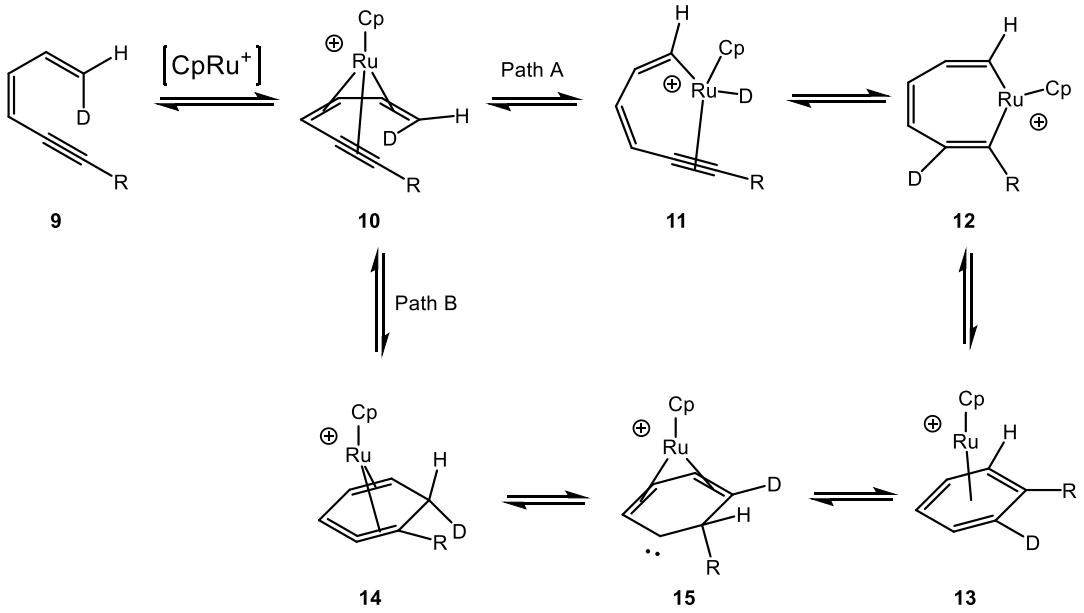

Scheme 2-4. Proposed reaction pathways for the ruthenium-mediated cyclizations of dienynes.[5]

The second pathway would proceed via η^4-bound *iso*benzene **14** by a disrotatory 6π-electrocyclization from **10** (Scheme 2-4, Path B). From **14** the metal center could assist in the [1,2]-hydride migration to form **15** and a second [1,2]-hydride migration to form the arene product, **13**. If carbene **15** is nucleophilic in nature, it could be protonated by H_2O. This could explain the results observed with **6-d**. In addition, **14** could proceed directly to **13** via a metal assisted [1,5]-hydride

migration, which could have metal hydride character.[7] Path B is similar to the accepted thermal pathway for this cyclization, but now mediated by complexation to the ruthenium center.

The purpose of the current research is to further elucidate the mechanism of this interesting organometallic transformation. Can the two pathways in Scheme 2-4 be distinguished? Herein we describe the synthesis and reactivity studies of dienyne substrates with a mono-deuterium label selectively placed at either the *E* or *Z* hydrogen position of the distal alkene. In addition, extension of the reaction to dienyne substrates containing phenyl substitutions is explored.

2-2 Ruthenium-Mediated Cycloaromatization of Dienynes

2-2.1 Dienynes Containing a Single Deuterium Atom.

The first objective was the synthesis of dienyne substrates ***E*-16-d** and ***Z*-16-d** (Scheme 2-5).

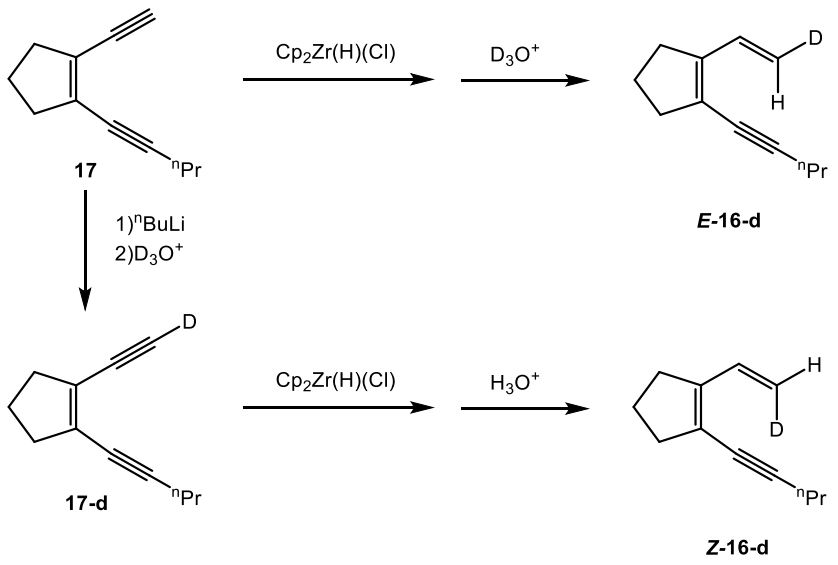

Scheme 2-5. Synthesis of mono-deuterium-labeled dienyne isotopologues.

Known enediyne **17** was reacted with Schwartz's reagent in benzene at rt and the reaction mixture was quenched with CF_3CO_2D diluted in D_2O to give ***E*-16-d** in 80% yield with 85% deuterium incorporation. Alternatively, deprotonation of **17** with ^{n}BuLi in THF at -78 °C, followed by quenching with CF_3CO_2D diluted in D_2O gave **17-d** in 90% yield with > 98% deuterium incorporation. Following the same procedure as that employed for the reaction of **17** with Schwartz's reagent, but quenching with CF_3CO_2H in H_2O, led to ***Z*-16-d** in 80% yield with > 98% deuterium incorporation. Dienyne ***E*-16-d** exhibited characteristic ^{1}H NMR ($CDCl_3$) resonances at δ 5.11 (d, $^3J_{HH}$ = 17.1 Hz) and 6.82 (d, $^3J_{HH}$ = 17.1 Hz), which integrated as 1:1.15 (Figure 2-2). The magnitude of the coupling constant is consistent with *trans* coupling and the integration indicates approximately 85% deuterium incorporation. Dienyne ***Z*-16-d** exhibited characteristic ^{1}H NMR ($CDCl_3$) spectral resonances at δ 5.11 (d,

$^3J_{HH}$ = 10.7 Hz) and 6.82 (d, $^3J_{HH}$ = 10.7 Hz) which integrated as 1:1. The magnitude of the coupling constant is consistent with *cis* coupling and the integration showed a very high degree of deuterium incorporation.

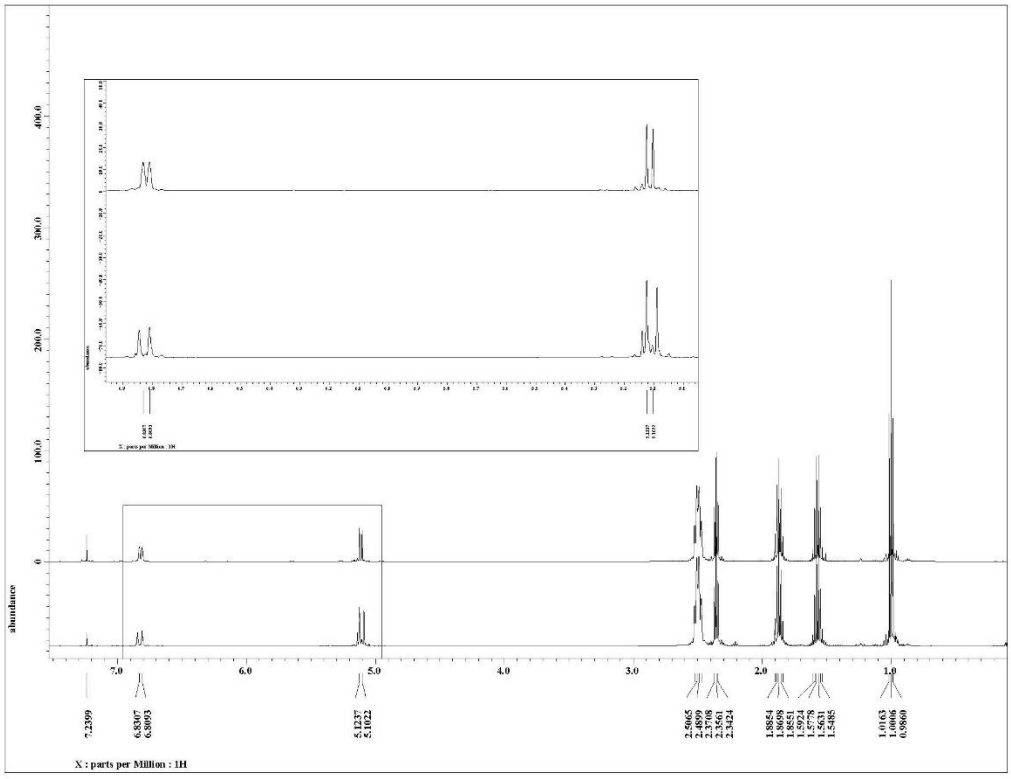

Figure 2-2. ^{1}H NMR spectra (500 MHz, $CDCl_3$) of ***E*-16-d** (bottom) and ***Z*-16-d** (top).

The reactions of ***E*-16-d** and ***Z*-16-d** (20 μmol) with **5** (20 μmol) in $CDCl_3$ (750 μL) were monitored by ^{1}H NMR spectroscopy. As shown in Figure 2-3, when ***E*-16-d** reacts with **5**, the product arene has a pair of doublets at δ 5.80 and 5.53 and a broad singlet at 5.65 with much lower intensity. This is consistent with deuterium migration from the *E*-position, with the observed singlet at 5.65 ppm attributed to a

small amount of protium present in the *E*-position of ***E*-16-d**. When ***Z*-16-d** reacts with **5**, the product arene exhibited a pair of singlets at δ 5.80 and 5.65 and a barely observable doublet at 5.53. This is consistent with a protium migration from the *E*-position and the retention of deuterium on the same carbon throughout the reaction (Scheme 2-6).

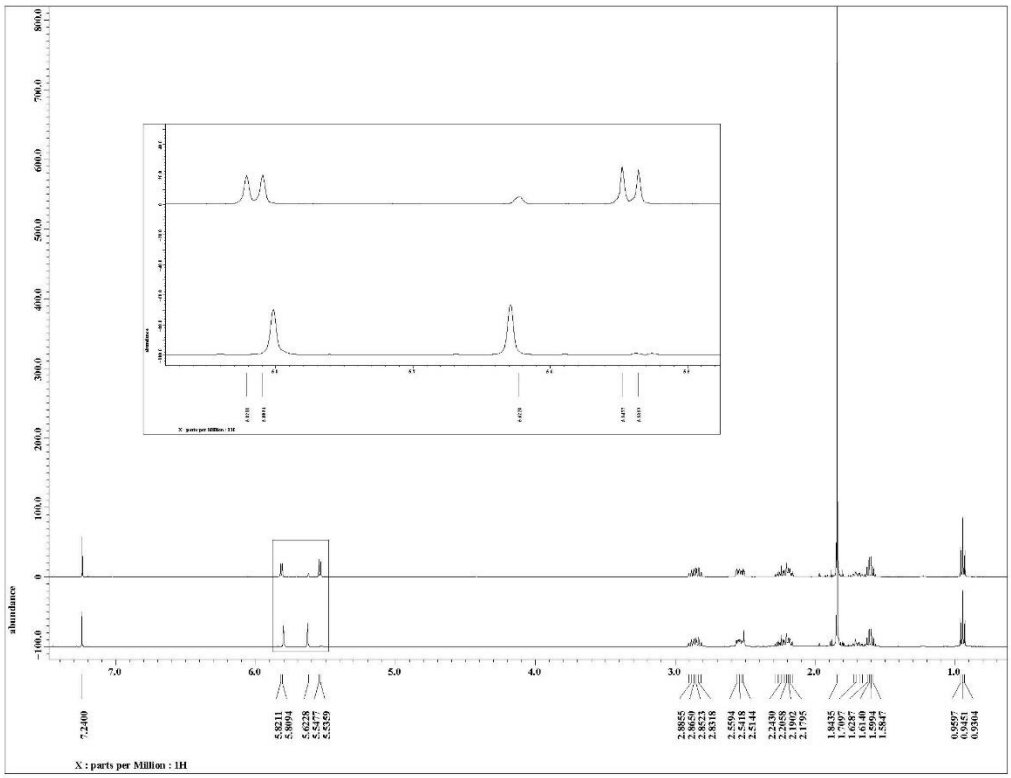

Figure 2-3. ^{1}H NMR spectra (500 MHz, $CDCl_3$) of the reaction of ***E*-16-d** (top) and ***Z*-16-d** (bottom) with $[Cp^*Ru]^+$.

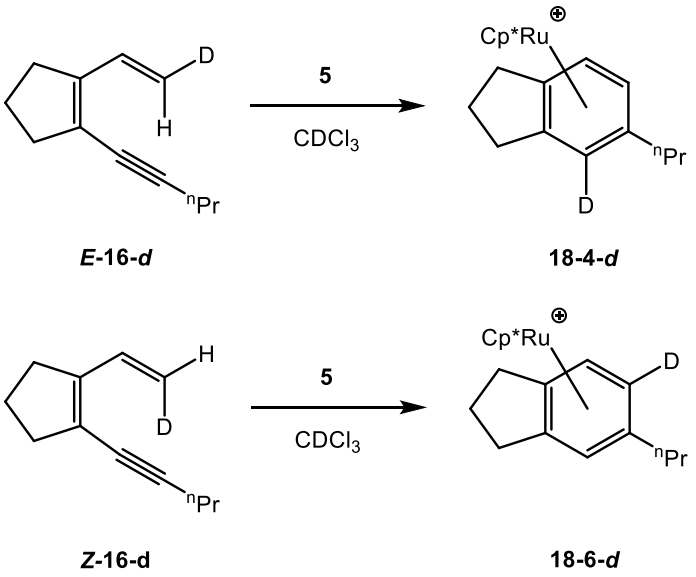

Scheme 2-6. Deuterium migration studies.

Deuterated internal distal alkenes were also prepared (Scheme 2-7). Enediyne **17** was reduced with Schwartz's reagent in benzene followed by treatment with NBS to give **20** in 70% yield following aqueous workup and silica gel chromatography (Scheme 2-7). Lithium-halogen exchange of **20** with ^{t}BuLi in Et_2O at -78 °C and quenching with MeI led to **21-*E*** in 85% yield after purification. Carrying out the same reaction sequence on **17-*d*** (> 95% deuterium enrichment) led to **21-*E*-d** in similar yields with > 95% deuterium incorporation. Addition of alkyne **22** to a suspension of Lindlar's catalyst in benzene with quinoline under an atmosphere of H_2 led to **23** in 95% yield after silica gel chromatography. Homologation of **23**, followed by deprotonation with ^{n}BuLi and quenching with ^{n}PrBr led to **21-*Z*** in 50% yield over two steps.

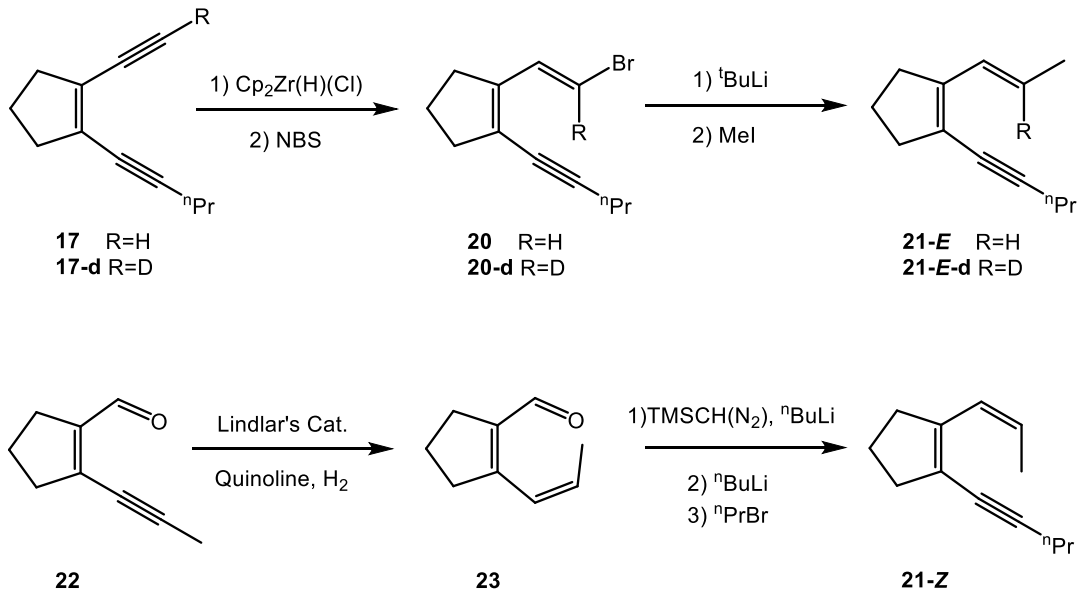

Scheme 2-7. Synthesis of internal distal alkenes.

The reactions of **21-*E*** (20 μmol) and **21-*Z*** (20 μmol) with **19** (20 μmol) in $CDCl_3$ (1 mL) were followed by ^{1}H NMR spectroscopy, and both dienynes proceeded to the same arene product (**24**) in 82% and 90% yield, respectively (Scheme 2-8). The reaction of **21-*E*** appeared to generate a Cp-containing side-product in approximately 10% yield, which was not observed in the reaction of **21-*Z***. This side product was easily separated from **24** by chromatography.

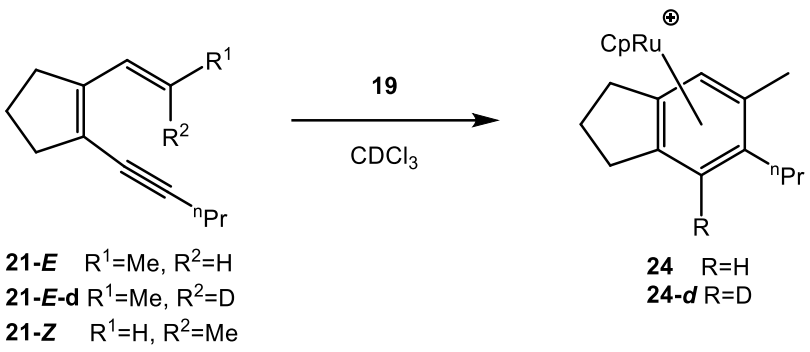

Scheme 2-8. Reactions of internal dienynes with $[CpRu]^+$.

The reaction of **21-*E*-*d*** (20 μmol) with **19** (20 μmol) in $CDCl_3$ (1 mL) proceeded to give arene product **24-*d*** in 85% yield with > 95% deuterium enrichment at the 4-position and the same side-product observed as in the case of **21-*E***. A competition KIE experiment of **21-*E*** and **21-*E*-*d*** with **19** under pseudo-first-order conditions in **19** was then attempted. A solution of **21-*E*** and **21-*E*-*d*** (0.35 mmol of each) in DCM (5 mL, 0.14 M in dienyne) was added to **19** (30 μmol) and the mixture was allowed to react overnight. The solution was then concentrated under vacuum and the residue was recrystallized from acetone/Et_2O to give a yellow crystalline product. The expected arene resonances were not observed by ^{1}H NMR spectroscopy ($CDCl_3$), but a new resonance at δ 5.12 was consistent with a Cp ligand bound to ruthenium. Additional resonances at δ 4.12 (singlet) and 5.61 (t, $^3J_{HH}$ = 2.2 Hz) were observed, which are more consistent with vinyl hydrogens of an olefin bound to ruthenium. To eliminate the possibility that deuterium incorporation into the product led to errors in the ^{1}H NMR spectral interpretation, a fresh synthesis was undertaken with **21-*E***. A solution of **21-*E*** (0.35 mmol) in DCM (3 mL, 0.12 M in dienyne) was

added to **19** (30 μmol) and the resulting mixture was allowed to react overnight. The solution was concentrated under vacuum and the residue recrystallized from acetone/Et_2O to give **25** in 65% yield. A single crystal X-ray study was undertaken to determine the structure of **25**. From the solid-state structure it is clear that the reaction involves dimerization of **21-*E*** (Figure 2-4). The structure shows ruthenium bound to the substrate through two allylic moieties and the generation of three new rings (Scheme 2-9). One key feature of **25** is the presence of a carbon atom bearing a hydrogen and propyl group, which was not observed in **21-*E***. This would be consistent with a hydrogen migration event.

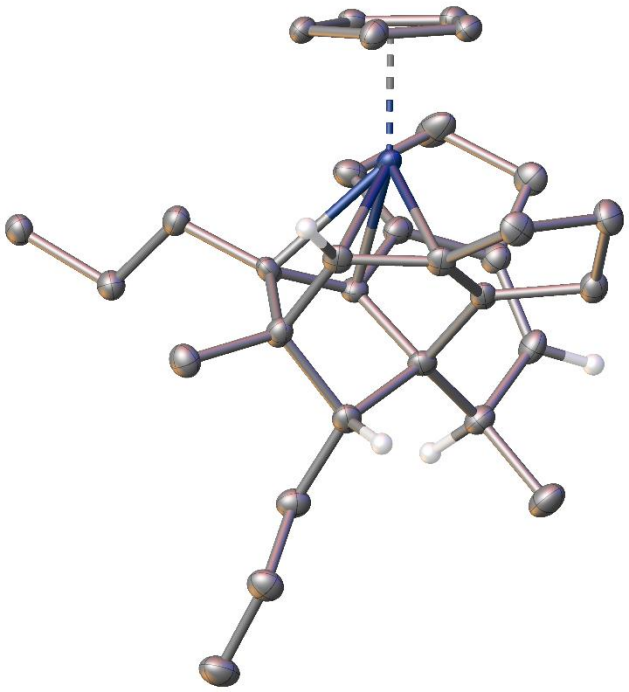

Figure 2-4. X-ray structure of **25**. Counter-ion and most hydrogens have been omitted for clarity.

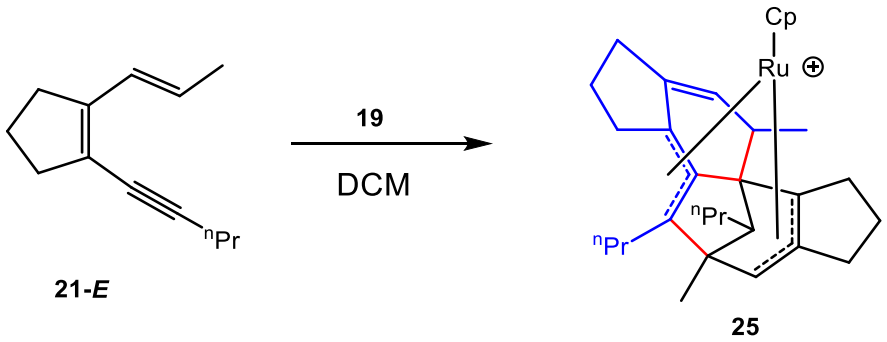

21-*E* 25

Scheme 2-9. Synthesis of **25**.

Attempting the competition KIE experiment at lower concentrations of dienynes (35 mM and 3.5 mM) in DCM resulted in the formation of **25**.

To determine if this unusual reaction pathway is unique to the *E* isomer, a similar reaction with the *Z* isomer was undertaken. A solution of **21-*Z*** (0.35 mmol) in DCM (3 mL, 0.12 M in dienyne) was added to **19** (30 μmol) and the resulting mixture was allowed to react overnight. The solution was concentrated under vacuum and the residue recrystallized from acetone/Et_2O to give **24** in 83% yield.

Next, dienynes with terminal acetylenes were prepared in order to test for possible hydrogen migration pathways (Scheme 2-10). Aldehyde **26** was added to a solution of methylenetriphenylphosphane in THF at rt and allowed to react for 2 h. The solution was concentrated under vacuum and the residue was purified by column chromatography to give dienyne **27** in 70% yield (Scheme 2-10). The TMS group was removed by reaction with K_2CO_3 in MeOH/THF for 1 h. The solution was diluted in H_2O and extracted with Et_2O. The organic solution was concentrated under vacuum and the residue was purified by silica gel chromatography with pentane eluant to give

dienyne **28** in 90% yield. Deprotonate of **28** by ^{n}BuLi in THF at -78 °C and subsequent quenching with D_3O^+ gave **28-*d*** in 90% yield with > 98% D incorporation.

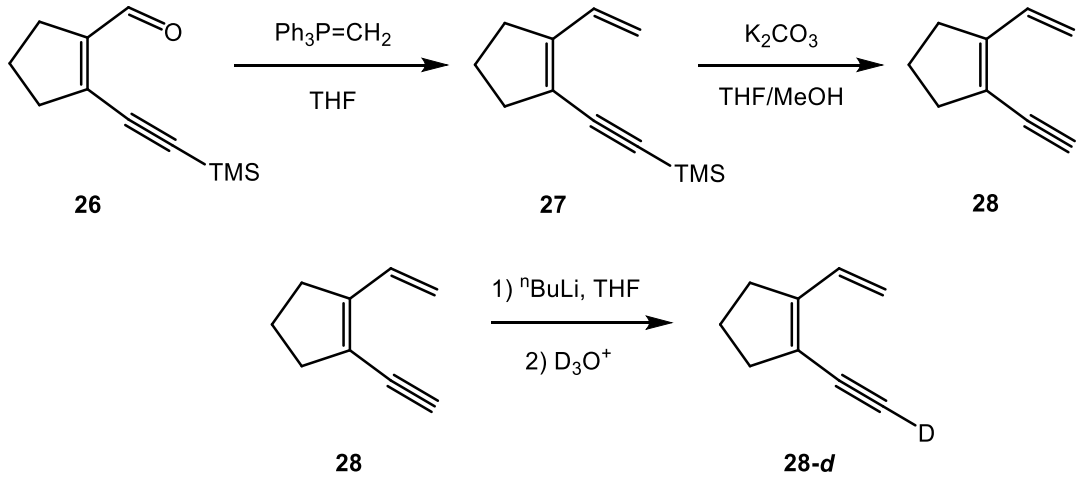

Scheme 2-10. Synthesis of terminal acetylenic dienynes **28** and **28-*d***.

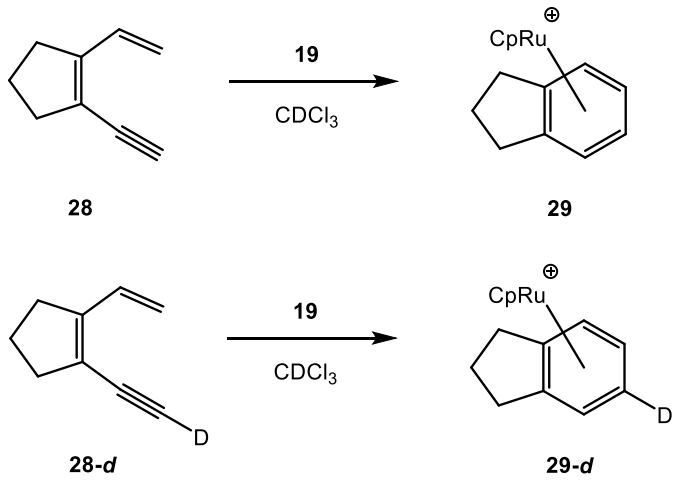

Scheme 2-11. Reaction of **28** and **28-*d*** with $[CpRu]^+$.

The reaction of **28** (20 μmol) with **19** (20 μmol) in $CDCl_3$ (1 mL) was monitored by ^{1}H NMR spectroscopy. Within 15 min, the reaction had proceed to

CpRu(indane)$^+$ (**29**) in 70% NMR yield as evidenced by the appearance of a pair resonances at δ5.60 and 5.80 (Scheme 2-11). An insoluble red side-product was also formed. The contents of the NMR tube were filtered through a pad of Celite and the solution concentrated to approximately 0.5 mL under vacuum. Then Et_2O was added to precipitate **29** as an off-white solid. The reaction of **28-*d*** (20 μmol) with **19** (20 μmol) in $CDCl_3$ (1 mL) was also monitored by ^{1}H NMR spectroscopy. As with **28**, the reaction was complete within 15 min as evidenced by the appearance of resonances at δ 5.60 and 5.80, which integrated as 1:2, with > 95% deuterium incorporation. The position of the deuterium on the indane ligand is consistent with the deuterium remaining on the same carbon through the reaction.

2-2.2 Cycloaromatization of Phenyl-Substituted Dienynes.

One of the reasons that **5** and **19** were selected initially for the cyclization of enediynes was because they had been shown to be super "areneophiles", as evidenced by the formation of stable ruthenium-arene complexes.[8] Previously it was shown that enediynes that were substituted with aryl groups at the terminal alkyne positions cyclized upon reaction with **5**, with little ruthenium complexation at the aryl substituents (Scheme 2-12).[3] When the enediyne was benzannulated; however, i.e. the alkene of the enediyne was incorporated into an arene ring, the ruthenium preferred complexation to the arene ring of the enediyne.

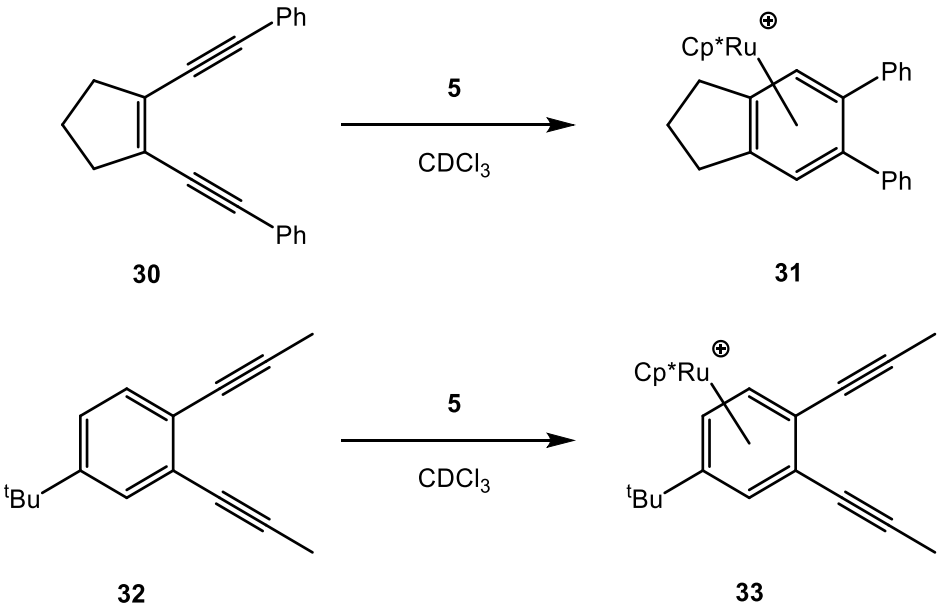

Scheme 2-12. Cycloaromatization of phenyl-substituted enediynes by $[Cp^*Ru]^+$.[3]

A question that was posed was will a phenyl-substituted dienyne also cyclize or will the ruthenium prefer complexation to the aromatic ring of the starting material? To answer this question a number of phenyl-substituted dienynes were synthesized. Aldehyde **34** was allowed to react with methylenetriphenylphosphane in THF at 0 °C for two h, followed by evaporation of volatiles and purification of the residue on a silica gel column with hexanes as eluant to give **35** in 70% yield (Scheme 2-13).

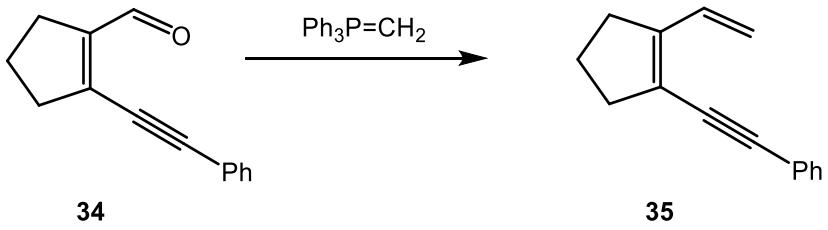

Scheme 2-13. Synthesis of **35**.

A homologation of aldehyde **36** led to terminal alkyne **37** in 80% yield following aqueous workup and silica gel chromatography (Scheme 2-14). Deprotonation of **37** with ^{n}BuLi in THF at -78 °C and quenching of the lithium acetylenide with MeI led to dienyne **38-*Z*** in 85% yield after aqueous workup and silica gel chromatography. Reacting aldehyde **39** with benzylidenetriphenylphosphane in THF at rt for 4 h led to dienyne **38-*E*** in 60% yield after silica gel chromatography.

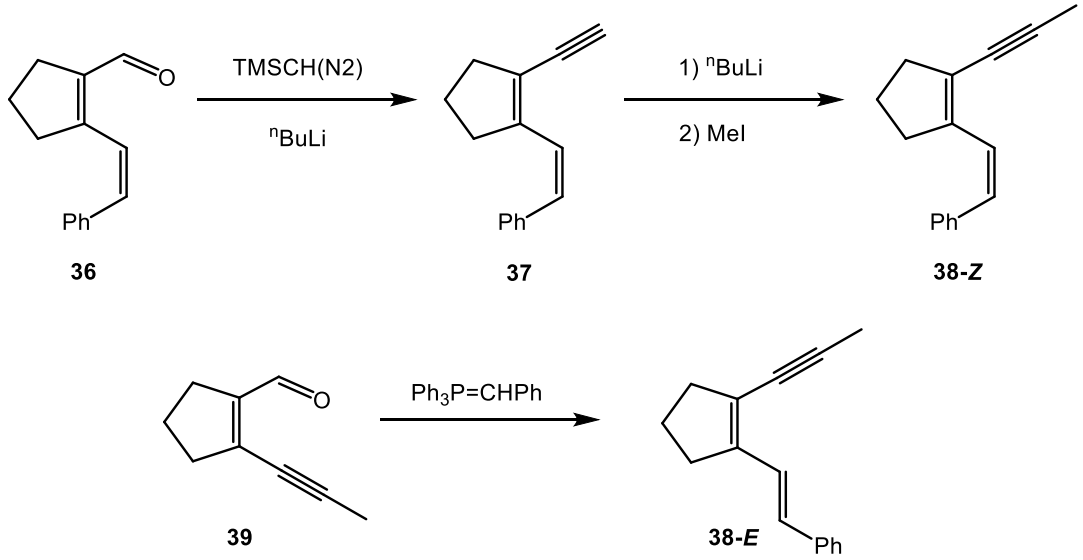

Scheme 2-14. Synthesis of **38**.

The reaction of **35** (20 μmol) with **19** (20 μmol) in $CDCl_3$ (1 mL) was monitored by ^{1}H NMR spectroscopy, and nearly quantitative conversion to **40** was observed over the course of 20 min, as evidenced by the appearance of arene resonances at δ5.60 and 5.80 and a singlet at 5.72 (Scheme 2-15).

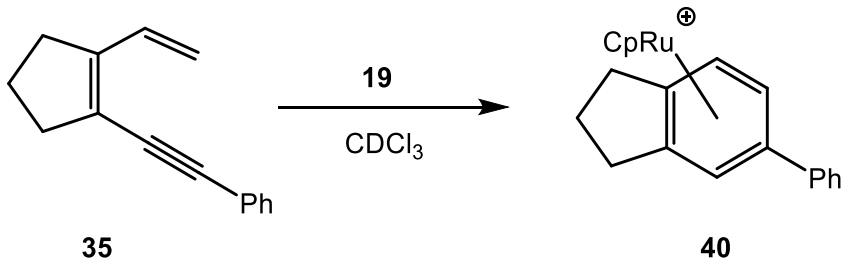

35 **40**

Scheme 2-15. Reaction of **35** with $[CpRu]^+$.

The reaction of **38-*E*** (20 μmol) with **19** (20 μmol) in $CDCl_3$ (1 mL) was monitored by ^1H NMR spectroscopy and nearly complete consumption of **38-*E*** was observed within 20 min. The formation of cyclized product **41** was observed in 90% yield, as indicated by new singlet resonances at δ 5.60 and 5.72 (Scheme 2-16). The five-membered-ring hydrogen resonances indicated a loss-of-symmetry, consistent with coordination of a metal complex to one face of the unsaturated system.

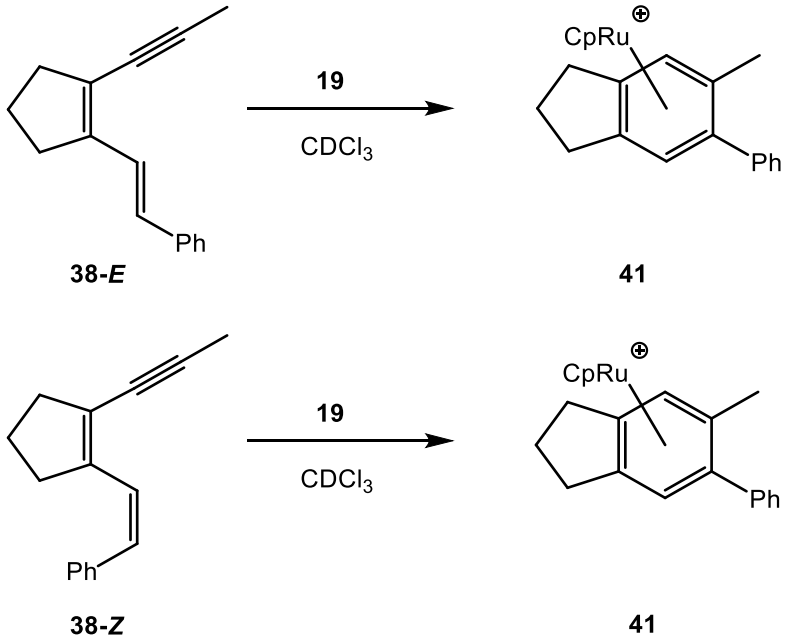

38-*E* **41**

38-*Z* **41**

Scheme 2-16. Reactions of **38** with $[CpRu]^+$.

The reaction of **38-*Z*** (20 μmol) with **19** (20 μmol) in $CDCl_3$ (1 mL) was monitored by ^1H NMR spectroscopy and **41** was observed to form in 90% yield within 1 h.

The reaction of the more sterically demanding ruthenium complex **5** (20 μmol) with **38-*E*** (20 μmol) in $CDCl_3$ (1 mL) was monitored by ^1H NMR spectroscopy and the formation of cycloaromatized product **42** was observed in 90% yield within 20 min (Scheme 2-17).

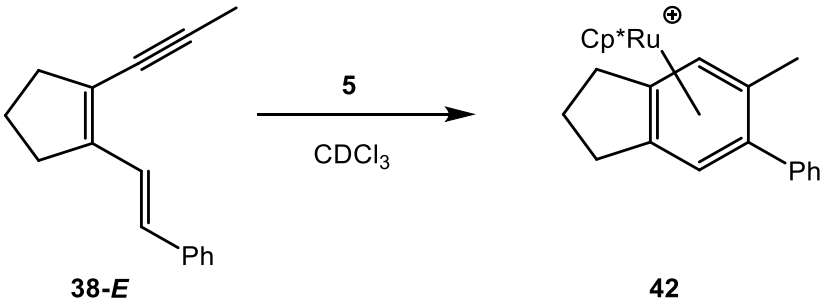

38-*E* **42**

Scheme 2-17. Reaction of **38-*E*** with $[Cp^*Ru]^+$.

2-2.3 Attempts to Intercept Reactive Intermediates

If the ruthenium-mediated cyclization of dienynes proceeds through a metal-mediated thermal pathway, it may proceed through an η^4-bound *iso*benzene. In an attempt to intercept this putative intermediate, the reaction of **16** with **19** in $CDCl_3$ was carried out in the presence of cyclopentadiene (CpH) or furan.[9] In the presence of CpH, the formation of ruthenocene was the only observed product. When the reaction was carried out in the presence of furan, the expected arene product **18** was the only observed product. In addition, the reaction was carried out in the presence of

[NHCCu(NCMe)]BF_4 (NHC=1,3-bis(diisopropylphenyl)-imidazol-2-ylidene), as a transition metal trap for an *iso*benzene intermediate.[10] The only observed product was the expect arene product **18**.

2-3 Mechanistic Proposal Revisited

Previously it was proposed that the ruthenium-mediated cycloaromatization of dienynes could proceed through two different pathways (Scheme 2-18). Both paths proceed from an η^6-dienyne intermediate, **10,** which was demonstrated by NMR spectroscopy and solid-state X-ray structure analysis. The first path proceeds via C-H bond activation of the hydrogen in the *Z*-position to give Ru(IV) hydride **11**. This was supported by the close proximity of this hydrogen to the metal center in the X-ray structure. The hydride then does a *trans* migratory insertion followed by a reductive ring contraction to give metal-bound arene product. The second pathway proceeds through a 6π-electrocyclization from **10** to give an η^4-*iso*benzene adduct, **14**. From **14** there are two main proposed pathways for a formal [1,5]-hydride shift. The first, as shown, is a series of two sequential [1,2]-hydride shifts, with the formation of carbene intermediate **15**. The other possibility is the formation of an agostic interaction, as shown for **14**, followed by a metal-mediated [1,5]-hydride shift to give product **13**.

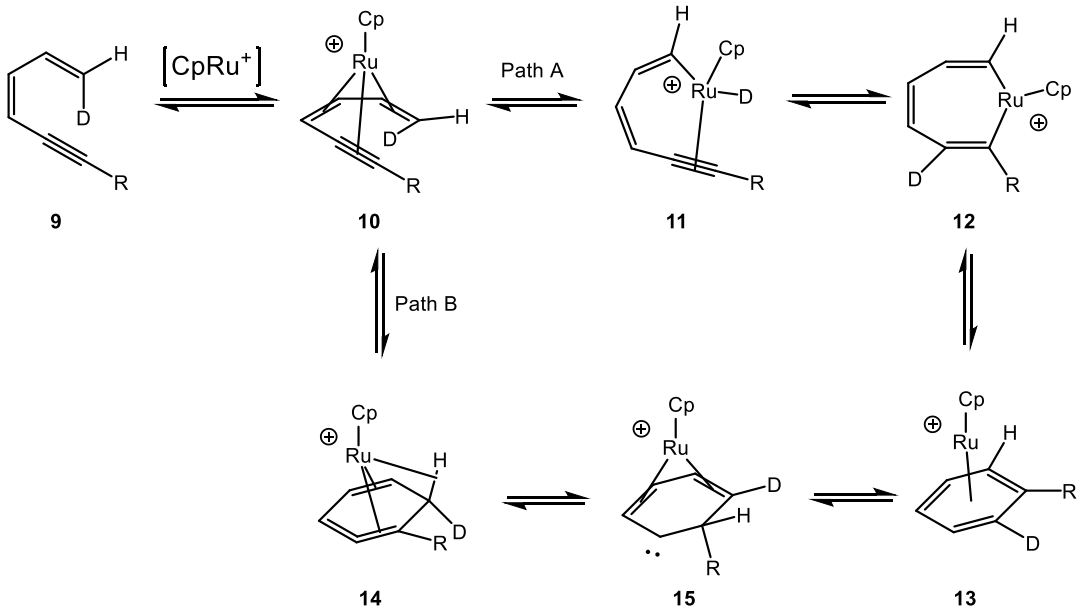

Scheme 2-18. Previously proposed mechanism.

Deuterium labeling studies conclusively demonstrated that the migrating hydrogen originates at the *E*-position and not in the *Z*-position as would be necessary for the reaction to proceed through pathway A.

The reaction of **19** with the internal distal alkenes **21** clearly demonstrates that the cyclization can proceed with a hydrogen in either position of the alkene, but substrates with a hydrogen in the *E*-position undergo faster reaction. When a group other than hydrogen is present in this position, the intermediates in the reaction pathway can be intercepted by a second equivalent of the substrate, as was demonstrated by the formation of **25**. One of the key features that was observed in **25** was the presence of a hydrogen on a carbon bearing a propyl group, which was not present in the starting substrate. The formation of **25** is proposed to begin with 6π-

electrocyclization of η^6-bound dienyne **50** to form an η^4-*iso*benzene **51** (Scheme 2-19).

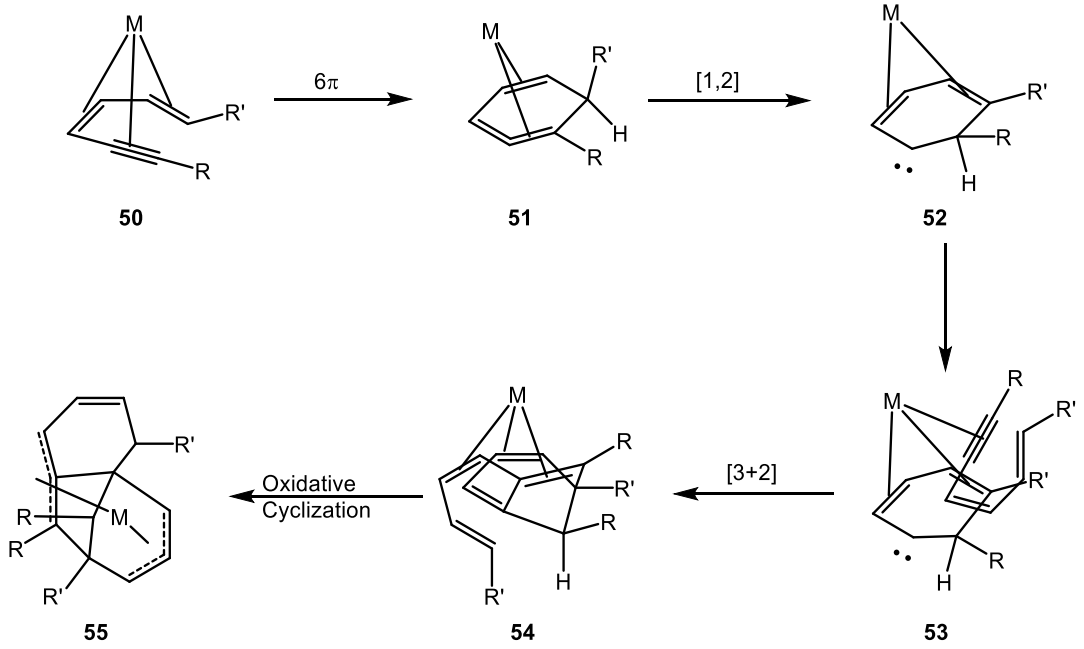

Scheme 2-19. Proposed mechanism for the formation of **25**.

Lacking a hydrogen *endo* to the metal, **51** undergoes a [1,2]-hydride shift to give carbene **52**. The hydrogen remains *exo* to the metal during the migration and now is present on a carbon bearing a propyl group as was observed in **25**. Coordination of a second equivalent of substrate will give **53**. It should be noted that coordination of the second equivalent of substrate could occur prior to the [1,2]-hydride shift but it shown after for clarity. Complex **53** could then undergo a [5+2] cycloaddition[11] to the carbene substrate to give **54**, which then undergoes an oxidative cyclization to give the product **55**.[12]

When **21-*Z*** was used instead of **21-*E***, the formation of a dimerized product was not observed, even in the presence of 20 equivalents of substrate. This clearly contrasts with **21-*E***, where as little as 5 equivalents were need to push the reaction to nearly complete dimerization over arene formation. This is evidence that the metal must be assisting in the migration of the hydrogen. A comparison could be made to ruthenium-pentadienyl systems studied by Roulet.[13] The protonation of **56** with triflic acid generates ruthenium-pentadiene **57** which equilibrates through ruthenium-hydride **58** (Scheme 2-20).

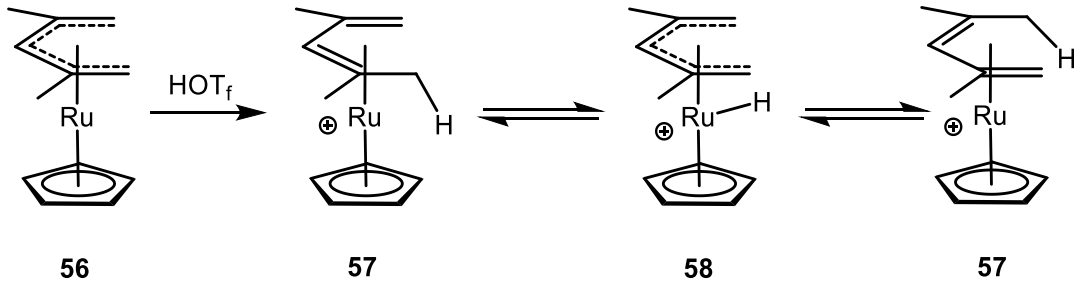

Scheme 2-20. Roulet's work with pentadienyl ligands.[13]

Through coalescence temperature measurements, Roulet estimated the activation barrier for the interconversion of pentadiene complexes to be < 7.2 kcal mol^{-1}. The formal [1,5]-hydride shift was fluxional even at 145K - the lower temperature limit of the NMR spectrometer used in the studies. More recent computational work on this subject by Tamm gave an activation barrier for this process of 5.1 kcal mol^{-1}.[14] Thus when a hydrogen in present in the *E*-position of the dienyne, the [1,5]-hydride shift should be facile.

The ruthenium-mediated cyclization of the phenyl-substituted dienynes were shown to proceed when the phenyl was attached to the alkyne or either position of the alkene. This result is not unexpected as the kinetic product for coordination of $CpRu^+$ to unsaturated systems would be predicted to be an alkene or alkyne over an arene, as aromaticity does not have to be disrupted.[15]

2-4 Conclusion

Through a number of synthetic studies, the mechanism of the ruthenium-mediated cycloaromatization of dienyne is clearer. The reaction starts with the formation of a ruthenium-η^6-dienyne complex, **10**, which was previously demonstrated (Scheme 2-21). Complex **10** then undergoes a disrotatory 6π-electrocyclization with torquoselectivity for the *E*-position to come toward the metal, to form *iso*benzene **14**.[16] Then a metal-mediated [1,5]-hydride shift gives the expect arene product, **13**, with selectivity for hydrogen migration from the *E*-position of the starting dienyne.[13, 14]

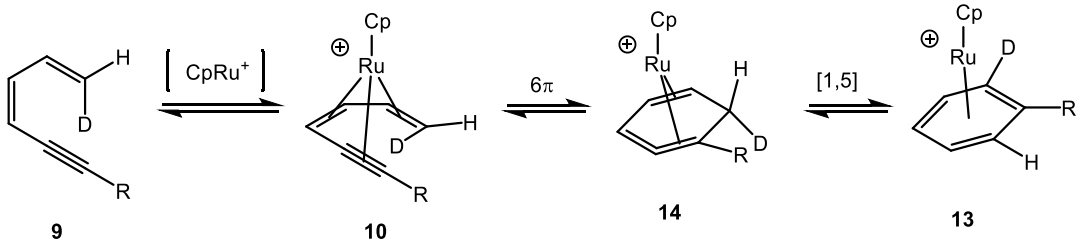

Scheme 2-21. Proposed mechanism with a hydrogen present in the *E*-position of the distal alkene.

The reaction can still proceed if the *E*-position is blocked with a small non-hydrogen group. In this case, the hydrogen, now *exo* to the metal in the *iso*benzene undergoes a [1,2]-hydride shift to give carbene **15**, which can undergo a second [1,2]-hydride shift to give **13** (Scheme 2-22).

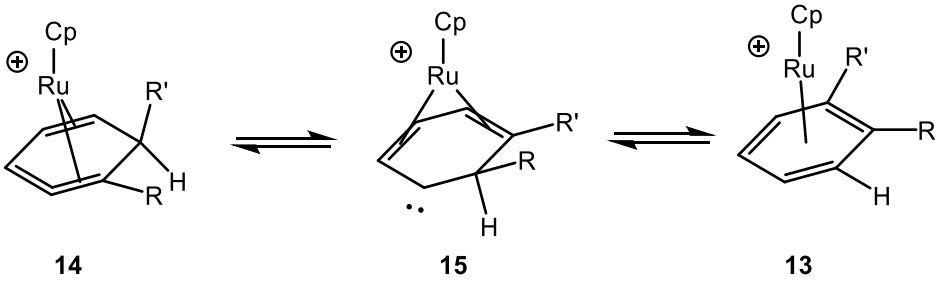

Scheme 2-22. Proposed mechanism when a hydrogen is not present in the *E*-position of the distal alkene.

2-5 Experimental

2-5.1 General Procedures

All manipulations were performed using standard Schlenk technique or in nitrogen-filled Vacuum Atmospheres or MBraun glovebox, unless otherwise stated. ^{1}H and ^{13}C NMR spectra were recorded on Varian Mercury 400 MHz, Varian VX 500 MHz, or JOEL ECA 500 MHz instruments. ^{1}H and ^{13}C NMR chemical shifts (δ) are reported in parts per million (ppm). Spectra were referenced to the residual solvent peak. Infrared spectra were obtained on a Nicolet iS10 FT-IR. High resolution mass spectra analyses were performed at either the mass spectrometer facility at UC San

Diego or UC Riverside. THF, ethyl ether, DCM, benzene, hexanes, and pentane used as reaction solvents were dried either by a solvent dispensing system equipped with two neutral alumina columns under argon atmosphere or by 3 Å activated molecular sieves. Chloroform-*d* and benzene-d_6 were dried over 3 Å activated molecular sieves and then distilled under static vacuum into oven-dried Schlenk storage tubes. Deuterated solvents were degassed using a Freeze-Pump-Thaw procedure, typically 5 cycles. NMR reactions were performed in 5 mm J-Young NMR tubes equipped with a Teflon needle valve. All literature compounds were prepared according to the indicated references or purchased from commercial suppliers and used as received.

2-5.2 Synthesis and Characterization Data

1-(ethynyl-*d*)-2-(pent-1-yn-1-yl)cyclopent-1-ene (17-*d*): Enediyne **17** (500 mg, 3.16 mmol) was dissolved in THF (10 mL) in an oven-dried side-arm flask equipped with a stir bar and rubber septum under dry N_2. The solution was cooled to -78 °C on a dry ice/acetone bath and ^{n}BuLi (4 mL, 1.25 M in hexanes, 5 mmol) was added dropwise to the solution. The resulting solution was stirred at -78 °C for 30 min and was then quenched with CF_3CO_2D (0.75 mL, 9.8 mmol, diluted to 5 mL with D_2O). The solution was allowed to warm to rt and stirred for 10 min at rt. The layers were partitioned and the aqueous layer was extracted with Et_2O (3 x 25 mL). The combined organic extracts were washed with $NaHCO_3$ (2 x 20 mL), H_2O (15 mL), brine (15 mL) and dried over $MgSO_4$. The volatiles were removed under vacuum and the

residue was purified on a silica column with hexanes elaunt to give **17-*d*** as a clear oil (475 mg, 2.98 mmol, 94% yield, > 98% deuterium incorporation as determined by ^{1}H NMR spectroscopy). ^{1}H NMR (500 MHz, $CDCl_3$) δ 1.00 (t, $^{3}J_{HH}$ = 7.4 Hz, 3H), 1.57 (sextet, $^{3}J_{HH}$ = 7.4 Hz, 2H), 1.89 (p, $^{3}J_{HH}$ = 7.5 Hz, 2H), 2.37 (t, $^{3}J_{HH}$ = 7.4 Hz, 2H), 2.50 (t, $^{3}J_{HH}$ = 7.5 Hz, 2H), 2.52 (t, $^{3}J_{HH}$ = 7.5 Hz, 2H). ^{13}C NMR (125 MHz, $CDCl_3$) δ 13.7; 22.0; 22.4; 23.1; 36.8; 37.5; 77.2; 80.3 (t, $^{2}J_{CD}$ = 7.4 Hz); 82.8 (t, $^{1}J_{CD}$ = 38.2 Hz); 98.3; 127.2; 133.1. HRMS(APCI): Calcd for ($C_{12}H_{14}D_1$+CH_3OH): 192.1495. Found: 192.1495.

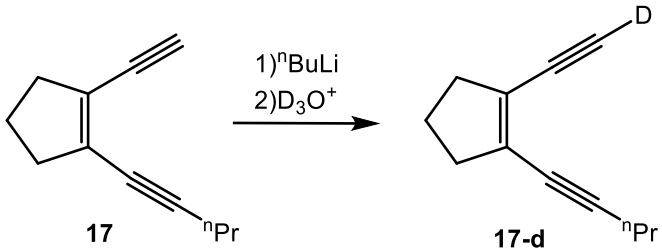

(*E*)-1-(pent-1-yn-1-yl)-2-(vinyl-2-*d*)cyclopent-1-ene (*E*-16-d): Enediyne **17** (100 mg, 0.63 mmol) dissolved in benzene (3 mL) was added to a suspension of $Cp_2Zr(H)(Cl)$ (163 mg, 0.63 mmol) in benzene (5 mL) in a side-arm flask equipped with a stir bar and rubber septum under dry N_2. The resulting light yellow suspension was allowed to stir for 1 h, whereupon the solution became homogeneous and red. The solution was then quenched with CF_3CO_2D (0.25 mL, 3.3 mmol diluted to 5 mL with D_2O) and allowed to stir for 5 min. The layers were partitioned and the aqueous layer was extracted with Et_2O (3 x 25 mL). The combined organic extracts were washed with $NaHCO_3$ (2 x 15 mL), H_2O (15 mL), brine (15 mL) and dried over $MgSO_4$. The volatiles were removed under vacuum and the residue was purified on a

silica gel column with hexanes eluant to give ***E*-16-d** as a clear oil (86 mg , 0.53 mmol, 84% yield, 85% deuterium incorporation as determined by ^{1}H NMR spectroscopy). ^{1}H NMR (500 MHz, $CDCl_3$) δ 1.01 (t, $^3J_{HH}$ = 7.4 Hz, 3H), 1.58 (h, $^3J_{HH}$ = 7.4 Hz, 2H), 1.88 (p, $^3J_{HH}$ = 7.5 Hz, 2H), 2.36 (t, $^3J_{HH}$ = 7.4 Hz, 2H), 2.50 (t, $^3J_{HH}$ = 7.5 Hz, 2H), 2.51 (t, $^3J_{HH}$ = 7.5 Hz, 2H), 5.11 (d, $^3J_{HH}$ = 17.1 Hz, 1H), 6.83 (d, $^3J_{HH}$ = 17.1 Hz, 1H). ^{13}C NMR (125 MHz, $CDCl_3$) δ 13.7, 21.9, 22.3, 22.5, 31.6, 37.6, 77.2, 97.1, 115.0 (t, $^1J_{CD}$ = 22.9 Hz), 123.3, 132.1, 146.1, 152.2. HRMS (APCI-TOFMS): Calcd for ($C_{12}H_{16}D$): 162.1388. Found: 162.1388.

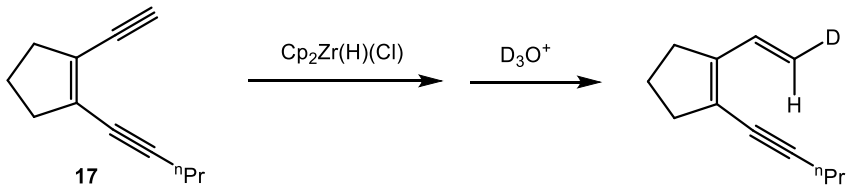

16-*E*

(*Z*)-1-(pent-1-yn-1-yl)-2-(vinyl-2-*d*)cyclopent-1-ene (*Z*-16-d): Enediyne **17-*d*** (100 mg, 0.63 mmol) dissolved in benzene (3 mL) was added to a suspension of $Cp_2Zr(H)(Cl)$ (163 mg, 0.63 mmol) in benzene (5 mL) in a side-arm flask equipped with a stir bar and rubber septum under dry N_2. The resulting light yellow suspension was allowed to stir for 1 h, whereupon the solution became homogeneous and red. The solution was then quenched with CF_3CO_2H (1 mL diluted to 5 mL in H_2O) and allowed to stir for 5 min. The layers were partitioned and the aqueous layer was extracted with Et_2O (3 x 25 mL). The combined organic extracts were washed with $NaHCO_3$ (2 x 15 mL), H_2O (15 mL), brine (15 mL) and dried over $MgSO_4$. The volatiles were removed under vacuum and the residue was purified on a silica gel

column with hexanes eluant to give ***Z*-16-d** as a clear oil (86 mg, 0.53 mmol, 84% yield, > 98% deuterium incorporation as determined by ^{1}H NMR spectroscopy). ^{1}H NMR (500 MHz, $CDCl_3$) δ 1.00 (t, $^{3}J_{HH}$ = 7.4 Hz, 3H), 1.57 (h, $^{3}J_{HH}$ = 7.4 Hz, 2H), 1.87 (p, $^{3}J_{HH}$ = 7.5 Hz, 2H), 2.36 (t, $^{3}J_{HH}$ = 7.4 Hz, 2H), 2.49 (t, $^{3}J_{HH}$ = 7.5 Hz, 2H), 2.51 (t, $^{3}J_{HH}$ = 7.5 Hz, 2H), 5.11 (d, $^{3}J_{HH}$ = 10.7 Hz, 1H), 6.82 (d, $^{3}J_{HH}$ = 10.7 Hz, 1H). ^{13}C NMR (125 MHz, $CDCl_3$) δ 13.7, 21.9, 22.3, 22.5, 31.6, 37.6, 77.2, 97.1, 115.0 (t, $^{1}J_{CD}$ = 22.9 Hz), 123.3, 132.1, 146.1, 152.2. HRMS (APCI-TOFMS): Calcd for ($C_{12}H_{16}D$): 162.1388. Found: 162.1387.

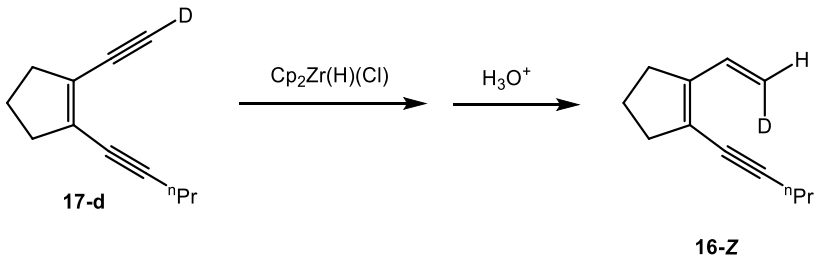

(η^5-pentamethylcyclopentadienyl)(η^6-(5-propyl-2,3-dihydro-1*H*-indene-4-*d*)ruthenium(II) hexafluorophosphate (**18-4-*d***): Diene ***E*-16-d** (3.5 mg, 22 μmol) and **19** (11.1 mg, 22 μmol) were weighed into an oven-dried J. Young tube and then placed under vacuum on a high vacuum line. Then $CDCl_3$ (550 μL) was distilled into the tube on the high-vacuum line and the resulting solution was allowed to warm to rt. The solution was allowed to react for 60 min and then a ^{1}H NMR spectrum of the sample showed complete consumption of ***E*-16-d** and the presence of **18-4-*d***. Quantitative conversion of ***E*-16-d** to **18-4-*d*** had occurred with 85% deuterium incorporation at the 4-position. The contents of the tube were poured into a vial and Et_2O (10 mL) was added to precipitate **18-4-*d***. The solution was filtered through a

pad of Celite, which was then rinsed with Et_2O (2 x 1 mL). The Celite was rinsed with DCM (3 x 1 mL) which was collected in a fresh vial. The volatiles were removed under vacuum to give **18-4-*d*** as a white powder (11.0 mg, 20 μmol, 92% yield). ^{1}H NMR (500 MHz, $CDCl_3$) δ 0.94 (t, $^3J_{HH}$ = 7.3 Hz, 3H), 1.58-1.64 (m, 3H), 1.84 (s, 15H), 2.16-2.27 (m, 3H), 2.50-2.57 (m, 2H), 2.80-2.91 (m, 2H), 5.52 (d, $^3J_{HH}$ = 6.2 Hz, 1H), 5.63 (s, 0.15H), 5.78 (d, $^3J_{HH}$ = 6.2 Hz, 1H). ^{13}C NMR (125 MHz, $CDCl_3$) δ 10.2; 13.7; 23.4; 25.3; 29.1; 29.3; 35.1; 84.3 (t, $^1J_{CD}$ = 27.1 Hz); 84.4; 86.8; 94.8; 103.3; 106.5; 107.5. HRMS (APCI-TOFMS): Calcd for ($C_{22}H_{30}DRu$): 392.1559. Found: 392.1554.

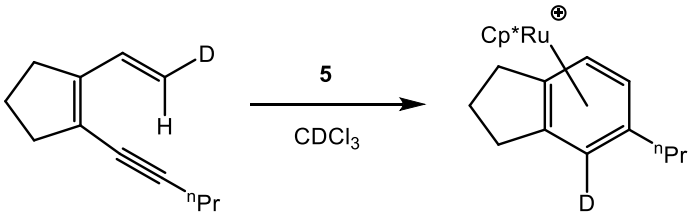

16-*E* **18-4-*d***

(η^5-pentamethylcyclopentadienyl)(η^6-(5-propyl-2,3-dihydro-1*H*-indene-6-*d*)ruthenium(II) hexafluorophosphate (**18-6-*d***): Diene ***Z*-16-d** (3.6 mg, 23 μmol) and **19** (11.3 mg, 23 μmol) were weighed into an oven-dried J. Young tube and then placed under vacuum on a high vacuum line. Then $CDCl_3$ (550 μL) was distilled into the tube on the high-vacuum line and the resulting solution was allowed to warm to rt. The solution was allowed to react for 60 min and then a ^{1}H NMR spectrum of the sample showed complete consumption of ***Z*-16-d** and the presence of **18-6-*d***. Quantitative conversion of ***Z*-16-d** to **18-6-*d*** had occurred with > 95% deuterium

incorporation at the 6-position. The contents of the tube were poured into a vial and Et_2O (10 mL) was added to precipitate **18-6-*d***. The solution was filtered through a pad of Celite, and the Celite rinsed with Et_2O (2 x 1 mL). The Celite was rinsed with DCM (3 x 1 mL) which was collected in a fresh vial. The volatiles were removed under vacuum to give **18-6-*d*** as a white powder (11.0 mg, 20 μmol, 92% yield). ^{1}H NMR (500 MHz, $CDCl_3$) δ 0.95 (t, $^3J_{HH}$ = 7.3 Hz, 3H), 1.56-1.69 (m, 3H), 1.84 (s, 15H), 2.16-2.30 (m, 3H), 2.49-2.58 (m, 2H), 2.81-2.92 (m, 2H), 5.63 (s, 1H), 5.78 (s, 1H). ^{13}C NMR (125 MHz, $CDCl_3$) δ 10.2; 13.7; 23.4; 25.3; 29.1; 29.3; 35.1; 84.3; 84.4; 86.5 (t, $^1J_{CD}$ = 27.2 Hz); 94.8; 103.3; 106.5; 107.6. HRMS (APCI-TOFMS): Calcd for ($C_{22}H_{30}DRu$): 392.1559. Found: 392.1556.

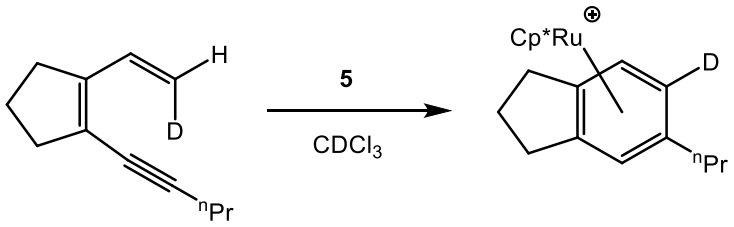

16-*Z* **18-6-*d***

(η^5-cyclopentadienyl)(η^6-(5-methyl-6-propyl-2,3-dihydro-1*H*-indene)ruthenium(II) hexafluorophosphate (**24**): **3** (8 mg, 18.4 μmol) and **21-*E*** (3.2 mg, 18.4 μmol) were weighed into an oven-dried J.Young tube (cooled to rt under vacuum). Then $CDCl_3$ (800 μL) was distilled into the tube on the high vacuum line and the reaction was allowed to proceed for 1 h at rt. Then a ^{1}H NMR spectrum showed consumption of the starting diene **7** and resonances expected for the product arene. The solution was passed through a pad of Celite and then Et_2O (12 mL) was

added to precipitate **8**. The resulting suspension was passed through a pad of Celite, rinsed through with Et_2O (2 x 2 mL) and then the Celite was rinsed with DCM (3 x 3 mL) which was collected in a fresh vial. The volatiles were removed under vacuum and the residue was purified on a pipette silica column with acetone in DCM (0 → 5%) to give **24** as a white powder (8.0 mg, 16.5 μmol, 90% yield). ^{1}H NMR (500 MHz, CD_2Cl_2) δ 1.03 (t, $^3J_{HH}$ = 7.4 Hz, 3H), 1.51-1.90 (m, 3H), 2.24-2.37 (m, 1H), 2.32 (s, 3H), 2.62-2.71 (m, 4H), 2.81-2.88 (m, 4H), 5.13 (s, 5H), 6.12 (s, 1H), 6.18 (s, 1H). ^{13}C NMR (125 MHz, CD_2Cl_2) δ 14.1, 19.1, 24.5, 25.2, 31.1, 31.4, 31.5, 81.1, 84.6, 85.2, 99.9, 104.5, 108.1, 108.3. HRMS (ESI-TOFMS): Calcd for ($C_{18}H_{23}Ru$): 341.0843. Found: 341.0840.

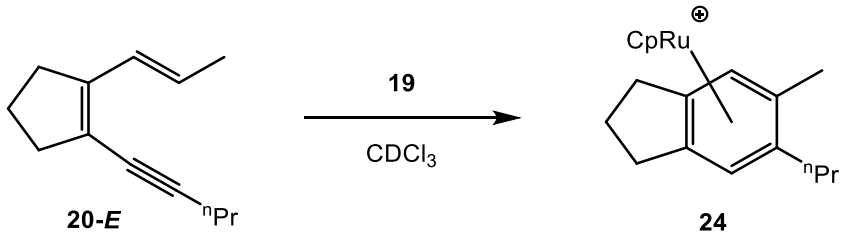

20-*E* 24

(*E*)-1-(2-bromovinyl-2-*d*)-2-(pent-1-yn-yl)cyclopent-1-ene (**20-*d***): Enediyne **17-*d*** (260 mg, 1.63 mmol) dissolved in benzene (5 mL) and added to a suspension of $Cp_2Zr(H)(Cl)$ (421 mg, 1.63 mmol) in benzene (20 mL) in a side-arm flask equipped with a stir bar and rubber septum under dry N_2. The resulting light yellow suspension was allowed to stir for 1 h, whereupon the solution became homogeneous and red. Then NBS (295 mg, 1.65 mmol) was added all-at-once and the resulting solution was stirred at rt for 30 min. The solution was poured into saturated solution of NH_4Cl (30 mL) and allowed to stir for 5 min. The layers were partitioned and the aqueous layer

was extracted with Et_2O (3 x 25 mL). The combined organic extracts were washed with $NaHCO_3$ (2 x 15 mL), H_2O (15 mL), brine (15 mL) and dried over $MgSO_4$. The volatiles were removed under vacuum and the residue was purified on a silica column with hexanes eluant to give **20-*d*** as a clear oil (282 mg, 1.17 mmol, 72% yield, > 98% deuterium incorporation as determined by ^{1}H NMR spectroscopy) ^{1}H NMR (500 MHz, $CDCl_3$) δ 1.01 (t, $^3J_{HH}$ = 7.4 Hz, 3H), 1.58 (h, $^3J_{HH}$ = 7.4 Hz, 2H), 1.88 (p, $^3J_{HH}$ = 7.5 Hz, 2H), 2.36 (t, $^3J_{HH}$ = 7.4 Hz, 2H), 2.45 (t, $^3J_{HH}$ = 7.5 Hz, 4H), 7.19 (s, 1H). ^{13}C NMR (125 MHz, $CDCl_3$) δ 13.8; 22.0; 22.4; 22.5; 31.8; 37.4; 76.9; 91.2; 108.1 (t, $^1J_{CD}$ = 29.1Hz); 124.5; 133.3; 143.3. HRMS (APCI-TOFMS): Calcd for ($C_{12}H_{15}DBr$): 240.0498. Found: 240.0497.

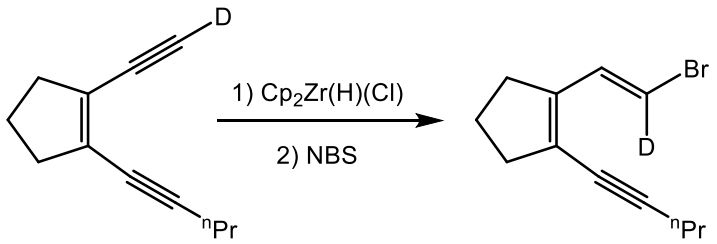

17-d **19-d**

(*E*)-1-(2-bromovinyl)-2-(pent-1-yn-yl)cyclopent-1-ene (**20**): Enediyne **17** (260 mg, 1.63 mmol) dissolved in benzene (5 mL) was added to a suspension of $Cp_2Zr(H)(Cl)$ (421 mg, 1.63 mmol) in benzene (20 mL) in a side-arm flask equipped with a stir bar and rubber septum under dry N_2. The resulting light yellow suspension was allowed to stir for 1 h, whereupon the solution became homogeneous and red. Then NBS (295 mg, 1.65 mmol) was added all-at-once and the resulting solution was stirred at rt for 30 min. The solution was poured into a saturated solution of NH_4Cl (30 mL) and allowed to stir for 5 min. The layers were partitioned and the aqueous layer was

extracted with Et_2O (3 x 25 mL). The combined organic extracts were washed with $NaHCO_3$ (2 x 15 mL), H_2O (15 mL), brine (15 mL) and dried over $MgSO_4$. The volatiles were removed under vacuum and the residue was purified on a silica column with hexanes eluant to give **20** as a clear oil (282 mg, 1.17 mmol, 72% yield) ^{1}H NMR (500 MHz, $CDCl_3$) δ 1.01 (t, $^3J_{HH}$ = 7.4 Hz, 3H), 1.58 (h, $^3J_{HH}$ = 7.4 Hz, 2H), 1.88 (p, $^3J_{HH}$ = 7.5 Hz, 2H), 2.36 (t, $^3J_{HH}$ = 7.4 Hz, 2H), 2.45 (t, $^3J_{HH}$ = 7.5 Hz, 4H), 6.25 (d, $^3J_{HH}$ = 13.9 Hz, 1H), 7.19 (d, $^3J_{HH}$ = 13.9 Hz, 1H). ^{13}C NMR (125 MHz, $CDCl_3$) δ 13.8; 22.0; 22.4; 22.5; 31.8; 37.4; 76.9; 91.2; 108.3; 124.5; 133.3; 143.3. HRMS (APCI-TOFMS): Calcd for ($C_{12}H_{16}Br$): 239.0430. Found: 239.0430.

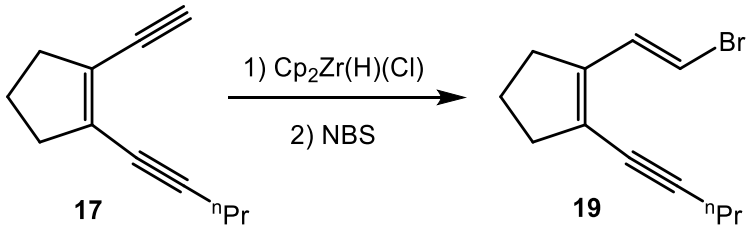

(*E*)-1-(pent-1-yn-1-yl)-2-(prop-1-en-1-yl-2-*d*)cyclopent-1-ene (**21-*E*-*d***): ^{t}BuLi (1.5 M in pentane, 1.6 mL, 2.4 mmol) was added to Et_2O (20 mL) cooled to -78 °C in a 50 mL side-arm flask equipped with a magnetic stir bar and rubber septum under N_2. Then vinyl bromide **20-*d*** (282 mg, 1.17 mmol), diluted in Et_2O (2 mL) was added dropwise and the resulting solution was stirred at -78 °C for 30 min. Then the cold bath was switched for an ice water bath. The solution was stirred at 0 °C for 45 min and then MeI (250 μL, 4 mmol) was added all-at-once. The cooling bath was removed and the solution was allowed to stir at rt overnight. The solution was then poured into a saturated solution of NH_4Cl (30 mL) and the layered partitioned. The aqueous layer

was extracted with Et_2O (2 x 30 mL). The combined organic extracts were washed with H_20 (20 mL), brine (20 mL) and dried over $MgSO_4$. The volatiles were removed under vacuum and the residue was purified on a silica column with hexanes eluant to give **21-*E*-*d*** as a clear oil (152 mg, 0.87 mmol, 74% yield, > 98% deuterium incorporation as determined by ^{1}H NMR spectroscopy). ^{1}H NMR (500 MHz, $CDCl_3$) δ 1.03 (t, $^3J_{HH}$ = 7.4 Hz, 3H), 1.60 (sextet, $^3J_{HH}$ = 7.4 Hz, 2H); 1.82 (s, 3H); 1.86 (t, $^3J_{HH}$ = 7.4 Hz, 2H); 2.38 (t, $^3J_{HH}$ = 7.3 Hz, 2H); 2.48 (m, 4H); 6.54 (s, 1H). ^{13}C NMR (125 MHz, $CDCl_3$) δ 13.8, 18.8, 22.0, 22.5, 29.6, 32.4, 37.4, 77.6, 96.4, 119.9, 127.2, 128.0 (t, $^1J_{CD}$ = 22.5 Hz), 146.1.

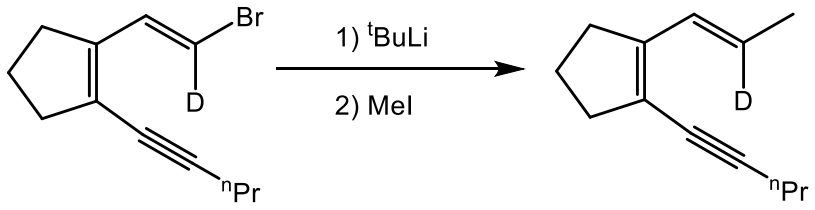

19-d **20-*E*-d**

(*E*)-1-(pent-1-yn-1-yl)-2-(prop-1-en-1-yl)cyclopent-1-ene (**21-*E***): ^{t}BuLi (1.5 M in pentane, 1.6 mL, 2.4 mmol) was added to Et_2O (20 mL) cooled to -78 °C in a 50 mL side-arm flask equipped with a magnetic stir bar and rubber septum under N_2. Then vinyl bromide **20** (282 mg, 1.17 mmol), diluted in Et_2O (2 mL) was added dropwise and the resulting solution was stirred at -78 °C for 30 min and then the cold bath was switched for an ice water bath. The solution was stirred at 0 °C for 45 min and then MeI (250 μL, 4 mmol) was added all-at-once. The cooling bath was removed and the solution was allowed to stir at rt overnight. The solution was then poured into a saturated solution of NH_4Cl (30 mL) and the layered partitioned. The aqueous layer

was extracted with Et_2O (2 x 30 mL). The combined organic extracts were washed with H_2O (20 mL), brine (20 mL) and dried over $MgSO_4$. The volatiles were removed under vacuum and the residue was purified on a silica column with hexanes eluant to give **21-*E*** as a clear oil (152 mg, 0.87 mmol, 74% yield). ^{1}H NMR (500 MHz, $CDCl_3$) δ 1.03 (t, $^3J_{HH}$ = 7.4 Hz, 3H), 1.60 (sextet, $^3J_{HH}$ = 7.4 Hz, 2H); 1.82 (d, $^3J_{HH}$ = 6.9 Hz, 3H); 1.86 (t, $^3J_{HH}$ = 7.4 Hz, 2H); 2.38 (t, $^3J_{HH}$ = 7.3 Hz, 2H); 2.48 (m, 4H); 5.65 (m, 1H); 6.54 (d, $^3J_{HH}$ = 15.6 Hz, 1H). ^{13}C NMR (125 MHz, $CDCl_3$) δ 13.8, 18.8, 22.0, 22.5, 29.6, 32.4, 37.4, 77.6, 96.4, 119.9, 127.2, 128.0, 146.1. HRMS (APCI-TOFMS): Calcd for ($C_{13}H_{19}$): 175.1481. Found: 175.1483.

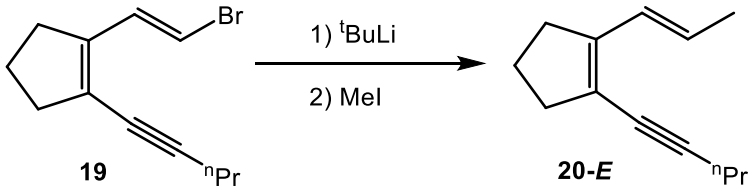

(η^5-cyclopentadienyl)(η^6-(5-methyl-6-propyl-2,3-dihydro-1*H*-indene)ruthenium(II) hexafluorophosphate (**24-*d***): **3** (8 mg, 18.4 μmol) and **21*E*-*d*** (3.2 mg, 18.4 μmol) were weighed into an oven-dried J.Young tube (cooled to rt under vacuum). Then $CDCl_3$ (800 μL) was distilled into the tube on the high vacuum line and the reaction was allowed to proceed for 1 h at rt. A ^{1}H NMR spectrum indicated consumption of the starting diene **21*E*-*d*** and resonances expected for the product arene. The solution was passed through a pad of Celite and then Et_2O (12 mL) was added to precipitate **24-*d***. The resulting suspension was passed through a pad of Celite, rinsed through was Et_2O (2 x 2 mL) and then the Celite was rinsed with DCM (3 x 3 mL) which was collected in a fresh vial. The volatiles were removed

under vacuum and the residue was purified on a pipette silica column with acetone in DCM (0 → 5%) to give **24-*d*** as a white powder (8.0 mg, 16.5 μmol, 90% yield, > 95% deuterium incorporation as determined by ^{1}H NMR spectroscopy). ^{1}H NMR (500 MHz, CD_2Cl_2) δ 1.03 (t, $^{3}J_{HH}$ = 7.4 Hz, 3H), 1.51-1.90 (m, 3H), 2.24-2.37 (m,1H), 2.32 (s,3H), 2.62-2.71 (m, 4H), 2.81-2.88 (m, 4H), 5.13 (s, 5H), 6.12 (s, 0.05H), 6.18 (s, 1H). ^{13}C NMR (125 MHz, CD_2Cl_2) δ 14.1, 19.1, 24.5, 25.2, 31.1, 31.4, 31.5, 81.1, 83.4 (m), 84.6 (d), 99.9, 104.5, 108.1, 108.3. HRMS (ESI-TOFMS): Calcd for ($C_{18}H_{22}DRu$): 342.0905. Found: 342.0908.

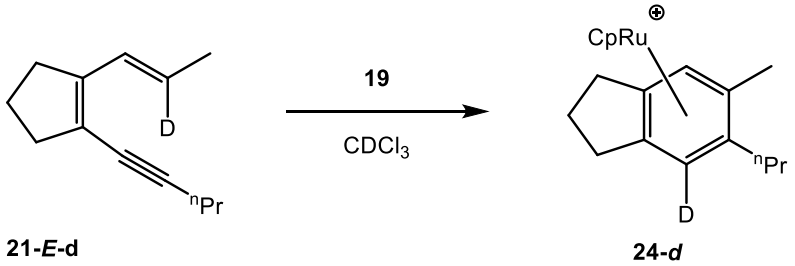

21-*E*-d **24-*d***

((2-vinylcyclopent-1-en-1-yl)ethynyl)benzene (35): ^{n}BuLi (1.25 M in hexanes, 2 mL, 2.5 mmol) was added dropwise to a suspension of methyl triphenylphosphonium bromide (890 mg, 2.5 mmol) in THF (40 mL) cooled to 0 °C under N_2. The resulting red solution was stirred at 0 °C for 45 min and then **34** (440 mg, 2.24 mmol) dissolved in THF (5 mL) was added dropwise. The resulting solution was stirred at rt overnight and then the volatiles were removed under vacuum. The residue was loaded onto a silica gel column and the reaction purified with hexanes to give **35** as a clear oil (400 mg, 2.06 mmol, 90% yield). ^{1}H NMR (500 MHz, $CDCl_3$) δ 1.90 (p, $^{3}J_{HH}$ = 7.8 Hz, 2H); 2.52 (t, $^{3}J_{HH}$ = 7.8 Hz, 2H); 2.60 (t, $^{3}J_{HH}$ = 7.8 Hz, 2H); 5.16 (d, $^{3}J_{HH}$ = 17Hz, 1H); 5.17 (d, $^{3}J_{HH}$ = 11.9 Hz, 1H); 6.90 (dd, $^{3}J_{HH}$ = 17 Hz, 11.9Hz, 1H); 7.22-7.26

(m, 3H); 7.4 (m, 2H). ^{13}C NMR (125 MHz, $CDCl_3$) δ 22.6; 32.0; 37.4; 86.19; 96.1; 116.28; 122.7; 123.8; 128.3; 128.5; 131.6; 132.2; 146.9; 148.1; 153.8. HRMS (ESI): Calcd for ($C_{15}H_{15}$): 195.1168. Found: 195.1169.

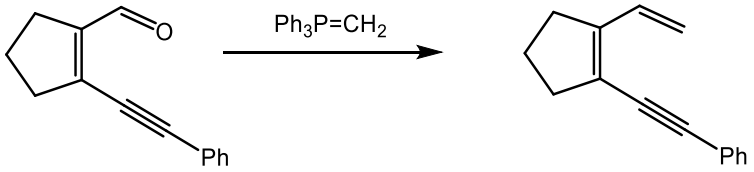

34 **35**

(η^5-pentamethylcyclopentadienyl)(η^6-(5-Phenyl-2,3-dihyrdo-1*H*-indene))ruthenium(II) hexafluorophosphate (**40**): **5** (10 mg, 23 μmol) and dienyne **35** (6 mg, 31 μmol) were weighed into an oven-dried J.Young tube and $CDCl_3$ (1 mL) was distilled into the tube on the high vacuum line. The solution was warmed to rt and a ^{1}H NMR spectrum was taken approximately 15 min after the addition of solvent. The spectrum showed the appearance of peaks associated with product **40** and the complete consumption of **35**. The solution was added to a 20 mL vial and then Et_2O (10 mL) was added to the solution to precipitate out **40**. The solution was filtered through a plug of Celite, and rinsed with Et_2O (2 x 2 mL). The Celite was rinsed with DCM (3 x 1 mL) which was collected in a fresh vial and the volatiles were removed under vacuum to give **40** as a white powder (10 mg, 19.8 μmol, 86% yield). ^{1}H NMR (500 MHz, CD_2Cl_2) δ 1.71 (s, 15H); 1.77-1.83 (m, 1H); 2.26-2.32 (m, 1H); 2.59-2.67 (m, 2H); 2.94-3.05 (m, 2H); 5.86 (d, $^3J_{HH}$ = 6.1 Hz, 1H), 6.08 (d, $^3J_{HH}$ = 6.1 Hz, 1H); 6.27 (s, 1H); 7.51-7.56 (m, 3H); 7.60-7.62 (m, 2H). ^{13}C NMR (125 MHz, CD_2Cl_2) δ

10.1, 23.7, 29.5, 29.9, 81.7, 83.4, 84.1, 95.6, 100.9, 108.1, 108.1, 127.3, 130.1, 130.9, 132.6. HRMS (ESI): Calcd for ($C_{25}H_{29}Ru$): 431.1313. Found: 431.1314.

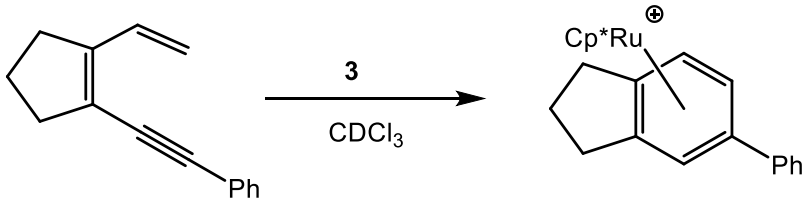

35 **40**

(η^5-cyclopentadienyl)(η^3,η^3-5,10-dimethyl-4,12-dipropyl-1,2,3,3a,5,6,7,8,9,10-decahydro-5,9b,methanoideno[5,4-*e*]azulenyl)ruthenium(II) hexafluorophosphate (25): **19** (16 mg, 37 μmol) was weighed into a 20 mL vial equipped with a rubber septum and was then blown out with an argon balloon. Meanwhile diene **21-*E*** (78 mg, 448 μmol, 12 eq.) was weighed into a 20 mL vial equipped with a rubber septum under argon and was dissolved in degassed DCM (3 mL). Then the solution of **21-*E*** was added to the vial containing **19** and the resulting solution was allowed to react overnight. Then the solution was concentrated to approximately 0.5 mL and Et_2O (15 mL) was added to precipitate **25**. The solution was filtered through a plug of Celite, which was then rinsed with additional Et_2O (2 x 2 mL). The Celite was rinsed with DCM (3 x 1 mL) which was collected in a fresh vial. The volatiles were removed under vacuum to give **25** as a yellow powder (12mg, 18 μmol, 50% yield). ^{1}H NMR (500 MHz, $CDCl_3$) δ 0.69 (dd, $^3J_{HH}$ = 8.3 Hz, 2.3 Hz, 1H); 0.86 (t, $^3J_{HH}$ = 7.6 Hz, 3H); 0.89 (t, $^3J_{HH}$ = 7.6 Hz, 3H); 0.97 (s, 3H); 0.99 (s, 3H); 1.00-1.26 (m, 2H); 1.42 (m, 1H); 1.58 (s, 3H); 1.73 (m, 1H); 1.81-1.92 (m, 3H);

2.12 (m, 2H); 2.21-2.24 (m, 2H); 2.29-2.36 (m, 3H); 2.45-2.52 (m, 2H); 2.63 (m, 2H); 2.72-2.82 (m, 2H); 4.12 (s, 1H); 5.12 (s, 5H); 5.61 (t, $^{3}J_{HH}$ = 2.2 Hz, 1H). ^{13}C NMR (125 MHz, $CDCl_3$) δ 14.4; 14.9; 15.2; 15.3; 19.1; 20.7; 22.9; 23.5; 26.4; 26.5; 27.3; 28.6; 29.7; 31.2; 32.1; 33.3; 33.4; 35.4; 49.7; 49.8; 51.4; 53.5; 58.2; 68.3; 83.1; 90.0; 107.4; 108.3; 126.5; 126.6; 146.7; 146.8.

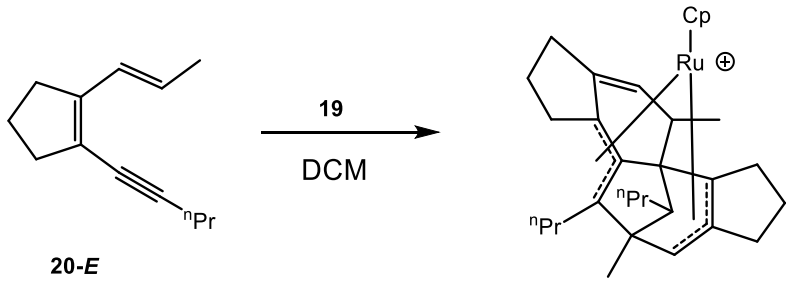

20-*E* **25**

(*Z*)-2-(prop-1-en-1-yl)cyclopent-1-ene-1-carbaldehyde (**23**): H_2 was bubbled through a suspension of Lindlar's catalyst (1.02 g) and quinoline (0.10 mL, 0.85 mmol) in hexanes (100 mL) for 5 min. Then alkyne **21** (1.3 g, 9.7 mmol, 2 M in EtOAc) was added via syringe and the reaction was stirred under one atmosphere of H_2 for 2 h. The reaction mixure was filter through a pad of Celite and the volatiles were removed under vacuum. The residue was purified on a silica column with EtOAc in hexanes (0 → 2%) to give **23** as a clear oil (1.25 g, 9.6 mmol, 98% yield). ^{1}H NMR (500 MHz, $CDCl_3$) δ 1.82 (d, $^{3}J_{HH}$ = 7.4 Hz, 3H); 1.91 (p, $^{3}J_{HH}$ = 7.4 Hz, 2H); 2.57 (bt, $^{3}J_{HH}$ = 7.4Hz, 4H); 5.89 (dq, $^{3}J_{HH}$ = 11.9 Hz, 7.3 Hz, 1H); 6.50 (d, $^{3}J_{HH}$ = 11.9 Hz, 1H), 9.96 (s, 1H). ^{13}C NMR (125 MHz, $CDCl_3$) δ 15.9; 22.4; 29.9; 39.0; 122.75;

132.8; 140.0; 159.3; 189.3. HRMS (APCI-TOFMS): Calcd for ($C_9H_{13}O$): 137.0961. Found: 137.0959.

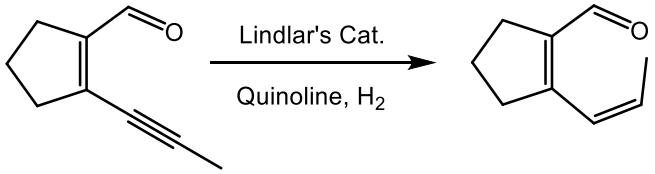

22 **23**

(*Z*)-1-ethynyl-2-(prop-1-en-1-yl)cyclopent-1-ene (23): ^{n}BuLi (2 mL, 1.25 M in hexanes, 2.5 mmol) was added dropwise to a stirred solution of TMS diazomethane (1.25 mL, 2 M in Et_2O, 2.5 mmol) in dry THF (35 mL) cooled to -78 °C under N_2. The resulting solution was stirred at this temperature for 45 min and then aldehyde **23** (270 mg, 2 mmol) dissolved in dry THF (6 mL) was added dropwise. The resulting solution was stirred at -78 °C for 30 min and then the cold bath was removed and the solution was allowed to warm to rt over the course of an hour. The reaction mixture was allowed to stir at rt for 1 h and then the reaction was quenched with a saturated solution of NH_4Cl (30 mL). The layers were partitioned and the aqueous layer was extracted with Et_2O (3 x 25 mL). The combined organic extracts were washed with H_2O (15 mL), brine (15 mL), dried over $MgSO_4$, and the volatiles removed under vacuum. The residue was purified on a silica column with hexanes eluant to give **23** as a clear oil (220 mg, 1.67 mmol, 85% yield.) ^{1}H NMR (500 MHz, $CDCl_3$) δ 1.85 (d, $^{3}J_{HH}$ = 7.0 Hz, 3H); 1.91 (p, $^{3}J_{HH}$ = 7.6 Hz, 2H); 2.49 (t, $^{3}J_{HH}$ = 7.6 Hz, 2H); 2.75 (t, $^{3}J_{HH}$ = 7.6 Hz); 3.30 (s, 1H); 5.60 (dq, $^{3}J_{HH}$ = 11.6 Hz, 7.0 Hz, 1H); 6.40 (d, $^{3}J_{HH}$ = 11.6 Hz, 1H). ^{13}C NMR (125 MHz, $CDCl_3$) δ 13.6, 20.7, 34.7, 41.1, 81.1, 90.7,

121.2, 130.4, 134.4, 148.7. HRMS (ESI): Calcd for ($C_{10}H_{13}$): 133.1012. Found: 133.1011.

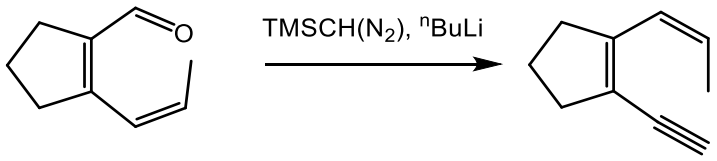

22 **23**

(*Z*)-1-(pent-1-yn-1-yl)–2–(prop-1-en-1-yl)cyclopent-1-ene (21-*Z*): ^{n}BuLi (2 mL, 1.25 M in hexanes, 2.5 mmol) was added dropwise to a stirred solution of alkyne **23** (220 mg, 1.67 mmol) dissolved in dry THF (5 mL) cooled to -78 °C under dry N_2. The resulting solution was stirred at this temperature for 30 min and then warmed to 0 °C on an ice/water bath for 15 min before being cooled back to -78 °C. Then ^{n}PrBr (450 μL, 5 mmol) was added all-at-once. The solution was stirred at -78 °C for 30 min and then the cooling bath was removed allowing the reaction to warm to rt over the course on 1 h. The solution was then quenched with a saturated solution of NH_4Cl (30 mL) and the aqueous solution was extracted with Et_2O (3 x 25 mL). The combined organic extracts were washed with H_2O (15 mL), brine (15 mL), dried over $MgSO_4$ and the volatiles were removed under vacuum. The residue was purified on a silica column with hexanes eluant to give **20-*Z*** as a clear oil (200 mg, 1.15 mmol, 69% yield). ^{1}H NMR (500 MHz, $CDCl_3$) δ 0.99 (t, $^{3}J_{HH}$ = 7.6 Hz, 3H); 1.56 (sextet, $^{3}J_{HH}$ = 7.6 Hz, 2H); 1.83 (d, $^{3}J_{HH}$ = 7.3 Hz, 3H); 1.87 (p, $^{3}J_{HH}$ = 7.4 Hz, 2H); 2.35 (t, $^{3}J_{HH}$ = 7.6 Hz, 2H); 2.43 (t, $^{3}J_{HH}$ = 7.4 Hz, 2H); 2.72 (t, $^{3}J_{HH}$ = 7.4 Hz, 2H); 5.52 (dq, $^{3}J_{HH}$ = 11.7 Hz, 7.3 Hz, 1H); 6.37 (d, $^{3}J_{HH}$ = 11.7 Hz, 1H). ^{13}C NMR (125 MHz, $CDCl_3$) δ

13.8; 15.4; 22.0; 22.7; 23.5; 35.8; 36.4; 77.9; 97.3; 125.5; 126.6; 127.3; 128.0. HRMS (APCI-TOFMS): Calcd for ($C_{13}H_{19}$): 175.1481. Found: 175.1483.

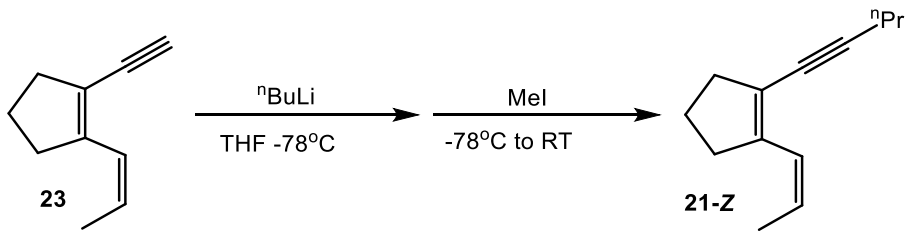

Trimethyl((2-vinylcyclopent-1-en-1-yl)ethynyl)silane (27): ^{n}BuLi (1.25 M in hexanes, 2 mL, 2.5 mmol) was added dropwise to a suspension of methyl triphenylphosphonium bromide (890 mg, 2.5 mmol) in THF (40 mL) cooled to 0 °C under N_2. The resulting red solution was stirred at 0 °C for 45 min and then **26** (440 mg, 2.24 mmol) dissolved in THF (5 mL) was added dropwise. The resulting solution was stirred at rt overnight and then the volatiles were removed under vacuum. The residue was loaded onto a silica column and the reaction purified with hexanes eluant to give **27** as a clear oil (400 mg, 2.06 mmol, 90% yield). ^{1}H NMR (500 MHz, $CDCl_3$) δ 0.19 (s, 9H); 1.88 (p, $^{3}J_{HH}$ = 7.6 Hz, 2H); 2.50 (t, $^{3}J_{HH}$ = 7.6 Hz, 2H); 2.55 (t, $^{3}J_{HH}$ = 7.6 Hz, 2H); 5.18 (d, $^{3}J_{HH}$ = 18.4 Hz, 1H); 5.19 (d, $^{3}J_{HH}$ = 9.6 Hz, 1H); 6.83 (dd, $^{3}J_{HH}$ = 18.4 Hz, 9.6 Hz, 1H). ^{13}C NMR (125 MHz, $CDCl_3$) δ 0.4; 22.5; 31.9; 37.3; 101.2; 101.8; 116.5; 122.6; 132.1; 149.4. HRMS (APCI-TOFMS): Calcd for ($C_{12}H_{19}Si$): 191.1251. Found: 191.1252.

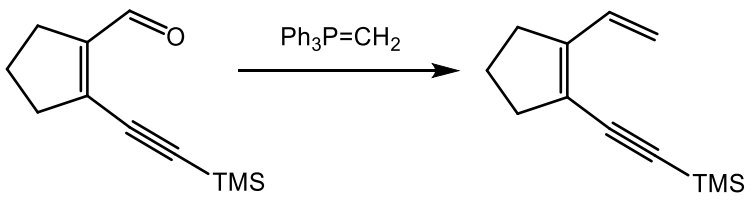

26 **27**

1-Ethynyl-2-vinylcyclopent-1-ene (28): A solution of **27** (400 mg, 2.06 mmol) and K_2CO_3 (50 mg, 0.36 mmol) in THF/MeOH (10 mL, 1:1) was stirred at rt for 1 h. Then the solution was diluted with H_2O (50 mL) and the aqueous solution was extracted with Et_2O (3 x 20 mL). The combined organic extracts were washed with brine (15 mL), dried over $MgSO_4$ and the volatiles were removed under vacuum. The resulting residue was purified on a silica column with pentane eluant to give **28** as a clear oil (145 mg, 1.23 mmol, 60% yield). ^{1}H NMR ($CDCl_3$, 500 MHz) δ 1.90 (p, $^3J_{HH}$ = 7.6 Hz, 2H); 2.52 (t, $^3J_{HH}$ = 7.6 Hz, 2H); 2.56 (t, $^3J_{HH}$ = 7.6 Hz, 2H); 3.28 (s, 1H); 5.20 (d, $^3J_{HH}$ = 17.5 Hz, 1H); 5.20 (d, $^3J_{HH}$ = 10.6 Hz, 1H); 6.84 (dd, $^3J_{HH}$ = 17.5 Hz, 10.6 Hz, 1H). ^{13}C NMR (125 MHz, $CDCl_3$) δ 22.4; 31.9; 37.2; 80.5; 83.6; 116.9; 121.4; 131.8; 149.7. HRMS (APCI-TOFMS): Calcd for (C_9H_{11}): 119.0855. Found: 119.0854.

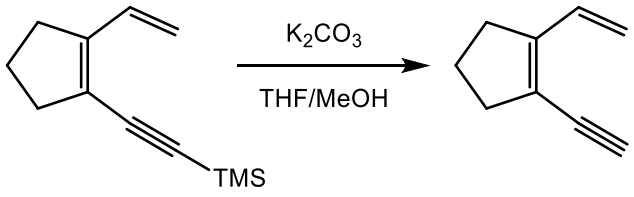

27 **28**

1-(Ethynyl-*d*)-2-vinylcyclopent-1-ene (28-*d*): Enediyne **28** (100 mg, 0.85 mmol) was dissolved in THF (5 mL) in an oven-dried side-arm flask equipped with a stir bar and rubber septum under dry N_2. The solution was cooled to -78 °C on a dry

ice/acetone bath and then ^{n}BuLi (1 mL, 1.25 M in hexanes, 1.25 mmol) was added dropwise to the solution. The resulting solution was stirred at -78 °C for 30 min and was then quenched with CF_3CO_2D (0.75 mL, 9.8 mmol, diluted to 5 mL with D_2O). The solution was allowed to warm to rt and stir for 10 min at rt. The layers were partitioned and the aqueous layer was extracted with Et_2O (3 x 25 mL). The combined organic extracts were washed with $NaHCO_3$ (2 x 20 mL), H_2O (15 mL), brine (15 mL) and dried over $MgSO_4$. The volatiles were removed under vacuum and the residue was purified on a silica column with pentane eluant to give **28-*d*** as a clear oil (65 mg, 0.55 mmol, 65% yield, > 98% deuterium incorporation as determined by ^{1}H NMR spectroscopy). ^{1}H NMR (500 MHz, $CDCl_3$) δ 1.90 (p, $^3J_{HH}$ = 7.6 Hz, 2H); 2.52 (t, $^3J_{HH}$ = 7.6 Hz, 2H); 2.56 (t, $^3J_{HH}$ = 7.6 Hz, 2H); 3.28 (s, 1H); 5.20 (d, $^3J_{HH}$ = 17.5 Hz, 1H); 5.20 (d, $^3J_{HH}$ = 10.6 Hz, 1H); 6.84 (dd, $^3J_{HH}$ = 17.5 Hz, 10.6 Hz, 1H). ^{13}C NMR (125 MHz, $CDCl_3$) δ 22.4; 31.9; 37.2; 80.5 (t, $^2J_{CD}$ = 7.5 Hz); 83.6 (t, $^1J_{CD}$ = 38.2 Hz); 116.9; 121.4; 131.8; 149.7. HRMS (APCI-TOFMS): Calcd for ($C_9H_{10}D_1$): 120.0924. Found: 120.0918.

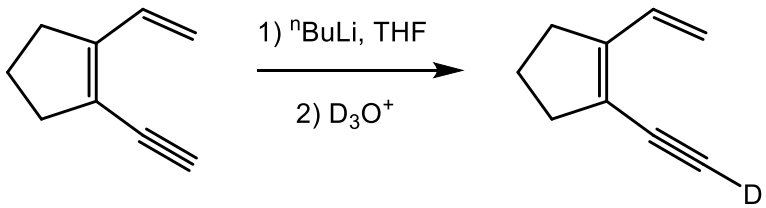

28 **28-*d***

(η^5-cyclopentadienyl)(η^6-(2,3-dihyrdo-1*H*-indene))ruthenium(II) hexafluorophosphate (**29**): **19** (10 mg, 23 μmol) and dienyne **28** (3.7 mg, 31 μmol) were weighed into an oven-dried J.Young tube and $CDCl_3$ (750 μL) was distilled into

the tube on the high vacuum line. The solution was warmed to rt and a ^{1}H NMR spectrum was taken approximately 15 min after the addition of solvent. The spectrum showed the appearance of peaks associated with product **29** and the complete consumption of **28**. The solution was added to a 20 mL vial and then Et_2O (10 mL) was added to the solution to precipitate **29**. The solution was filtered through a plug of Celite, which was rinsed with Et_2O (2 x 2 mL). The Celite was rinsed with DCM (3 x 1 mL) which was collected in a fresh vial and the volatiles were removed under vacuum to give **29** as a white powder (7 mg, 16 μmol, 70% yield). ^{1}H NMR (500 MHz, CD_2Cl_2) δ 1.82-1.89 (m, 1H); 2.25-2.31 (m, 1H); 2.68-2.73 (m, 2H); 2.86-2.93 (m, 2H); 5.27 (s, 5H); 5.96 (dd, J = 4.3 Hz, 2.3 Hz, 2H); 6.23 (dd, J = 4.3 Hz, 2.3 Hz). ^{13}C NMR (125 MHz, CD_2Cl_2) δ 25.0, 31.8, 80.9, 82.8, 84.5, 109.3. HRMS (ESI): Calcd for ($C_{14}H_{15}Ru$): 285.0217. Found: 285.0215.

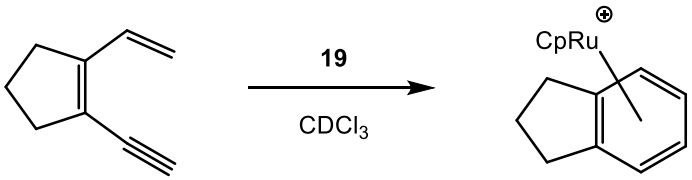

28 **29**

(η^5-cyclopentadienyl)(η^6-(2,3-dihyrdo-1*H*-indene-5-*d*))ruthenium(II) hexafluorophosphate (**29-*d***): **5** (10 mg, 23 μmol) and dienyne **28-*d*** (3.4 mg, 29 μmol) were weighed into an oven-dried J.Young tube and $CDCl_3$ (750 μL) was distilled into the tube on the high vacuum line. The solution was warmed to rt and a ^{1}H NMR spectrum was taken approximately 15 mins after the addition of solvent. The spectrum showed the appearance of peaks associated with product **29-*d*** and the

complete consumption of **28-*d***. The solution was added to a 20 mL vial and then Et_2O (10 mL) was added to the solution to precipitate **29-*d***. The solution was filtered through a plug of Celite, which was rinsed with Et_2O (2 x 2 mL). The Celite was rinsed with DCM (3 x 1 mL) which was collected in a fresh vial and the volatiles were removed under vacuum to give **29-*d*** as a white powder (7 mg, 16 μmol, 70% yield, > 95% deuterium incorporation). ^{1}H NMR (CD_2Cl_2, 500 MHz) δ 1.82-1.89 (m, 1H); 2.25-2.31 (m, 1H); 2.68-2.73 (m, 2H); 2.86-2.93 (m, 2H); 5.27 (s, 5H); 5.96 (m, 1H); 6.23 (m, 2H). ^{13}C NMR (125 MHz, CD_2Cl_2) δ 25.0, 31.8, 80.9, 82.8 (m), 84.5 (m), 109.3. HRMS (ESI): Calcd for ($C_{14}H_{14}DRu$): 286.0278. Found: 286.0277.

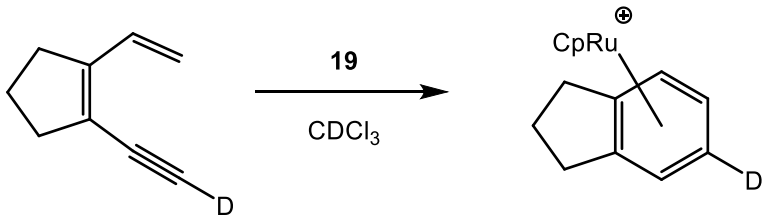

28-*d* 29-*d*

(*E*)-(2-(2-(prop-1-yn-1-yl)cyclopen-1-en-1-yl)vinyl)benzene (38-*E*): ^{n}BuLi (1.25 M in hexanes, 2 mL, 2.5 mmol) was added dropwise to a suspension of benzyl triphenylphosphonium bromide (1.083 g, 2.5 mmol) in THF (40 mL) cooled to 0 °C under N_2. The resulting red solution was stirred at 0 °C for 45 min and then **39** (268 mg, 2.0 mmol) dissolved in THF (5 mL) was added dropwise. The resulting solution was stirred at rt overnight and then the volatiles were removed under vacuum. The residue was loaded onto a silica column and the reaction purified with hexanes eluant to give **38-*E*** as a yellow oil (333 mg, 1.60 mmol, 80% yield). ^{1}H NMR ($CDCl_3$, 500 MHz) δ 1.86 (p, $^3J_{HH}$ = 7.5 Hz, 2H); 2.03 (s, 3H); 2.49 (t, $^3J_{HH}$ = 7.5 Hz, 2H); 2.55 (t,

$^{3}J_{HH}$ = 7.5 Hz, 2H); 6.41 (d, $^{3}J_{HH}$ = 16.3 Hz, 1H); 7.3-7.5 (m, 5H); 7.40 (d, $^{3}J_{HH}$ = 9.0 Hz, 2H). ^{13}C NMR (125 MHz, $CDCl_3$) δ 5.1; 22.6; 32.3; 37.8; 76.8; 93.5; 123.9; 124.3; 126.8; 127.6; 128.8; 130.4; 137.9; 146.0. HRMS (APCI-TOFMS): Calcd for ($C_{16}H_{17}$): 209.1325. Found: 209.1325.

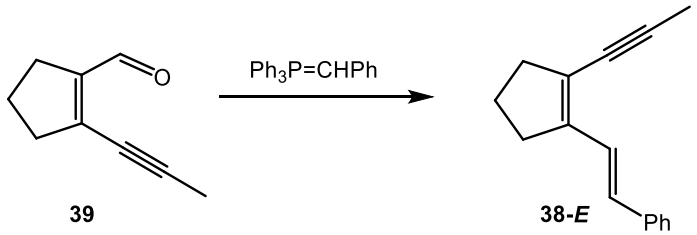

(*Z*)-(2-(2-ethynylcyclopent-1-en-1-yl)vinyl)benzene (37): ^{n}BuLi (2 mL, 1.25 M in hexanes, 2.5 mmol) was added dropwise to a stirred solution of TMS diazomethane (1.25 mL, 2 M in Et_2O, 2.5 mmol) in dry THF (35 mL) cooled to -78 °C under N_2. The resulting solution was stirred at this temperature for 45 min and then aldehyde **36** (270 mg, 2 mmol) dissolved in dry THF (6 mL) was added dropwise. The resulting solution was stirred at -78 °C for 30 min and then the cold bath was removed and the solution was allowed to warm to rt over the course of an hour. The reaction mixture was allowed to stir at rt for 1 hour and then the reaction was quenched with a saturated solution of NH_4Cl (30 mL). The layers were partitioned and the aqueous layer was extracted with Et_2O (3 x 25 mL). The combined organic extracts were washed with H_2O (15 mL), brine (15 mL), dried over $MgSO_4$ and the volatiles removed under vacuum. The residue was purified on a silica column with hexanes eluant to give **37** as a clear oil (220 mg, 1.67 mmol, 85% yield). ^{1}H NMR ($CDCl_3$, 500 MHz) δ 1.84 (p, $^{3}J_{HH}$ = 7.5 Hz, 2H); 2.23 (t, $^{3}J_{HH}$ = 7.5 Hz, 2H); 2.55 (t, $^{3}J_{HH}$ = 7.5 Hz, 2H); 3.24

(s, 1H); 6.71 (d, $^{3}J_{HH}$ = 12.1 Hz, 1H); 6.78 (d, $^{3}J_{HH}$ = 12.1 Hz, 1H); 7.3-7.5 (m, 5H). ^{13}C NMR (125 MHz, $CDCl_3$) δ 23.8; 34.8; 36.7; 76.3; 93.9; 126.2; 126.4; 127.8; 129.2; 130.4; 138.8; 145.7. HRMS (ESI): Calcd for ($C_{15}H_{15}$): 195.1168. Found: 195.1169.

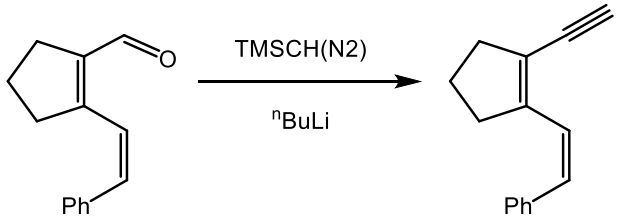

36 **37**

(*Z*)-(2-(2-(prop-1-yn-1-yl)cyclopent-1-en-1-yl)vinyl)benzene (38-*Z*): ^{n}BuLi (2 mL, 1.25 M in hexanes, 2.5 mmol) was added dropwise to a stirred solution of **37** (220 mg, 1.67 mmol) dissolved in dry THF (5 mL) cooled at -78 °C under N_2. The resulting solution was stirred at this temperature for 30 min and then warmed to 0 °C on an ice/water bath for 15 min before being cooled back to -78 °C. Then MeI (450 μL, 5 mmol) was added all-at-once. The solution was stirred at -78 °C for 30 min and then the cooling bath was removed allowing the reaction to warm to rt over the course of 1 h. The solution was then quenched with a saturated solution of NH_4Cl (30 mL) and the aqueous solution was extracted with Et_2O (3 x 25 mL). The combined organic extracts were washed with H_2O (15 mL), brine (15 mL), dried over $MgSO_4$ and the volatiles were removed under vacuum. The residue was purified on a silica column with hexanes eluant to give **38-*Z*** as a clear oil (200 mg, 1.60 mmol, 92% yield). ^{1}H NMR (500 MHz, $CDCl_3$) δ 1.84 (p, $^{3}J_{HH}$ = 7.5 Hz, 2H); 2.18 (s, 3H); 2.23 (t, $^{3}J_{HH}$ = 7.5 Hz, 2H); 2.55 (t, $^{3}J_{HH}$ = 7.5 Hz, 2H); 6.71 (d, $^{3}J_{HH}$ = 12.1 Hz, 1H); 6.78 (d, $^{3}J_{HH}$

= 12.1 Hz, 1H); 7.3-7.5 (m, 5H). ^{13}C NMR (125 MHz, $CDCl_3$) δ5.0; 23.8; 34.8; 36.7; 76.9; 93.9; 126.2; 126.4; 127.8; 129.2; 130.4; 138.8; 145.7. HRMS (APCI-TOFMS): Calcd for ($C_{16}H_{17}$): 209.1325. Found: 209.1326.

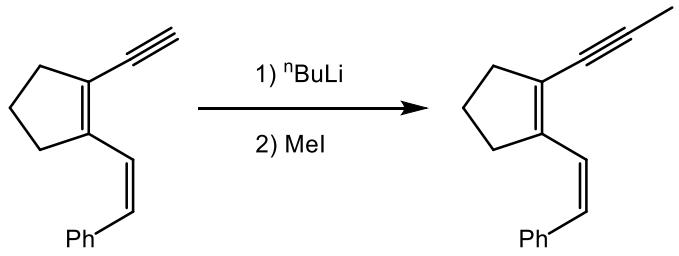

37 **38-*Z***

(η^5-cyclopentadienyl)(η^6-(5-methyl-6-phenyl-2,3-dihyrdo-1*H*-indene))ruthenium(II) hexafluorophosphate (**41**): **19** (10 mg, 23 μmol) and dienyne **38-*E*** (3.4 mg, 29 μmol) were weighed into an oven-dried J.Young tube and $CDCl_3$ (750 μL) was distilled into the tube on the high vacuum line. The solution was warmed to rt and a ^{1}H NMR spectrum was taken approximately 15 min after the addition of solvent. The spectrum showed the appearance of peaks associated with product **41** and the complete consumption of **38-*E***. The solution was added to a 20 mL vial and then Et_2O (10 mL) was added to the solution to precipitate **41**. The solution was filtered through a plug of Celite, which was rinsed through with Et_2O (2 x 2 mL). The Celite was rinsed with DCM (3 x 1 mL) which was collected in a fresh vial, and the volatiles were removed under vacuum to give **41** as a white powder (7 mg, 16 μmol, 70% yield). ^{1}H NMR ($CDCl_3$, 500 MHz) δ1.85 (m, 2H); 2.24 (s, 3H); 2.79 (m, 4H); 5.26 (s, 5H); 6.20 (s, 1H); 6.47 (s, 1H); 7.32 (d, $^3J_{HH}$ = 7.7 Hz, 2H); 7.42 (m, 3H). ^{13}C NMR (125 MHz, $CDCl_3$) δ20.3; 24.9; 31.0; 81.8; 84.4; 84.5; 99.8;

106.7; 107.5; 108.7; 129.2; 129.6; 130.1; 134.7. HRMS (APCI-TOFMS): Calcd for ($C_{21}H_{21}Ru$): 375.0687. Found: 375.0688.

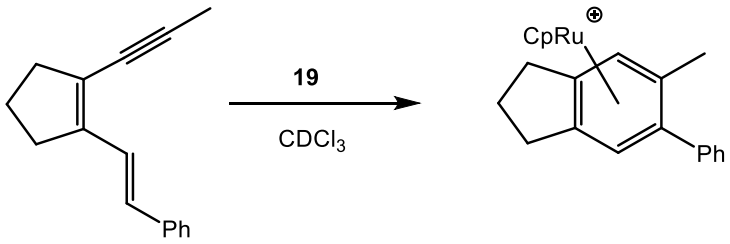

38-*E* **41**

(η^5-cyclopentadienyl)(η^6-(5-methyl-6-phenyl-2,3-dihyrdo-1*H*-indene))ruthenium(II) hexafluorophosphate (**41**): **19** (10 mg, 23 μmol) and dienyne **38-*Z*** (3.4 mg, 29 μmol) were weighed into an oven-dried J.Young tube and $CDCl_3$ (750 μL) was distilled into the tube on the high vacuum line. The solution was warmed to rt and a ^1H NMR spectrum was taken approximately 15 min after the addition of solvent. The spectrum showed the appearance of peaks associated with product **41** and the complete consumption of **38-*Z***. The solution was added to a 20 mL vial and then Et_2O (10 mL) was added to the solution to precipitate **38-*Z***. The solution was filtered through a plug of Celite, which was rinsed with Et_2O (2 x 2 mL). The Celite was rinsed with DCM (3 x 1 mL) which was collected in a fresh vial, and the volatiles were removed under vacuum to give **41** as a white powder (7 mg, 16 μmol, 70% yield).

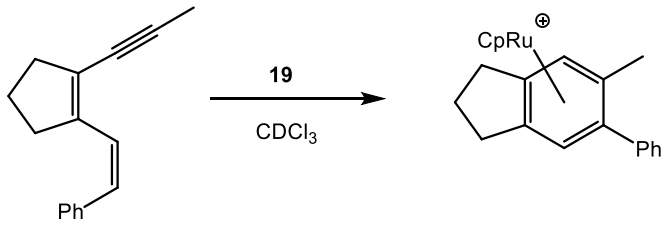

38-*Z* **41**

(η^5-pentamethylcyclopentadienyl)(η^6-(5-methyl-6-phenyl-2,3-dihyrdo-1*H*-indene))ruthenium(II) hexafluorophosphate (**42**): **5** (10 mg, 23 μmol) and dienyne **38-*E*** (3.4 mg, 29 μmol) were weighed into an oven-dried J.Young tube and $CDCl_3$ (750 μL) was distilled into the tube on the high vacuum line. The solution was warmed to rt and a ^{1}H NMR spectrum was taken approximately 15 min after the addition of solvent. The spectrum showed the appearance of peaks associated with product **42** and the complete consumption of **38-*E***. The solution was added to a 20 mL vial and then Et_2O (10 mL) was added to the solution to precipitate **42**. The solution was filtered through a plug of Celite, which was rinsed with Et_2O (2 x 2 mL). The Celite was rinsed with DCM (3 x 1 mL) which was collected in a fresh vial, and the volatiles were removed under vacuum to give **42** as a white powder (7 mg, 16 μmol, 70% yield). ^{1}H NMR ($CDCl_3$, 500 MHz) δ 1.74 (m, 1H); 1.80 (s, 15H); 2.17 (s, 3H); 2.21 (m, 1H); 2.61 (m, 2H); 2.91 (m, 2H); 5.85 (s, 1H); 5.97 (s, 1H); 7.37 (d, $^3J_{HH}$ = 7.2 Hz, 2H); 7.44 (m, 3H). ^{13}C NMR (125 MHz, $CDCl_3$) δ 10.0; 18.8; 23.3; 28.9; 29.1; 85.8; 86.1; 94.5; 105.8; 106.4; 108.6; 129.1; 129.5; 129.6; 134.3. HRMS (ESI-TOFMS): Calcd for ($C_{26}H_{31}Ru$): 445.1471. Found: 445.1470.

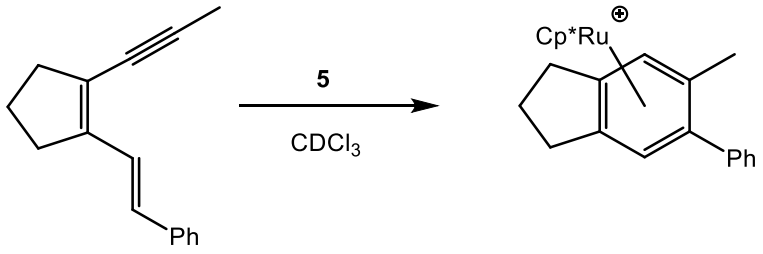

38-*E* **42**

2-5.3 ^{1}H and ^{13}C NMR Spectroscopic Data

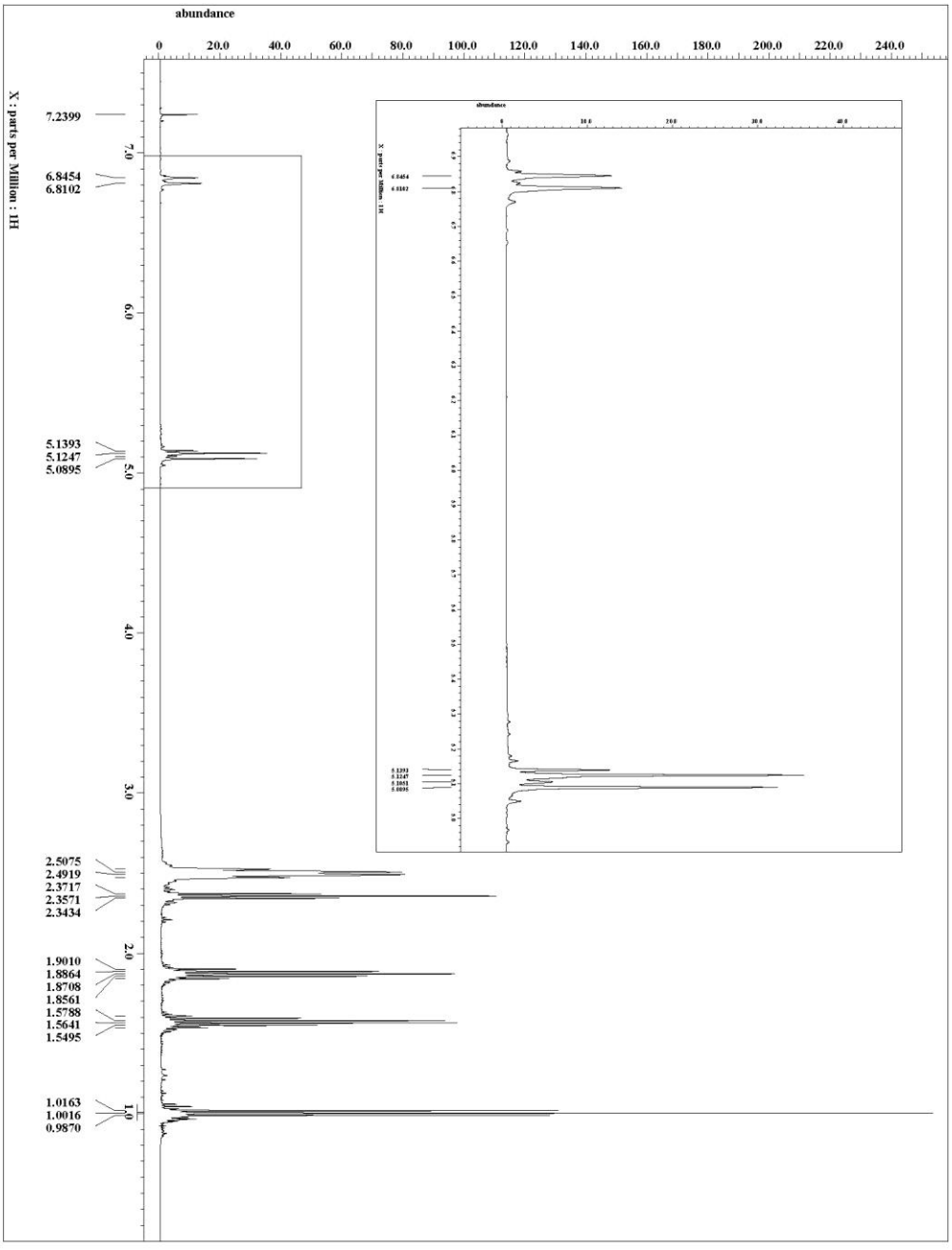

Figure 2-5. *E*-16-d ^{1}H NMR spectrum (500 MHz, $CDCl_3$).

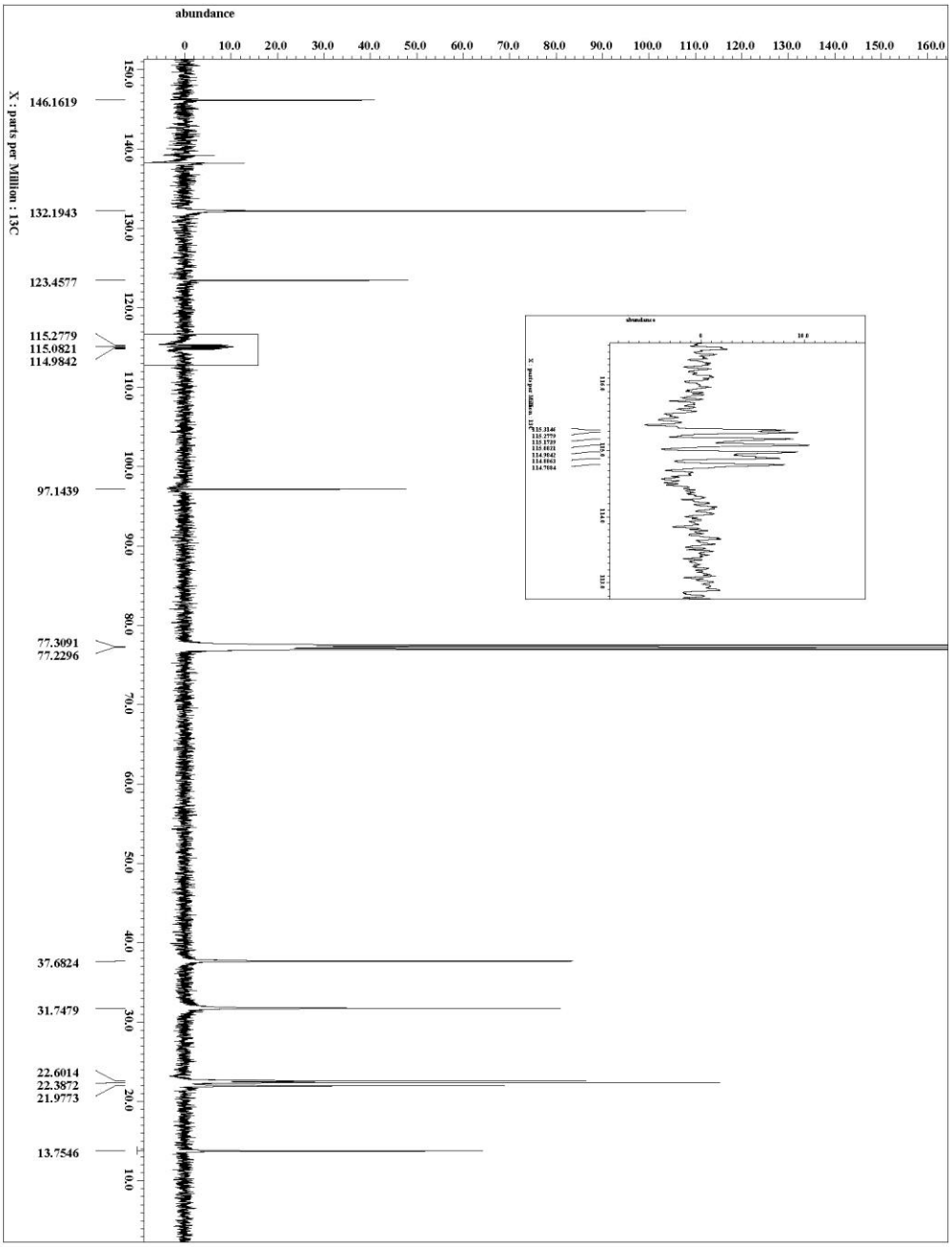

Figure 2-6. *E*-16-d ^{13}C NMR spectrum (125 MHz, $CDCl_3$).

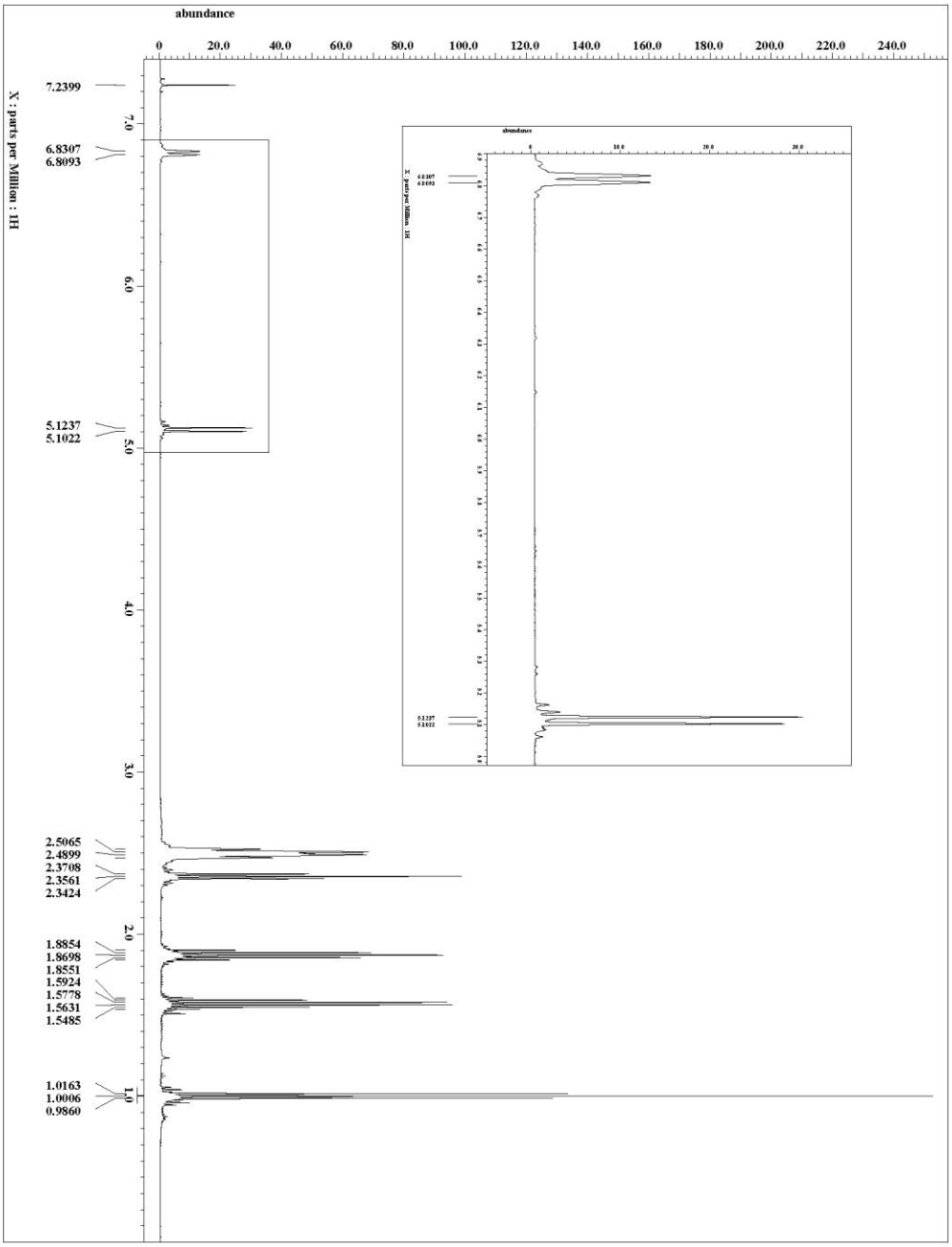

Figure 2-7. *Z*-16-d ^{1}H NMR spectrum (500 MHz, $CDCl_3$).

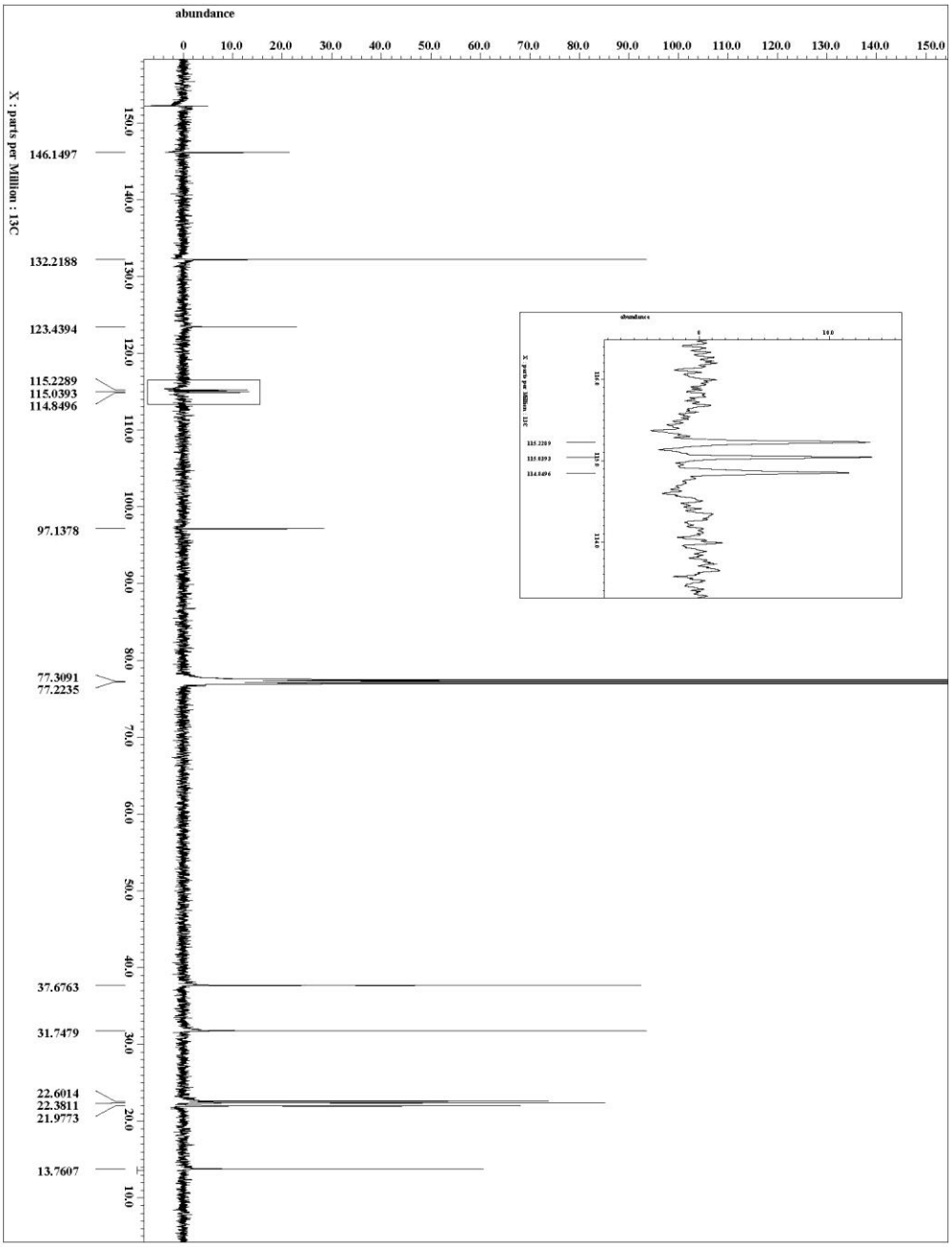

Figure 2-8. *Z*-16-d ^{13}C NMR spectrum (125 MHz, $CDCl_3$).

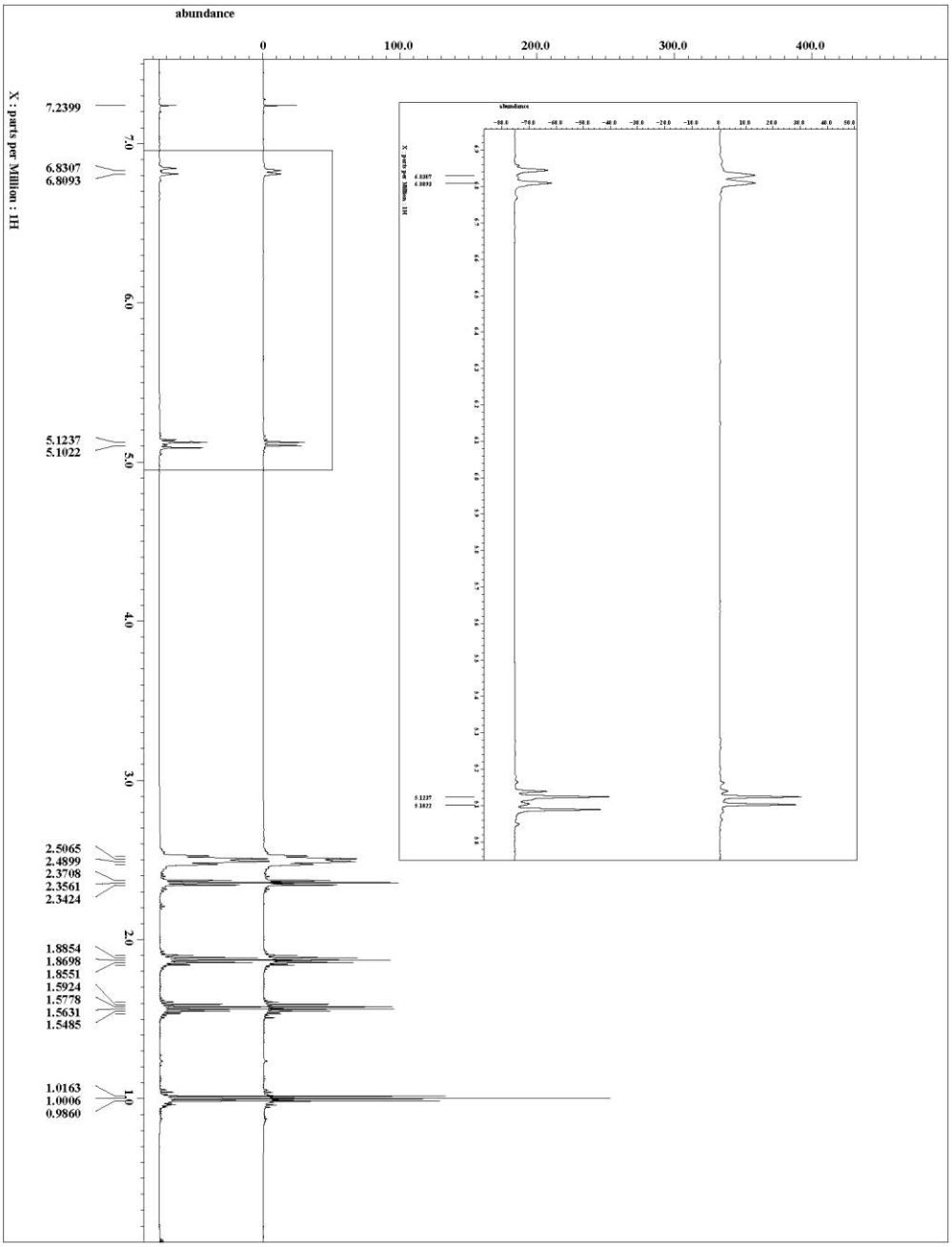

Figure 2-9. ***E*-16-d** (bottom) and ***Z*-16-d** (top) ^{1}H NMR spectra (500 MHz, $CDCl_3$).

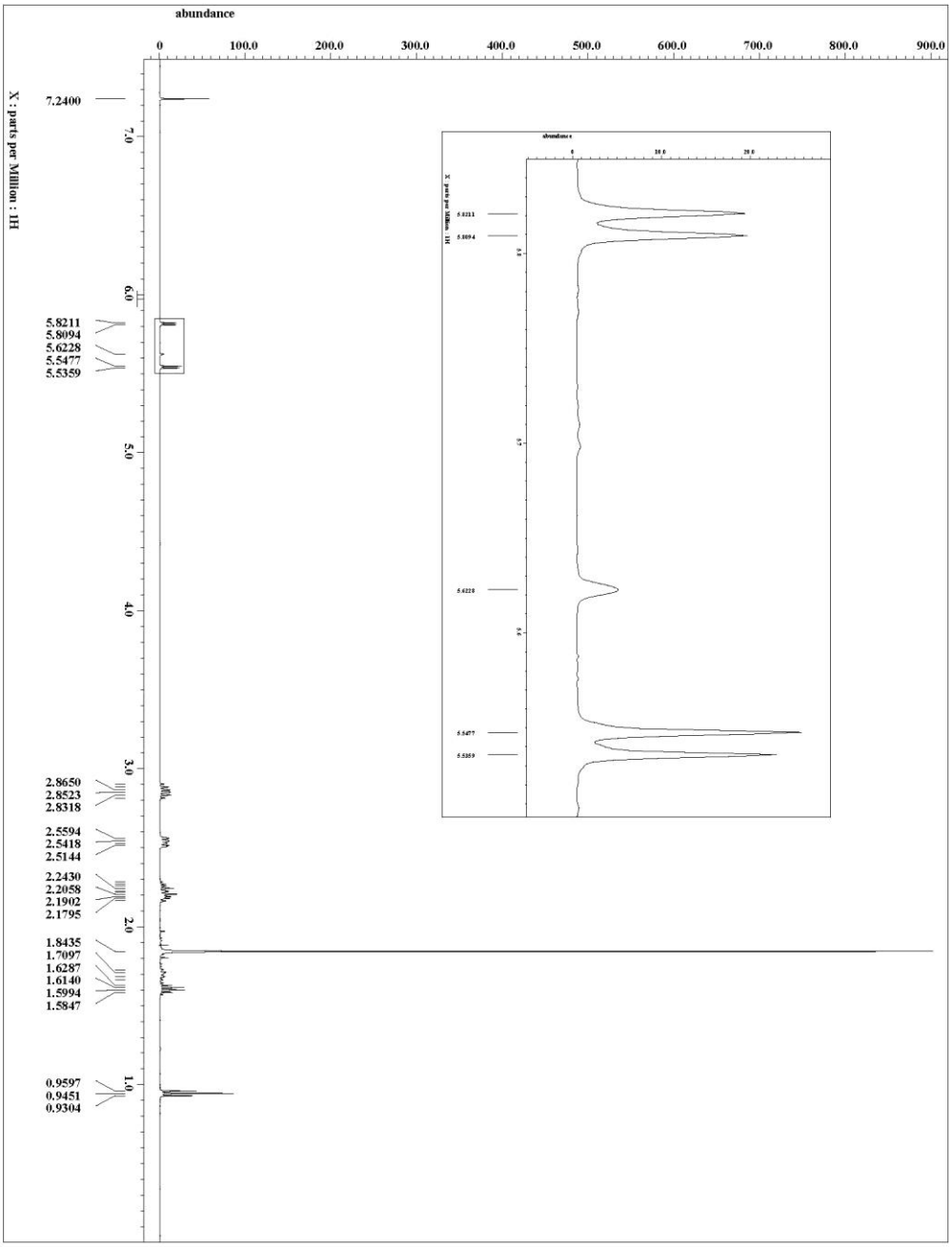

Figure 2-10. 18-4*d* from ***E*-16-d** ^{1}H NMR spectrum (500 MHz, $CDCl_3$).

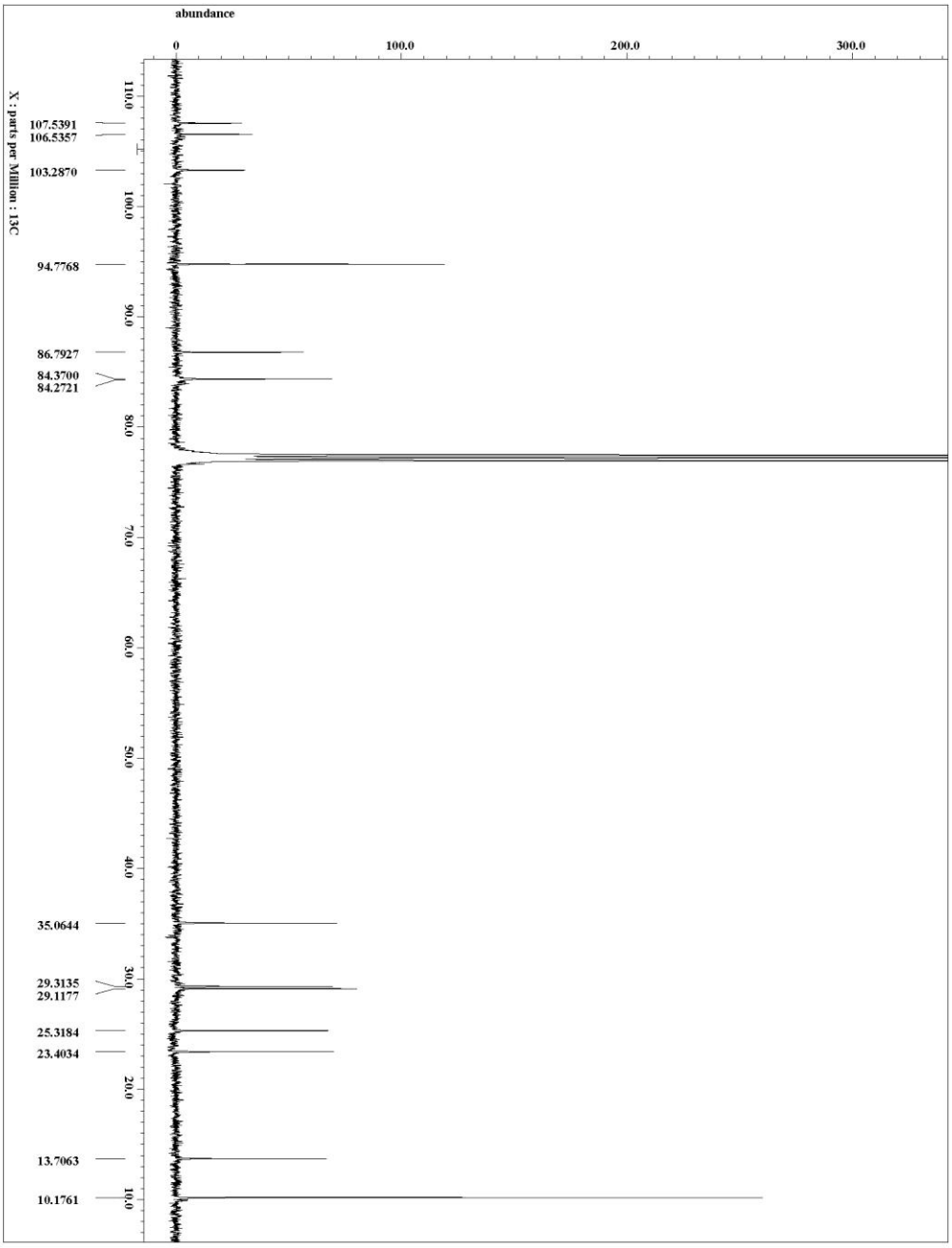

Figure 2-11. 18-4*d* from ***E*-16-d** ^{13}C NMR spectrum (125 MHz, $CDCl_3$).

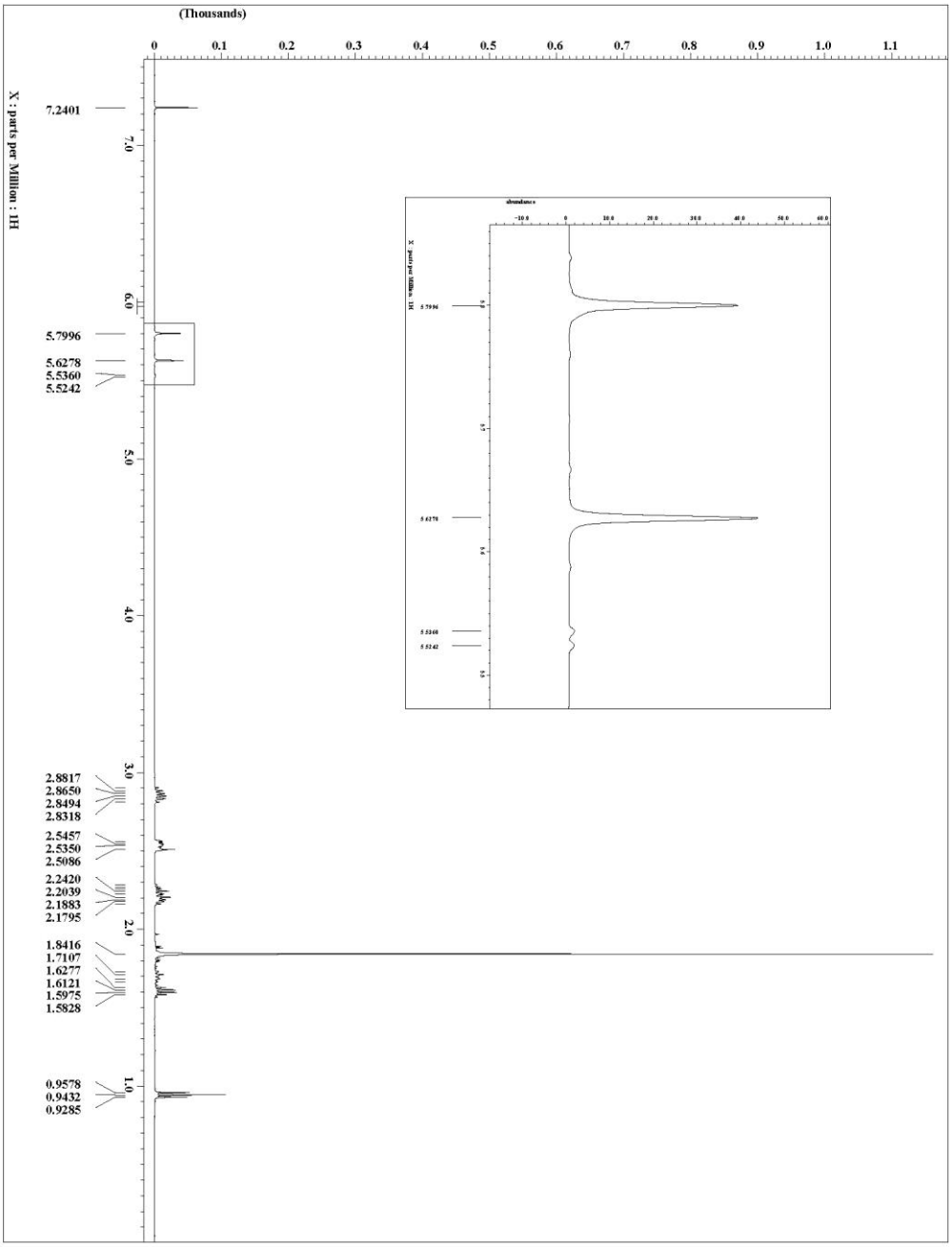

Figure 2-12. 18-6*d* from ***Z*-16-d** ^{1}H NMR spectrum (500 MHz, $CDCl_3$).

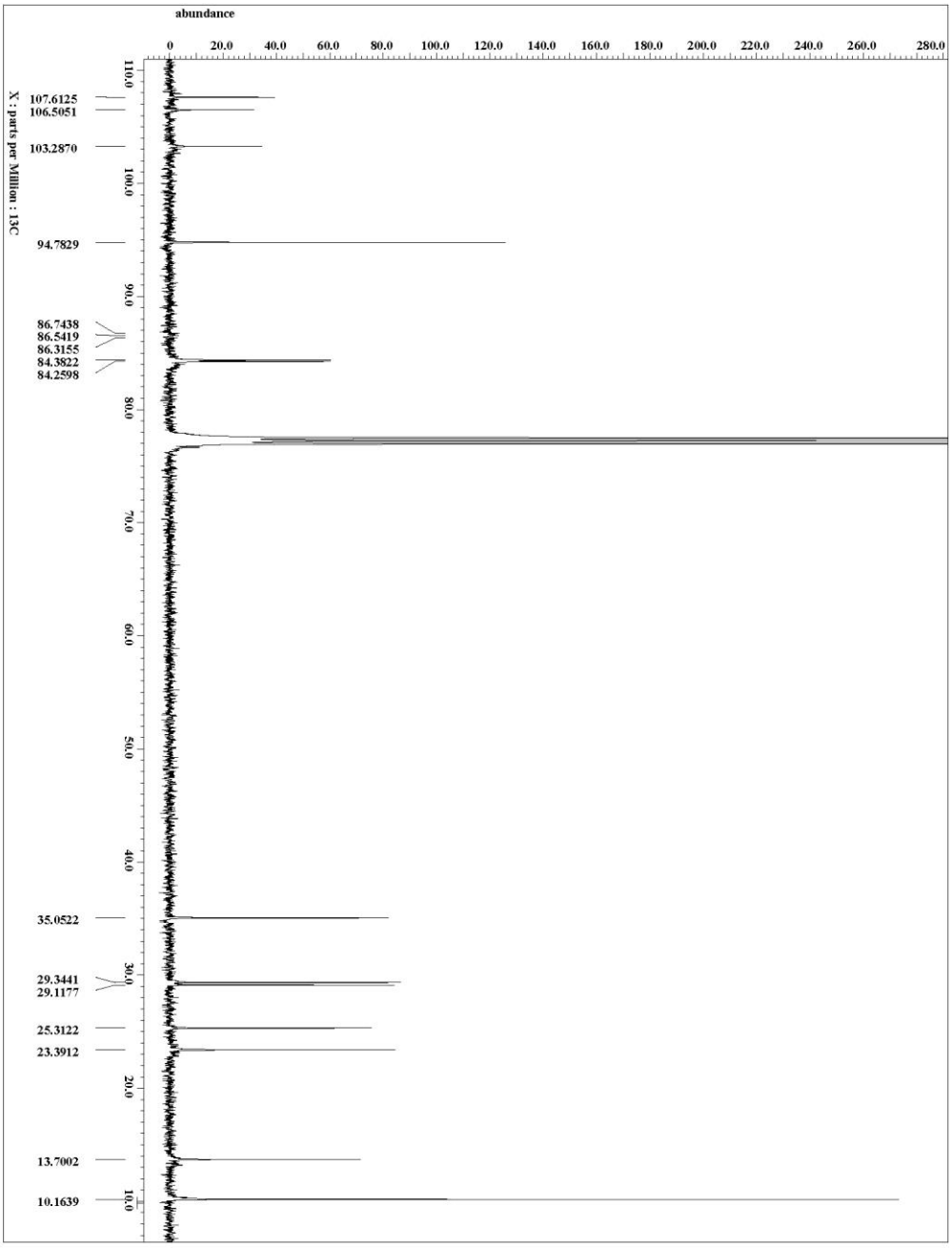

Figure 2-13. 18-6*d* from ***Z*-16-d** ^{13}C NMR spectrum (125 MHz, $CDCl_3$).

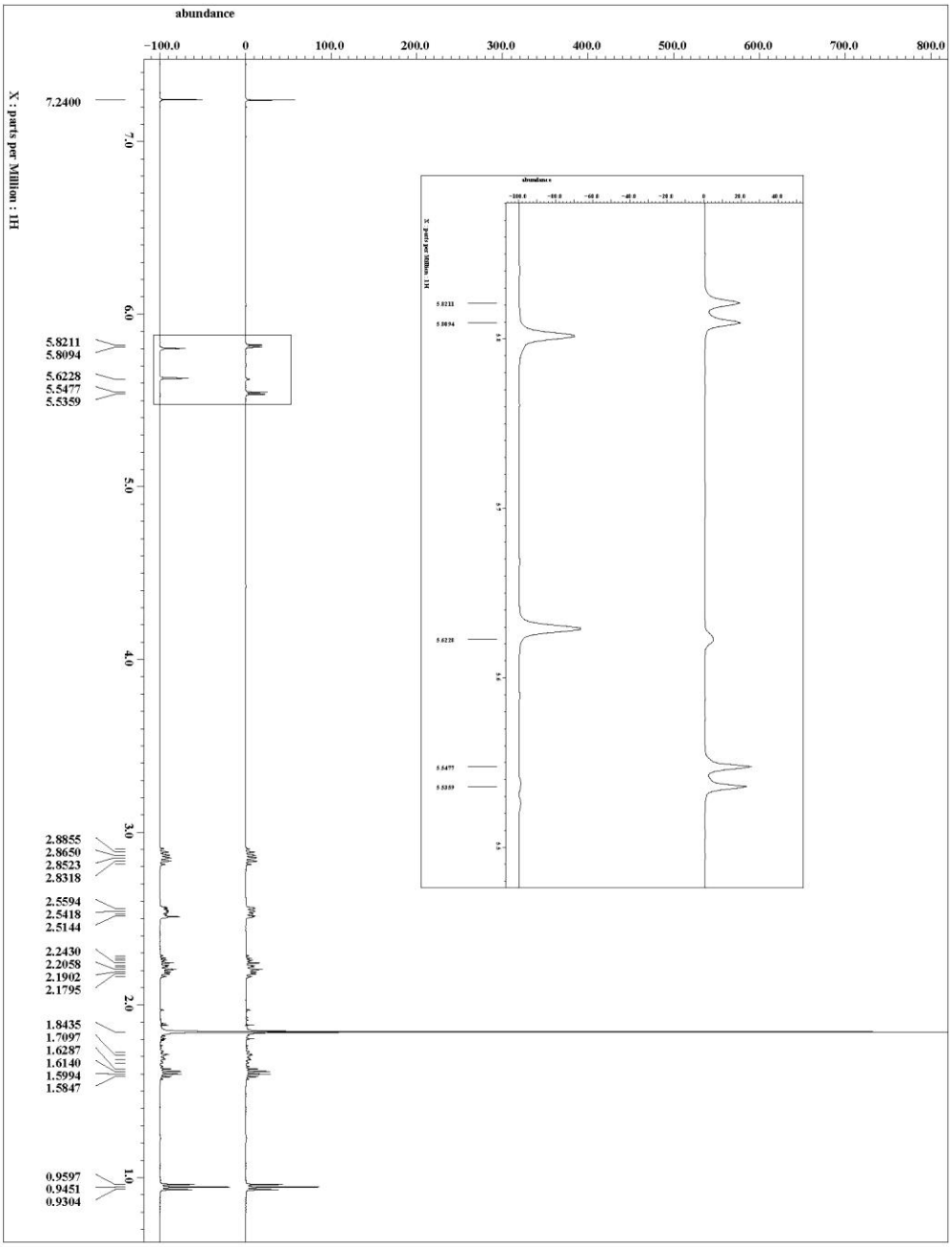

Figure 2-14. 18 from ***Z*-16-d** (bottom) and ***E*-16-d** (top) ^{1}H NMR spectra (500 MHz, $CDCl_3$).

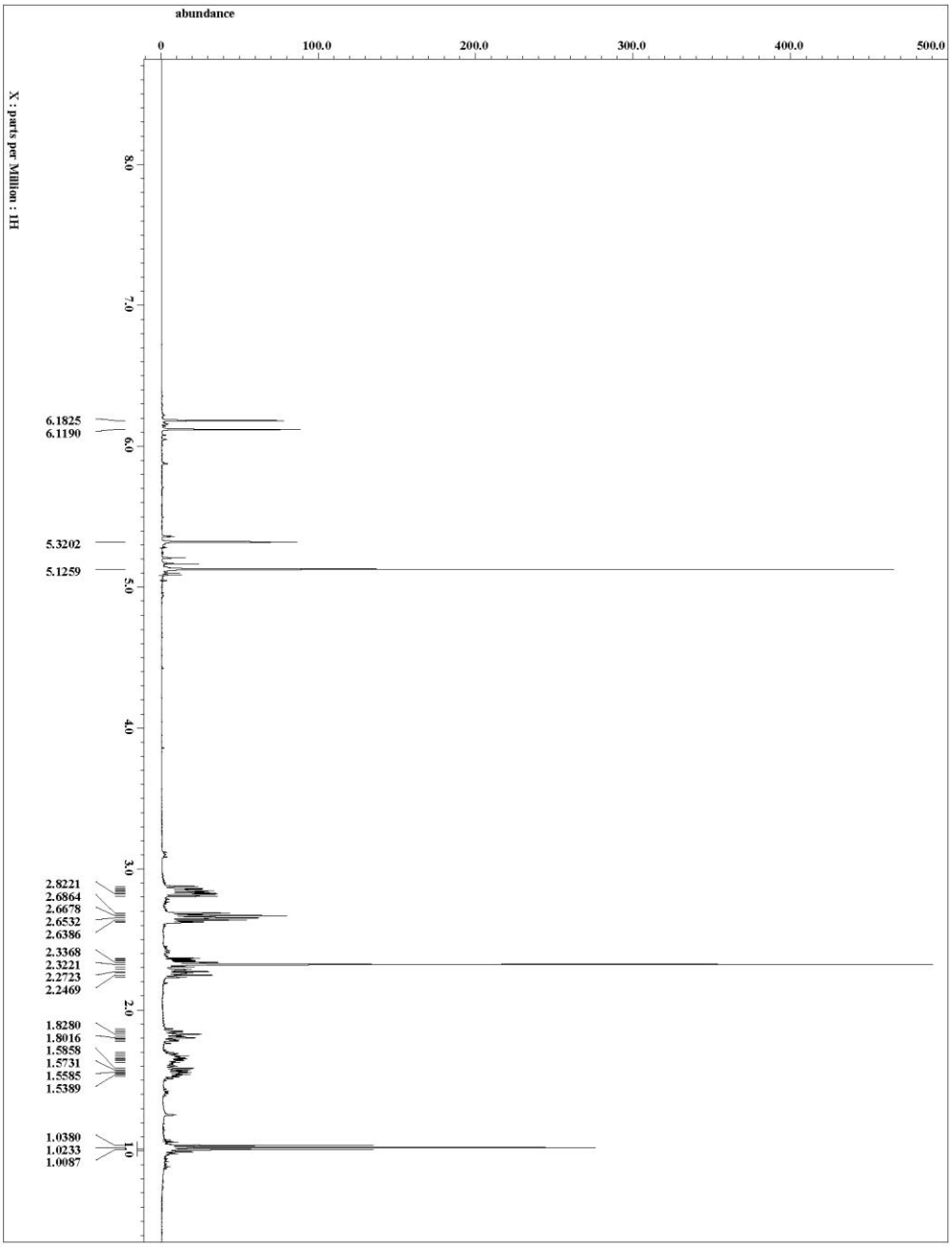

Figure 2-15. 24 ^{1}H NMR spectrum (500 MHz, CD_2Cl_2).

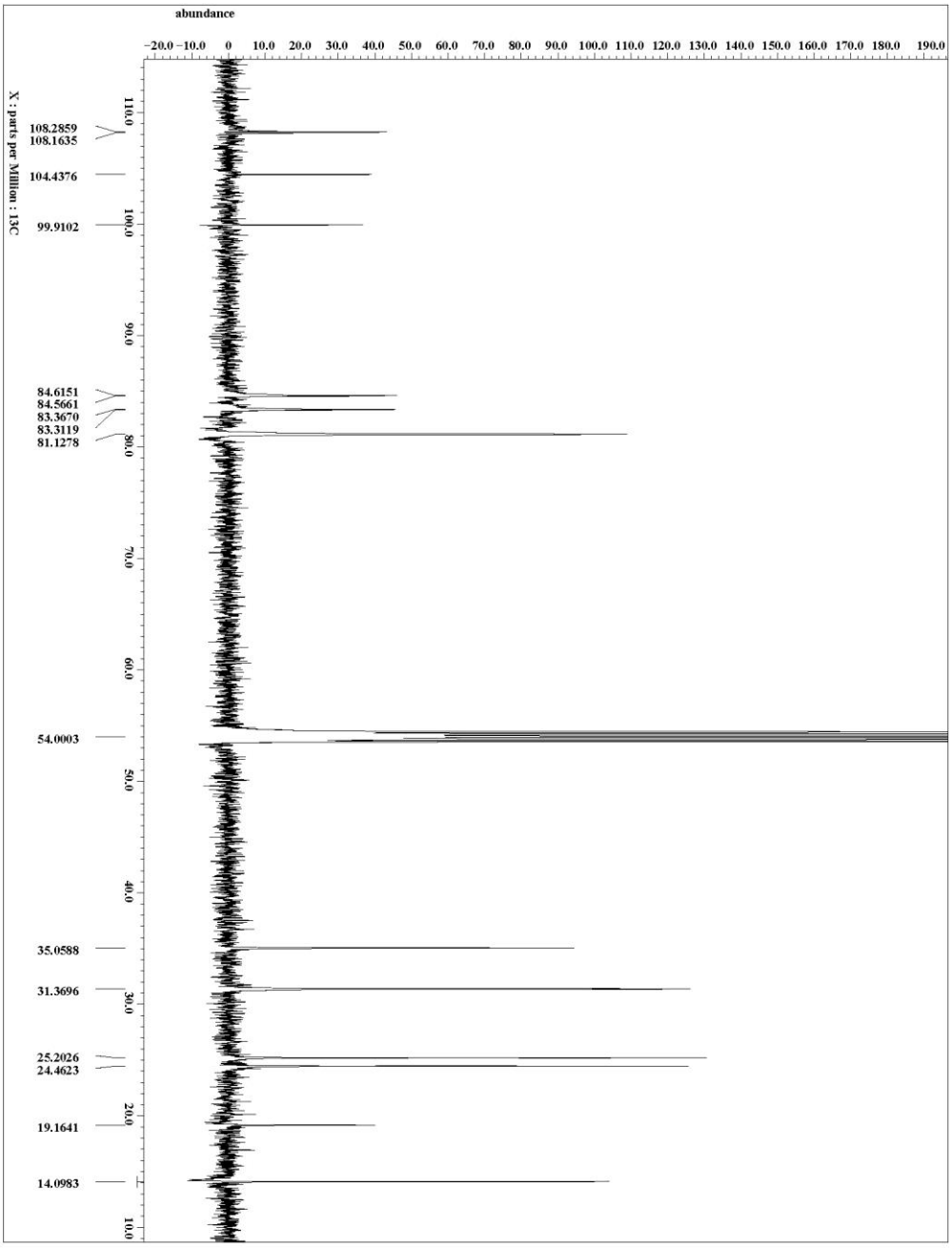

Figure 2-16. 24 ^{13}C NMR spectrum (125 MHz, CD_2Cl_2).

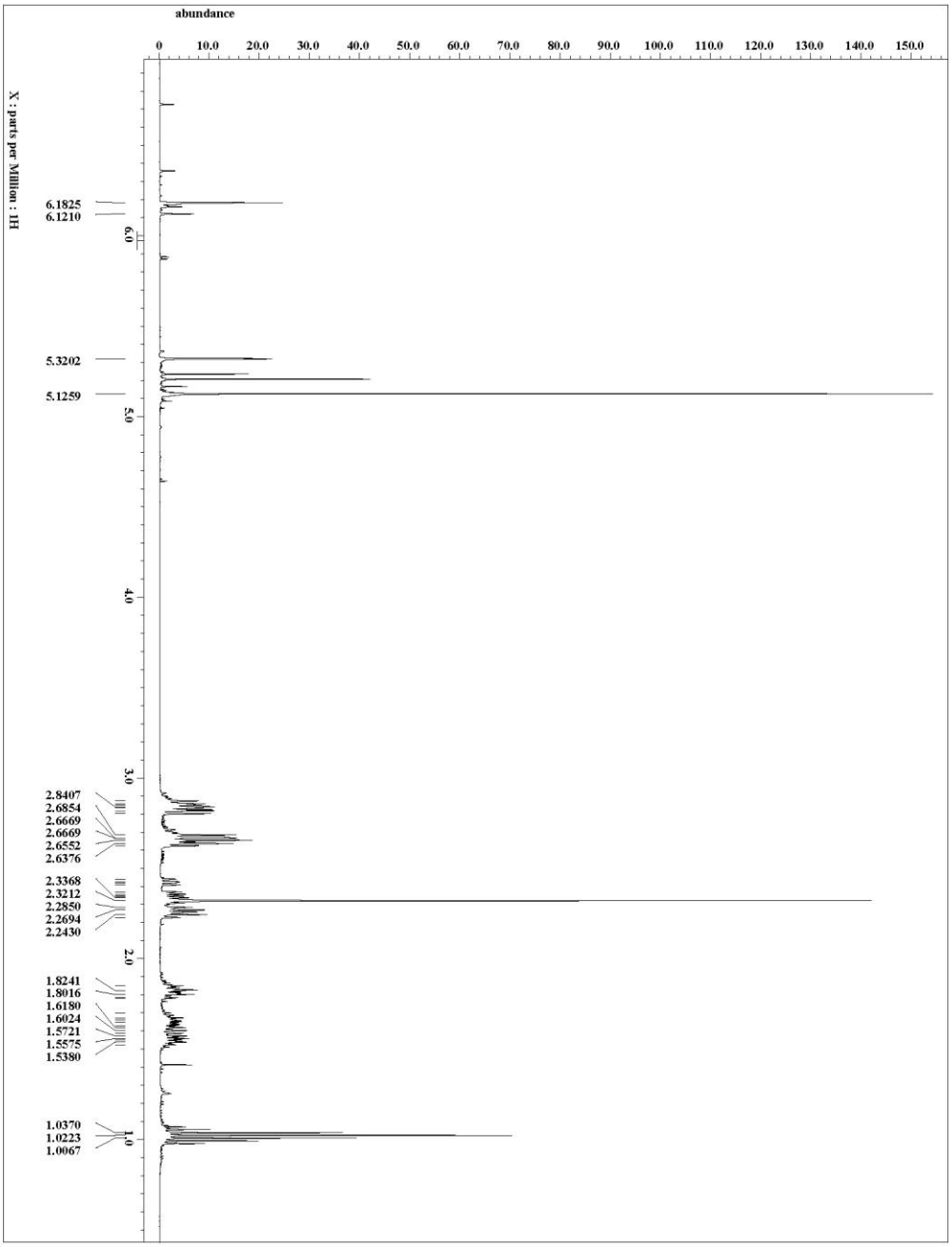

Figure 2-17. 24-*d* ^{1}H NMR spectrum (500 MHz, CD_2Cl_2).

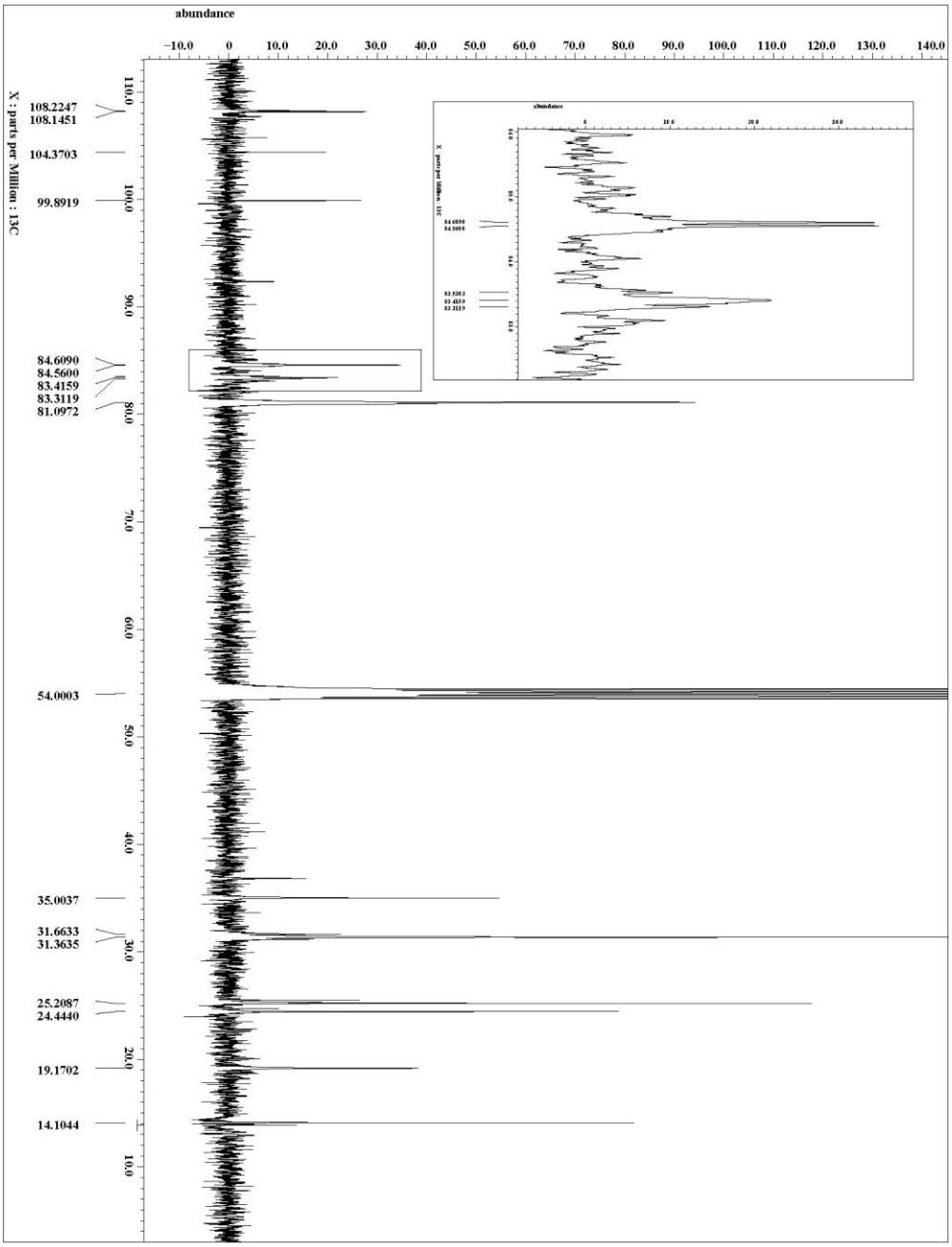

Figure 2-18. 24-*d* ^{13}C NMR spectrum (125 MHz, CD_2Cl_2).

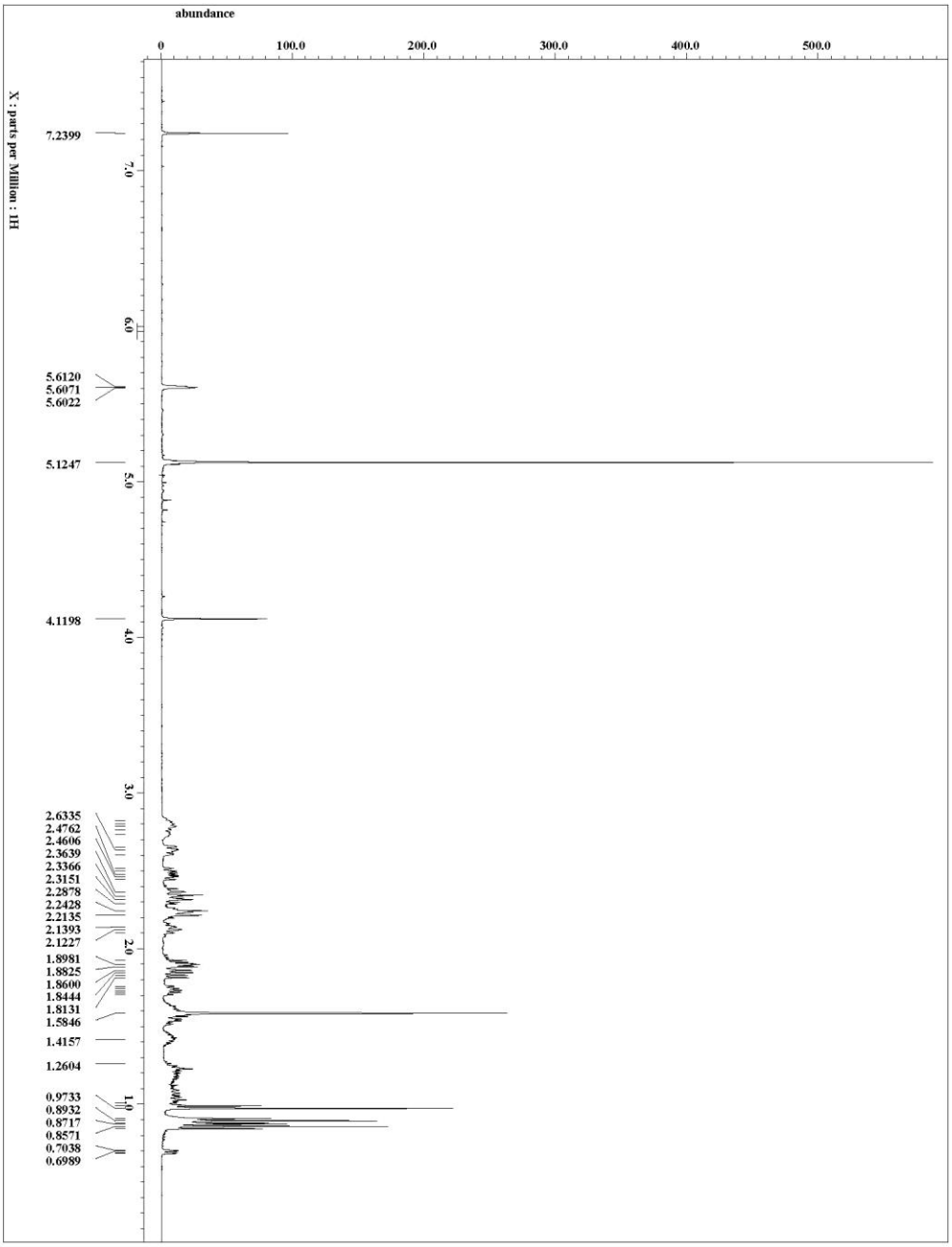

Figure 2-19. 25 ^{1}H NMR spectrum (500 MHz, $CDCl_3$).

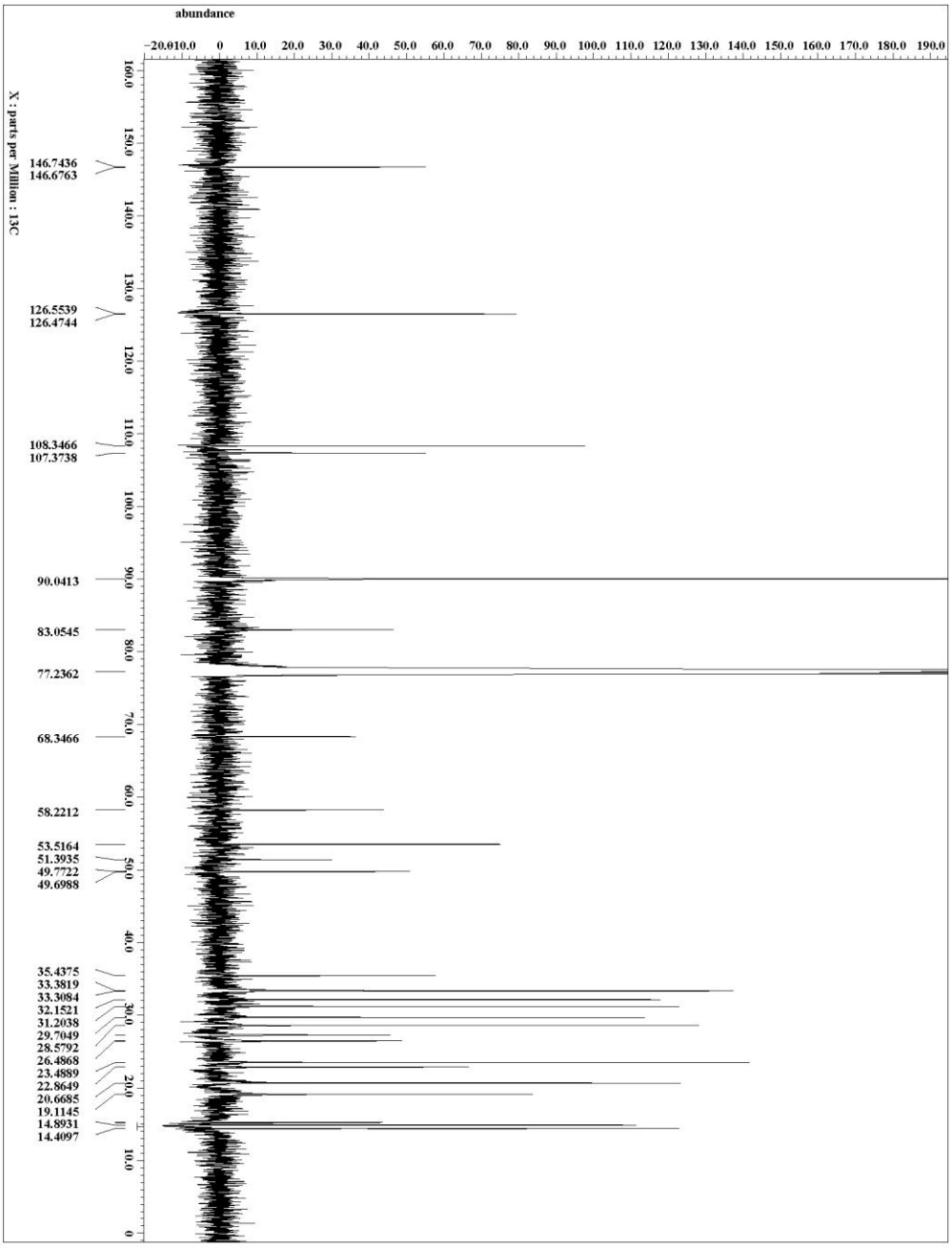

Figure 2-20. 25 ^{13}C NMR spectrum (125 MHz, $CDCl_3$).

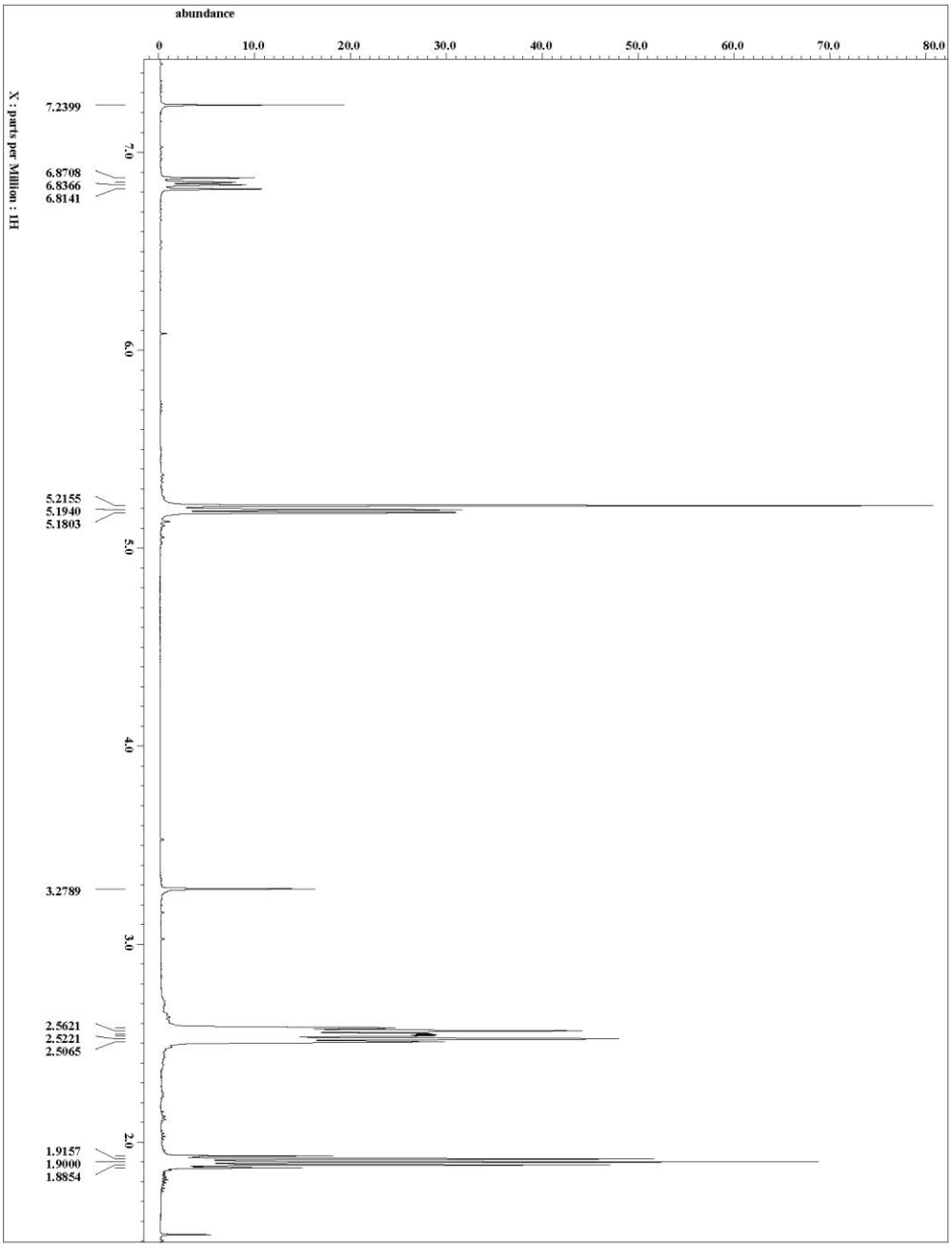

Figure 2-21. 28 ^{1}H NMR spectrum (500 MHz, $CDCl_3$).

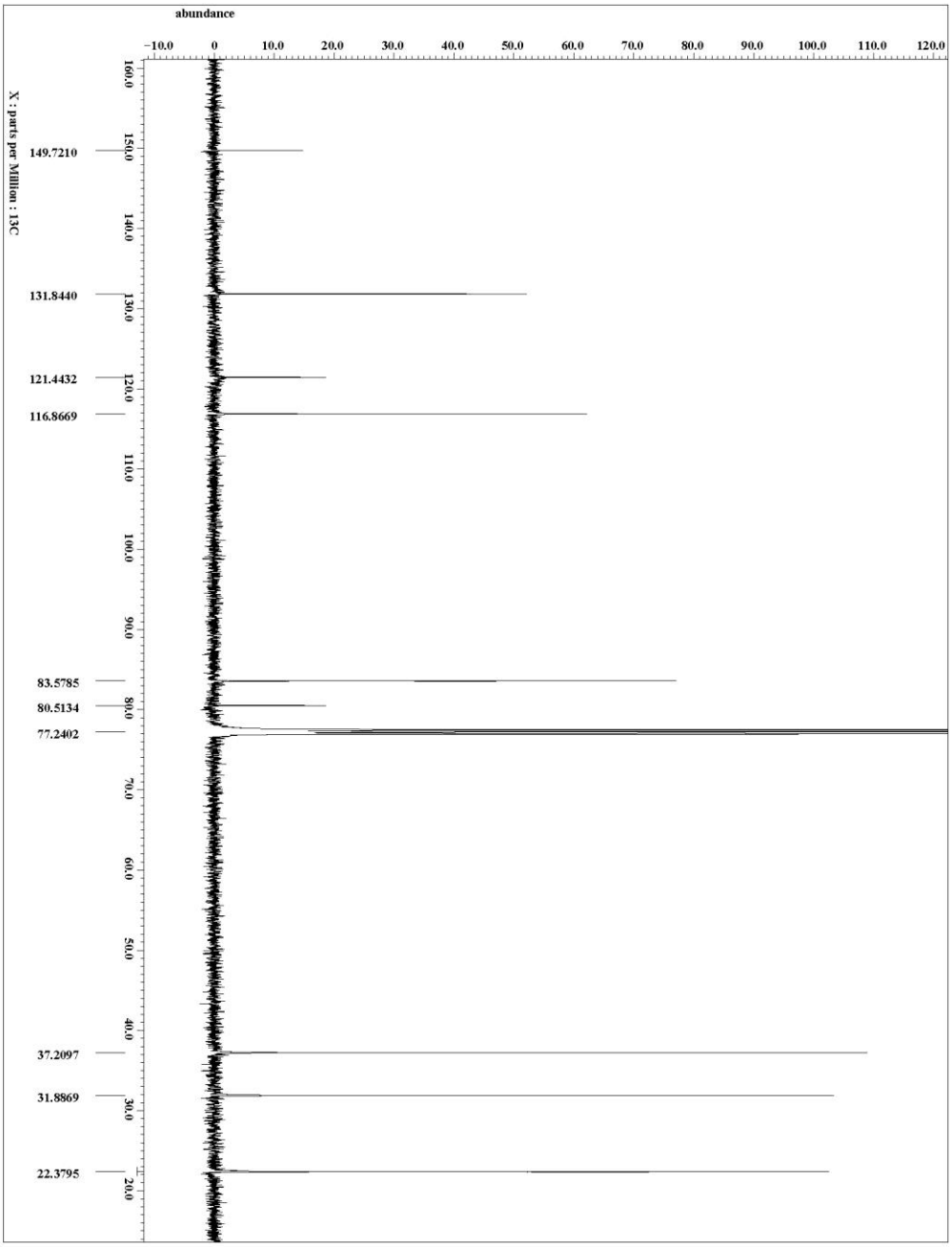

Figure 2-22. 28 ^{13}C NMR spectrum (125 MHz, $CDCl_3$).

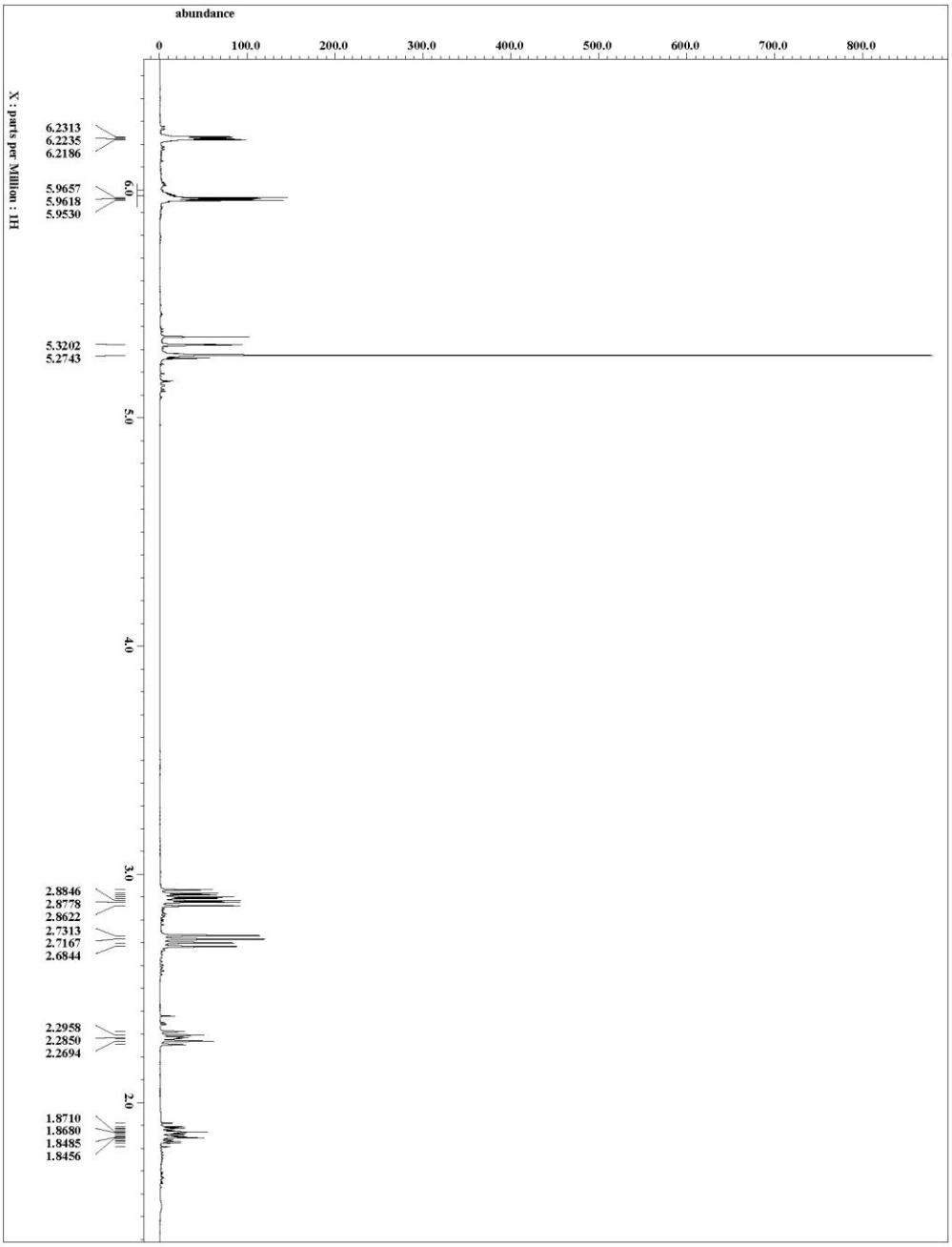

Figure 2-23. 29 ^{1}H NMR spectrum (500 MHz, CD_2Cl_2).

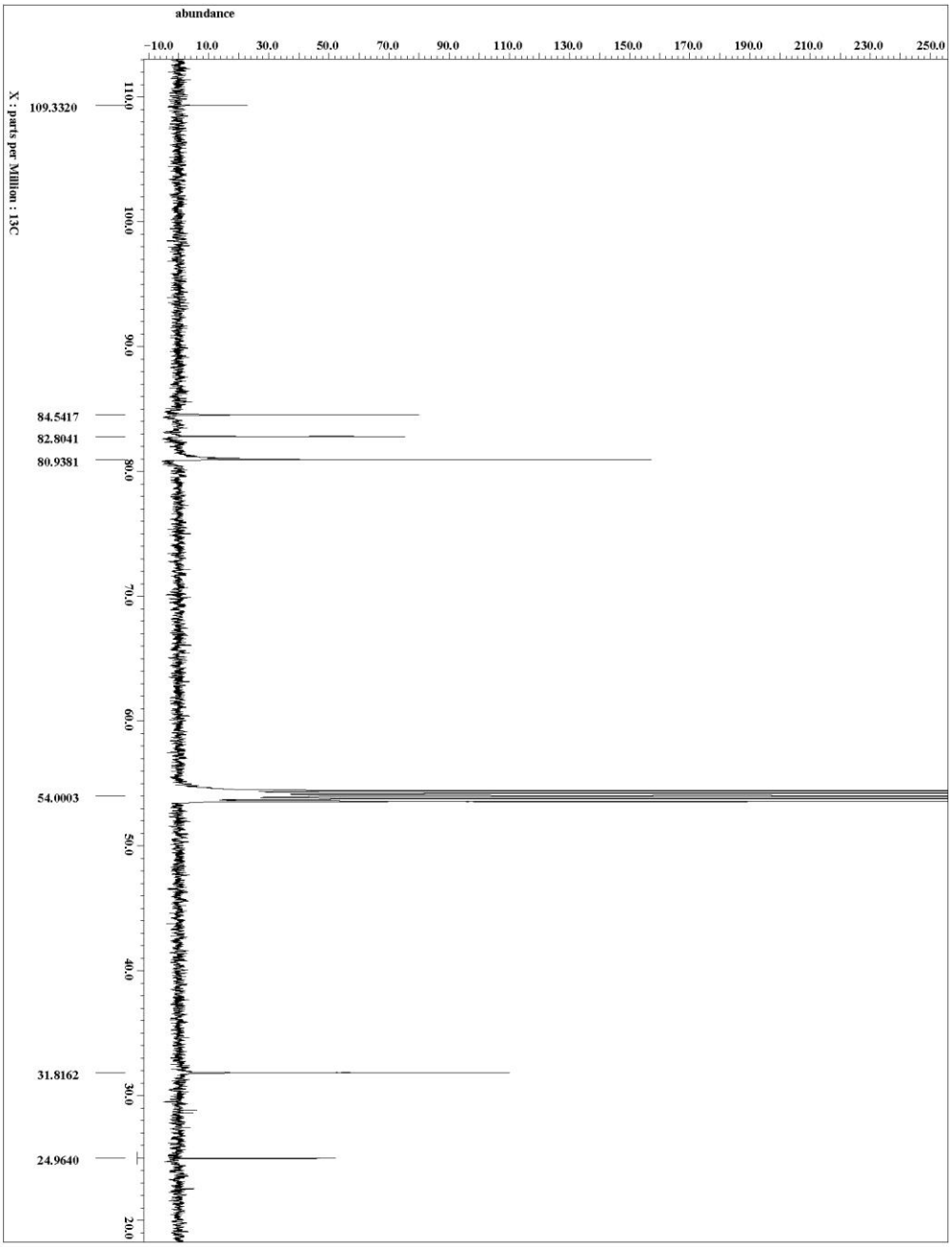

Figure 2-24. 29 ^{13}C NMR spectrum (125 MHz, CD_2Cl_2).

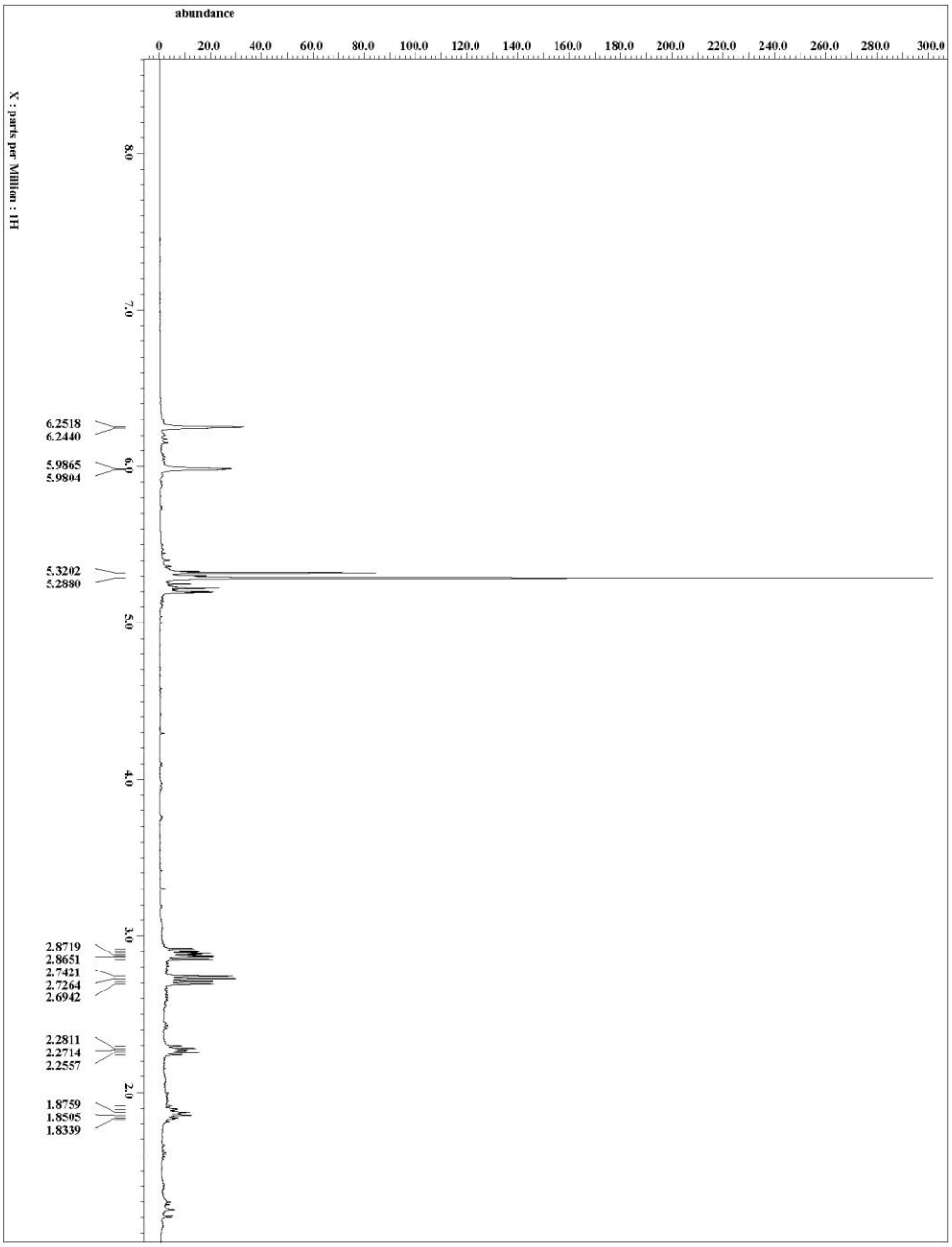

Figure 2-25. 29-*d* ^{1}H NMR spectrum (500 MHz, CD_2Cl_2).

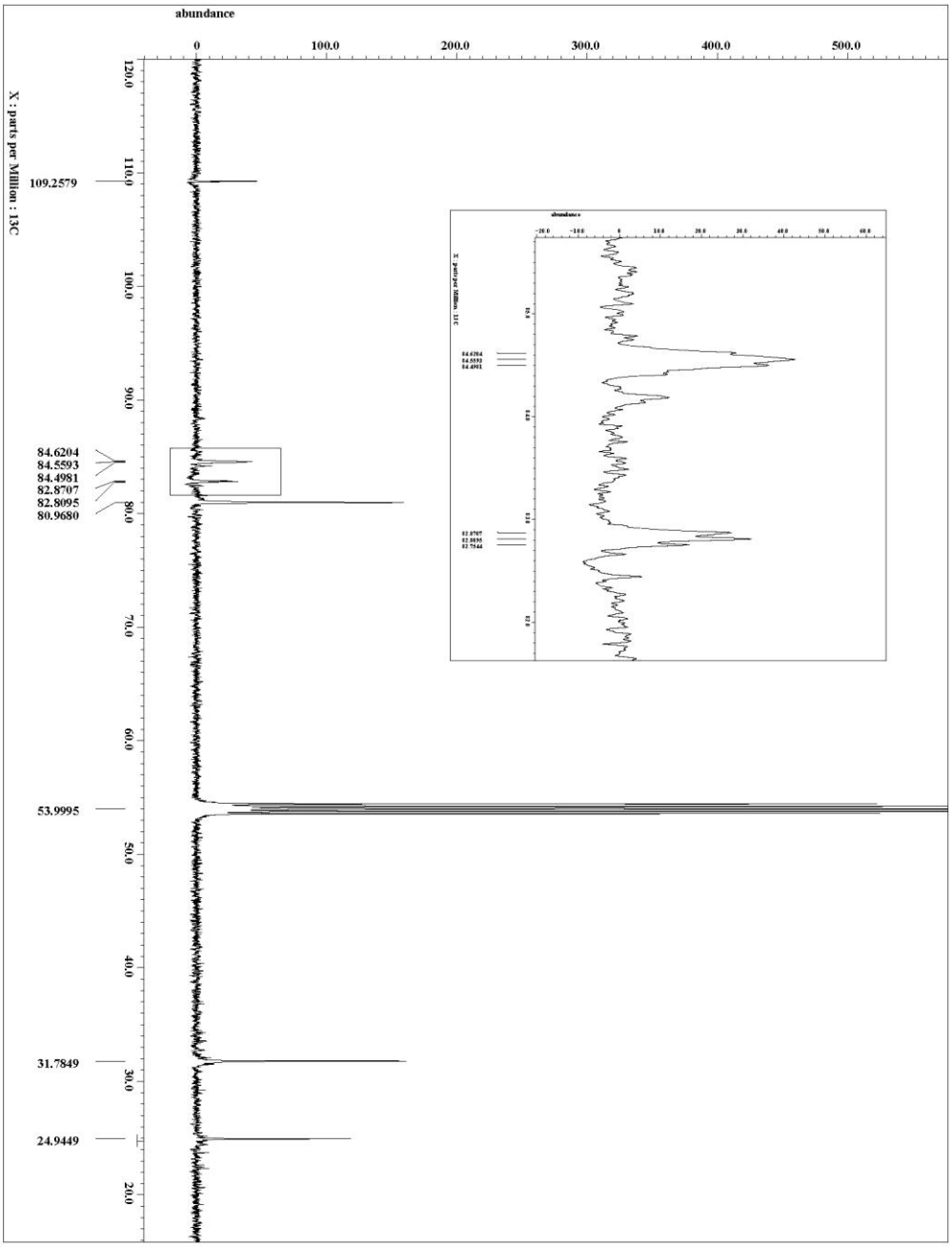

Figure 2-26. 29-*d* ^{13}C NMR spectrum (125 MHz, CD_2Cl_2).

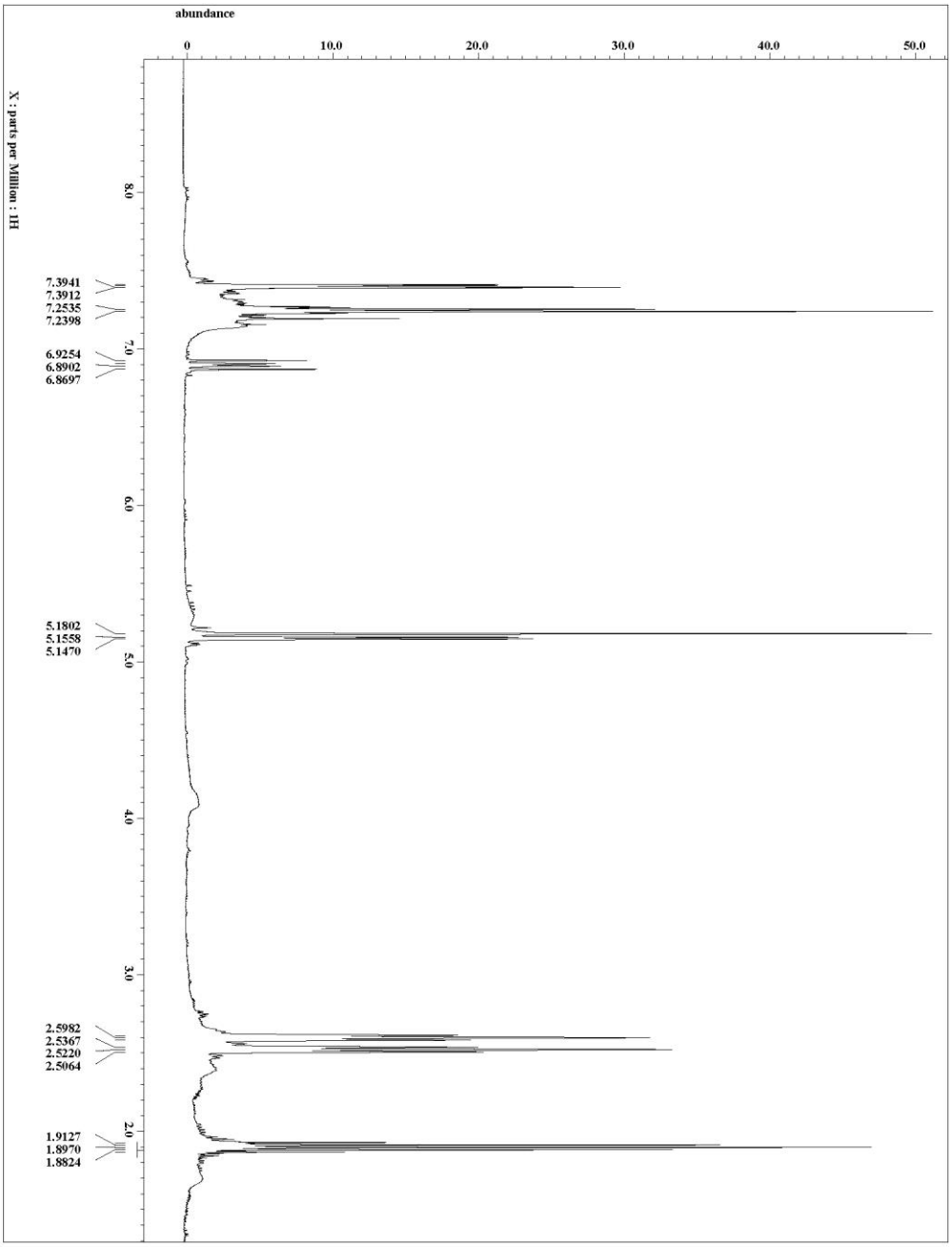

Figure 2-27. 35 ^{1}H NMR spectrum (500 MHz, $CDCl_3$).

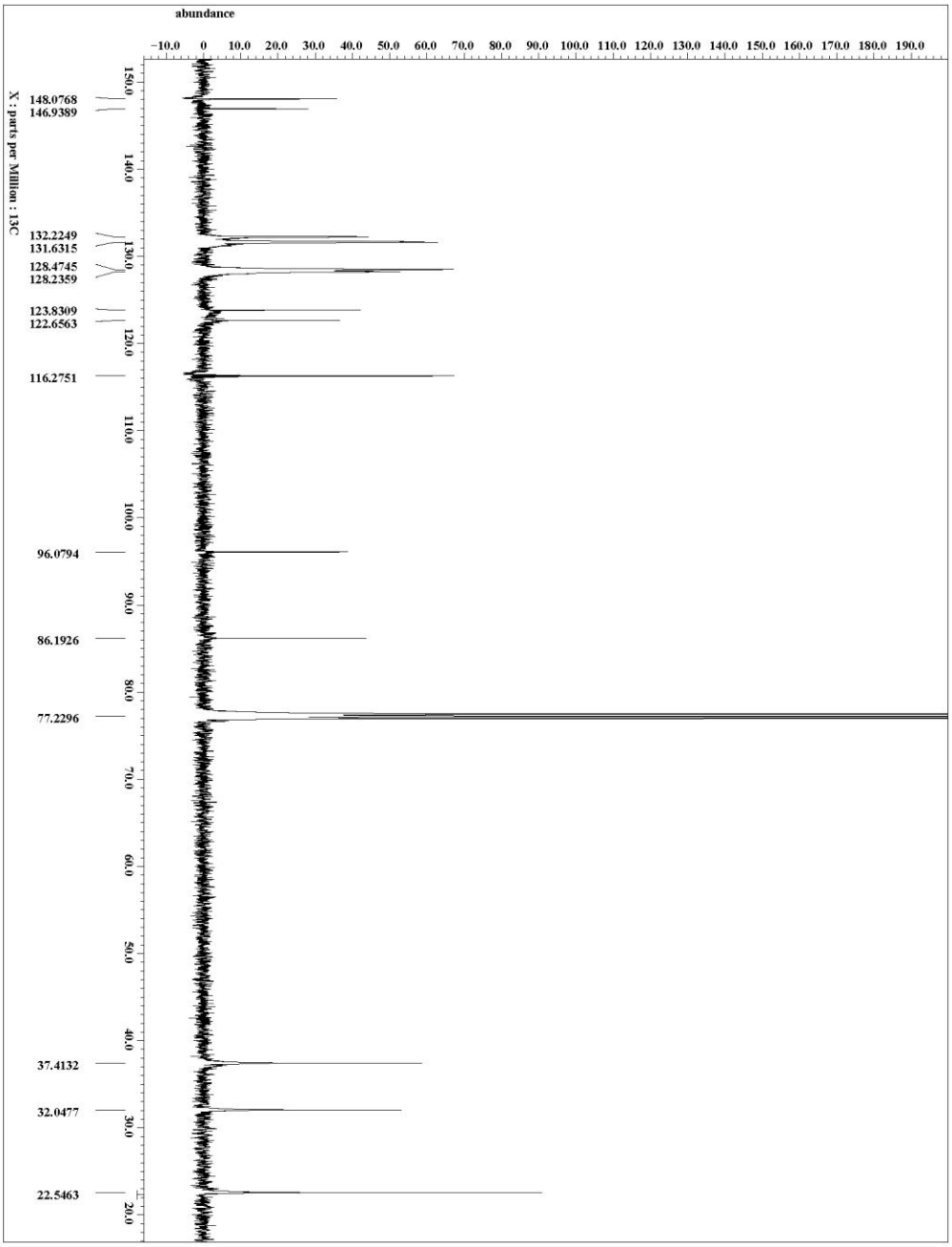

Figure 2-28. 35 ^{13}C NMR spectrum (125 MHz, $CDCl_3$).

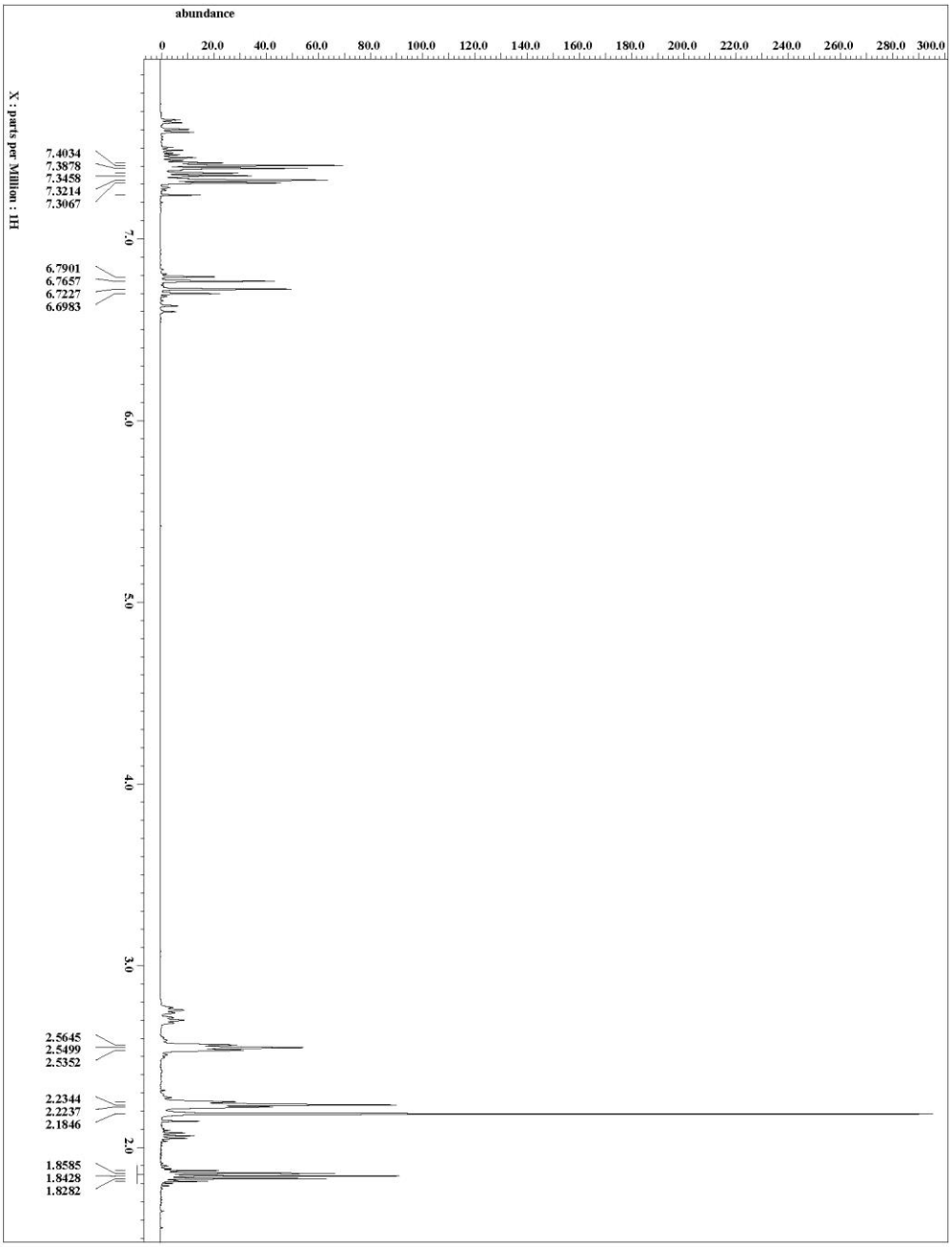

Figure 2-29. 38-*Z* ^{1}H NMR spectrum (500 MHz, $CDCl_3$).

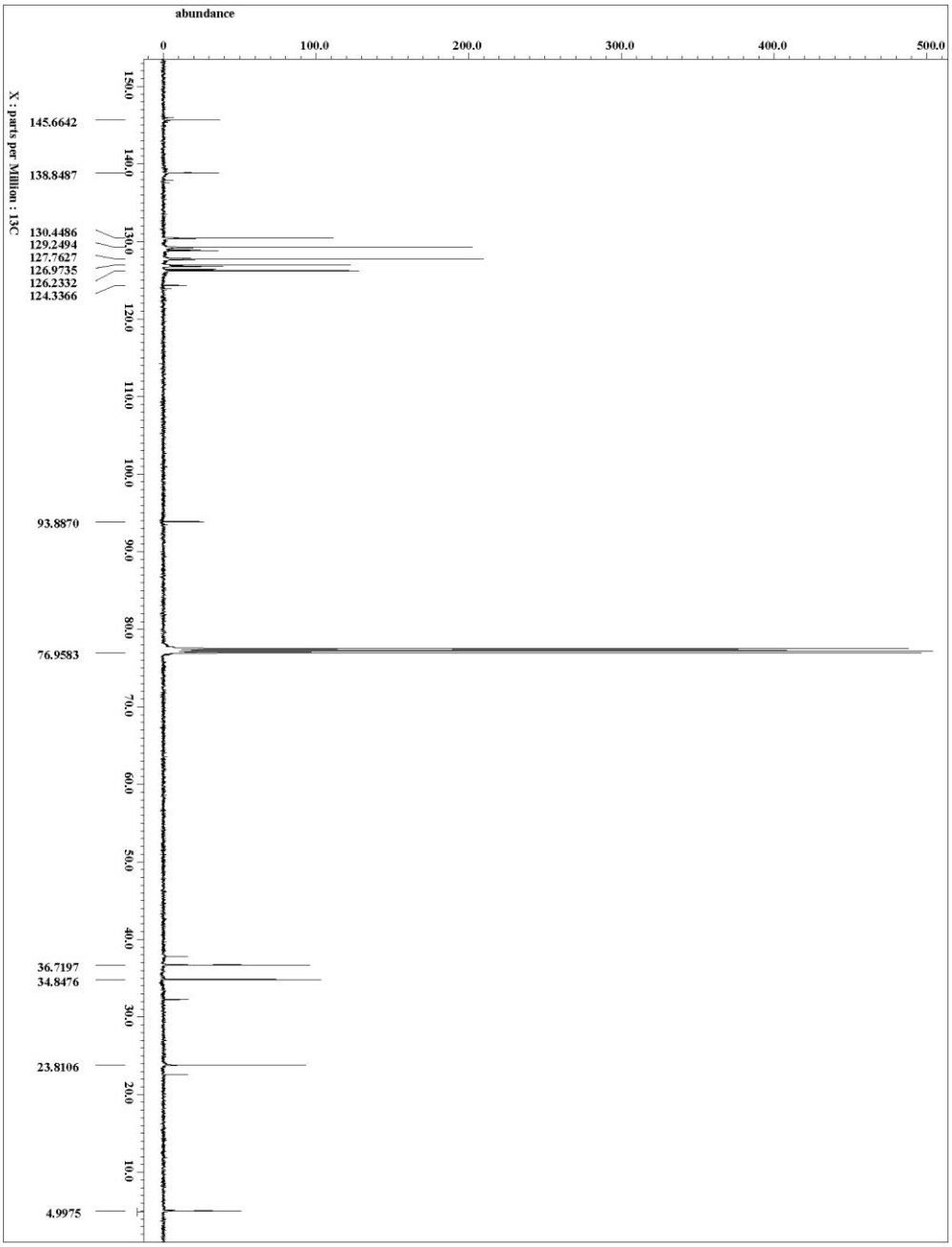

Figure 2-30. 38-*Z* ^{13}C NMR spectrum (125 MHz, $CDCl_3$).

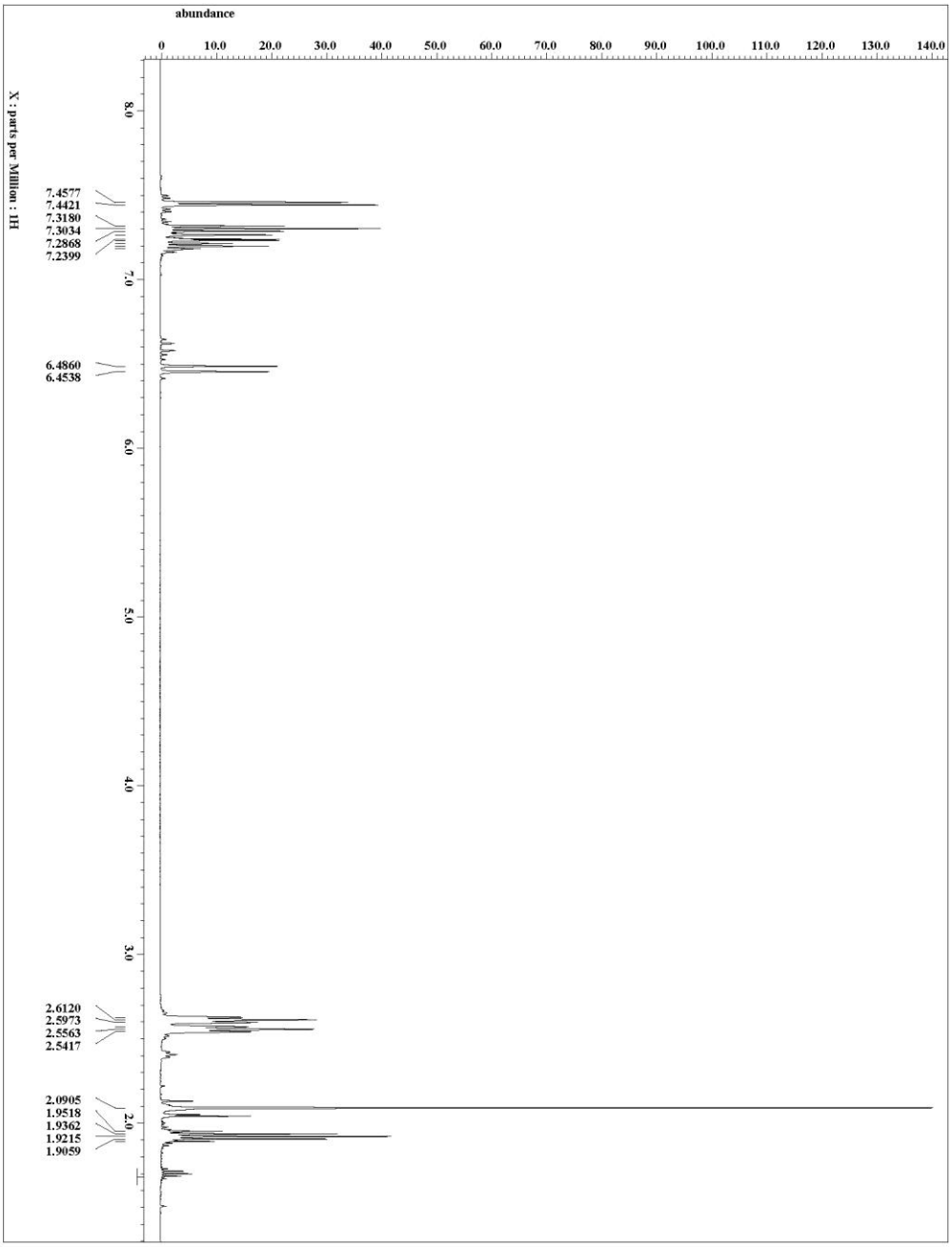

Figure 2-31. 38-*E* ^{1}H NMR spectrum (500 MHz, $CDCl_3$).

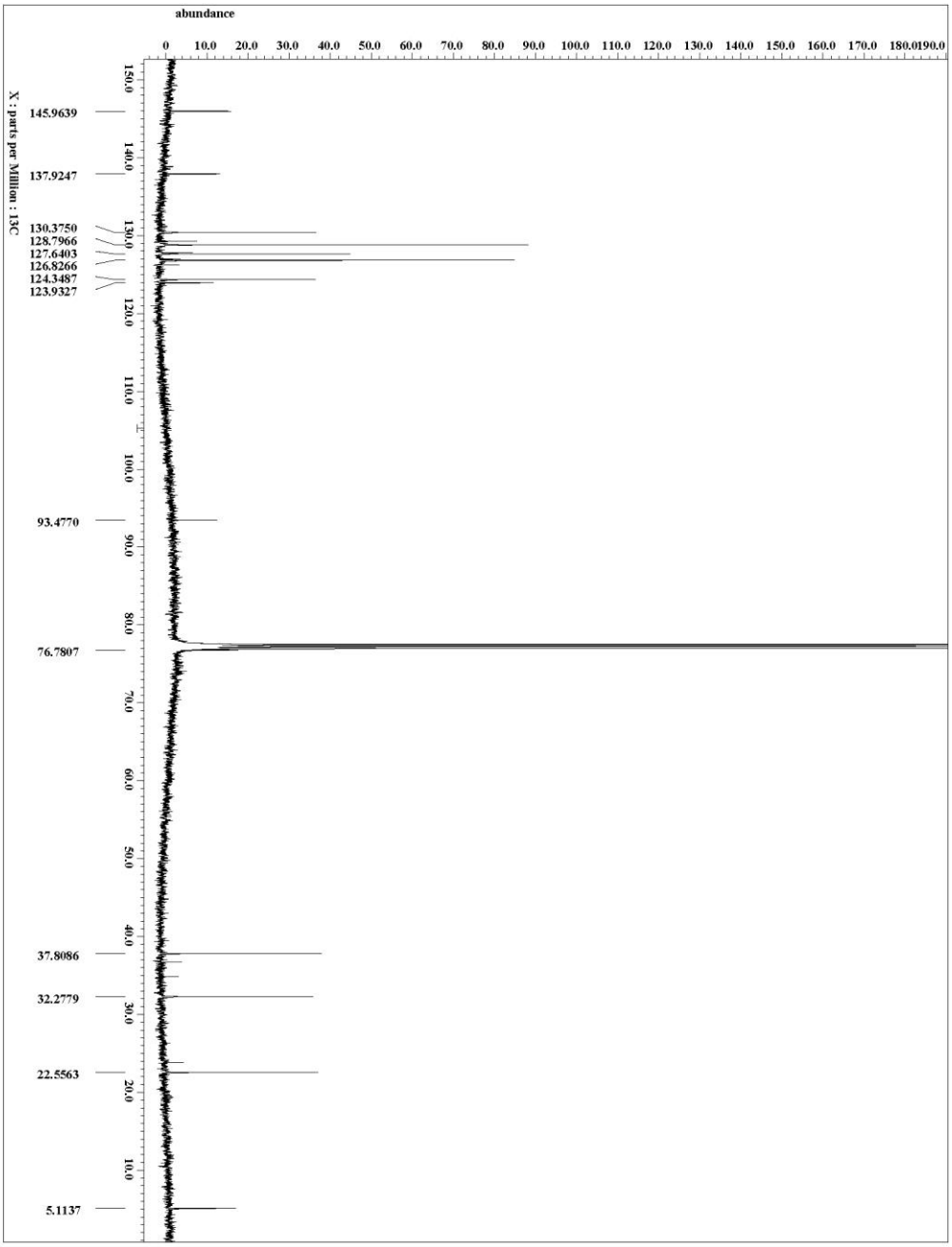

Figure 2-32. 38-*E* ^{13}C NMR spectrum (125 MHz, $CDCl_3$).

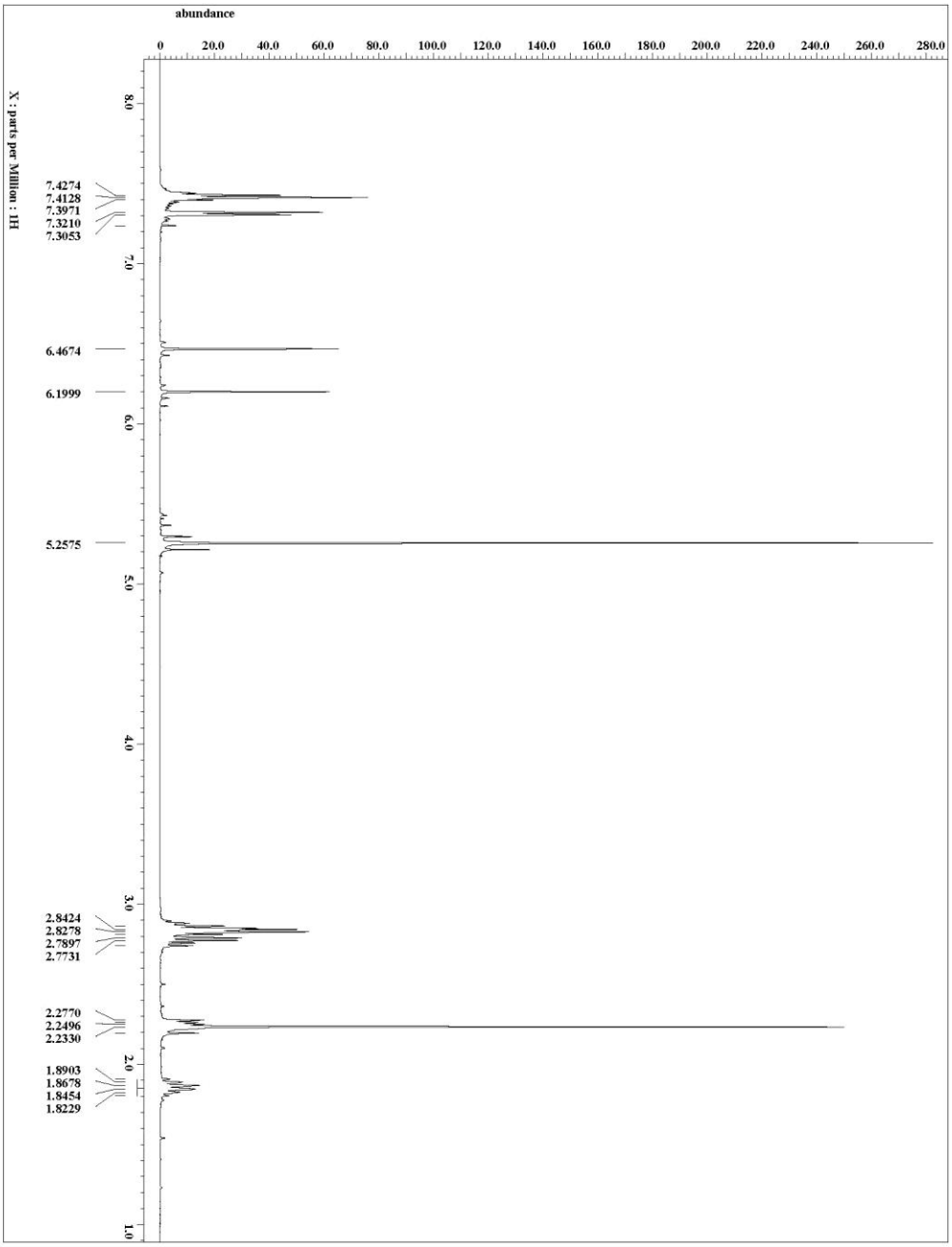

Figure 2-33. 41 ^{1}H NMR spectrum (500 MHz, $CDCl_3$).

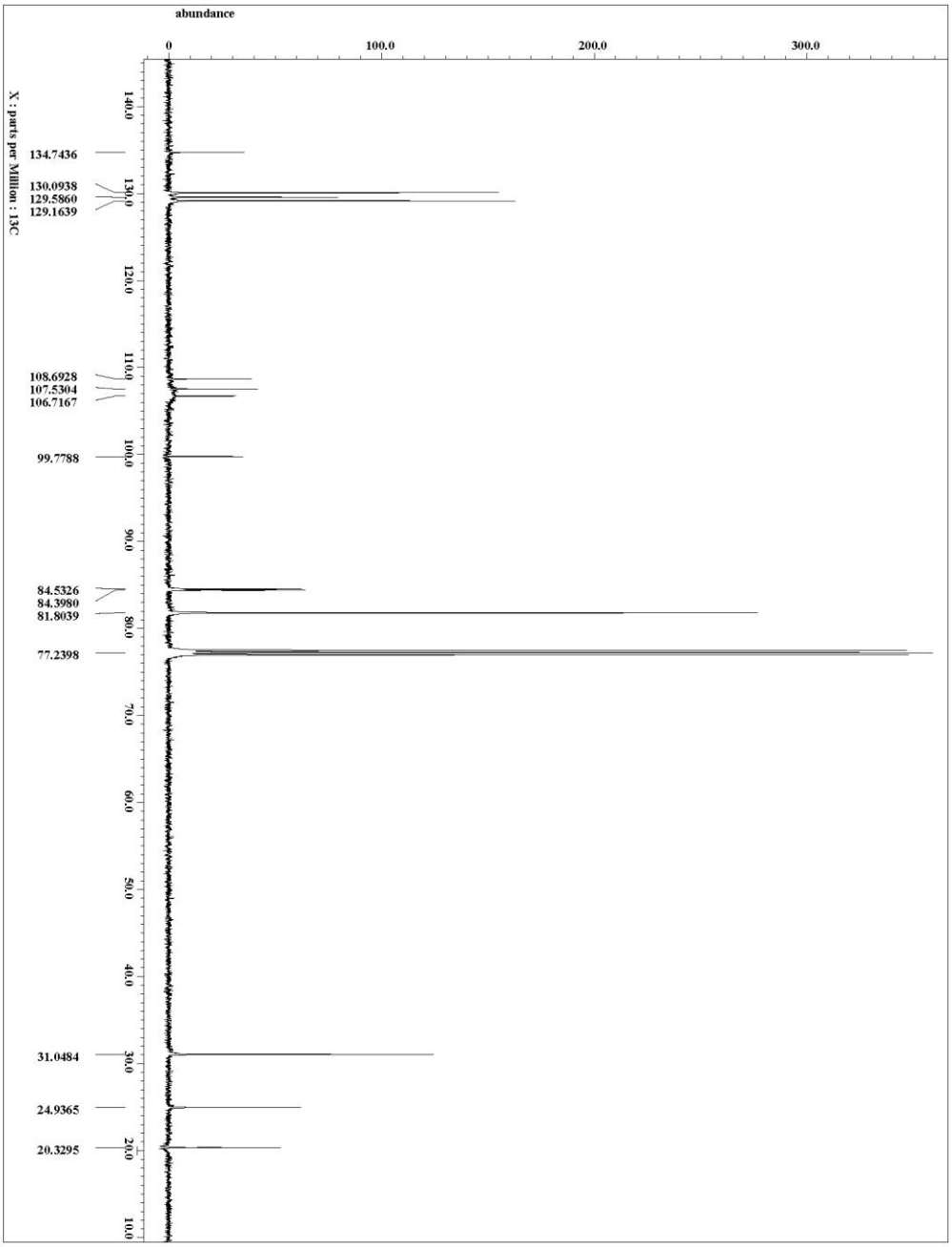

Figure 2-34. 41 ^{13}C NMR spectrum (125 MHz, $CDCl_3$).

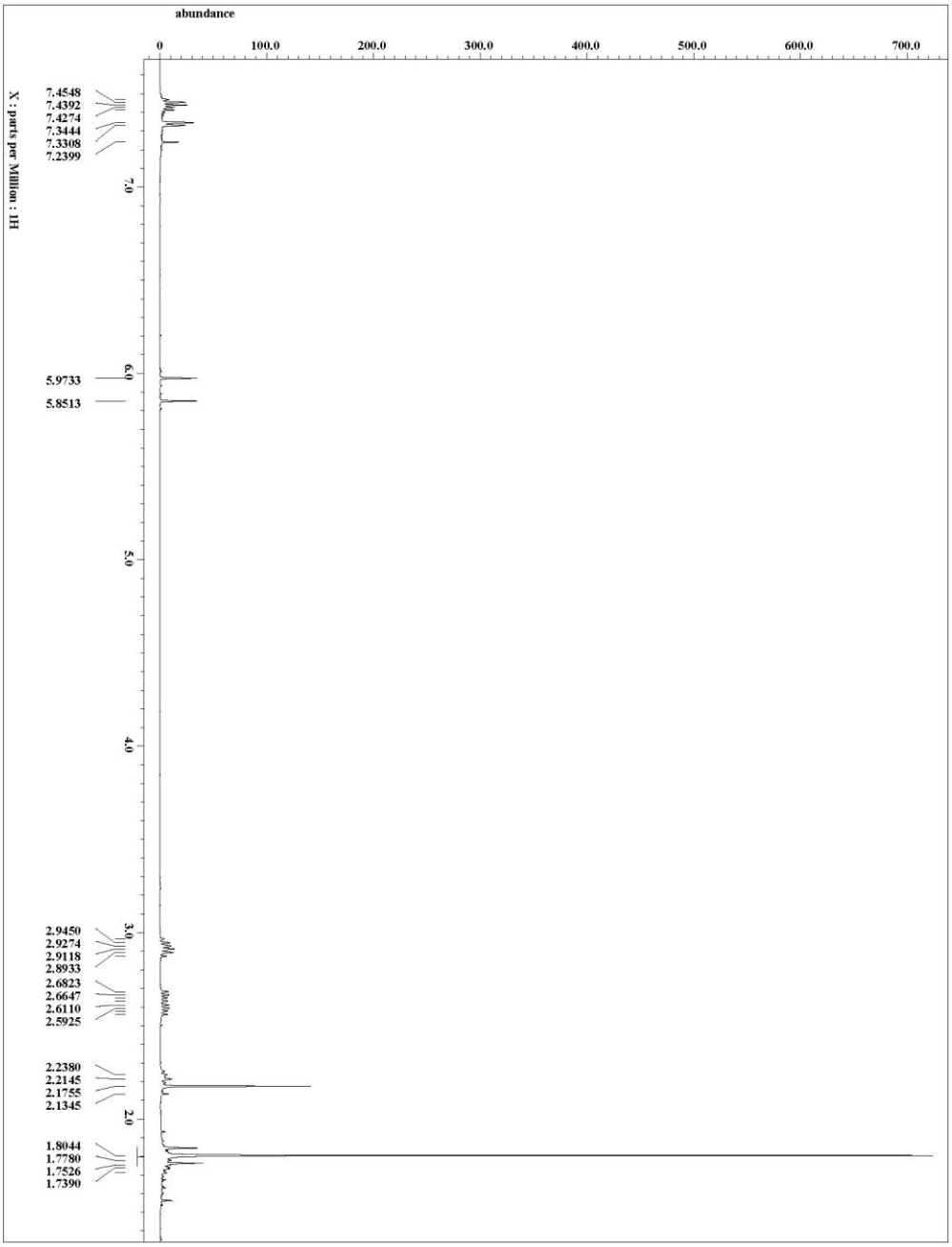

Figure 2-35. 42 ^{1}H NMR spectrum (500 MHz, $CDCl_3$).

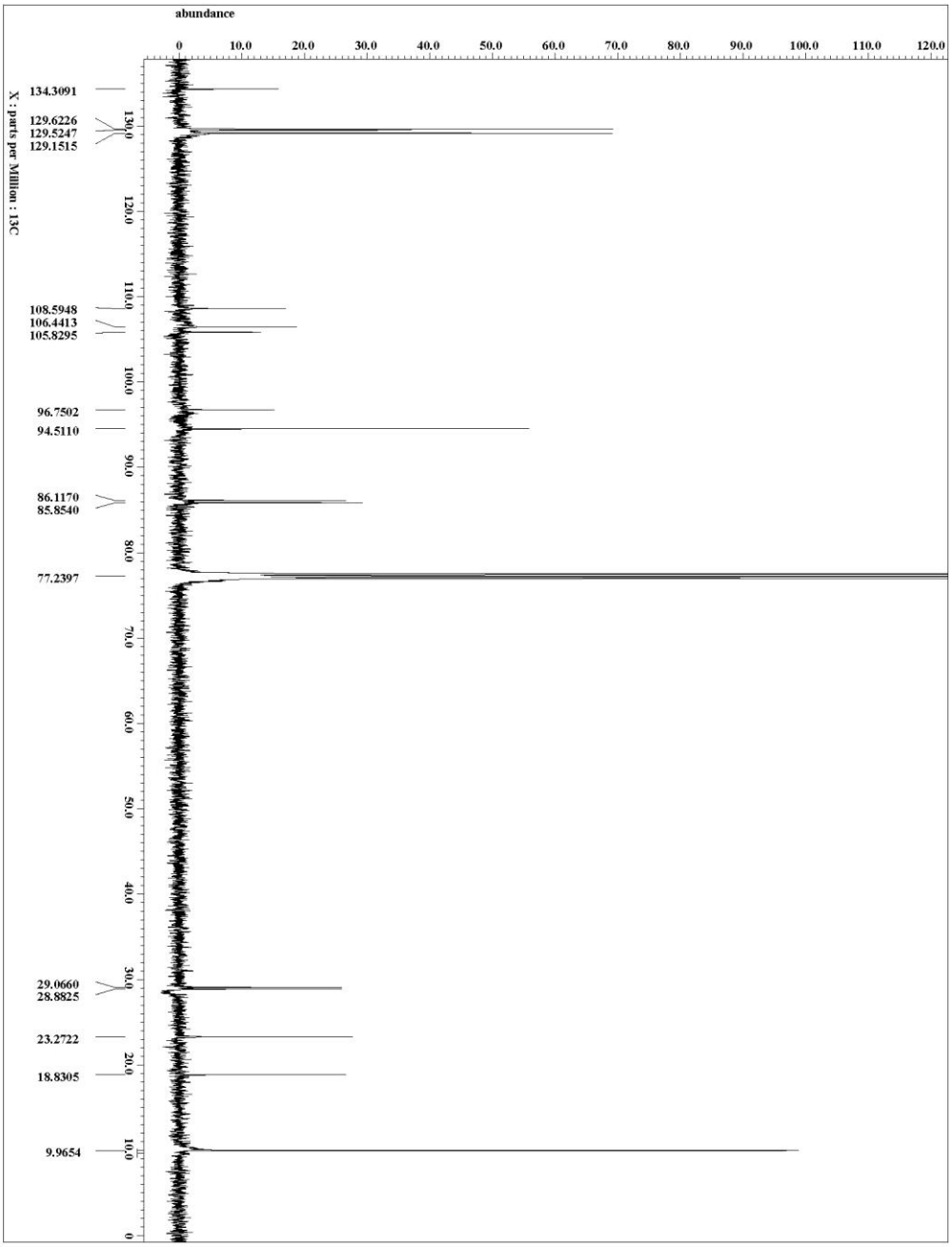

Figure 2-36. 42 ^{13}C NMR spectrum (125 MHz, $CDCl_3$).

2-5.4 X-ray Crystallographic Summary for Complex 25.

General Experimental for X-ray Structure Determinations.

A single crystal with general dimensions of *a* x *b* x *c* was immersed in Paratone and placed on a Cryoloop. Data were collected on a Bruker SMART (APEX) CCD diffractometer using a graphite monochromator with Mo or Cu Kα radiation (λ = 0.71073 or 1.54178 Å) at the defined temperature. The data were integrated using the Bruker SAINT software program and scaled using the SADABS software program. Solution by direct methods (SIR-2004) produced a complete heavy-atom phasing model consistent with the proposed structure. All non-hydrogen atoms were refined anisotropically by full-matrix least squares (SHELXL-97). All hydrogen atoms were placed using a riding model. Their positions were constrained relative to their parent atom using the appropriate HFIX command in SHELXL-97.

Table 2-1. Crystallographic Data Collection and Refinement Information for **25.**

	25
Formula	$C_{31}H_{41}F_6PRu$
Crystal System	Monoclinic
Space Group	*C* 1 21/c 1
a, Å	12.9972(14)
b, Å	9.8847(12)
c, Å	22.358(3)
α, deg	90
β, deg	103.245(5)
γ, deg	90
V, Å^3	2796.0(6)
Z	4
Radiation (λ, Å)	Mo-Kα, 0.71073
ρ (calcd.), g/cm^3	1.567
μ, mm^{-1}	0.678
Temp, K	100(2)
θ max, deg	25.448
data/parameters	5150 / 90 / 352
R_1	0.0568
wR_2	0.1127
GOF	1.128

2-6 Acknowledgements

The material in Chapter 2, in part, is currently being prepared for submission for publication with the following authors: Cope, S.K.; O'Connor, J.M. The dissertation author was the primary investigator and author of this material.

2-7 References

1. Höpf, H.; Musso, H. *Angew. Chem. Int. Ed. Engl.* **1969**, *8*, 680

2. Hitt, D.M.; O'Connor, J.M. *Chem. Rev.* **2011**, *111*, 7904.

3. (a) O'Connor, J.M.; Lee, L.I.; Gantzel, P.; Rheingold, A.L.; Lam, K.C. *J. Am. Chem. Soc.* **2000**, *122*, 12057. (b) O'Connor, J.M.; Friese, S.J.; Tichenor, M. *J. Am. Chem. Soc.* **2002**, *124*, 3506. (c) O'Connor, J. M.; Friese, S.J.; Rodgers, B.L. *J. Am. Chem. Soc.* **2005**, *127*, 16342, (d) O'Connor, J.M.; Friese, S.J. *Organomet.* **2008**, *27*, 4280.

4. O'Connor, J.M.; Friese, S.J.; Rodgers, B.L.; Rheingold, A.L.; Zakharov, L. *J. Am. Chem. Soc.* **2005**, *127*, 9346.

5. Friese, S.; PhD. Dissertation, University of California, San Diego **2004**.

6. (a) Yamamoto, Y.; Kitahara, H.; Ogawa, R.; Itoh, K. *Chem. Comm.* **2000**, 549 (b) Lindener, E.; Jansen, R.-M.; Mayer, H.A.; Hiller, W.; Fawzi, R. *Organomet.* **1989**, *8*, 2355. (c) Yi, L.S.; Torres-Lubian, J.R.; Liu, N.; Rheingold, A.L.; Guzei, I.A. *Organomet.* **1998**, *17*, 1257.

7. (a) Masuda, K.; Ohkita, H.; Kurumatani, S.; Itoh, K. *Organomet.* **1993**, *12*, 2221. (b) Itoh, K.; Masuda, K.; Fukahori, T.; Nakano, K.; Aoki, K.; Nagashima, H. *Organomet.* **1994**, *13*, 1020

8. Fagan, P.J.; Ward, M.D.; Calabrese, J.C. *J. Am. Chem. Soc.* **1989**, *111*, 1698.

9. Christl, M.; Braun, M.; Muller, G. *Angew. Chem. Int. Ed. Engl.* **1992**, *31*, 473.

10. Fructos, M.R.; Fremont, P.; Nolan, S.P.; Diaz-Requejo, M.M.; Perez, P.J. *Organomet.* **2006**, *25*, 2237.

11. Mango, F.D. *Coord. Chem. Rev.* **1975**, *15*, 109.

12. (a) Abley, P.; McQuillen, F.J. *Chem. Comm.* **1969**, 1503. (b) Khan, A.M.; McQuillen, F.J.; Jardine, I. *J. Chem. Soc. C* **1967**, 136. (c) Mitsui, S.; Kudo, Y.; Kobayashi, M. *Tetrahedron* **1969**, *25*, 1921.

13. Cox, D.N.; Roulet, R. *J. Chem. Soc., Chem. Comm.* **1989**, 175.

14. Gloge, T.; Jess, K.; Bannenberg, T.; Jones, P.G.; Langenscheidt-Dabringhausen, N.; Salzer, A.; Tamm, M. *Dalt. Trans.* **2015**, *44*, 11717.

15. Perekalin, D.S.; Kudinov, A.R. *Coord. Chem. Rev.* **2014**, *276*, 153.

16. (a) Mango, F.D. *Advan. Catalysis* **1969**, *20*, 291. (b) Mango, F.D. *Tet. Lett.* **1973**, *17*, 150.

Chapter 3 Cycloaromatization of Acyclic Conjugated Trienes Mediated by Ruthenium

3-1 Introduction

The thermal cyclization of trienes to cyclohexadienes has had a relatively long history in synthetic organic chemistry.[1] The stereochemical outcome of this reaction, and the ring-opening reverse reaction, were laid out in the seminal work by Woodward and Hoffmann entitled The Conservation of Orbital Symmetry.[2] It was postulated that the thermal cyclization of trienes, **1**, proceed in a disrotatory fashion (Scheme 3-1).

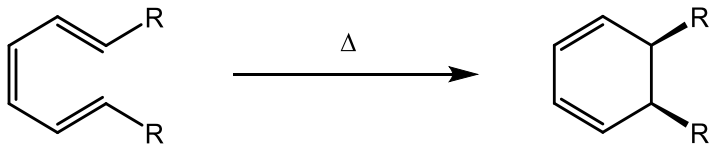

1 **2**

Scheme 3-1. Thermal electrocyclization of trienes.[2]

In contrast to the cyclization of enediynes and dienynes discussed above, the cyclization of trienes proceeds under milder conditions, ~ 100 °C.[1] The 1,3-cyclohexadiene product **2** can be isolated, or can be oxidized to the corresponding arene under mild conditions by simply opening the reaction flask to air.[3]

Drawing inspiration from the previous work with enediynes[4] and dienynes,[5] we proposed that $CpRu(NCMe)_3PF_6$ (**3**) or $Cp^*Ru(NCMe)_3PF_6$ (**4**) would trigger the cyclization of trienes at room temperature. In this chapter the synthesis of trienes with specific stereochemistry is reported, along with triene cyclization mediated by **3** and **4**. The isolation and characterization (NMR spectroscopy and X-ray crystallography)

of a purported intermediate is reported. In addition, the mechanism of triene cycloaromatization is addressed with deuterium labeling and NMR spectroscopy studies.

3-2 Synthesis of Trienes

A rapid stereospecific synthesis of trienes was desired for this project. Two main pathways were chosen to selectively access *EZE* (**5**) or *ZZZ* (**8**) trienes in good yield with high stereoselectivity (Figure 3-1). In the first pathway to **5**, a Heck reaction was utilized to install R^2 onto vinyl bromide **6** (step A). In step B a Wittig reaction was used to install R^1 from **7,** which in turn was generated from cyclopentanone under Vilsmeyer-type conditions. The cyclopentene core was chosen to prevent the photo-induced isomerization of the central alkene.

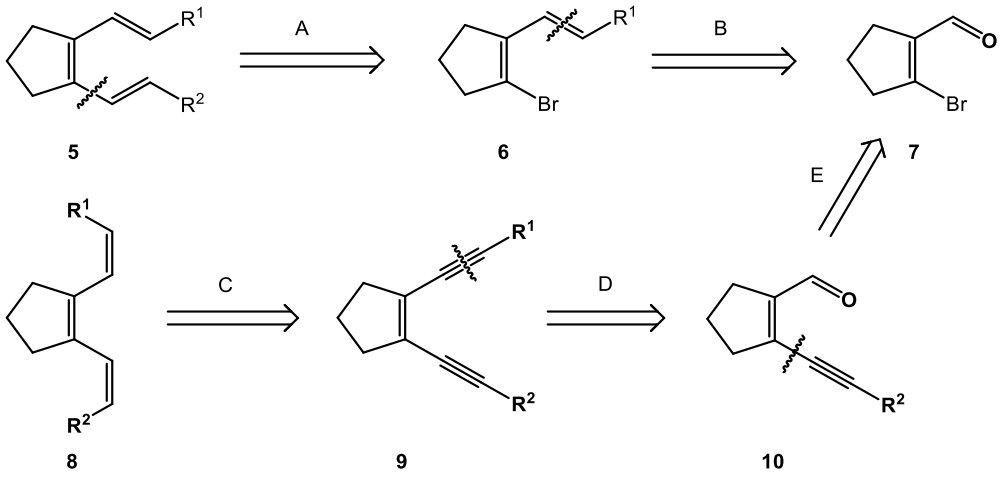

Figure 3-1. Retrosynthetic scheme for the synthesis of *EZE* and *ZZZ* trienes.

For the synthesis of triene **8**, a reduction of enediyne **9** provided the desired *ZZ* stereochemistry (Step C). A homologation of **10**, followed by installation of R^1, for groups other than hydrogen, generated **9**. A Sonogashira coupling installed R^2 on the common starting material **7** (Step E). Alternatively, we employed a literature route to **9** that involved a double Sonogashira coupling onto 1,2-dibromo-1-cyclopentene.[6]

Following a literature procedure, phenyl-substituted analogues of **5** were synthesized.[7] As a representative procedure, **7** (1 mmol) was reacted with benzylidene triphenyl-phosphane (1.2 mmol) in THF (30 mL) at rt overnight (Scheme 3-2). The crude reaction mixture was concentrated under vacuum and the residue was purified on a silica gel column to give **11** in 70% yield. Then **11** was reacted with styrene in the presence of $Pd(OAc)_2$, PPh_3, and NEt_3 in DMF at 80 °C for 16 h. The reaction was cooled to rt, diluted in H_2O and extracted into Et_2O. The organic solution was concentrated under vacuum and the residue was purified on a silica gel column to give **12** as a light yellow fluffy solid in 75% yield.

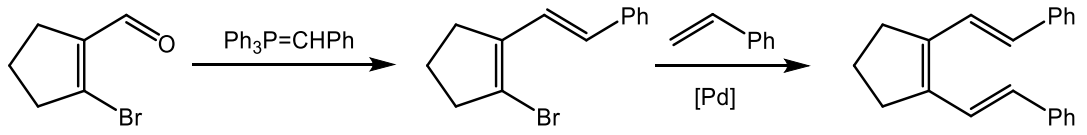

7 **11** **12**

Scheme 3-2. Synthetic path to **12**.[7]

Recrystallization of **12** from ethanol gave yellow needles which were subjected to an X-ray crystallography study. Unfortunately, a weak diffraction pattern led to a low quality X-ray structure which confirmed connectivity but did not provide useful bond

metrics data. Attempts to grow higher quality crystals for X-ray crystallography failed.

The *ZZZ* analogue of **12** was generated by the partial reduction of **14**, which was in turn generated by a double Sonogashira coupling on dibromocyclopentene **13** (Scheme 3-3).[6] As a representative reaction, a degassed solution of **13** (1 mmol) in benzene (20 mL) with NEt_3 (2.2 mmol) was treated with $PdCl_2(PPh_3)_2$ (5 mol %) and CuI (5 mol %) under N_2. Phenylacetylene (2.2 mmol) was then added and the resulting solution was allowed to stir at rt. After 2 h the mixture was passed through a pad of Celite and concentrated under vacuum. The residue was purified on a silica gel column to give **14** in 60% yield, with a 30% yield of mono-substituted cyclopentene byproduct. When the mono-substituted product was resubjected to the reaction conditions, the formation of **14** was seen in only a few percent yield with predominant decomposition of the catalyst system and recovery of the starting monosubstituted cyclopentene. Reduction was achieved by addition of enediyne **14** to a suspension of Pd on $CaCO_3$/Pb in benzene with quinoline under an atmosphere of H_2.[8] The resulting solution was stirred at rt for 2 h and then passed through a pad of Celite. The solution was concentrated under vacuum and the residue was purified on a silica gel column to give **15** in 70% yield.

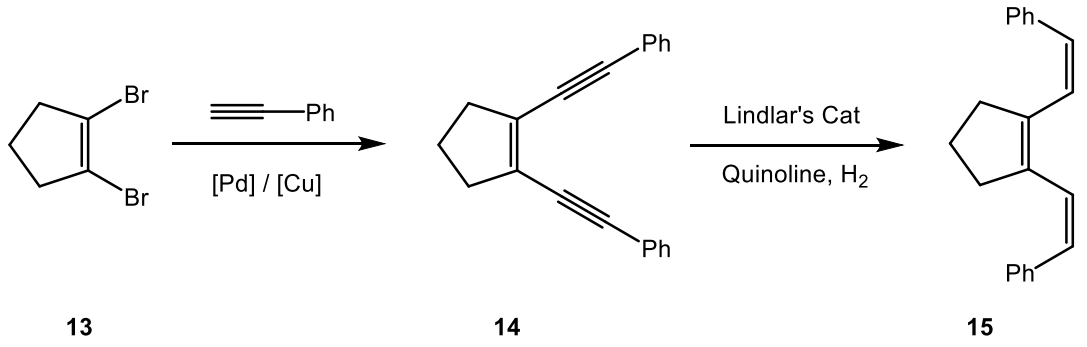

13 **14** **15**

Scheme 3-3. Synthetic path to **15**.

The trienes **12** and **15** showed similar ^{1}H NMR ($CDCl_3$) spectroscopic data with aromatic hydrogen signals, an allylic methylene hydrogen triplet at δ 2.4 and a pentet at 1.8. The characteristic feature for each was a pair of doublets at δ 6.54 ($^3J_{HH}$ = 15.9 Hz) and 7.40 ($^3J_{HH}$ = 15.9 Hz) for **12** and 6.65 ($^3J_{HH}$ = 11.5 Hz) and 6.71 ($^3J_{HH}$ = 11.5 Hz) for **15**. The magnitude of the coupling constants is consistent with *trans* and *cis* coupling, respectively.

To gain insight into the stereochemistry of cyclization and aromatization, dideutero-substituted trienes were prepared. A double Sonogashira coupling of TMS-acetylene onto **13** generated the previously known enediyne **19** (Scheme 3-4).[9] Desilylation of **19** was accomplished by stirring **19** in THF/MeOH (1:1) in the presence of K_2CO_3 for 1 h and then diluting the solution in H_2O. The aqueous solution was extracted with Et_2O and the organic solution was concentrated under vacuum. The residue was purified by silica gel chromatography to give **20** in 60% yield. Terminal enediyne **20** is volatile and care was taken in handling it to prevent loss due to evaporation. Deprotonation of **20** with ^{n}BuLi in THF at -78 °C for 30 min and

subsequent quenching with D_3O^+, gave **20-*d*** in 80% yield after aqueous workup and silica gel chromatography. A ^1H NMR spectrum ($CDCl_3$) showed > 98% deuterium incorporation in **20-*d***, as evidenced by the lack of a resonance at δ 3.12.

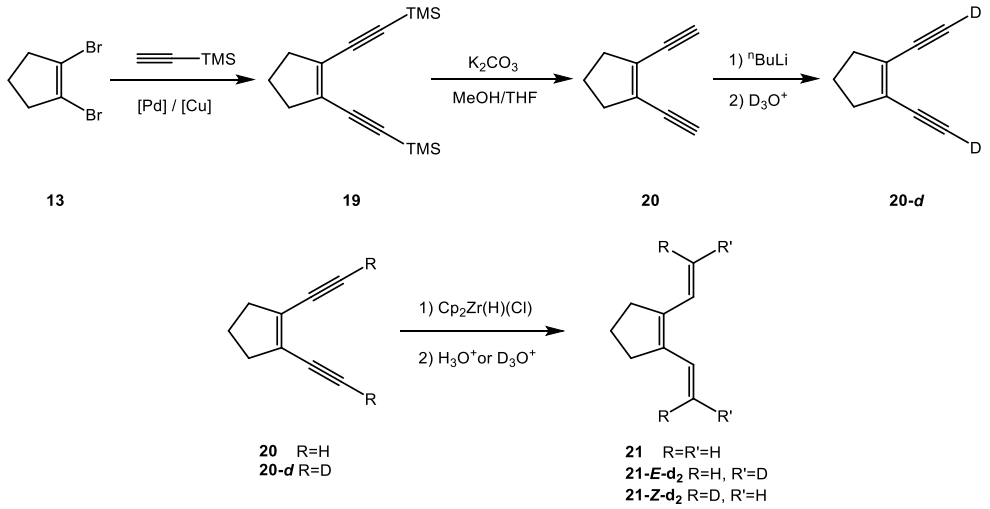

Scheme 3-4. Synthetic route to **21**.

A double Schwartz reduction of **20** in benzene at rt and subsequent quenching of the vinyl zirconium intermediate with D_3O^+ gave **21-*E*-d$_2$** in 80% yield after aqueous workup and silica gel chromatography. The analogous reaction with **20-*d*** and quenching with H_3O^+ gave **21-*Z*-d$_2$** in the same 80% yield. Due to spectral overlap in the ^1H NMR spectrum ($CDCl_3$) of the vinyl resonances, the % deuterium incorporation was taken as the ratio of the internal vinyl resonance to the terminal vinyl resonance. For **21-*E*-d$_2$** the % deuterium incorporation was 85% at each of the enriched vinyl positions, in line with results from the synthesis of deuterium labeled dienynes in Chapter 2, and for **21-*Z*-d$_2$** the % deuterium incorporation was > 98%, in line with the % deuterium incorporation observed for **20-*d***.

Finally, a trisubstituted alkene was prepared to determine the scope of the cyclization chemistry. Reaction of dienaldehyde **22** (1 mmol) with triphenyl(propan-2-ylidene)phosphane in THF (30 mL) for 1 h at rt gave **23** in 70% yield after silica gel chromatography (Scheme 3-5).

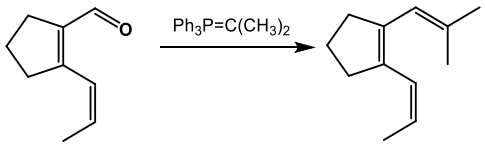

22 **23**

Scheme 3-5. Synthetic route to **23**.

3-3 Reactions of Trienes with Ruthenium

The reaction of **12** (20 μmol) with ruthenium complex **3** in $CDCl_3$ (1 mL) was monitored by ^1H NMR spectroscopy (Scheme 3-6). The initial light yellow solution turned orange after 5 min and a ^1H NMR spectrum of the crude reaction mixture indicated the formation of a new compound, **24**. The ^1H NMR spectroscopic data ($CDCl_3$) for **24** indicate the desymmetrization of the methylene hydrogens of the alicyclic five-membered ring, the appearance of a new pair of vinyl hydrogen doublets at δ4.10 and 6.92, with a $^3J_{HH}$ = 10.3 Hz, and a cyclopentadienyl hydrogen resonance at 5.00. A ^{13}C NMR spectrum ($CDCl_3$) exhibited vinyl carbon resonances at δ77.7, 83.0, and 119, which are consistent with metal coordination to the alkene.[10] For comparison, triene **12** exhibited ^1H NMR ($CDCl_3$) resonances at δ6.54 and 7.40, $^3J_{HH}$ = 15.9 Hz, and vinyl-carbon resonances at δ 122.5, 129.9, and 139.8. A proton-

coupled ^{13}C NMR spectrum ($CDCl_3$) of **24** showed resonances at δ 77.7 (d, $^1J_{CH}$ = 164.7 Hz) and 83.0 (d, $^1J_{CH}$ = 165.8 Hz) which contrast with the vinyl resonances of **12** at δ 122.5 (d, $^1J_{CH}$ = 149.1 Hz) and 129.9 (d, $^1J_{CH}$ = 153.1 Hz). When the tube was left to stand overnight, the formation of orange block crystals was observed. A single crystal X-ray diffraction study provided a solid-state structure which confirmed that $CpRu^+$ is coordinated to **12** through all six sp^2 carbons of the triene system (Figure 3-2).

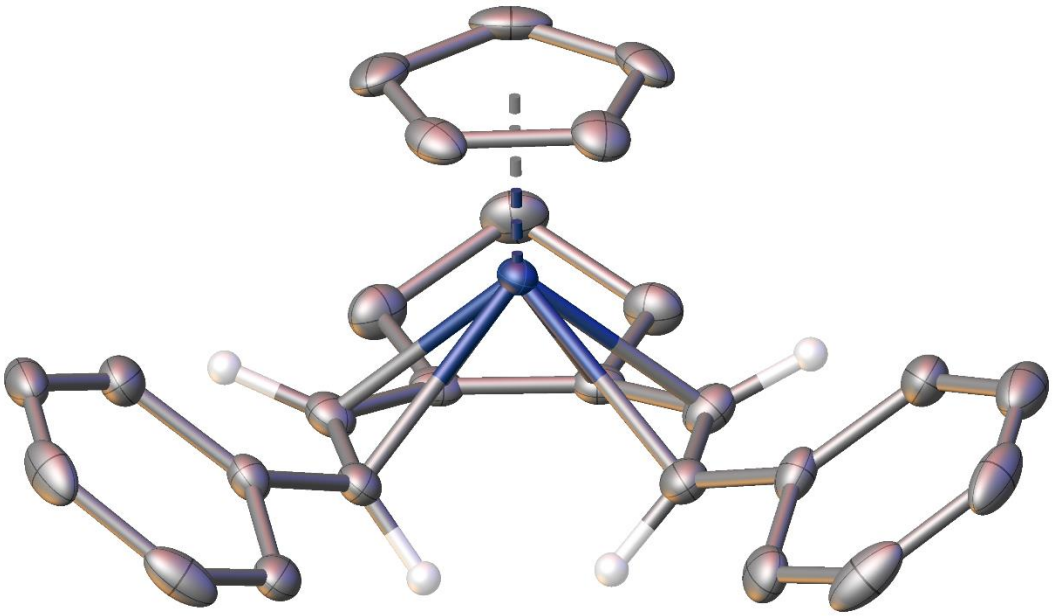

Figure 3-2. X-ray structure of CpRu(η^6-**12**)$^+$ (**24**). Most hydrogens and the counter-ion have been omitted for clarity.

Table 3-1. Selected Bond Distance (Å) and Angle (deg) Data for **24**.

Bond (A-B)	Distance (Å)	Angle (A-B-C)	Degrees (°)
C1-C2	1.388(8)	C13-C1-C2	123.1(5)
C2-C3	1.423(7)	C1-C2-C3	126.9(5)
C3-C4	1.412(5)	C2-C3-C4	131.6(5)
C4-C5	1.420(5)	C3-C4-C5	131.1(5)
C5-C6	1.382(5)	C4-C5-C6	127.6(5)
C1-C6	2.821(5)	C5-C6-C7	123.0(4)

Table 3-2. Selected Ruthenium-carbon Distances (Å) in **24**.

Bond (A-B)	Distance (Å)	Bond (A-B)	Distance (Å)
C1-Ru	2.313(5)	C22-Ru	2.211(7)
C2-Ru	2.204(4)	C23-Ru	2.185(5)
C3-Ru	2.237(5)	C24-Ru	2.195(6)
C4-Ru	2.235(6)	C25-Ru	2.211(8)
C5-Ru	2.190(8)	C26-Ru	2.195(6)
C6-Ru	2.294(6)		

Table 3-3. Selected Torsion Angles (deg) for **24**.

A-B-C-D	Torsion angle	A-B-C-D	Torsion angle
C13-C1-C2-H2	1(3)	C7-C6-C5-H5	5(2)
H1-C1-C2-H2	156(4)	H6-C6-C5-H5	145(3)
H2-C2-C3-C19	16(3)	H5-C5-C4-C21	10(2)
H1-C1-C2-C3	36(3)	H6-C6-C5-C4	44(3)

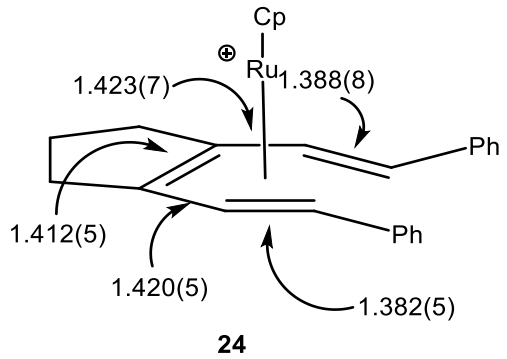

24

Figure 3-3. Selected bond distances (Å) for triene complex **24**.

One of the key features from this structure is that all of the bond lengths in the triene system are nearly equivalent at 1.40 ± 0.02 Å (Figure 3-3). This length is remarkably similar to the bond length observed in benzene at 1.39 Å. A second key feature is that all six of the sp^2-carbons of the triene lie in the same plane, with only a slight deviations from the mean plane at carbons 2 (0.099 Å) and 5 (0.093 Å). The phenyl substituents are 0.40 and 0.43 Å above the mean plane and the hydrogens connected to carbons 2 and 5 are 0.51 and 0.50 Å above the mean plane. The

hydrogens connected to carbons 1 and 6 are 0.91 and 0.89 Å below the mean plane. This demonstrates the twisting of the alkenes in the structure.

The reaction of **15** (20 μmol) with **3** (20 μmol) in acetone·d_6 (1 mL) was monitored by ^{1}H NMR spectroscopy. The initially light yellow solution color turned forest green after approximately 5 min and then a tan color developed over the course of 1 h. The ^{1}H NMR spectrum during this time was difficult to decipher as all of the resonances were broadened out and a number of the resonances overlapped. After 1 h, the spectrum sharpened, showing desymmetrization of methylene hydrogens of the alicyclic five-membered ring, and a new resonance was observed at δ 6.72 in a 2:5 ratio to the Cp resonance at 5.65. Thus the product is assigned as the cycloaromatized product, **25** (Scheme 3-6).[4]

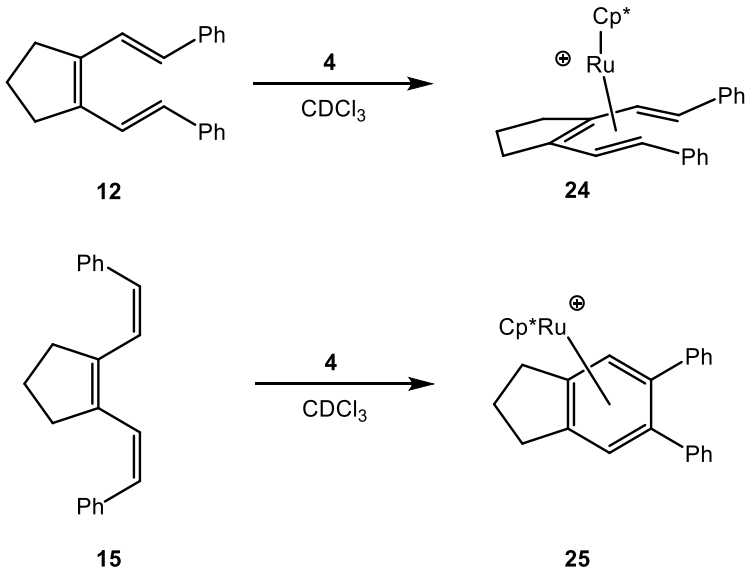

Scheme 3-6. Reactions leading to **24** and **25**.

The reaction of **21** (20 μmol) with **4** (20 μmol) in $CDCl_3$ (1 mL) was monitored by ^{1}H NMR spectroscopy. Upon addition of solvent, the solution turned to brownish-green and the spectral data indicated desymmetrization of the alicyclic five-membered ring. Other broad new resonances were observed, but due to spectral overlap no clear assignments were made. When the reaction was allowed to stand overnight at rt, the formation of Cp*Ru(indane)$^+$ was observed in the ^{1}H NMR spectrum, as evidenced by a singlet at δ 1.90 and a pair of resonances at 5.57 (dd) and 5.72 (dd), with a $^3J_{HH}$ = 4.2 Hz and $^4J_{HH}$ = 2.3 Hz (Scheme 3-7). The reaction was carried out again to get better NMR data on the possible intermediate. The reaction was allowed to proceed for 20 min after the addition of solvent, then the volatiles were removed under vacuum. Fresh solvent was distilled into the tube on the high vacuum line and the volatiles were again removed under vacuum. Fresh deuterated solvent was distilled into the tube and a ^{1}H NMR spectrum showed the formation of **27**. The complexes exhibited limited solubility in $CDCl_3$, so the reaction was repeated with CD_2Cl_2. The complexes appear to be more soluble in CD_2Cl_2, but the spectrum remained complicated by spectral overlap. The existence of possible intermediate **26** (Scheme 3-7) could not be confirmed due to spectral overlap and broad signals in the ^{1}H NMR spectrum.

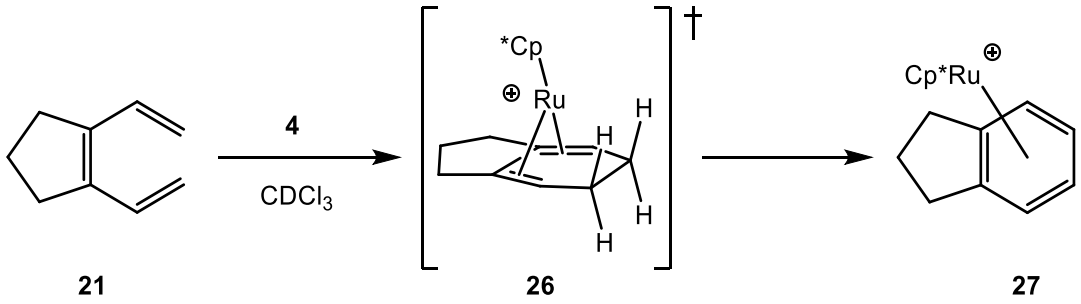

Scheme 3-7. Reaction of **21** with $[Cp^*Ru]^+$. (The open-coordination site on ruthenium is most likely engaged in an agostic interaction to a methylene hydrogen.)

The reaction of **21-*E*-d$_2$** (20 μmol) with **4** (20 μmol) in $CDCl_3$ (1 mL) was monitored by ^{1}H NMR spectroscopy. The solution changed color, as had been observed for **21,** and the ^{1}H NMR spectral data were similar to those for **21**, including evidence for desymmetization of the five-membered ring. When this reaction was allowed to stand overnight, the formation of **27** was observed by ^{1}H NMR spectroscopy (Scheme 3-8). The aromatic hydrogen resonances of the product were observed in a ratio of 1.5:1.5:15 for the signals at δ 5.72: 5.57: 1.90 (C_5Me_5). This signaled a loss of one protium and one deuterium from **21-*E*-d$_2$** on the path of aromatization, and the rearrangement of the remaining deuterium over the two aromatic-positions. A ^{13}C NMR spectrum of this product showed a complex feature for the resonances at δ 84.3 and 86.0, consistent with the partial incorporation of deuterium in these positions.

The reaction of **21-*Z*-d$_2$** (20 μmol) with **3** (20 μmol) in $CDCl_3$ (1 mL) was monitored by ^{1}H NMR spectroscopy. This solution changed color, as had been

observed for **21**, and the observed ^{1}H NMR spectral data was similar to that observed for **21**, including evidence for desymmetization of the five-membered ring. When this reaction was allowed to stand overnight, the formation of **27** was observed by ^{1}H NMR spectroscopy. The aromatic hydrogen signals of the product showed a ratio of 2:1:15 for the signals at δ 5.72: 5.57: 1.90 (C_5Me_5). This observation is consistent with a loss of one protium and one deuterium from **21-*Z*-d$_2$** on the path of aromatization. A ^{13}C NMR spectrum ($CDCl_3$) of this product showed a complex feature for the resonance at δ 84.3, consistent with the incorporation of deuterium in the 5-position of **27**.

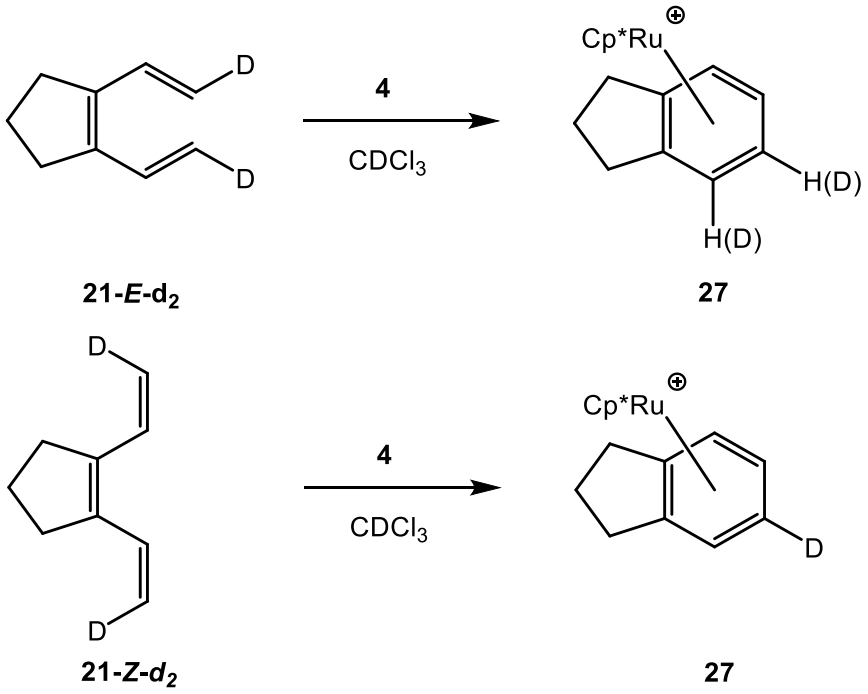

Scheme 3-8. Reactions of **21-*E*-d$_2$** and **21-*Z*-d$_2$** with $[Cp^*Ru]^+$.

The reaction of **23** (20 μmol) with **4** (20 μmol) in $CDCl_3$ (1 mL) was monitored by ^1H NMR spectroscopy (Scheme 3-9). The color of the solution changed as had been observed for **21**, and the ^1H NMR spectrum exhibited new resonances at δ -8.46 (d, 19.4 Hz, 1H), 0.40 (s, 3H), 1.15 (s, 3H), 1.38 (s, 3H), 2.07 (d, 19.4 Hz, 1H), and 4.81 (s, 1H). This is consistent with the formation of an η^4-cyclohexadiene complex,[11] where the initially formed cyclohexadiene **28** rearranges via a [1,5]-hydride shift to give **29**. The volatiles were removed from the NMR tube under vacuum and fresh solvent was distilled into the tube on the high-vacuum line.

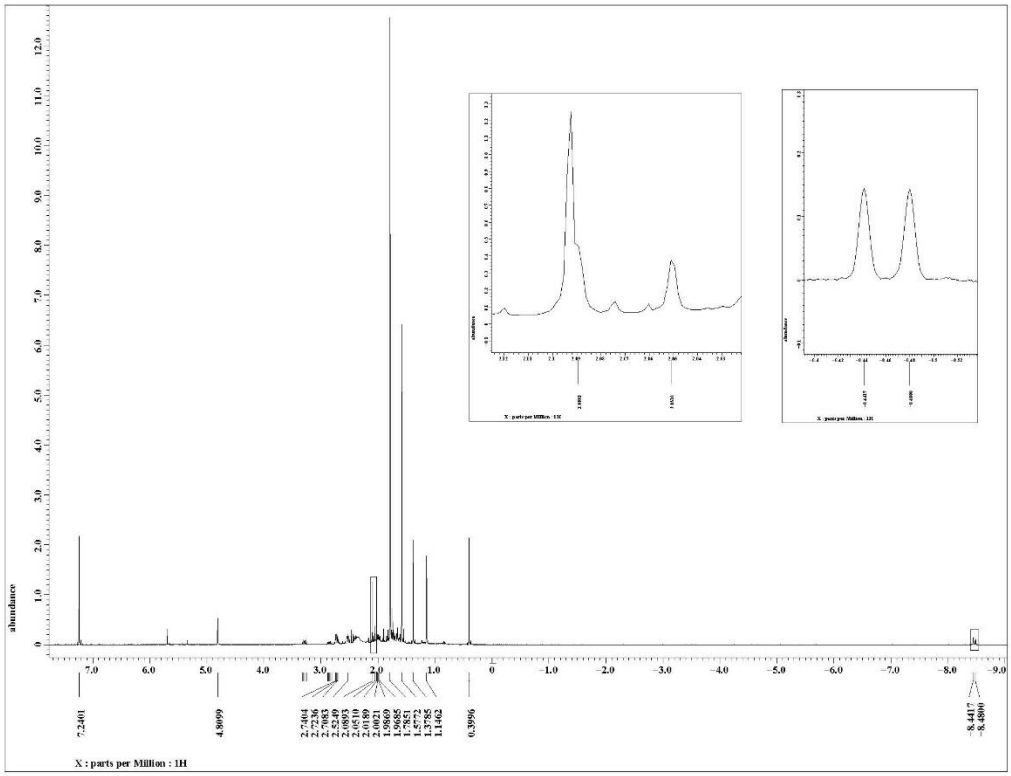

Figure 3-4. ^1H NMR spectrum (500 MHz, $CDCl_3$) of the reaction of **23** with **4**.

The volatiles were again removed under vacuum and fresh deuterated solvent was distilled into the tube. Complex **29** appeared to be stable in solution for several days under N_2.

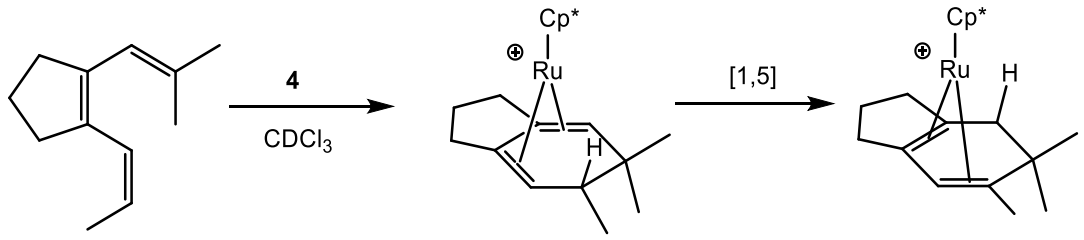

23 **28** **29**

Scheme 3-9. Reaction of **23** with $[Cp^*Ru]^+$. (The open-coordination site on ruthenium is most likely engaged in an agostic interaction to the hydrogen on the aliphatic carbon.)

When the tube was opened to air and isolation of the complex was attempted, a ^1H NMR spectrum showed the formation of dimethyl indane product **30**. Simply opening the NMR tube to air resulted in the formation of **30** (Scheme 3-10). The isolation of **29** was attempted by addition of Et_2O to the NMR tube and cooling the solution. The brownish-green solution slowly turned light tan and the formation of crystals of **30** was observed. The experiment was repeated with pentane in place of Et_2O, with the same result.

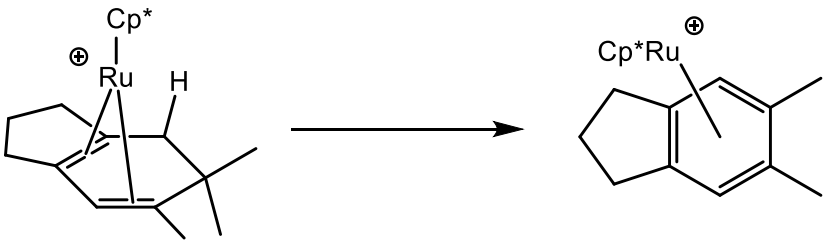

29 **30**

Scheme 3-10. Formation of **30**. (The open-coordination site on ruthenium is most likely engaged in an agostic interaction to the hydrogen on the aliphatic carbon.)

When **23** was reacted with **4** in $CDCl_3$ without removing the volatiles and was allowed to stand overnight, the formation of **30** was observed as the only product.

3-4 Discussion

At the initiation of this project the cyclization of linear trienes was proposed to proceed via η^6-coordination of a $CpRu^+$ fragment, as shown for complex **32** (Scheme 3-11). The hexahapto-coordination would distort the ground state geometry and energy of the triene, leading to a disrotatory 6π-electrocyclization[14] and formation of η^4-cyclohexadiene **33**. This disrotatory ring-closure was proposed to proceed with torquoselectivity to bring the groups in the *E*-position *endo* to the metal. Then through an *endo* C-H bond activation, a ruthenium-hydride species, **34**, could form. A subsequent sigma bond metathesis would then generate the product arene **35** and H_2.

Thus, both hydrogens in the dihydrogen byproduct originate at the *E*-position of the starting triene.

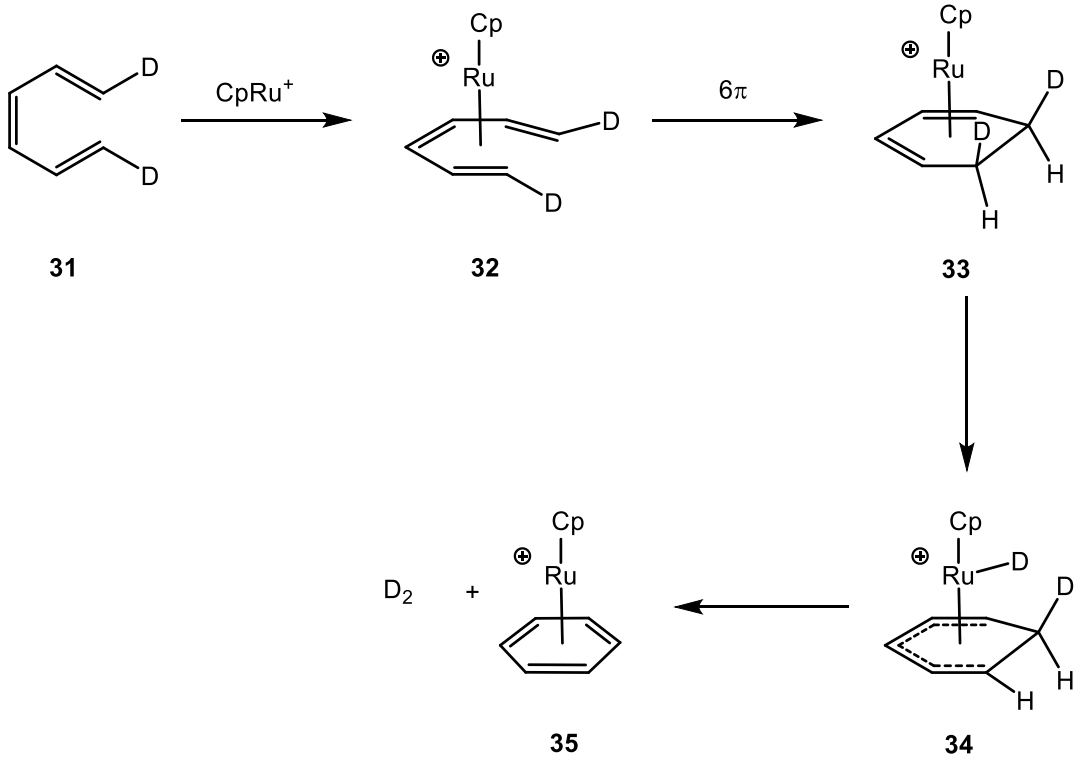

Scheme 3-11. Proposal at the initiation of the project.

3.4-1 η^6-Coordination Studies

When triene **12** was reacted with **3**, the formation of ruthenium-η^6-triene complex **24** was observed by NMR spectroscopy and then confirmed by X-ray crystallography (Figure 3-5). The X-ray structure demonstrated a pronounced twisting of the disubstituted alkenes of 156(4)°, as measured by the torsion angle between the hydrogens on C1 and C2. The six carbons of the triene lie in the same

plane, with C2 and C5 puckered above the plane by 0.09 Å. The hydrogens attached to C2 and C5 are twisted toward the metal center, distorted above the mean plane of the triene by 0.5 Å. The phenyl substituents deviate from the mean plane of the triene by 0.4 Å, consistent with the rotation of the hydrogens at C2 and C5 above the plane. The phenyl substituents and hydrogens at C2 and C5 showed a torsion angle of 1(3)° and 5(2)°, whereas the phenyl *ipso* carbon to C1-C2-C3 showed a torsion angle of 167.1(5)°. The twisting of the alkene is more pronounced for the hydrogens at C1 and C6, which deviate from the mean plane of the triene by 0.9 Å. The hydrogens at C1 and C6 show a torsion angle to the hydrogens at C2 and C5 of 156(4)° and 145(3)° and to C3 and C4 of 36(3)° and 44(3)°.

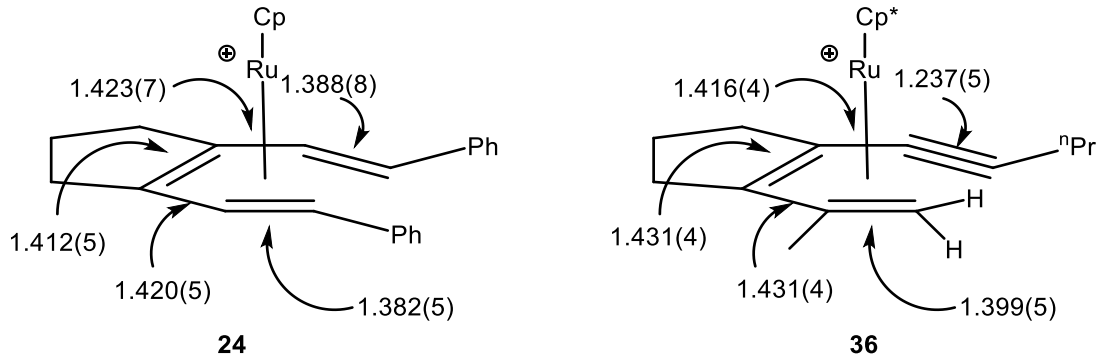

Figure 3-5. Selected bond distances (Å) in η^6-triene complex **24** and η^6-dienyne complex **36**.

The remarkable similarity of the bond lengths in the triene of **24** signals a significant delocalization. These values are similar to the values observed previously

in the solid-state structure of Cp*Ru(η^6-dienyne)$^+$ (**36**, Figure 3-5). Interestingly, the observed non-bonding C1-C6 distance of 2.797(5) Å for **36** is quite similar to the observed non-bonding C1-C6 distance of 2.821(5) Å for **24**.

In addition, comparison to a known ruthenium-η^6-cycloheptatriene complex is informative (Figure 3-6).

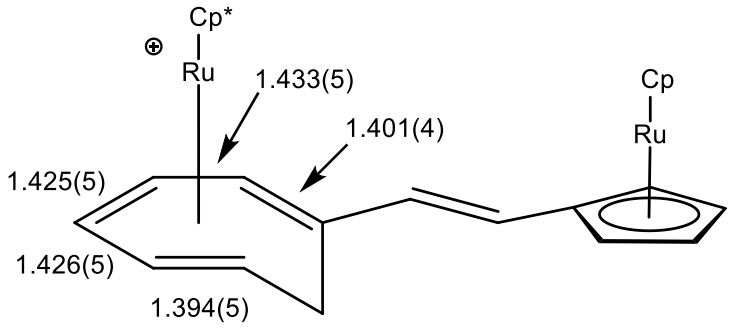

37

Figure 3-6. Selected bond distances (Å) of known cyclic triene **37**.[12]

The triene of **37**[12] has an average bond distance of 1.416(5) Å, with a maximum and minimum bond distance of 1.426(5) Å and 1.394(5) Å, respectively. Complex **24** has an average bond distance of 1.405(8) Å, with a maximum and minimum bond distance of 1.423(7) Å and 1.382(5) Å, respectively. The C1-C6 non-bonding distance in **37** is 2.42(3) Å, substantially shorter than what is observed for **24** as a consequence of the triene's incorporation into a seven-membered ring.

Trienes in cycloheptatrienes are known to undergo 6π-electrocyclization under thermal conditions,[15] but to the best of our knowledge there are no known

examples of cycloheptatrienes bound to ruthenium, as in **37**, undergoing an electrocyclization. Linear triene **12** is known to undergo electrocyclization under thermal conditions,[6] but does not undergo electrocyclization upon coordination to ruthenium, most likely due to steric clashing of the phenyl substituents with the ruthenium center and Cp ligand. When the stereochemistry of the triene is changed from *EZE* to *ZZZ* (**15**) the triene cleanly undergoes cyclization followed by aromatization to give **25**. If an η^6-triene structure such as **24** lies on the pathway to cyclization of trienes by ruthenium, it is hard to see how **15** would form a similar structure. Coordination to generate an η^6-complex with **15** would place phenyls in the positions on H1 and H6 in **24**, generating a large degree of steric clashing.

Structure **24** appears, at least qualitatively, like an η^6-bound triene undergoing a disrotatory 6π-electrocyclic ring-closing which has been arrested before ring-closure by steric clashing with the metal center. This provides good evidence for a disrotatory electrocyclic ring-closing of trienes induced by η^6-coordination to ruthenium.

3-4.2 Deuterium Labeling Studies

When triene **21** was allowed to react with **3** in $CDCl_3$ overnight, the cycloaromatization of **21** was observed as the only organic product. At shorter times, the formation of possible intermediates were observed by ^{1}H NMR spectroscopy, but

could not be confirmed. Stryker[13] generated both *cis* and *trans* hexamethyl cyclohexa-1,3-diene complexed to ruthenium, **38** (Figure 3-7).

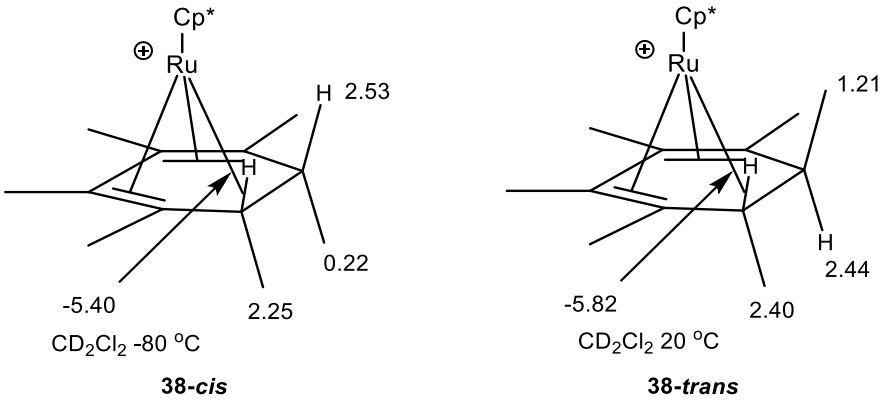

Figure 3-7. Selected ^{1}H NMR chemical shifts (CD_2Cl_2, ppm) for **38**.[13]

When **21** was allowed to react overnight with **3** in $CDCl_3$ the loss of H_2 and aromatization was observed. When **21-*E*-d$_2$** was allowed to react under the same conditions, the loss of a protium and a deuterium was observed and the remaining deuterium was incorporated into two-positions of the newly formed arene. When **21-*Z*-d$_2$** was allowed to react under the same conditions, the loss of a protium and a deuterium was again observed and this time the remaining deuterium was incorporated into a single position on the arene consistent with no migration occurring. These results would not be consistent with our initial proposal that H_2 could be lost by formation of a ruthenium-hydride then sigma-bond metathesis, which would lead to D_2 loss from **21-*E*-d$_2$** and H_2 loss from **21-*Z*-d$_2$**.

In work on the aromatization of cyclohexadienes by ruthenium, Stryker showed that the addition of H_2O or MeOH to **38-*trans*** resulted in the elimination of H_2 and the formation of hexamethylbenzene.[13] When H_2O was added to **38-*cis***, the formation of methane and pentamethylbenzene were observed. In addition, they were unable to resolve the coupling of the upfield signal which that attributed to persistent fluxionality even at -80 °C, caused by [1,5]-hydride shifts.[16] They propose an initial deprotonation of the ruthenium-hydride complex by the added base to generate a cyclohexadienyl ligand, as in **39** (Scheme 3-12). The *exo*-hydrogen is then removed via a ruthenium-assisted protolytic C-H cleavage by the liberated Brønsted acid. This pathway worked even when a methyl was present in the *exo*-position of **39**, liberating methane via a ruthenium-assisted protolytic C-C bond cleavage.

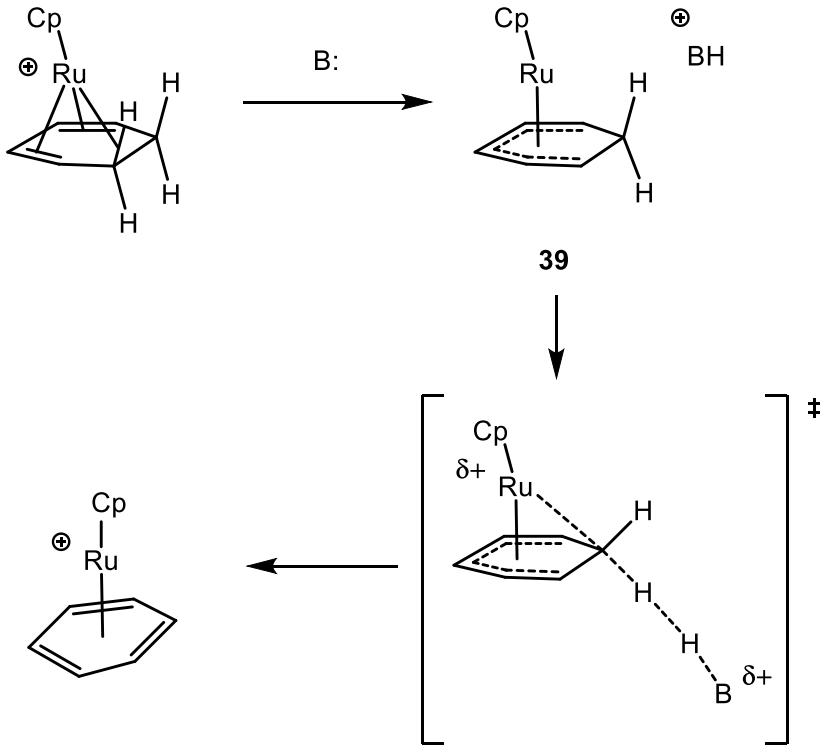

Scheme 3-12. Stryker's proposed mechanism for aromatization of **39**.[13]

The results from **20-*E*-d$_2$** and **20-*Z*-d$_2$** would be consistent with this mechanism for the loss of H-D in each case. In the case of **20-*E*-d$_2$**, the initial deprotonation involves a deuterium which would be *endo* to the metal following a disrotatory 6π-electrocyclization (Scheme 3-13). Before this deprotonation event, the deuterium could migrate to the carbons next to the five-membered ring,[16] thereby explaining the scrambling of the deuterium signal across both positions of the product arene. Then cleavage of the *exo* protium bonds leads to the observed product. In the case of **20-*Z*-d$_2$**, the initial deprotonation occurs on an *endo* protium and then cleavage of the *exo* deuterium by the protonated base.

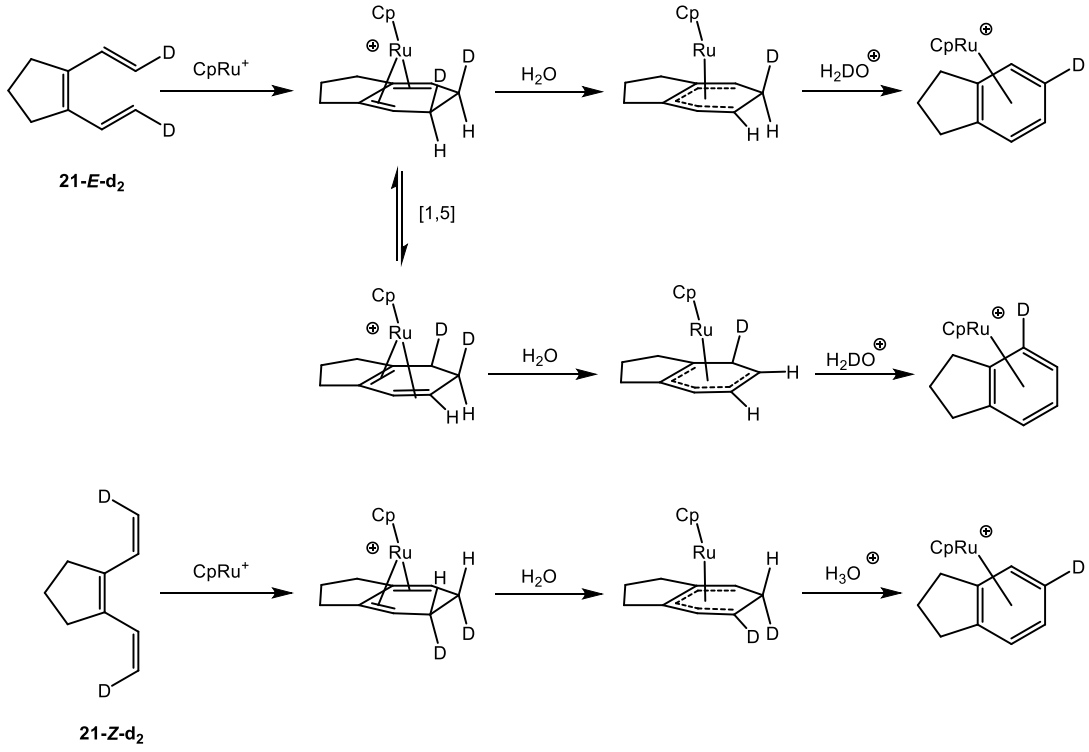

Scheme 3-13. Mechanism for the reaction of **21-*E*-d$_2$** and **21-*Z*-d$_2$** with $CpRu^+$.

The reaction of **23** with **4** is also consistent with these pathways, both in product formation and intermediates. The initial cyclized species **28** rapidly undergoes a [1,5]-hydride shift[16] to give **29**, as this minimizes eclipsing methyl interactions (Scheme 3-14). In addition, **29** should be thermodynamically favored over **28** as it has a tetrasubstituted and trisubstituted alkene versus two trisubstituted alkenes in **28**. The presumed base involved in the formation of **30** is proposed to be advantageous water.

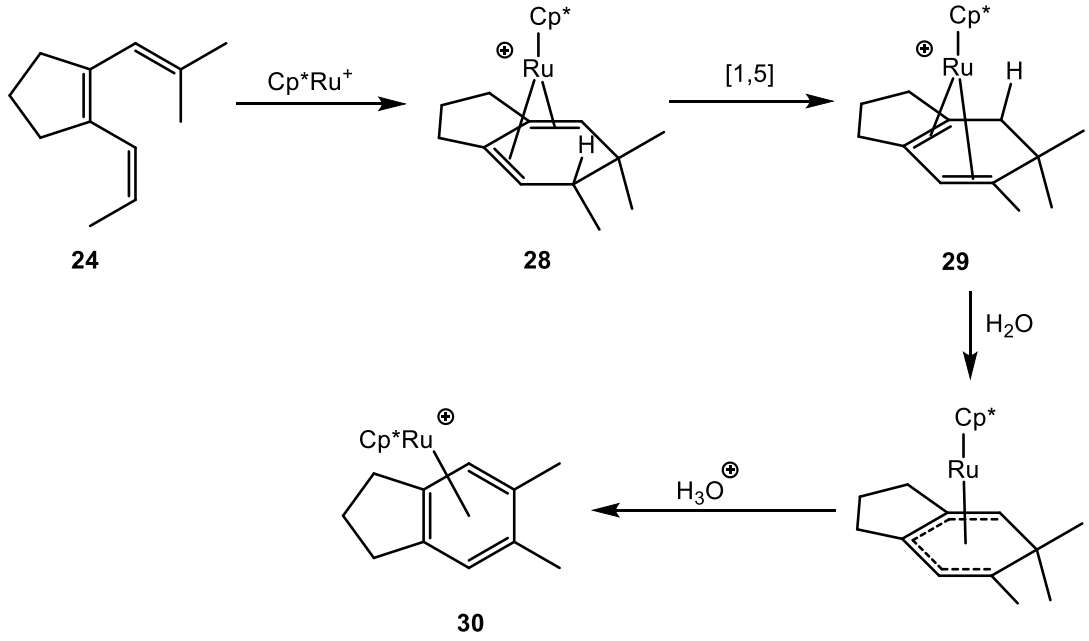

Scheme 3-14. Mechanism for the formation of **30** from **24** and $[Cp^*Ru]^+$.

3-5 Conclusion

The room temperature cyclization and aromatization of linear trienes by $CpRu^+$ and Cp^*Ru^+ was demonstrated. The reaction is proposed to start by η^6-

coordination of ruthenium to the triene (Scheme 3-15), as demonstrated unambiguously in the related complex **24**. The η^6-bound triene then undergoes a disrotatory 6π-electrocyclization with torquoselectivity to bring the groups in the *E*-positions of the triene toward the metal. Then the deprotonation of a ruthenium-hydride intermediate by base generates a cyclohexadienyl intermediate **40**. Finally, a ruthenium-assisted protolytic cleavage of the *exo* bond by Brønsted acid, leads to the formation of arene product.

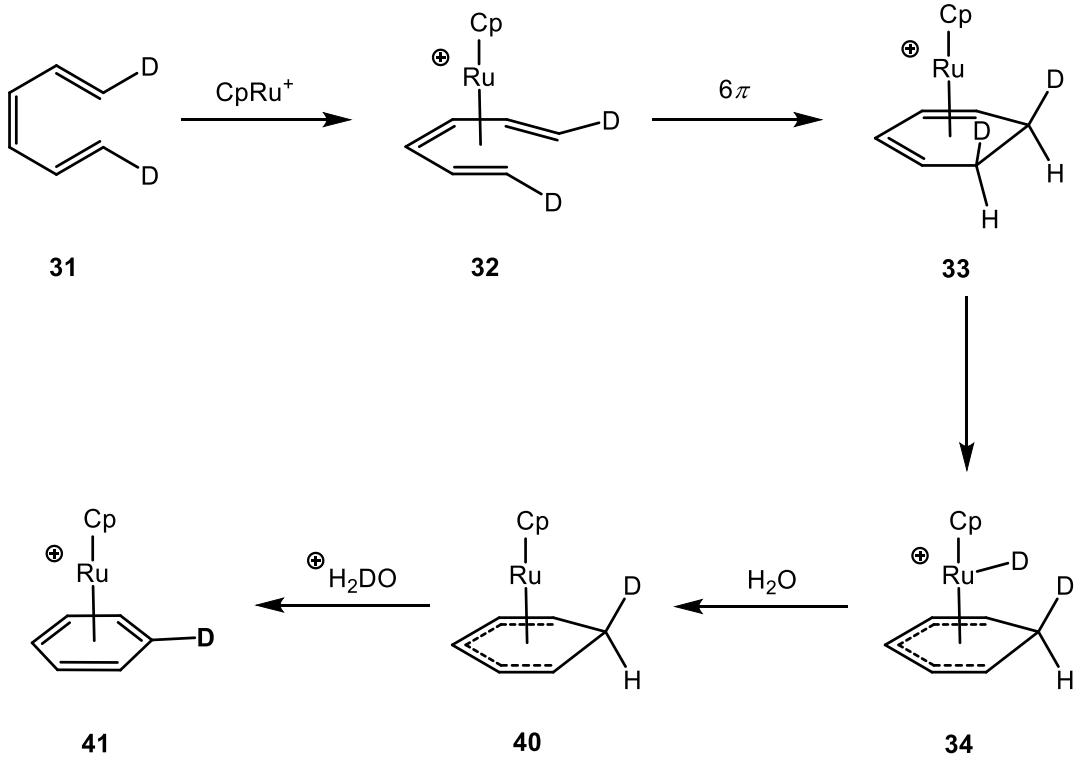

Scheme 3-15. Proposed mechanism for the ruthenium-mediated cycloaromatization of linear trienes.

In the future, more extensive studies into the scope and limitations of the cyclization of trienes by ruthenium should be undertaken. The limits of steric size of groups in the *E*-position of trienes should be explored as well as the possibility of catalytic turnover by incorporation of non-hydrogen groups in the *E*-position. In addition, the exploration of the reactivity pattern of η^6-bound linear triene **24** should be undertaken. It has been well demonstrated that complexation of transition metals changes the observed reactivity patterns of arenes,[17] but no such study has been undertaken with linear η^6-triene complexes.

3-6 Experimental

3-6.1 General Procedures

All manipulations were performed using standard Schlenk technique or in nitrogen filled Vacuum Atmospheres or MBraun glovebox, unless otherwise stated. ^{1}H and ^{13}C NMR spectra were recorded on Varian Mercury 400 MHz, Varian VX 500 MHz, or JOEL ECA 500 MHz instruments. ^{1}H and ^{13}C NMR chemical shifts (δ) are reported in parts per million (ppm). Spectra were referenced to the residual solvent peak. Infrared spectra were obtained on a Nicolet iS10 FT-IR. High resolution mass spectra analyses were performed at either the mass spectrometer facility at UC San Diego or UC Riverside. Photolysis was performed in a Rayonett photo-reactor equipped with UV lamps centered at 254 nm. THF, ethyl ether, DCM, benzene,

hexanes, and pentane used as reaction solvents were dried either by a solvent dispensing system equipped with two neutral alumina columns under argon atmosphere or by 3 Å activated molecular sieves. Chloroform-*d* and benzene-d_6 were dried over 3 Å activated molecular sieves and then distilled under static vacuum into oven-dried Schlenk storage tubes. Deuterated solvents were degassed using a Freeze-Pump-Thaw procedure, typically 5 cycles. NMR reactions were performed in 5 mm J-Young NMR tubes equipped with a Teflon needle valve. All literature compounds were prepared according to the indicated references or purchased from commercial suppliers and used as received.

3-6.2 Preparation and Characterization Data

1,2-di((*Z*)-styryl)cyclopent-1-ene (15): Enediyne **14** (250 mg, 0.92 mmol) and quinoline (20 μL) were dissolved in hexanes/EtOAc (10 mL, 3:1) in a 25 mL side-arm flask under N_2. The resulting solution was sparged with argon for 15 min and then Lindlar's Cat. (200 mg) was added. The flask was equipped with a rubber septum. Then H_2 was bubbled through the solution for 5 min and the solution was stirred at rt for 45 min under an atmosphere of H_2, at which time TLC (silica, hexanes) indicated complete consumption of **14**. The solution was filtered through a plug of Celite, and the Celite rinsed with hexanes. The volatiles were removed under vacuum and the residue was purified on a silica gel column with hexanes eluant to give **14** as a clear oil (234 mg, 0.86 mmol, 90% yield). ^{1}H NMR ($CDCl_3$, 500 MHz) δ 1.84 (p,

$^3J_{HH}$ = 7.5 Hz, 2H), 2.21 (t, $^3J_{HH}$ = 7.5 Hz, 4H), 6.65 (d, $^3J_{HH}$ = 11.5 Hz, 2H), 6.71 (d, $^3J_{HH}$ = 11.5 Hz, 2H), 7.3-7.5 (m, 10H). ^{13}C NMR (125 MHz, $CDCl_3$) δ 23.8, 35.0, 126.2, 126.4, 127.8, 129.2, 130.4, 138.8, 145.7. HRMS(EI): Calcd for ($C_{21}H_{20}$): 272.1565. Found 272.1563.

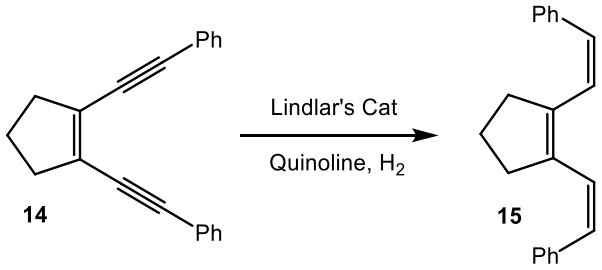

1,2-bis(ethynyl-*d*)cyclopent-1-ene (20-*d*): Enediyne **20** (250 mg, 2.15 mmol) was dissolved in THF (10 mL) in an oven-dried side-arm flask equipped with a stir bar and rubber septum under dry N_2. The solution was cooled to -78 °C on a dry ice/acetone bath and then ^{n}BuLi (4 mL, 1.25 M in hexanes, 5 mmol) was added dropwise to the solution. The resulting solution was stirred at -78 °C for 30 min and then quenched with CF_3CO_2D (0.75 mL, 9.8 mmol, diluted to 5 mL with D_2O). The solution was allowed to warm to rt and stirred for 10 min at rt. The layers were partitioned and the aqueous layer was extracted with Et_2O (3 x 25 mL). The combined organic extracts were washed with $NaHCO_3$ (2 x 20 mL), H_2O (15 mL), brine (15 mL) and dried over $MgSO_4$. The volatiles were removed under vacuum and the residue was purified on a silica gel column with hexanes eluant to give **20-*d*** as a clear oil (230 mg, 1.95 mmol, 90% yield, > 98% deuterium incorporation as determined by ^{1}H NMR spectroscopy) ^{1}H NMR (500 MHz, $CDCl_3$) δ 1.91 (p, $^3J_{HH}$ = 7.5 Hz, 2H),

2.51 (t, $^{3}J_{HH}$ = 7.5 Hz, 4H), 3.38 (s, 0.02H). ^{13}C NMR (125 MHz, $CDCl_3$) δ19.4, 33.4, 81.1 (t, $^{1}J_{CD}$ = 38 Hz), 82.9 (t, $^{2}J_{CD}$ = 7 Hz), 134.1.

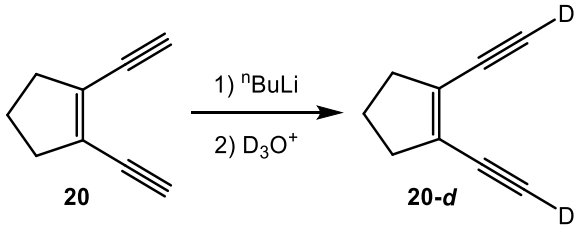

1,2-bis((*E*)-vinyl-2-*d*)cyclopent-1-ene (21-*E*-d$_2$): Enediyne **20** (100 mg, 0.86 mmol) dissolved in benzene (3 mL) was added to a suspension of $Cp_2Zr(H)(Cl)$ (443 mg, 1.72 mmol) in benzene (8 mL) in a side-arm flask equipped with a stir bar and rubber septum under dry N_2. The resulting light yellow suspension was allowed to stir for 1 h, whereupon the solution became homogeneous and red. The solution was then quenched with CF_3CO_2D (0.75 mL, diluted to 5 mL with D_2O) and allowed to stir for 5 min. The layers were partitioned and the aqueous layer was extracted with Et_2O (3 x 25 mL). The combined organic extracts were washed with $NaHCO_3$ (2 x 15 mL), H_2O (15 mL), brine (15 mL) and dried over $MgSO_4$. The volatiles were removed under vacuum and the residue was purified on a silica column with hexanes eluant to give **21-*E*-d$_2$** as a clear oil (84 mg, 0.7 mmol, 82% yield, 85% deuterium incorporation as determined by ^{1}H NMR spectroscopy) ^{1}H NMR (500 MHz, $CDCl_3$) δ1.87 (p, $^{3}J_{HH}$ = 7.5 Hz, 2H), 2.57 (t, $^{3}J_{HH}$ = 7.5 Hz, 4H), 5.12 (d, $^{3}J_{HH}$ = 17.2 Hz, 2.36H), 6.84 (d, $^{3}J_{HH}$ = 17.2 Hz, 2H). ^{13}C NMR ($CDCl_3$, 125 MHz) δ21.4; 33.3; 114.7 (t, $^{1}J_{CD}$ = 24.4 Hz); 130.3; 139.2. HRMS (APCI-TOFMS): Calcd for ($C_{19}H_{11}D_2$): 123.1138. Found: 123.1137.

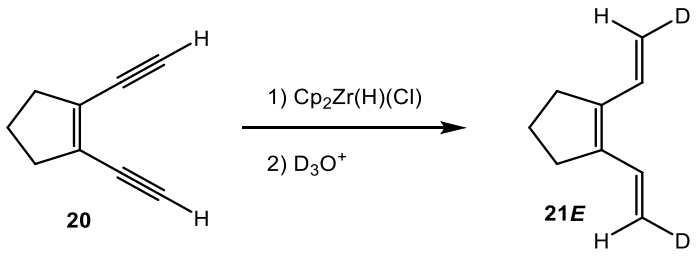

1,2-bis((*Z*)-vinyl-2-*d*)cyclopent-1-ene (21-*Z*-d$_2$): Enediyne **20-*d*** (100 mg, 0.86 mmol) dissolved in benzene (3 mL) was added to a suspension of $Cp_2Zr(H)(Cl)$ (443 mg, 1.72 mmol) in benzene (8 mL) in a side-arm flask equipped with a stir bar and rubber septum under dry N_2. The resulting light yellow suspension was allowed to stir for 1 h, whereupon the solution became homogeneous and red. The solution was then quenched with CF_3CO_2H (0.75 mL, diluted to 5 mL with H_2O) and allowed to stir for 5 min. The layers were partitioned and the aqueous layer was extracted with Et_2O (3 x 25 mL). The combined organic extracts were washed with $NaHCO_3$ (2 x 15 mL), H_2O (15 mL), brine (15 mL) and dried over $MgSO_4$. The volatiles were removed under vacuum and the residue was purified on a silica gel column with hexanes eluant to give **21-*Z*-d$_2$** as a clear oil (84 mg, 0.7 mmol, 82% yield, > 98% deuterium incorporation as determined by ^{1}H NMR spectroscopy) ^{1}H NMR (500 MHz, $CDCl_3$) δ 1.87 (p, $^3J_{HH}$ = 7.5 Hz, 2H), 2.57 (t, $^3J_{HH}$ = 7.5 Hz, 4H), 5.11 (d, $^3J_{HH}$ = 10.4 Hz, 2.02H), 6.84 (dt, $^3J_{HH}$ = 17.2 Hz, $^3J_{HD}$ = 2.3 Hz, 2H). ^{13}C NMR ($CDCl_3$, 125 MHz) δ 21.4; 33.3; 114.7 (t, $^1J_{CD}$ = 24.4 Hz); 130.3; 139.2. HRMS (APCI-TOFMS): Calcd for ($C_{19}H_{11}D_2$): 123.1138. Found: 123.1137.

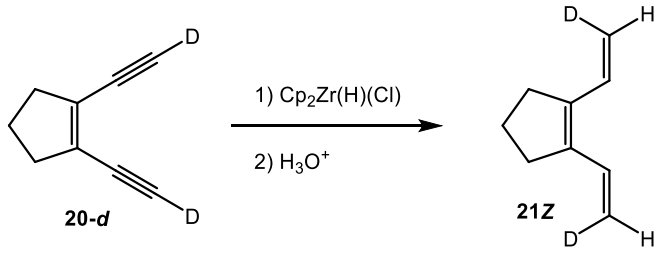

(*Z*)-1-(2-methylprop-1-en-1-yl)-2-(prop-1-en-1-yl)cyclopent-1-ene (**24**): Isopropyl triphenyl phosphonium bromide (500 mg, 1.3 mmol) was weighed into an oven-dried 100 mL side-arm flask under N_2 and suspensed in dry THF (30 mL). The suspension was cooled on an ice water bath and then ^{n}BuLi (1 mL, 1.25 M solution in hexanes, 1.25 mmol) was added dropwise. The resulting solution was stirred at 0 °C for 45 min and then aldehyde **3** (150 mg, 1.1 mmol, diluted in 5 mL THF) was added dropwise. The resulting solution was stirred at 0 °C for 30 min and then warmed to rt. The solution was stirred at rt for 2 h and then silica gel was added to the solution and the volatiles were removed under vacuum. The reaction mixture absorbed on silica gel was then placed on top of a silica gel column and the product separated and purified with hexanes elaunt to give **23** as a clear oil (140 mg, 0.86 mmol, 78% yield) ^{1}H NMR (500 MHz, $CDCl_3$) δ 1.72 (s, 3H); 1.76 (d, $^{3}J_{HH}$ = 11. Hz, 3H); 1.79 (s, 3H); 1.83 (p, $^{3}J_{HH}$ = 7.2 Hz, 2H), 2.54 (t, $^{3}J_{HH}$ = 7.2 Hz, 2H), 2.64 (t, $^{3}J_{HH}$ = 7.2 Hz, 2H); 5.44 (m, 1H); 5.87 (s, 1H); 6.06 (d, $^{3}J_{HH}$ = 11.8 Hz, 1H) ^{13}C NMR ($CDCl_3$, 125 MHz) δ 20.3; 23.8; 27.6; 29.9; 36.2; 36.3; 121.2; 124.8; 125.7; 134.6; 136.6; 139.1.

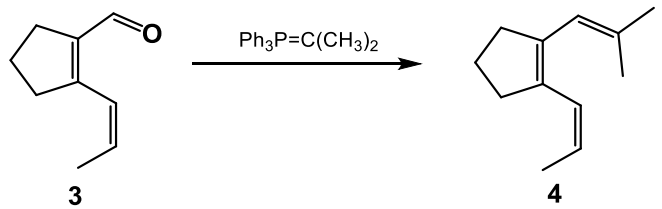

(η^5-cyclopentadienyl)(η^6-1,2-di((*Z*)-styryl)cyclopent-1-ene)ruthenium(II) hexafluorophosphate (25): A solution of **12** (18 mg, 66 μmol) in $CDCl_3$ (1 mL) was added to a vial containing **19** (20.5 mg, 47.2 μmol) via syringe. The solution was swirled to mix and dissolve all of the solids. The solution was allowed to stand at 0 °C for 1 h, after which time orange block crystals formed on the bottom of the vial. The mother liquor was decanted and the crystals were dried under vacuum for 1 h to give **24** as orange crystalline solid (14.5 mg, 38.8 μmol, 83% yield). ^{1}H NMR (acetone·d_6, 500 MHz) δ 4.10 (d, $^3J_{HH}$ = 10.3 Hz, 2H); 5.00 (s, 5H); 6.92 (d, $^3J_{HH}$ = 10.3 Hz, 2H); 7.41 (t, $^3J_{HH}$ = 7.6 Hz, 4H); 7.49 (t, $^3J_{HH}$ = 7.6 Hz, 2H); 7.88 (d, $^3J_{HH}$ = 7.6 Hz, 4H). ^{13}C NMR (acetone·d_6, 125 MHz) δ 24.3 (t, $^1J_{CH}$ = 134.8 Hz); 39.8 (t, $^1J_{CH}$ = 131.8 Hz); 77.7 (d, $^1J_{CH}$ = 164.7 Hz); 83.0 (d, $^1J_{CH}$ = 165.8 Hz); 89.7 (dp, $^1J_{CH}$ = 183.1 Hz; 6.8 Hz); 119.0 (s); 127.9 (dq, $^1J_{CH}$ = 157.3 Hz; 5.0 Hz); 129.4 (t, $^1J_{CH}$ = 161.9 Hz; 7.7 Hz); 130.4 (t, $^1J_{CH}$ = 160.8 Hz; 7.8 Hz); 140.9 (s). HRMS(ESI): Calcd for ($C_{26}H_{25}Ru$): 439.1001. Found 439.1002.

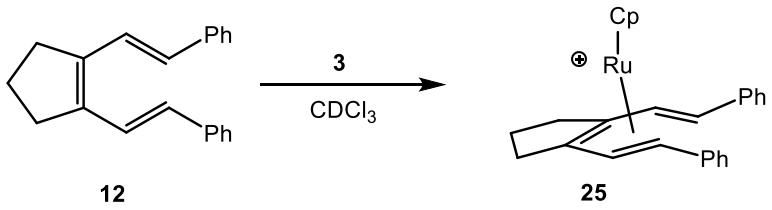

12 **25**

(η^5-pentamethylcyclopentadienyl)(η^6-indane)ruthenium(II) hexafluorophosphate (28): A solution of indane (100 μL, 0.81 mmol) in DCM (5 mL) was added to a vial containing **4** (100 mg, 0.2 mmol) under an argon balloon. The resulting solution was allowed to stir at rt for 1 h and then the solution was

concentrate under vacuum to approximately 0.5 mL. Then Et_2O (10 mL) was added to precipitate out **28** and the resulting suspension was filtered through a Celite plug, which was rinsed with Et_2O (2 x 2 mL). Then the Celite was rinsed with DCM (3 x 3 mL) which was collected in a fresh vial. The volatiles were removed under vacuum to give **28** as a white powder (92 mg, 0.18 mmol, 92% yield). ^{1}H NMR (CD_2Cl_2, 500 MHz) δ 1.68 (m, 1H); 1.90 (s, 15H); 2.19 (m, 1H); 2.53-2.58 (m, 2H); 2.86-2.93 (m, 2H); 5.57 (dd, $^3J_{HH}$ = 4.2 Hz, $^4J_{HH}$ = 2.3 Hz, 2H); 5.72 (dd, $^3J_{HH}$ = 4.2 Hz, $^4J_{HH}$ = 2.3 Hz, 2H). ^{13}C NMR (CD_2Cl_2, 125 MHz) δ 10.6; 23.5; 29.8; 84.3; 86.0; 96.0; 107.6. HRMS (ESI-TOFMS): Calcd for ($C_{19}H_{25}Ru$): 355.1000. Found: 355.0999.

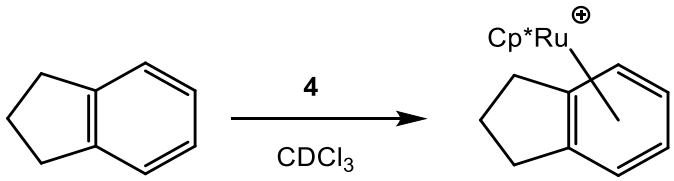

28

3-6.3 NMR-Scale reactions

Reaction of 21 with 4. Complex **4** (7.5 mg, 15 μmol) and **21** (3 mg, 24 μmol) were weighed into an oven-dried J. Young tube on the bench. The tube was closed with a Teflon needle valve and placed on the high-vacuum line. The tube was cooled on a dry ice/IPA bath and opened to vacuum. Then $CDCl_3$ (750 μL) was distilled into the tube under static vacuum, the tube was closed and the solution was warmed to rt on a H_2O bath. A ^{1}H NMR spectrum was collected and the mixture was left to react

overnight. A second ^{1}H NMR spectrum was collected, which showed the appearance of **28** in 90% NMR yield.

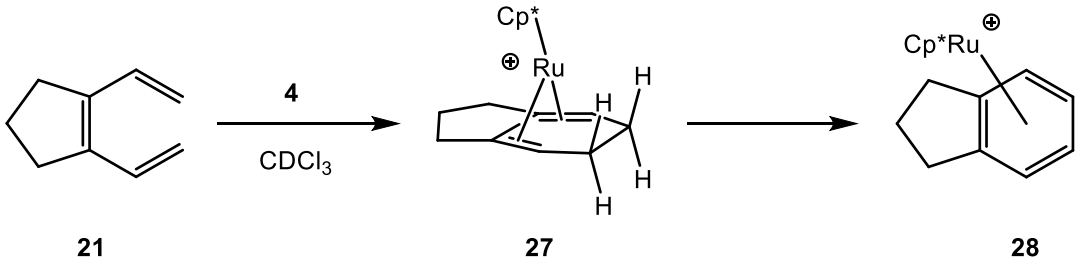

21 **27** **28**

Reaction of 21-*E*-d$_2$ with 4. Complex **4** (7.5 mg, 15 μmol) and **21-*E*-d$_2$** (3 mg, 24 μmol) were weighed into an oven-dried J. Young tube on the bench. The tube was closed with a Teflon needle valve and placed on the high-vacuum line. The tube was cooled on a dry ice/IPA bath and opened to vacuum. Then $CDCl_3$ (750 μL) was distilled into the tube under static vacuum, the tube was closed and the solution was warmed to rt on a H_2O bath. A ^{1}H NMR spectrum was collected and the mixture was left to react overnight. A second ^{1}H NMR spectrum was collected, which showed the appearance of **28** in 90% NMR yield. ^{1}H NMR (CD_2Cl_2, 500 MHz) δ 1.68 (m, 1H); 1.90 (s, 15H); 2.19 (m, 1H); 2.53-2.58 (m, 2H); 2.86-2.93 (m, 2H); 5.57 (dd, $^3J_{HH}$ = 4.2 Hz, $^4J_{HH}$ = 2.3 Hz, 1.5H); 5.72 (dd, $^3J_{HH}$ = 4.2 Hz, $^4J_{HH}$ = 2.3 Hz, 1.5H). ^{13}C NMR (CD_2Cl_2, 125 MHz) δ 10.6; 23.5; 29.8; 84.3 (m); 86.0 (m); 96.0; 107.6. HRMS (APCI-TOFMS): Calcd for ($C_{19}H_{25}D_1Ru$): 357.1140. Found: 357.1125.

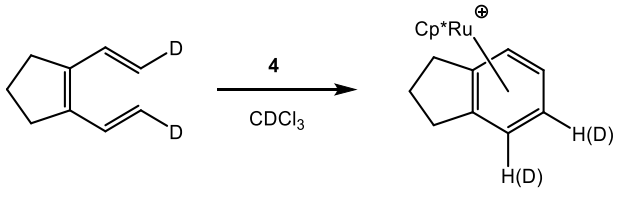

21-*E*-d$_2$ **28**

Reaction of 21-*Z*-d$_2$ with 4. Complex **4** (12.5 mg, 25 μmol) and **21-*Z*-d$_2$** (4.5 mg, 37 μmol) were weighed into an oven-dried J. Young tube on the bench. The tube was closed with a Teflon needle valve and placed on the high-vacuum line. The tube was cooled on a dry ice/IPA bath and opened to vacuum. Then $CDCl_3$ (750 μL) was distilled into the tube under static vacuum, the tube was closed and the solution was warmed to rt on a H_2O bath. A ^{1}H NMR was collected and the mixture was left to react overnight. A second ^{1}H NMR spectrum was collected, which showed the appearance of **28** in 90% NMR yield. ^{1}H NMR (CD_2Cl_2, 500 MHz) δ 1.68 (m, 1H); 1.90 (s, 15H); 2.19 (m, 1H); 2.53-2.58 (m, 2H); 2.86-2.93 (m, 2H); 5.57 (dd, $^3J_{HH}$ = 4.2 Hz, $^4J_{HH}$ = 2.3 Hz, 2H); 5.72 (dd, $^3J_{HH}$ = 4.2 Hz, $^4J_{HH}$ = 2.3 Hz, 1H). ^{13}C NMR (CD_2Cl_2, 125 MHz) δ 10.6; 23.5; 29.8; 84.3 (m); 86.0; 96.0; 107.6. HRMS (APCI-TOFMS): Calcd for ($C_{19}H_{25}D_1Ru$): 356.1062. Found: 356.1083.

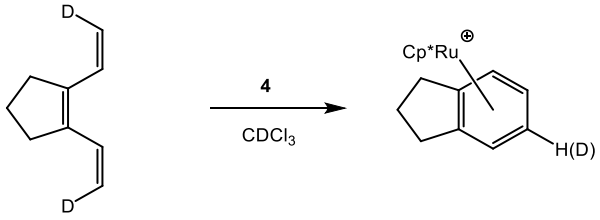

21-*Z*-d$_2$ **28**

Reaction of 15 with 3. Complex **3** (12 mg, 24 μmol) and **15** (7.2 mg, 26 μmol) were weighed into an oven-dried J. Young tube on the bench. The tube was closed with a Teflon needle valve and placed on the high-vacuum line. The tube was cooled on a dry ice/IPA bath and opened to vacuum. Then $CDCl_3$ (750 μL) was distilled into the tube under static vacuum, the tube was closed and the solution was warmed to rt on a H_2O bath. A ^{1}H NMR spectrum was collected and the mixture was left to react

overnight. A second ^{1}H NMR spectrum was collected, which showed the appearance of **28** in 90% NMR yield. The product exhibited spectroscopic properties identical to those reported in literature.[4]

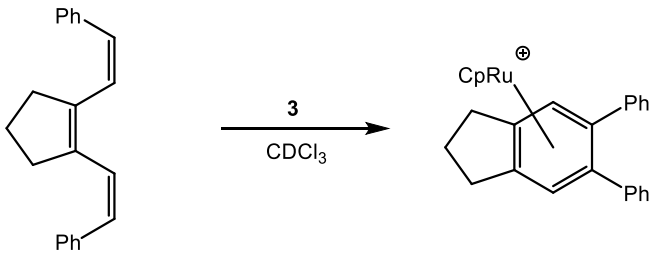

15 **26**

Reaction of 24 with 4. Complex **4** (12 mg, 24 μmol) and **24** (5 mg, 30 μmol) were weighed into an oven-dried J. Young tube on the bench. The tube was closed with a Teflon needle valve and placed on the high-vacuum line. The tube was cooled on a dry ice/IPA bath and opened to vacuum. Then $CDCl_3$ (750 μL) was distilled into the tube under static vacuum, the tube was closed and the solution was warmed to rt on a H_2O bath. A ^{1}H NMR spectrum was collected and the mixture was left to react overnight. A second ^{1}H NMR spectrum was collected, which showed the appearance of **28** in 90% NMR yield. The product exhibited spectroscopic properties identical to those reported in literature.[4]

A second tube was setup as above, then after 15 mins the volatiles were removed under vacuum and fresh $CDCl_3$ (750 μL) was distilled into the tube. A ^{1}H NMR spectrum was taken showing resonances associated with **30**. (**30**) ^{1}H NMR ($CDCl_3$, 500 MHz) δ -8.46 (d, $^2J_{HH}$ = 19.1 Hz, 1H); 0.40 (s, 3H); 1.15 (s, 3H); 1.38 (s, 3H);

1.79 (s, 15H); 2.07 (d, $^{2}J_{HH}$ = 19.1 Hz, 1H), 4.81 (s, 1H). ^{13}C NMR ($CDCl_3$, 125 MHz) δ9.9; 17.5; 23.0; 26.8; 29.1; 29.9; 31.6; 49.1; 79.9; 80.8; 86.0; 90.3; 94.8; 98.9; 114.4.

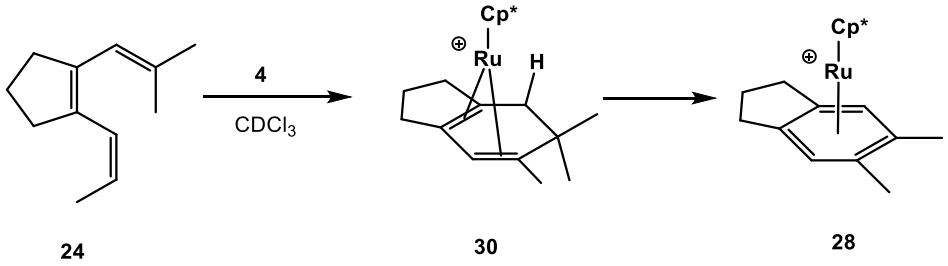

24 **30** **28**

3-6.4 ^{1}H and ^{13}C NMR Spectroscopic Data

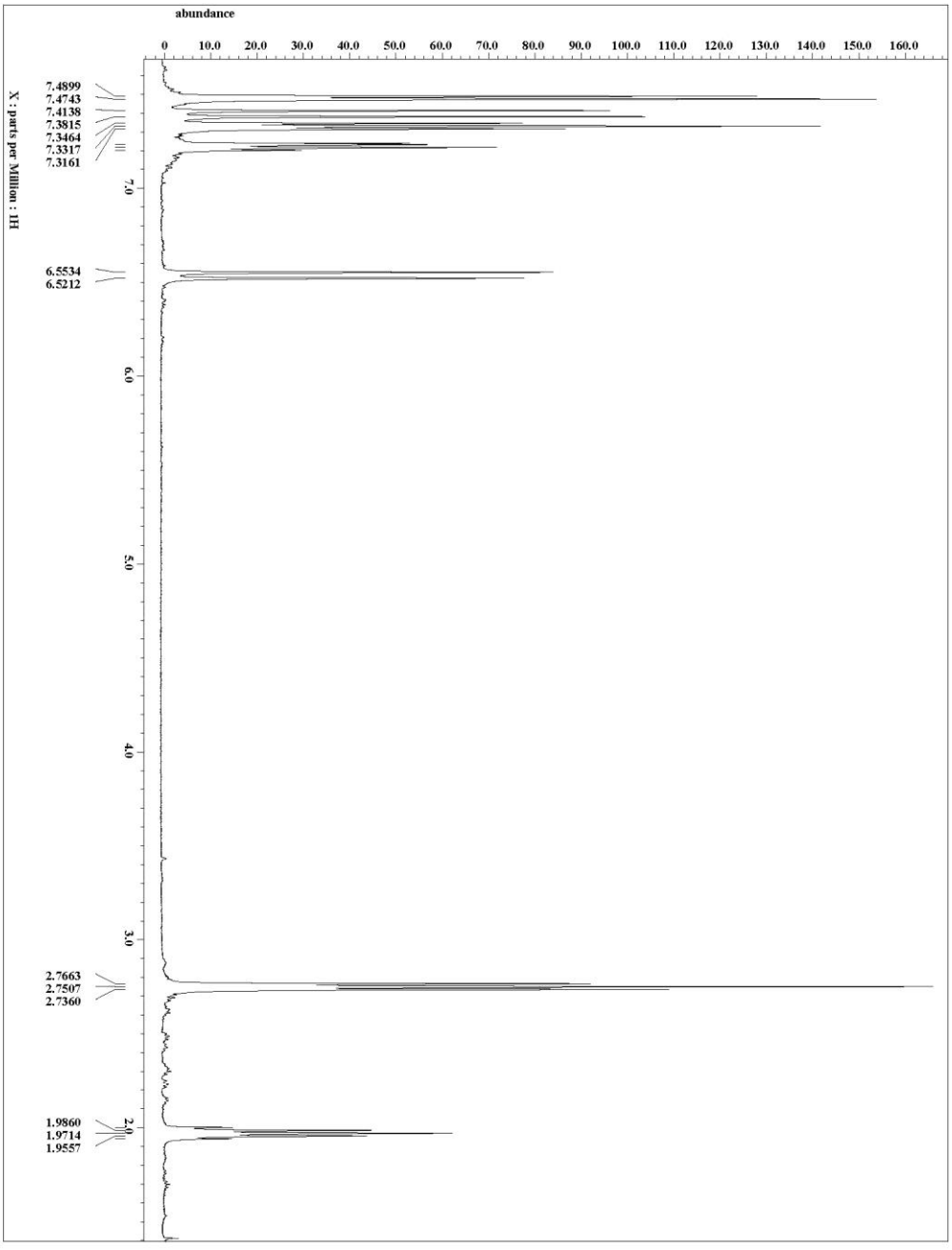

Figure 3-8. 15 ^{1}H NMR spectrum (500 MHz, $CDCl_3$).

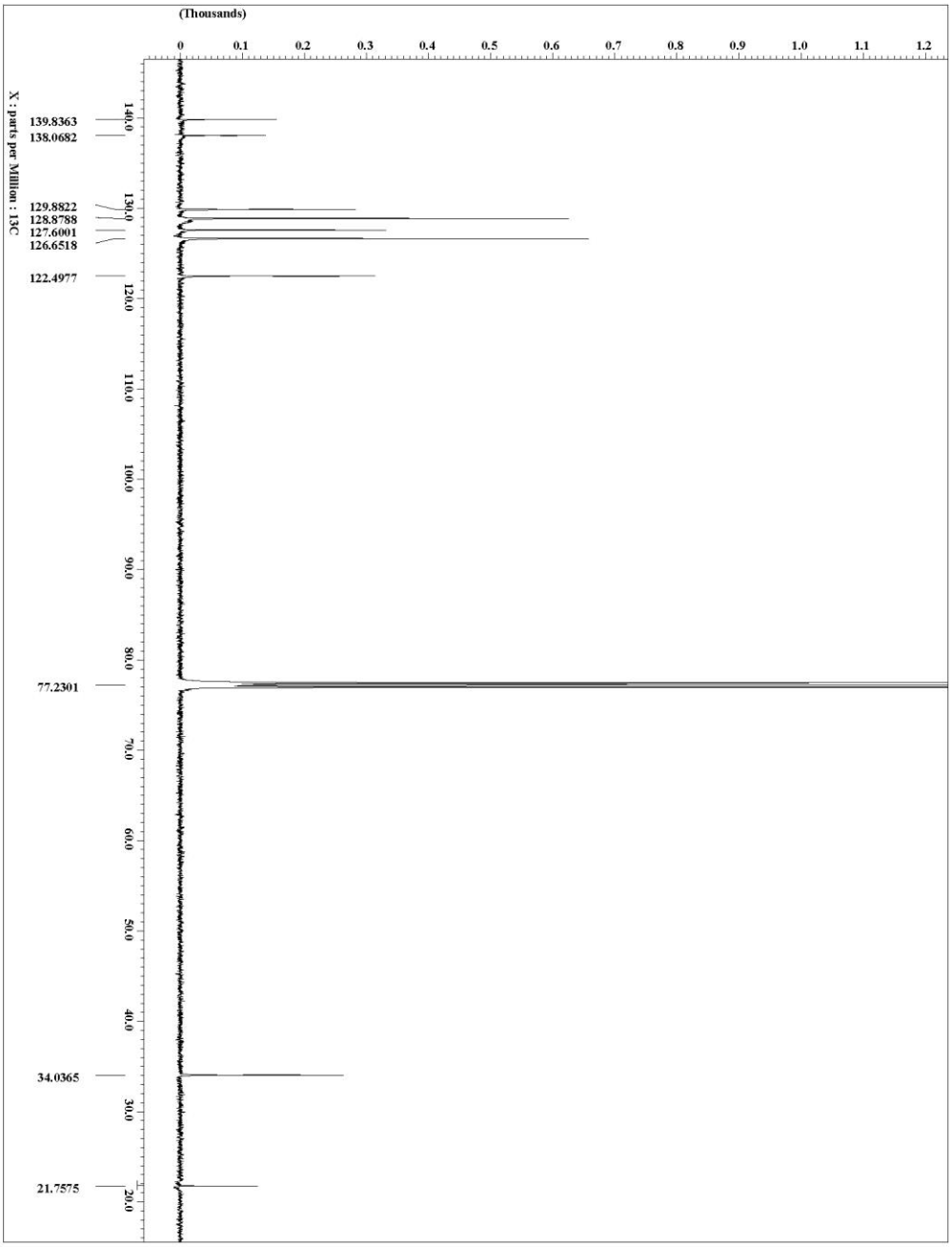

Figure 3-9. 15 ^{13}C NMR spectrum (125 MHz, $CDCl_3$).

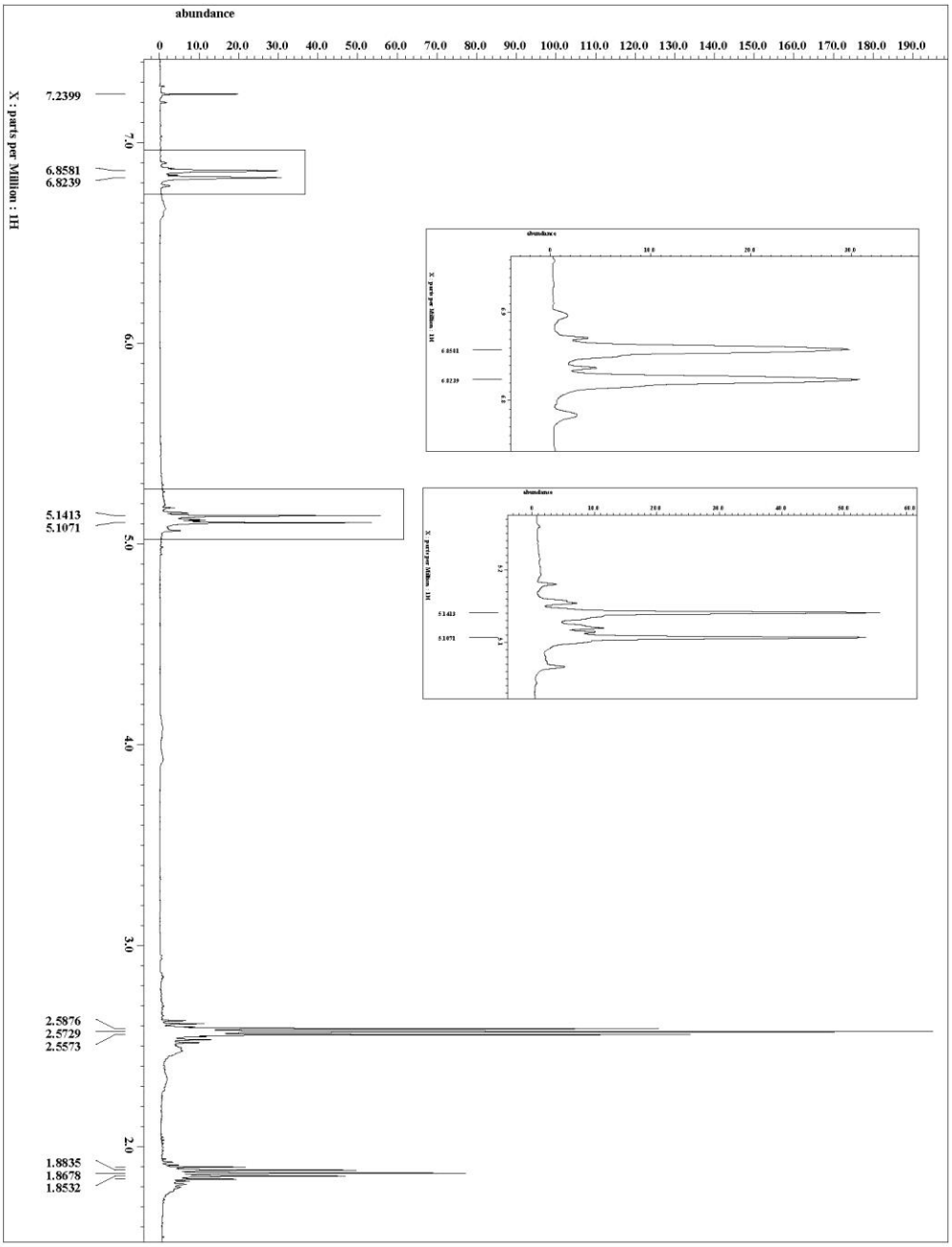

Figure 3-10. 21-*E*-d$_2$ ^{1}H NMR spectrum (500 MHz, $CDCl_3$).

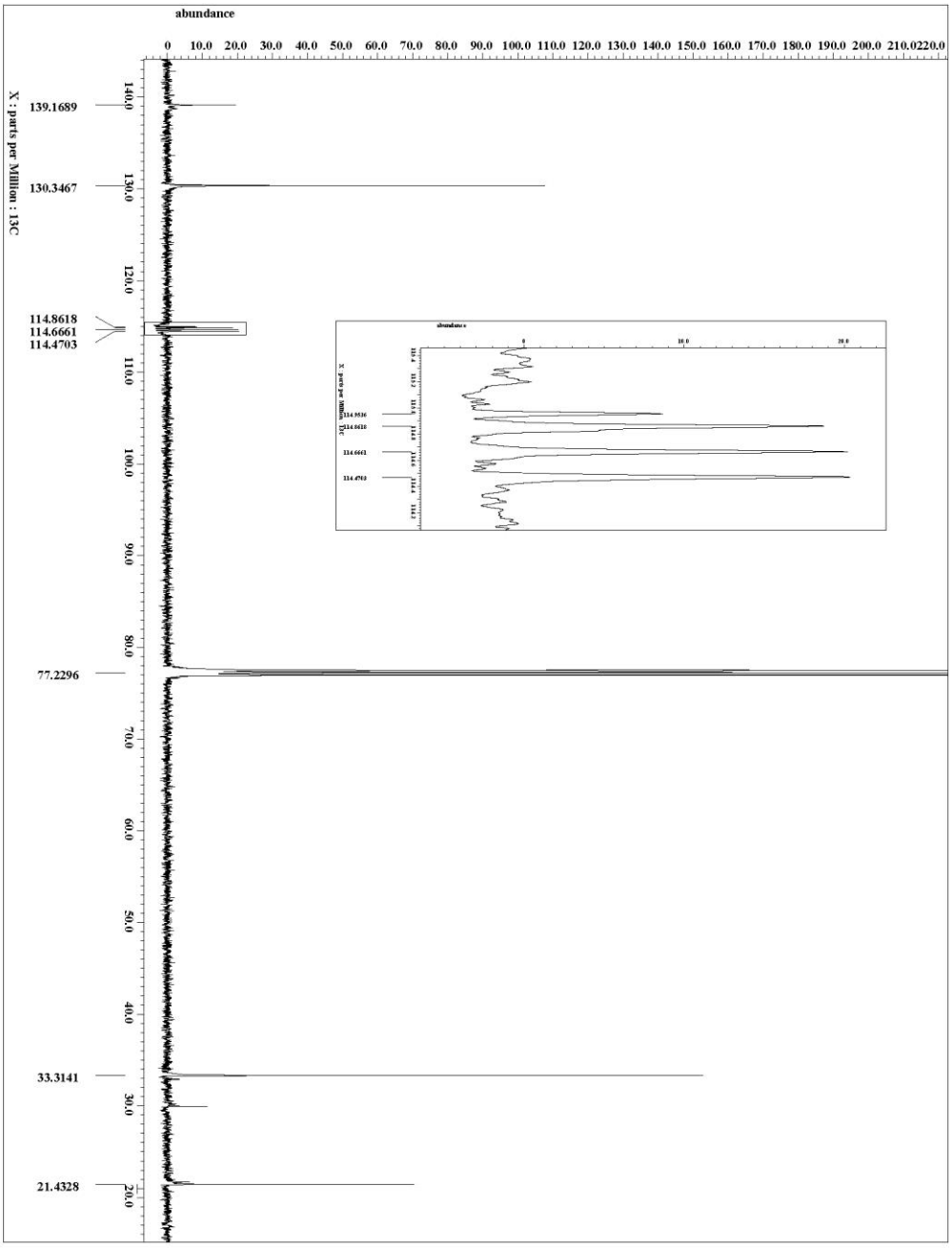

Figure 3-11. 21-*E*-d$_2$ ^{13}C NMR spectrum (125 MHz, $CDCl_3$).

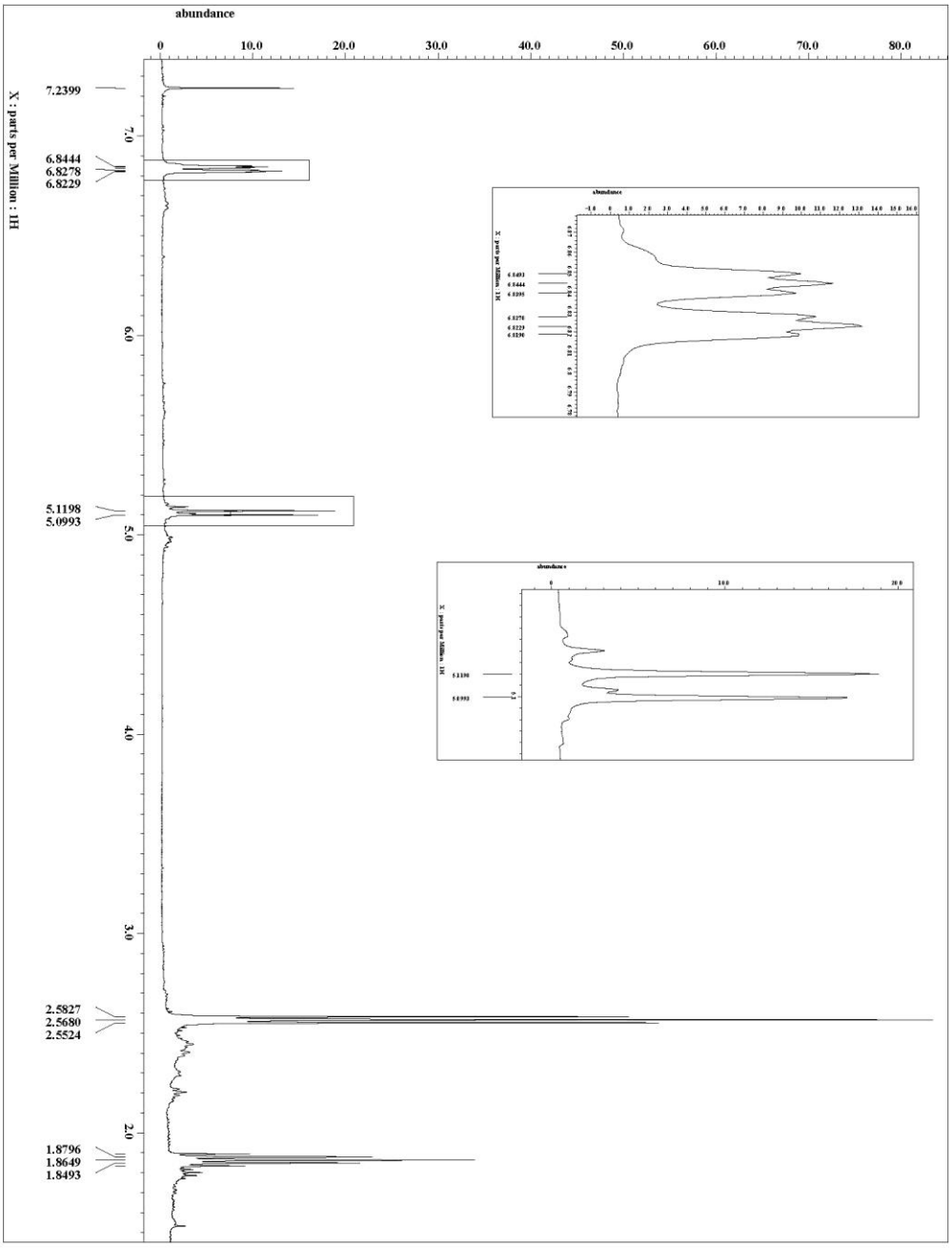

Figure 3-12. 21-*Z*-d$_2$ ^{1}H NMR spectrum (500 MHz, $CDCl_3$).

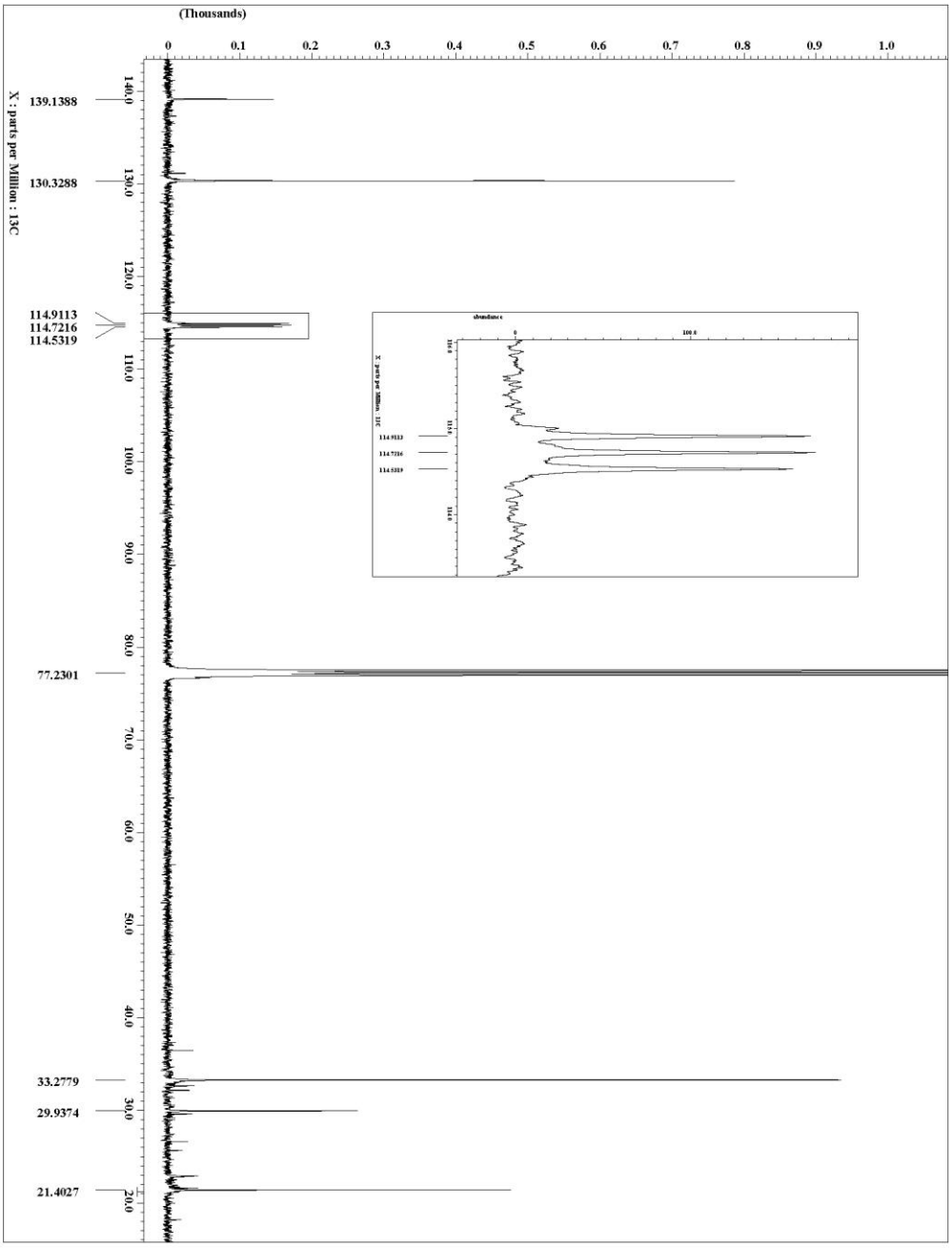

Figure 3-13. 21-*Z*-d$_2$ ^{13}C NMR spectrum (125 MHz, $CDCl_3$).

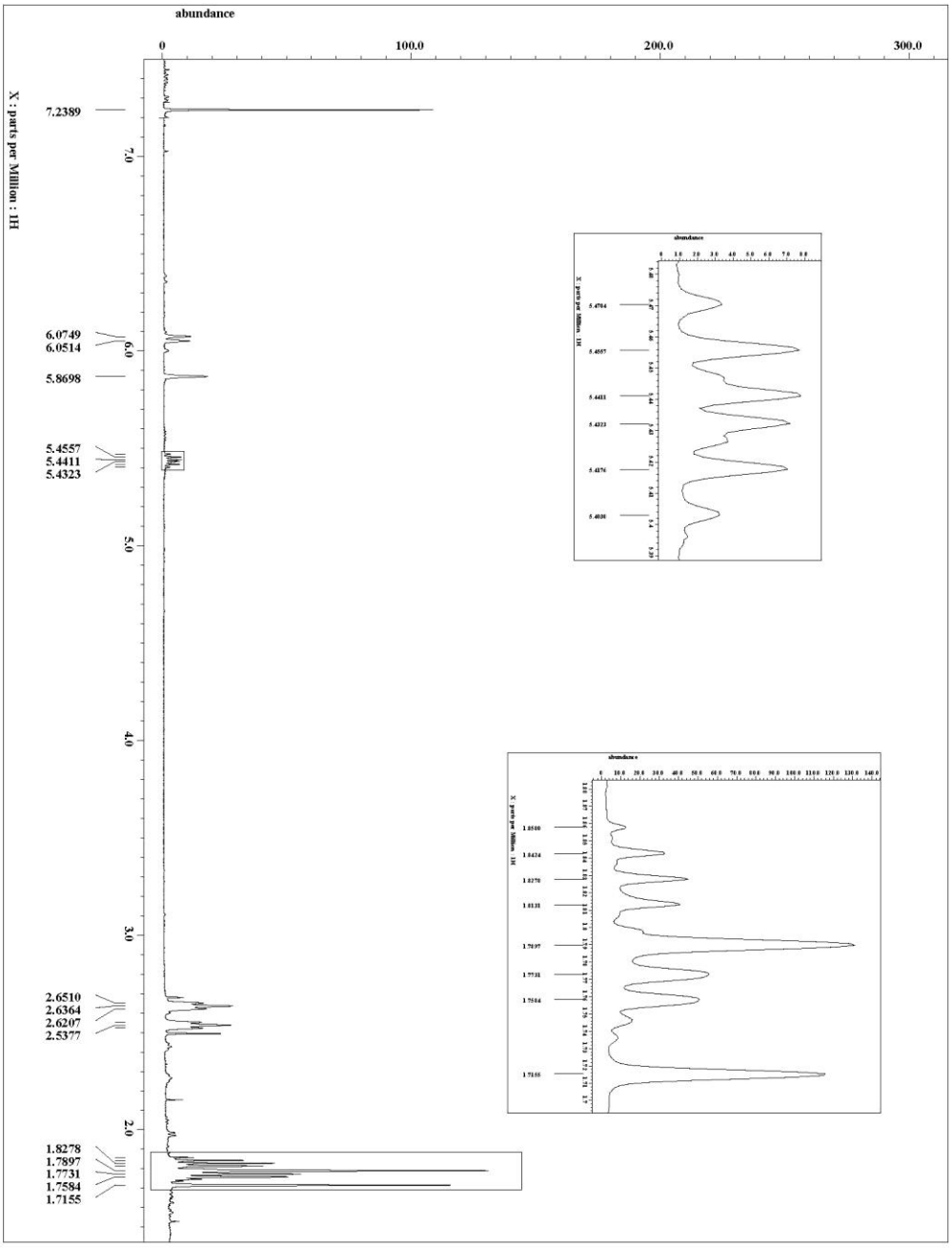

Figure 3-14. 24 ^{1}H NMR spectrum (500 MHz, $CDCl_3$).

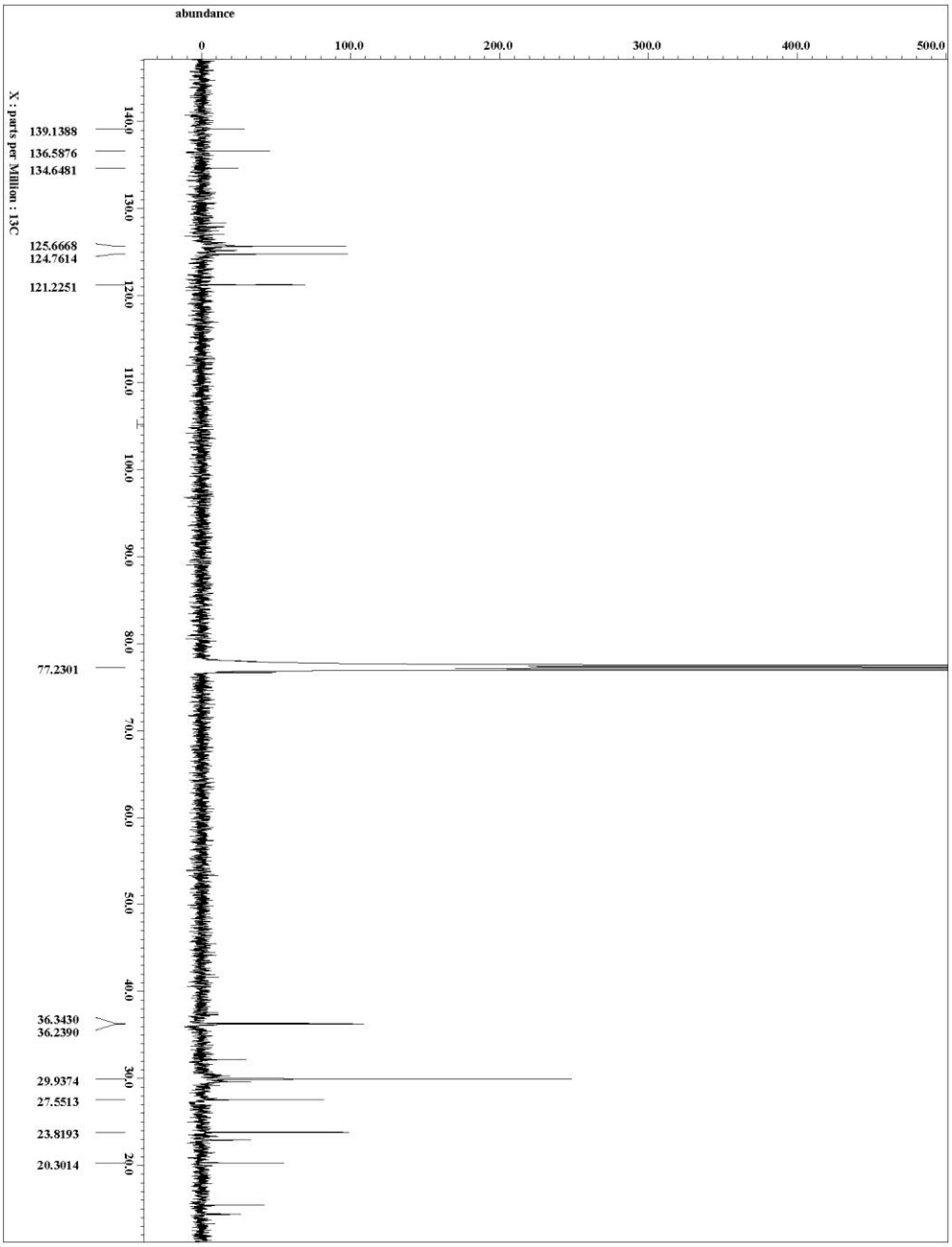

Figure 3-15. 24 ^{13}C NMR spectrum (125 MHz, $CDCl_3$).

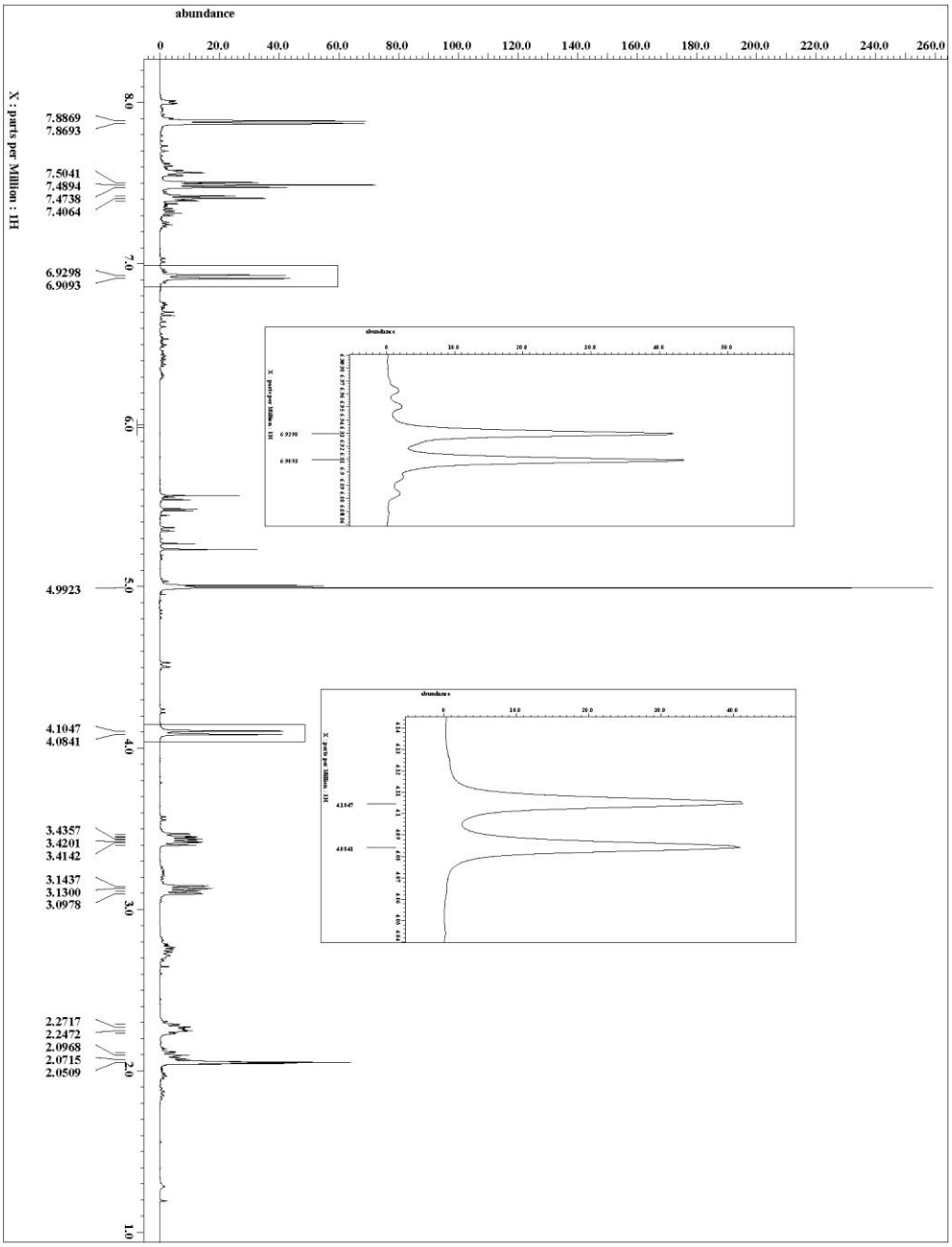

Figure 3-16. 25 ^{1}H NMR spectrum (500 MHz, acetone-d_6).

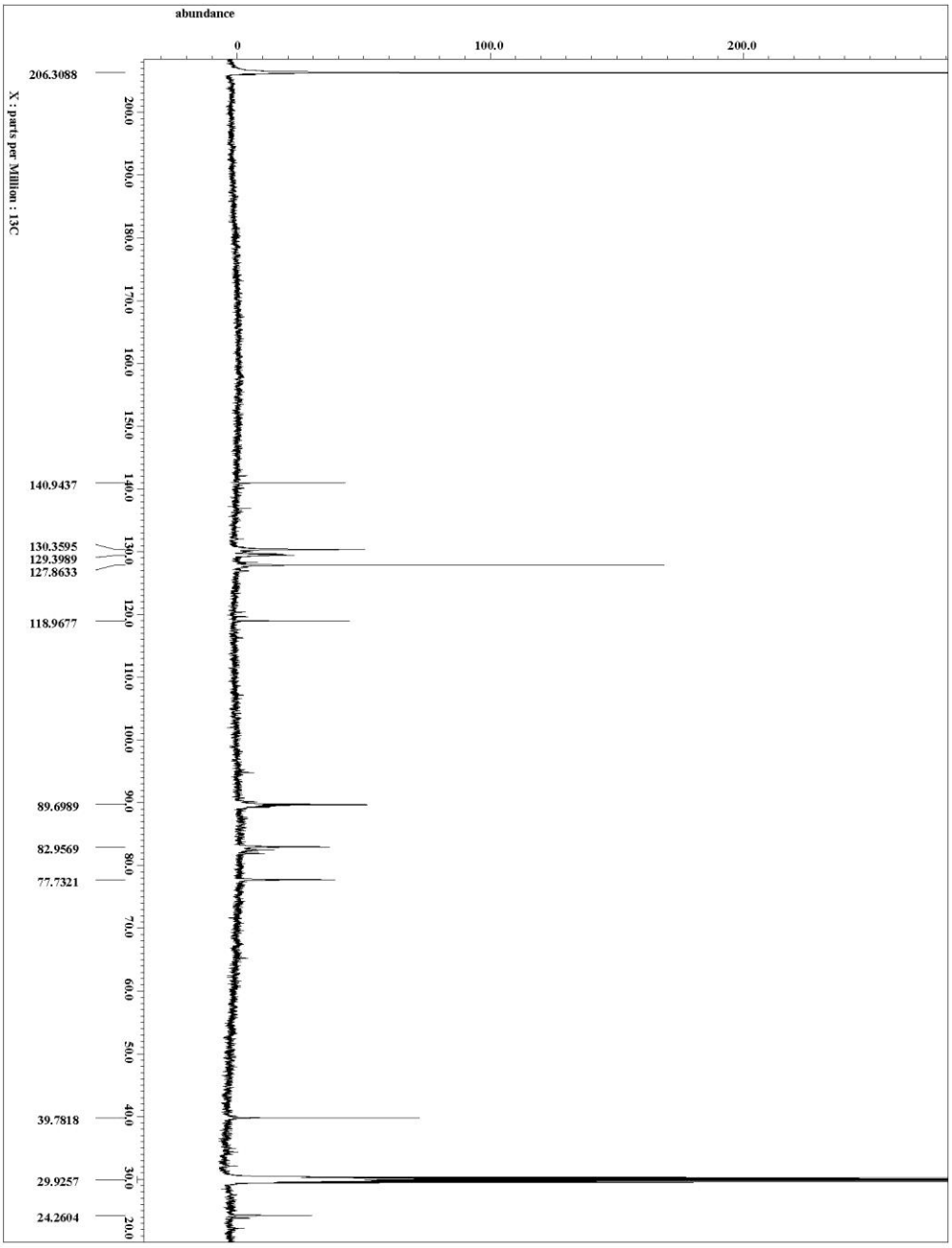

Figure 3-17. 25 ^{13}C NMR spectrum (125 MHz, acetone-d_6).

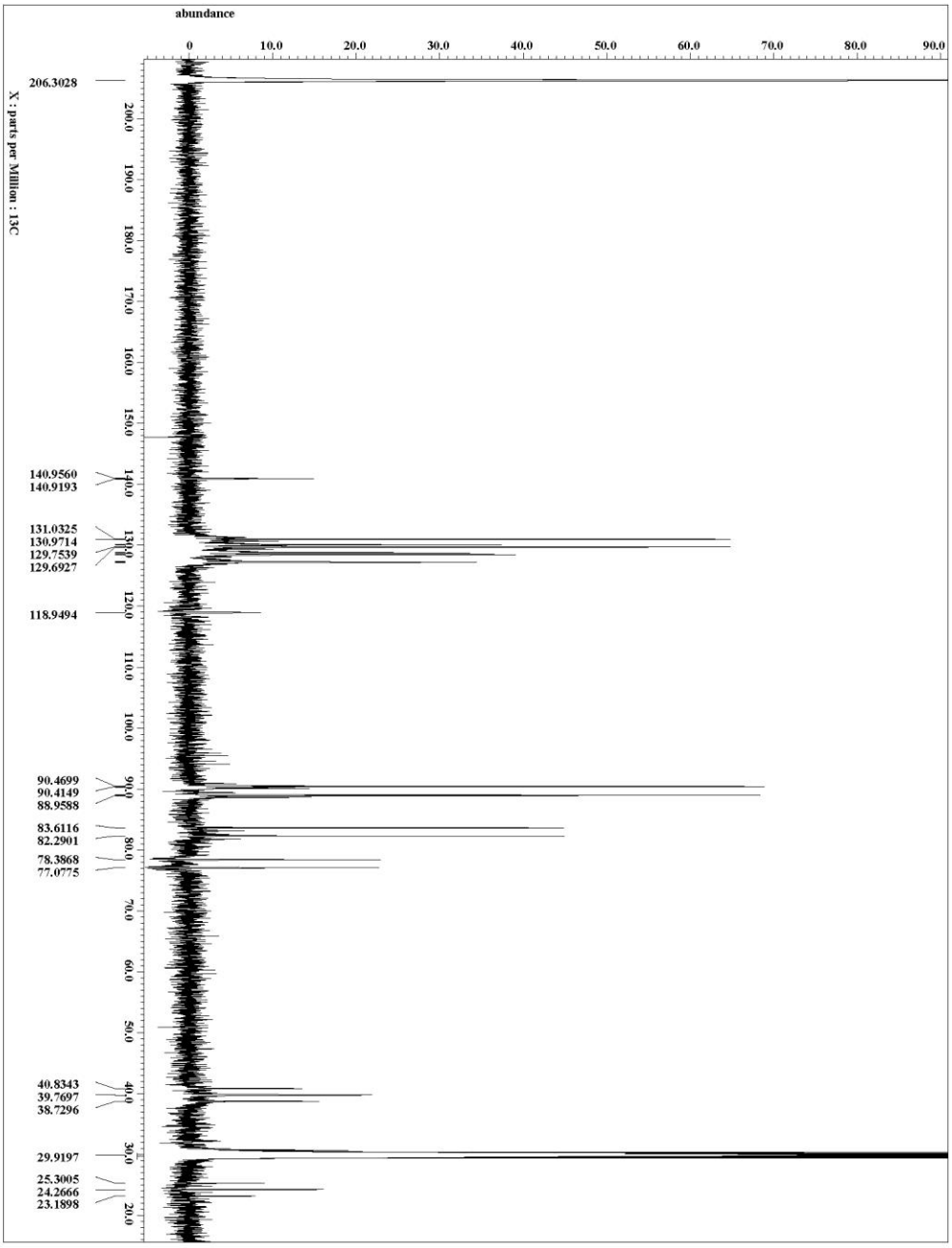

Figure 3-18. 25 $^{13}C\{^{1}H\}$ NMR spectrum (125 MHz, acetone-d_6).

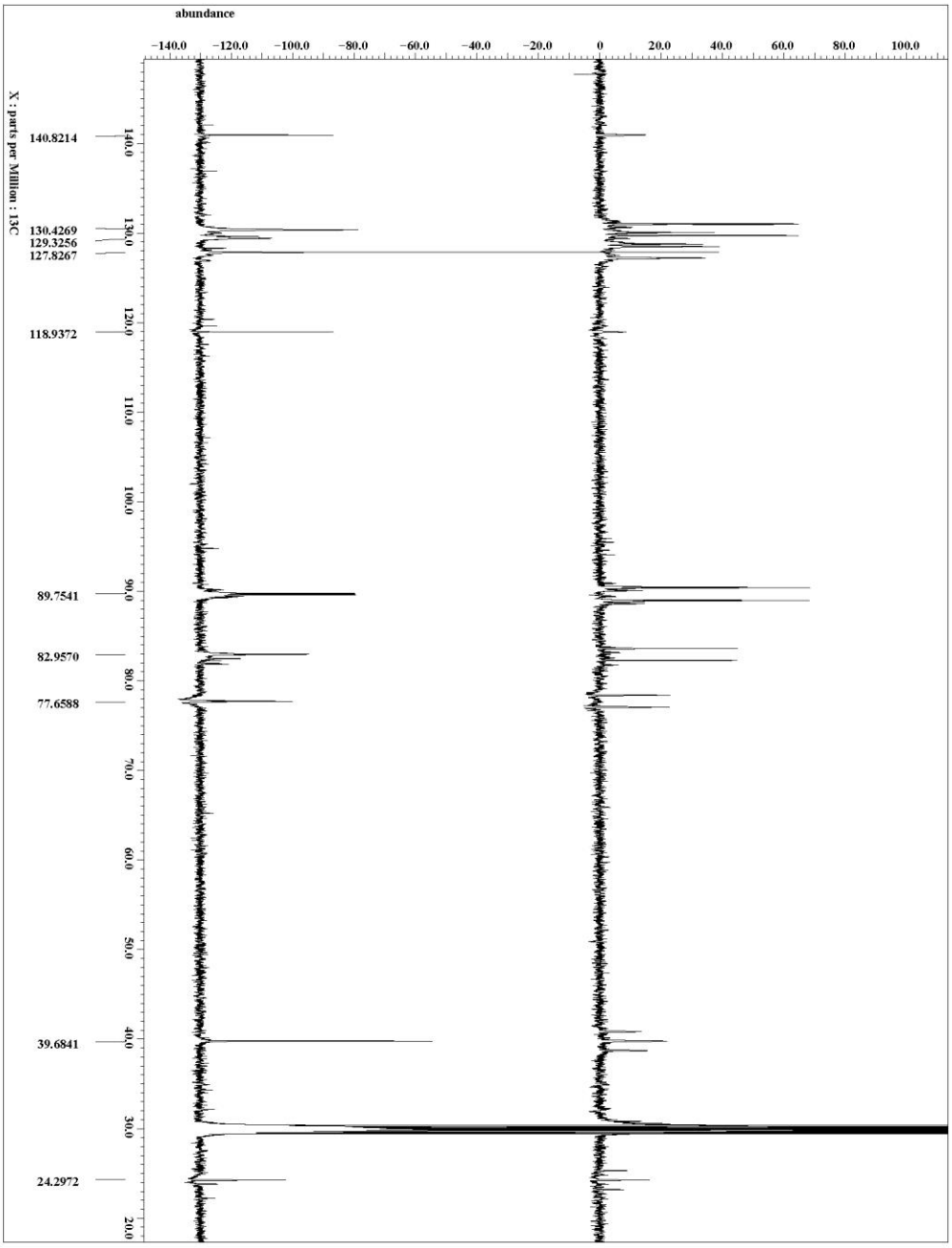

Figure 3-19. 25 ^{13}C NMR spectrum (top) and ^{13}C{^{1}H} NMR spectrum (bottom) (125 MHz, acetone-d_6).

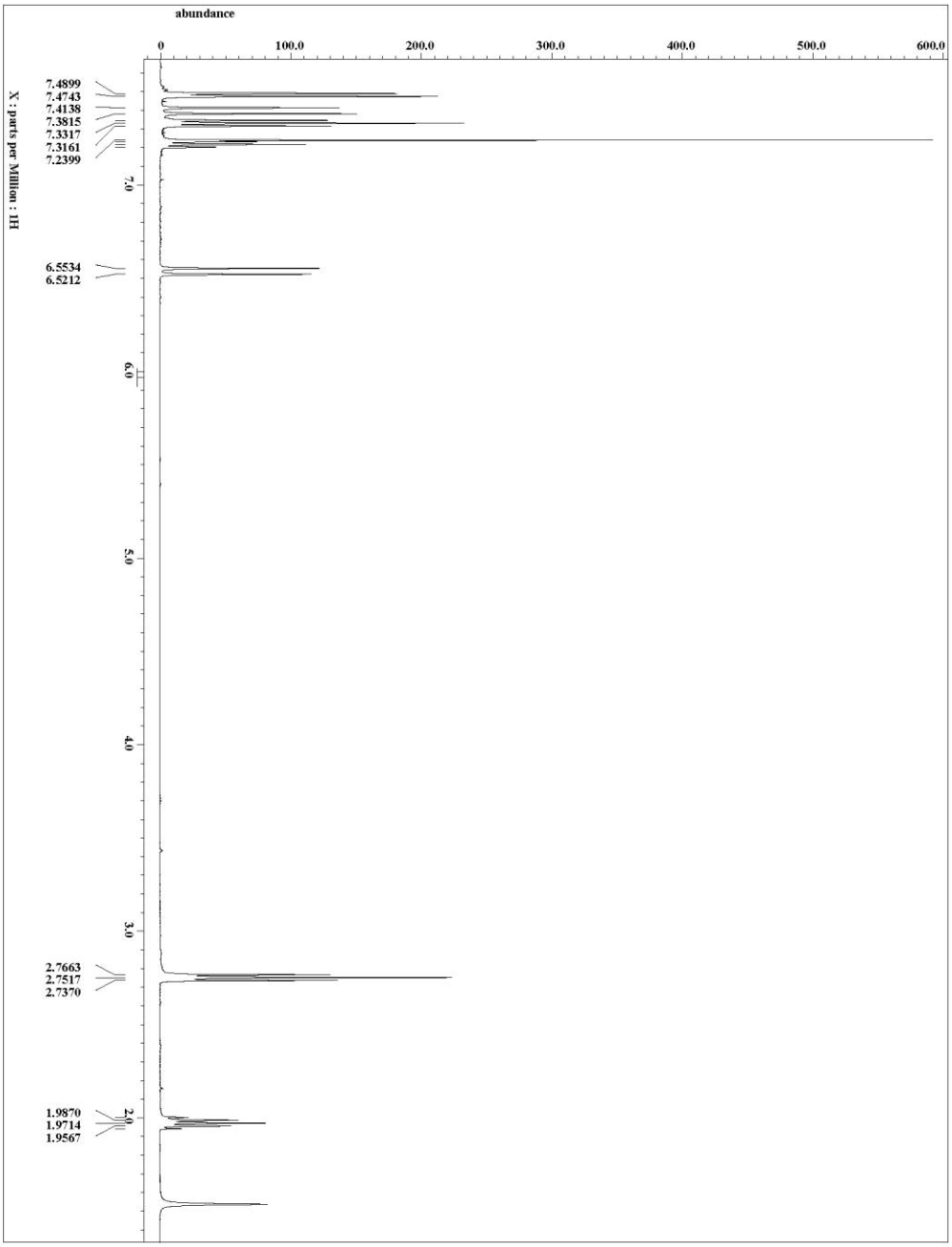

Figure 3-20. 12 ^{1}H NMR spectrum (500 MHz, $CDCl_3$).

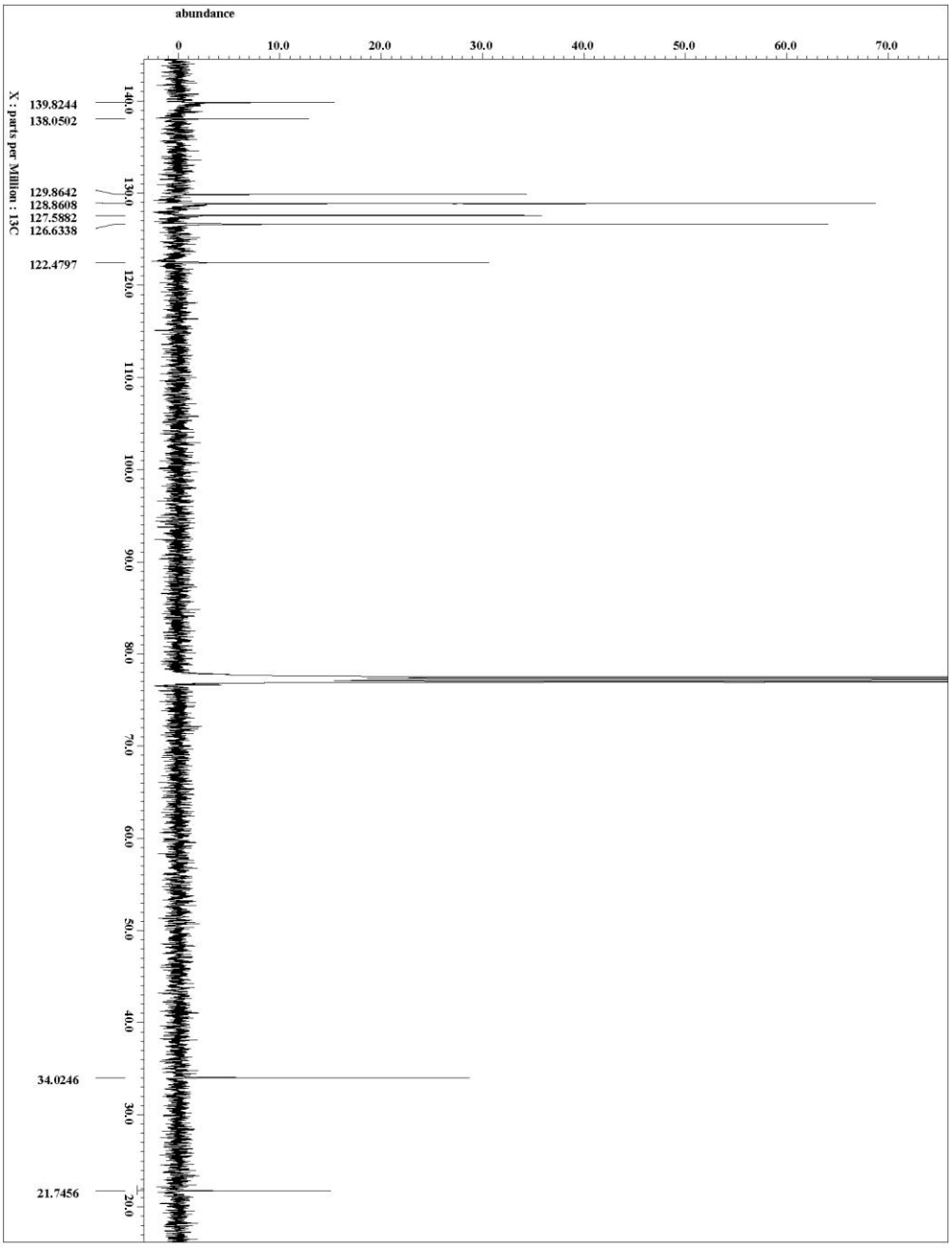

Figure 3-21. 12 ^{13}C NMR spectrum (125 MHz, $CDCl_3$).

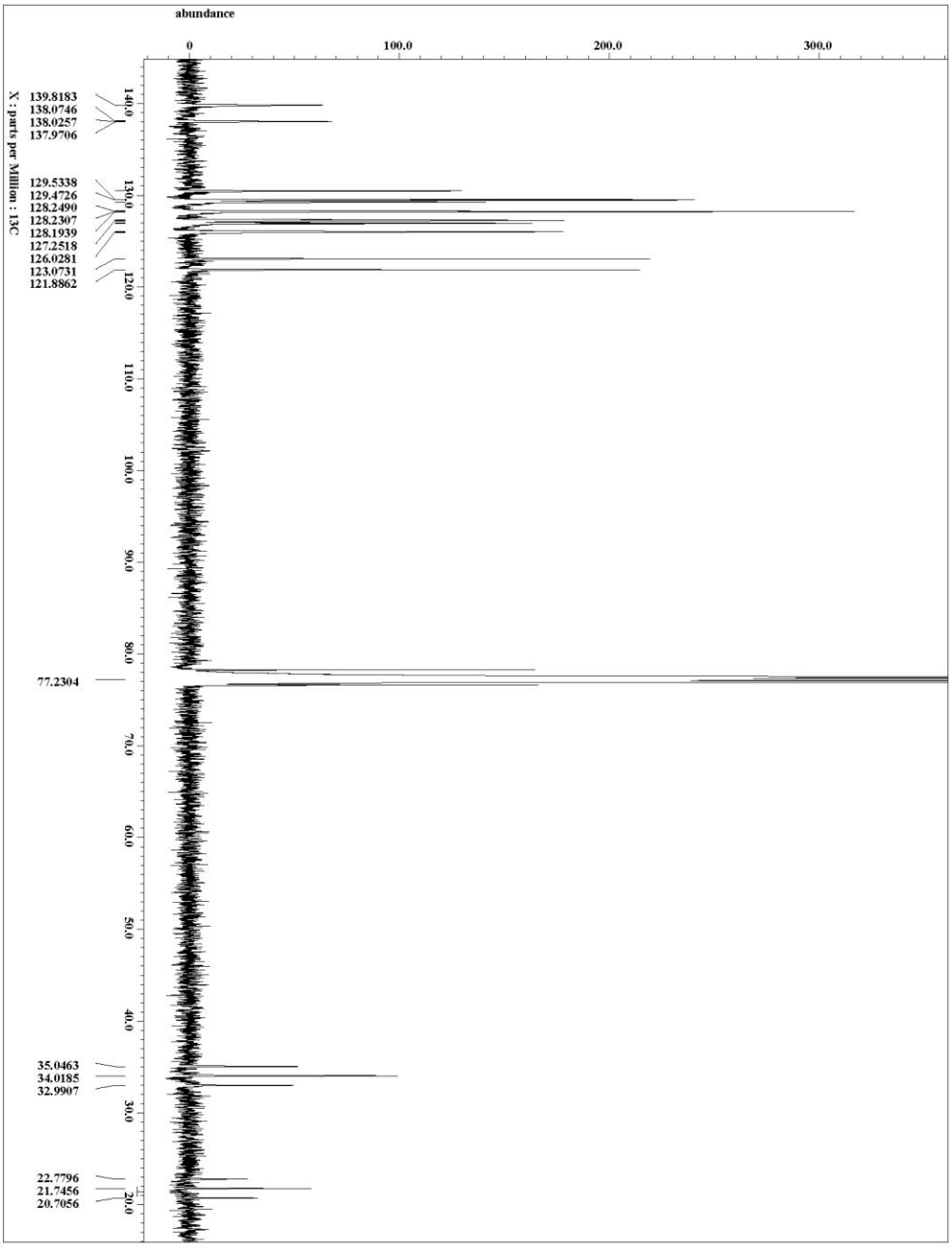

Figure 3-22. 12 $^{13}C\{^{1}H\}$ NMR spectrum (125 MHz, $CDCl_3$).

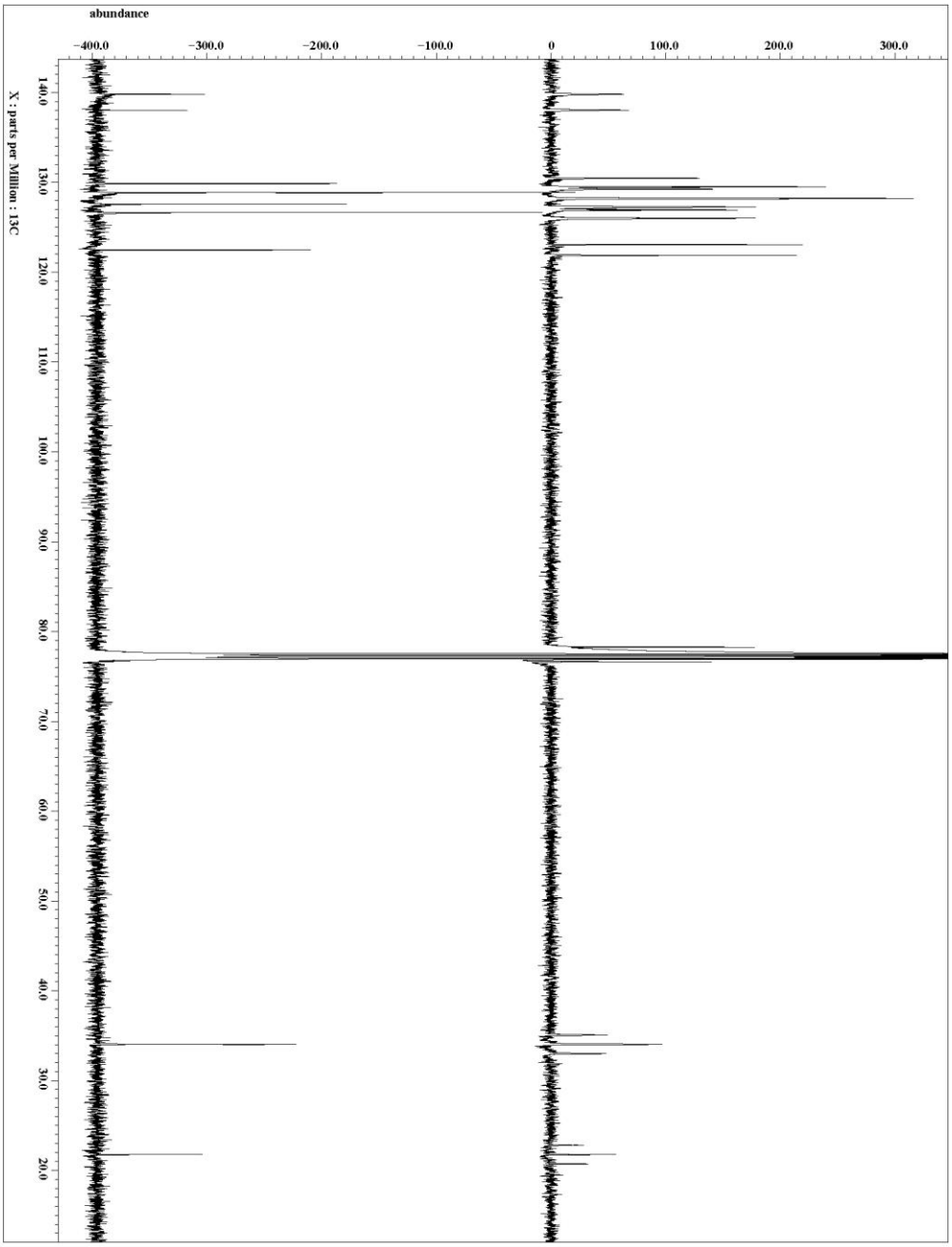

Figure 3-23. 12 ^{13}C NMR spectrum (bottom) and $^{13}C\{^{1}H\}$ NMR spectrum (top) (125 MHz, $CDCl_3$).

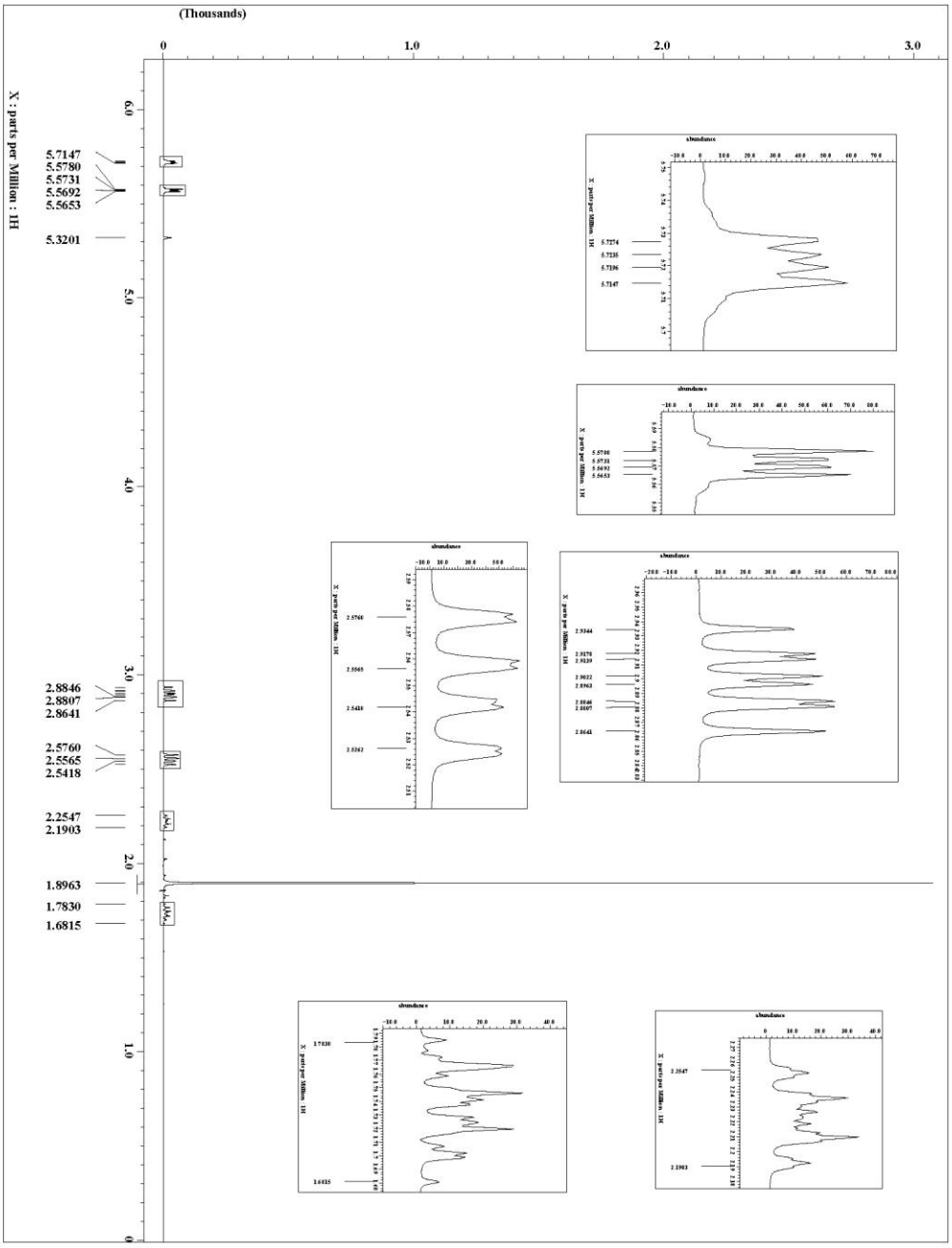

Figure 3-24. 28 ^{1}H NMR spectrum (500 MHz, CD_2Cl_2).

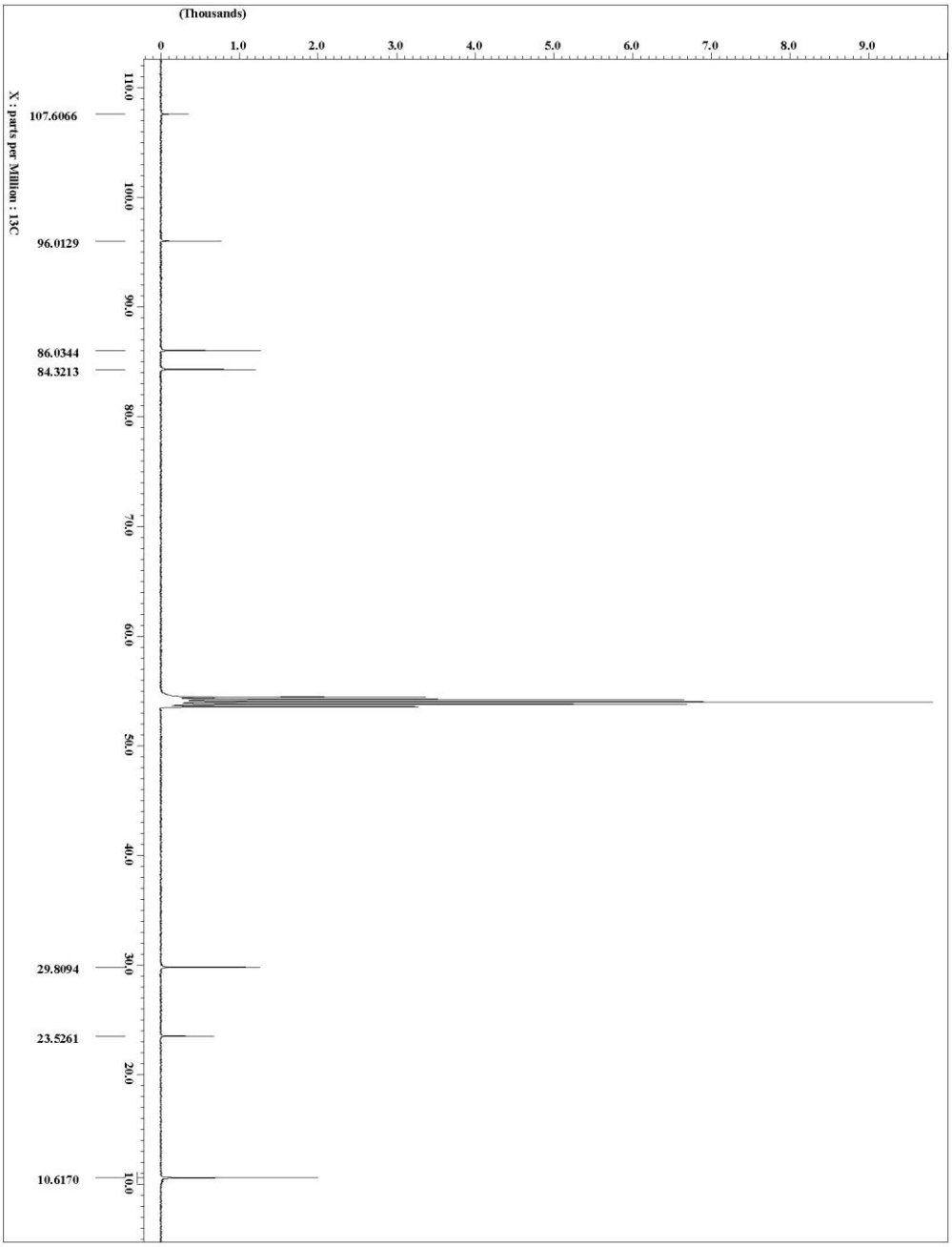

Figure 3-25. 28 ^{13}C NMR spectrum (125 MHz, CD_2Cl_2).

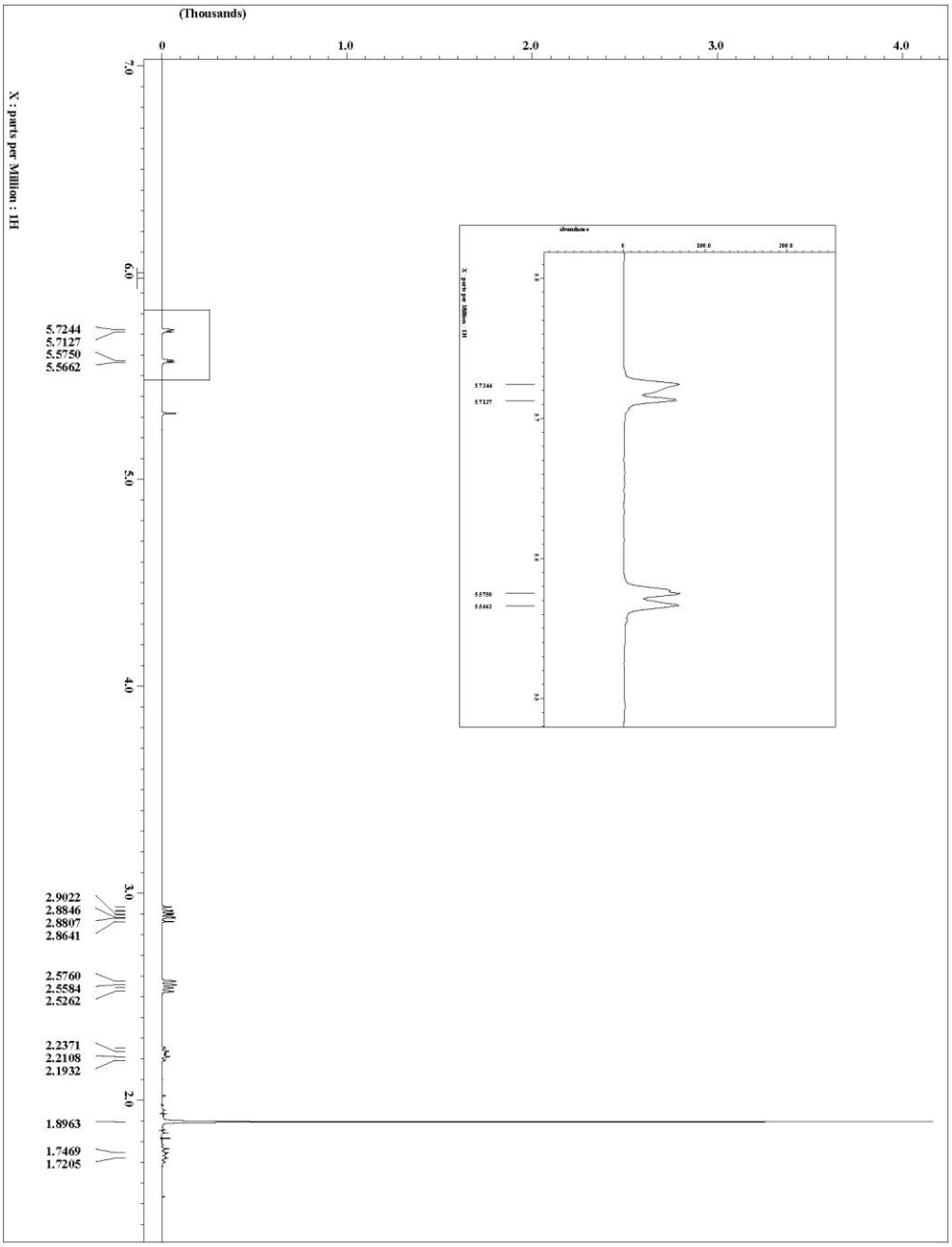

Figure 3-26. 28 from **21-*E*-d$_2$** ^{1}H NMR spectrum (500 MHz, CD_2Cl_2).

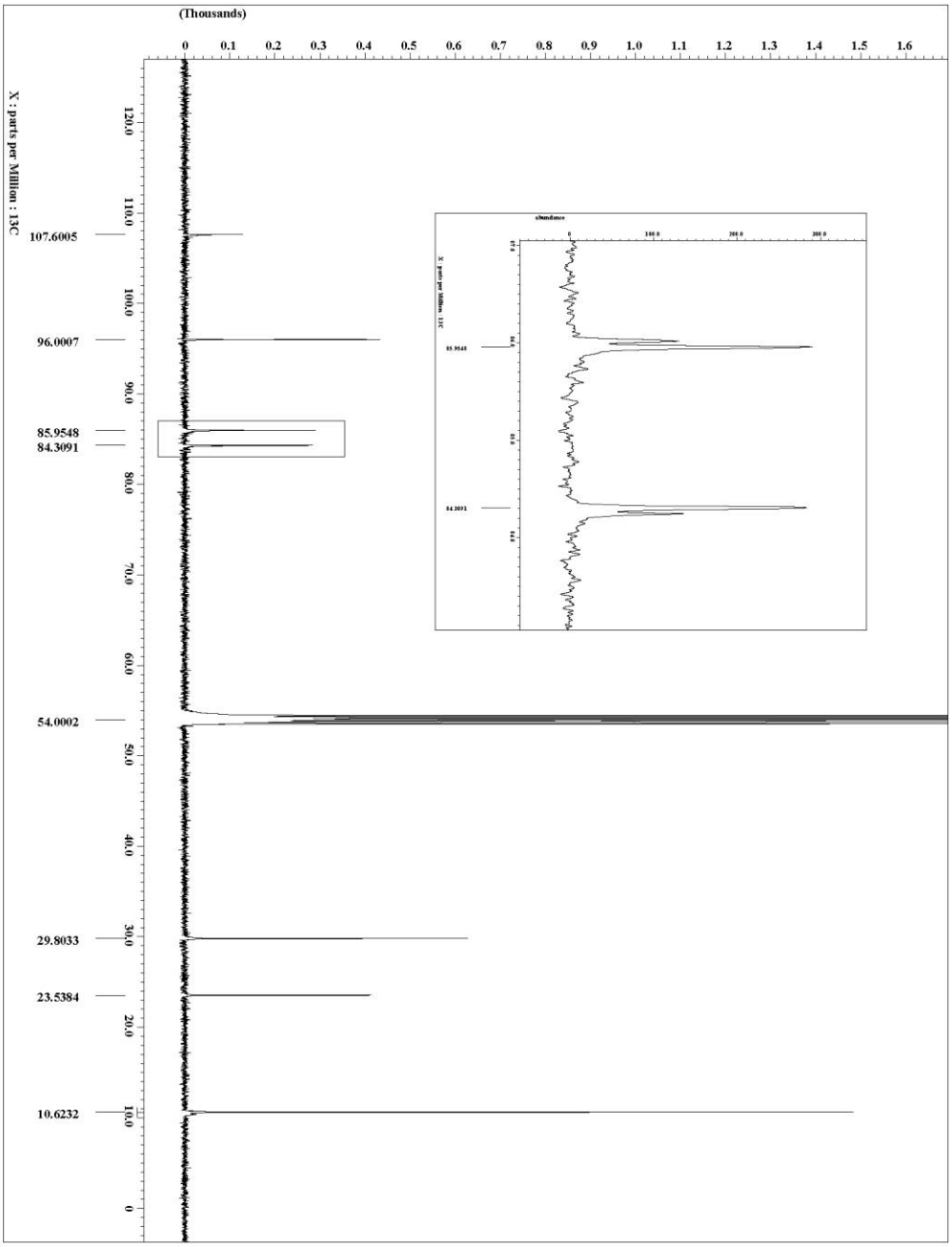

Figure 3-27. 28 from **21-*E*-d$_2$** ^{13}C NMR spectrum (125 MHz, CD_2Cl_2).

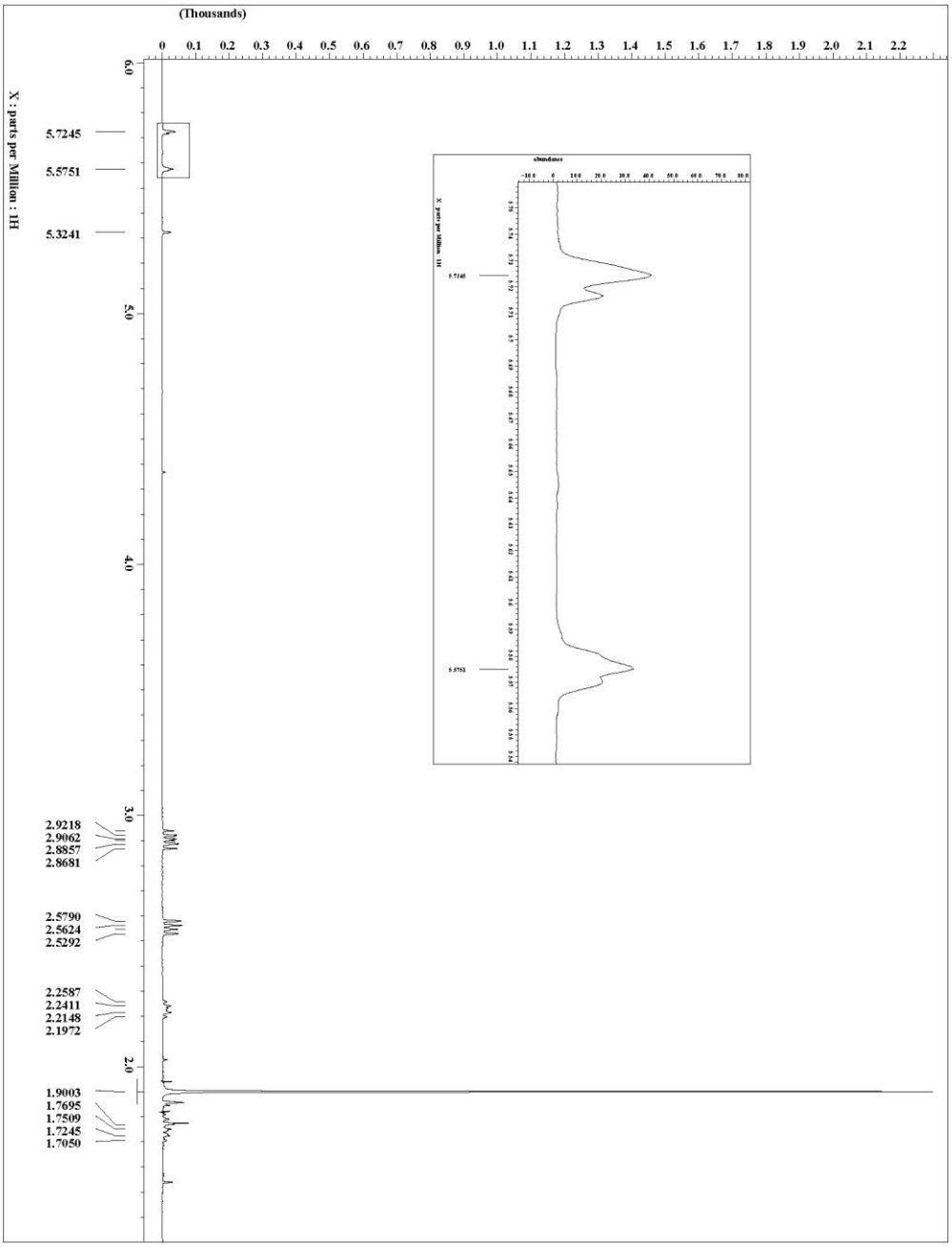

Figure 3-28. 28 from **21-*Z*-d$_2$** ^{1}H NMR spectrum (500 MHz, CD_2Cl_2).

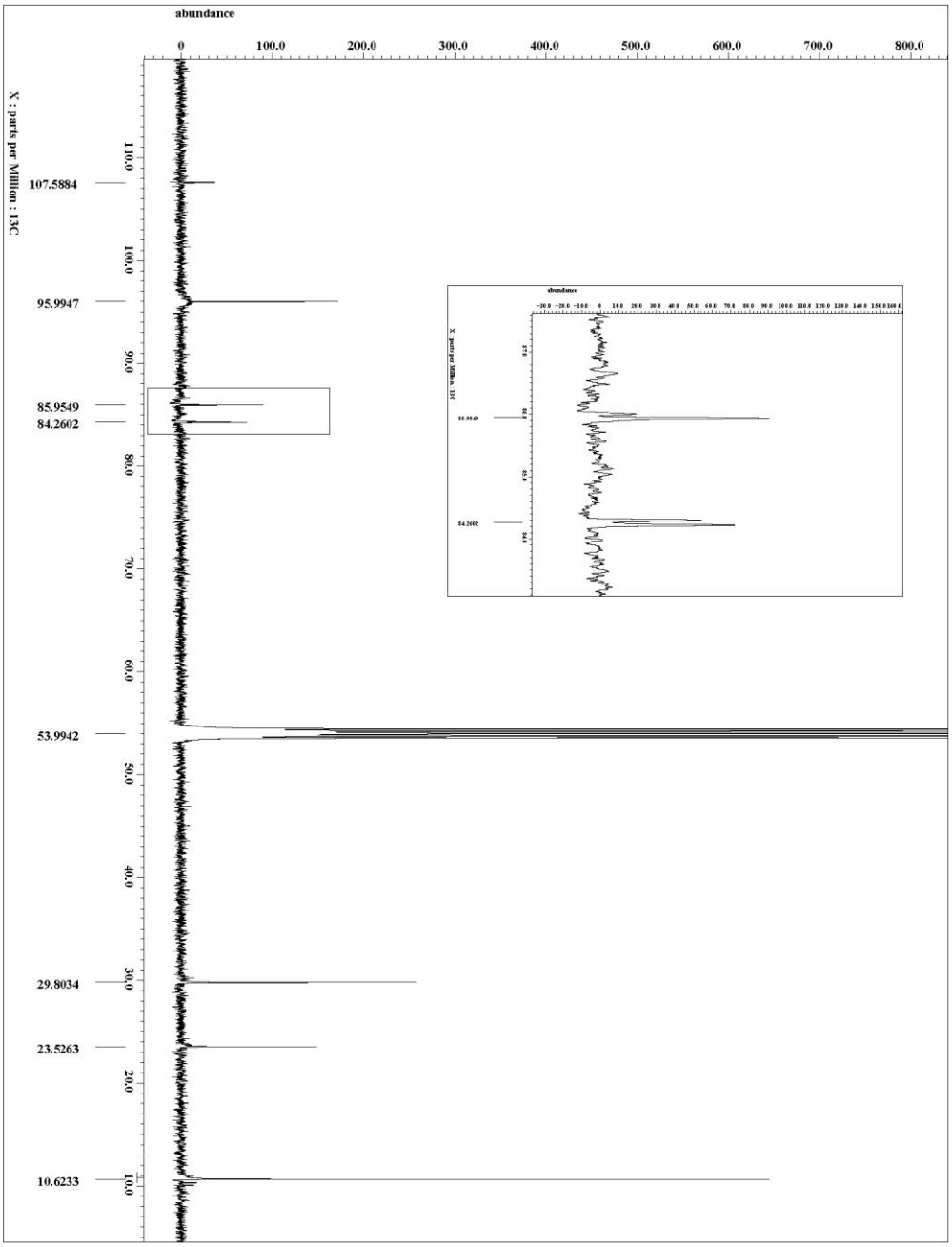

Figure 3-29. 28 from **21-*Z*-d$_2$** ^{13}C NMR spectrum (125 MHz, CD_2Cl_2).

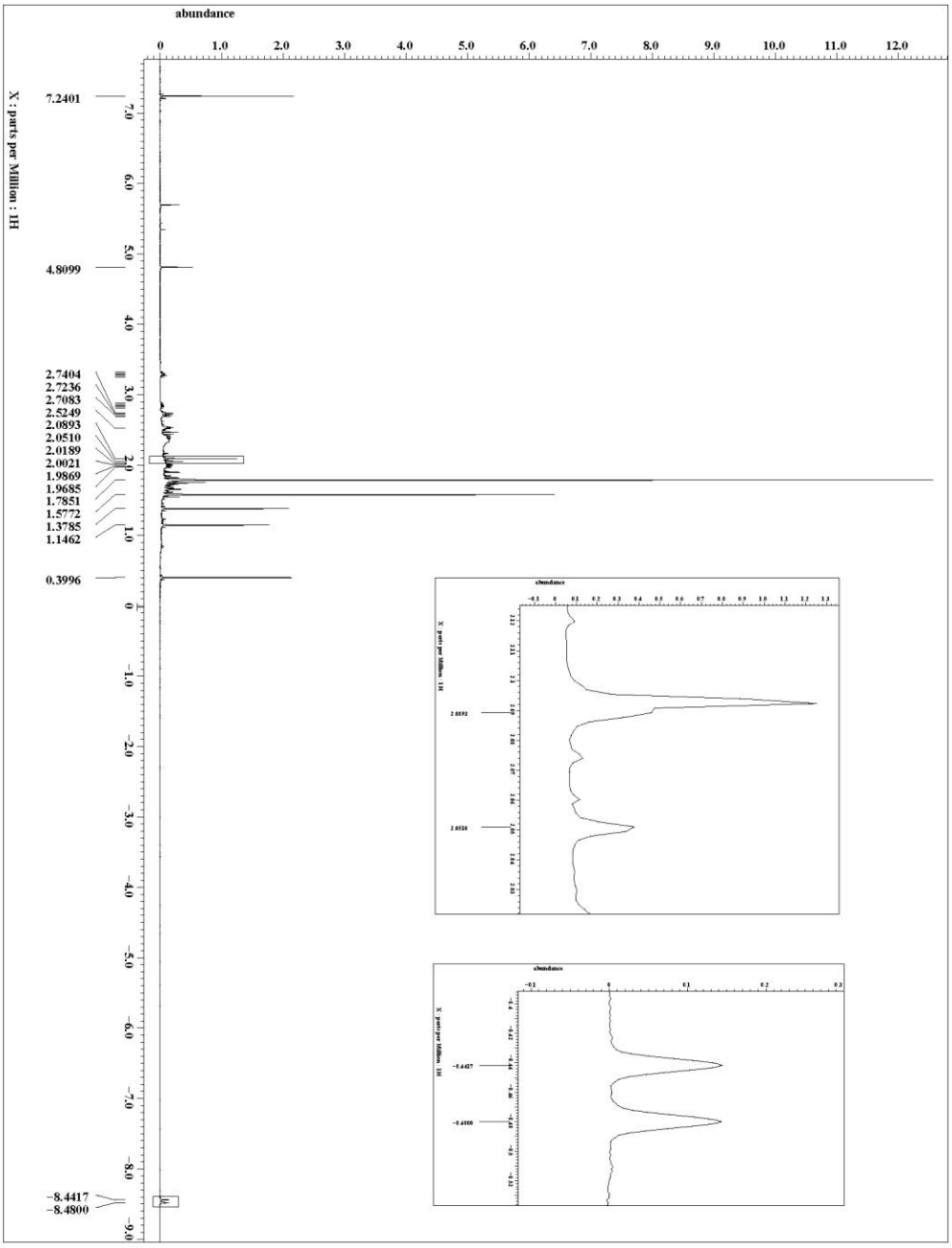

Figure 3-30. 30 ^{1}H NMR spectrum (500 MHz, $CDCl_3$).

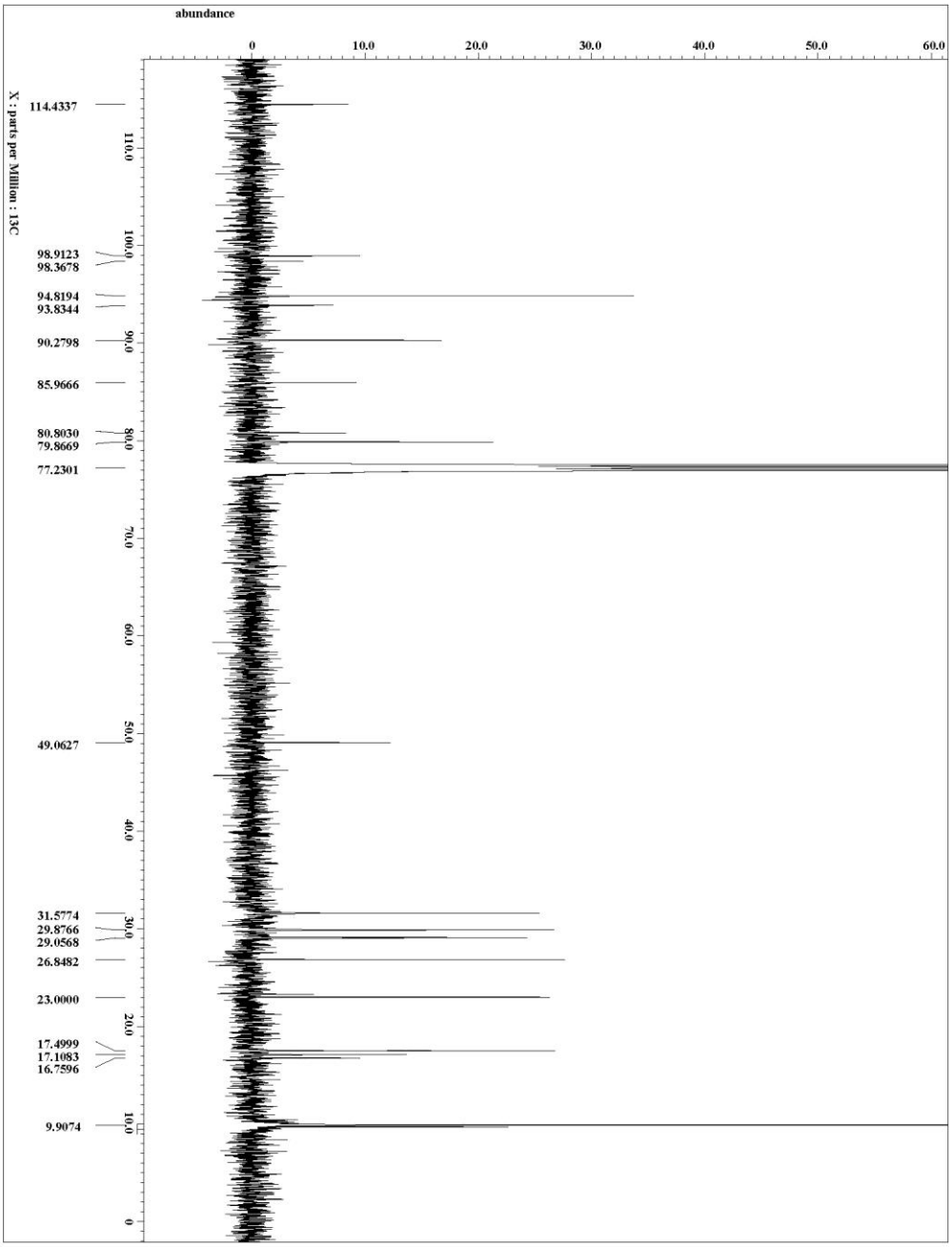

Figure 3-31. 30 ^{13}C NMR spectrum (125 MHz, $CDCl_3$).

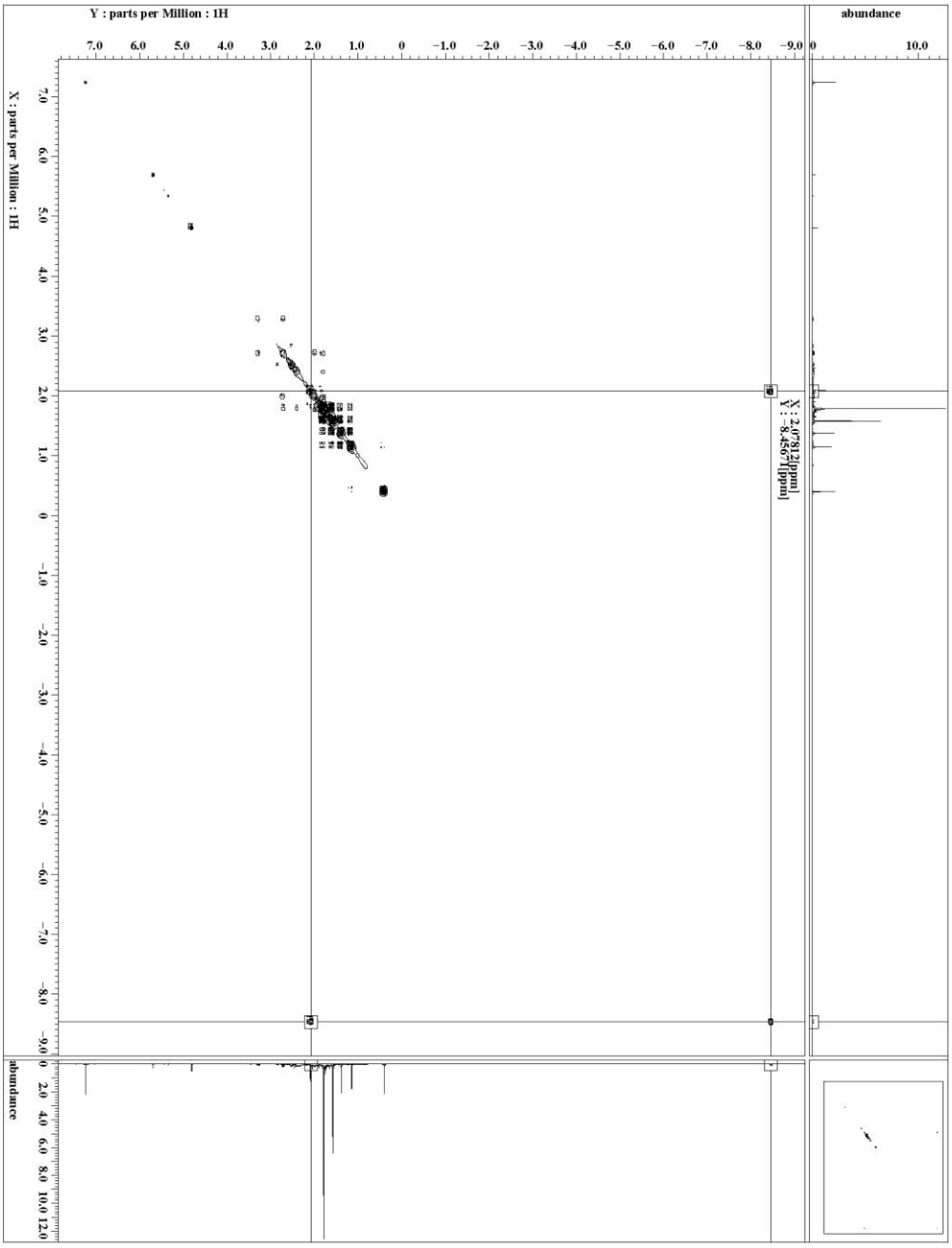

Figure 3-32. 30 COSY spectrum (500 MHz, $CDCl_3$).

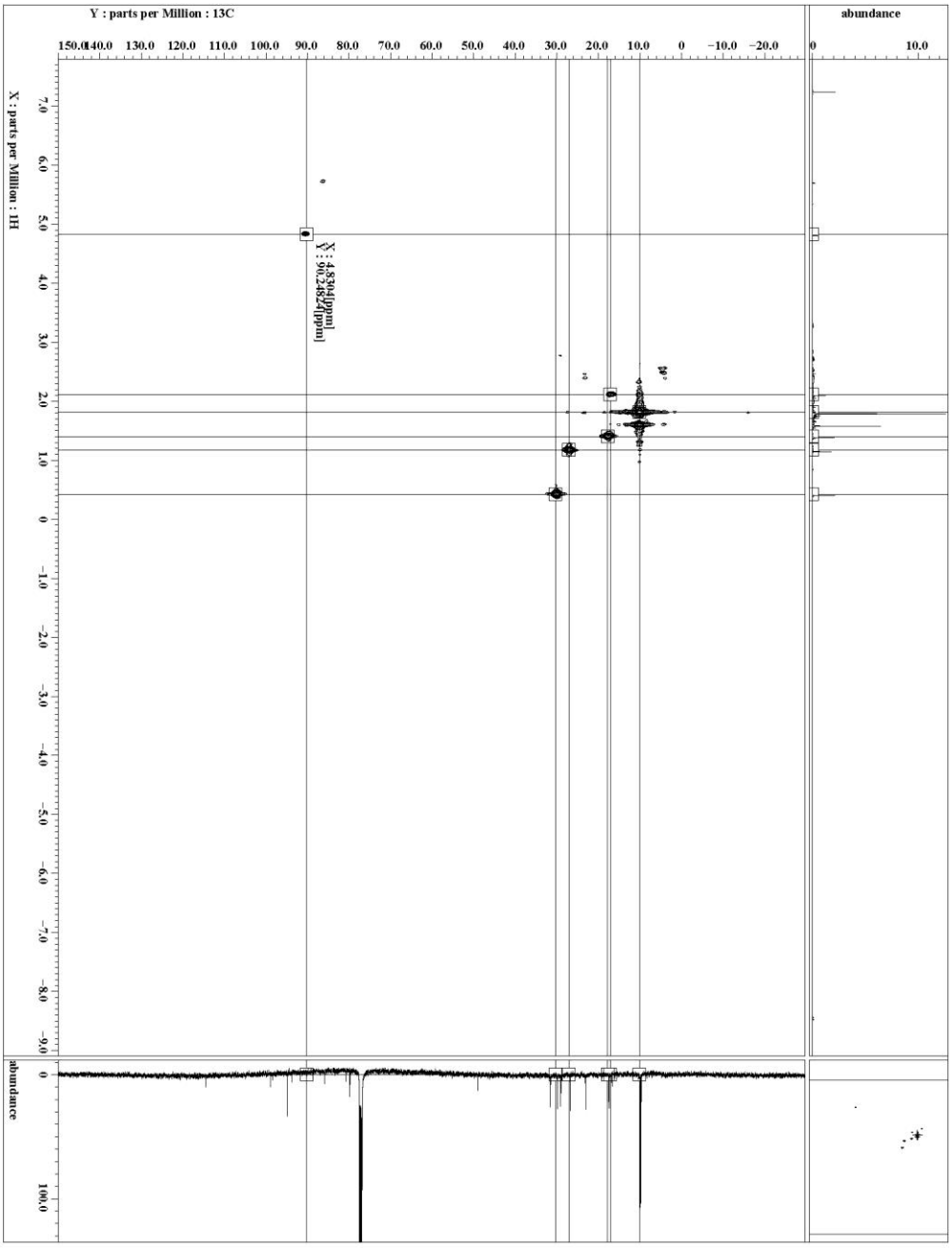

Figure 3-33. 30 HMQC spectrum (500 MHz, $CDCl_3$).

3-6.5 X-ray Crystallographic Summary for Complex 25.

General Experimental for X-ray Structure Determinations.

A single crystal with general dimensions of *a* x *b* x *c* was immersed in Paratone and placed on a Cryoloop. Data were collected on a Bruker SMART (APEX) CCD diffractometer using a graphite monochromator with Mo or Cu Kα radiation (λ = 0.71073 or 1.54178 Å) at the defined temperature. The data were integrated using the Bruker SAINT software program and scaled using the SADABS software program. Soltuion by direct methods (SIR-2004) produced a complete heavy-atom phasing model consistent with the proposed structure. All non-hydrogen atoms were refined anisotropically by full-matrix least squares (SHELXL-97). All hydrogen atoms were placed using a riding model. Their positions were constrained relative to their parent atom using the appropriate HFIX command in SHELXL-97.

Table 3-4. Crystallographic Data Collection and Refinement Information for **24.**

	24
Formula	$C_{26}H_{25}F_6PRu$
Crystal System	Monoclinic
Space Group	*C* 1 2/c 1
a, Å	20.5879(10)
b, Å	18.3160(9)
c, Å	16.0287(12)
α, deg	90
β, deg	129.602(2)
γ, deg	90
V, Å^3	4657.0(5)
Z	8
Radiation (λ, Å)	Mo-Kα, 0.71073
ρ (calcd.), g/cm^3	1.664
μ, mm^{-1}	0.803
Temp, K	100(2)
θ max, deg	26.435
data/parameters	4793 / 63 / 334
R_1	0.0413
wR_2	0.0992
GOF	1.075

3-7 Acknowledgement

The material in Chapter 3, in part, is currently being prepared for submission for publication with the following authors: Cope, S.K.; O'Connor, J.M. The dissertation author was the primary investigator and author of this material.

3-8 References

1. Busse, P. *Z. Physiol.* **1933**, *214*, 211.

2. Woodward, R.B.; Hoffmann, R. "Conservation of Orbital Symmetry," Verlag Chemie, Weinhiem, **1970**.

3. Schiess, P.; Seegar, R.; Sulter, C. *Helv. Chim. Acta* **1970**, *53*, 1713.

4. (a) O'Connor, J.M.; Friese, S.J.; Rodgers, B.L. *J. Am. Chem. Soc.* **2005**, *127*, 16342. (b) O'Connor, J.M.; Friese, S.J. *Organomet.* **2008**, *27*, 4280. (c) O'Connor, J.M.; Friese, S.J.; Tichenor, M. *J. Am. Chem. Soc.* **2002**, *124*, 3506.

5. O'Connor, J.M.; Friese, S.J.; Rodgers, B.L.; Rheingold, A.L.; Zakharov, L. *J. Am. Chem. Soc.* **2005**, *127*, 9346.

6. Boydston, A; Laskoski, M.; Bunz, U.H.F.; Haley, M.M. *Synlett.* **2002**, 981.

7. Voigt, K.; Zezschwitz, P.V.; Rosauer, K.; Lansky, A.; Adams, A.; Reiser, O.; de Meijere, A. *Eur. J. Org. Chem.* **1998**, 1521.

8. Lindlar, H.; Dubuis, R. *Org. Syn.* **1996**, *46*, 89.

9. Ashe III, A.J.; Drone, F.J. *J. Am. Chem. Soc.* **1987**, *109*, 1879.

10. Crabtree, R.H. "The Organometallic Chemistry of the Transition Metals," John Wiley and Sons, **2009**.

11. Calculations on triene were performed using Spartan '14 version 1.1.9; Wavefunction, Inc. Irvine, CA. DFT RB3LYP method with a 6-31G(*) basis set.

12. Meyer-Friedrichsen, T.; Wong, H.; Prosenc, M.H.; Heck, J. *Eur. J. Inorg. Chem.* **2003**, 936.

13. Older, C.M.; Stryker, J.M. *J. Am. Chem. Soc.* **2000**, *122*, 2784.

14. (a) Mango, F.D. *Advan. Catalysis* **1969**, *20*, 291. (b) Mango, F.D. *Tet. Lett.* **1973**, *17*, 1509.

15. Maier, G. *Angew. Chem. Int. Ed. Engl.* **1967**, *6*, 402.

16. Gloge, T.; Jess, K.; Bannenberg, T.; Jones, P.G.; Langenscheidt-Dabringhausen, N.; Salzer, A.; Tamm, M. *Dalt. Trans.* **2015**, *44*, 11717.

17. Pike, R.D.; Sweigart, D.A. *Coord. Chem. Rev.* **1999**, *187*, 183.

Chapter 4 Stereoelectronic Effects in Ruthenium-Mediated Cycloaromatization of Enediynes

4-1 Introduction

Bergman and Jones[1] demonstrated the thermal cyclization of *cis*-1,5-hexadiyn-3-ene (**1**), which formed benzene (**2**) when heated in the presence of a sufficient hydrogen atom source (Scheme 4-1). The reaction is proposed to proceed via an equilibrium between **1** and *p*-benzyne diradical, **3**, whose existence was inferred by scrambling of deuterium atoms between acetylenic and vinylic positions. The diradical **3** can then abstract hydrogen atoms to form benzene.

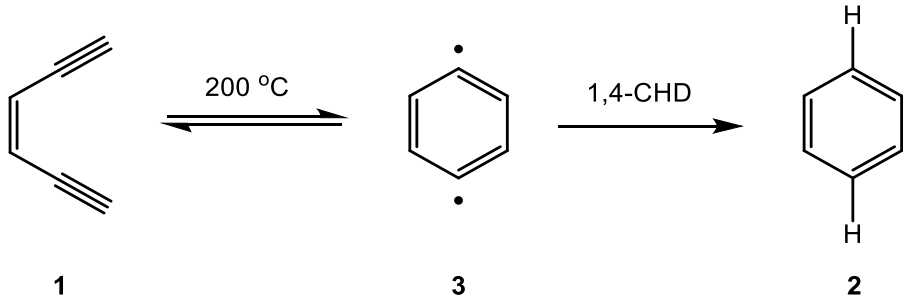

Scheme 4-1. Bergman cyclization. (1,4-CHD is 1,4-cyclohexadiene)[1]

In recent years, interest in this unique reaction has increased due to marine natural products[2] which are proposed to undergo cyclization to species like **3** and abstract hydrogen atoms from the sugar backbone of DNA.[3] This atom abstraction leads to double stranded DNA cleavage and cell death, leading to hopes for therapeutic agents in cancer treatment and antibiotics. Due to the high temperatures necessary for the reaction to occur and the low yields typically observed for the reaction, the reaction has had little utility in organic synthesis.

Previously, the O'Connor research group[4] demonstrated the cycloaromatization of enediynes by the complexation of $CpRu^+$ or Cp^*Ru^+ to the enediyne (Scheme 4-2). When enediyne **4** was reacted with $[CpRu(NCMe)_3]PF_6$ (**5**) or $[Cp^*Ru(NCMe)_3]PF_6$ (**6**) in $CDCl_3$ in the presence of 1,4-CHD, the formation of arene product **7** was observed in 61% and 64% yield, respectively.

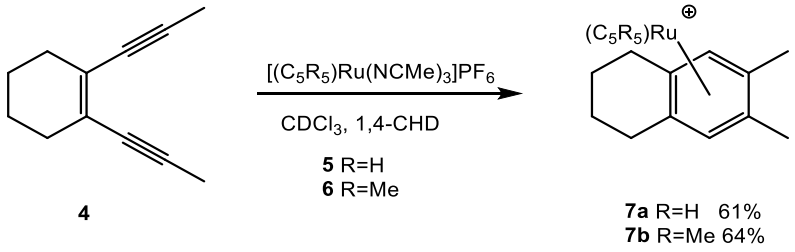

Scheme 4-2. Previous work on ruthenium-mediated cyclization of enediynes.[4]

This reaction was demonstrated to tolerate a variety of substituents and proceed to arene products in moderate to good isolated yields. The major drawback in this work was the stoichiometric use of ruthenium and the limitations on the decomplexation of ruthenium from the arene, especially for electron-rich arenes.

They then demonstrated the ability of $[Cp^*Fe(NCMe)_3]PF_6$ (**8**) to cyclize **4** in acetone·d_6 in the presence of 1,4-CHD to give **9** in 71% yield (Scheme 4-3).

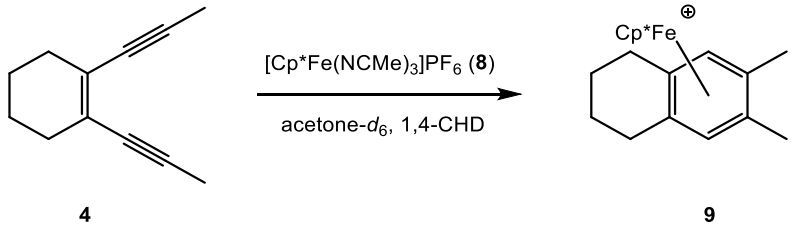

Scheme 4-3. Iron-mediated cyclization of enediynes.[4]

They followed this work by demonstrating the ability of iron-arene complex **10** to undergo arene-decomplexation under photolytic conditions and cyclize enediyne **11** by action of *in situ* generated Cp*Fe$^+$ (Scheme 4-4).[4a] The reaction mixture was photolyzed for 6 days and arene **12** was observed in 91% yield, representing a TON of 3.9.

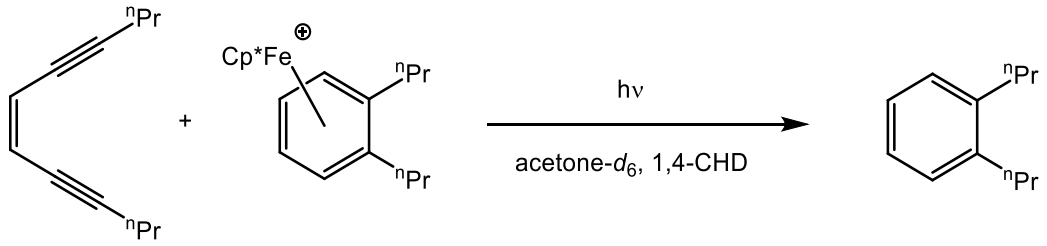

Scheme 4-4. Previous catalytic cycloaromatization of an enediyne by iron under photolytic conditions.[4a]

The reaction suffered from low turnover of the active catalyst which was attributed to the intrinsic low quantum efficiency for photolytic arene release from Cp*Fe$^+$ complexes. Mann and McNair[5] showed the quantum efficiency for arene release from Cp and Cp* ligated iron and ruthenium complexes to be affected by a number of variables including solvent, temperature, arene substitution, counter-ion, metal and ligand substitution. As an example, the quantum efficiency of release of hexamethylbenzene in acetonitrile at rt decreases from CpFe$^+$ (0.41) > CpRu$^+$ (0.014) > Cp*Ru$^+$ (0.0019) > Cp*Fe$^+$ (0.00002). The Cp*Fe$^+$ was demonstrated to have the lowest quantum efficiency of arene release, but the CpRu$^+$ and Cp*Ru$^+$ were shown to have lower activity in the catalytic reaction. When [CpFe(*p*-xylene)]PF$_6$ (**13**) was

used in the place of **10**, the formation of **12** was not observed. Instead the formation of Cp_2Fe (**14)** and $[Fe(NCMe)_6][PF_6]_2$ (**15**) were observed (Scheme 4-5).[4] These results were consistent with previous reports on the attempted synthesis of $[CpFe(NCMe)_3]PF_6$. The mechanism for this disproportionation reaction is unclear.[6]

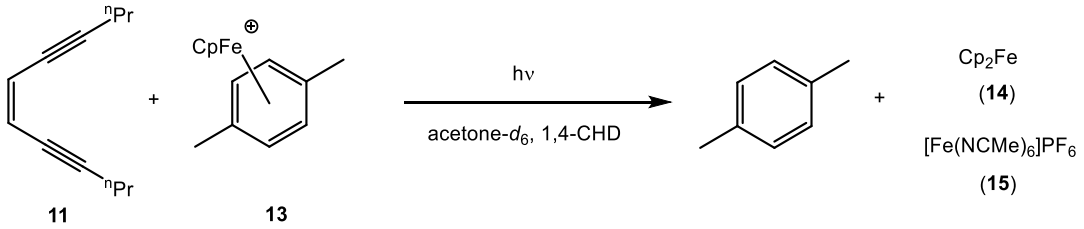

Scheme 4-5. Attempted reaction with $CpFe^+$.[4]

The quantum efficiency of arene release in this series is proposed to be dominated by electronic features of the Cp-ligand set. In 1992, Gassman[7] reported the synthesis of 1,2,3,4-tetramethyl-5-trifluoromethyl-cyclopentadiene (**16**) ($Cp^‡H$) in a similar fashion to Cp*H. He reasoned that CF_3 was electron-withdrawing to approximately the same degree as four CH_3 are electron-releasing; so the ligand should be electronically similar to Cp but sterically similar to Cp*. A number of iron complexes of $Cp^‡$ were synthesized and the ligand bonding energies were measured to demonstrate the electronic similarities between $Cp^‡$ and Cp (Table 4-1, Scheme 4-6).

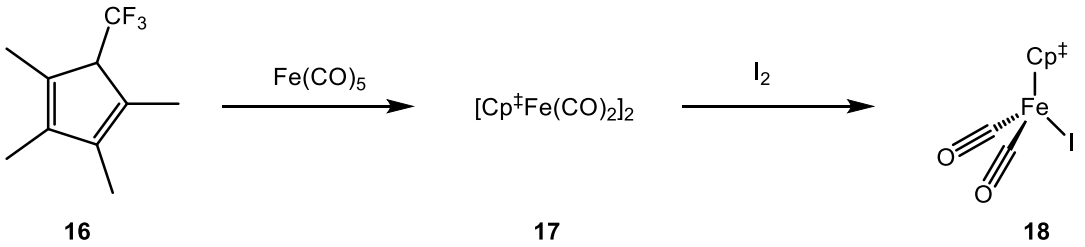

16 17 18

Scheme 4-6. Gassman's work with $Cp^{‡}$.[7]

Table 4-1. X-ray Photoelectron Binding Energies (in eV).[7]

	17	**18**
$Cp^{‡}$	708.1	709.0
Cp	708.1	709.0
Cp*	707.7	708.5

In this chapter, the chemistry of [$Cp^{‡}Ru^{+}$] complexes is explored. $Cp^{‡}Ru^{+}$ is shown to cycloaromatize enediynes in good yields and show results similar to $CpRu^{+}$ complexes. In addition, attempts toward the synthesis of [$Cp^{‡}Fe(NCMe)_3$]PF_6 and [$Cp^{‡}Fe(arene)$]PF_6 will be discussed. The unique formation of a (diphenylmethyl)cyclopentadiene ligand by C-F bond activation will also be discussed.

4-2 Results

4-2.1 Synthesis of [$Cp^{‡}Fe$] Complexes

Following the two step procedure outlined by Gassman,[7] **16** was made in 70% yield. Then following the procedure from Gassman, **17** was made by refluxing **16** (20 mmol) with $Fe(CO)_5$ (50 mmol) in octane (150 mL) for 2 days. Filtering and evaporation of the solution gave a residue of **17**, which was recrystallized from CH_2Cl_2/hexanes to give **17** (7 mmol) as a purple microcrystalline solid in 35% yield. Then **17** (1 mmol) was reacted with $[Cp_2Fe]PF_6$ (1 mmol) in DCM/MeCN (9 mL, 2:1) overnight.[8] The initially purple solution turned yellow-orange and the volatiles were removed under vacuum. The residue was washed with Et_2O to remove Cp_2Fe and the residue was recrystallized from acetone/Et_2O to give **19** (0.9 mmol) in 90% yield as a bright yellow powder (Scheme 4-7).

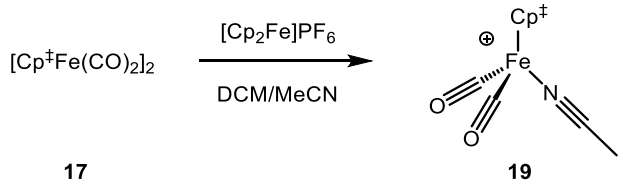

Scheme 4-7. Synthesis of **19**.

Recrystallization by slow diffusion of Et_2O into a solution of **19** in acetone gave crystals of good quality for X-ray diffraction studies. The refinement of the diffraction data gave a monoclinic unit cell in the P2(1) space group with a final refinement value of 3.8%. The solid-state structure exhibited the expected piano-stool geometry. A ^{1}H NMR spectrum (500 MHz, acetone-d_6) showed singlet resonances at δ 1.72, 2.07 and 2.35, which integrated as 2:2:1. An IR spectrum (thin-film) of **19** showed stretches at 2075 and 2032 cm^{-1} ; which compare more favorably with

$[CpFe(CO)_2(NCMe)]PF_6$[9] which exhibits stretches at 2077 and 2033 cm^{-1} ($CHCl_3$) than with $[Cp^*Fe(CO)_2(NCMe)]PF_6$[8] which exhibits stretches at 2065 and 2010 cm^{-1} ($CHCl_3$).

A yellow solution of **19** (0.2 mmol) in MeCN (20 mL) in a sealed flask was photolyzed for 2 h, during which time the color of the solution turned bright red. The volatiles were removed under vacuum and the residue was recrystallized from $MeCN/Et_2O$ to give **20** in 90% yield (Scheme 4-8).

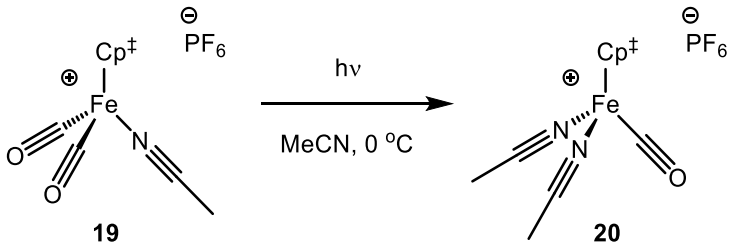

19 **20**

Scheme 4-8. Synthesis of **20**.

Recrystallization by slow diffusion of Et_2O into a solution of **20** in acetone gave crystals of good quality for X-ray diffraction studies. The refinement of the diffraction data gave a monoclinic unit cell in the P2(1)/m space group with a final refinement value of 3.4%. The solid-state structure showed the expected piano stool geometry, with two MeCN ligands and one CO ligand. A ^1H NMR spectrum (500 MHz, acetone-d_6) of **20** showed singlet resonances at δ1.75, 2.08 and 2.45 which integrated as 1:1:1. An IR spectrum (thin-film) of **20** showed stretches at 2079 and 2000 cm^{-1}; compared with $[CpFe(CO)(NCMe)_2]PF_6$[10] which exhibits stretches at 2190 and 1980 cm^{-1}

($CHCl_3$) and $[Cp^*Fe(CO)(NCMe)_2]PF_6$[8] which exhibits stretches at 2308 and 1976 cm^{-1} ($CHCl_3$).

A yellow solution of **19** in MeCN was photolyzed at -10 °C for 3 h under a constant flow of N_2, during which time the solution changed first to red and then slowly to deep purple. The color is consistent with the formation of $[Cp^{‡}Fe(NCMe)_3]PF_6$ (**21**) as both **8**[8] and $[CpFe(NCMe)_3]PF_6$[6] are purple in MeCN. Below -10 °C in MeCN the solution was relatively stable for a few hours but upon warming to 0 °C the solution turned from purple to faint yellow over the course of 10 min. The purple solution was made again and then at -15 °C the solution was concentrated under vacuum to give a purple film on the inside of the flask. Upon warming the residue again decomposed to a yellow film. Attempts to recrystallize the yellow film yielded colorless block crystals which were identified as $Fe(NCMe)_6(PF_6)_2$[11] by X-ray crystallography. The purple solution was produced again and concentrated to a minimal volume under vacuum at -15 °C. Then the solution was layered with clean dry Et_2O via cannula under argon. The solution was then left at -15 °C for several hours, during which time the solution again turned yellow. No farther attempts toward the isolation of $[Cp^{‡}Fe(NCMe)_3]PF_6$ were made.

Next **17** (1 mmol) was reacted with Br_2 (1 mmol) in DCM/$CHCl_3$ (1:2) at 0 °C to give $Cp^{‡}Fe(CO)_2Br$, **22**, in 90% yield following recrystallization from hot EtOH (Scheme 4-9).[12]

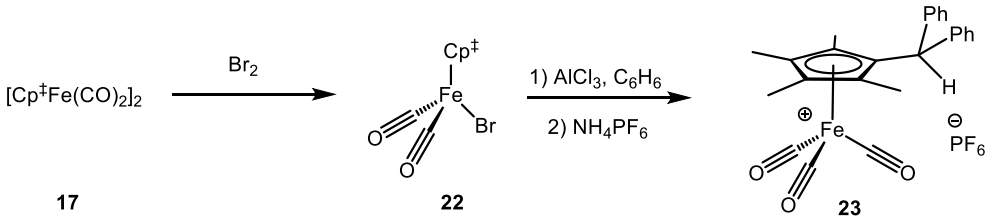

Scheme 4-9. Synthesis of **22** and **23**.

A single crystal X-Ray diffraction study was undertaken on **22**. The unit cell is monoclinic in the P2(1)/m space group with a single molecule in the unit cell. The solid-state structure exhibited the expected piano-stool geometry with two CO ligands and one bromide. A ^{1}H NMR spectrum (500MHz, $CDCl_3$) showed a pair of singlets at δ 1.70 and 2.08 which integrated 1:1. An IR spectrum (thin-film) of **22** showed stretches at 2040 and 1960 cm^{-1}; compared with $CpFe(CO)_2Br$[13] which exhibits stretches at 2077 and 2033 cm^{-1} ($CHCl_3$) and $Cp^*Fe(CO)_2Br$[12] which exhibits stretches at 2008 and 1957 cm^{-1} ($CHCl_3$).

Complex **22** (0.3 mmol) was refluxed in C_6H_6 (1 mL) in the presence of $AlCl_3$ (1.1 mmol) under N_2 overnight. The reaction was cooled to rt and quenched with H_2O. The solution was filter through Celite and then the iron complex was precipitated by salt metathesis with NH_4PF_6. The orange precipitate was collected on a frit and washed with H_2O, MeOH and Et_2O. The powder was then recrystallized from CH_2Cl_2/Et_2O to give orange block crystals of compound **23**. A ^{1}H NMR spectrum (500 MHz, CD_2Cl_2) of **23** showed the expected methyl resonances as singlets at δ 1.72 and 2.07, but also resonances in the aromatic region at δ 7.14 (d, J = 7.5 Hz) and 7.38 (m) and a singlet at δ 5.22. A ^{19}F NMR (470 MHz, CD_2Cl_2) spectrum of **23**

showed only a doublet at δ-65 with a coupling constant of 707 Hz, which is consistent with the PF_6^- counter-ion. IR spectroscopy (thin-film) showed stretches at 2105 and 2059 cm^{-1}. A X-ray diffraction study on the compound was undertaken. The diffraction data was refined in a monoclinic unit cell with a P2(1)/n space group with two identical molecules in the unit cell.

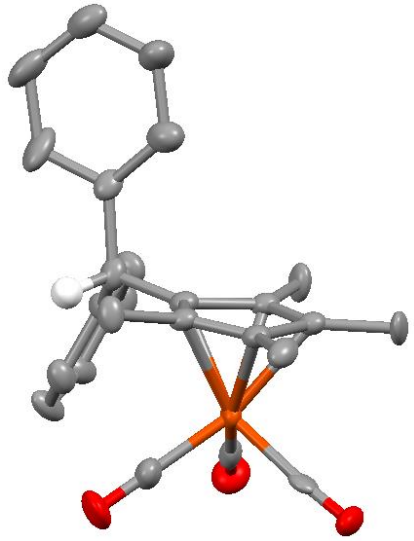

Figure 4-1. X-ray structure of **23**. (Most hydrogens and the counter-ion have been omitted for clarity).

As is shown in the X-ray structure (Figure 4-1), the three fluorines of the trifluoromethyl group have been substituted with two phenyls and a hydrogen. In addition, the bromide has been replaced with a carbonyl, most likely from a disproportionation reaction with a second iron carbonyl species in solution. With a structure and molecular formula in hand, **23** was formed in 37% yield.

4-2.2 Synthesis of [Cp‡Ru] Complexes

Following a known procedure[15] Cp‡H (2.5 mmol) was refluxed with $RuCl_3 \cdot (H_2O)_x$ (1 mmol) in EtOH (20 mL) under argon for 3 h and then the solution was cooled to rt and then 0 °C. The precipitate was then collected on a frit and washed with ice cold EtOH and Et_2O (Scheme 4-10). The microcrystalline black solid **24** was then dried overnight under vacuum (10^{-4} mmHg), to give **24** (0.3 mmol, 30% yield). Then **24** (0.3 mmol) was suspended in dry, degassed MeCN (12 mL) under N_2 and Zn^0 dust (1 mmol) was added.[16] The solution was stirred for 1 h and $NaPF_6$ (0.35 mmol) was added to the solution. The solution was then allowed to stir overnight under N_2 and the volatiles were removed under vacuum. The residue was suspended in dry degassed CH_2Cl_2 and passed through a pad of Celite to remove Zn and excess $NaPF_6$. The volatiles were removed under vacuum and the residue was dissolved in a minimal amount of MeCN, then precipitated by the addition of Et_2O, to give **25**[17] (0.28 mmol) as a bright yellow microcrystalline solid in 95% yield.

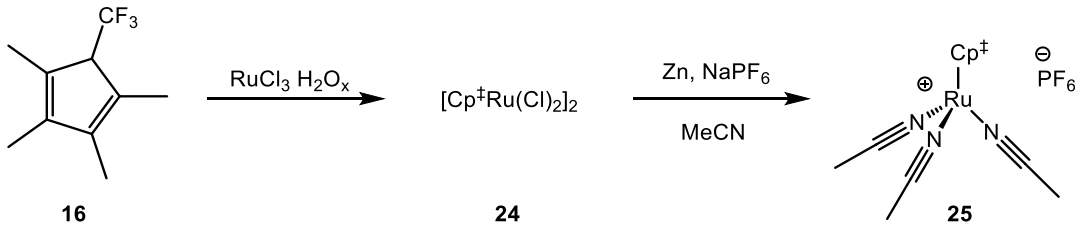

Scheme 4-10. Synthesis of **25**.

Then **25** (0.3 mmol) was added to a solution of naphthalene (3 mmol) in DCM (10 mL) at rt under N_2 and the resulting solution was stirred at rt for 2 h.[5c] The

volatiles were removed under vacuum and the residue was washed with Et_2O to remove excess naphthalene. The residue was recrystallized from acetone/Et_2O to give pale yellow crystals of **26**[17] in near quantitative yield (Scheme 4-11).

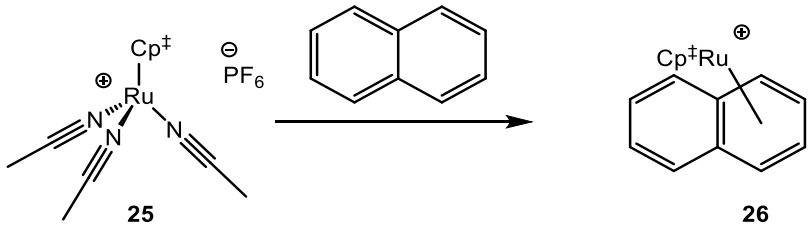

Scheme 4-11. Synthesis of **26**.

A single crystal X-ray diffraction study was carried out on **26**. Refinement of the diffraction data showed an orthorhombic unit cell in the Pbca space group with a single molecule in the unit cell. From the X-ray structure the ruthenium is clearly bound η^5 to the $Cp^‡$ ligand and η^6 to one ring of the naphthalene. The $Cp^‡$-centroid to ruthenium distance is 1.801(4) Å and the arene-centroid to ruthenium distance is 1.726(5) Å. These values are similar to the values observed for [CpRu(naphthalene)]PF_6[18] (**27**) 1.811(2) Å and 1.719(2) Å, respectively, and for [Cp*Ru(naphthalene)]PF_6[19] (**28**) 1.803(4) Å and 1.727(8) Å.

4-2.3 Reactions of [Cp‡Ru] Complexes

The reaction of **25** (30 μmol) with acyclic enediyne **29** (30 μmol) and 1,4-CHD (60 μmol) in $CDCl_3$ (1 mL) was monitored by ^1H NMR spectroscopy (Scheme

4-12). Within 20 min the formation of [Cp‡Ru(η^6-*o*-xylene)]PF_6 was observed to form in 68% yield as indicated by resonances at δ 1.56 (s, 6H), 1.72 (s, 6H), 2.15 (s, 6H), and 6.20-6.25 (m, 4H). The contents of the NMR tube were poured into a vial and concentrated to a minimal volume and Et_2O was added to precipitate **30** as a white solid (Scheme 4-12).

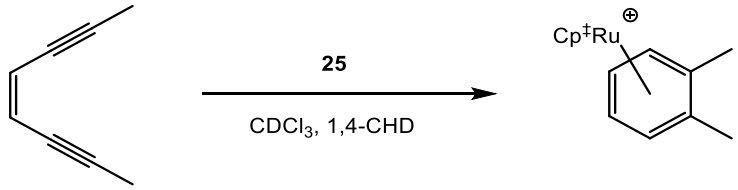

29 **30**

Scheme 4-12. Formation of **30**.

Recrystallization of **30** by slow diffuse of Et_2O into a $CDCl_3$ solution of **30** lead to crystals of sufficient quality for X-ray diffraction study. Refinement of the diffraction data lead to an orthorhombic unit cell in the Pna 2(1) space group, with a single molecule in the unit cell. The data refined to a 3.4% structure. The X-ray structure confirms the proposed structure with a cyclopentadienyl-centroid to ruthenium distance of 1.813(5) Å and an arene-centroid to ruthenium distance of 1.714(5) Å. These values are similar to the values observed for [CpRu(benzene)]PF_6,[20] of 1.85(3)Å and 1.67(3) Å, respectively, and for [Cp*Ru(benzene)]PF_6,[21] of 1.811(5) Å and 1.711(5) Å.

Showing that **25** mediated the room temperature Bergman cycloaromatization in comparable yields to $CpRu^+$ and Cp^*Ru^+, a question of stereoelectronic effects was asked. Previously, the O'Connor group undertook a series of experiments to explore

the possibility of facial selectivity in ruthenium-mediated cyclization of enediynes.[22] It was shown in this work that when racemic enediyne **31** was allowed to react with **5**, the product **32-H** was obtained in 30% yield in a 1:1 diastereomeric ratio. When the reaction was repeated with **6**, the yield increased to 56% with an 8:2 diastereomeric ratio (Scheme 4-13).

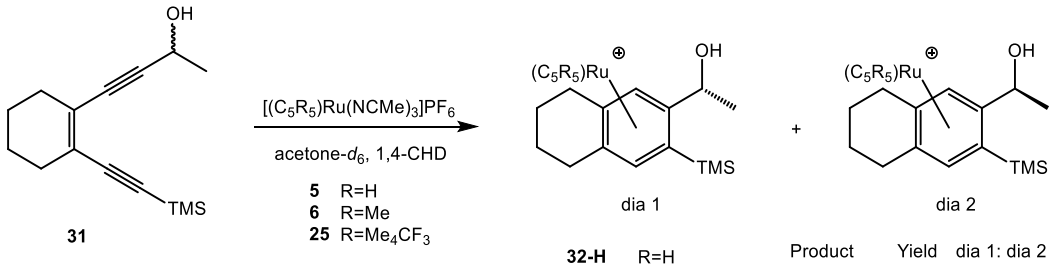

Product	Yield	dia 1: dia 2
32-H	30%	1:1
32-CH$_3$	56%	8:2
32-CF$_3$	32%	1:1

Scheme 4-13. Investigations into the stereoelectronic effects of diastereoselective reactions.[22]

A mixture of diastereomers of **32-CH$_3$** was separated by column chromatography. Solid-state structures of each diastereomer showed that the major isomer of **32-CH$_3$**, dia 1, placed the hydroxyl group toward the metal and the methyl group away from the trimethylsilyl group. This diastereomer exhibited ^{1}H NMR chemical shifts ($CDCl_3$) of the arene resonances at δ 5.28 and 6.00. The minor diastereomer exhibited arene resonances at δ 5.42 and 5.65 in the ^{1}H NMR spectrum ($CDCl_3$). The 3-D configuration of the diastereomers of **32-H** were unassigned. The arene resonances of the diastereomers of **32-H** appear at δ 5.72 and 6.34 for

diastereomer 1 and 5.83 and 6.25 for diastereomer 2 in the ^{1}H NMR spectrum ($CDCl_3$). While the pathway of stereoselectivity was unclear, several models were put forward to rationalize the observed selectivity involving both steric and electronic arguments. The separation of electronic and steric contributions of the selectivity could not be performed as the increased electron-density of Cp* is tied to the increase in steric bulk. The Cp‡ ligand was developed by Gassman for this very reason. When **31** was allowed to react with **25** under the same conditions, the product arene **32-CF$_3$** was obtained in 32% yield with a 1:1 diastereomeric ratio, as evidenced by singlet resonances at δ 5.55 and 6.11 for diastereomer 1 and 5.67 and 5.83 for diastereomer 2, which were assigned by comparison with **32-CH$_3$**. In addition, when a preparative scale (0.2 mmol) reaction was carried out, a third product was isolated and identified as the oxidation of the alcohol to a ketone **33** in 4% yield (Scheme 4-14).

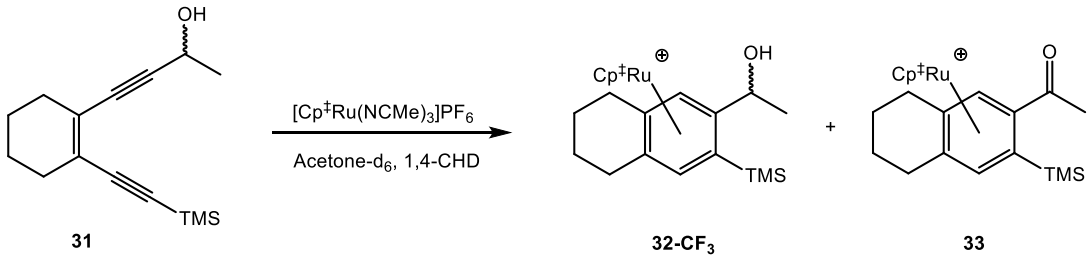

Scheme 4-14. Preparative scale reaction of **31** with [Cp‡Ru]$^+$.

This complex exhibited characteristic resonances by ^{1}H NMR spectroscopy at δ 5.84 and 6.55 and a ketone carbon resonance at δ 199.7. This ketone product was not observed in the NMR-scale reaction. The yield and diastereoselectivity of **25**

were more similar to **5** than to **6**, showing that electronic features of the reaction predominate in facial selectivity.

Previously it had been shown by Kudinov that CpRu(naphthalene)$^+$ would undergo arene exchange under photochemical conditions.[18] This led us to propose the reaction of Cp‡Ru(naphthalene)$^+$ (**26**) with enediyne **29** under photolysis. The reaction of **29** (30 μmol) with **26** (30 μmol) and 1,4-CHD (60 μmol) in acetone·d_6 (1 mL) was monitored by ^{1}H NMR spectroscopy. The solution was placed in a photo-reactor with UV lamps with a broad spectrum output centered at 254 nm. The solution was periodically removed from the photo-reactor and a ^{1}H NMR spectrum was collected. After 6 h there was approximately 95% conversion of **26** with an 88% yield of arene complex **30** (Scheme 4-15).

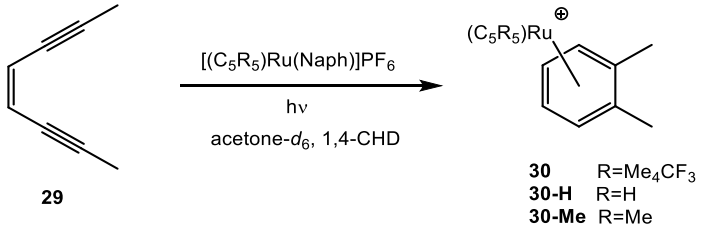

Product	Conversion	Yield
30	95%	88%
30-H	93%	92%
30-Me	97%	94%

Scheme 4-15. Photochemical reactions of ruthenium-naphthalene complexes with enediynes.

When the above reaction was repeated with CpRu(naphthalene)$^+$ (**27**) in place of **26**, after 6 h 93% conversion of **27** with a 92% yield of **30-H** was observed. Replacing **26** with Cp*Ru(naphthalene)$^+$ (**28**) lead to a 97% conversion after 6 h and a 94% yield of **30-Me**.

The reaction of CpRu(naphthalene)$^+$ (**27**, 30 μmol) with dienyne **33** (30 μmol) in acetone·d_6 (1 mL) was monitored by ^{1}H NMR spectroscopy. After an initial ^{1}H NMR spectrum was collected, the solution was placed in a photo-reactor with UV-lamps centered at 254 nm and the solution was photolyzed for 16 h. A ^{1}H NMR spectrum showed 96% conversion of **27** with a 95% yield of **34** (Scheme 4-16).

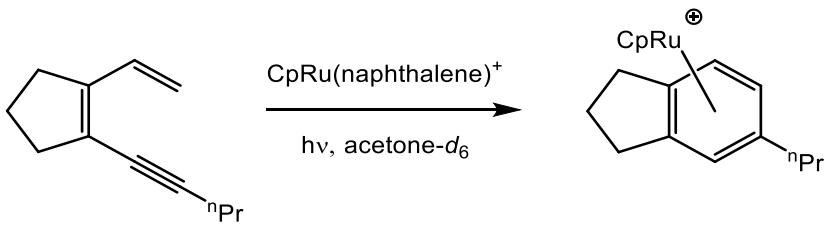

33 **34**

Scheme 4-16. Reaction of **33** with CpRu(naphthalene)$^+$ under photolytic conditions.

4-3 Discussion

The effects of sterics and electronics of the Cp and Cp* ligand sets is all too often a topic that is glossed over in research literature. The increase in steric bulk of the Cp* ligand is usually ascribed as the reason for differences in observed reactions, with no consideration of the electronic difference between the complexes. The Cp‡ ligand set was designed by Gassman[7] to allow for the dissection of the steric and electronic properties. Following known procedures [Cp‡Ru(NCMe)$_3$]PF$_6$ (**25**) was produced as a bright yellow microcrystalline powder. It was shown to react with enediyne substrates in the presences of 1,4-CHD to give arenes in yields comparable

to the previously studied complexes of [CpRu] and [Cp*Ru]. A comparison of bonding distances in ruthenium-arene complexes showed no statically significant difference between Cp‡, Cp, or Cp* ligand sets.

When the stereoelectronic impact of the diastereoselective reaction between ruthenium and enediynes bearing a chiral center was explored, the results pointed to the electronic features of Cp* having the largest influence. A comparison of the arene resonances for **32-CH$_3$** and **32-CF$_3$** showed a trend wherein one diastereomer has a larger difference in chemical shift between the resonances and the other diastereomer exhibits resonances that are closer together (Table 4-2). Based on this comparison **32-CF$_3$** dia 1 is proposed to have the same relative stereochemistry as **32-CH$_3$** dia 1, which was the major isomer in the previous studies. This isomer places the hydroxyl group toward the metal in a solid-state structure and the methyl group away from the trimethylsilyl group in **32-CH$_3$**.

Table 4-2. ^{1}H NMR Chemical Shifts (δ) of the Arene Resonances for **32-H**, **32-CH$_3$**, and **32-CF$_3$**.[22]

	Dia 1		Dia 2	
32-H	5.72	6.34	5.83	6.25
32-CH$_3$	5.28	6.00	5.42	5.65
32-CF$_3$	5.55	6.11	5.67	5.83

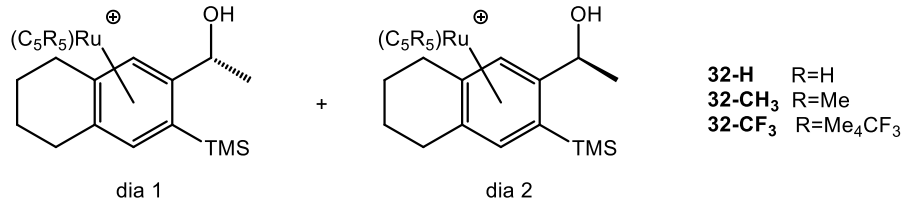

Figure 4-2. Ruthenium-arene **32**.

When $[CpRu]^+$ was used the reaction proceeded in 30% yield with 1:1 DR, whereas $[Cp^*Ru]^+$ led to 56% yield and 8:2 DR.[22] When $[Cp^‡Ru]^+$ was used the yield dropped to 32%, approximately the same as observed for $[CpRu]^+$ and the facial selectivity dropped to 1:1, again as seen for $[CpRu]^+$. There were several models previously put forth for the observed stereoselectivity based on equilibriums and irreviersible steps (Scheme 4-17). Previous studies had suggested that the rate-limiting step in the cycloaromatization of enediyne by ruthenium occurs during the conversion of η^4-diyne intermediate (e.g. **35**). They based this conclusion on kinetic studies which showed an inverse second order dependence on the concentration of acetonitrile and the observed build-up of this type of intermediate in low temperature NMR studies.[4e] There were two proposed equilibrating sets of species that were considered previously. The first was a pair of η^4-diyne diastereomers **35-d1** and **35-d2**. There could be either an unequal concentration of these species with the rate of cycloaromatization from each species being approximately equal. They could also have an approximately equal concentration of **35-d1** and **35-d2**, but the rate of cycloaromatization could be faster for one diastereomer over the other. The change in concentration and rate of aromatization was attributed to either steric interactions

of the substituents of the diyne with the methyl groups of the Cp* ligand or electrostatic interaction of the hydroxyl substituent with the ruthenium. Loss of acetonitrile from **35** and coordination of the metal to the alkene leads to a pair of diastereomeric η^6-enediynes, **36-d1** and **36-d2**, which could also equilibrate before the cyclization occurs.

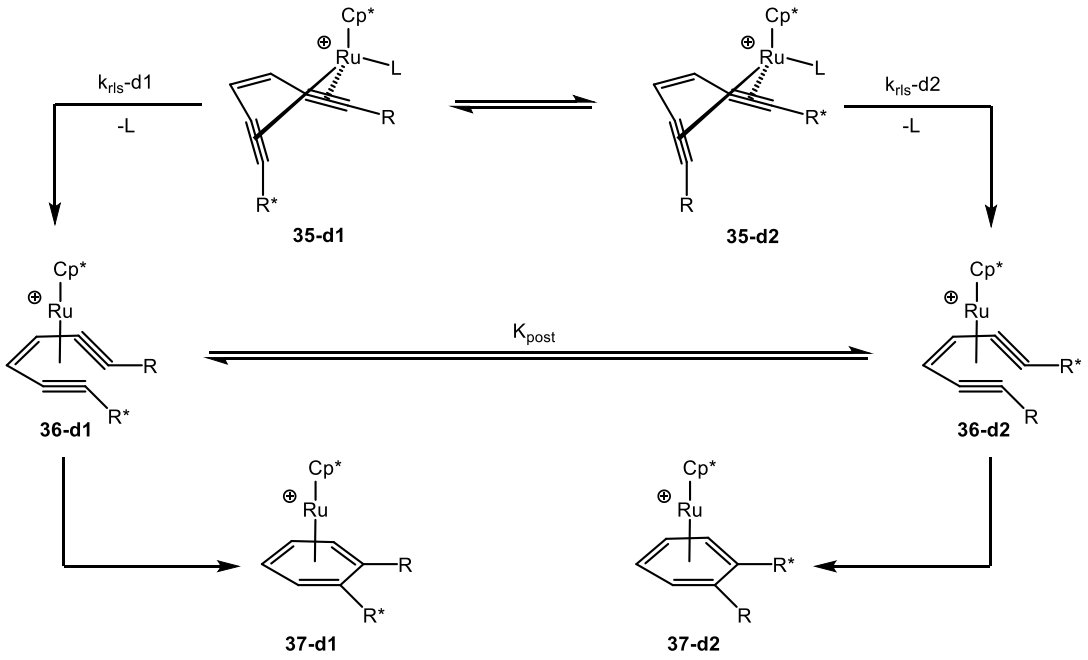

Scheme 4-17. Proposed models for selectivity.[22]

The change from the electron-rich and sterically encumbering Cp* ligand to the less electron-rich non-sterically encumbering Cp ligand or the less electron-rich but sterically encumbering Cp‡ ligand lead to a decrease in yield and a loss of stereoselectivity. Previously, it was shown that η^4-diyne **38** would rapidly exchange with enediyne **39** upon mixing in THF (Scheme 4-18).[4e]

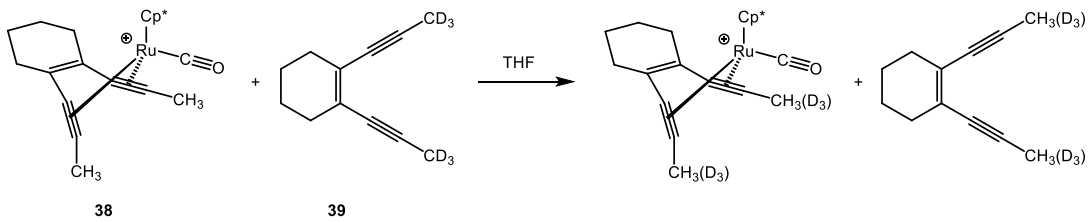

Scheme 4-18. Exchange experiment in η^4-enediyne ruthenium complexes.[4e]

This would suggest an equilibration between η^4-diynes **35-d1** and **35-d2** would be rapid. Unfortunately, a similar exchange experiment was not performed with $[CpRu]^+$ or $[Cp^{‡}Ru]^+$. It could be that exchange is much slower in the less electron-rich systems and cycloaromatization occurs from a mixture of **35-d1** and **35-d2** resulting from initial coordination of ruthenium to the enediyne. This initial coordination of the ruthenium to the enediyne should experience less steric pressure between the ruthenium and the substituents on the enediyne, giving near equal concentration of the diastereomers. In addition, a less electron-rich ruthenium center should not allow for a rapid equilibrium between η^6-enediyne complexes.

When the ruthenium-naphthalene complexes **26**, **27**, and **28** were reacted with enediynes under photolysis, the formation of arene products was observed in excellent yield with high conversion of naphthalene complex. The nature of the Cp ligand showed a minor effect on the rate of conversion and yield of the arene product. The UV-Vis spectra (acetonitrile) for the [CpRu(benzene)]PF_6 series has been shown to have little variation in the λ_{max}; [CpRu] 320 nm, [Cp*Ru] 321 nm, and $[Cp^{‡}Ru]$ 321 nm.[17] The quantum efficiency of the release of benzene was shown to be similar for [CpRu] and $[Cp^{‡}Ru]$ at approximately 0.34, with [Cp*Ru] being lower at 0.19.[17] The

yield of arene product is higher using the naphthalene complexes under photo-conditions than the reactions of the ruthenium tris-acetonitrile complexes.[4] This is attributed to the slower production of $[CpRu]^+$. The exchange rate of MeCN in $[CpRu(NCMe)_3]PF_6$ is known to be $k = 4.1\ s^{-1}$ and the exchange undergo a dissociative mechanism.[23] The loss of one MeCN leads to an open-coordination site which can then bind to enediyne, leading to η^6-coordination and cycloaromatization. In the naphthalene complexes, the generation of ruthenium bis-solvate complexes which can interact with enediyne is slower and the generation of the proposed *p*-benzyne intermediate would be in lower concentrations than observed for the tris-acetonitrile complexes. The lower concentration of reactive *p*-benzyne could lead to lower amounts of side-products and less oligomerization of substrate. It is not known if the ruthenium-naphthalene complexes react with enediynes from a tris-solvate complex **40** or from an η^4-naphthalene intermediate **41**, Scheme 4-19.

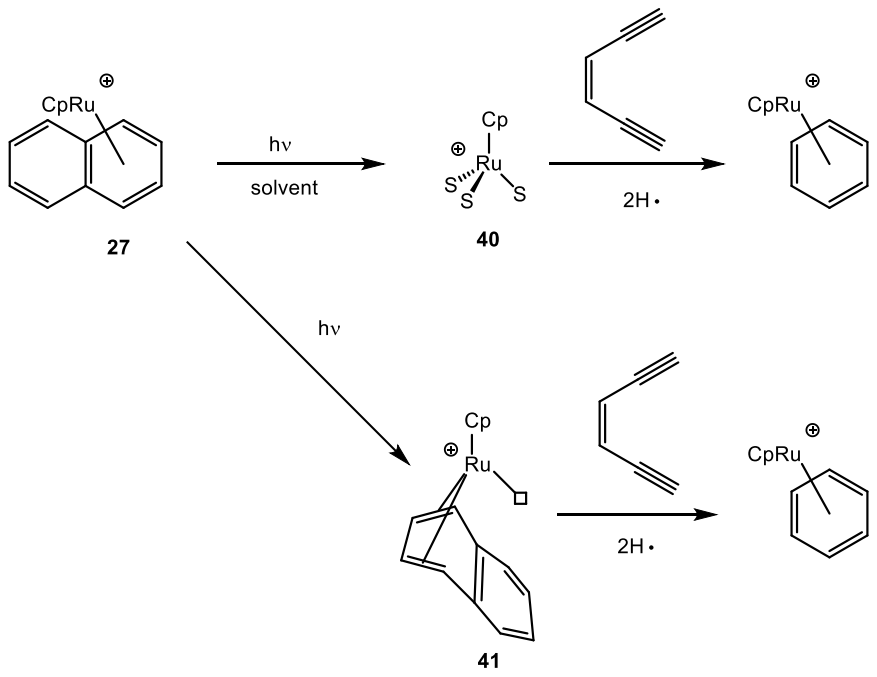

Scheme 4-19. Possible $CpRu^{+}$ complexes from $CpRu(naphthalene)^{+}$.

One other advantage for the use of **26**, **27**, and **28**, is that since they are ruthenium sandwich complexes, they are bench- and air-stable. The tris-acetonitrile complexes **5**, **6**, and **25** are air-sensitive even in the solid-state, requiring special consideration for reactions and storage of the complexes. The naphthalene complexes have been stored on the bench, protected from light, for several months with no observed decomposition or loss in reactivity. The one precaution when using these reagents in reactions is to use deoxygenated solvents, since the $[CpRu]^{+}$ generated during the course of the reaction are oxygen-sensitive.

The reaction of **27** with dienyne under photolysis gave arene product in excellent yield with high conversion of **27**. The reactions of dienynes with **5** give

similar high yields to those obtained with **27**. The main advantage, as discussed previously, is the air-stable **27** is easier to work with compared to **5**.

As was seen by Gassman[7] during the development of the $Cp^{‡}$ ligand, the synthesis of $[Cp^{‡}Fe(CO)_2]_2$ from $Cp^{‡}H$ and $Fe(CO)_5$ proceeded in lower yield than the Cp*H analogue. The dimer underwent clean oxidization by ferrocenium to give $[Cp^{‡}Fe(CO)_2MeCN]PF_6$ which showed similar IR (thin-film) stretches to those observed in the [CpFe] analogue[9] but different from the [Cp*Fe] analogue.[8] This is consistent with lower electron density at the metal center, which then back-bonds less to the carbonyl ligands, which results in stronger C-O bonds for $Cp^{‡}$ and Cp. Photolysis of $[Cp^{‡}Fe(CO)_2MeCN]PF_6$ in N_2-saturated MeCN in a sealed flask led to $[Cp^{‡}Fe(CO)(MeCN)_2]PF_6$ as a red solid. Again the CO IR (thin-film) stretches are consistent with lower electron density on the metal center. The photolysis of $[Cp^{‡}Fe(CO)_2MeCN]PF_6$ in MeCN under a constant stream of N_2 below -10 °C led to a purple solution, which is consistent with the formation of $[Cp^{‡}Fe(NCMe)_3]PF_6$ by analogy to $[Cp^{*}Fe(NCMe)_3]PF_6$.[8] Several attempts were made to isolate and characterize this complex, but decomposition of the complex was a constant problem.

The dimer $[Cp^{‡}Fe(CO)_2]_2$ was also oxidized with Br_2 in DCM/$CHCl_3$ to give $Cp^{‡}Fe(CO)_2Br$ by analogy to $[Cp^{*}Fe(CO)_2]_2$. $Cp^{*}Fe(CO)_2Br$ is known to react with $AlCl_3$ in aromatic solvents to give $[Cp^{*}Fe(arene)]^{+}$ complexes. When $Cp^{‡}Fe(CO)_2Br$ was reacted with $AlCl_3$[14] in refluxing benzene overnight, the expected benzene complex was not observed. Instead, the product from activation and substitution of

all three of the C-F bonds was observed to give **23** as confirmed by X-ray crystallography (Scheme 4-20).

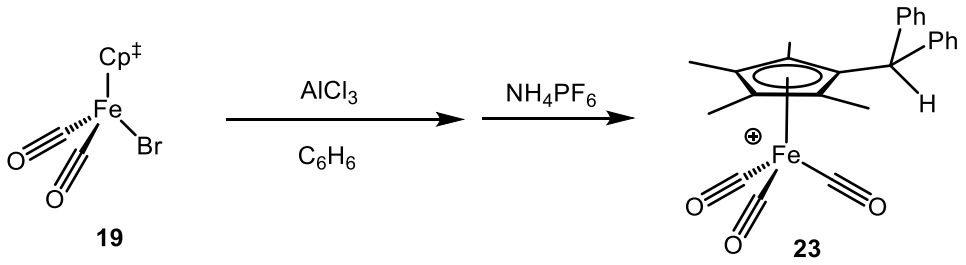

Scheme 4-20. Synthesis of **23**.

The formation of this unusual product is proposed to start by removal of the bromide from iron by $AlCl_3$ to generate the unsaturated metal complex **42** (Scheme 4-21). Then through an intramolecular C-F activation, iron-fulvene **43** could be formed, which is one resonance form with the other maintaining the cyclopentadienyl ring and placing a carbocation at the carbon bearing the fluorines. This electrophile is then attacked by the solvent benzene, by analogy to Friedel-Crafts chemistry, to give **44**. Repetition of this cycle initiated by fluoride abstract from **44** by $AlCl_3$ leads to **45** which could be attacked by a hydride generated in solution[24] by hydride abstraction from a methyl group by $AlCl_3$ to give **46**. Then fluoride abstract of **46** by $AlCl_3$ leads to **47** which can form **23** by CO abstraction from another iron-CO complex in solution. The mechanism for the CO abstraction is unclear, but it could proceed via an $AlCl_3$-mediated pathway or a direct disproportionation with another iron-CO complex in solution.

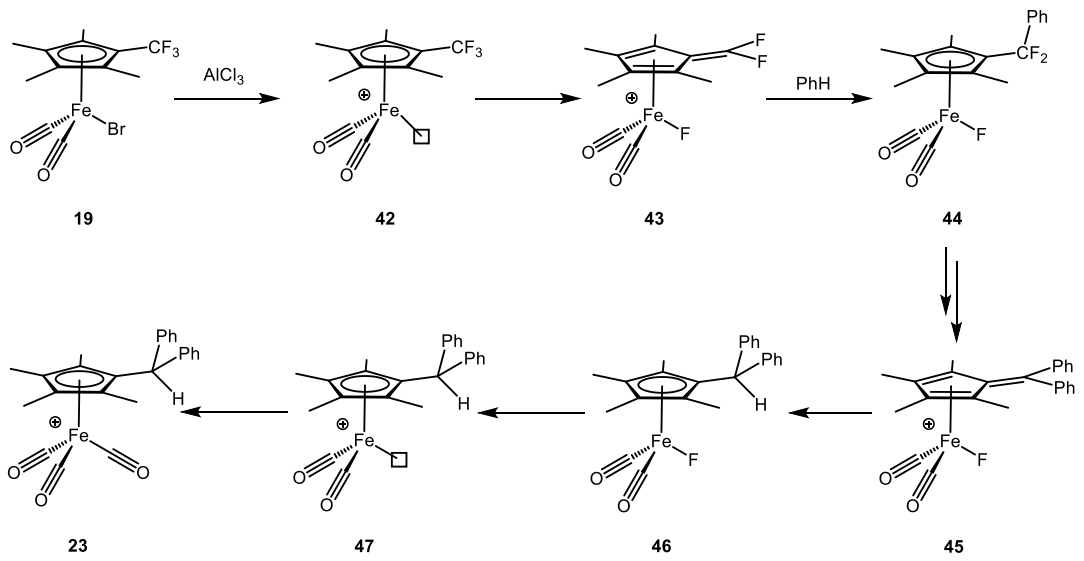

Scheme 4-21. Proposed mechanism for the formation of **23**.

The close proximity and unsaturated nature of the iron in intermediate **42** would make the migratory defluorination a preferable path over fluoride abstraction by aluminum. The presence of aluminum-hydrides in solution under such strongly acidic, both Lewis acidic and increasingly Brönsted acidic as the reaction progresses, has been proposed before in $AlCl_3$-mediated rearrangements of hydrocarbons.[24] The preparation of 1-chloronorbornane[25] is accomplished by an aluminum chloride catalyzed rearrangement of 2,2-dichloronornornane in pentane (Scheme 4-22). If the reaction is carried out in pentane·d_{12}, there is ~50% incorporation of a mono-deuterium observed. The only source of deuterium under the reactions conditions is pentane.[26]

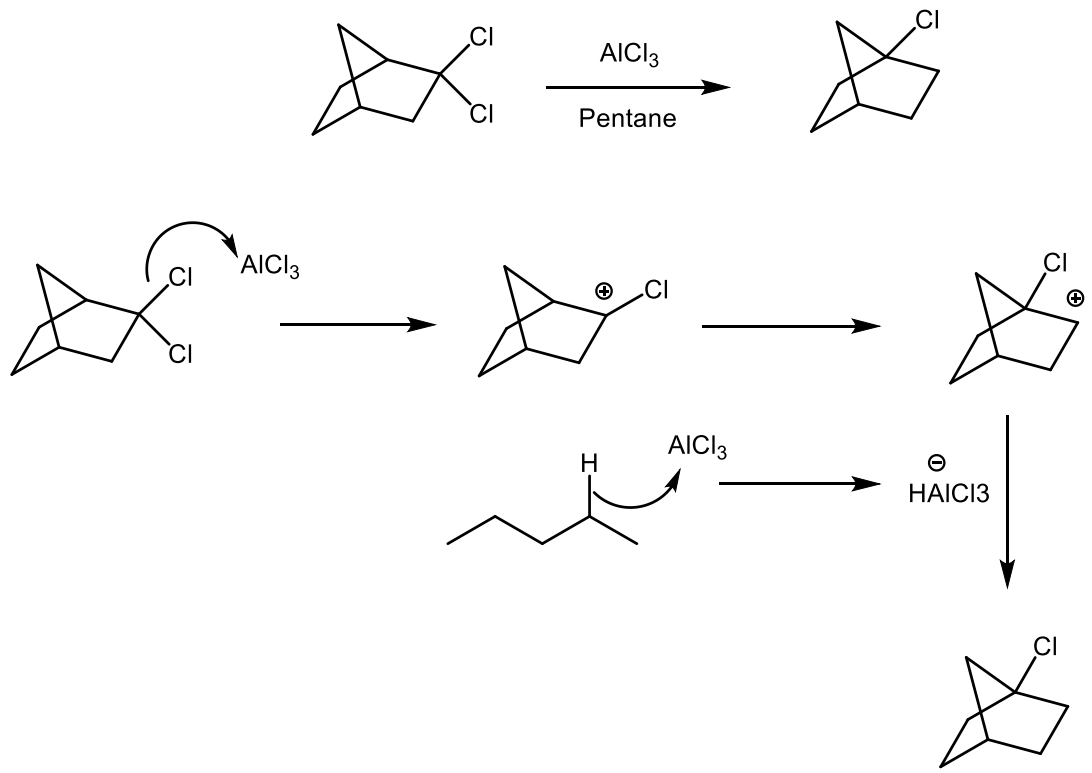

Scheme 4-22. Synthesis of 1-chloronorbornane.

4-4 Conclusion

The ruthenium complexes of $Cp^{‡}$ mediate the cycloaromatization of enediyne and dienyne substrates in good yields. In addition, it was shown that the facial selectivity in cyclization of enediynes bearing a chiral center is primarily influenced by electronic effects not steric effects of Cp ligands. Several iron complexes bearing the $Cp^{‡}$ ligand were synthesized and data collected reinforced the electronic similarity between $Cp^{‡}$ and Cp. When the synthesis of a $Cp^{‡}Fe(arene)^{+}$ complex was attempted

under Lewis acid conditions, the unexpected activation of three C-F bonds and the formation of a tetramethyl(diphenylmethyl)cyclopentadienyl ligand was observed.

4-5 Experimental

4-5.1 General Procedures

All manipulations were performed using standard Schlenk technique or in nitrogen filled Vacuum Atmospheres or MBraun glovebox, unless otherwise stated. ^{1}H and ^{13}C NMR spectra were recorded on Varian Mercury 400 MHz, Varian VX 500 MHz, or JOEL ECA 500 MHz instruments. ^{1}H and ^{13}C NMR chemical shifts (δ) are reported in parts per million (ppm). Spectra were referenced to the residual solvent peak. Infrared spectra were obtained on a Nicolet iS10 FT-IR. High resolution mass spectra analyses were performed at either the mass spectrometer facility at UC San Diego or UC Riverside. Photolyses was performed in a Rayonett photo-reactor equipped with UV lamps centered at 254 nm. THF, ethyl ether, DCM, benzene, hexanes, and pentane used for reaction solvents were dried either by a solvent dispensing system equipped with two neutral alumina columns under argon atmosphere or by 3 Å activated molecular sieves. Chloroform-*d* and benzene-d_6 were dried over 3 Å activated molecular sieves and then distilled under static vacuum into oven-dried Schlenk storage tubes. Deuterated solvents were degassed using a Freeze-Pump-Thaw procedure, typically 5 cycles. NMR reactions were performed in 5 mm

J-Young NMR tubes equipped with a Teflon needle valve. All literature compounds were prepared according to the indicated references or purchased from commercial suppliers and used as received.

4-5.2 Preparation and Characterization Data

{[η^5-$C_5(CF_3)(CH_3)_4$]Fe(CO)$_2$(NCMe)}PF_6 (19): A degassed solution of DCM/MeCN (60 mL, 2:1) was added via cannula to a side arm flask containing **17** (411 mg, 0.68 mmol) and $[Cp_2Fe]PF_6$ (450 mg, 1.37 mmol) under N_2. The resulting blue suspension was allowed to stir overnight at rt under N_2, during which time the color changed to yellow-orange and a homogenous solution was obtained. The volatiles were removed under vacuum and the residue was dissolved in minimal amount of acetone. The addition of Et_2O caused the precipitation of a bright yellow powder which was collected on a frit and the washed with Et_2O (3 x 25 mL) until the filtrate remained clear colorless. The collected solid was then recrystallized from DCM/Et_2O to give **19** as a yellow solid (458 mg, 0.94 mmol 70% yield). ^{1}H NMR ($CDCl_3$, 500 MHz) δ 1.85 (s, 6H); 1.97 (s, 6H), 2.26 (s, 3H). ^{13}C NMR ($CDCl_3$, 125 MHz) δ 4.5, 9.3, 10.2, 78.7 (q, $^2J_{C\text{-}F}$ = 36.7 Hz), 101.0, 104.5, 124.0 (q, $^1J_{C\text{-}F}$ = 273.7 Hz), 135.3, 207.1. HRMS (ESI): Calcd for ($C_{14}H_{16}F_3FeNO_2$): 342.0399. Found 342.0402. IR (thin film, cm^{-1}): 2075, 2032.

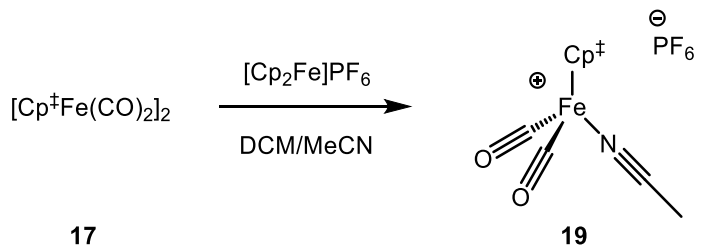

17 19

{[η^5-$C_5(CF_3)(CH_3)_4$]Fe(CO)$(NCMe)_2$}PF_6 (20): MeCN (20 mL, sparged with argon for 10 mins) was added to side-arm flask containing **19** (100 mg, 0.24 mmol) under N_2. The flask was closed and placed in an ice water bath in the photo-reactor. The solution was then photolyzed for 1 h, during which time the yellow solution turned to bright red. The volatiles were removed under vacuum and the residue was recrystallized from acetone/Et_2O to give **20** as a red solid (56 mg, 0.13 mmol, 50% yield). ^{1}H NMR (acetone·d_6, 500 MHz) δ 1.83 (s, 6H), 1.88 (s, 6H), 2.62 (s, 6H). ^{13}C NMR (acetone·d_6, 125 MHz) δ 3.8, 8.6, 9.6, 70.0 (q, $^2J_{C\text{-}F}$ = 36.3 Hz), 93.7, 99.0, 126.4 (q, $^1J_{C\text{-}F}$ = 271.9 Hz), 134.9, 214.7. HRMS (ESI): Calcd for ($C_{15}H_{18}F_3FeN_2O$): 355.0721. Found 355.0721. IR (thin film, cm^{-1}): 2079, 2000.

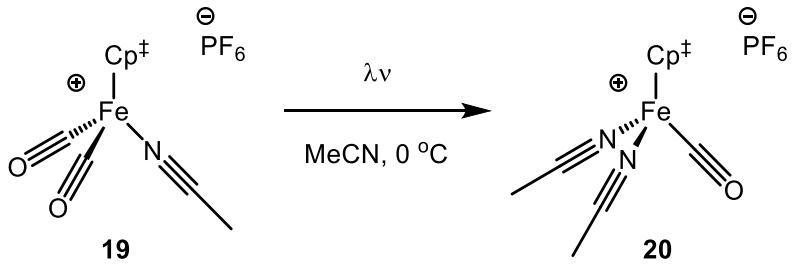

19 20

[η^5-$C_5(CF_3)(CH_3)_4$]Fe$(CO)_2$Br (22): A solution of **17** (225 mg, 0.37 mmol) in $CHCl_3$/DCM (10 mL, 2:1) was cooled to 0 °C on an ice water bath and then Br_2 (20 μL, 0.38 mmol) dissolved in $CHCl_3$ (2 mL) was added dropwise over 5 min. The resulting solution was allowed to stir at rt for 3 h. The solution was then washed with

$Na_2S_2O_3$ (3 x 10 mL), H_2O (2 x 10 mL) and brine (10 mL) and dried over $MgSO_4$. The volatiles were removed under vacuum and the residue was recrystallized from hot ethanol, to give **22** as deep red needle crystals (225 mg, 0.6 mmol, 81% yield). ^{1}H NMR ($CDCl_3$, 500 MHz) δ 1.92 (s, 6H), 2.06 (s, 6H). ^{13}C NMR ($CDCl_3$, 125 MHz) δ 9.9, 10.6, 99.7, 100.6, 124.7 (q, $^1J_{C\text{-}F}$ = 271.9 Hz), 211.9. HRMS (ESI): Calcd for ($C_{12}H_{12}BrF_3FeO_2$): 379.9322. Found 379.9320. IR (thin film, cm^{-1}): 2040, 1960.

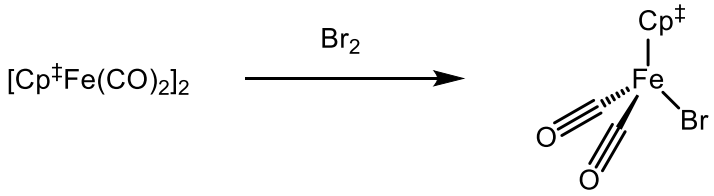

17 **22**

[η^5-C$_5$(Ph2CH)(CH$_3$)$_4$]Fe(CO)$_3$}PF$_6$ (23): Benzene (5 mL) was added to a side-arm flask containing $AlCl_3$ (145 mg, 1.09 mmol) under N_2, and then under stirring **22** (103 mg, 0.27 mmol) was added. The flask was topped with a reflux condenser and the solution was brought to reflux under N_2 for 16 h. The solution was cooled to rt and poured into ice water (10 mL) and then NH_4PF_6 (310 mg, 2 mmol) dissolved in H_2O (5 mL) was added. The aqueous solution was extracted with DCM (3 x 30 mL). The combined organic extracts were washed with brine, dried over $MgSO_4$ and volatiles removed under vacuum. The residue was then recrystallized from acetone/Et_2O to give **23** as orange crystals (45 mg, 0.079 mmol, 30% yield). ^{1}H NMR (CD_2Cl_2, 500 MHz) δ 1.72 (s, 6H), 2.08 (s, 6H), 5.24 (s, 1H), 7.15 (d, $^3J_{H\text{-}H}$ = 8.4 Hz, 4H), 7.36-7.43 (m, 6H). ^{13}C NMR (CD_2Cl_2, 125 MHz) δ 10.3, 11.3, 48.5, 89.7, 104.0, 110.6,

128.8, 129.7, 129.8, 138.9, 204.7. HRMS (ESI): Calcd for ($C_{25}H_{24}FeO_3$): 427.0991. Found 427.0993. IR (thin film, cm^{-1}): 2105, 2059.

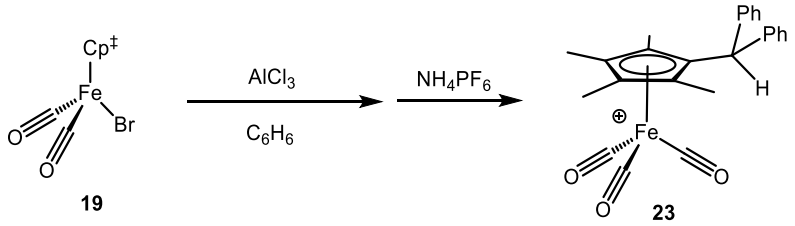

(*Z*)-Octa-4-en-2,6-diyne (29): *Cis*-1,2-dichloroethylene (1 mL, 13.2 mmol) was added to a degassed solution of benzene (100 mL) and NEt_3 (2.5 mL) in a side-arm flask under N_2. Then $PdCl_2(PPh_3)_2$ (400 mg, 0.56 mmol) and CuI (150 mg, 0.8 mmol) were added all-at-once and the resulting solution was stirred at rt for 5 min. Then propyne (from a balloon) was bubbled through the solution for 2 min, and then the flask was closed off and the solution stirred under an atmosphere of propyne for 2 h. The solution was then filter through a pad of Celite, which was rinsed with EtOAc (2 x 20 mL) and the volatiles removed under vacuum. The residue was then purified on a silica column with hexanes eluant to give **29** as a clear colorless oil (1 g, 10 mmol, 76% yield). ^{1}H NMR ($CDCl_3$, 500 MHz) δ 1.93 (s, 3H); 5.59. (s, 1H) ^{13}C NMR ($CDCl_3$, 125 MHz) δ 3.8, 79.4, 88.1, 120.3. HRMS (EI): Calcd for (C_8H_9) 105.0704. Found 105.0706.

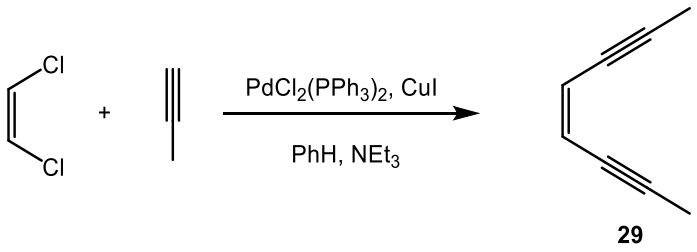

(η^5-Trifluoromethyltetramethylcyclopentadienyl)(η^6-*o*-xylene)ruthenium(II) hexafluorophosphate (30): A degassed solution of **29** (20 mg, 0.2 mmol) and 1,4-CHD (47 μL, 0.5 mmol) in CH_2Cl_2 (10 mL) was added to a flask containing **25** (110 mg, 0.2 mmol) under N_2. The resulting solution was stirred at rt under N_2 for 2 h and then the solution was concentrated to ~0.5 mL under vacuum. Addition of Et_2O (10 mL) caused a precipitate and the suspension was filtered thru a pad of Celite, which was rinsed with Et_2O (3 x 2 mL). Then the Celite was rinsed with acetone (3 x 3 mL) which was collected in a fresh vial. The volatiles were removed under vacuum and the residue was purified on a short silica gel column with acetone in DCM (2%) to give **30** as a colorless solid (70 mg, 0.13 mmol, 65% yield). ^{1}H NMR (acetone·d_6, 500 MHz) δ 2.07 (s, 6H); 2.12 (bs, 6H); 2.30 (s, 6H); 6.20-6.25 (m, 4H). ^{13}C NMR (acetone·d_6, 125 MHz) δ 10.1, 10.4, 17.0, 85.8 (q, $^2J_{CF}$ = 36.7 Hz), 89.4, 91.3, 94.8, 98.9, 103.5, 126.3 (q, $^1J_{CF}$ = 271.6 Hz). HRMS (ESI): Calcd for ($C_{18}H_{22}F_3Ru$): 397.0717. Found 397.0716.

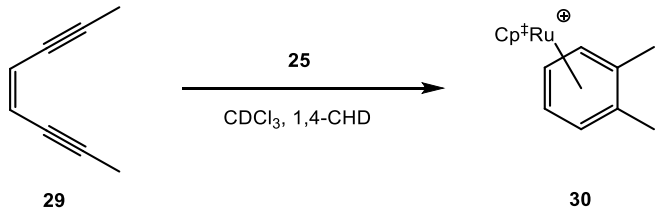

(η^5-Tetramethyl(trifluoromethyl)cyclopentadienyl)(η^6-6-(1-hydroxyethyl)-7-trimethylsilyl-tetralinyl)ruthenium(II) hexafluorophosphate (32): **25** (10.8mg, 21 μmol) was added to a solution of **31** (4.9 mg, 19.9 mmol), 1,4-CHD (4 μL, 42 mmol), and 1,3,5-tri-^{t}butylbenzene (0.8 mg, 3.2 μmol) in acetone·d_6 (1 mL) in a J.Young tube in the glovebox. The ratio of diastereomers was determined by integration of

distinguishable ^{1}H NMR resonances of **32** at δ 6.13(s, 1H) and 5.56 (s, 1H) for diastereomer A; and δ 5.82 (s, 1H) and 5.68 (s, 1H) for diastereomer B. Yield 32%(NMR yield) of a 1:1 mixture of diastereomer A to B.

Preparative scale synthesis of 32: Ruthenium complex **25** (100 mg, 180 μmol) was added to a solution of **31** (50 mg, 200 μmol) in acetone:THF (10 mL, 1:1) in the glovebox. The mixture was allowed to react for 60 min and then concentrated under vacuum. The residue was dissolved in methylene chloride and then ruthenium complexes precipitated upon addition of Et_2O. The precipitate was collected on a fine frit and washed with Et_2O. The precipitate was loaded onto a silica gel column and eluted with acetone in CH_2Cl_2 (0→2%). Three bands came off of the column. The first was identified as **33** (4.5 mg, 7.2 μmol, 4% yield), the second band was **32**-dia**1** (14.7 mg, 23.4 μmol, 13% yield), and the final band **32**-dia**2** (15.9 mg, 25.2 μmol, 14% yield). Each product was obtained as a white powder. The observed chemical shifts were comparable to the shifts reported for the CpRu and Cp*Ru complexes previously reported.[22] (**32**-dia**1**) ^{1}H NMR (500 MHz, $CDCl_3$) δ 0.43 (s, 9H, TMS), 1.54 (d, $^{3}J_{HH}$ = 6.5 Hz, 3H, CH(OH)C*H*$_3$), 1.65-1.79 (m, 4H, 2,3-CH_2), 1.91 (s, 3H, Cp‡C*H*$_3$), 1.94 (bs, 3H, Cp‡C*H*$_3$), 1.96 (s, 3H, Cp‡C*H*$_3$), 2.05 (bs, 3H, Cp‡C*H*$_3$), 2.39-2.52 (m, 2H, 1,4-CH_2^{syn}), 2.69-2.75 (m, 1H, 1,4-CH_2^{anti}), 2.84 (dt, $^{2}J_{HH}$ = 17.9Hz $^{3}J_{HH}$ = 5.6Hz, 1H, 1,4-CH_2^{anti}), 3.10 (d, $^{3}J_{HH}$ = 6.5 Hz, 1H, O*H*), 4.69 (p, $^{3}J_{HH}$ = 6.5 Hz, 1H), 5.55 (s, 1H, ArH), 6.11 (s, 1H, ArH). ^{13}C NMR (125 MHz, $CDCl_3$) δ 0.69 (TMS), 10.0 (Cp‡*C*H$_3$), 10.1 (Cp‡*C*H$_3$), 10.4 (Cp‡*C*H$_3$), 11.4 (Cp‡*C*H$_3$), 21.2 (CH_2), 21.5 (CH_2), 25.3 (CH_2), 26.5 (CH_2), 26.7 (CH_2), 65.7 (*C*H(OH)), 84.6 (q, $^{1}J_{CF}$ = 270 Hz,

$C^{Cp}CF_3$), 84.8 ($C^{Ar}H$), 89.3 ($C^{Ar}H$), 92.6 ($C^{Cp}CH_3$), 94.2 ($C^{Cp}CH_3$), 95.4 ($C^{Ar}TMS$), 97.4 ($C^{Cp}CH_3$), 98.3 ($C^{Cp}CH_3$), 103.4 ($C^{Ar}CH_2$), 104.32 ($C^{Ar}CH_2$), 114.2 ($C^{Ar}CH(OH)$), 125.3 (q, $^1J_{CF}$ = 270 Hz, CF_3). ^{19}F NMR (470 MHz, $CDCl_3$) δ -54.40 (CF_3), -72.2 (d, $^1J_{PF}$ = 712.8 Hz, PF_6^-). HRMS (ESI): Calcd for ($C_{25}H_{36}F_3ORuSi$ – PF_6): 539.1538, found 539.1525. (**32**-dia**2**) ^{1}H NMR (500 MHz, $CDCl_3$) δ 0.38 (s, 9H, TMS), 1.55 (d, $^3J_{HH}$ = 6.4 Hz, CH(OH)C*H*$_3$), 1.71 (m, 2H, 2,3-CH_2), 1.82 (m, 2H, 2,3-CH_2), 1.87 (s, 3H, Cp‡C*H*$_3$), 1.88 (s, 3H, Cp‡C*H*$_3$), 1.93 (bs, 3H, Cp‡C*H*$_3$), 1.98 (bs, 3H, Cp‡C*H*$_3$), 2.38-2.50 (m, 2H, 1,4-CH_2^{syn}), 2.73 (dt, $^2J_{HH}$ = 17.4 Hz, $^3J_{HH}$ = 6.6 Hz, 1H, 1,4-CH_2^{anti}), 2.84 (dt, $^2J_{HH}$ = 17.7 Hz, $^3J_{HH}$ = 6.5 Hz, 1H, 1,4-CH_2^{anti}), 3.15 (bs, 1H, OH), 4.58 (q, $^3J_{HH}$ = 6.4 Hz, 1H, C*H*(OH)CH_3), 5.67 (s, 1H, ArH), 5.83 (s, 1H, ArH). ^{13}C NMR (125 MHz, $CDCl_3$) δ 1.5 (TMS), 10.1 (Cp‡*C*H$_3$), 10.3 (Cp‡*C*H$_3$), 10.4 (Cp‡*C*H$_3$), 11.1 (Cp‡*C*H$_3$), 21.4 (CH_2), 21.5 (CH_2), 21.9 (CH(OH)*C*H$_3$), 25.4 (CH_2), 26.2 (CH_2), 66.9 (*C*H(OH)CH_3), 84.3 (q, 36.5 Hz, $C^{Cp}CF_3$), 86.1 ($C^{Ar}H$), 91.8 ($C^{Ar}H$), 92.6 ($C^{Cp}CH_3$), 93.8 ($C^{Cp}CH_3$), 96.6 ($C^{Ar}TMS$), 96.7 ($C^{Cp}CH_3$), 98.9 ($C^{Cp}CH_3$), 103.7 ($C^{Ar}CH_2$), 104.6 ($C^{Ar}CH_2$), 110.6 ($C^{Ar}CH_2$), 125.1 (q, $^1J_{CF}$ = 272.3 Hz, CF_3). ^{19}F NMR (470 MHz, $CDCl_3$) δ -54.6 (CF_3), -72.2 (d, $^1J_{PF}$ = 712.2 Hz, PF_6^-) HRMS (ESI): Calcd for ($C_{25}H_{36}F_3ORuSi$ – PF_6): 539.1538, found 539.1537. (**33**) ^{1}H NMR (500 MHz, $CDCl_3$) δ 0.33 (s, 9H, TMS), 1.71 (m, 2H, 2,3-CH_2), 1.82 (s, 3H, Cp‡C*H*$_3$), 1.85 (m, 2H, 2,3-CH_2), 1.88 (bs, 3H, Cp‡C*H*$_3$), 1.91 (s, 3H, Cp‡C*H*$_3$), 1.92 (bs, 3H, Cp‡C*H*$_3$), 2.47 (dt, $^2J_{HH}$ = 17.7 Hz, $^3J_{HH}$ = 6.0 Hz, 1H, 1,4-CH_2^{syn}), 2.62 (dt, $^2J_{HH}$ = 18.1 Hz, $^3J_{HH}$ = 6.7 Hz, 1H, 1,4-CH_2^{syn}), 2.81 (dt, $^2J_{HH}$ = 17.7 Hz, $^3J_{HH}$ = 6.7 Hz, 1H, 1,4-CH_2^{anti}), 2.97 (dt, $^2J_{HH}$ = 18.1 Hz, $^3J_{HH}$ = 6.5 Hz, 1H, 1,4-CH_2^{anti}), 5.84

(s, 1H, ArH), 6.55 (s, 1H, ArH). ^{13}C NMR (125 MHz, $CDCl_3$) δ 1.1 (TMS), 9.7 ($Cp^{‡}CH_3$), 9.8 ($Cp^{‡}CH_3$), 10.0 ($Cp^{‡}CH_3$), 10.6 ($Cp^{‡}CH_3$), 21.3 (CH_2), 21.5 (CH_2), 25.1 (CH_2), 26.5 (CH_2), 29.9 (C(O)CH_3), 85.2 (q, $^2J_{CF}$ = 36.9 Hz, $C^{Cp}CF_3$), 88.8 (ArH), 92.9 (ArH), 94.1 ($C^{Cp}CH_3$), 95.2 ($C^{Cp}CH_3$), 98.0 ($C^{Cp}CH_3$), 98.1 ($C^{Cp}CH_3$), 98.3 ($C^{Ar}CH_2$), 100.4 (C^{Ar}TMS), 105.6 ($C^{Ar}CH_2$), 105.9 (C^{Ar}C(O)CH_3), 124.8 (q, $^1J_{CF}$ = 273.8 Hz, CF_3), 199.7 (C(O)CH_3. ^{19}F NMR (470 MHz, $CDCl_3$) δ -55.0 (CF_3), -72.2 (d, $^1J_{PF}$ = 712.2 Hz, PF_6^-).

31 **32-CF$_3$** R=Me$_4$CF$_3$

4-5.3 Procedures for NMR-Scale Reactions

General procedure for photochemical reactions. Substrate, 1,3,5-tri-*tert*-butylbenzene (0.5-1 mg), ruthenium complex and H-atom donor were weighed into a J. Young tube and then acetone-d_6 (750 μL) was distilled into the tube on the high vacuum line. The solution was subjected to 2 Freeze-Pump-Thaw cycles and an initial ^{1}H NMR spectrum was collected (4 scans, 60 second recycle delay). The tube was then placed in the photo-reactor and photolyzed for the indicated time. Then a ^{1}H NMR spectrum was collected (4 scans, 60 second recycle delay), the % conversion was calculated by the disappearance of bound naphthalene resonances at δ 6.5 and

7.1 and the appearance of free naphthalene at δ 7.8 and 7.9. The % yield was based on the % conversion of the naphthalene complex.

Reaction of 29 with 26. **29** (3 mg, 29 μmol), **26** (16 mg, 29 μmol) and 1,4-CHD (6 μL, 60 μmol). The solution was photolyzed for 6 h. A ^{1}H NMR spectrum showed 95% conversion and 88% yield of **30**.

Reaction of 29 with 27. **29** (3 mg, 29 μmol), **27** (12.5 mg, 29 μmol) and 1,4-CHD (6 μL, 60 μmol). The solution was photolyzed for 6 h. A ^{1}H NMR spectrum showed 93% conversion and 92% yield of **30-H**. The contents of the tube was poured into a vial and **30-H** was precipitated by the addition of Et_2O (10 mL). The solution was filtered through a Celite pad, which was rinsed with Et_2O (2 x 2 mL). The Celite pad was then rinsed with DCM (3 x 2 mL) which was collected in a fresh vial. The volatiles were removed under vacuum to give **30-H** as a white powder (12 mg, 25 μmol, 86% yield). (**30-H**) ^{1}H NMR (acetone·d_6, 500 MHz) δ 2.45 (s, 6H), 5.45 (s, 5H), 6.19 (dd, $^{3}J_{H\text{-}H}$ = 4.3 Hz, $^{4}J_{H\text{-}H}$ = 2.4 Hz, 2H), 6.35 (dd, $^{3}J_{H\text{-}H}$ = 4.3 Hz, $^{4}J_{H\text{-}H}$ = 2.4 Hz, 2H). ^{13}C NMR (acetone·d_6, 125 MHz) δ 19.0, 81.6, 85.5, 88.4, 103.0. HRMS (ESI): Calcd for ($C_{13}H_{15}Ru$): 273.0215, found 273.0216.

Reaction of 29 with 26. **29** (3 mg, 29 μmol), **28** (14.6 mg, 29 μmol) and 1,4-CHD (6 μL, 60 μmol). The solution was photolyzed for 6 hrs. A ^{1}H NMR spectrum showed 97% conversion and 94% yield of **30-Me**. The product exhibited spectroscopic properties identical to those reported in literature.[27]

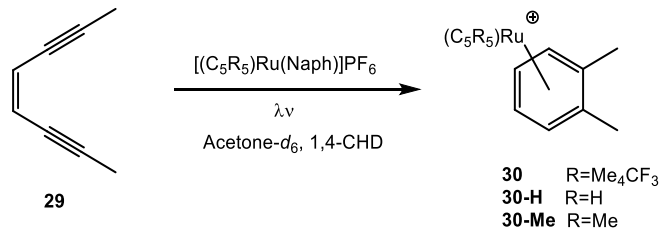

Reaction of 33 with 27. **33** (4.6 mg, 29 μmol) and **26** (12.5 mg, 29 μmol). The solution was photolyzed for 16 hrs. A ^{1}H NMR spectrum showed 95% conversion and 88% yield of **34**.

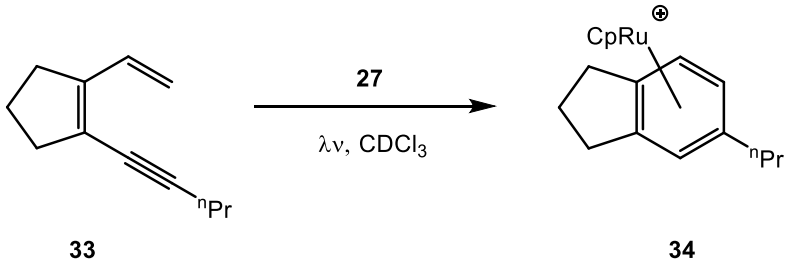

4-5.4 ^{1}H and ^{13}C NMR Spectroscopic Data

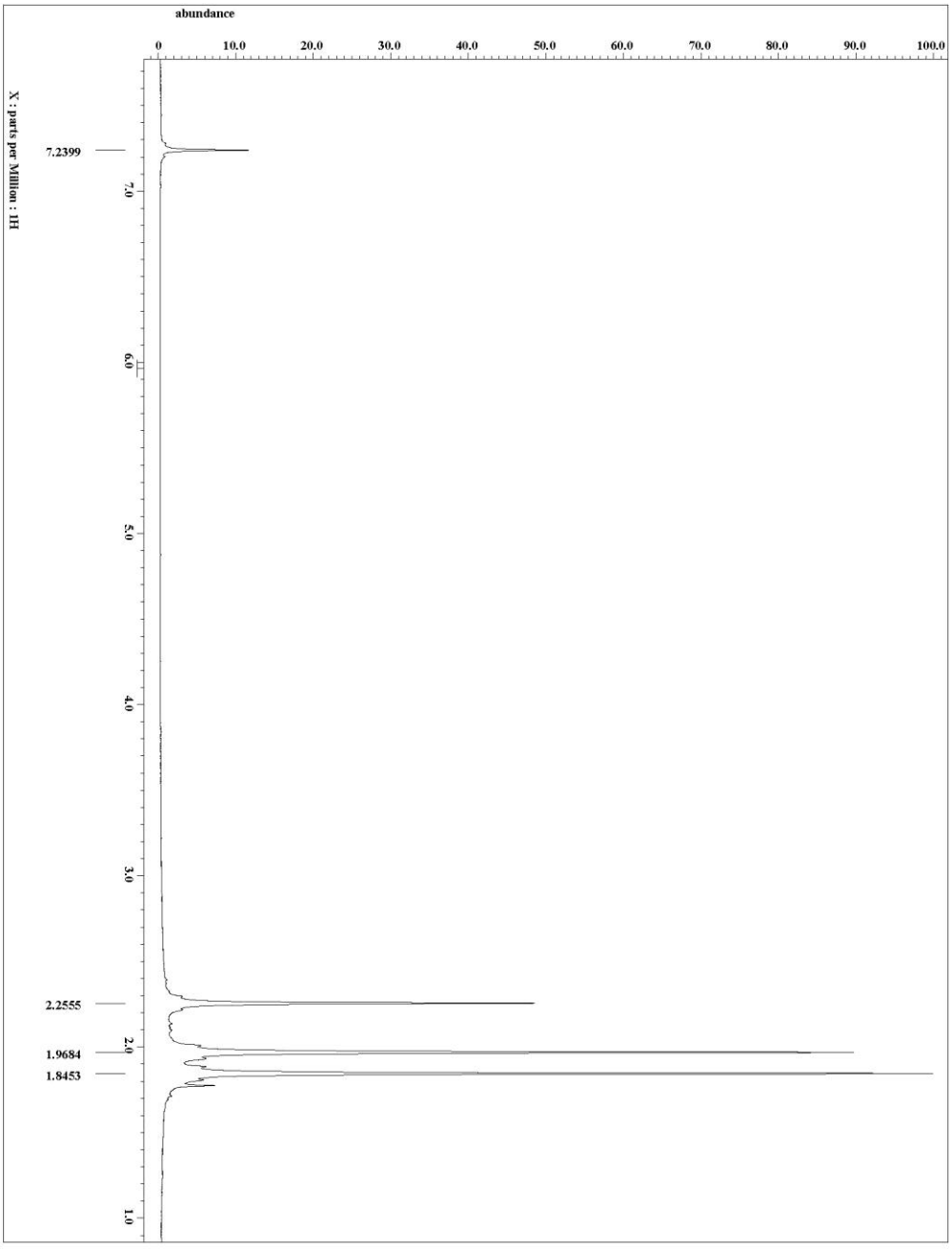

Figure 4-3. 19 ^{1}H NMR spectrum (500 MHz, $CDCl_3$).

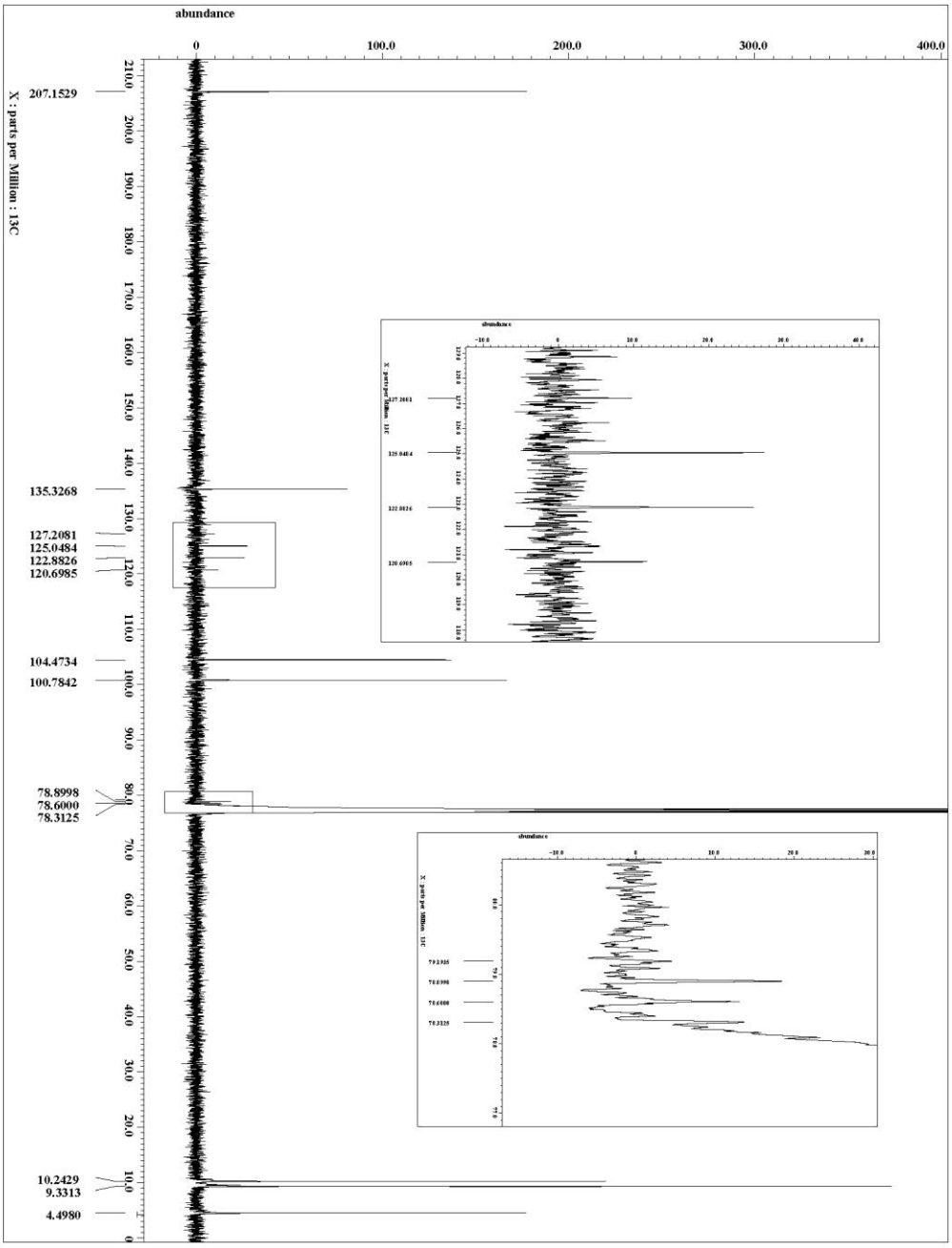

Figure 4-4. 19 ^{13}C NMR spectrum (125 MHz, $CDCl_3$).

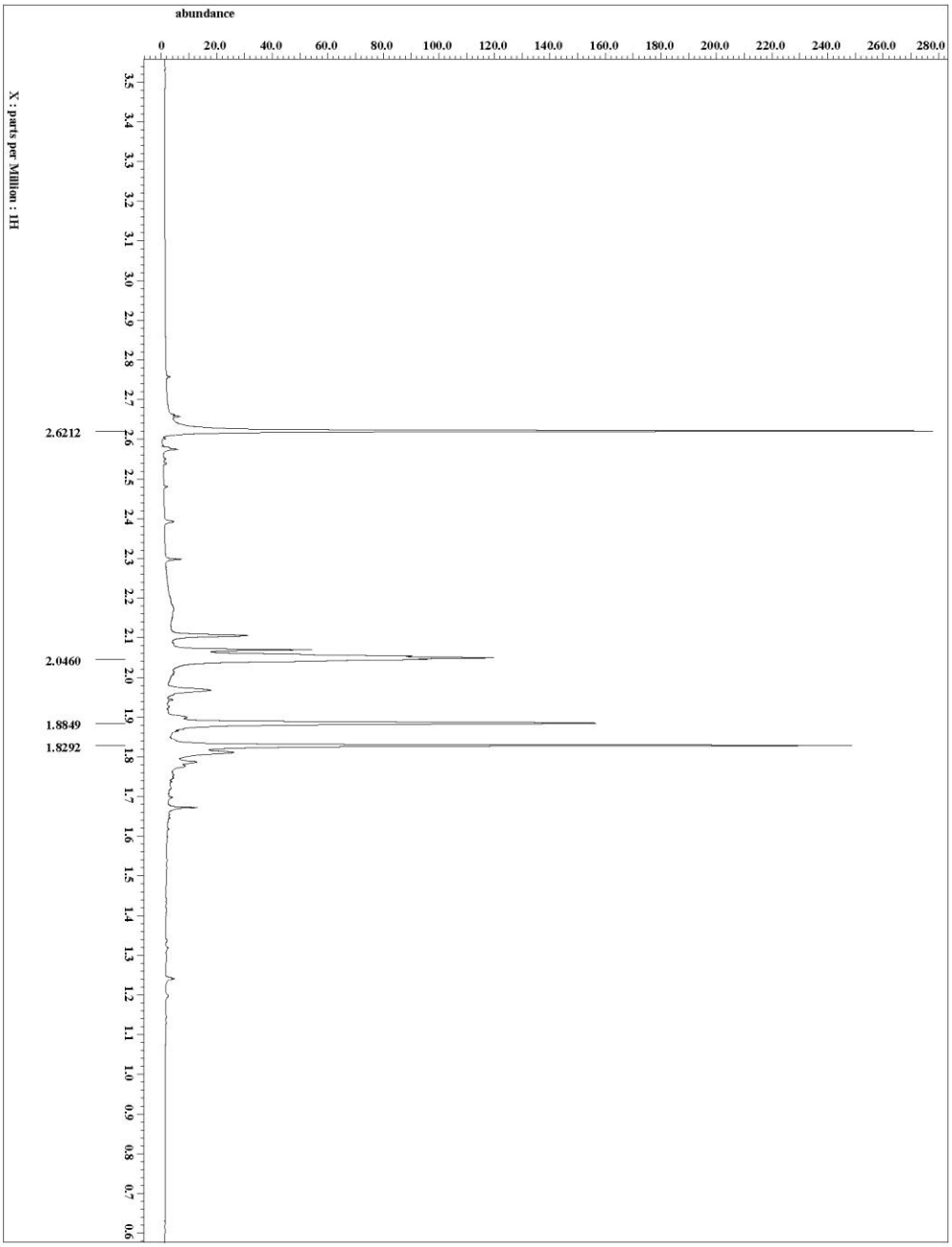

Figure 4-5. 20 ^{1}H NMR spectrum (500 MHz, acetone-d_6).

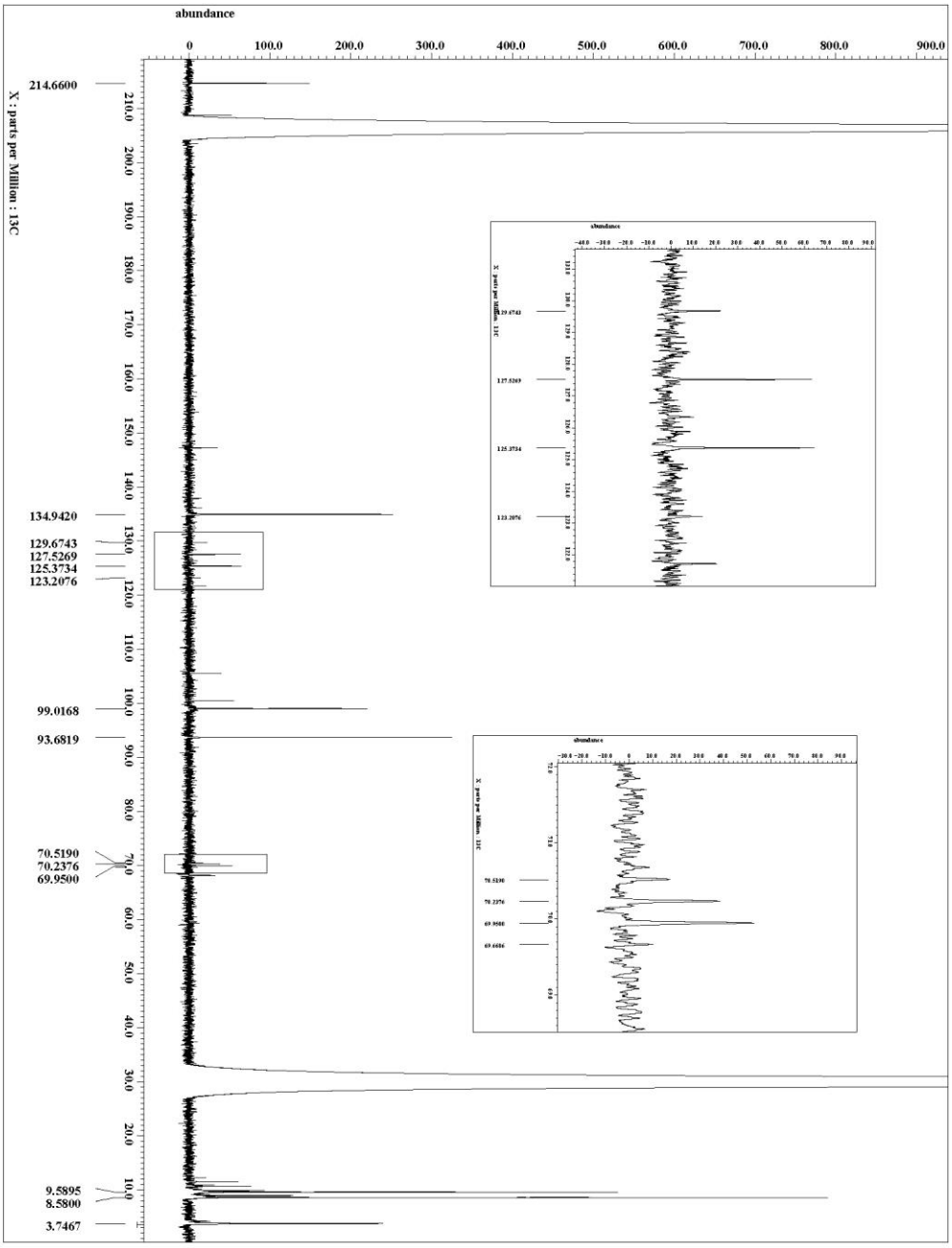

Figure 4-6. 20 ^{13}C NMR spectrum (125 MHz, acetone-d_6).

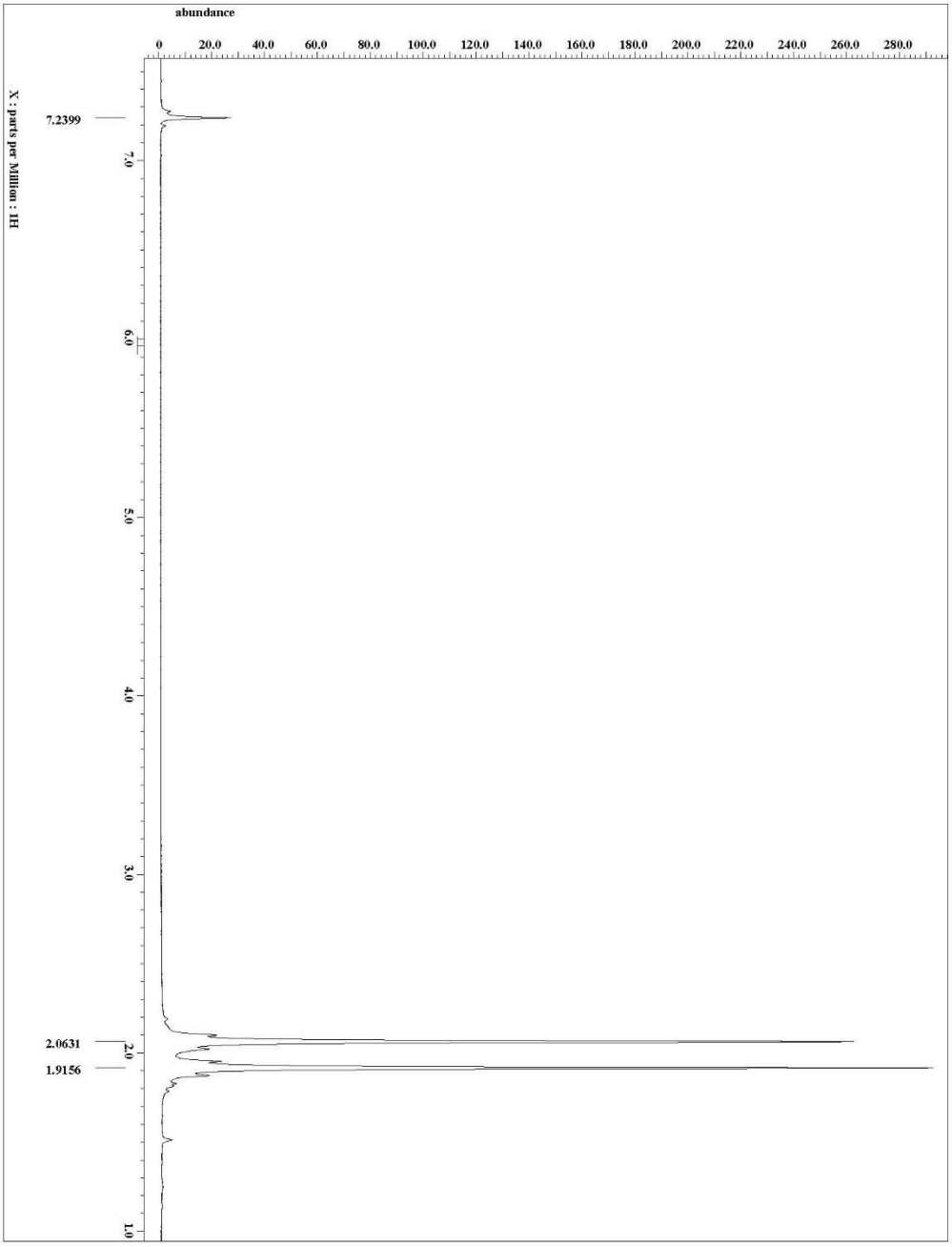

Figure 4-7. 22 ^{1}H NMR spectrum (500 MHz, $CDCl_3$).

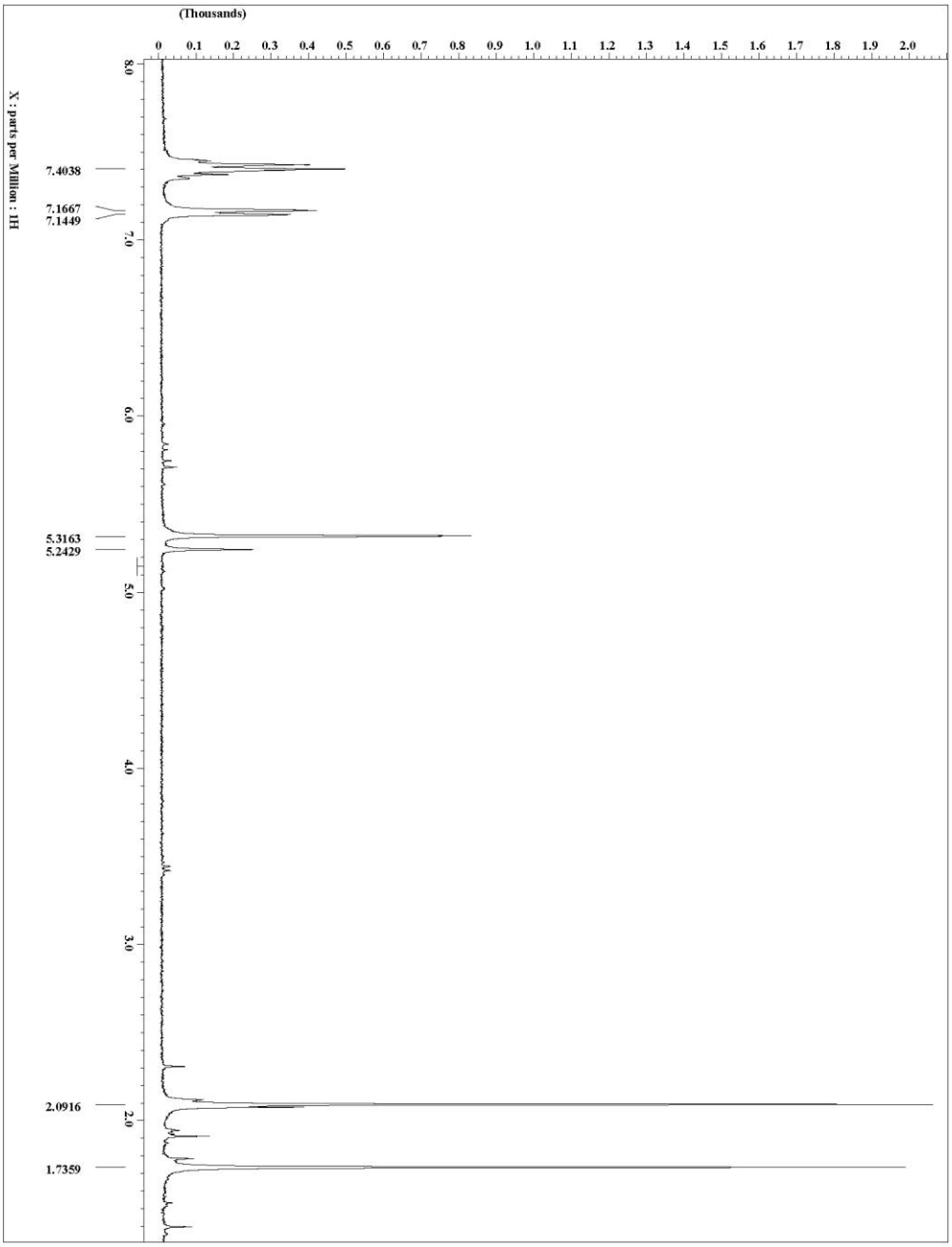

Figure 4-8. 23 ^{1}H NMR spectrum (500 MHz, CD_2Cl_2).

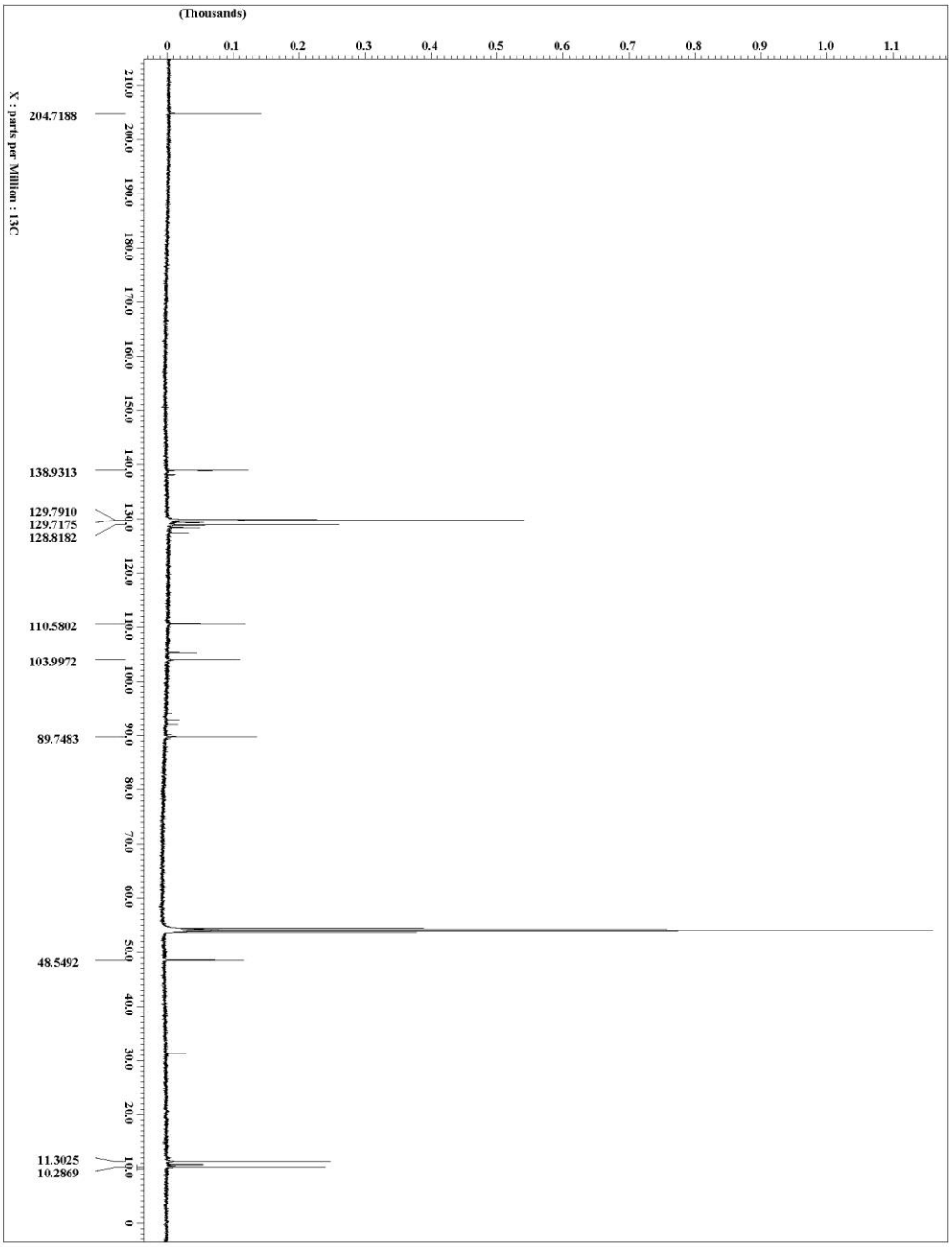

Figure 4-9. 23 ^{13}C NMR spectrum (125 MHz, CD_2Cl_2).

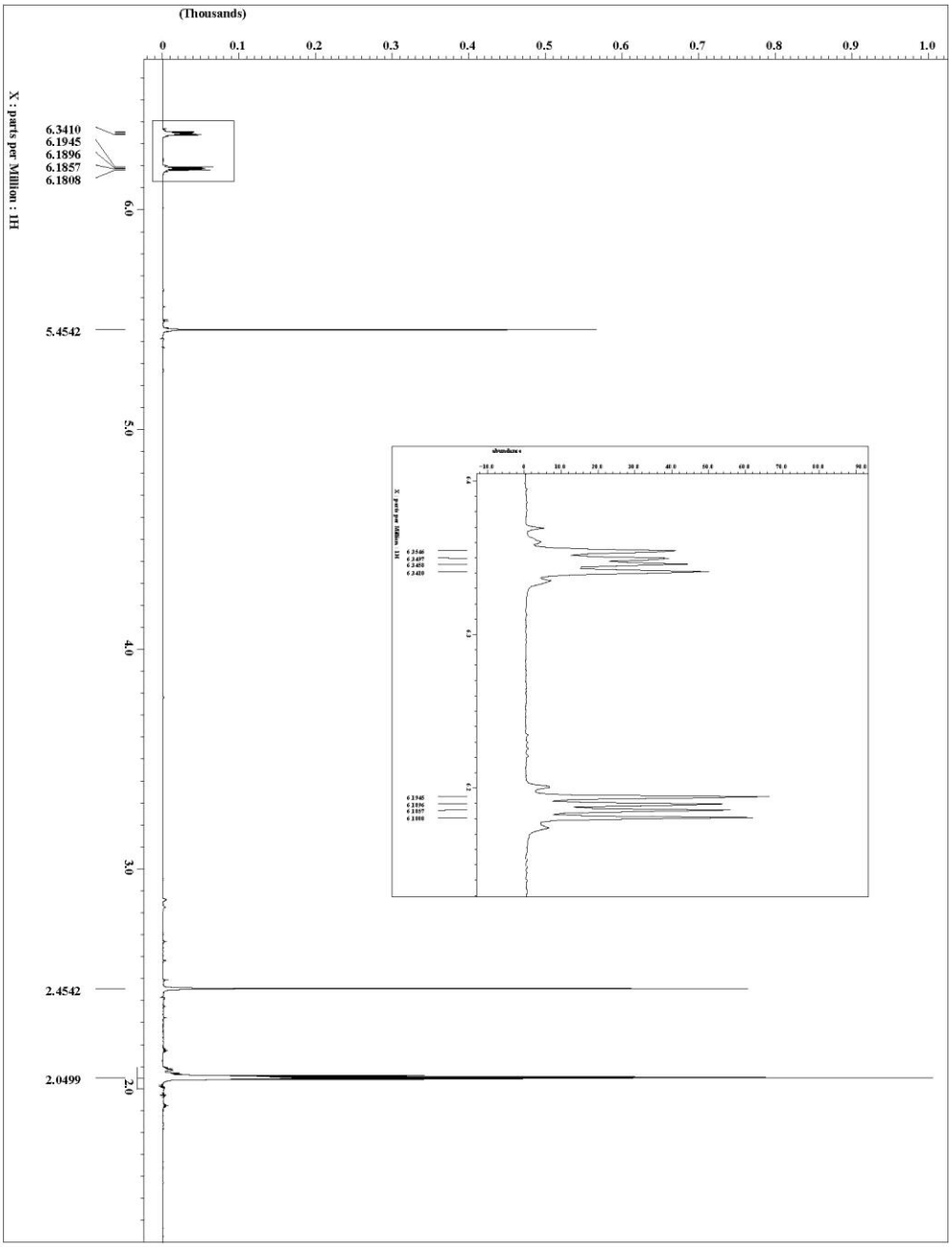

Figure 4-10. 30-H ^{1}H NMR spectrum (500 MHz, acetone-d_6).

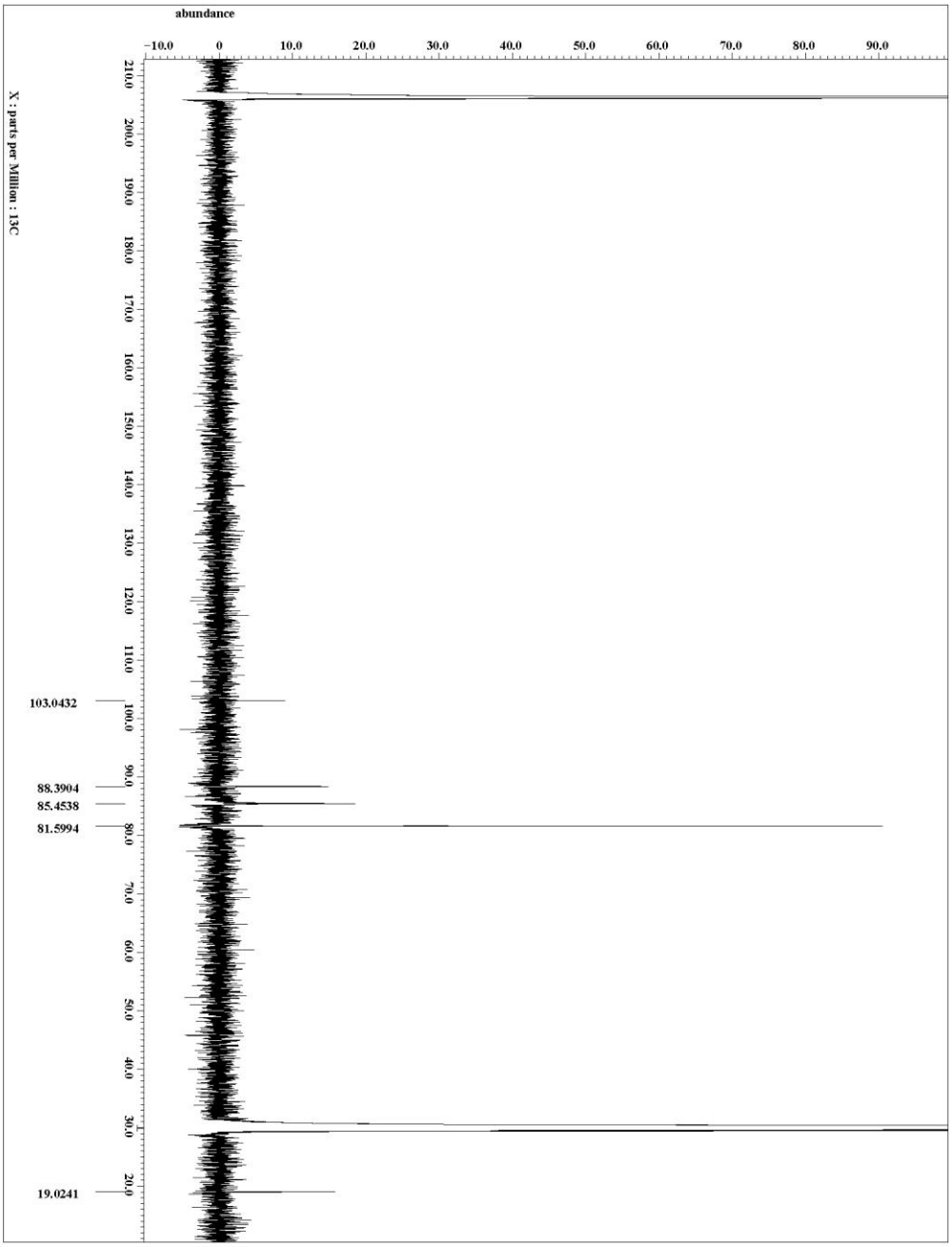

Figure 4-11. 30-H ^{13}C NMR spectrum (125 MHz, acetone-d_6).

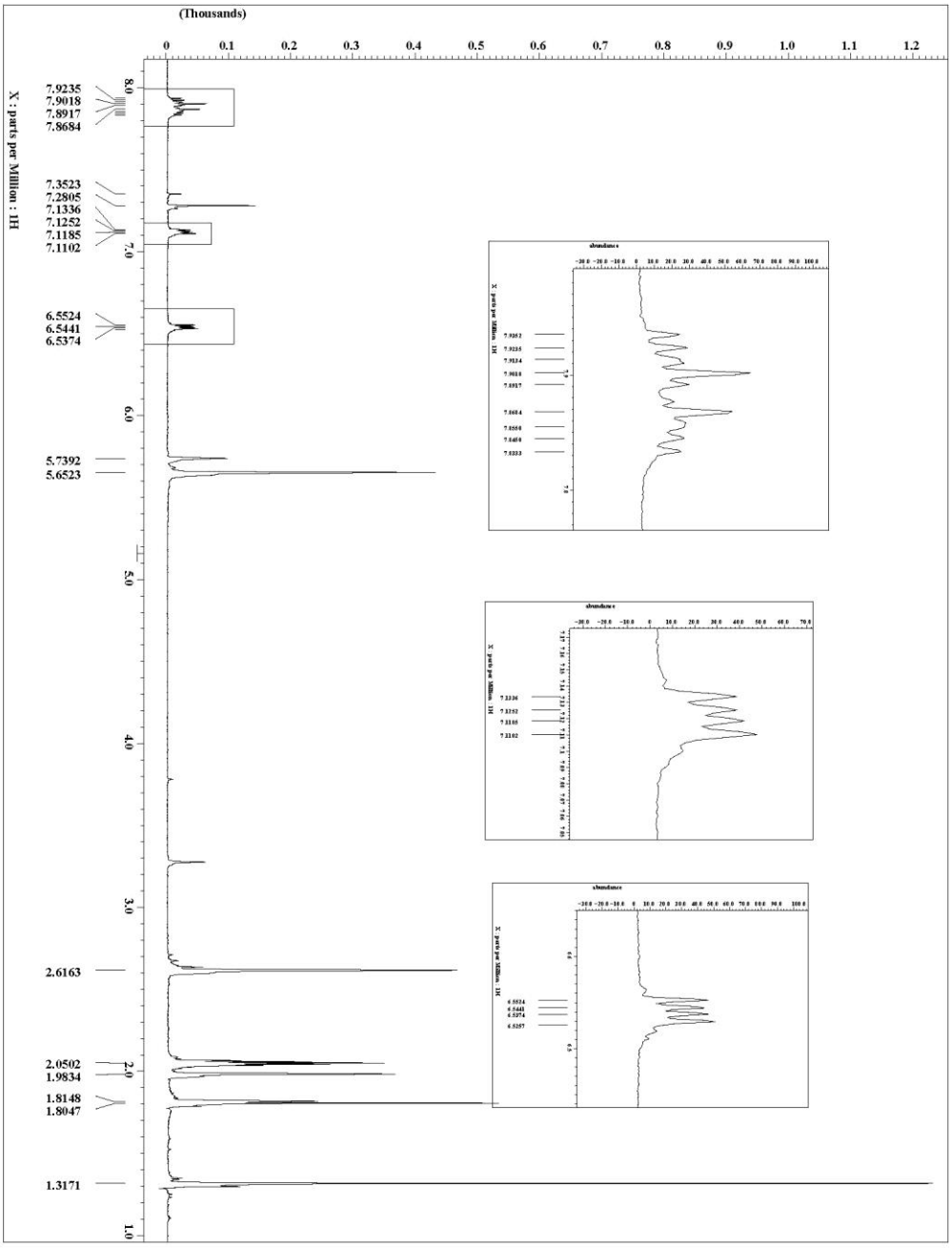

Figure 4-12. 26 plus **29** ^{1}H NMR spectrum initial (400 MHz, acetone-d_6).

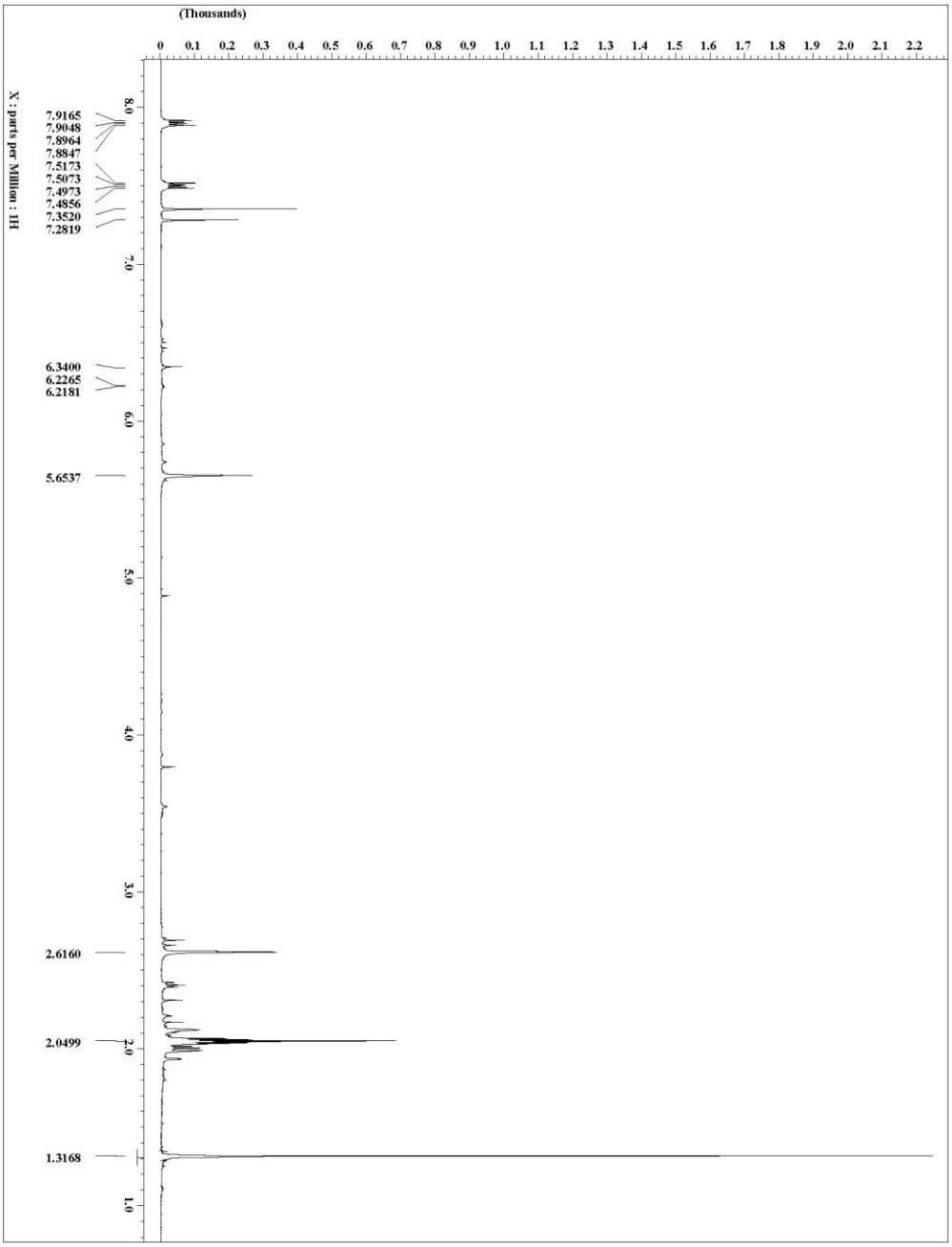

Figure 4-13. 26 plus **29** ^{1}H NMR spectrum final (400 MHz, acetone-d_6).

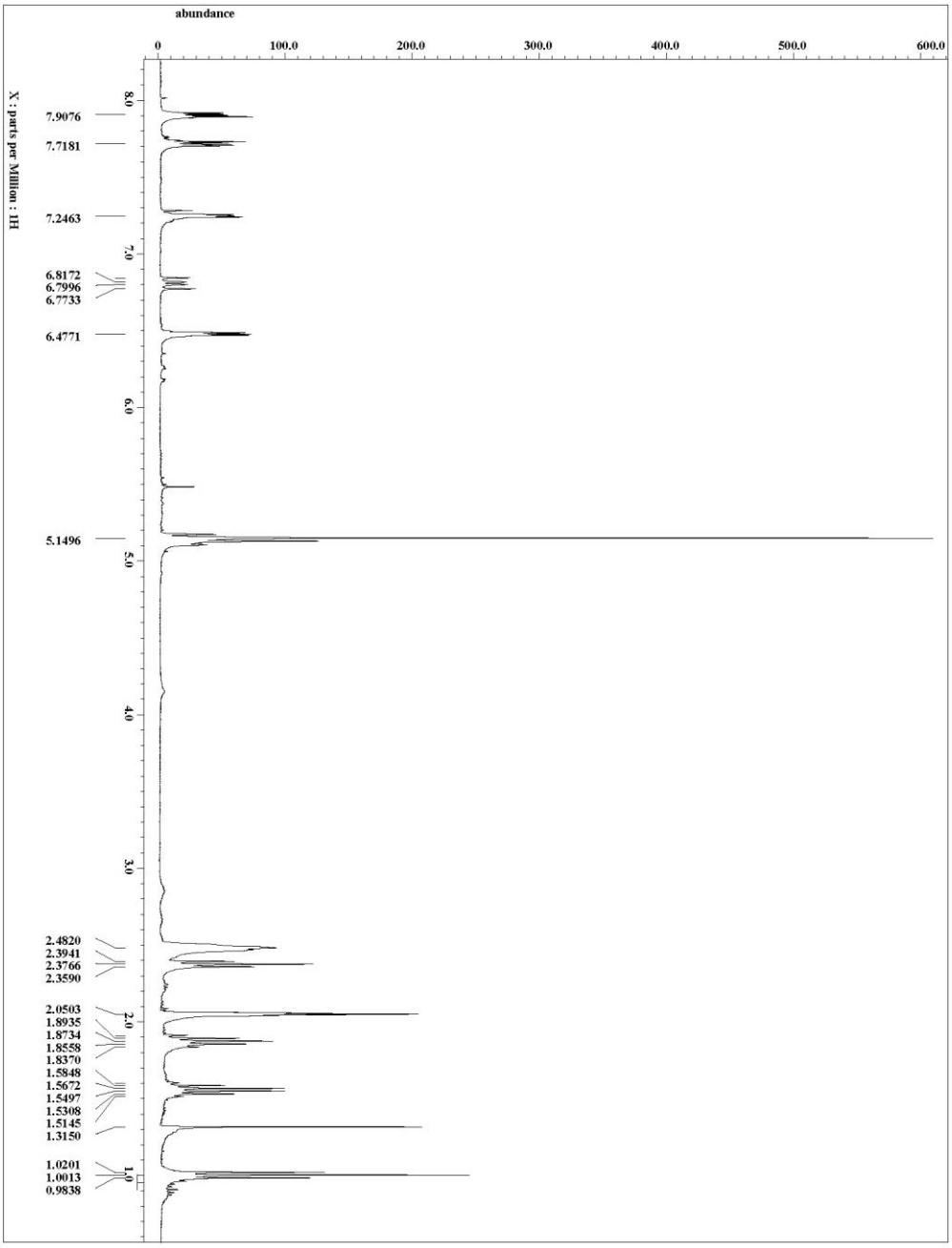

Figure 4-14. 27 plus **33** ^{1}H NMR spectrum initial (400 MHz, acetone-d_6).

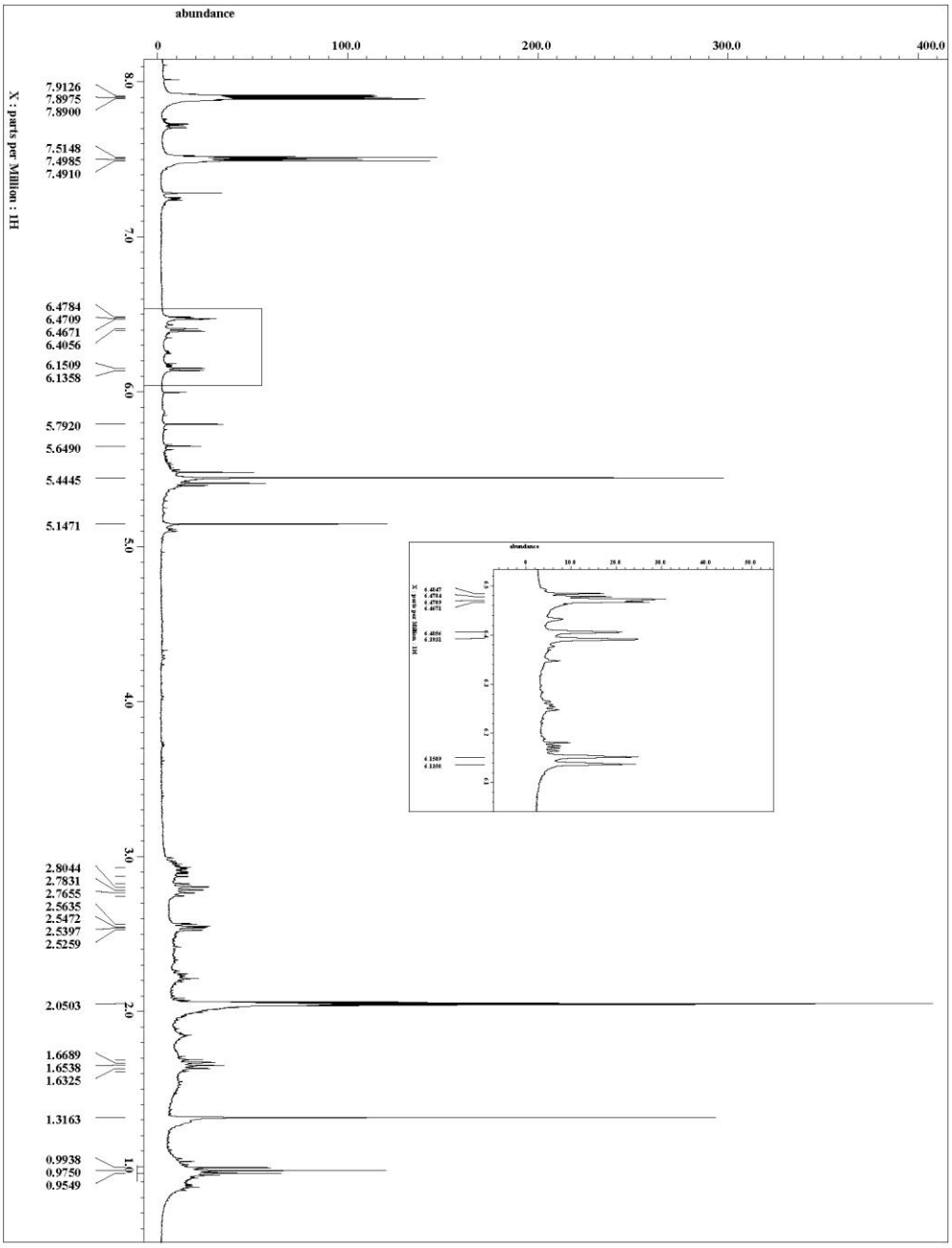

Figure 4-15. 27 plus **33** ^{1}H NMR spectrum final (400 MHz, acetone-d_6).

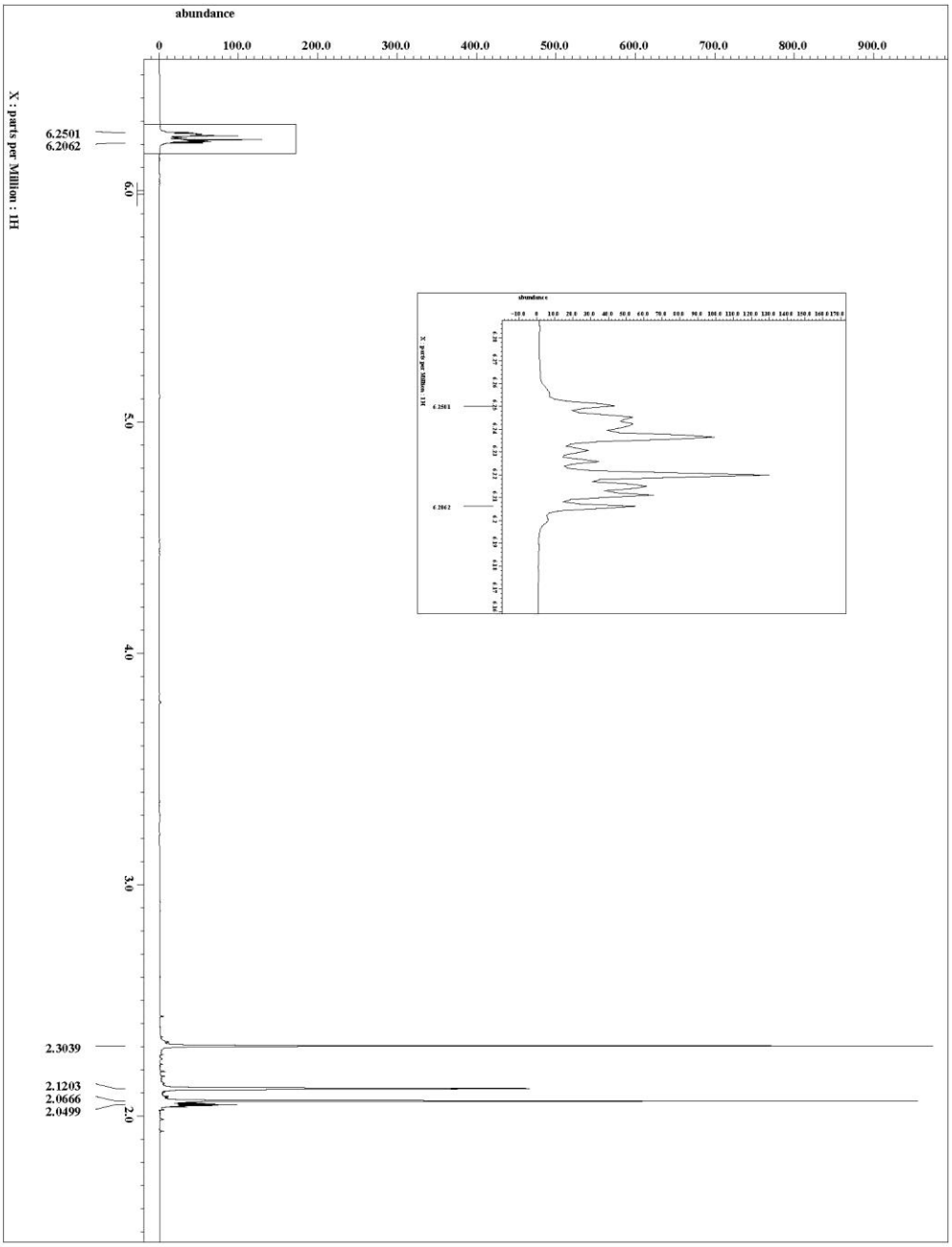

Figure 4-16. 30 ^{1}H NMR spectrum (500 MHz, acetone-d_6).

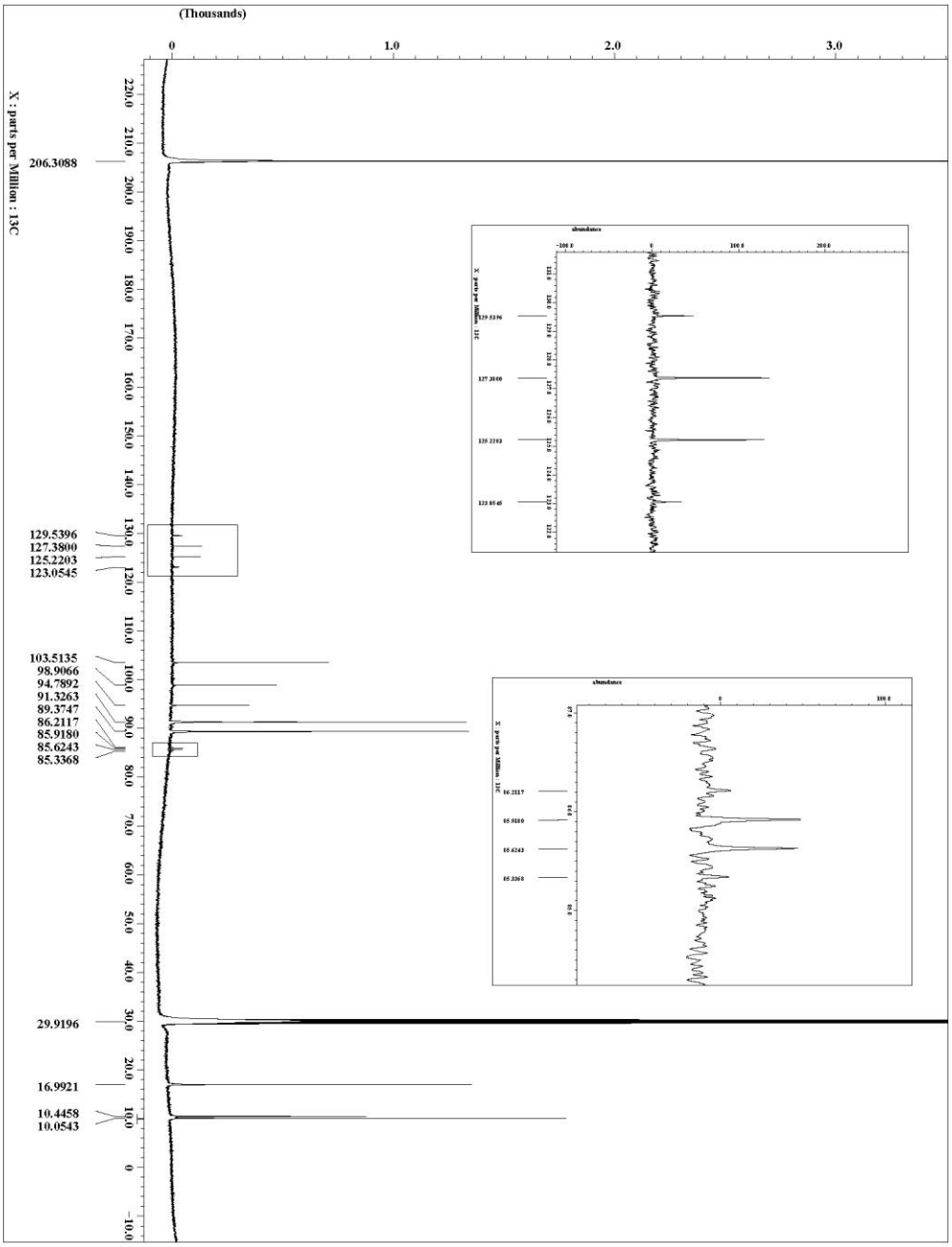

Figure 4-17. 30 ^{13}C NMR spectrum (125 MHz, acetone-d_6).

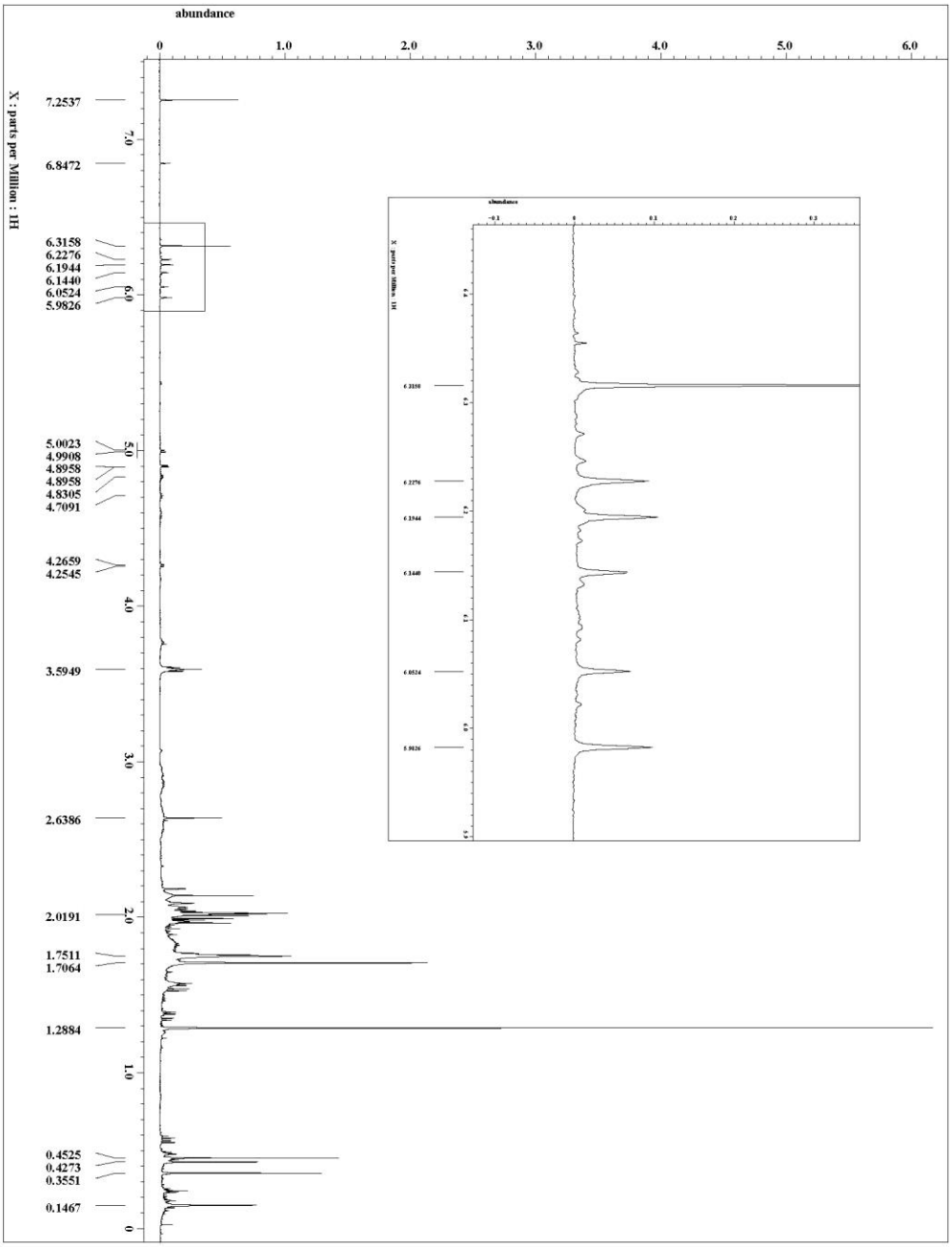

Figure 4-18. 32 crude reaction mixture ^{1}H NMR spectrum (500 MHz, $CDCl_3$).

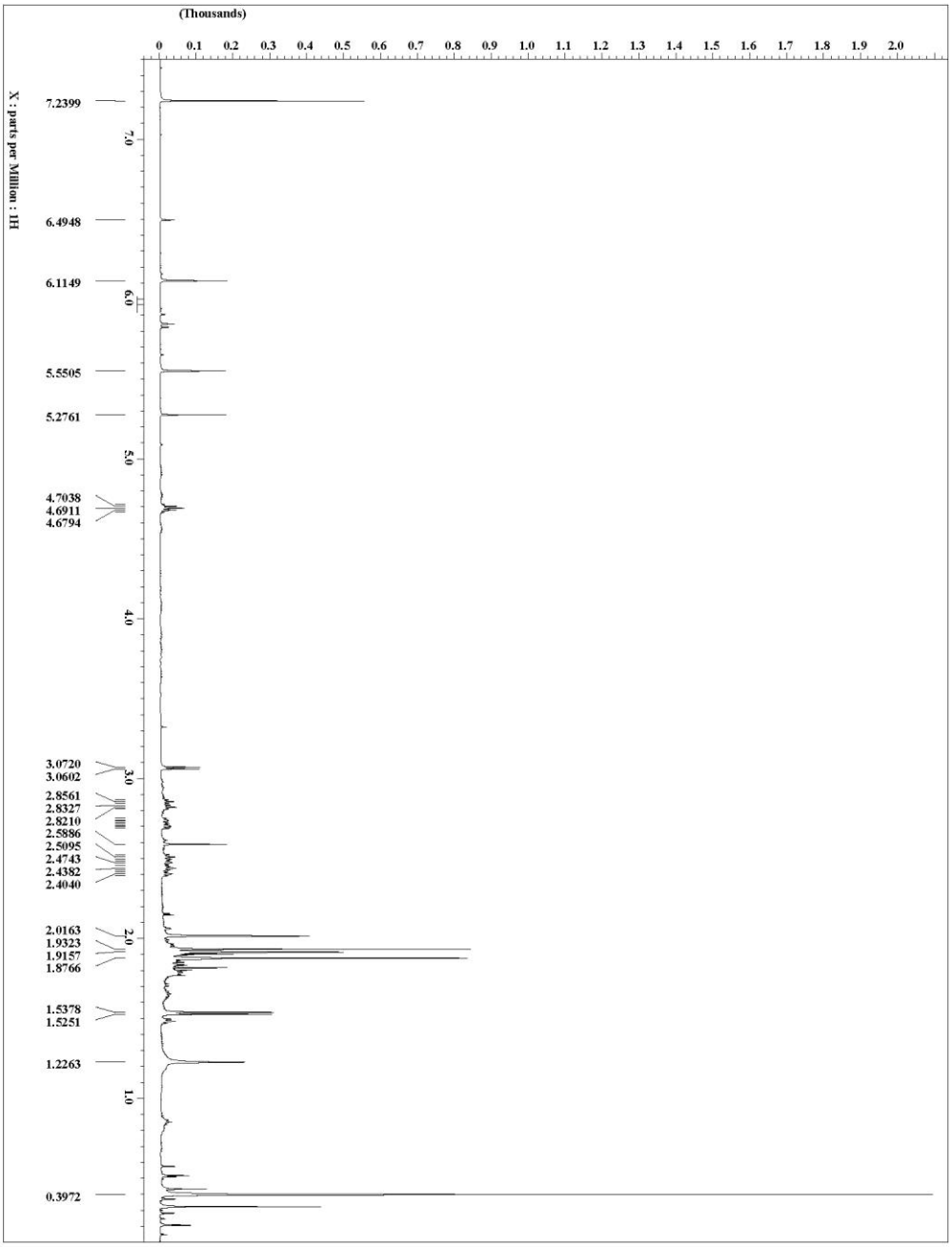

Figure 4-19. 32-diaA ^{1}H NMR spectrum (500 MHz, $CDCl_3$).

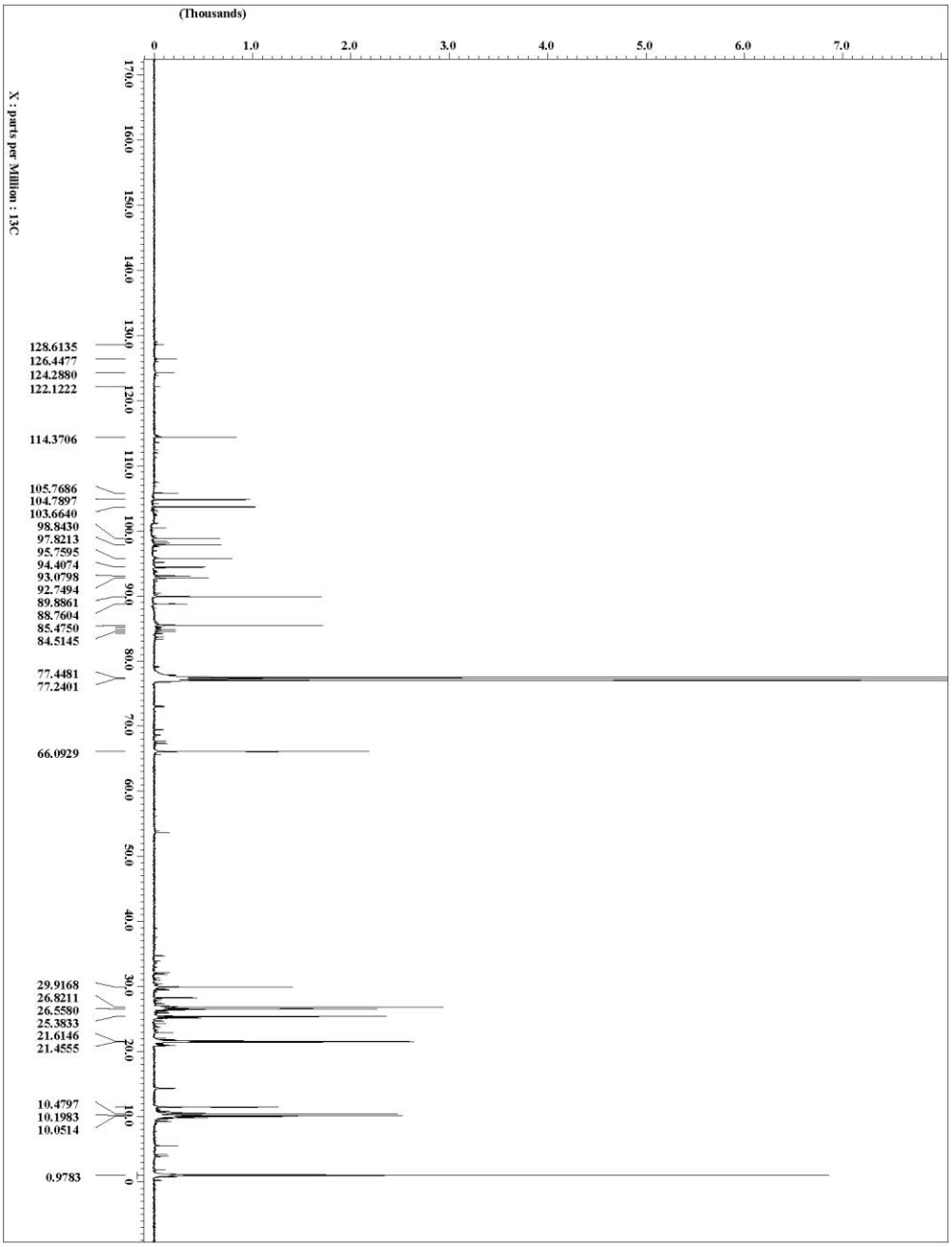

Figure 4-20. 32-diaA ^{13}C NMR spectrum (125 MHz, $CDCl_3$).

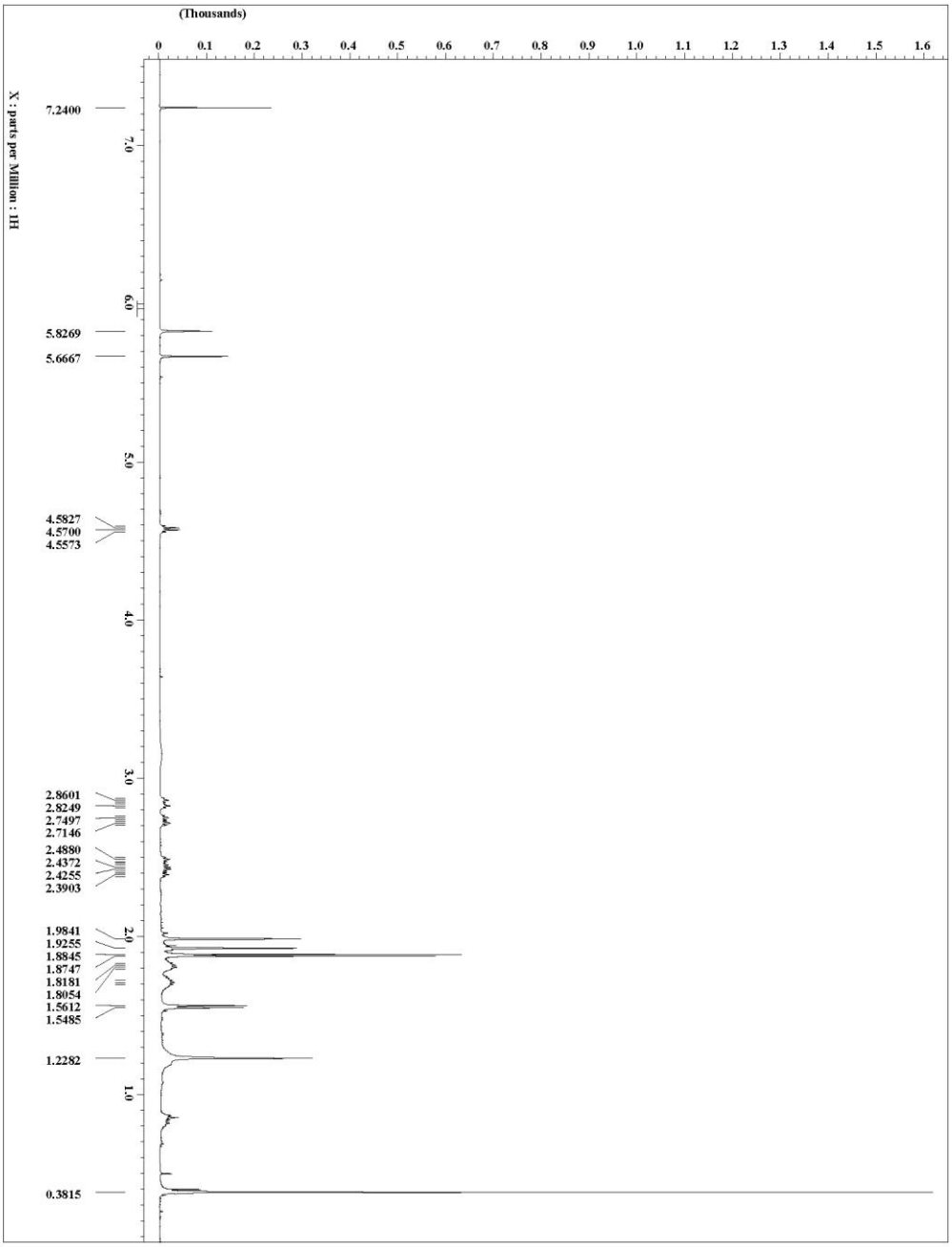

Figure 4-21. 32-diaB ^{1}H NMR spectrum (500 MHz, $CDCl_3$).

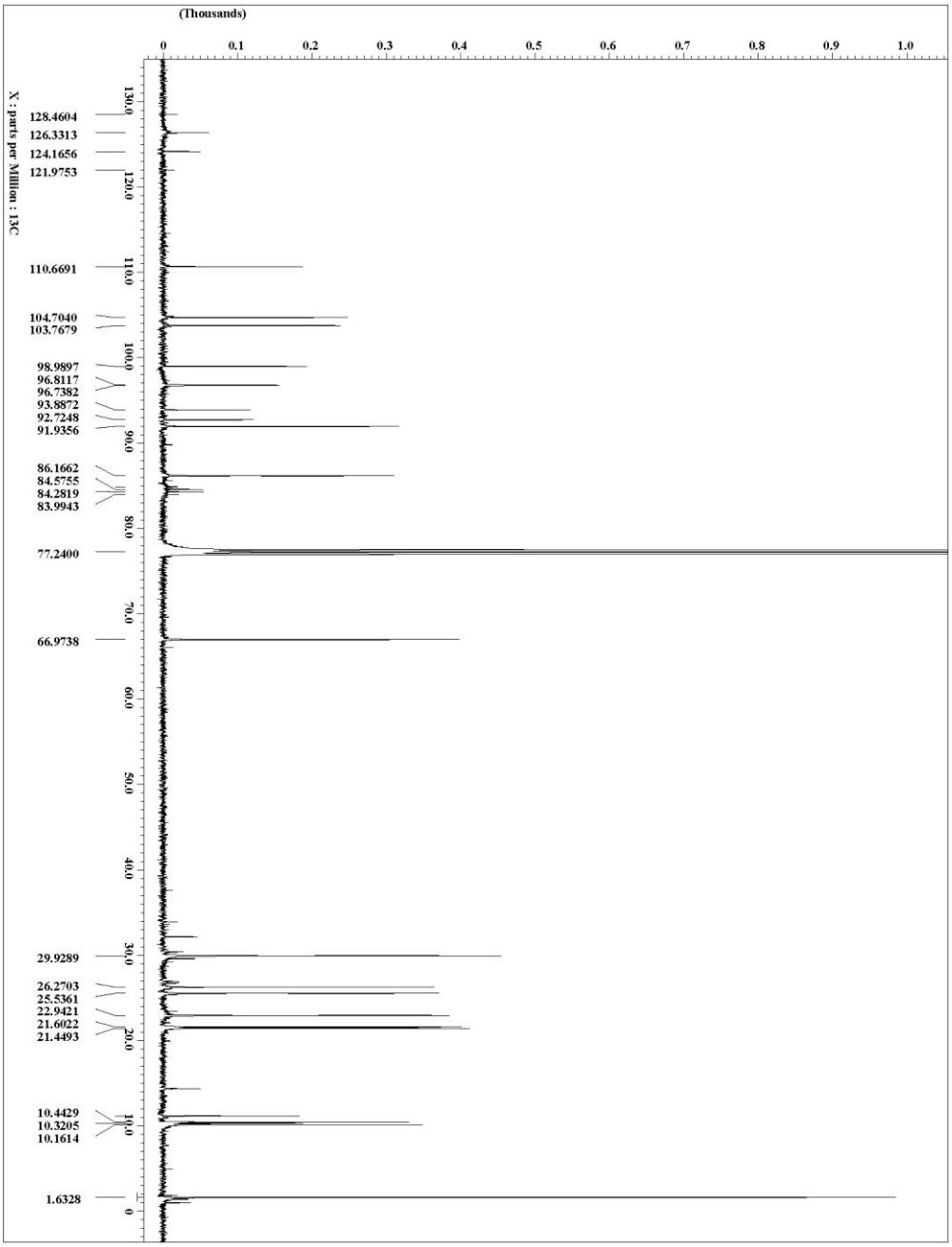

Figure 4-22. 32-diaB ^{13}C NMR spectrum (125 MHz, $CDCl_3$).

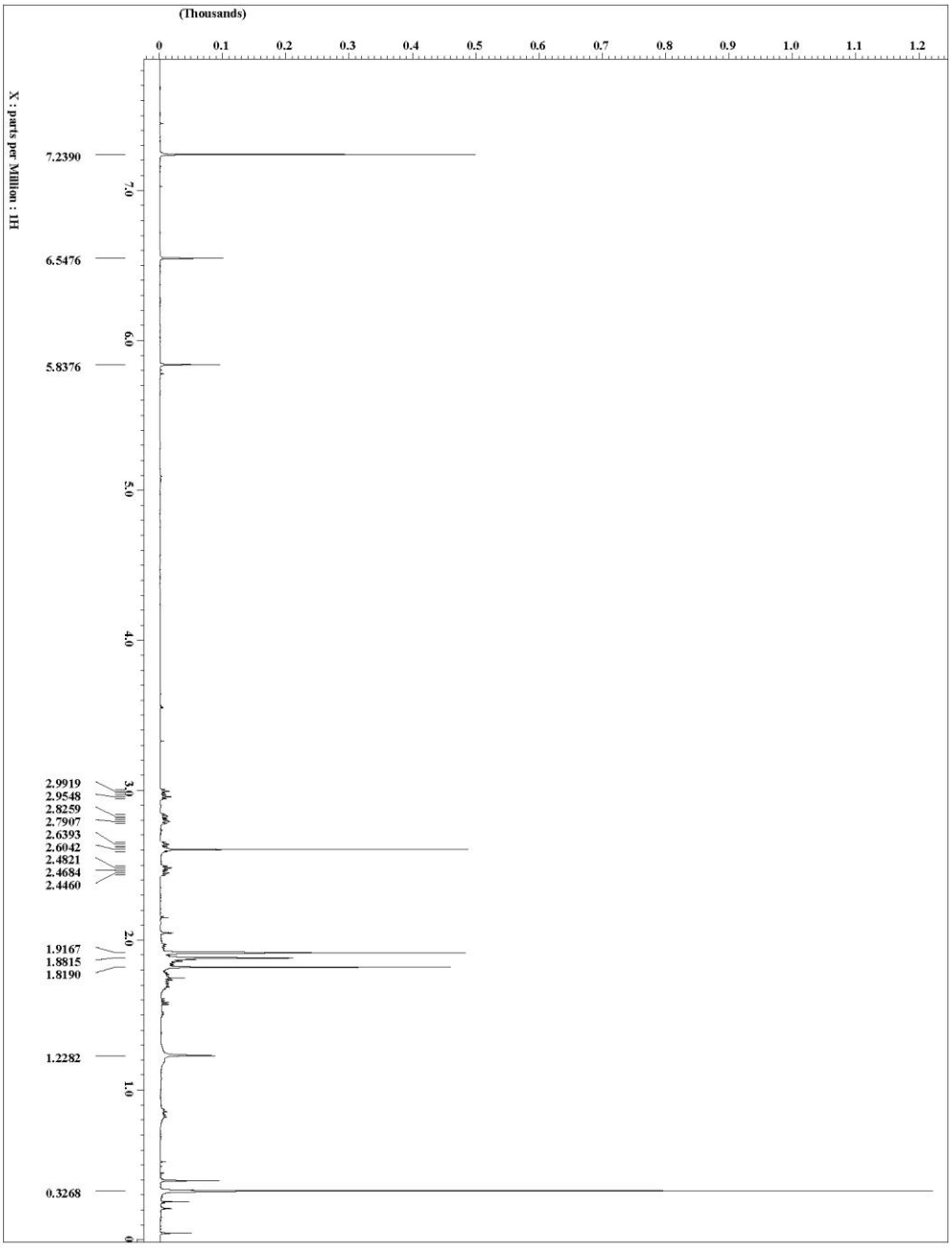

Figure 4-23. 33 ^{1}H NMR spectrum (500 MHz, $CDCl_3$).

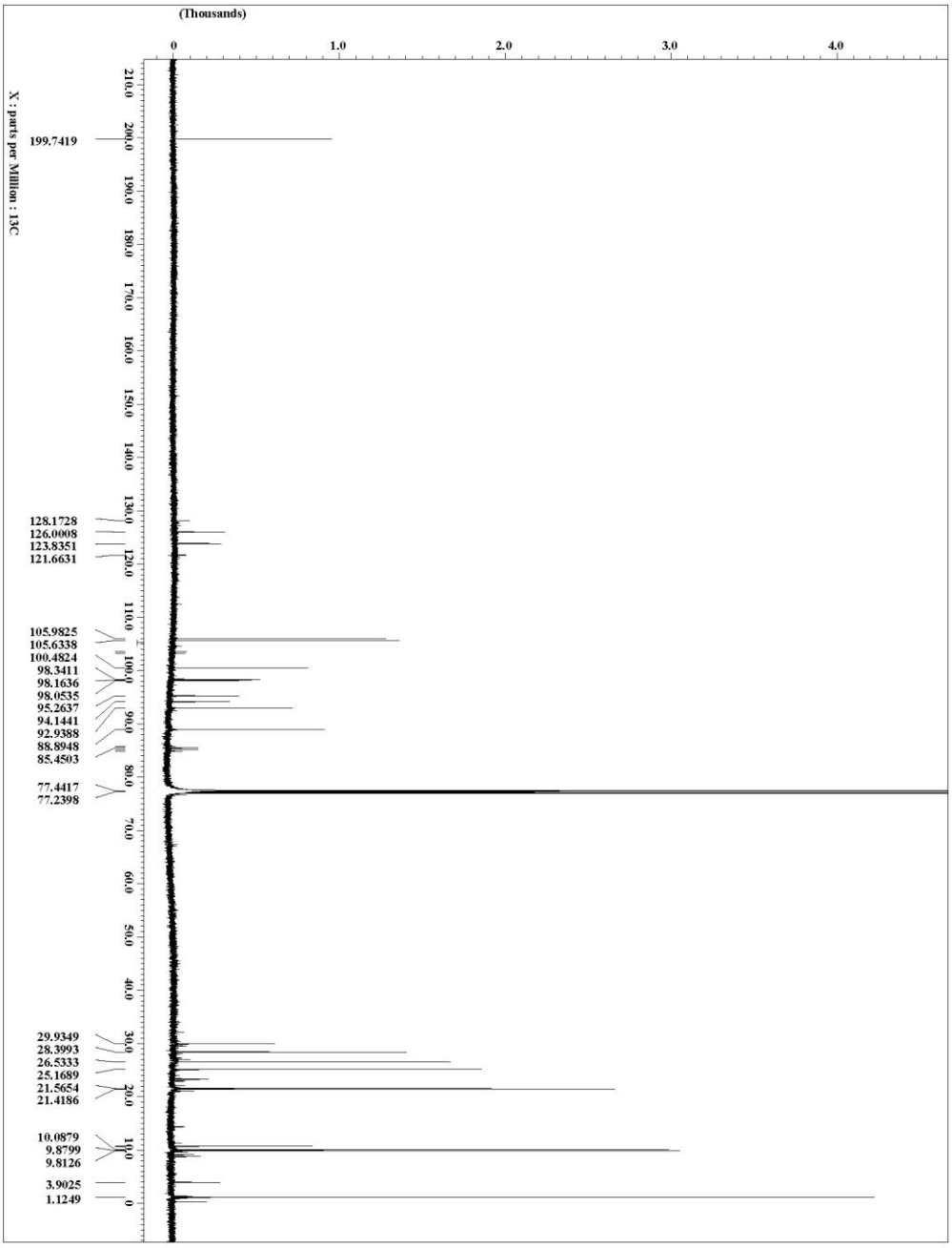

Figure 4-24. 33 ^{13}C NMR spectrum (125 MHz, $CDCl_3$).

4-5.5 X-ray Crystallographic Summaries for Complexes 19, 20, 22, 23, 26, and 30.

General Experimental for X-Ray Structure Determinations.

A single crystal with general dimensions of *a* x *b* x *c* was immersed in Paratone and placed on a Cryoloop. Data were collected on a Bruker SMART (APEX) CCD diffractometer using a graphite monochromator with Mo or Cu Kα radiation (λ = 0.71073 or 1.54178 Å) at the defined temperature. The data were integrated using the Bruker SAINT software program and scaled using the SADABS software program. Soltuion by direct methods (SIR-2004) produced a complete heavy-atom phasing model consistent with the proposed structure. All non-hydrogen atoms were refined anisotropically by full-matrix least squares (SHELXL-97). All hydrogen atoms were placed using a riding model. Their positions were constrained relative to their parent atom using the appropriate HFIX command in SHELXL-97.

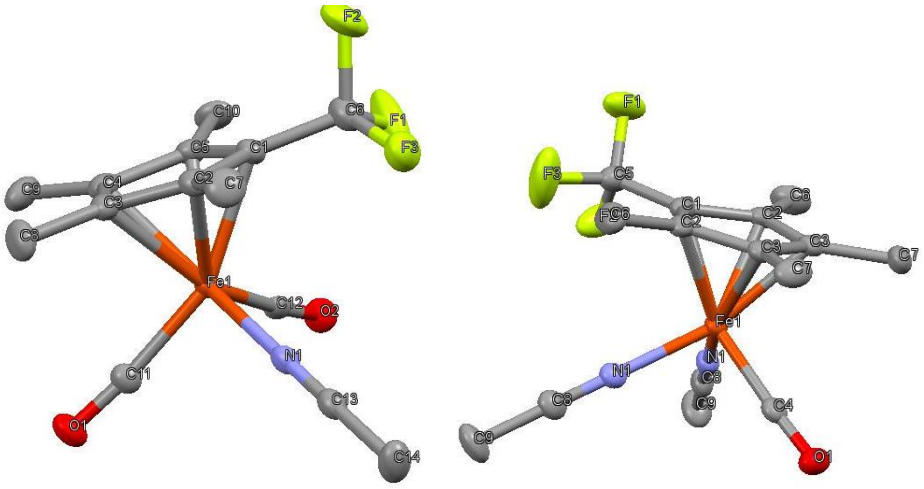

Figure 4-25. X-ray structures of **19** and **20**. (Hydrogens and the counter-ions are omitted for clarity).

Table 4-3: Selected Bond Distance (Å) data for **19**.

Bond (A-B)	Distance (Å)	Bond (A-B)	Distance (Å)
C_1-Fe	2.055(3)	C_5-Fe	2.136(3)
C_2-Fe	2.086(4)	C_{11}-Fe	1.806(4)
C_3-Fe	2.100(3)	C_{12}-Fe	1.792(3)
C_4-Fe	2.116(3)	N_1-Fe	1.925(2)

Table 4-4: Selected Bond Distance (Å) data for **20**.

Bond (A-B)	Distance (Å)	Bond (A-B)	Distance (Å)
C_1-Fe	2.059(3)	C_5-Fe	2.108(3)
C_2-Fe	2.108(4)	C_{11}-Fe	1.792(4)
C_3-Fe	2.102(3)	N_1-Fe	1.939(3)
C_4-Fe	2.102(3)	N_2-Fe	1.939(2)

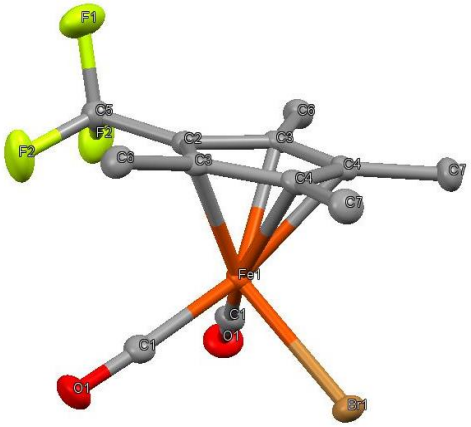

Figure 4-26. X-ray structure of **22.** (Hydrogens are omitted for clarity).

Table 4-5: Selected Bond Distance (Å) data for **22**.

Bond (A-B)	Distance (Å)	Bond (A-B)	Distance (Å)
C_1-Fe	2.037(3)	C_5-Fe	2.121(3)
C_2-Fe	2.121(4)	C_{11}-Fe	1.779(4)
C_3-Fe	2.142(3)	C_{12}-Fe	1.779(3)
C_4-Fe	2.142(3)	Br_1-Fe	2.421(2)

Table 4-6. Crystallographic Data Collection and Refinement Information for **19, 20,** and **22**.

	19	**20**	**22**
Formula	$C_{14}H_{15}F_9FeNO_2P$	$C_{15}H_{18}F_9FeN_2OP$	$C_{12}H_{12}BrF_3FeO_2$
Crystal System	Monoclinic	Monoclinic	Monoclinic
Space Group	*P*2(1)	*P*2(1)/m	*P*2(1)/m
a, Å	8.0127(4)	7.2476(4)	6.7596(2)
b, Å	12.9837(6)	11.5086(6)	11.5790(4)
c, Å	8.7967(4)	11.7889(6)	8.8010(3)
α, deg	90	90	90
β, deg	95.325(3)	100.387(2)	98.012(2)
γ, deg	90	90	90
V, Å^3	911.21(7)	967.19(9)	682.12(4)
Z	2	2	2
Radiation (λ, Å)	Mo-Kα, 0.71073	Mo-Kα, 0.71073	Mo-Kα, 0.71073
ρ (calcd.), g/cm^3	1.775	1.717	1.855
μ, mm^{-1}	1.026	0.955	4.062
Temp, K	90(2)	90(2)	90(2)
θ max, deg	29.82	29.15	30.45
data/parameters	3946 / 1 / 259	2348 / 0 / 184	1769 / 0 / 97
R_1	0.0378	0.0341	0.0233
wR_2	0.0703	0.0827	0.0596
GOF	1.002	1.033	1.030

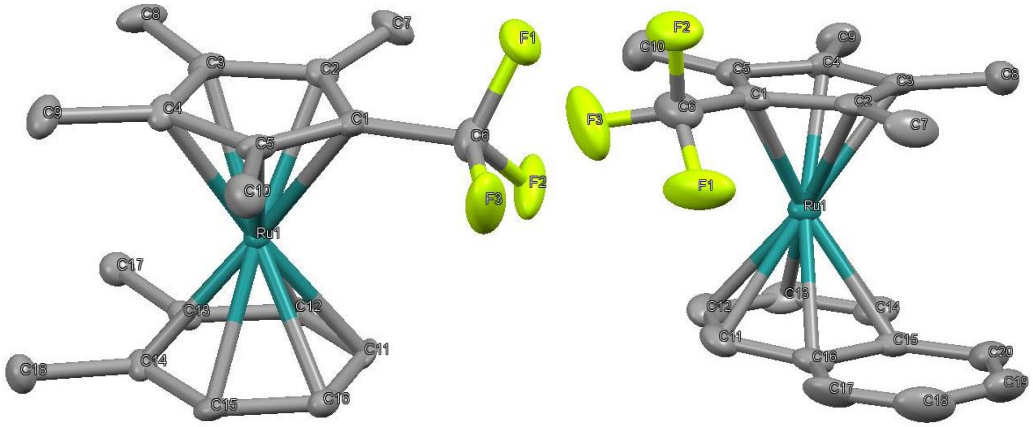

Figure 4-27. X-ray structures of **30** and **26**. (Hydrogens and the counter-ions omitted for clarity.)

Table 4-7. Selected Bond Distance (Å) Data for **26**.

Bond (A-B)	Distance (Å)	Bond (A-B)	Distance (Å)
C_1-C_2	1.441(6)	C_1-C_6	1.479(6)
C_2-C_3	1.424(6)	C_2-C_7	1.516(6)
C_3-C_4	1.426(5)	C_3-C_8	1.495(6)
C_4-C_5	1.435(6)	C_4-C_9	1.504(5)
C_5-C_1	1.431(6)	C_5-C_{10}	1.500(6)
C_{11}-C_{12}	1.398(7)	C_{16}-C_{17}	1.431(6)
C_{12}-C_{13}	1.407(7)	C_{17}-C_{18}	1.353(8)
C_{13}-C_{14}	1.402(7)	C_{18}-C_{19}	1.412(7)
C_{14}-C_{15}	1.424(6)	C_{19}-C_{20}	1.350(7)
C_{15}-C_{16}	1.443(6)	C_{15}-C_{20}	1.435(6)
C_{16}-C_{11}	1.424(6)	C_6-F_1	1.342(6)
C_6-F_2	1.320(6)	C_6-F_3	1.350(6)

Table 4-8: Selected Ruthenium-carbon Distances (Å) for **26**, **27**[18], and **28**.[19]

Bond (A-B)	**26**	**27**	**28**
C_1-Ru	2.140(4)	2.190(2)	2.192(2)
C_2-Ru	2.182(4)	2.1824(19)	2.175(2)
C_3-Ru	2.195(3)	2.172(2)	2.175(2)
C_4-Ru	2.178(3)	2.180(2)	2.164(2)
C_5-Ru	2.176(4)	2.179(2)	2.173(2)
C_6-Ru	2.284(3)	2.2836(19)	2.191(2)
C_7-Ru	2.215(4)	2.218(2)	2.210(3)
C_8-Ru	2.210(3)	2.221(2)	2.217(3)
C_9-Ru	2.208(5)	2.218(2)	2.206(3)
C_{10}-Ru	2.208(5)	2.004(19)	2.206(3)
C_{11}-Ru	2.267(4)	2.2615(18)	2.184(3)

Table 4-9. Selected Angle (deg) Data for **26**.

Angle (A-B-C)	Degrees (°)	Angle (A-B-C)	Degrees (°)
Ru-C_1-C_6	125.3(3)	Ru-C_2-C_7	125.1(3)
Ru-C_3-C_8	128.1(3)	Ru-C_4-C_9	125.6(3)
Ru-C_5-C_{10}	127.7(3)	C_6-C_1-C_2	122.6(4)
C_6-C_1-C_5	127.9(4)	C_7-C_2-C_3	125.3(4)
C_7-C_2-C_1	127.8(4)	C_8-C_3-C_2	125.4(4)
C_8-C_3-C_4	126.0(4)	C_9-C_4-C_3	125.3(3)
C_9-C_4-C_5	125.7(3)	C_{10}-C_5-C_4	125.1(4)
C_{10}-C_5-C_1	128.5(4)	C_5-C_1-C_2	109.4(3)
C_1-C_2-C_3	106.9(3)	C_2-C_3-C_4	108.4(3)
C_3-C_4-C_5	109.0(3)	C_4-C_5-C_1	106.3(3)
C_{11}-C_{12}-C_{13}	119.6(4)	C_{12}-C_{13}-C_{14}	120.6(4)
C_{13}-C_{14}-C_{15}	120.8(4)	C_{14}-C_{15}-C_{16}	118.7(4)
C_{15}-C_{16}-C_{11}	118.8(3)	C_{16}-C_{11}-C_{12}	121.4(4)
C_{15}-C_{16}-C_{17}	118.6(4)	C_{16}-C_{17}-C_{18}	120.1(5)
C_{17}-C_{18}-C_{19}	121.3(5)	C_{18}-C_{19}-C_{20}	121.4(5)
C_{19}-C_{20}-C_{15}	120.0(4)	C_{20}-C_{15}-C_{16}	118.7(4)

Table 4-10. Selected Bond Distance (Å) Data for **30**.

Bond (A-B)	Distance (Å)	Bond (A-B)	Distance (Å)
C_1-C_2	1.418(7)	C_1-C_6	1.505(7)
C_2-C_3	1.419(7)	C_2-C_7	1.510(7)
C_3-C_4	1.437(6)	C_3-C_8	1.507(6)
C_4-C_5	1.439(7)	C_4-C_9	1.502(7)
C_5-C_1	1.421(8)	C_5-C_{10}	1.519(7)
C_{11}-C_{12}	1.414(7)	C_{12}-C_{13}	1.430(7)
C_{13}-C_{14}	1.420(7)	C_{14}-C_{15}	1.425(6)
C_{15}-C_{16}	1.398(7)	C_{16}-C_{11}	1.417(7)
C_{13}-C_{17}	1.503(6)	C_{14}-C_{18}	1.505(7)
C_6-F_1	1.330(5)	C_6-F_2	1.337(5)
C_6-F_3	1.327(6)		

Table 4-11: Selected Ruthenium-carbon Distances (Å) for **30**, [CpRu(benzene)]PF_6[20], and [Cp*Ru(benzene)]PF_6.[21]

Bond (A-B)	**30**	$CpRu^+$	Cp^*Ru^+
C_1-Ru	2.141(5)	2.19(3)	2.183(2)
C_2-Ru	2.182(5)	2.20(3)	2.179(2)
C_3-Ru	2.194(4)	2.22(3)	2.179(2)
C_4-Ru	2.204(5)	2.22(3)	2.178(3)
C_5-Ru	2.189(5)	2.21(3)	2.191(3)
C_6-Ru	2.210(5)	2.16(2)	2.205(2)
C_7-Ru	2.219(5)	2.16(2)	2.214(2)
C_8-Ru	2.216(5)	2.17(2)	2.221(2)
C_9-Ru	2.241(3)	2.19(2)	2.218(2)
C_{10}-Ru	2.245(5)	2.19(3)	2.226(3)
C_{11}-Ru	2.215(4)	2.17(2)	2.216(3)

Table 4-12. Selected Angle (deg) Data for **30**.

Angle (A-B-C)	Degrees (°)	Angle (A-B-C)	Degrees (°)
Ru-C_1-C_6	125.4(3)	Ru-C_2-C_7	127.8(4)
Ru-C_3-C_8	127.5(3)	Ru-C_4-C_9	126.6(3)
Ru-C_5-C_{10}	127.9(3)	C_6-C_1-C_2	123.3(4)
C_6-C_1-C_5	126.3(4)	C_7-C_2-C_3	125.0(4)
C_7-C_2-C_1	128.2(4)	C_8-C_3-C_4	125.0(4)
C_8-C_3-C_2	125.8(4)	C_9-C_4-C_5	126.2(4)
C_9-C_4-C_3	126.5(4)	C_{10}-C_5-C_1	130.1(5)
C_{10}-C_5-C_4	123.0(4)	C_5-C_1-C_2	110.3(4)
C_1-C_2-C_3	106.6(4)	C_2-C_3-C_4	109.2(4)
C_3-C_4-C_5	107.2(4)	C_4-C_5-C_1	106.8(4)
C_{11}-C_{12}-C_{13}	121.1(4)	C_{12}-C_{13}-C_{14}	118.7(4)
C_{13}-C_{14}-C_{15}	119.5(4)	C_{14}-C_{15}-C_{16}	121.4(4)
C_{15}-C_{16}-C_{11}	119.6(4)	C_{16}-C_{11}-C_{12}	119.7(4)
C_{17}-C_{13}-C_{12}	119.6(4)	C_{17}-C_{13}-C_{14}	121.8(4)
C_{18}-C_{14}-C_{13}	120.9(4)	C_{18}-C_{14}-C_{15}	119.6(4)

Table 4-13. Crystallographic Data Collection and Refinement Information **30, 26,** and **23.**

	30	**26**	**23**
Formula	$C_{18}H_{22}F_9PRu$	$C_{20}H_{20}F_6PRu$	$C_{25}H_{23}F_6FeO_3P$
Crystal System	Orthorhombic	Orthorhombic	Monoclinic
Space Group	*P*na2(1)	*P*bca	*P*2(1)/n
a, Å	14.8864(4)	15.2283(3)	21.8309(13)
b, Å	8.6896(3)	16.4149(3)	10.9180(7)
c, Å	15.3701(5)	16.6124(4)	21.8377(14)
α, deg	90	90	90
β, deg	90	90	112.893(2)
γ, deg	90	90	90
V, Å^3	1988.23(11)	4152.62(15)	4795.0(5)
Z	4	8	8
Radiation (λ, Å)	Mo-Kα, 0.71073	Mo-Kα, 0.71073	Mo-Kα, 0.71073
ρ (calcd.), g/cm^3	1.809	1.802	1.585
μ, mm^{-1}	0.769	0.916	0.952
Temp, K	90(2)	90(2)	90(2)
θ max, deg	26.38	26.38	25.00
data/parameters	4015 / 1 / 269	4239 / 0 / 290	8366 / 0 / 604
R_1	0.0340	0.0419	0.0675
wR_2	0.0450	0.0548	0.1397
GOF	1.030	1.039	1.018

4-6 Acknowledgements

The material in Chapter 4, in part, is currently being prepared for submission for publication with the following authors: Cope, S.K.; O'Connor, J.M. The dissertation author was the primary investigator and author of this material.

4-7 References

1. (a) Jones, R.R.; Bergman, R.G. *J. Am. Chem. Soc.* **1972**, *94*, 660. (b) Mohamed, R.K.; Peterson, P.W.; Alabugin, I.V. *Chem. Rev.* **2013**, *113*, 7089.

2. Maiese, W.M.; Lechevalier, M.P.; Lechevalier, H.A.; Korshalla, J.; Kuck, N.; Fantini, A.; Wildey, M.J.; Thomas, J.; Greenstein, M. *J. Anibiotics* **1989**, *42*, 558.

3. Walker, S.; Landovitz, R.; Ding, W.D.; Ellestad, G.A.; Kahne, D. *Proc. Natl. Acad. Sci. U.S.A.* **1992**, *89*, 4608.

4. (a) O'Connor, J.M.; Friese, S.J. *Organometallics* **2008**, *27*, 4280. (b) O'Connor, J.M.; Friese, S.J.; Rodgers, B.L. *J. Am. Chem. Soc.* **2005**, *127*, 16342. (c) O'Connor, J.M.; Friese, S.J.; Tichenor, M. *J. Am. Chem. Soc.* **2002**, *124*, 3506. (d) O'Connor, J.M.; Lee, L.I.; Gantzel, P. *J. Am. Chem. Soc.* **2000**, *122*, 12057. (e) Friese, S.; PhD. Dissertation, University of California, San Diego **2004**.

5. (a) Schrenk, J.L.; McNair, A.M.; McCormick, F.B.; Mann, K.R. *Inorg. Chem.* **1986**, *25*, 3501. (b) McNair, A.M.; Boyd, D.C.; Bohling, D.A.; Gill, T.P.; Mann, K.R *Inorg. Chem.* **1987**, *26*, 1182. (c) McNair, A.M.; Mann, K.R. *Inorg. Chem.* **1986**, *25*, 2519. (d) McNair, A.M.; Schrenk, J.L.; Mann, K.R. *Inorg. Chem.* **1984**, *23*, 2633.

6. Kuhn, N.; Zauder, E. *J. Organomet. Chem.* **1988**, *340*, C1.

7. (a) Gassman, P.G.; Mickelson, J.W.; Sowa Jr., J.R. *J. Am. Chem. Soc.* **1992**, *114*, 6942. (b) Gassman, P.G.; Sowa Jr., J.R.; Hill, M.G.; Mann, K.R. *Organomet.* **1995**, *14*, 4879.

8. Catheline, D.; Astruc, D. *Organomet.* **1984**, *3*, 1094.

9. Schmidt, E.K.G.; Thiel, C.H. *J. Organomet. Chem.* **1981**, *209*, 373.

10. Callan, B.; Manning, A.R.; Stephens, F.S. *J. Organomet. Chem.* **1987**, *331*, 357.

11. Barbour, C.J.; Cameron, J.H.; Winfield, J.M. *J. Chem. Soc., Dal. Trans.* **1980**, *10*, 2001.

12. Barras, J.P.; Davies, S.G.; Metzler, M.R.; Edwards, A.J.; Humphreys, V.M.; Prout, K. *J. Organomet. Chem.* **1993**, *461*, 157.

13. Kumar, R.; Manning, A.R.; Murray, P.T. *J. Organomet. Chem.* **1987**, *323*, 53.

14. Hamon, J.R.; Astruc, D.; Michaud, P. *J. Am. Chem. Soc.* **1981**, *103*, 758.

15. Gusev, O.V.; Levlev, M.A.; Lyssenko, K.A.; Petrovskii, P.V.; Ustynyuk, N.A.; Maitlis, P.M. *Inorg. Chim. Acta* **1998**, *280*, 249.

16. Mercier, A.; Yeo, W.C.; Chou, J.; Chaudhuri, P.D.; Bernardinelli, G.; Kundig, E.P. *Chem. Comm.* **2009**, 5227.

17. Evju, J.K.; Mann, K.R. *Organomet.* **2002**, *21*, 993.

18. (a) Karslyan, E.E.; Perekalin, D.S.; Petrovskii, P.V.; Borisova, A.O.; Kudinov, A.R.; *Russ. Chem. Bull., Int. Ed.* **2009**, *58*, 585. (b) Karslyan, E.E.; Perekalin, D.S.; Petrovskii, P.V.; Lyssenko, K.A.; Kudinov, A.R. *Russ. Chem. Bull., Int. Ed.* **2008**, *57*, 2201.

19. Loughrey, B.T.; Cunning, B.V.; Healy, P.C.; Brown, C.L.; Parsons, P.G.; Williams, M.L. *Chem. Asian J.* **2012**, *7*, 112.

20. Grepioni, F.; Cojazzi, G.; Braga, D.; Marseglia, E.; Scaccianoce, L.; Johnson, B.F.G. *J. Chem. Soc., Dal. Trans.* **1999**, 553.

21. Gemel, C.; Mereiter, K.; Schmid, R.; Kirchner, K. *Organomet.* **1996**, *15*, 532.

22. Hitt, D.; PhD. Dissertation, University of California, San Diego **2011**.

23. Luginbuhl, W.; Zbinden, P.; Pittet, P.A.; Armbruster, T.; Burgi, H.B.; Merbach, A.E.; Ludi, A. *Inorg. Chem.* **1991**, *30*, 2350.

24. (a) Olah, G.A.; Mathew, T.; Marinez, E.R.; Esteves, P.M.; Etzkorn, M.; Rasul, G.; Surya Prakash, G.K. *J. Am. Chem. Soc.* **2001**, *123*, 11556. (b) Ma, M.; Johnson, K.E. *J. Am. Chem. Soc.* **1995**, *117*, 1508.

25. Rieke, R.D.; Bales, S.E.; Hudnall, P.M.; Burns, T.P.; Poindexter, G.S. *Org. Synth.* **1979**, *59*, 85.

26. Smith, K.; Conley, N.; Hondrogiannis, G.; Glover, L.; Green, J.F.; Mamantov, A.; Pagni, R.M. *J. Org. Chem.* **2004**, *69*, 4843.

27. Masuda, K.; Ohkita, H.; Kurumatani, S.; Itoh, K. *Organomet.* **1993**, *12*, 2221.

Chapter 5 Novel Non-aryne Cycloaromatization of Enediynes with Incorporation of H-X from Haloforms

5-1 Introduction

As an extension of the metal-mediated cycloaromatization of enediynes in the O'Connor group[1], a comparison of the thermal activation parameters for the cyclization of enediyne **1** was attempted in $CDCl_3$ at 190 °C. After 20 h the expected cyclization product **2** was not observed, instead the novel cycloaromatization product **3** was observed (Scheme 5-1).[2]

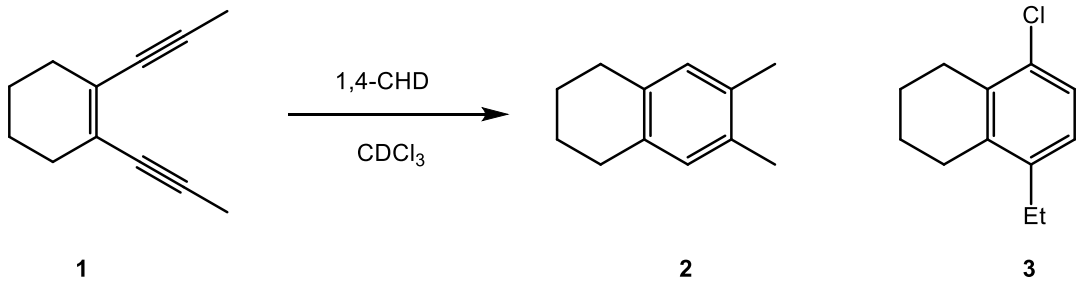

Scheme 5-1. Reaction of **1** in the presence of 1,4-CHD in $CDCl_3$.[2]

The incorporation of HCl was revealed by mass spectrometry and the connectivity of the product was determined by reaction with $[Cp^*Ru(NCMe)_3]PF_6$ to give the Cp^*Ru sandwich complex **4** (Scheme 5-2). A solid-state structure was determined for **4** which established a *para*-arrangement of the Cl and ethyl groups.

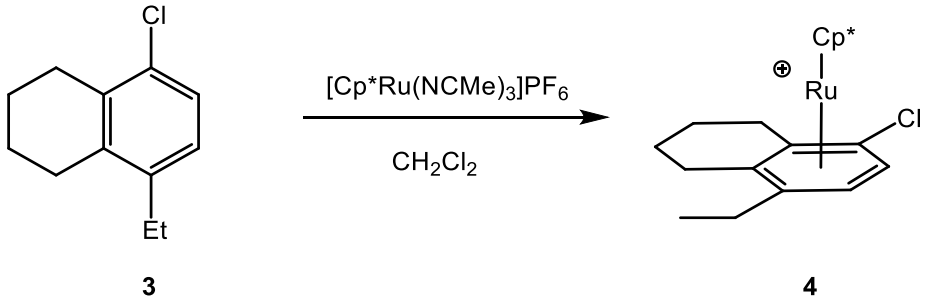

3 **4**

Scheme 5-2. Synthesis of **4**, allowing connectivity of **3**.[2]

When **1** was heated to 150 °C in the presence of HCl (0.5 eq, 12 M aqueous) in $CDCl_3$ for 46 h, the formation of **3** was observed in 55% NMR yield along with a new species, **5**, with chemical shifts at δ 5.72 (q, J = 7 Hz, 1H), 1.95 (s, 3H) and 1.62 (d, J = 7 Hz, 3H) in the ^{1}H NMR spectrum. Compound **5** was assigned as a vinyl chloride with undetermined stereochemistry (Scheme 5-3).

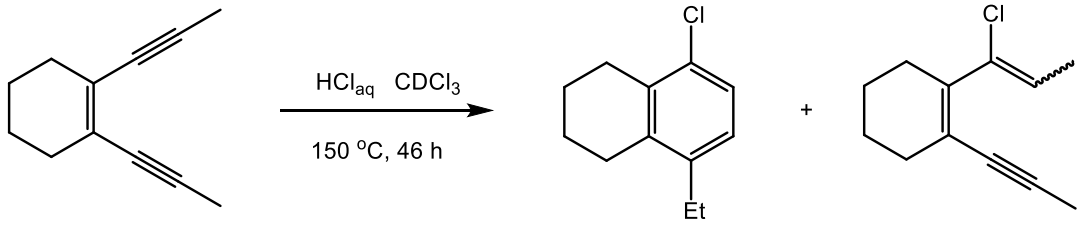

1 **3** **5**

55% Yield(NMR) 12% Yield(NMR)

Scheme 5-3. Addition of HCl to **1**.[2]

Interestingly, when the reaction above was repeated at rt, there was no observed formation of **3** or **5** after 24 h, but upon warming to 50 °C the formation of **5** was observed in 76% NMR yield based on 9% conversion of **1**, with no observed

formation of **3**. This result was attributed to the addition reaction between HCl and **1** being faster than the cyclization reaction.

In a final experiment, compound **1** was prepared with ^{13}C-enrichment in the propargylic methyl groups (Scheme 5-4). The ^{13}C-enriched **1** was heated to 140 °C in $CDCl_3$ in the presences of HCl for 3 days. The product arene showed ^{13}C-enrichment at an arene position and the methyl carbon of the ethyl group.

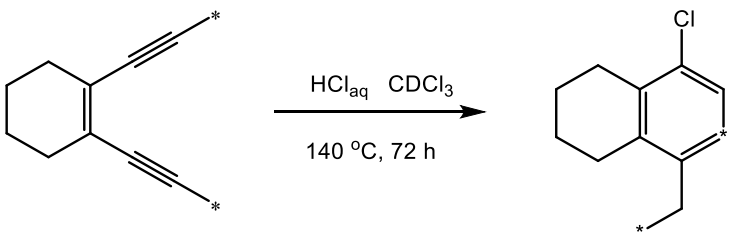

Scheme 5-4. Cyclization of ^{13}C-enriched **1**.[2]

With these results, the cyclization of **1** to **3** was proposed to begin with HCl addition to **1** to give a mixture of **5-*E*** and **5-*Z*** of unknown ratio (Scheme 5-5). The HCl was proposed to be generated from the reaction of $CDCl_3$ with 1,4-CHD to give HCl, benzene and $CHDCl_2$. Then **5-*E*** would undergo a [1,7]-hydride shift to give intermediate **I**. A 6π-electrocyclization of **I** would led to **II**, which could undergo a formal [1,3]-hydride shift to give **3**.

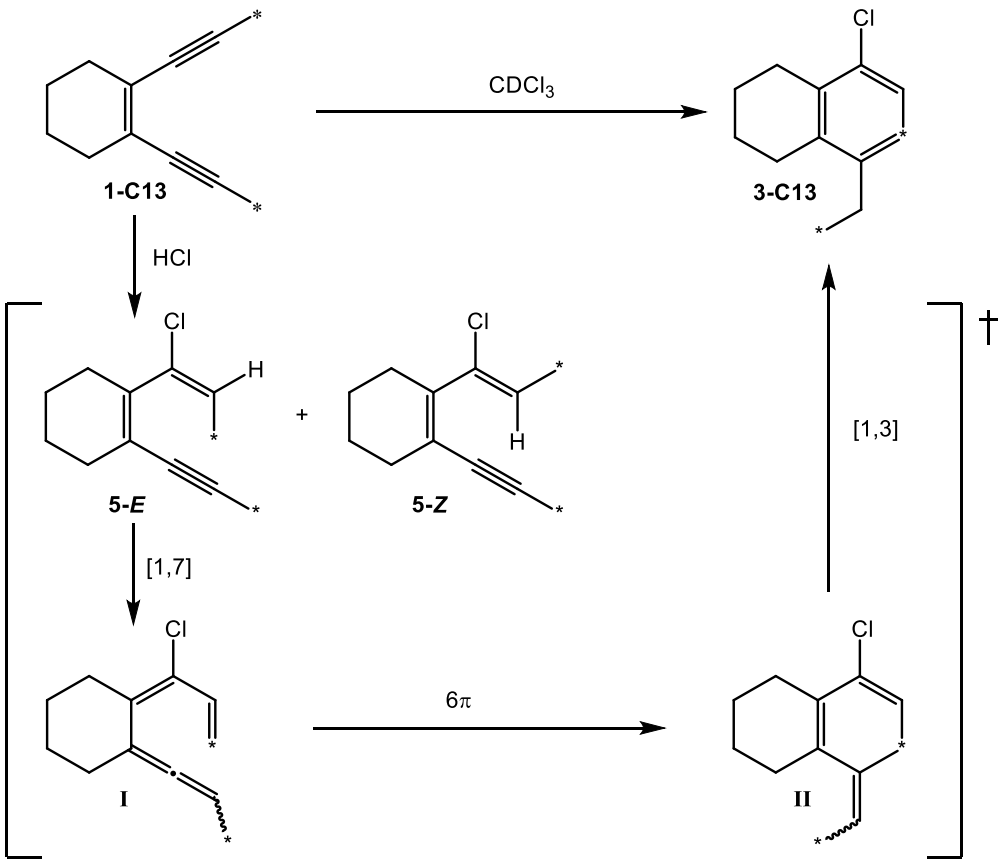

Scheme 5-5. Proposed mechanism for the transformation of **1** to **3**. [2]

In this chapter the mechanism of this reaction is explored further. The synthesis and characterization of intermediate **5** were undertaken and the relevant thermal chemistry of **5** was explored. In addition the reaction of enediynes with other haloforms was examined.

5-2 Results

5-2.1 Reactions Involving $CDCl_3$

Recognizing that the earlier synthesis of **5** was undertaken with aqueous HCl in $CDCl_3$, we speculated that the yields could be improved by use of a non-aqueous source of HCl. When HCl (0.64 mmol, 2 M in Et_2O) was added to a solution of **1** (0.64 mmol) in $CHCl_3$ (10 mL) under argon at 0 °C, the solution turned opaque purple-black and the formation of a new compound was observed by TLC. The solution was stirred for 45 min and the complete consumption of **1** was observed by TLC. The volatiles were removed under vacuum and the residue was purified on a silica gel column with hexanes as eluant. A ^{1}H NMR ($CDCl_3$) spectrum of the product showed two vinyl resonances at δ 5.70 (q, 7.3 Hz) and 5.87 (q, 6.7 Hz) in a 3:1 ratio (Scheme 5-6). The more upfield vinyl resonance was attributed to **5-*E*** and the downfield vinyl resonance was attributed to **5-*Z***, based on computations which give a vinyl resonance of δ 5.78 for **5-*E*** and 6.20 for **5-*Z***.[3]

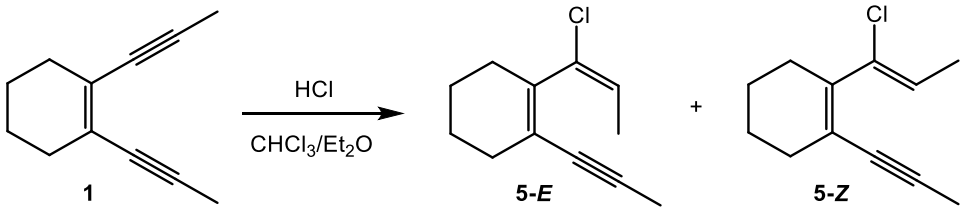

Scheme 5-6. Synthesis of **5** by HCl addition to **1**.

Interestingly, if $CDCl_3$ is used as solvent instead of $CHCl_3$, the reaction proceeds to form a mixture of **5-*E*** and **5-*Z*** in a 98:2 ratio.

When **5** (30 μmol, 3:1 mix of *E*/*Z*) dissolved in $CDCl_3$ (600 μL) was heated at 165 °C in a flame-sealed NMR tube for 16 h, the formation of **3** was observed by ^{1}H NMR spectroscopy along with new resonances at δ 6.78, 2.28, and 2.23 which

integrated as 1:3:3. The second species is proposed to be **6** (Scheme 5-7). Interestingly, upon re-examining the spectra collected for the thermolysis of **1** with 1,4-CHD in $CDCl_3$, the formation of **6** was observed in ~ 5% yield. A 93% conversion of **5-*E*** was observed with a 93% yield of **3** (based on conversion of **5-*E***) and the complete consumption of **5-*Z*** with a > 75% yield of **6** (based on isomer **5-*Z***). To minimize any possible side reactions based on possible production of HCl from $CDCl_3$, the reaction was attempted in C_6D_6. When **5** (30 μmol, 3:1 mix of *E*/*Z*) dissolved in C_6D_6 (600 μL) was heated at 165 °C in a flame-sealed NMR tube for 40 h, the complete consumption of **5-*E*** was observed by ^{1}H NMR spectroscopy along with a 94% yield of **3** (based on conversion of **5-*E***). The minor isomer showed 75% conversion and the formation of **6** was observed in approximately 50% yield, but exact quantitation by ^{1}H NMR spectroscopy was not possible due to overlap of resonances.

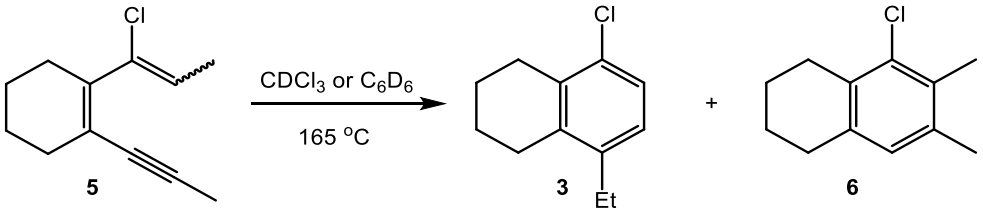

Scheme 5-7. Cyclization of isolated **5**.

When **5** (30 μmol, 98:2 *E*:*Z*) dissolved in C_6D_6 (600 μL) in a flame-sealed NMR tube was heated at 165 °C for 42 h, the complete consumption of **5** was observed along with the formation of **3** in 93% NMR yield. The formation of **6** was not observed by ^{1}H NMR spectroscopy.

A re-examination of the ^{1}H NMR spectrum of the thermal reaction of **1** in $CDCl_3$ and 1,4-CHD showed in addition to **3** the appearances of a broad signal at δ 5.30. In an effort to determine if this signal is due to the proposed $CHDCl_2$ produced in the formation of HCl, the thermal reaction was repeated. Enediyne **1** (30 μmol) and 1,4-CHD (60 μmol) were dissolved in $CDCl_3$ (600 μL) in a medium-walled NMR tube and the tube was flame sealed. The tube was submerged in an oil-bath maintained at 165 °C for 16 h and then the tube was removed and allowed to cool to rt. A ^{1}H NMR spectrum showed the expected formation of **3** along with a signal at δ 5.27 (t, J = 1 Hz), which is consistent with the formation of $CHDCl_2$.[4] A ^{13}C NMR spectrum of the mixture exhibited a resonance at δ 53.35 (t, J = 27.3 Hz), again consistent with the formation of $CHDCl_2$. Next, 1,4-CHD (60 μmol) in $CDCl_3$ (600 μL) in a flame-sealed NMR tube was heated at 165 °C for 16 h. A ^{1}H NMR spectrum of the reaction showed approximately 50% consumption of 1,4-CHD and the appearance of a signal at δ 5.27 (t, J = 1 Hz), consistent with earlier reactions (Scheme 5-8). In addition, a singlet was observed at δ 1.38 in an approximate 1:1 intensity ratio to the 5.27 resonance. This resonance is attributed to HCl, by comparison to the chemical shifts of MeOH in $CDCl_3$.[5] A ^{13}C NMR spectrum of this reaction also showed a triplet at δ 53.35 (J = 27.3 Hz), again consistent with the formation of $CHDCl_2$.

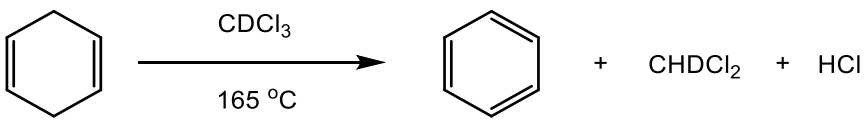

Scheme 5-8. Reaction of 1,4-CHD with $CDCl_3$.

To examine the effect of *c-d* distance of the starting enediyne on the reactions, the five-membered ring enediyne, **7**, was subjected to the above reaction conditions. From known solid-state structures of **1**[1] and **7**[6], the *c-d* distance is 4.203(2) Å and 4.635(3) Å, respectively (Figure 5-1).

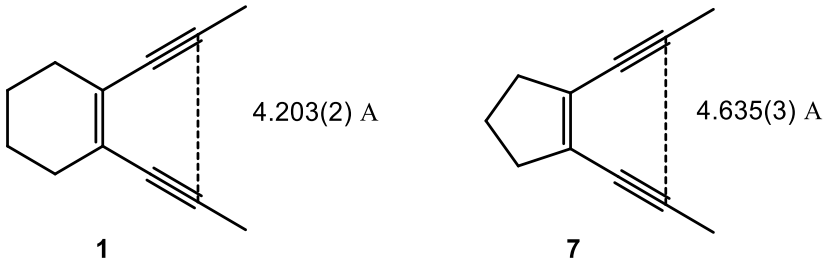

Figure 5-1. A comparison of the *c-d* distance in **1**[1] and **7**[6] (in Å).

Enediyne **7** (60 μmol) and 1,4-CHD (75 μmol) dissolved in $CDCl_3$ (600 μL) in a flame-sealed NMR tube were heated at 165 °C for 16 h. A ^{1}H NMR spectrum of the mixture showed a pair of doublets at δ 6.92 and 7.08 (J = 8.1 Hz) along with a quartet at 2.56 (J = 7.6 Hz) and triplet at 1.18 (J = 7.6 Hz), which integrated as 1:1:2:3. This is consistent with formation of the expected ethyl chloro indane **8** (Scheme 5-9). There was a second set of resonances observed in the ^{1}H NMR spectrum with singlets at δ 6.93, 2.27 and 2.29 which integrated as 1:3:3. These resonances are proposed to belong to a formal Höpf product, **9**. The ratio of **8** to **9** formed was determined to be 4:1.

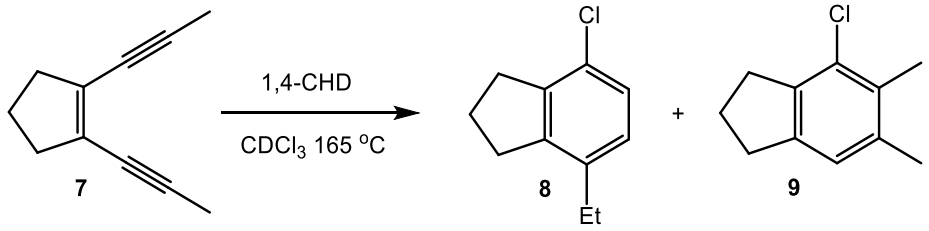

Scheme 5-9. Reaction of **7** with 1,4-CHD in $CDCl_3$.

Then HCl (0.7 mmol, 2.0 M in Et_2O) was added to a stirred solution of **7** (0.87 mmol) in $CDCl_3$ (4 mL) under argon and the resulting opaque solution was allowed to stir overnight. The volatiles were removed under vacuum and the residue was purified by silica chromatography with hexanes eluant, which showed two bands. The first band was the HCl addition product **10** (0.24 mmol) and the second band was recovered **7** (0.50 mmol). Vinyl chloride **10** was obtained as a 96:4 mixture of *E*:*Z* isomers as determined by comparing the integrals for the vinyl resonances at δ 5.81 (q, J = 7.3 Hz) and 6.22 (q, J = 6.9 Hz) in the ^{1}H NMR spectrum ($CDCl_3$, Scheme 5-10).

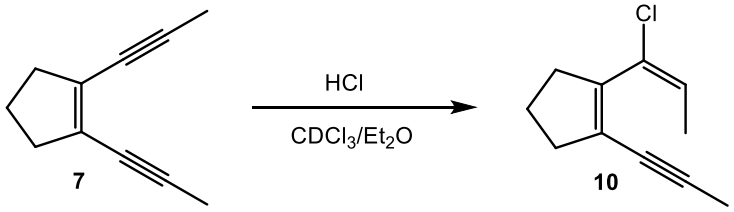

Scheme 5-10. Synthesis of **10**.

Vinyl chloride **10** (20 μmol) in C_6D_6 (600 μL) in a flame-sealed NMR tube was heated at 165 °C for 16 h. A ^{1}H NMR spectrum showed complete consumption

of **10** and the formation of **8** in 93% yield (Scheme 5-11). The formation of **9** was not observed in the ^{1}H NMR spectrum of the crude reaction mixture.

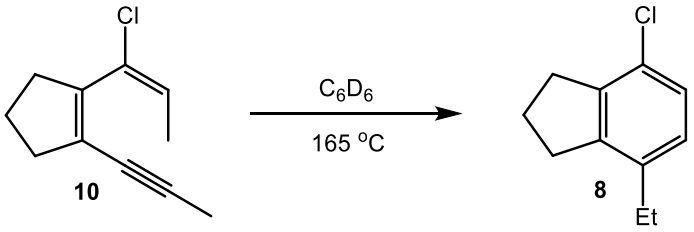

Scheme 5-11. Cyclization of **10**.

Next, **10** (22 μmol) in DCM (2 mL) was added to [CpRu(NCMe)$_3$]PF$_6$[1,7] (**11**) (22 μmol) under argon and the solution was allowed to react for 1 h. The solution was concentrated to ~0.5 mL under vacuum and then Et_2O (10 mL) was added to precipitate arene complex **12** (Scheme 5-12). A ^{1}H NMR spectrum in CD_3CN showed resonances consistent with the formation of **12** and then the solution was placed in a photoreactor and irradiated at 254 nm for 16 h. A ^{1}H NMR spectrum showed the disappearance of resonances of **12** and the appearance of peaks consistent with **9**. The contents of the NMR tube were poured into Et_2O to precipitate out ruthenium containing complexes and the solution was filtered. The volatiles were removed under vacuum and the residue was purified on a small silica gel column with hexanes eluant to give **9** (20 μmol) in 90% yield.

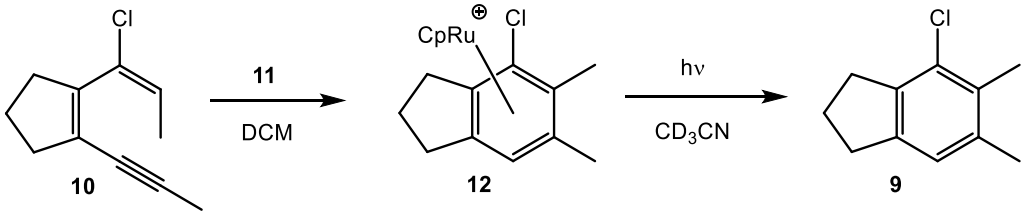

Scheme 5-12. Synthesis of **9**.

5-2.2 Reactions Involving the Other Haloforms

The ability to generate HCl *in situ* from $CDCl_3$ and 1,4-CHD and to subsequently use this HCl in a reaction was an interesting results. Calculations of ΔH^{o}_{rxn} for the reaction of 1,4-CHD with the haloforms to form benzene, dihalomethane, and hydrogen halide were performed (Scheme 5-13).[8] Details for the calculations of $\Delta H°_{rxn}$ and a listing of $\Delta H°_{f}$ can be find in the experimental (section 5-5.4).

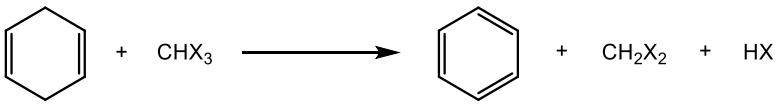

X	ΔH^{o}_{rxn} in kcal mol^{-1}
F	-11.6
Cl	-24.6
Br	-18.6
I	-25.6

Scheme 5-13. Energy of formation of HX from 1,4-CHD and CHX_3.[8]

It is clear from these numbers that the formation of HX is exothermic for all four halogens, most likely due to the formation of benzene as a product.

The first haloform chosen was bromoform. When a solution of **7** (30 μmol) and 1,4-CHD (45 μmol) in $CDBr_3$ (600 μL) in a flame-sealed NMR tube was heated at 165 °C for 16 h, the formation of a black gel was observed in the NMR tube. A ^1H NMR spectrum of the reaction mixture did not reveal any useful information as all the peaks were broad. Drawing inspiration from the previously studied chloro-substituted dienyne **10** in C_6D_6, and to minimize possible unproductive decomposition pathways of bromoform, further studies were performed in C_6D_6 with one equivalent of haloform. When **7** (60 μmol), $CHBr_3$ (60 μmol) and 1,4-CHD (66 μmol) in C_6D_6 in a flame-sealed NMR tube were heated at 165 °C for 16 h, the formation of arene products was observed by ^1H NMR spectroscopy. The ^1H NMR data indicated the formation of two arene species, **13** and **14**, in a ratio of 2.3:1. Much like as was seen with reactions in $CDCl_3$, we propose that **13** would arise from a [1,7]-hydride shift and **14** would form from a formal Höpf reaction (Scheme 5-14). A pair of doublets at δ 6.86 and 7.24 (J = 7.8 Hz, 1H), a quartet at 2.55 (J = 7.5 Hz, 2H) and a triplet at 1.18 (J = 7.5 Hz, 3H) are in the ^1H NMR spectrum of the sample are diagnostic of **13**. Singlets at δ 6.95 (1H), 2.33 (3H) and 2.29 (3H) characterize **14**.

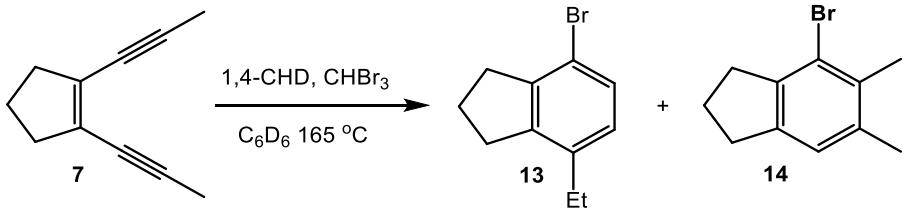

Scheme 5-14. Reaction of **7** in the presence of $CHBr_3$ and 1,4-CHD in C_6D_6.

Then by analogy to the above chemistry with chloroform, HBr (1.2 mmol, 8.9 M in H_2O) was added to a stirred solution of **7** (0.87 mmol) in $CDCl_3$ (4 mL) under argon and the resulting opaque solution was stirred vigorously for 16 h. The solution was diluted in Et_2O and neutralized with $NaHCO_3$. The organic layer was separated, dried over $MgSO_4$ and the volatiles removed under vacuum. The residue was purified on a silica gel column with hexanes as eluant to give vinyl bromide **15** (0.27 mmol, 31% yield) and **7** (0.45 mmol, 52% recovery). Compound **15** has characteristic ^{1}H NMR ($CDCl_3$) chemical shifts at δ 6.03 (q, J = 7.1 Hz, 1), 2.00 (s, 3H) and 1.66 (d, J = 7.1 Hz, 3H). The structure is assigned as *E* by analogy to **10** (Scheme 5-15)

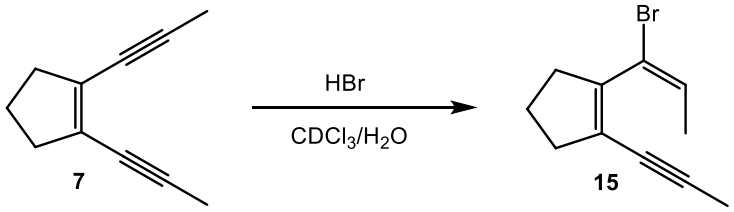

Scheme 5-15. Synthesis of **15** by HBr addition to **7**.

When **15** (45 μmol) in C_6D_6 (600 μmol) in a flame-sealed NMR tube was heated at 165 °C for 16 h, the complete consumption of **15** was observed by ^{1}H NMR spectroscopy along with the formation of **13** and **14** in a 9:1 ratio, in a 90% yield (Scheme 5-16).

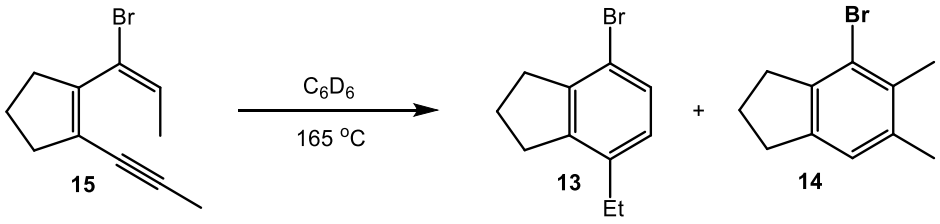

Scheme 5-16. Cyclization of **15**.

Vinyl bromide **15** (22 μmol) in DCM (2 mL) was added to $[CpRu(NCMe)_3]PF_6$ (**11**, 22 μmol) under argon and the solution was allowed to react for 1 h. The solution was concentrated to ~ 0.5 mL under vacuum and then Et_2O (10 mL) was added to precipitate intermediate **16** (Scheme 5-17). A ^1H NMR spectrum in CD_3CN showed ^1H NMR resonances consistent with the formation of intermediate **16** and then the solution was placed in a photoreactor and irradiated at 254 nm for 16 h. A ^1H NMR spectrum showed the disappearance of the resonances of **16** and the appearance of peaks consistent with **14**. The contents of the NMR tube were poured into Et_2O to precipitate out ruthenium-containing complexes and the solution was filtered. The volatiles were removed under vacuum and the residue was purified on a small silica gel column with hexanes eluant to give **14** (20 μmol, 90% yield).

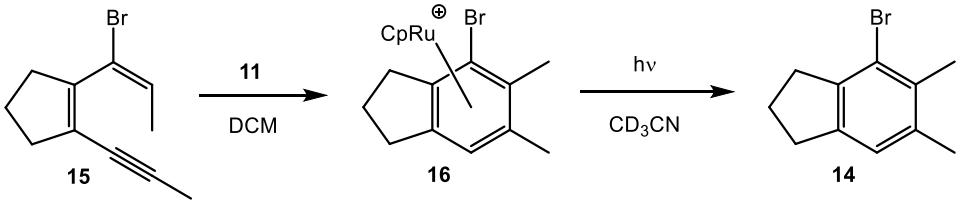

Scheme 5-17. Synthesis of **14** from **15**.

Next the reactions with iodoform were undertaken. When a solution of **7** (30 μmol), CHI_3 (30 μmol) and 1,4-CHD (33 μmol) in C_6D_6 (600 μL) in a flame-sealed NMR tube was heated at 165 °C for 16 h, the solution turned dark red and black material was observed on the inside of the tube. A ^1H NMR spectrum showed complete consumption of **7**, but the expected resonances of an iodo-analogue of **8** were not observed. Instead singlets at δ6.90 and 2.23 were observed which integrated as 1:3, along with broad peaks in the baseline. The contents of the tube were poured into an aqueous solution of $Na_2S_2O_3$, which removed the red color and the aqueous solution was extracted with Et_2O. The organic solution was dried over $MgSO_4$ and the volatiles were removed under vacuum. The residue was purified on a short silica gel plug with hexanes as eluant to give **17**[9] as the only isolated product in 75% yield (Scheme 5-18).

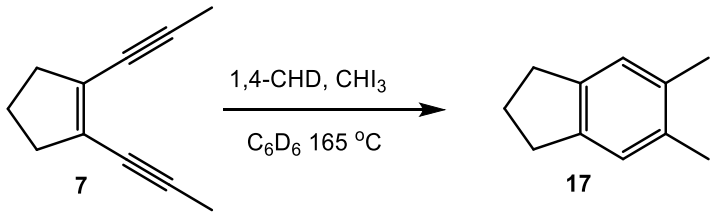

Scheme 5-18. Reaction of **7** with CHI_3 in the presences of 1,4-CHD.

Next a solution of **7** (30 μmol), CHI_3 (30 μmol) and 1,4-CHD (33 μmol) in C_6D_6 (600 μL) in a flame-sealed NMR tube was heated at 100 °C for 24 h, after which a ^1H NMR spectrum was taken which showed complete consumption of **7** and the appearance of a quartet at δ6.26 (J = 7.6 Hz, 1H), singlet at 1.55 (3H) and doublet at 1.57 (J = 7.6 Hz, 3H). This new species, **18**, was tentatively assigned as the *E*-vinyl

iodide analogue to **10** (Scheme 5-19) The tube was then placed in an oil bath at 165 °C for 3 h and a ^{1}H NMR spectrum showed the complete consumption of intermediate **18** and the appearance of resonances consistent with **17**. No iodo-analogue of **8** was observed in the ^{1}H NMR spectrum.

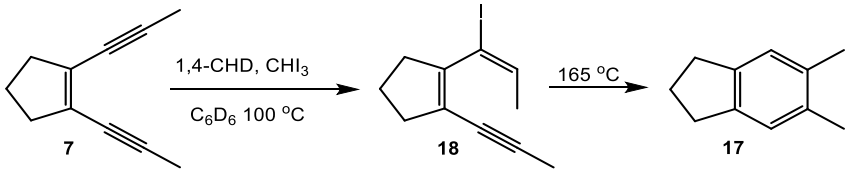

Scheme 5-19. Reaction of **7** with CHI_3 and 1,4-CHD at 100 °C and then 165 °C.

To compare the formation of **17** from **7** in the presence and absence of CHI_3, a flame-sealed NMR tube containing **7** (50 μmol) and 1,4-CHD (100 μmol) in C_6D_6 (600 μL) was heated at 165 °C. After 48 h at 165 °C, there was 35% conversion of **7** with a 44% yield of **17**, based on the conversion of **7**. After 260 h at 165 °C, there was an 87% conversion of **7** with a 42% yield of **17**, based on the conversion of **7**. After 450 h at 165 °C, there was 99.5% conversion of **7** with a 40% yield of **17**, based on the conversion of **7**. From this data, the cyclization of **7** was determined to have a half-life of 165 h at 165 °C.

The reaction of **7** with fluoroform presented unique challenges as it is a gas at rt, with a boiling point of -124 °C. An NMR tube with a Teflon needle valve was evacuated on the high vacuum line and then the gas manifold was purged with CHF_3 (1 atm) and the evacuated tube was opened to the gas manifold and was then sealed

again. The NMR tube was determined to have a volume of 3.3 mL to the Teflon valve seat.[10] Meanwhile a solution of **7** (30 μmol) and 1,4-CHD (40 μmol) in C_6D_6 was prepared on the high vacuum line and frozen on a liquid N_2 bath. The manifold was placed under static vacuum and the tube containing CHF_3 (140 μmol) was opened and the CHF_3 allowed to condense in the reaction tube. Then the tube was flame sealed while the solution was frozen on liquid N_2. The tube was then placed in an oil bath at 165 °C and the solution was checked periodically by ^{1}H NMR spectroscopy. After 48 h, a singlet resonance at δ 6.90 was observed, consistent with the formation of **17** (Scheme 5-20). The aliphatic resonance of **17** were obscured by broad baseline resonances, making integration unreliable but resonances in the correct chemical shifts and multiplicity were observed. There were no changes observed in the ^{19}F NMR spectrum from the initial spectrum which showed a resonance at δ -78.5 (d, J = 80 Hz). The reaction was allowed to proceed at 165 °C for 300 h and a ^{1}H NMR spectrum showed the near complete consumption of **7** and the formation of **17**. The NMR yield of **17** was not measured due to broad baseline resonances, which caused problems with reliable integrations. A ^{19}F NMR spectrum showed only a resonance at δ -78.5 (d, J = 80 Hz), consistent with unchanged CHF_3.[11]

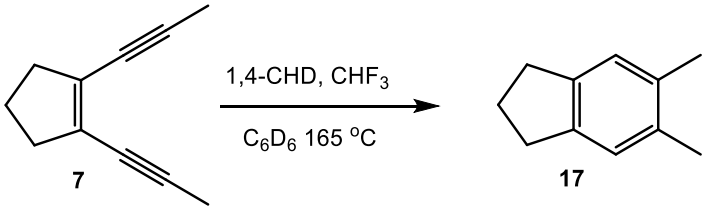

Scheme 5-20. Reaction of **7** in the presence of CHF_3 and 1,4-CHD.

5-3 Discussion

Heating of solution of 1,4-CHD in $CDCl_3$ at 165 °C was shown to generate benzene, $CHDCl_2$ and a ^1H NMR resonance at δ 1.47 consistent with the formation of HCl. The appearance of $CHDCl_2$ shows that the hydrogen of the HCl generated is from 1,4-CHD with the chlorine coming from chloroform. The most likely pathway for this reaction starts with homolytic cleavage of a carbon chlorine bond of $CDCl_3$ to give a chlorine radical and $CDCl_2$ radical, **i** (Scheme 5-21). The chlorine radical then abstracts a hydrogen from 1,4-CHD to give the cyclohexadienyl radical **ii** and HCl. Then **i** reacts with **ii** via hydrogen abstract to give $CHDCl_2$ and benzene.

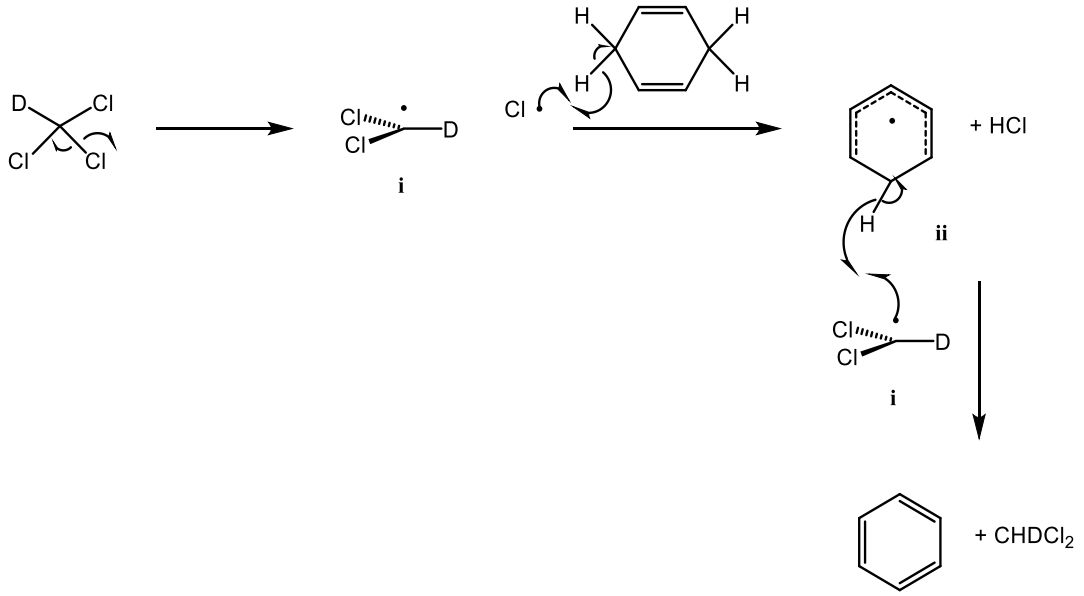

Scheme 5-21. Mechanism for the formation of HCl, benzene and $CHDCl_2$.

The cleavage of the C-Cl bond as the first step would be explained by the bond-dissociation energy of the C-Cl bond of chloroform (70 kcal mol^{-1})[12] versus the C-H bond of 1,4-CHD (75 kcal mol^{-1}).[13]

The *in situ* generated HCl is then proposed to add to one of the alkynes of **1** to give vinyl chloride **5**. The reaction of **1** with HCl in $CDCl_3$ gives **5** in moderate yield with excellent selectivity for one isomer, > 95:5, which we assign as the *E* isomer. Addition of HCl to alkynes has been shown to favor *syn* addition in non-polar solution[14], as would be present in this case. In addition, computationally the trend was for the *E* isomer to show an upfield vinyl resonance in ^{1}H NMR spectroscopy as compared to the *Z* isomer[3], as was observed in our system. Additionally, the calculated structures of **5-*E*** and **5-*Z*** showed only a 0.1 kcal mol^{-1} preference for **5-*E***, meaning little thermodynamic preference for the formation of either structure.[3]

The isolated vinyl chloride **5** was then heated in C_6D_6 at 165 °C and was observed to proceed to the rearranged product **3** in high yields with high conversions of **5** after 16 h. This shows that **5** is competent intermediate in the formation of **3** from **1**. The intermediates **I** and **II** (Scheme 5-22) were not isolated or observed, but their existence can be inferred from the formation of **3** from **5**. It would be difficult to propose a mechanism for this transformation without the intermediacy of **I** and **II**.

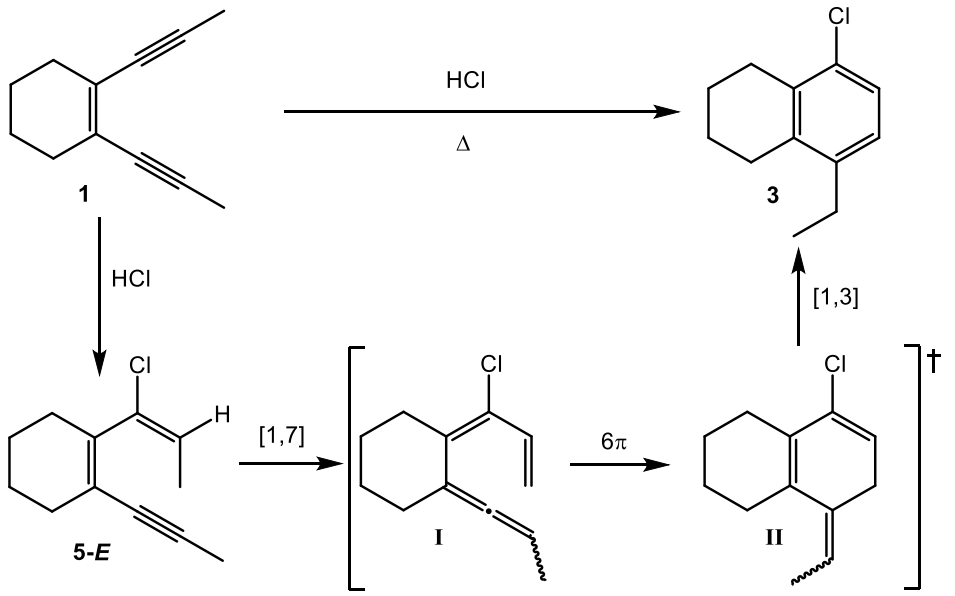

Scheme 5-22. Proposed mechanism for the formation of **3** from **1**.

The formation of a mixture of **8** and **9** (4:1) from the heating of **7** with 1,4-CHD in $CDCl_3$ is a curious result as the formation of **6** from the similar reaction with **1** was only observed as a trace product (Scheme 5-23).

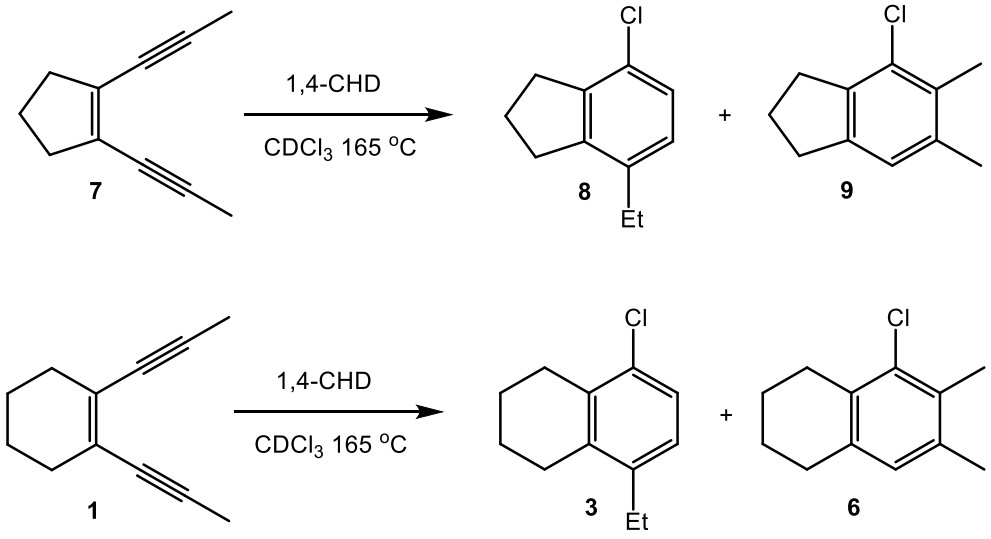

Scheme 5-23. Reaction of **1** and **7** in the presence of 1,4-CHD and $CDCl_3$.

When the vinyl chloride intermediate **10** (96:4 *E*/*Z*) was isolated and heated at 165 °C in C_6D_6, the clean formation of **8** was observed with no observation of **9** (Scheme 5-24)

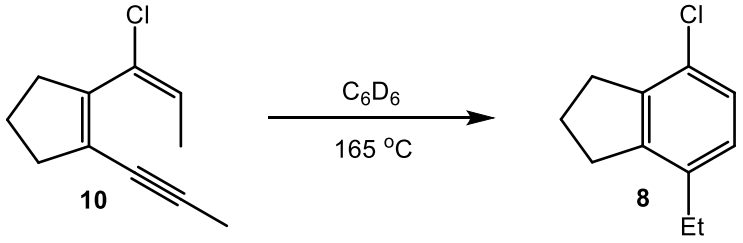

Scheme 5-24. Cyclization of **10**.

This would discredit an argument for the *Z* isomer being solely responsible for the formation of **9**, as one would suspect the formation of **9** during this reaction, albeit in very low yield. One possible explanation for the formation of **9** when in the presence of 1,4-CHD in $CDCl_3$, is the catalysis of the reaction by HCl. A second equivalent of HCl could interact with the alkyne, leading to nucleophilic attack by alkene. Then loss of a proton would lead to the observed product **9**, Scheme 5-25.

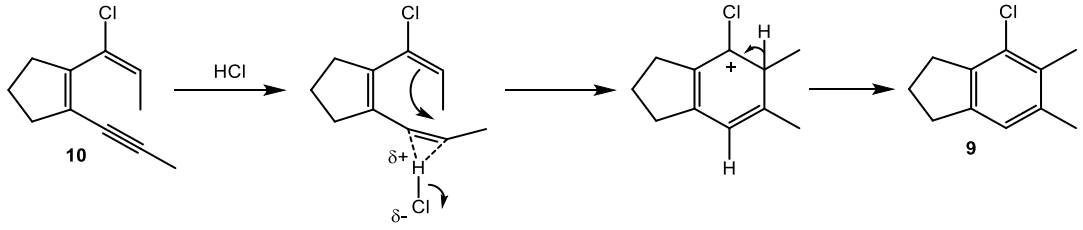

Scheme 5-25. Proposed mechanism for the formation of **9**.

This is similar to an example proposed by Shibata for the gold-catalyzed cyclization of aromatic enynes.[15]

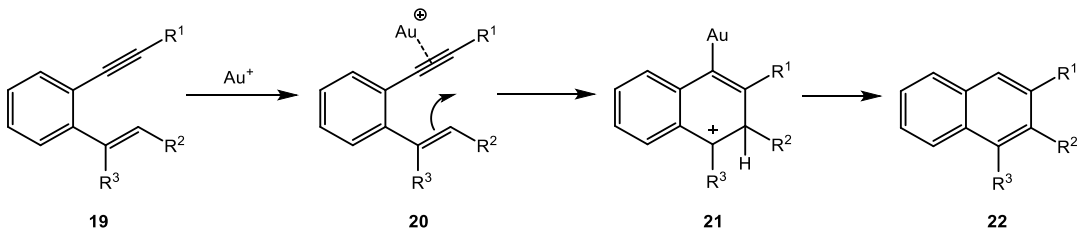

Scheme 5-26. Gold-catalyzed cyclization of aromatic enynes from Shibata.[15]

The coordination of a soluble source of gold cation, Ph_3PAuCl plus AgOTf to give $Ph_3PAuOTf$, to the alkyne activates the species to undergo a 6-*endo*-dig cyclization to give **21** (Scheme 5-26). Deprotonation of **21,** followed by protolytic removal of gold give naphthalene **22**. Another possibility comes from the Liu lab, in which the double addition of HCl to 1,2-diethynylcyclohexene, **23**, gives intermediate **24** (Scheme 5-27).[16] Which upon cyclization and lost of HCl lead to chloro-tetralin **25**.

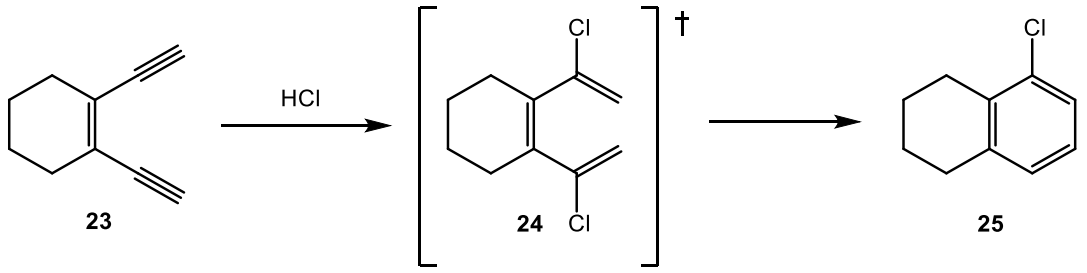

Scheme 5-27. Cyclization of enediynes observed by Liu.[16]

When the halide source was changed to $CHBr_3$, the ratio of product from the [1,7]-H shift, **13**, to the formal Höpf reaction, **14**, changed to 2.3:1 (Scheme 5-28). When the isolated vinyl bromide **15** (> 99% isomeric purity as determined by ^1H

NMR spectroscopy) was heated at 165 °C in C_6D_6, the formation of **13** and **14** was observed in a ratio of 9:1.

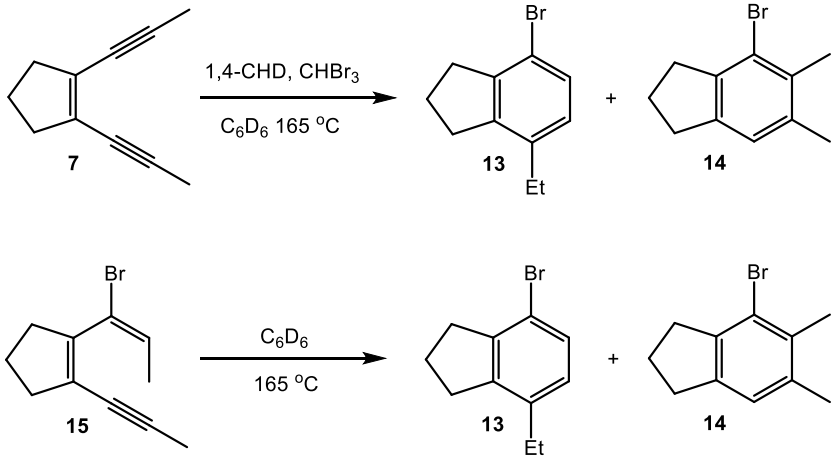

Scheme 5-28 Formation of **13** and **14**.

The difference in the ratio on going from the reaction mixture where HBr is generated to the reaction of isolated **15** can be explained by the mechanism discussed above for HCl. The increase in the formation of **14** as compared to the formation of **9** could be due to the higher acidity of HBr (-4.9 pKa in dichloroethane)[17] in non-aqueous solutions as compared to HCl (-0.4 pKa in dichloroethane). The formation of **14** from **15** in C_6D_6 may indicate a competition between the [1,7]-H shift and a 6π-electrocyclization from **15**. The larger effective steric size of chlorine (A value of 0.53)[18] compared to bromine (A value of 0.48), disfavors the dienyne of **10** from adopting a co-planar arrangement necessary for a 6π-electrocyclization to occur. In addition, the larger size of chlorine puts the unsaturated system is a canted arrangement that may favor the [1,7]-hydride shift. The higher effective withdrawing

nature of Br (σ_{meta} = +0.393)[19] as compared to Cl (σ_{meta} = +0.373) could also account for the increase in the rate of the 6π-electrocyclization. The electron-withdrawing nature lowers the HOMO-LUMO gap for the 6π-electrocyclization, thereby lowering the activation barrier of this process. To the best of our knowledge, this is the only example of a system which demonstrates a competition between a 6π-electrocyclization and [1,7]-hydride shift.

Heating a solution of **7** with CHI_3 and 1,4-CHD at 100 °C for 24 h cleanly led to the formation of ^{1}H NMR spectroscopy resonances consistent with vinyl iodide **18**, clearly indicating the generation of HI in solution (Scheme 5-29). When this sample was heated at 165 °C for 3 h the formation of **17** was observed as the only product. The formation of an iodo-analogue of **8** was not observed. The bond dissociation energy of vinyl iodides are known to be low (41 kcal mol^{-1} for 1-iodo-1-propene).[12] Heating of **18** may lead to hemolytic cleavage of the C-I bond and hydrogen abstraction from 1,4-CHD to give HI and dienyne **27**. Then HI addition to the alkyne in **27** leads to iodo-triene **28**, which undergoes a 6π-electrocyclization to give **29**. Loss of HI from **27** leads to the observed indane product **17**.

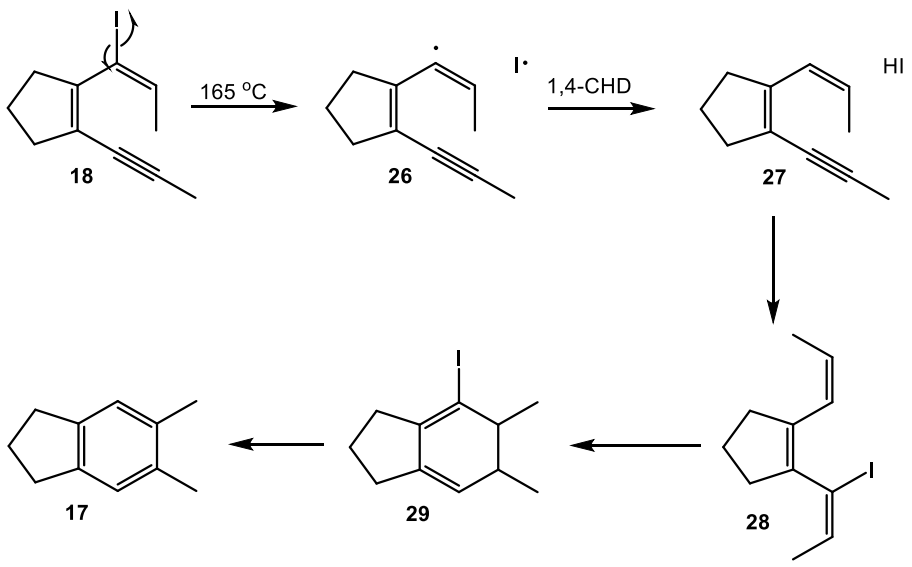

Scheme 5-29. Proposed mechanism for the formation of **17** from **7** in the presence of CHI_3 and 1,4-CHD.

The formation of **17** from **7** in the presence of CHF_3 and 1,4-CHD proceeds at approximately the same rate as the formation of **17** without added CHF_3. This result is not too surprising as the weakest bond in CHF_3[12] is the C-H bond at 106 kcal mol^{-1} versus the C-F bond at 125 kcal mol^{-1}. Radical chemistry initiated from CHF_3 seems unlikely with such strong bonds.

5-4 Conclusion

In conclusion, the previously discovered novel cycloaromatization of enediynes upon heating in $CDCl_3$ has been extended to other haloforms. The reaction had been proposed to proceed by generation of HCl via homolytic cleavage of C-Cl

bonds in $CDCl_3$ then H-atom abstraction. The HCl generated adds to an alkyne to give a chlorodienyne. Mixtures of chlorodienynes were synthesis and isolated. The isomer made in higher quantity was proposed to be the *E* isomer and this isomer was shown to form the arene product. The reaction was extended to enediynes containing a five-membered ring backbone. Under the reaction conditions in $CDCl_3$, these substrates were shown to form a mixture of arene products resulting from a [1,7]-hydride shift as a first step and from a 6π-electrocyclization as a first step. When isolated chlorodienyne intermediate was subjected to the same temperatures in C_6D_6 the formation of the product from [1,7]-hydride shift was the only product observed. The reaction was then extended to $CHBr_3$, which also showed a mixture of products resulting from a [1,7]-hydride shift as the first step and 6π-electrocyclization as a first step. When bromo dienyne intermediate was isolated and subjected to the conditions, a mixture of products was again observed, but in a different ratio, 9:1 as compared to 2.3:1. When the reaction was extended to CHI_3, the product of a formal Bergman cyclization was obtain as the only product in 75% yield. This product was proposed to be formed via multiple additions of HI to the substrate and homolytic cleavage of C-I bonds.

Future outlooks for this project are centered on the synthesis of dienyne substrates that resemble **9**, but with phenyl substituents in place of chlorine. The electronics of the phenyl group will then be varied by incorporation of different groups in the *para*-position. Then heating of these dienynes should give information of the electronic effects on the selectivity of 6π-electrocyclizations versus [1,7]-

hydride shifts in these substrates. In addition, the synthesis of analogous structures with substituents of different sizes should give information on the steric effects on product selectivity. In addition, there are ongoing efforts toward the extension of this reaction to benzanulated systems and heteroaromatic systems.

5-5 Experimental

5-5.1 General Procedures

All manipulations were performed using standard Schlenk technique or in nitrogen filled Vacuum Atmospheres or MBraun glovebox, unless otherwise stated. ^{1}H and ^{13}C NMR spectra were recorded on Varian Mercury 400 MHz, Varian VX 500 MHz, or JOEL ECA 500 MHz instruments. ^{1}H and ^{13}C NMR chemical shifts (δ) are reported in parts per million (ppm). Spectra were referenced to the residual solvent peak. Infrared spectra were obtained on a Nicolet Avatar 320 FT-IR. High resolution mass spectra analyses were performed at either the mass spectrometer facility at UC San Diego or UC Riverside. Photolyses was performed in a Rayonett photo-reactor equipped with UV lamps centered at 254 nm. THF, ethyl ether, DCM, benzene, hexanes, and pentane used for reaction solvents were dried either by a solvent dispensing system equipped with two neutral alumina columns under argon atmosphere or by 3 Å activated molecular sieves. Chloroform-*d* and benzene-d_6 were dried over 3 Å activated molecular sieves and then distilled under static vacuum into

oven-dried Schlenk storage tubes. Deuterated solvents were degassed using a Freeze-Pump-Thaw procedure, typically 5 cycles. NMR reactions were performed in 5 mm J-Young NMR tubes equipped with a Teflon needle valve. All literature compounds were prepared according to the indicated references or purchased from commercial suppliers and used as received.

5-5.2 Preparation and Characterization Data

E:Z*-1-(1-chloroprop-1-en-1-yl)-2-(prop-1-yn-1-yl)cyclohex-1-ene** (**5**): Endiyne(**1**) (100 mg, 0.63 mmol) was weighed into an oven-dried 50 mL side-arm Schlenk flask equipped with a stir bar and rubber septum under an atmosphere of N_2. Then 10 mL of $CHCl_3$ (distilled over CaH_2 under N_2) was added to the flask and the solution was cooled to 0 °C on an ice/water bath. Then HCl (2 M in Et_2O, 320 μL, 0.64 mmol) was added dropwise via syringe over 5 min, the solution immediately turned opaque purple-black. The resulting solution was allowed to stir at 0 °C for 45 min, at which time TLC (silica gel, hexanes) showed consumption of the starting alkyne **1**. The volatiles were then removed under vacuum and the residue purified on a silica gel column with hexanes eluant to give **5** as a colorless oil (151 mg, 78% of a 3:1mixture of *E:Z* isomer). (**2-*E) ^{1}H NMR (500 MHz, $CDCl_3$) δ 1.60 (d, $^3J_{HH}$ = 7.3 Hz, 3H, CHC*H*$_3$), 1.65-1.56 (m, 4H, 2,3-CH_2), 1.93 (s, 3H, CH_3), 2.22-2.14 (m, 4H, 1,4-CH_2), 5.70 (q, $^3J_{HH}$ = 7.3 Hz), 1H, C*H*CH_3). ^{13}C NMR (125 MHz, $CDCl_3$) δ4.7, 15.3, 22.2, 22.4, 27.7, 30.6, 79.7, 88.7, 121.3, 124.3, 132.0, 137.6. HRMS (ESI): Calcd for

($C_{12}H_{15}Cl$ + H): 195.0935, found 195.0932. (**2-*Z***) ^{1}H NMR (500 MHz, $CDCl_3$) δ1.65-1.56 (m, 4H, 2,3-CH_2), 1.79 (d, $^{3}J_{HH}$ = 6.7 Hz, 3H, CHC*H*$_3$), 1.91 (s, 3H, CH_3), 2.22-2.14 (m, 4H, 1,4-CH_2), 5.87 (q, $^{3}J_{HH}$ = 6.7 Hz, 1H, C*H*CH_3). ^{13}C NMR (125 MHz, $CDCl_3$) δ4.7, 14.5, 22.3, 22.3, 28.4, 31.2, 80.1, 88.5, 119.1, 123.8, 133.6, 140.5.

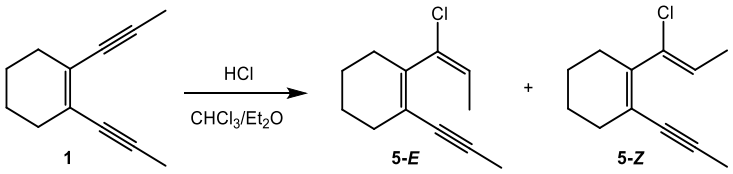

(*E*)-1-(1-chloroprop-1-en-1-yl)-2-(prop-1-yn-1-yl)cyclopent-1-ene (**10**): Enediyne **7** (125 mg, 0.87 mmol) was dissolved in $CDCl_3$ (4 mL) in a 20 mL vial equipped with a rubber septum and stir bar. Then HCl (0.35 mL, 2.0 M in Et_2O) was added and the resulting solution was stirred overnight at rt. Then the solution was dried over $MgSO_4$ and the suspension filtered and the volatiles removed under vacuum. The residue was then purified on a silica gel column with hexanes eluant. Vinyl chloride **7** was the first band to come off of the column, followed by unreacted starting material (recovered 74 mg of **7**). **10** was obtained as a colorless oil (61 mg, 0.27 mmol, 31% yield as a 96:4 mixture of (*E*:*Z*) as determined by ^{1}H NMR spectroscopy). (**10**) ^{1}H NMR (500 MHz, $CDCl_3$) δ1.69 (d, $^{3}J_{HH}$ = 7.3 Hz, 3H), 1.91 (p, $^{3}J_{HH}$ = 7.7 Hz, 2H), 2.00 (s, 3H), 2.55 (tt, $^{3}J_{HH}$ = 7.7 Hz, $^{5}J_{HH}$ = 2.1 Hz, 2H), 2.59 (tt, $^{3}J_{HH}$ = 7.7 Hz, $^{5}J_{HH}$ = 2.1 Hz, 2H), 5.81 (q, $^{3}J_{HH}$ = 7.3 Hz, 1H). ^{13}C NMR (125 MHz, $CDCl_3$) δ4.8, 16.0, 22.6, 35.5, 37.9, 76.5, 93.1, 125.1, 125.9, 127.7, 141.7. HRMS (APCI-TOFMS): Calcd for ($C_{11}H_{14}Cl$) : 181.0779, found 181.0780.

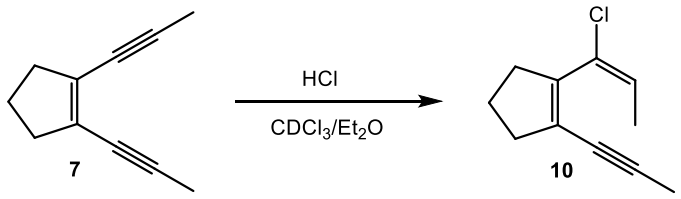

(*E*)-1-(1-bromoprop-1-en-1-yl)-2-(prop-1-yn-1-yl)cyclopent-1-ene (**15**): Enediyne **7** (125 mg, 0.87 mmol) was dissolved in $CDCl_3$ (4 mL) in a 20 mL vial equipped with a rubber septum and stir bar. Then aqueous HBr (0.130 mL, 8.9 M, 1.2 mmol) was added and the resulting solution was stirred overnight at rt. Then the solution was dried over $MgSO_4$ and the suspension filtered. Then silica gel was added to the solution and the volatiles were removed under vacuum. The reaction mixture absorbed on silica gel was loaded onto the top of a 10 cm column of silica gel and the mixture separated with hexanes elaunt. Vinyl bromide **15** was the first band to come off the column, followed by unreacted starting material (recovered 74 mg of **7)**. **15** was obtained as a colorless oil (61 mg, 0.27 mmol, 31% yield). (**15**) ^{1}H NMR (500 MHz, $CDCl_3$) δ 1.66 (d, $^3J_{HH}$ = 7.1 Hz, 3H), 1.91 (p, $^3J_{HH}$ = 7.7 Hz, 2H), 2.00 (s, 3H), 2.53 (tt, $^3J_{HH}$ = 7.7 Hz, $^5J_{HH}$ = 2.3 Hz, 2H), 2.60 (tt, $^3J_{HH}$ = 7.7 Hz, $^5J_{HH}$ = 2.3 Hz, 2H), 6.03 (q, $^3J_{HH}$ = 7.1 Hz, 3H). ^{13}C NMR (125 MHz, $CDCl_3$) δ 4.8, 17.1, 22.5, 36.1, 37.9, 76.5, 93.1, 117.8, 124.6, 129.7, 142.9. HRMS (APCI-TOFMS): Calcd for ($C_{11}H_{14}Br$) : 225.0273, found 225.0275.

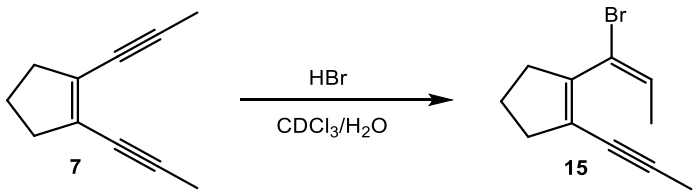

5-Chloro-8-ethyl-1,2,3,4-tetrahydronaphthalene (**3**): Dienyne(**5**) (3:1 *E*:*Z*, 15 mg, 77 μmol) and 1,3,5-tris(^{t}Bu)benzene (1 mg, 4 μmol) was weighed into an oven-dried medium-walled NMR tube and then $CDCl_3$ (600 μL) was distilled into the tube on a high-vacuum line. The resulting solution was frozen and then the tube was flame sealed. An initial ^{1}H NMR spectrum was collected and then the tube was submerged into a constant temperature oil bath held at 165 °C. The reaction was allowed to proceed for 22 h and then the tube was removed from the oil bath. A ^{1}H NMR spectrum was collected and showed consumption of the starting material **5** and the appearance of tetralin **3**. The tube was opened and the contents were poured into a vial, rinsing the NMR tube through with $CDCl_3$. The volatiles were removed under vacuum and the residue was loaded onto a silica gel column. The reaction mixture was then eluted with pentane to give **3** as a colorless oil (10 mg, 87% yield based upon consumption of *E* isomer). ^{1}H NMR (500 MHz, $CDCl_3$) δ 1.19 (t, $^3J_{HH}$ = 7.4 Hz, 3H, CH_2CH_3), 1.79 (bp, $^3J_{HH}$ = 3.3 Hz, 4H, 2,3-CH_2), 2.56 (q, $^3J_{HH}$ = 7.4 Hz, 2H, CH_2CH_3), 2.69 (bt, 2H, CH_2), 2.78 (bt, 2H, CH_2), 6.94 (d, $^3J_{HH}$ = 8.2 Hz, 1H, Ar*H*), 7.15 (d, $^3J_{HH}$ = 8.2 Hz, 1H, Ar*H*). ^{13}C NMR (125 MHz, $CDCl_3$) δ 14.4, 22.7, 22.9, 25.5, 26.7, 28.0, 126.1, 126.2, 132.3, 134.8, 137.3, 140.9. HRMS (EI+): Calcd for ($C_{12}H_{15}Cl$): 194.0857, found 194.0858.

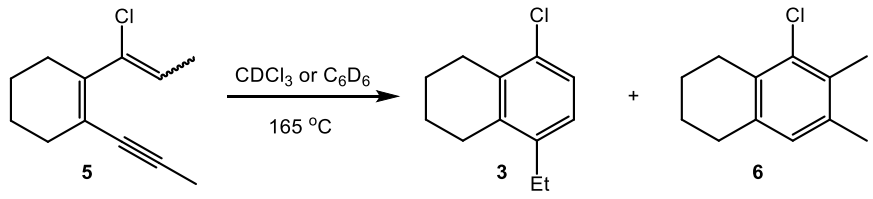

Thermal Reaction of 7 with 1,4-CHD in $CDCl_3$: Enediyne **7** (8.4 mg, 58 μmol, 1 eq) and 1,4-CHD (7.3 μL, 77 μmol, 1.3 eq) were weighed into an oven-dried medium-walled NMR tube, which was cooled to rt under vacuum. Then $CDCl_3$ (550 μL) was distilled into the tube on the high vacuum line and the tube was flame sealed under vacuum. An initial ^{1}H NMR spectrum was collected and the tube was submerged in a constant temperature oil-bath maintained at 165 °C for 15.5 h. The tube was removed from the oil bath, allowed to cool to rt and a ^{1}H NMR spectrum was collected. The spectrum showed complete consumption of **7**, with formation of benzene and a triplet (δ 5.29 ppm, $^2J_{HD}$ = 1.1 Hz) indicative of the formation of $CHDCl_2$. The tube was cracked open and the reaction mixture was separated on a silica gel plug with hexanes eluant. 95% NMR yield as a mixture of **8**:**9** in a ratio of 4:1.

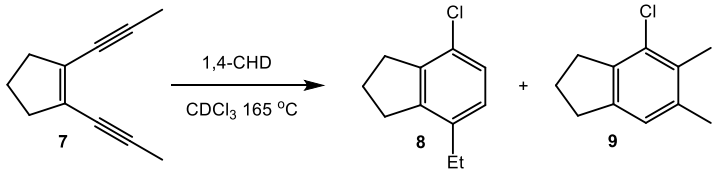

4-Chloro-7-ethyl-2,3-dihydro-1*H*-indene (**8**): Vinyl chloride **10** (5 mg, 28 μmol) was weighed into an oven-dried medium-walled NMR, which was allowed to cool to rt under vacuum. Then C_6D_6 (550 μL) was distilled into the tube on the high vacuum line. The resulting solution was frozen and the tube was flame sealed under vacuum. An initial ^{1}H NMR spectrum was collected of the solution and the tube was submerged in a constant temperature oil bath maintained at 165 °C for 16 h. The tube

was removed from the oil bath and allowed to cool to rt. A ^{1}H NMR spectrum was collected showing the complete conversion of **10**, and the observed formation of **8** without the formation of **9**. The tube was cracked open and the volatiles were removed under vacuum. The residue was then purified on a short plug of silica gel with hexanes eluant to give **8** as a colorless oil (4.7 mg, 26 μmol, 93% yield). (**7**) ^{1}H NMR (500 MHz, $CDCl_3$) δ 1.18 (t, $^{3}J_{HH}$ = 7.6 Hz, 3H), 2.09 (p, $^{3}J_{HH}$ = 7.4 Hz, 2H), 2.56 (q, $^{3}J_{HH}$ = 7.6 Hz, 2H), 2.92 (t, $^{3}J_{HH}$ = 7.4 Hz, 2H), 2.97 (t, $^{3}J_{HH}$ = 7.4 Hz, 2H), 6.92 (d, $^{3}J_{HH}$ = 8.1 Hz, 1H), 7.08 (d, $^{3}J_{HH}$ = 8.1 Hz, 1H). ^{13}C NMR (125 MHz, $CDCl_3$) δ 14.5, 24.2, 26.2, 32.1, 32.6, 126.5, 127.0, 128.0, 138.4, 142.1, 144.4. HRMS (EI): Calcd for ($C_{11}H_{13}Cl$): 180.0706, found 180.0704.

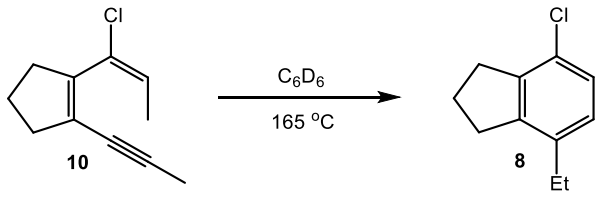

4-Chloro-5,6-dimethyl-2,3-dihydro-1*H*-indene (**9**): Vinyl chloride **10** (4 mg, 22 μmol) was dissolved DCM (2 mL) and the resulting solution was sparged with argon for 10 mins and then the solution was added to a vial charged with $[CpRu(MeCN)_3]PF_6$ (9.5 mg, 21 μmol) under argon. The resulting solution was allowed to react for 1 h at rt and then the solution was concentrated under vacuum to approximately 0.5 mL. Et_2O (10 mL) was added to the solution to precipitate **12** and the suspension was filter thru a short plug of Celite, which was rinsed with Et_2O (3 x 1 mL). The Celite was rinsed with acetone (3 x 1 mL) into a fresh vial, and the

volatiles were removed under vacuum. The resulting solids were added to a J. Young tube and CD_3CN (750 μL) was distilled into the tube on the high vacuum line. The solution was photolyzed in a Rayonett photo-reactor for 16 h, until **12** was completely consumed. Then the solution was poured into Et_2O (6 mL) and the resulting solution was passed through a short plug of Celite. The volatiles were removed under vacuum and the resulting residue was purified on a silica gel plug with hexanes eluant to give **9** as a colorless oil (3.6 mg, 20 μmol, 90% yield over 2 steps). (**9**) ^{1}H NMR (500 MHz, $CDCl_3$) δ 2.06 (p, $^3J_{HH}$ = 7.3 Hz, 2H), 2.27 (s, 3H), 2.29 (s, 3H) 2.91 (t, $^3J_{HH}$ = 7.3 Hz, 2H), 2.93 (t, $^3J_{HH}$ = 7.3 Hz, 2H), 6.93 (s, 1H). ^{13}C NMR (125 MHz, $CDCl_3$) δ 16.1, 21.1, 24.8, 33.0, 33.6, 124.0, 131.2, 131.7, 136.3, 140.3, 142.7 HRMS (EI): Calcd for ($C_{11}H_{13}Cl$): 180.0706, found 180.0704.

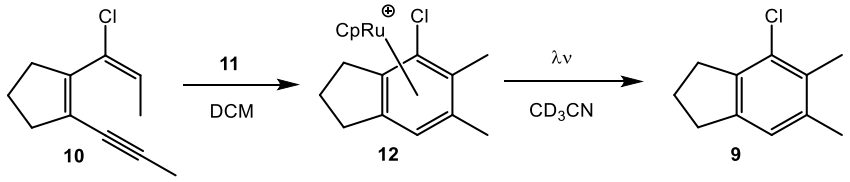

Thermal Reaction of 7 with 1,4-CHD and $CHBr_3$ in C_6D_6: Enediyne **7** (8.2 mg, 57 μmol, 1 eq), $CHBr_3$ (5 μL, 58 μmol, 1 eq) and 1,4-CHD (6 μL, 64 μmol, 1.1 eq) were weighed into an oven-dried medium-walled NMR tube, which was cooled to rt under vacuum. Then C_6D_6 (550 μL) was distilled into the tube on the high vacuum line and the tube was flame sealed under vacuum. An initial ^{1}H NMR spectrum was collected and then the tube was submerged in a constant temperature oil bath maintained at 165 °C for 19 h. The tube was then removed from the oil bath and allowed to cool to rt. A

^{1}H NMR spectrum collected of the reaction mixture in the sealed tube, showed complete consumption of **7** along with numerous new product peaks. An HMQC spectrum was collected on the reaction mixture with cross-peaks at ^{1}H δ 3.88 ppm and ^{13}C δ 19.24 ppm; which is consistent with the formation of CH_2Br_2. The tube was then cracked open and the reaction mixture was purified on a silica gel plug with hexanes eluant to give a colorless oil (8 mg, 37 μmol, 65% yield) of a 2.3:1 mixture of **13**:**14** as determined by ^{1}H NMR spectroscopy.

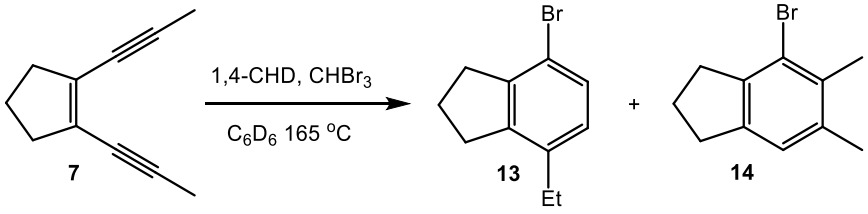

4-Bromo-7-ethyl-2,3-dihydro-1*H*-indene (**13**): Vinyl bromide **15** (10 mg, 44 μmol) was weighed into an oven-dried medium-walled NMR tube, which had been allowed to cool to rt under vacuum. Then C_6D_6 (550 μL) was distilled into the tube on the high vacuum line. The resulting solution was frozen and the tube was flame sealed under vacuum. An initial ^{1}H NMR spectrum was collected of the solution and the tube was submerged in a constant temperature oil bath maintained at 165 °C for 16 h. The tube was removed from the oil bath and allowed to cool to rt. A ^{1}H NMR spectrum was collected showing the complete conversion of **15**, and the observed formation of **13** with an approximate 10% formation of **14**. The tube was cracked open and the volatiles were removed under vacuum. The residue was absorbed on silica gel, which was loaded onto a short plug of silica and the reaction mixture separated with hexanes

eluant to give **13** as a colorless oil (8.9 mg, 39 μmol, 89% yield). (**13**) ^{1}H NMR (500 MHz, $CDCl_3$) δ 1.18 (t, $^{3}J_{HH}$ = 7.5 Hz, 3H), 2.09 (p, $^{3}J_{HH}$ = 7.6 Hz, 2H), 2.55 (q, $^{3}J_{HH}$ = 7.5 Hz, 2H), 2.96 (t, $^{3}J_{HH}$ = 7.6 Hz, 2H), 2.96 (t, $^{3}J_{HH}$ = 7.6 Hz, 2H), 6.86 (d, $^{3}J_{HH}$ = 7.8 Hz, 1H), 7.24 (d, $^{3}J_{HH}$ = 7.8 Hz, 1H). ^{13}C NMR (125 MHz, $CDCl_3$) δ 14.4, 24.0, 26.3, 32.4, 34.7, 117.0, 127.4, 129.5, 139.1, 144.2, 144.3. HRMS (EI): Calcd for ($C_{11}H_{13}Br$): 224.0201, found 224.0201.

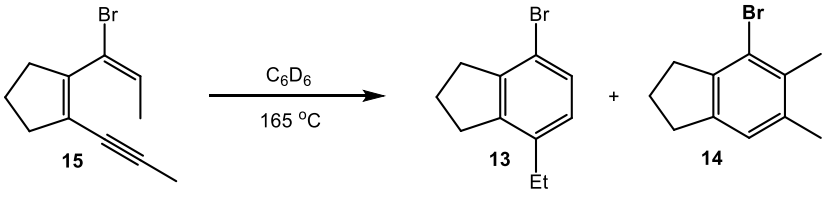

4-Bromo-5,6-dimethyl-2,3-dihydro-1*H*-indene (**14**): Vinyl bromide **15** (8 mg, 36 μmol) was dissolved in DCM (2 mL) and the resulting solution was sparged with argon for 10 mins and then the solution was added to a vial charged with $CpRu(MeCN)_3PF_6$ (9.5 mg, 21 μmol) under argon. The resulting solution was allowed to react for 1 h at rt and then the solution was concentrated under vacuum to approximately 0.5 mL. Then Et_2O (10 mL) was added to the solution to precipitate **16** and the suspension was filter thru a short plug of Celite, which was rinsed with Et_2O (3 x 1 mL). The Celite was rinsed with acetone (3 x 1 mL) into a fresh vial and the volatiles were removed under vacuum. The resulting solids were added to a J. Young tube and CD_3CN (750 μL) was distilled into the tube on the high vacuum line. The solution was photolyzed in a Rayonett photo-reactor for 16 h, until **16** was completely consumed. Then the solution was poured into Et_2O (6 mL) and the resulting solution was passed through a short plug of Celite. The volatiles were

removed under vacuum and the resulting residue was absorbed on silica gel. The reaction mixture absorbed on silica gel was loaded onto a short silica plug and run through with hexanes eluant to give **14** as a colorless oil (4.7 mg, 20 μmol, 90% yield over 2 steps). (**14**) ^{1}H NMR (500 MHz, $CDCl_3$) δ 2.06 (p, $^{3}J_{HH}$ = 7.3 Hz, 2H), 2.29 (s, 3H), 2.33 (s, 3H) 2.93 (t, $^{3}J_{HH}$ = 7.3 Hz, 2H), 2.96 (t, $^{3}J_{HH}$ = 7.3 Hz, 2H), 6.95 (s, 1H). ^{13}C NMR (125 MHz, $CDCl_3$) δ 19.3, 21.5, 24.5, 34.0, 35.5, 123.2, 124.7, 133.4, 136.2, 142.5, 142.7. HRMS (EI): Calcd for ($C_{11}H_{13}Br$): 224.0201, found 224.0203.

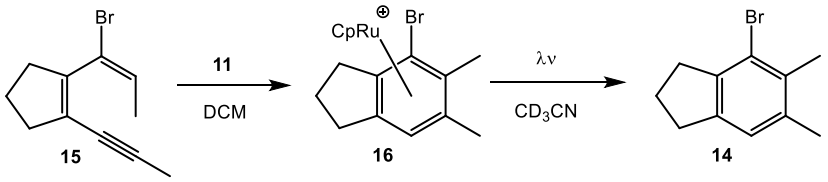

Thermal Reaction of 1,4-CHD in $CDCl_3$. 1,4-Cyclohexadiene (26.4 mg, 330 μmol) and $^{t}Bu_3$benzene (1mg, 4 μmol) were added to an oven-dried medium-walled NMR tube, which was cooled to rt under vacuum. Then, $CDCl_3$ (750 μL) was distilled into the tube on the high vacuum line. The tube was then flame sealed and an initial ^{1}H NMR spectrum was collected. Then the entire tube was submerged in a constant temperature oil bath maintained at 165 °C for 16 h and was then removed from the oil bath. The tube was allowed to cool to rt and a ^{1}H NMR spectrum was collected. The spectrum showed 55% conversion of starting 1,4-cyclohexadiene with formation of benzene, 95% yield of benzene based on conversion of 1,4-cyclohexadiene. In addition, a signal was observed at 5.26 ppm (t, J = 1.1 Hz) that integrated 1:6 with the benzene signal, which is consistent with $CHDCl_2$. A ^{13}C NMR spectrum was

collected on the reaction mixture which and showed a signal at 53.4 ppm (t, J = 27.3 Hz), again consistent with $CHDCl_2$. In addition, the ^1H NMR spectrum showed a broad signal at 1.42 ppm which integrates to 0.75:1 to the $CHDCl_2$. The chemical shift of this peak is consistent for HCl, with the broadening arising from ^1H coupling to ^{35}Cl & ^{37}Cl. To the best of our knowledge this is the first report of the ^1H NMR spectrum of HCl in a non-polar, non-oxygenated solvent. The ^1H NMR spectrum also showed small amounts of other aliphatic material, arising presumably from HCl addition to 1,4-cyclohexadiene.

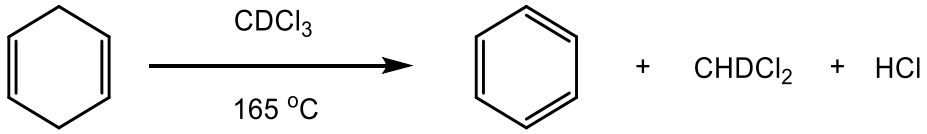

Thermal Reaction of 7 with 1,4-CHD and CHI_3 in C_6D_6: Enediyne **7** (7.4 mg, 51 μmol, 1 eq), CHI_3 (26 mg, 65 μmol, 1.3 eq) and 1,4-CHD (8μL, 84 μmol, 1.6 eq) were weighed into an oven-dried medium-walled NMR tube, which was cooled to rt under vacuum. Then C_6D_6 (550 μL) was distilled into the tube on the high vacuum line and the tube was flame sealed under vacuum. An initial ^1H NMR spectrum was collected and then the tube was submerged in a constant temperature oil bath maintained at 165 °C for 19 h. The tube was then removed from the oil bath and allowed to cool to rt. A ^1H NMR spectrum collected of the reaction mixture in the sealed tube, showed complete consumption of **6** along with numerous new product peaks. The tube was then cracked open and the reaction mixture was poured into a vial. The mixture was diluted with Et_2O and washed with $Na_2S_2O_3$ (3 x 2 mL) / H_2O

(2 mL) / brine (2 mL). The organic phase was then dried over $MgSO_4$ and the volatiles were removed under vacuum. The residue was purified on a silica plug with hexanes eluant to give **17** as a colorless oil (6 mg, 41 μmol, 81% yield). The product exhibited spectroscopic properties identical to those reported in literature.

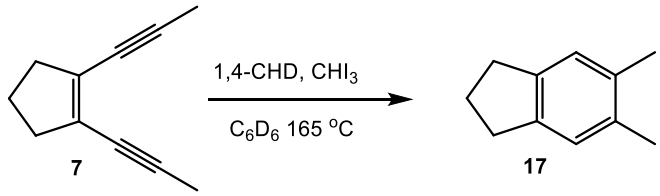

Reaction of 7 with 1,4-CHD and CHI_3 in C_6D_6 at 100 °C: Enediyne **7** (7.4 mg, 51 μmol, 1 eq), CHI_3 (26 mg, 65 μmol, 1.3 eq) and 1,4-CHD (8 μL, 84 μmol, 1.6 eq) were weighed into an oven-dried medium-walled NMR tube, which was cooled to rt under vacuum. Then C_6D_6 (550 μL) was distilled into the tube on the high vacuum line and the tube was flame sealed under vacuum. An initial ^{1}H NMR spectrum was collected and then the tube was submerged in a constant temperature oil bath maintained at 100 °C for 24 h. The tube was then removed from the oil bath and allowed to cool to rt. A ^{1}H NMR spectrum collected of the reaction mixture in the sealed tube, showed complete consumption of **7** along with formation of **18**. The tube was then placed in a constant temperature oil-bath maintained at 165 °C for 3 h. The tube was removed and allowed to cool to rt. A ^{1}H NMR spectrum showed complete consumption of **18** and the formation of **17**. (**18**) ^{1}H NMR (C_6D_6, 500 MHz) δ 1.54 (p, $^3J_{HH}$ = 7.4 Hz, 2H); 1.55 (s, 3H); 1.57 (d, $^3J_{HH}$ = 7.0 Hz, 3H); 2.33 (tt, $^3J_{HH}$ = 7.6 Hz, $^4J_{HH}$ = 2.4 Hz, 2H); 2.56 (bt, $^3J_{HH}$ = 7.6 Hz, 2H); 6.26 (q, $^3J_{HH}$ = 7.0 Hz, 1H). ^{13}C

NMR (C_6D_6, 125 MHz) δ 5.3, 19.3, 23.2, 38.0, 39.1, 78.2, 94.0, 94.6, 125.5, 138.9, 146.9.

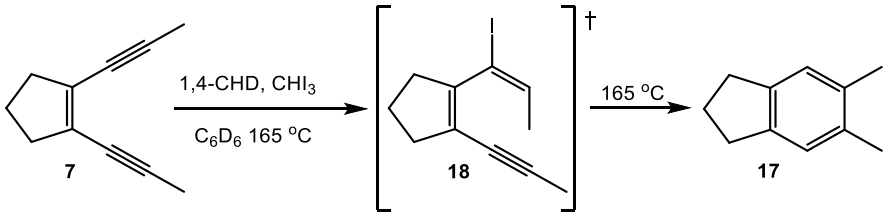

Reaction of 7 with 1,4-CHD in C_6D_6 at 165 °C: Enediyne **7** (6.3 mg, 44 μmol, 1 eq) and 1,4-CHD (8μL, 84 μmol, 2 eq) were weighed into an oven-dried medium-walled NMR tube, which was cooled to rt under vacuum. Then C_6D_6 (550 μL) was distilled into the tube on the high vacuum line and the tube was flame sealed under vacuum. An initial ^{1}H NMR spectrum was collected and then the tube was submerged in a constant temperature oil bath maintained at 165 °C. A ^{1}H NMR spectrum of the reaction collected periodically to monitor the progess of the reaction. The % yield of **17** was based on the % convserion of **7**. The reaction was determined to have a half-life of 165 h.

Time (h)	% Conversion of **7**	% Yield of **17**
48	35	44
192	79	40
260	87	42
450	99.5	40

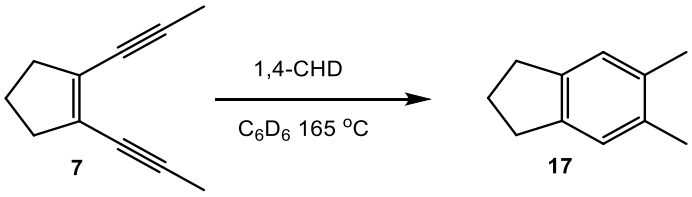

Thermal Reaction of 7 with 1,4-CHD and CHF_3 in C_6D_6: An oven-dried J-Young tube was cooled to rt under vacuum and was then closed. The gas manifold was purged with argon and then purged with CHF_3. The evacuated J-Young tube was opened to the gas manifold for several minutes and then closed, giving approximately 3.3 mL of CHF_3 gas (120 μmol). Then **7** (6.3 mg, 44 μmol, 1 eq) and 1,4-CHD (8 μL, 84 μmol, 2 eq) were weighed into an oven-dried heavy-walled NMR tube, which was cooled to rt under vacuum. C_6D_6 (550 μL) was distilled into the tube on the high vacuum line and the solution was frozen with N_2 (liq). The tube containing CHF_3 was opened to the manifold and allowed to freeze in the tube containing **7**. The tube was then flame sealed and ^1H and ^{19}F NMR spectra were collected of the mixture. The ^1H NMR resonance of CHF_3 overlapped with a resonance of 1,4-CHD, but showed a clean doublet resonance at δ-78.5 (J = 80 Hz) by ^{19}F NMR. The tube was submerged in a constant temperature oil bath maintained at 165 °C. After 48 h, a ^1H NMR spectrum showed approximately 40% conversion of **7** with a 30% yield of **17**-consistent with the rate observed for the thermolysis of **7** without added haloform and a ^{19}F NMR spectrum showed only the resonance of CHF_3 at δ-78.5.

5-5.3 ^{1}H and ^{13}C NMR Spectroscopic Data

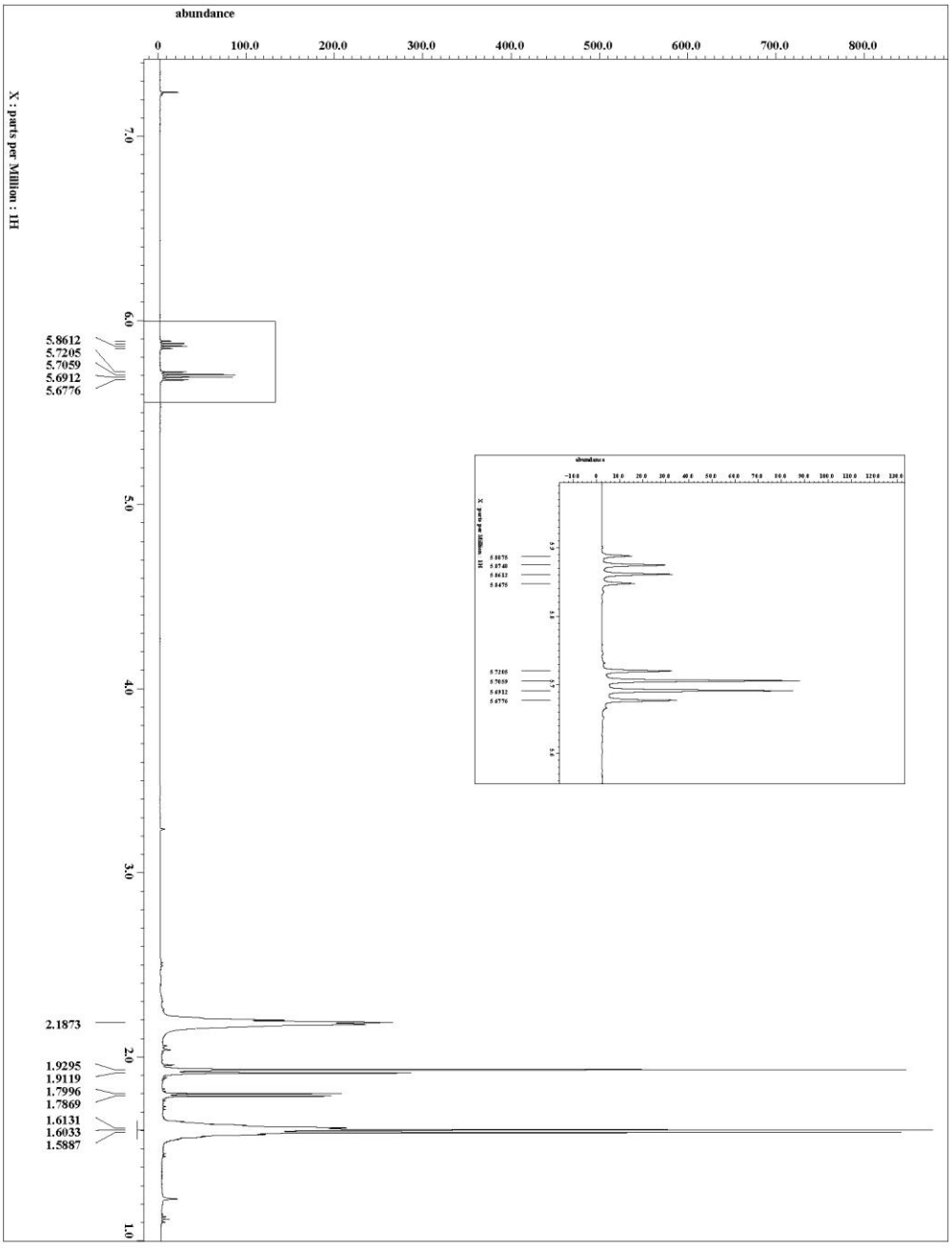

Figure 5-2. 5 3:1 *E*:*Z* ^{1}H NMR spectrum ($CDCl_3$, 500 MHz).

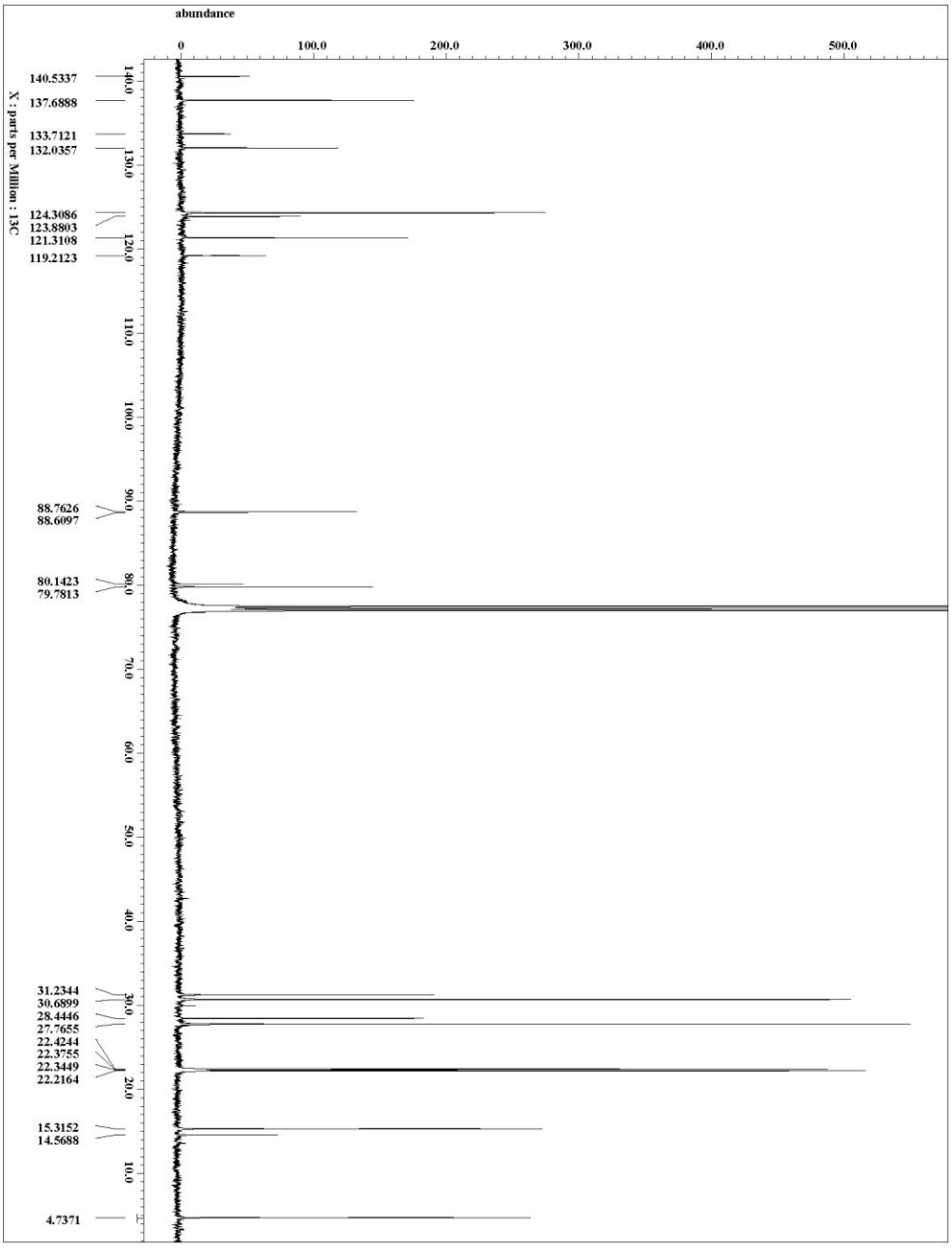

Figure 5-3. 5 3:1 *E*:*Z* ^{13}C NMR spectrum ($CDCl_3$, 125 MHz).

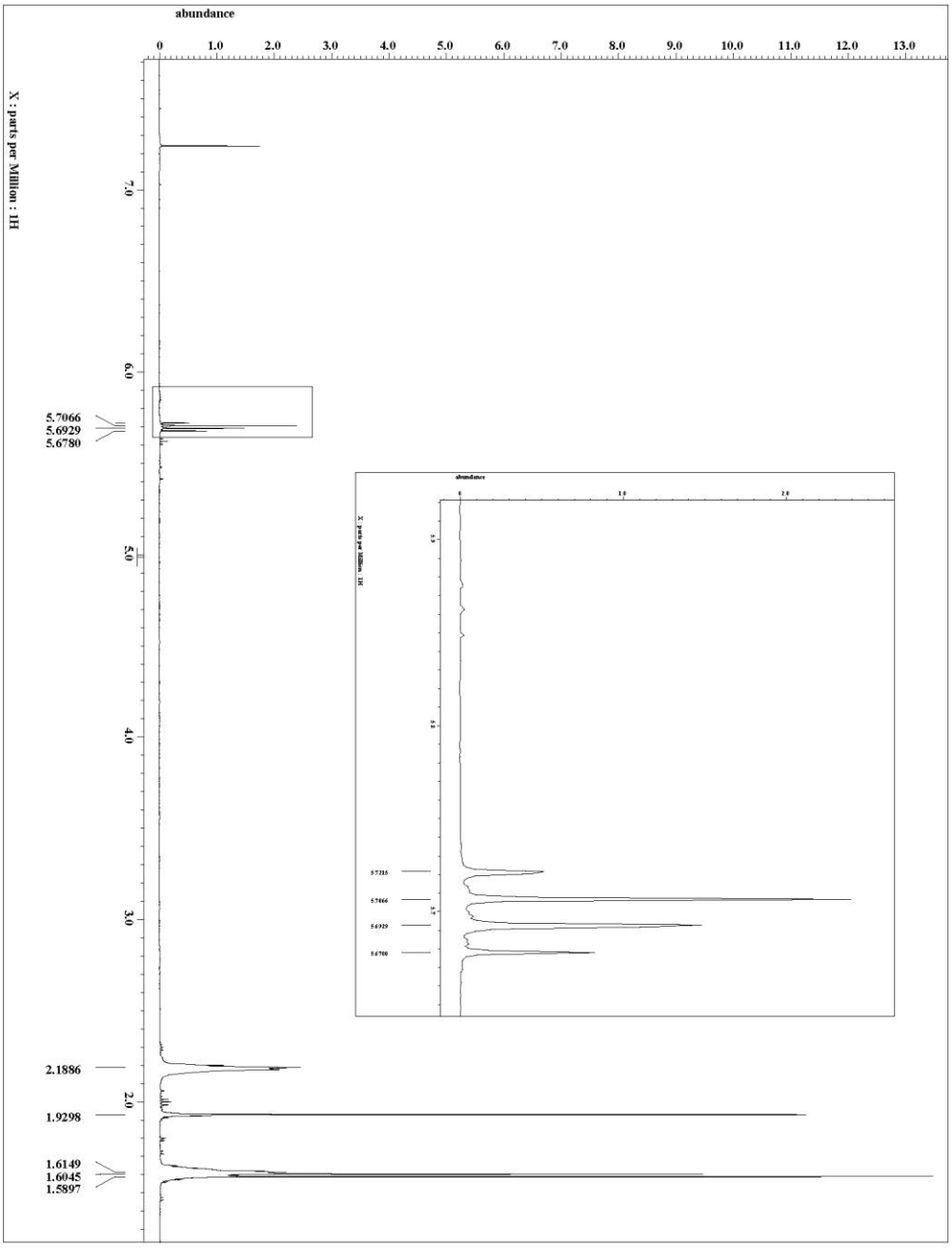

Figure 5-4. 5*E* ^{1}H NMR spectrum ($CDCl_3$, 500 MHz).

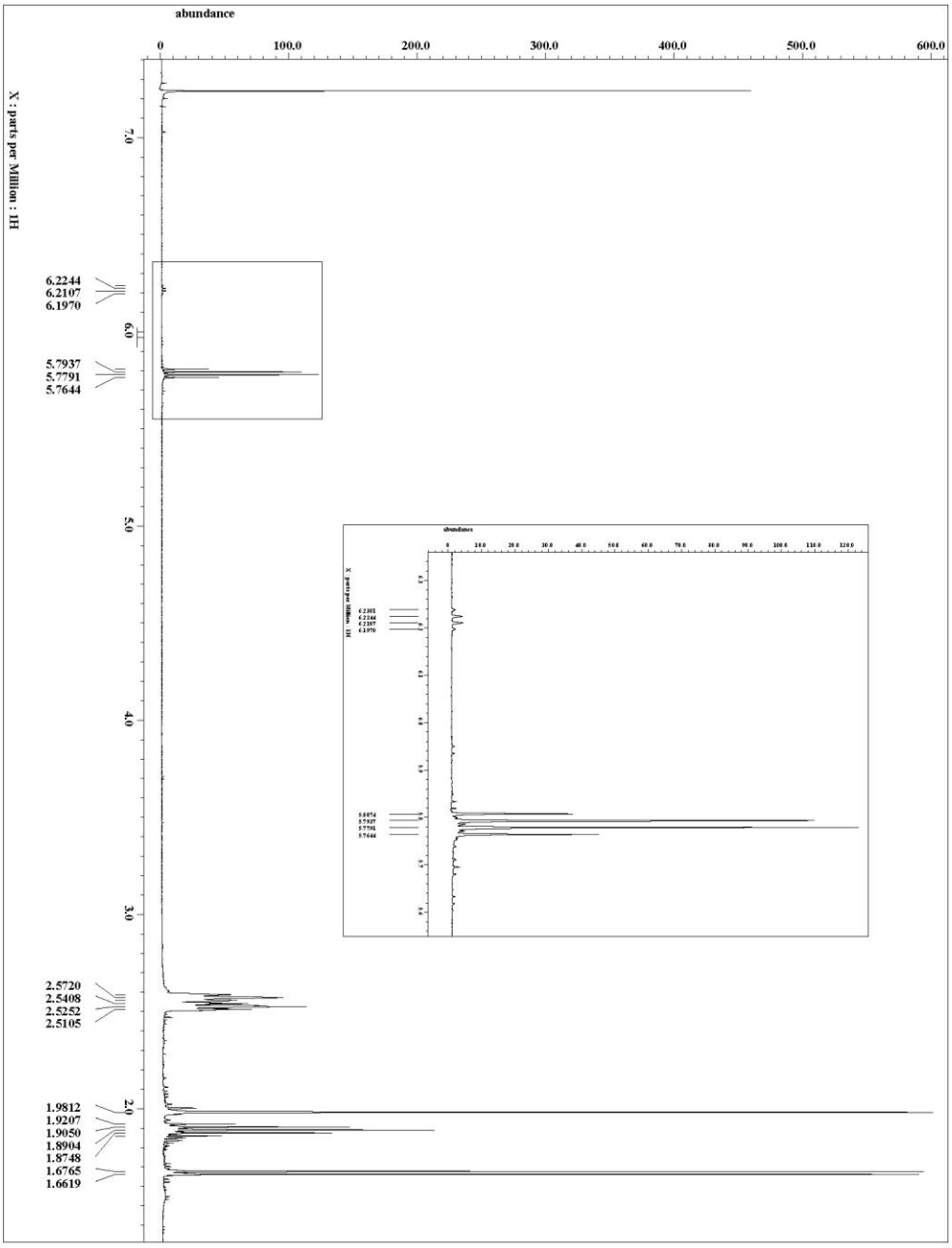

Figure 5-5. 10 ^{1}H NMR spectrum ($CDCl_3$, 500 MHz).

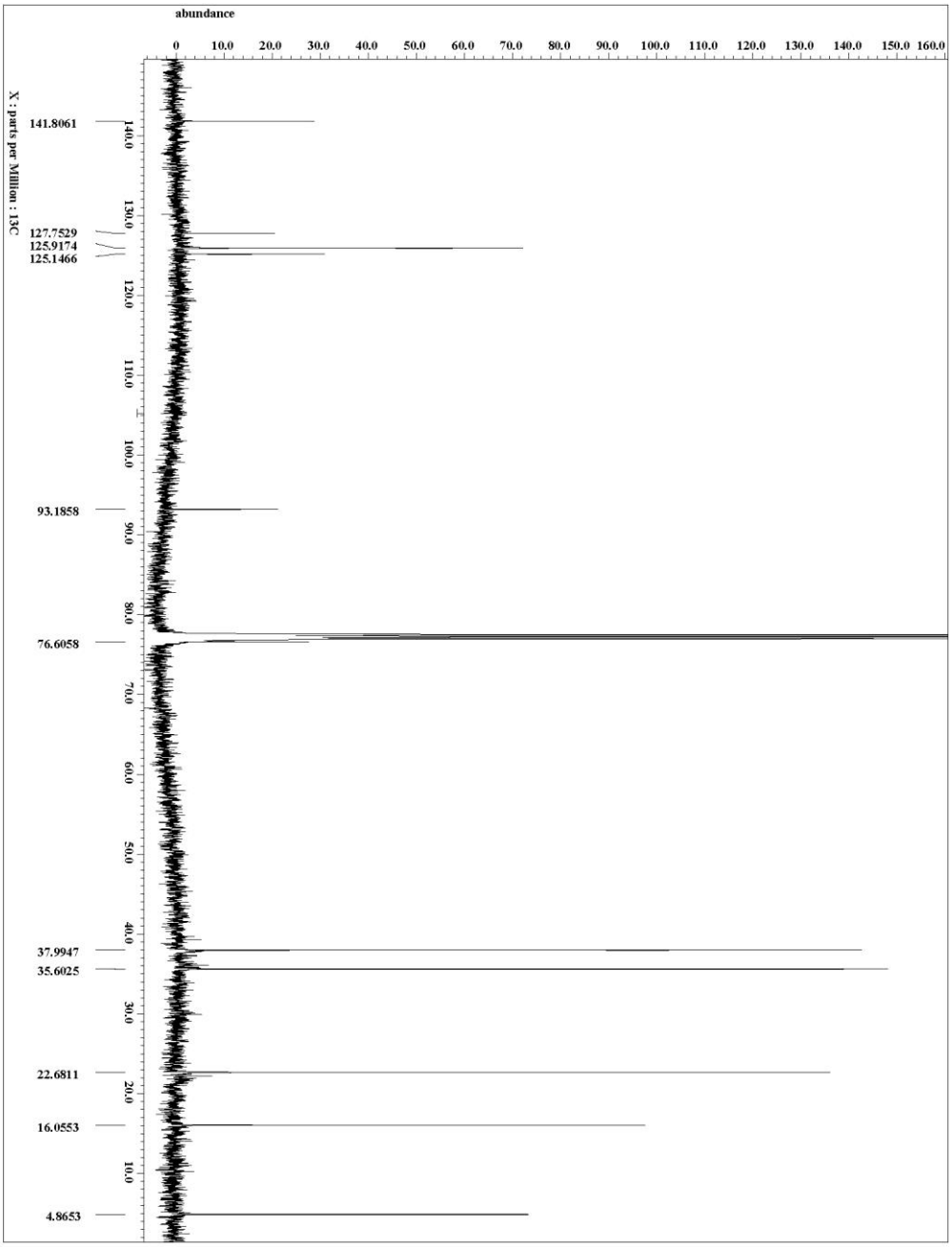

Figure 5-6. 10 ^{13}C NMR spectrum ($CDCl_3$, 125 MHz).

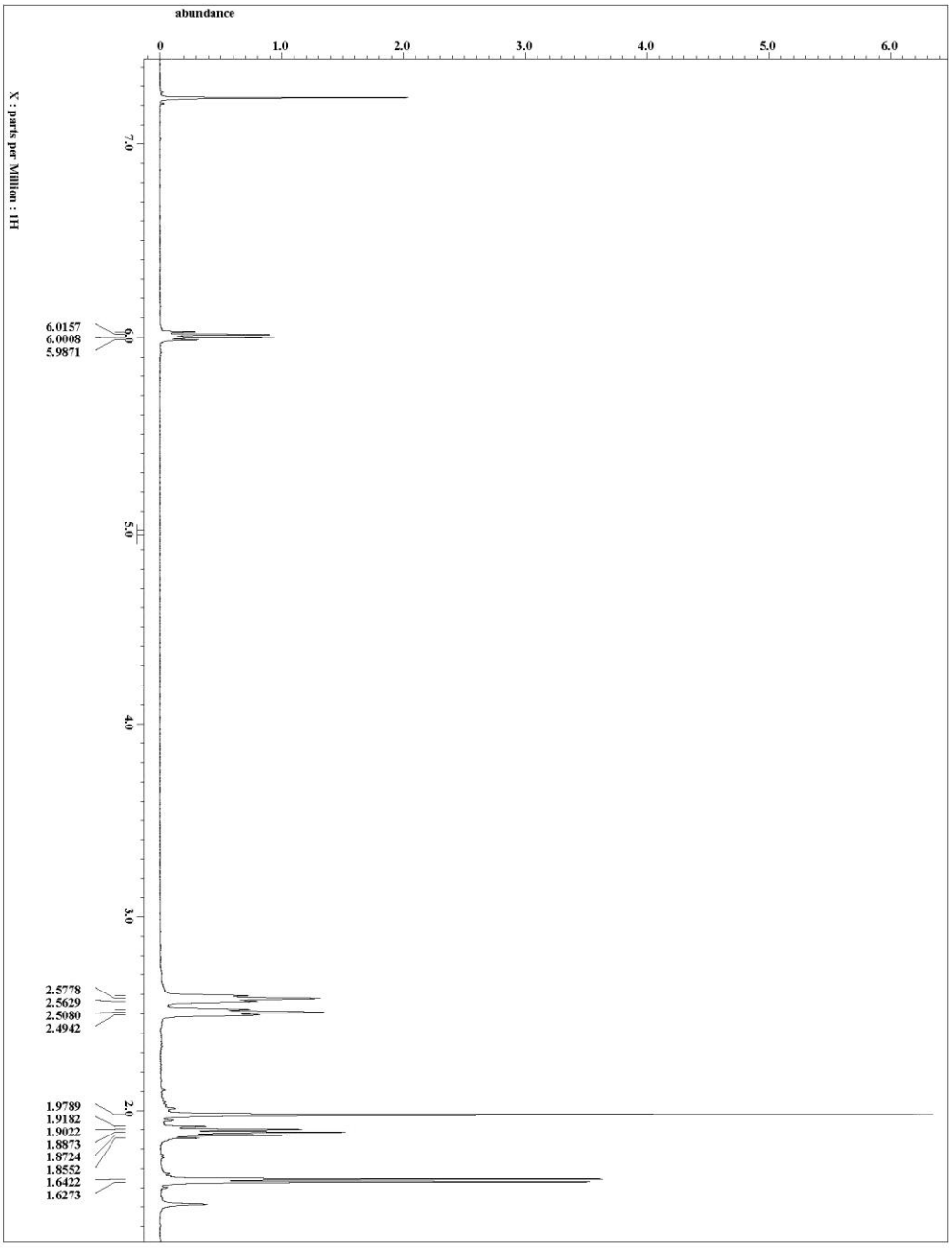

Figure 5-7. 15 ^{1}H NMR spectrum ($CDCl_3$, 500 MHz).

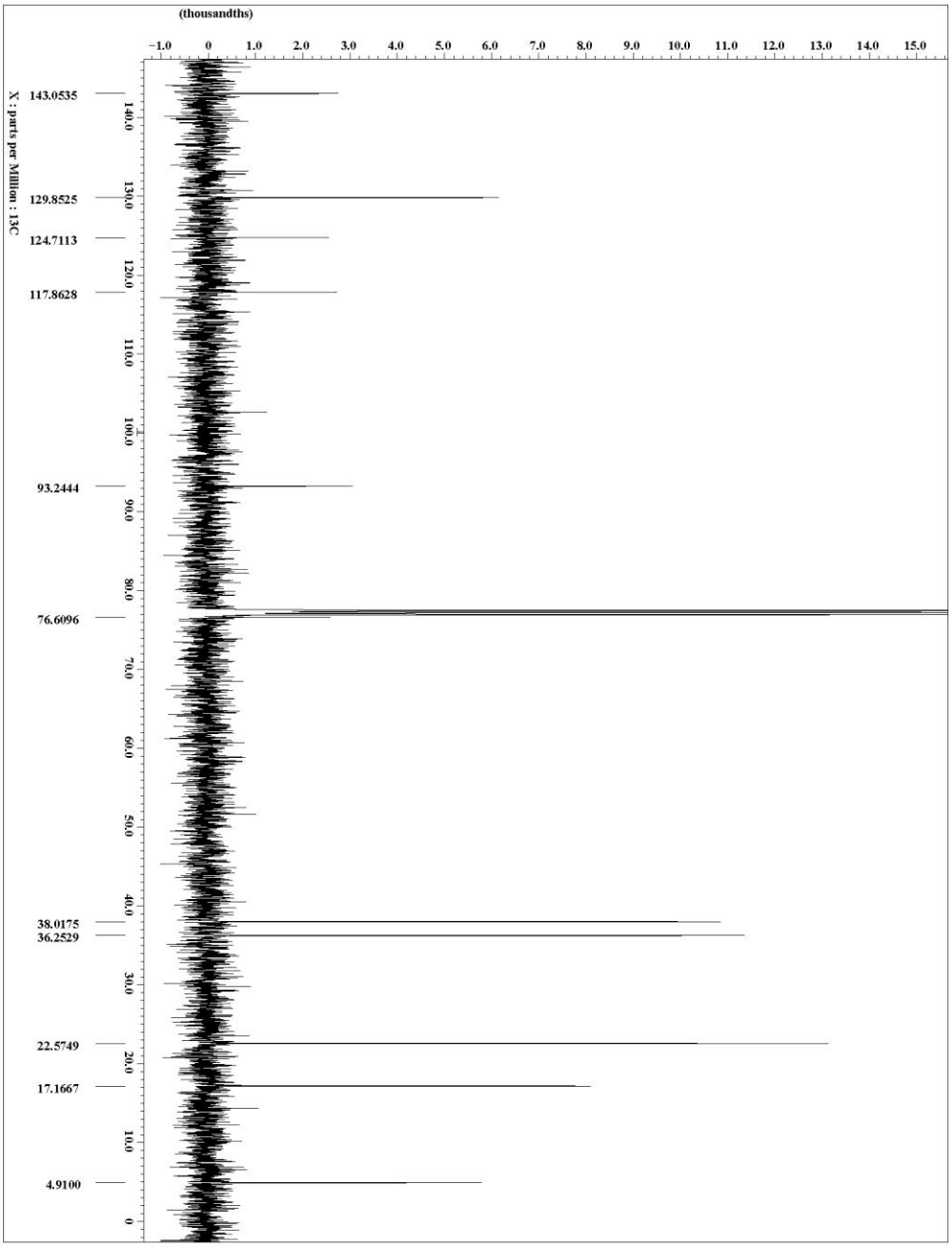

Figure 5-8. 15 ^{13}C NMR spectrum ($CDCl_3$, 125 MHz).

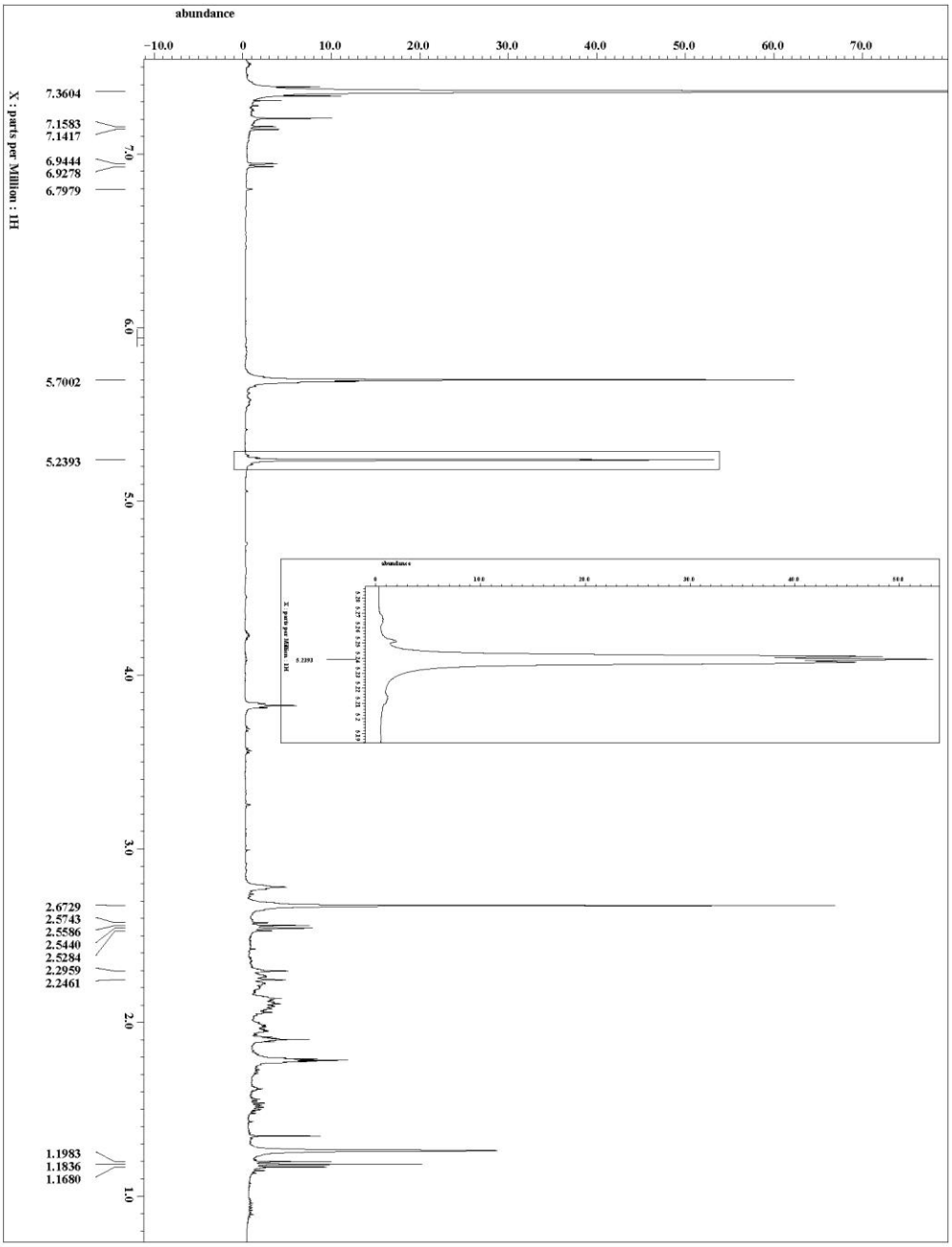

Figure 5-9. Reaction of **1** with 1,4-CHD in $CDCl_3$ at 165 °C ^1H NMR spectrum ($CDCl_3$, 500 MHz).

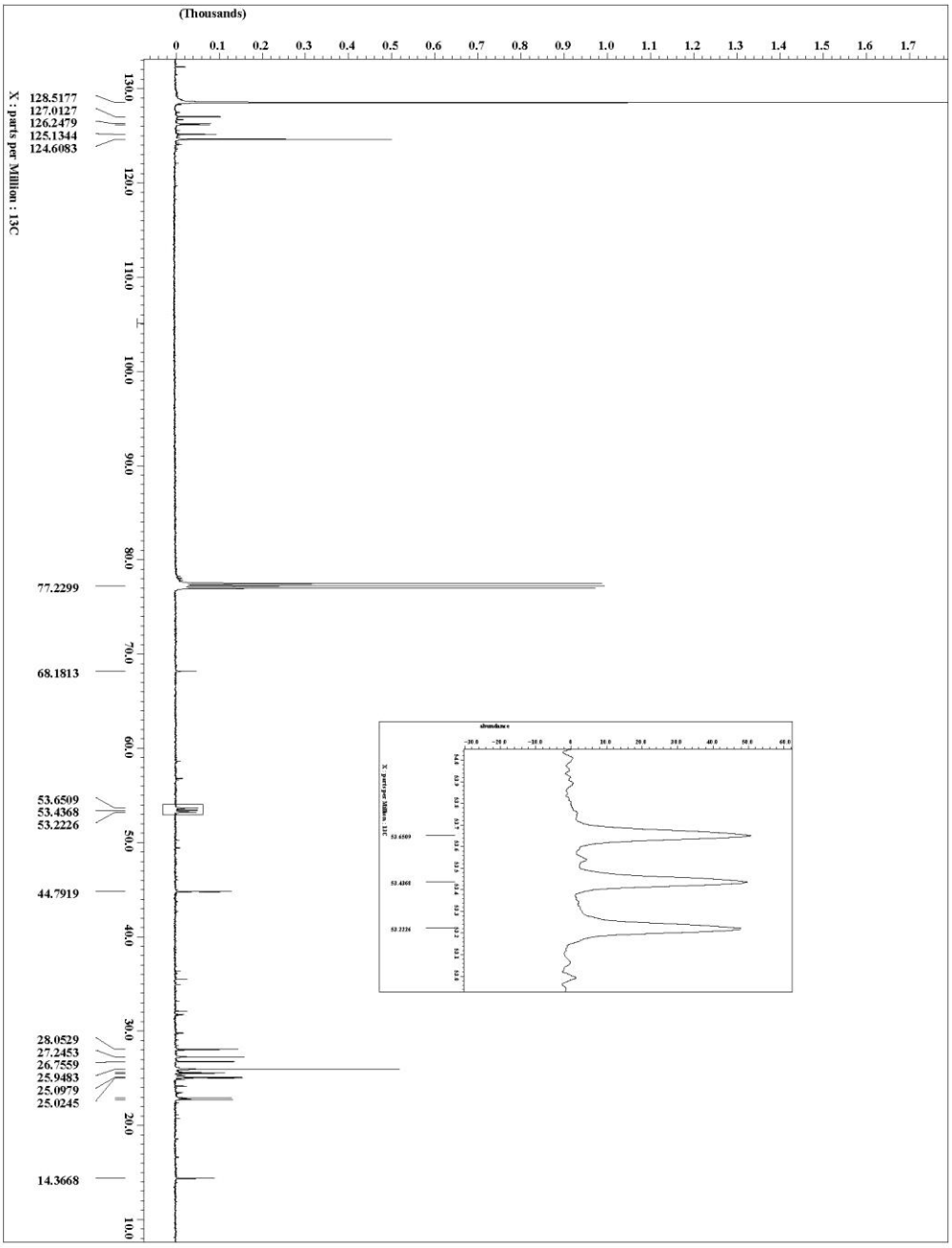

Figure 5-10. Reaction of **1** with 1,4-CHD in $CDCl_3$ at 165 °C ^{13}C NMR spectrum ($CDCl_3$, 125 MHz).

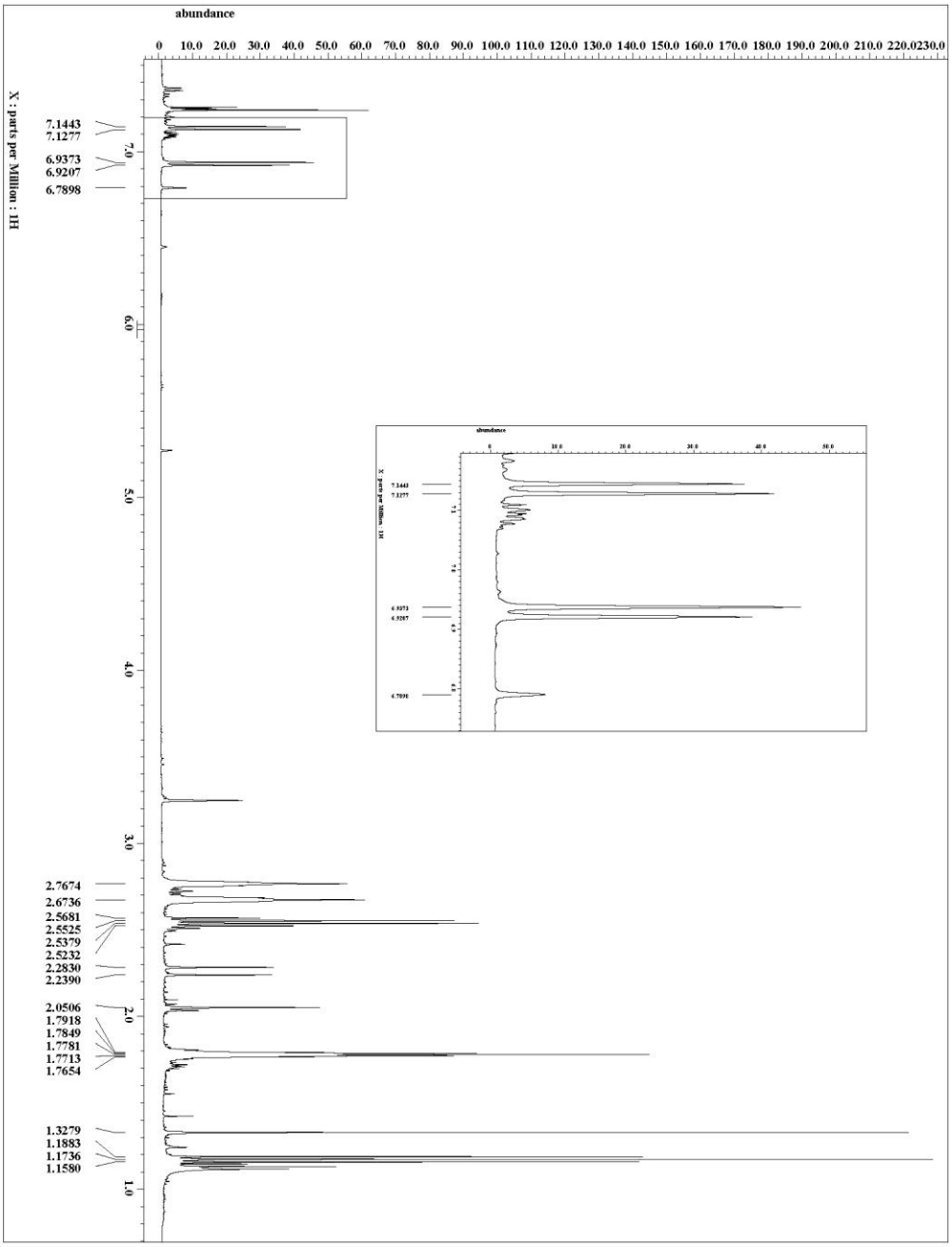

Figure 5-11. Cyclization of **5** (3:1 *E*:*Z*) in $CDCl_3$ at 165 °C ^1H NMR spectrum ($CDCl_3$, 500 MHz).

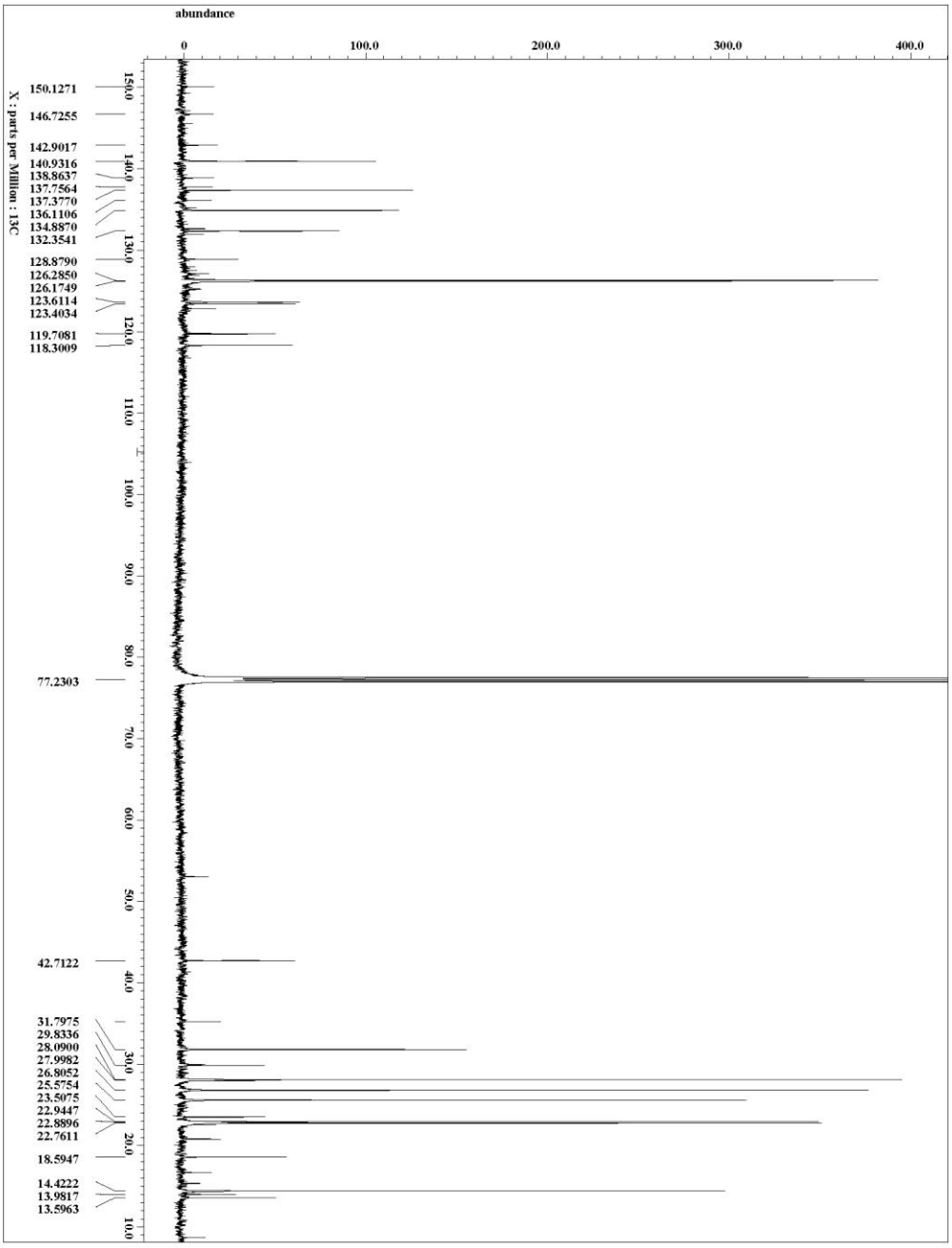

Figure 5-12. Cyclization of **5** (3:1 *E*:*Z*) in $CDCl_3$ at 165 °C ^{13}C NMR spectrum ($CDCl_3$, 125 MHz).

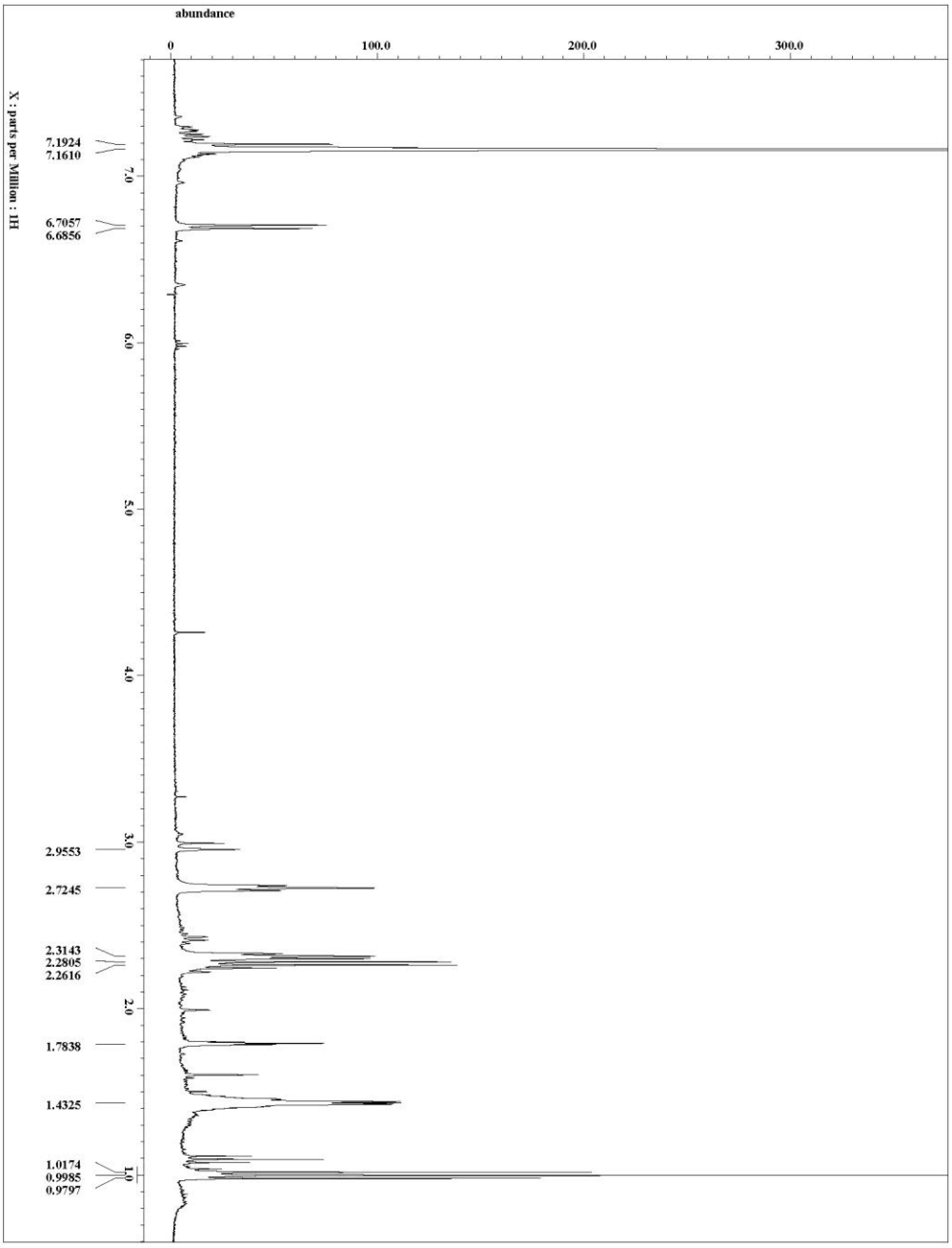

Figure 5-13. Cyclization of **5** (3:1 *E*:*Z*) in C_6D_6 at 165 °C ^{1}H NMR spectrum (C_6D_6, 500 MHz).

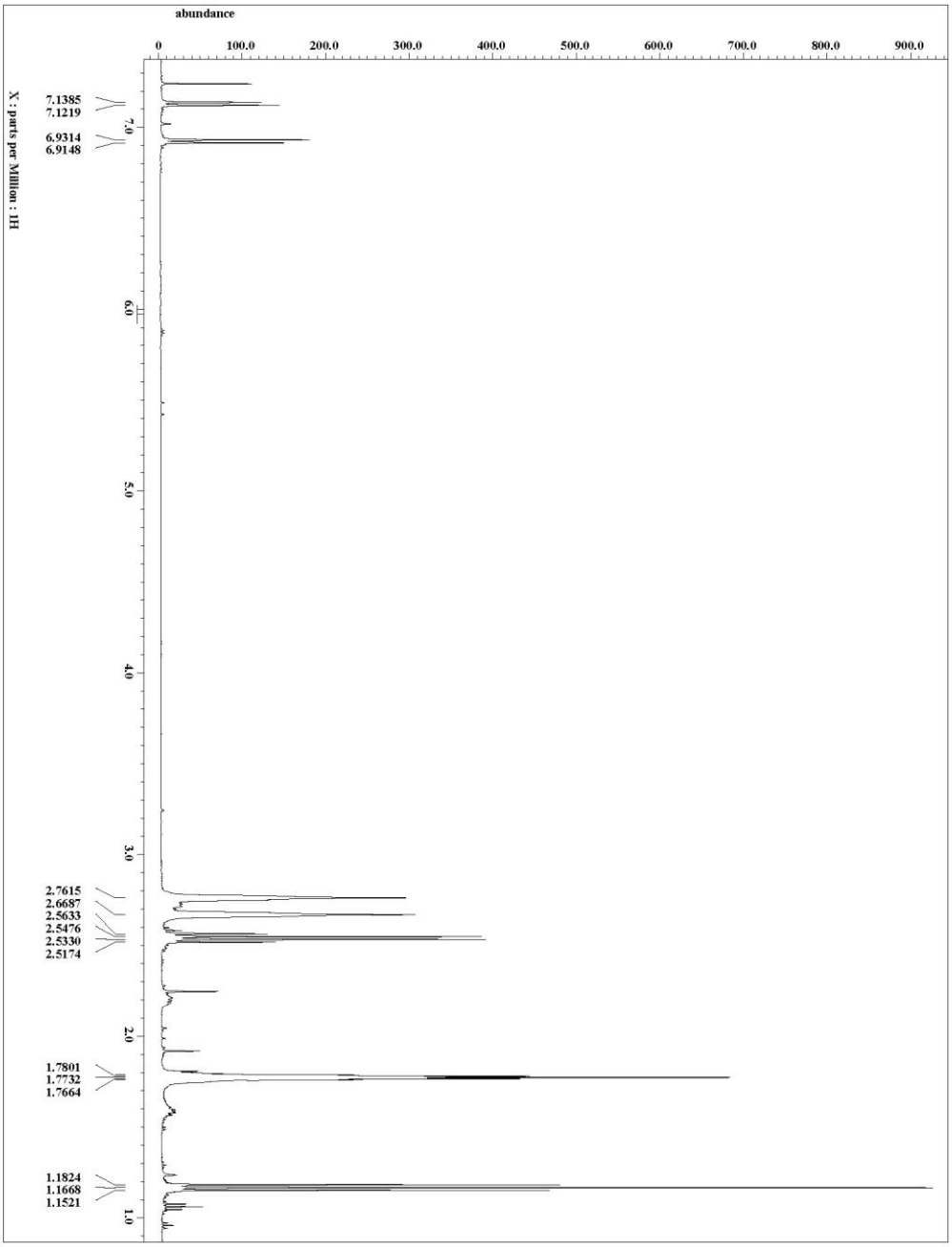

Figure 5-14. 3 from **5-*E*** in C_6D_6 ^1H NMR spectrum ($CDCl_3$, 500 MHz).

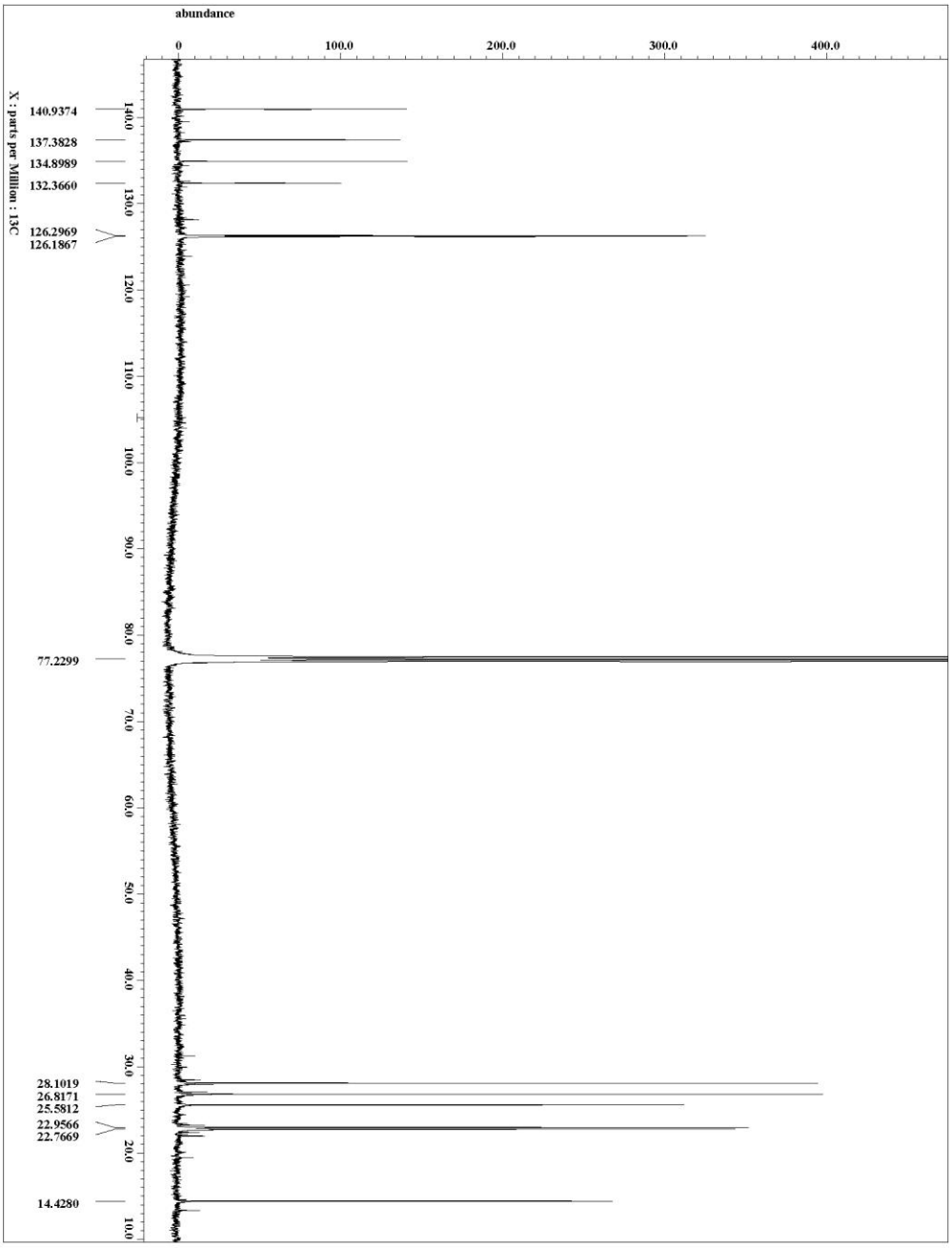

Figure 5-15. 3 from **5-*E*** in C_6D_6 ^{13}C NMR spectrum ($CDCl_3$, 125 MHz).

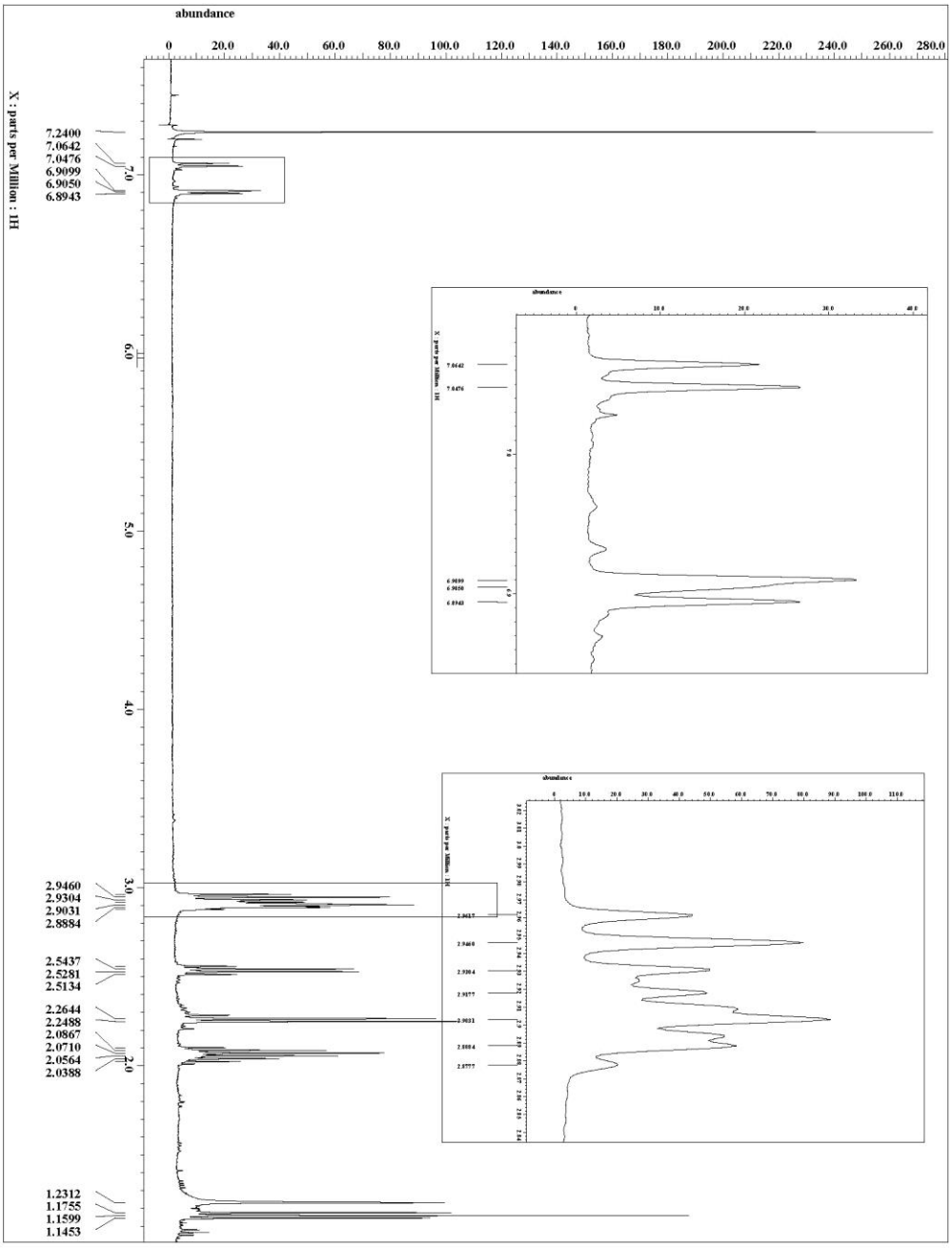

Figure 5-16. Reaction of **7** with 1,4-CHD in $CDCl_3$ at 165 °C ^1H NMR spectrum ($CDCl_3$, 500 MHz).

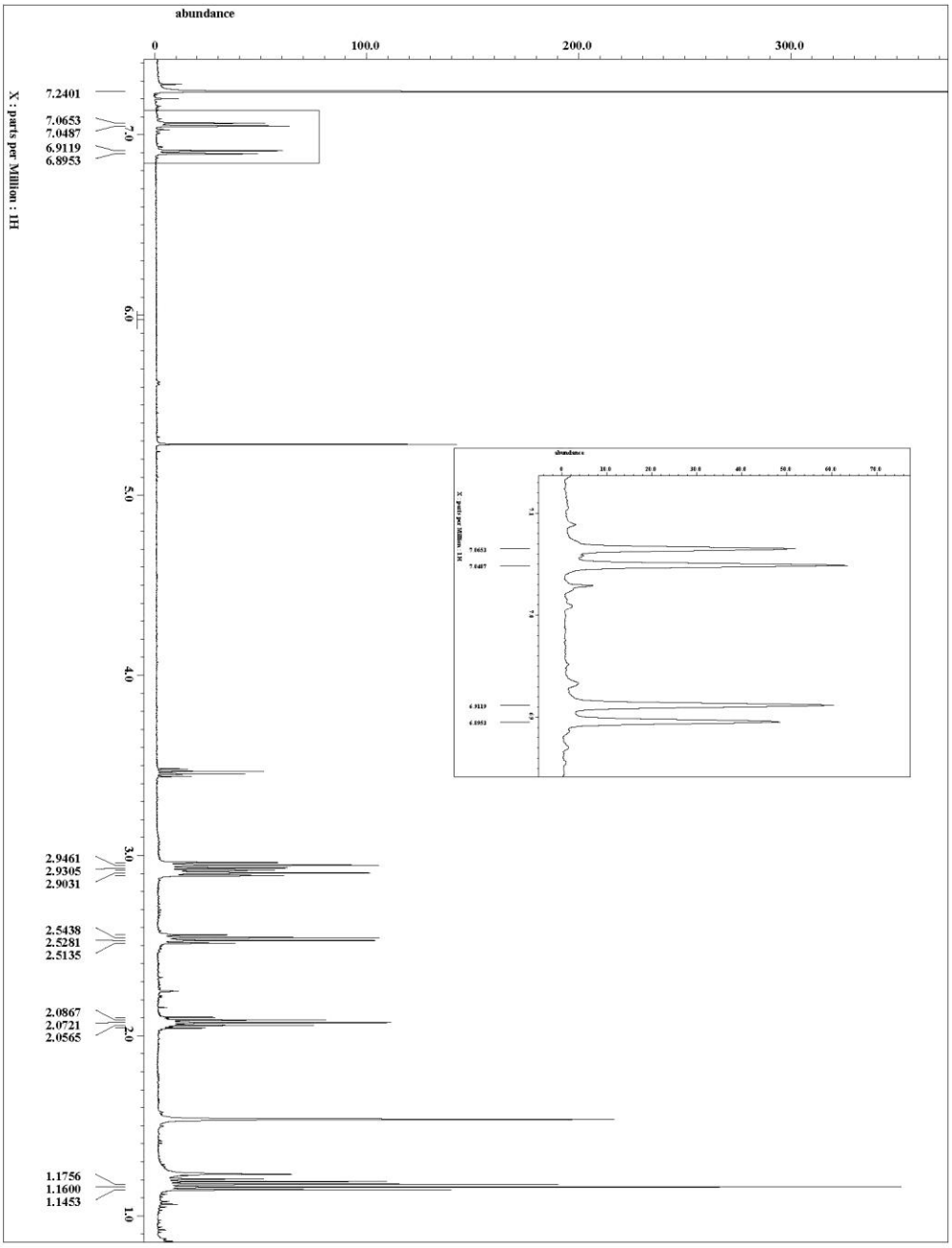

Figure 5-17. 8 ^{1}H NMR spectrum ($CDCl_3$, 500 MHz).

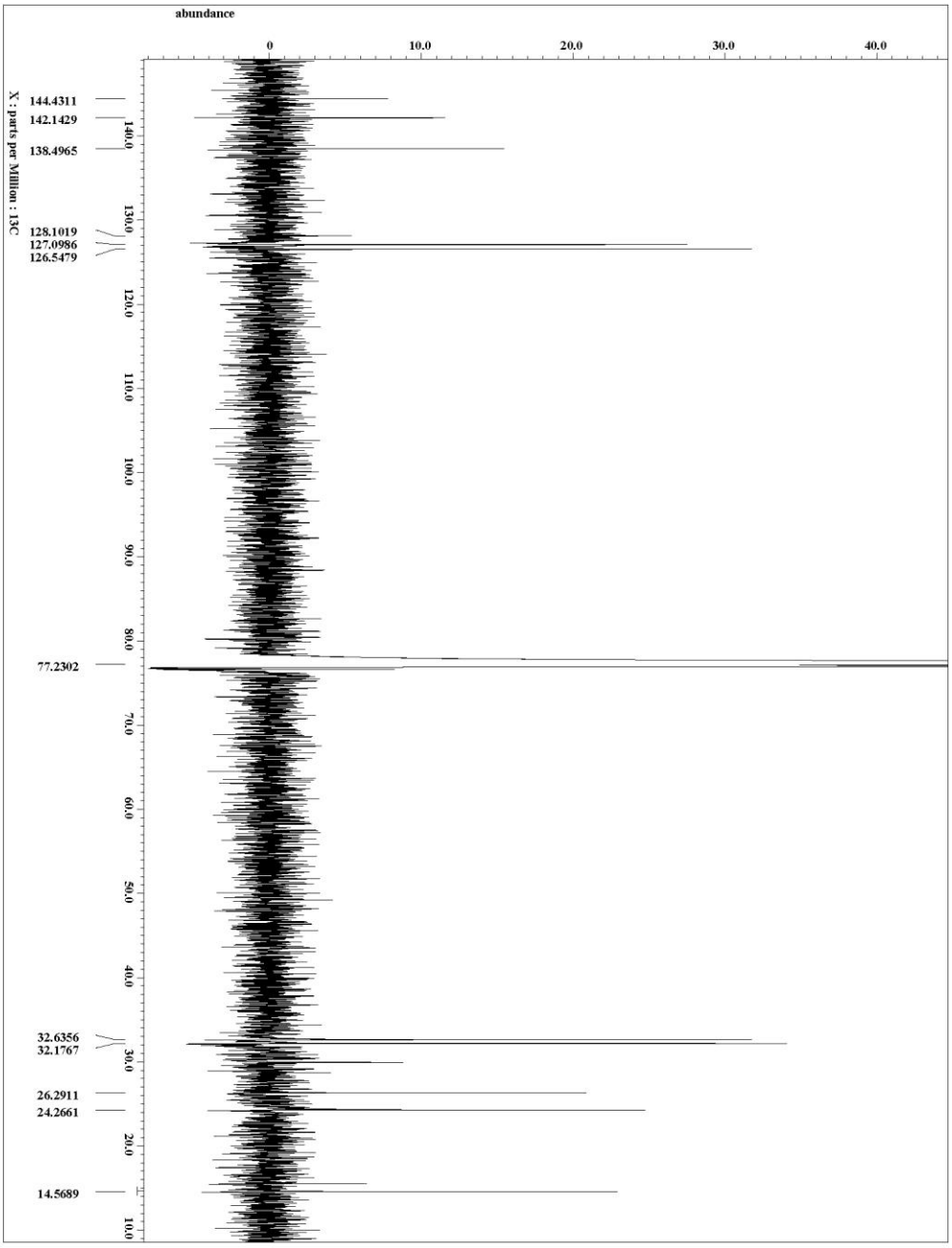

Figure 5-18. 8 ^{13}C NMR spectrum ($CDCl_3$, 125 MHz).

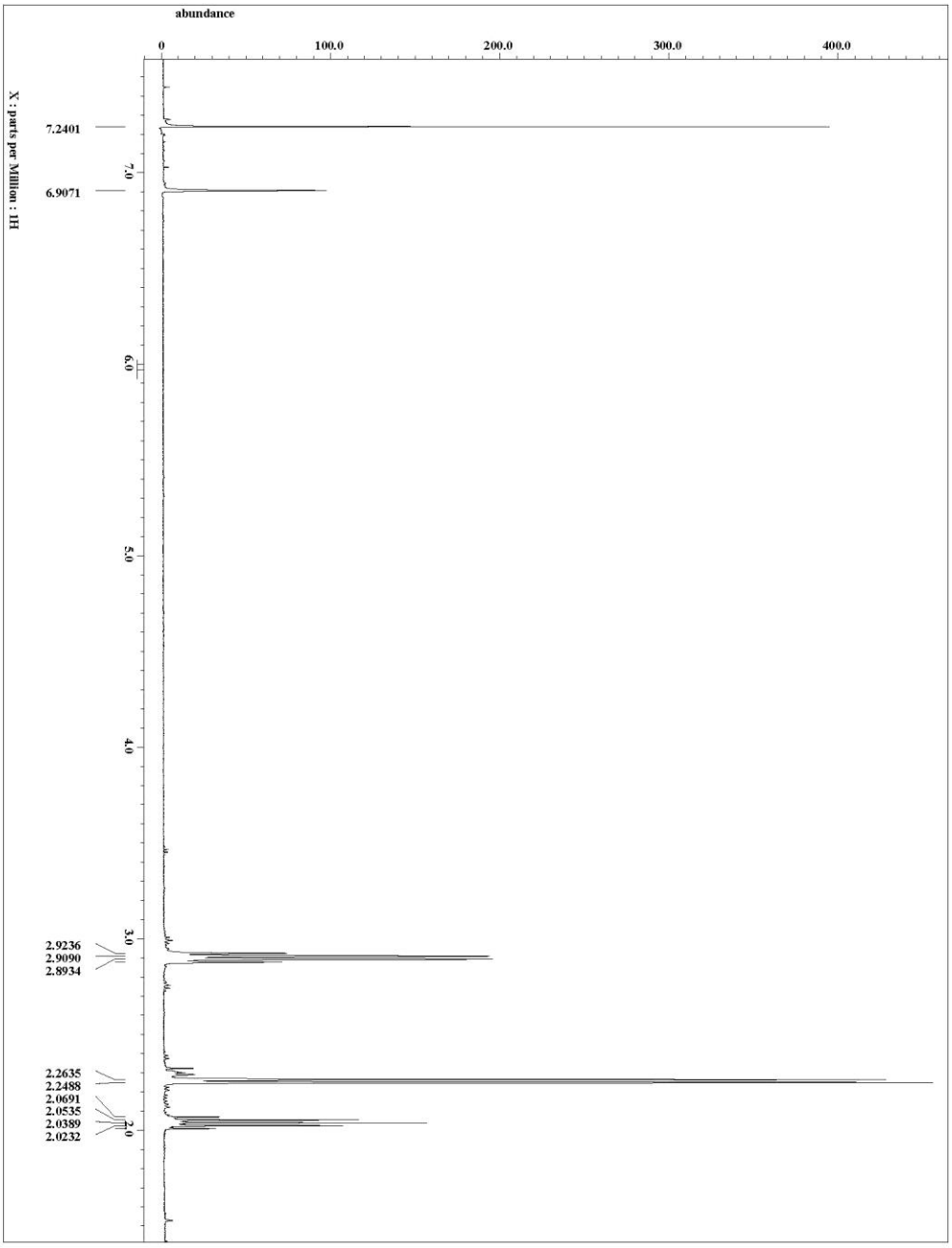

Figure 5-19. 9 ^{1}H NMR spectrum ($CDCl_3$, 500 MHz).

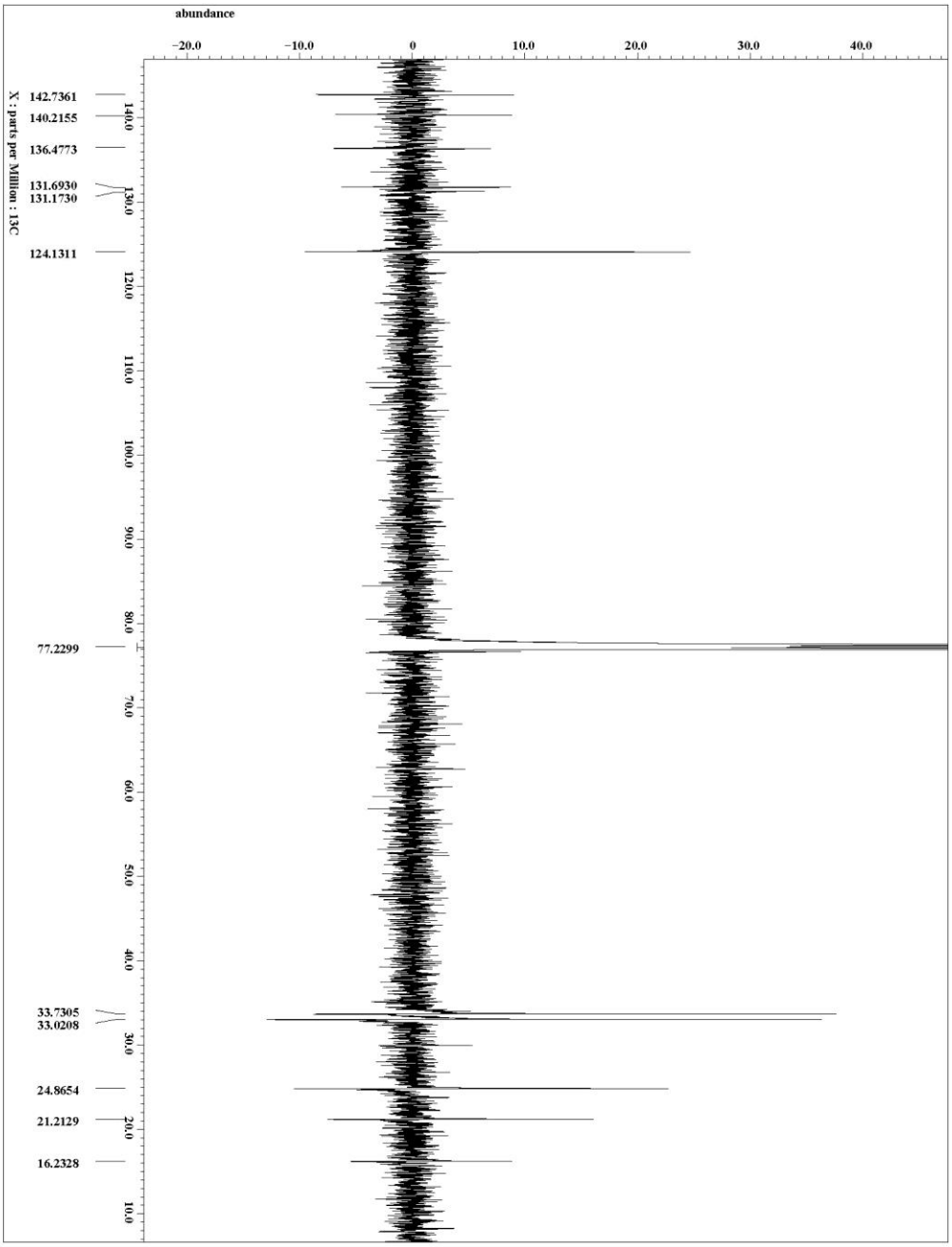

Figure 5-20. 9 ^{13}C NMR spectrum ($CDCl_3$, 125 MHz).

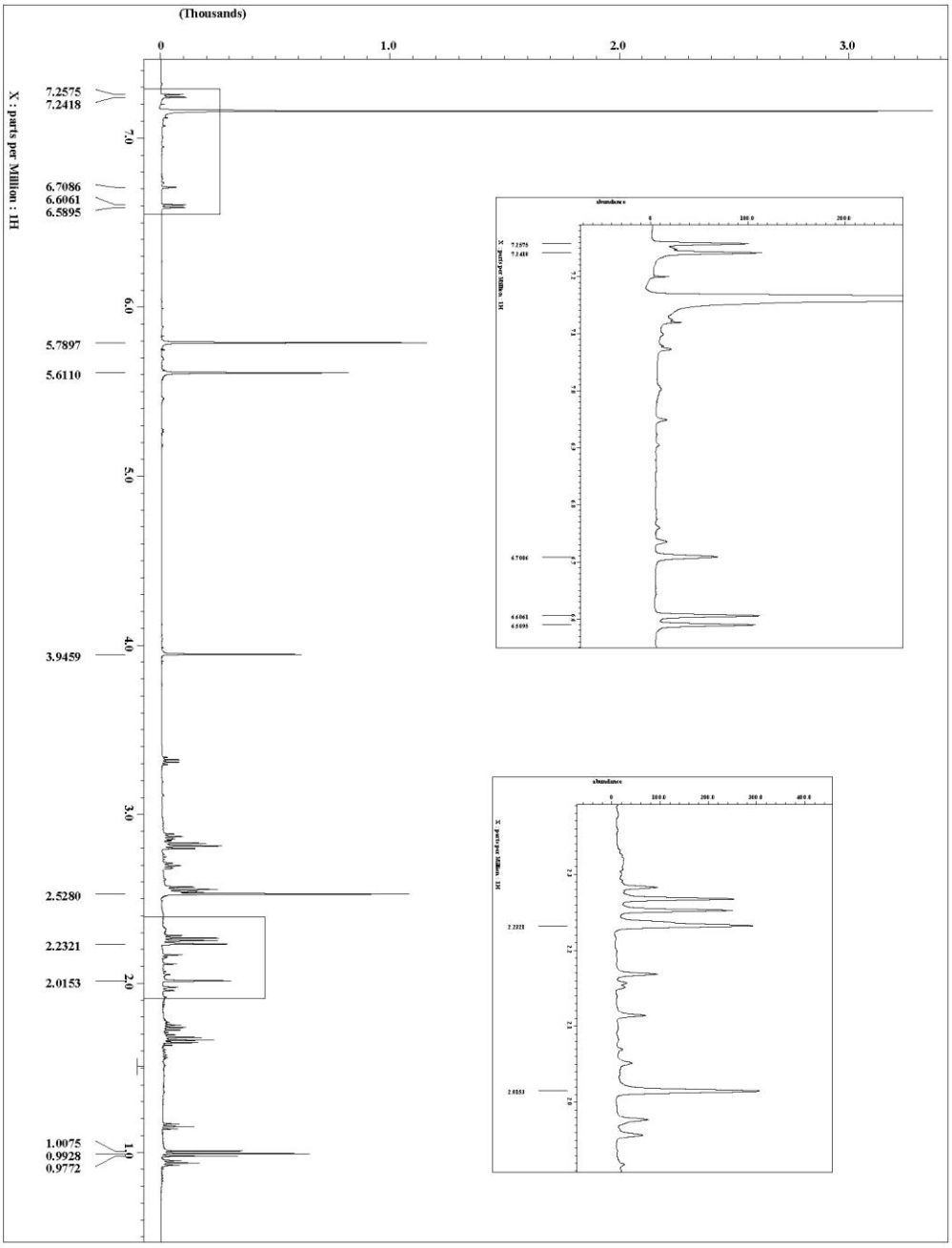

Figure 5-21. Reaction of **7** with 1,4-CHD and $CHBr_3$ in C_6D_6 at 165 °C ^1H NMR spectrum (C_6D_6, 500 MHz).

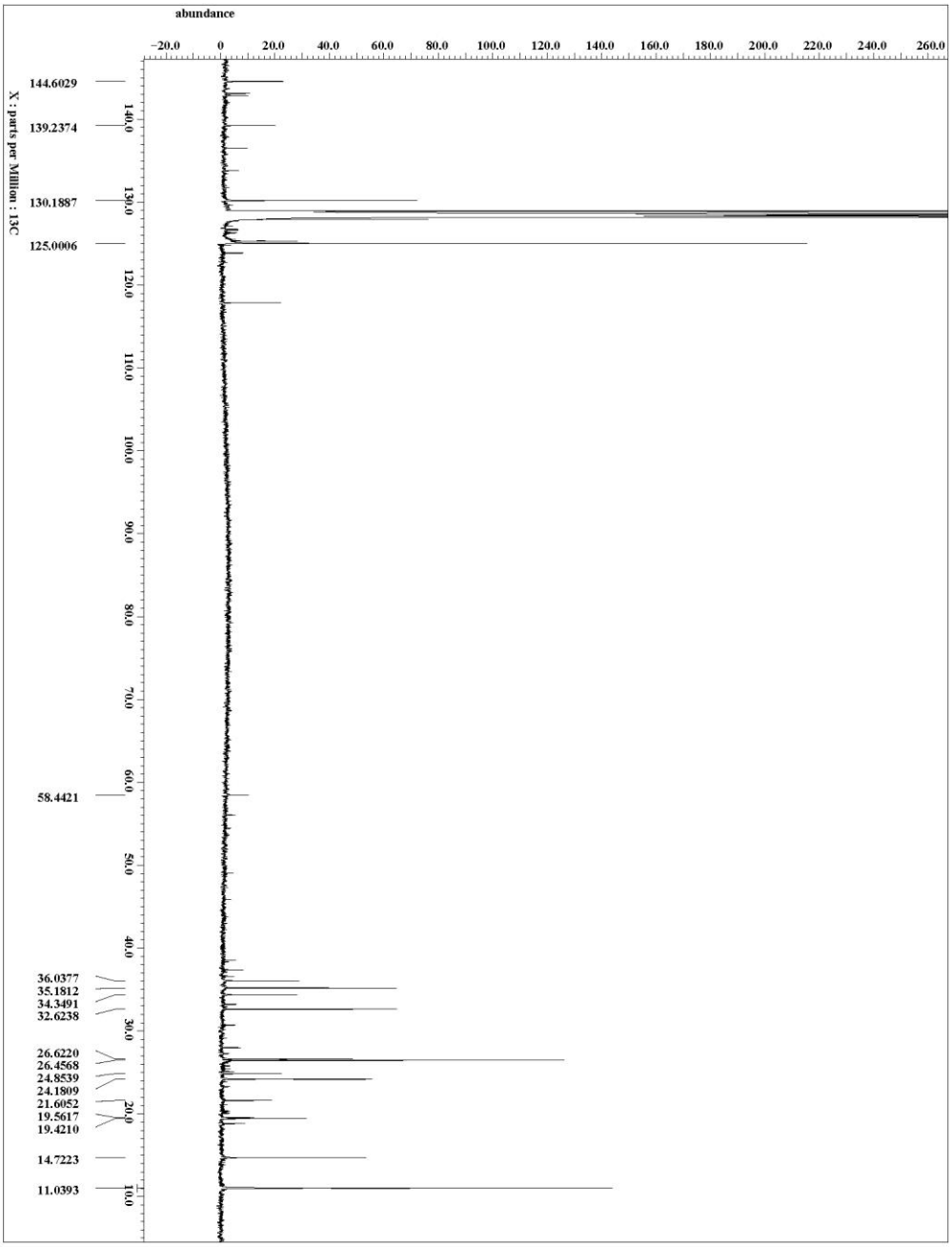

Figure 5-22. Reaction of **7** with 1,4-CHD and $CHBr_3$ in C_6D_6 at 165 °C ^{13}C NMR spectrum (C_6D_6, 125 MHz).

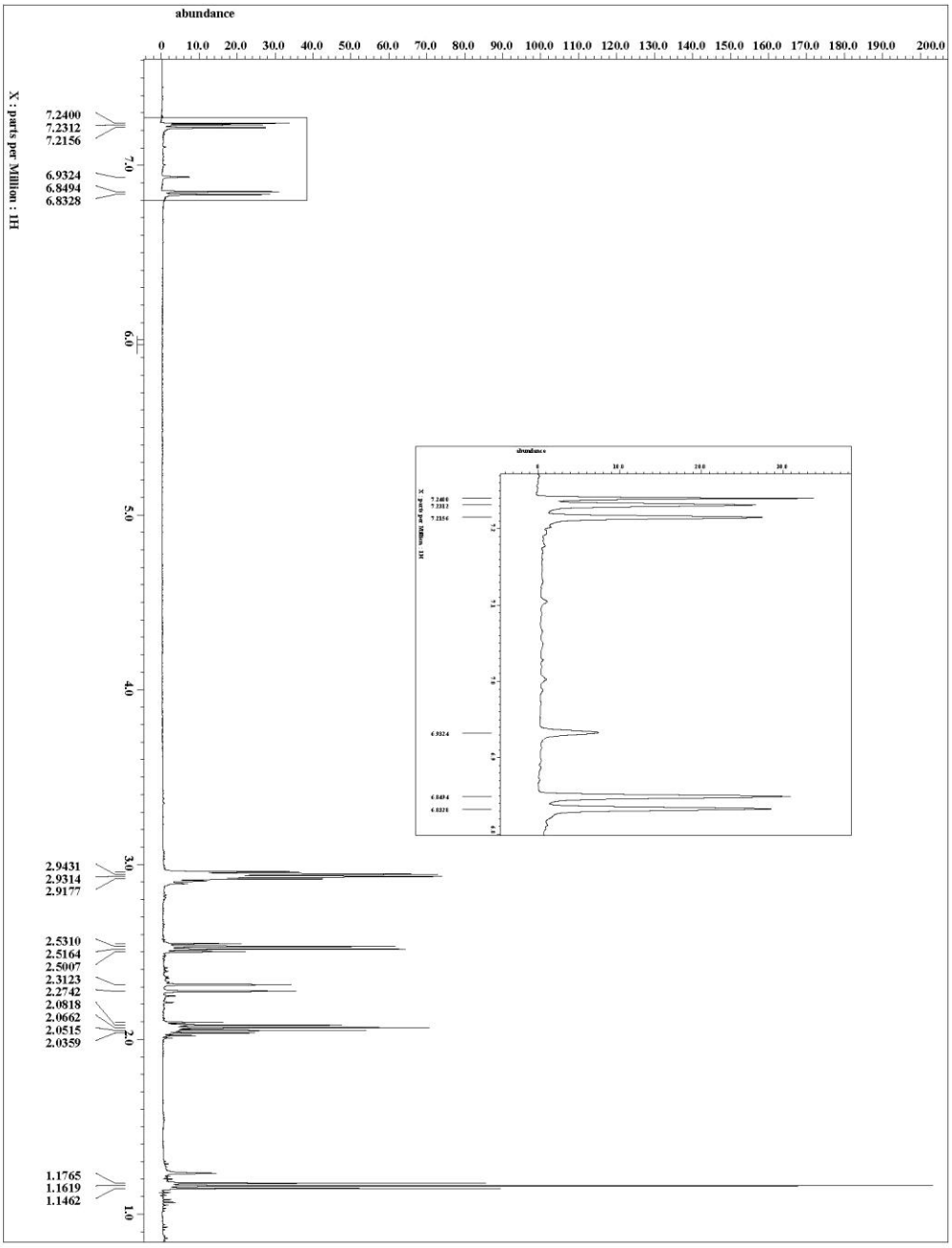

Figure 5-23. 13 ^{1}H NMR spectrum (CDCl3, 500 MHz).

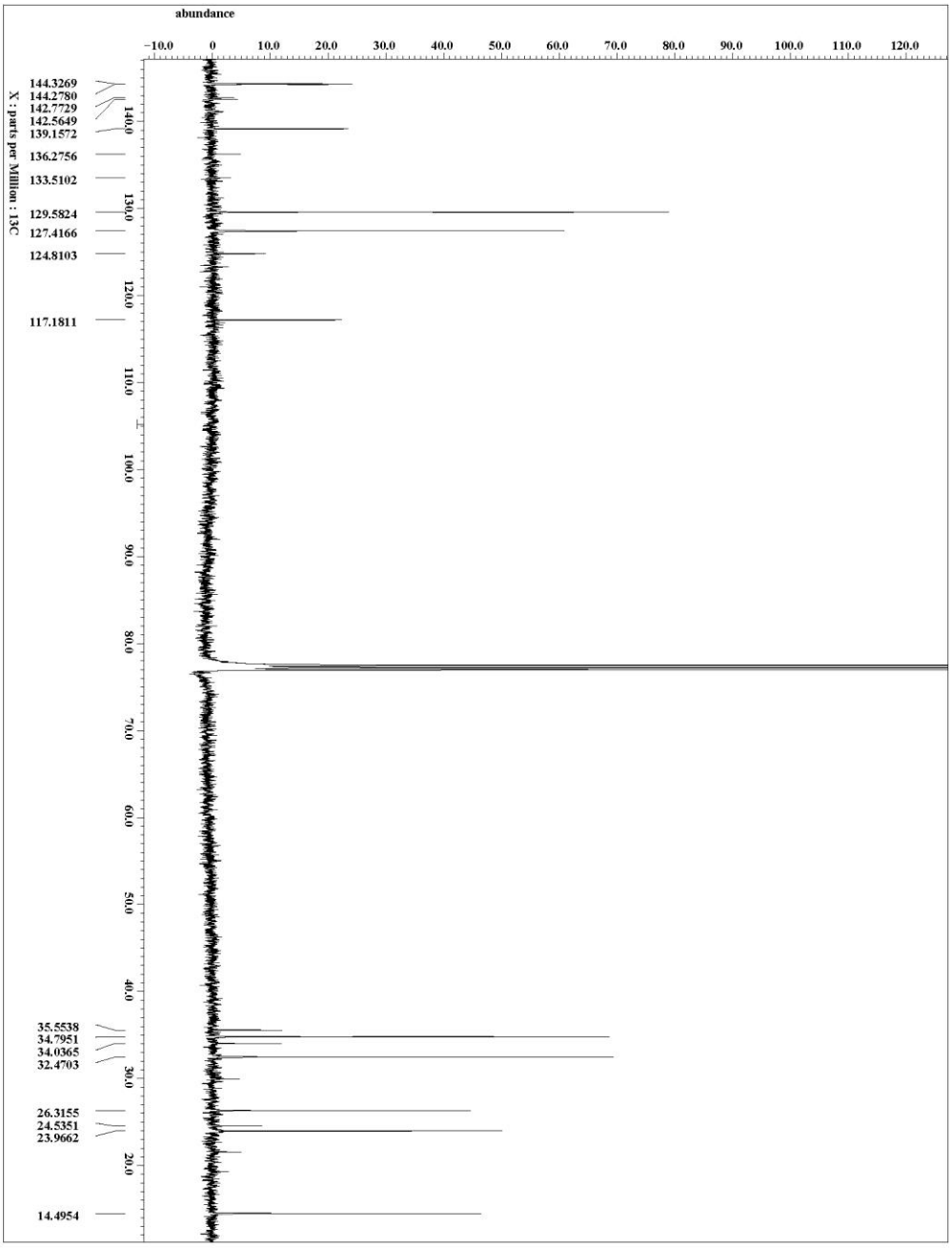

Figure 5-24. 13 ^{13}C NMR spectrum ($CDCl_3$, 125 MHz).

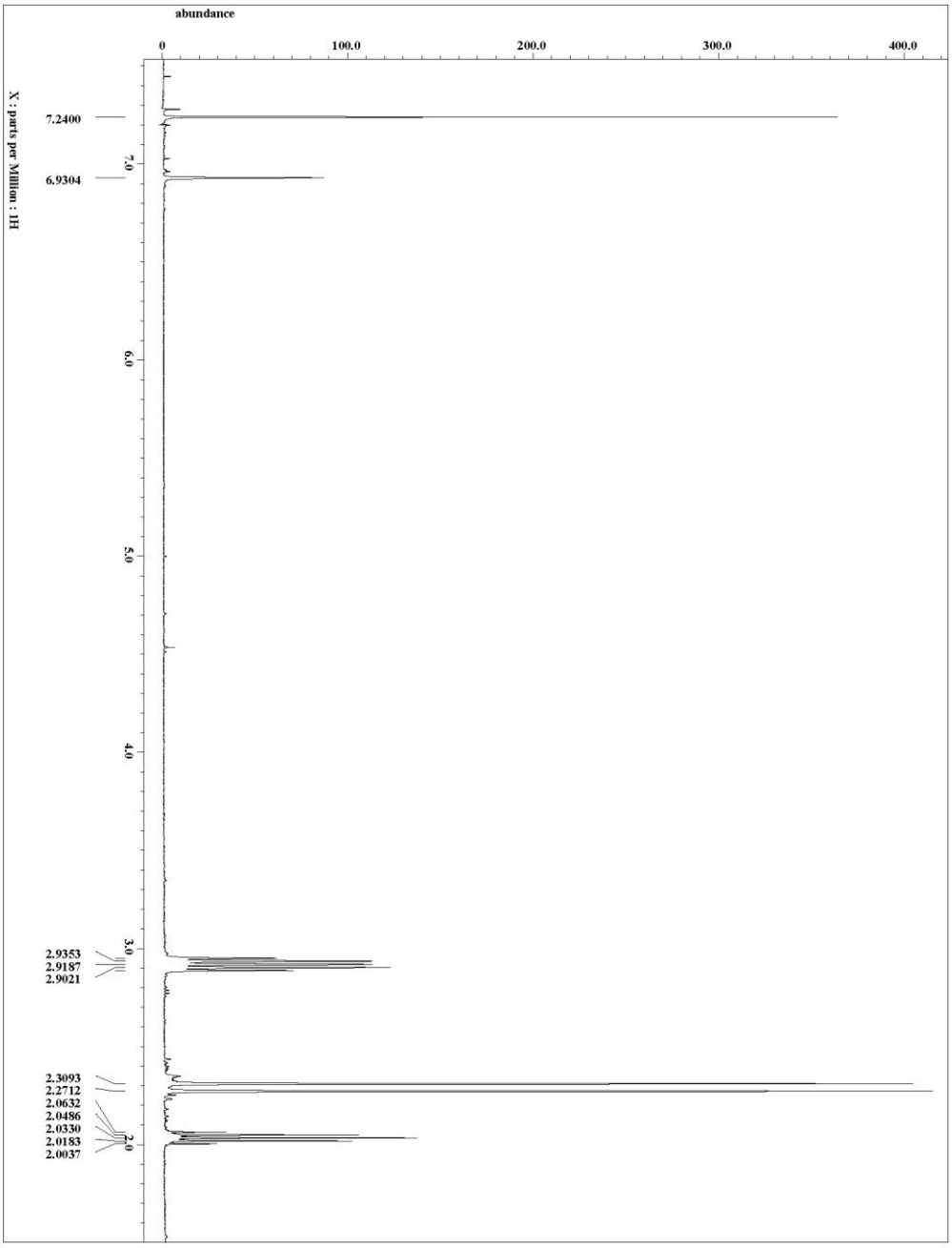

Figure 5-25. 14 ^{1}H NMR spectrum ($CDCl_3$, 500 MHz).

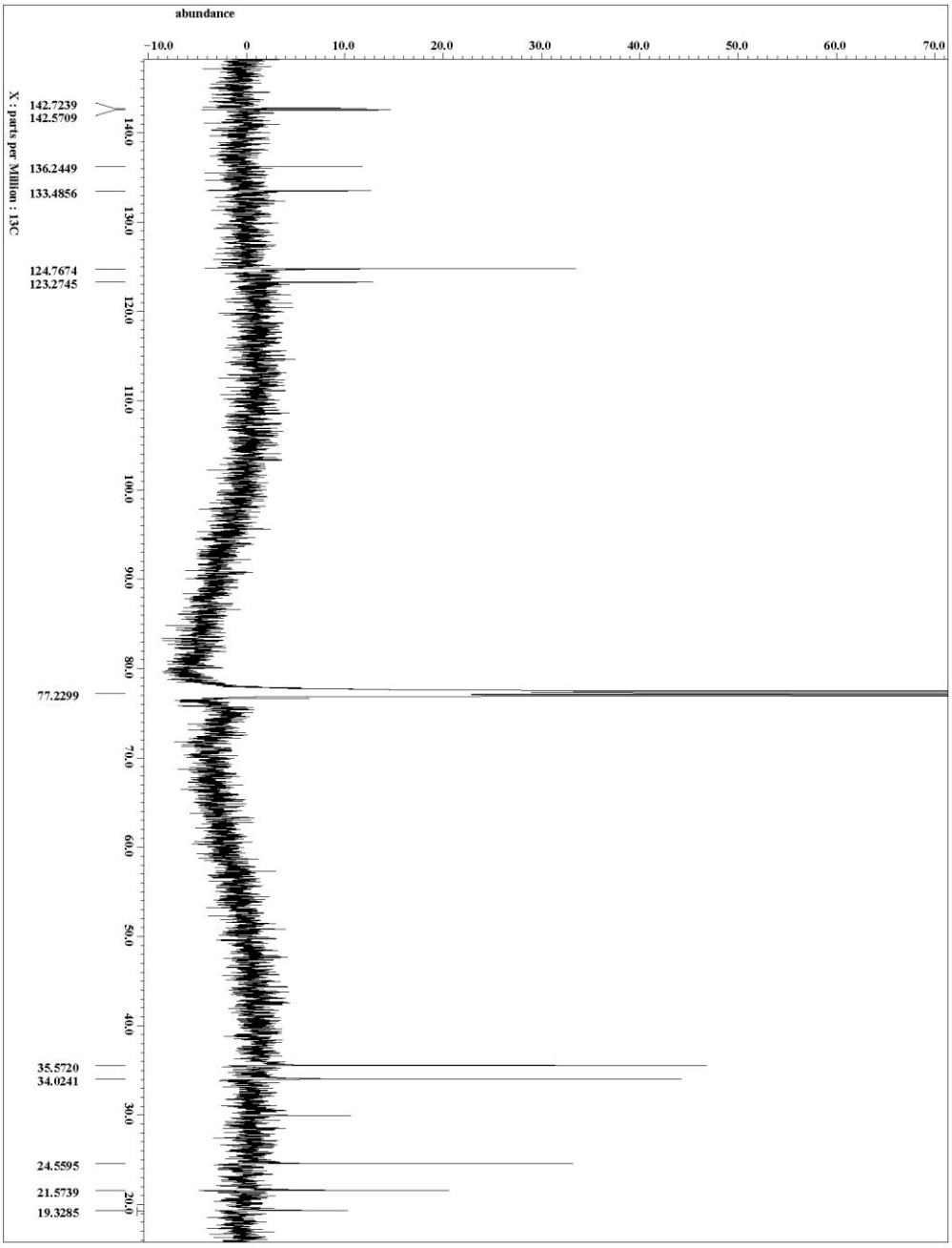

Figure 5-26. 14 ^{13}C NMR spectrum ($CDCl_3$, 125 MHz).

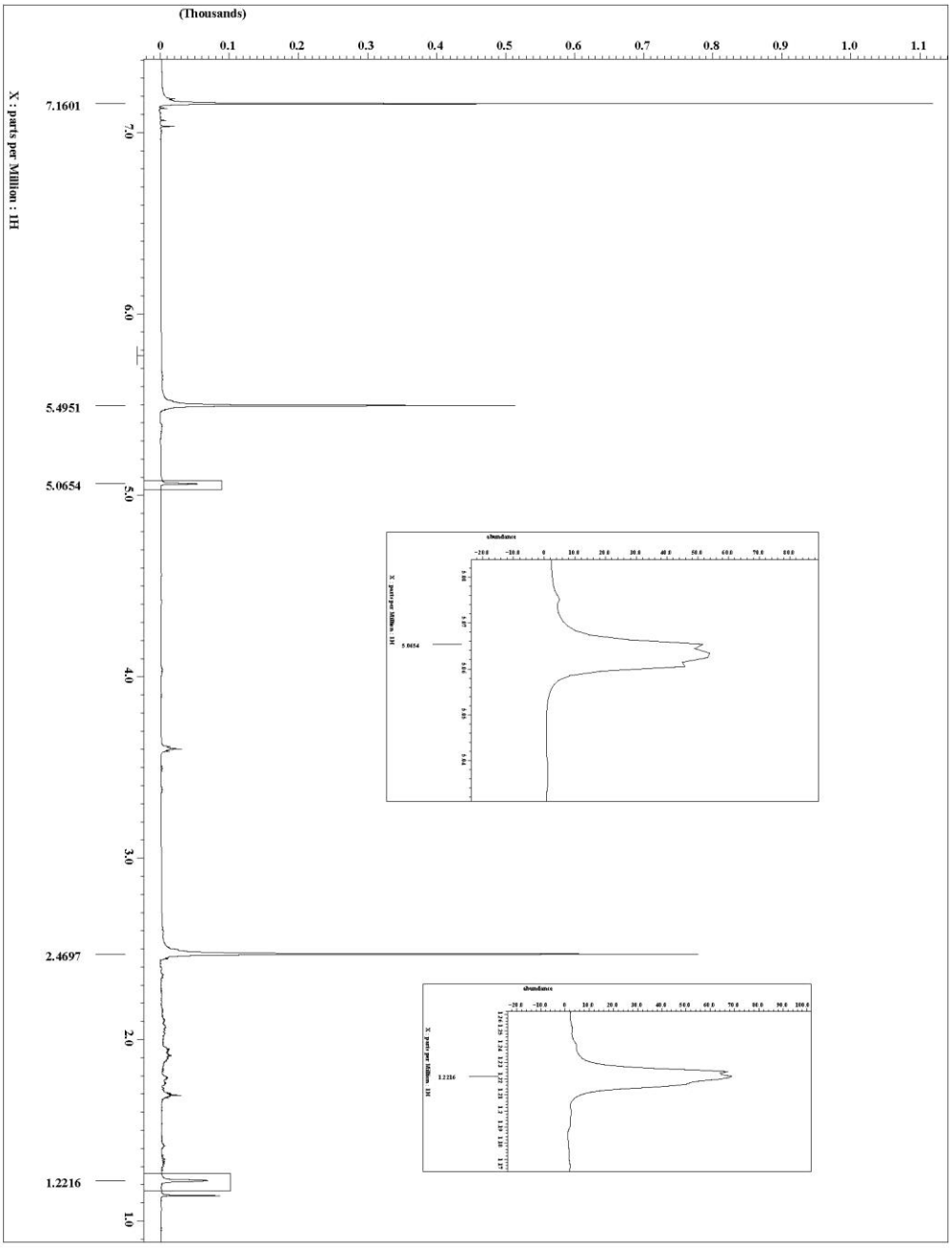

Figure 5-27. Reaction of 1,4-CHD in $CDCl_3$ at 165 °C ^1H NMR spectrum ($CDCl_3$, 500 MHz).

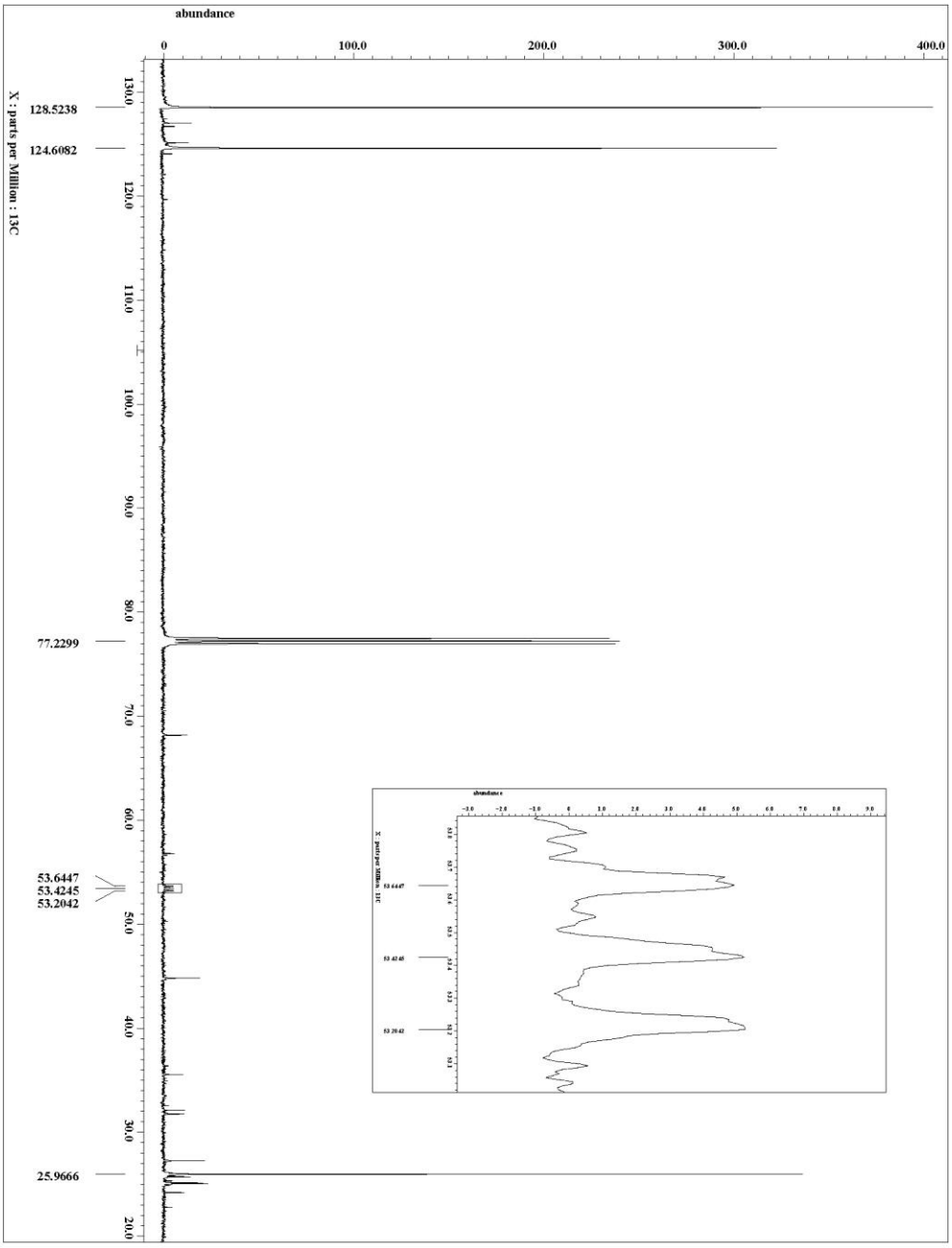

Figure 5-28. Reaction of 1,4-CHD in $CDCl_3$ at 165 °C ^{13}C NMR spectrum ($CDCl_3$, 125 MHz).

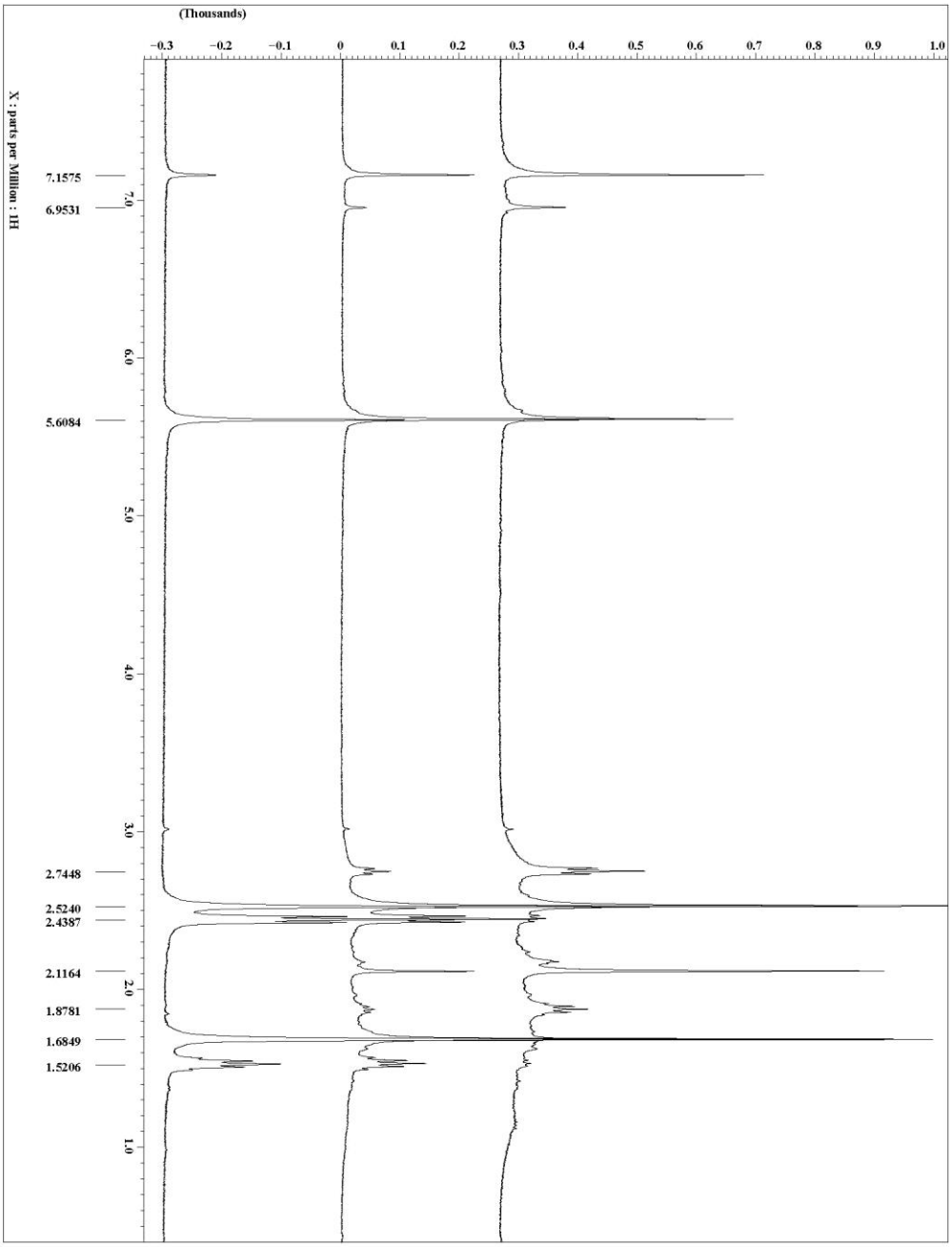

Figure 5-29. Reaction of **7** with CHF_3 and 1,4-CHD at 165 °C at time 0 (bottom), 48 h (middle), and 220 h (top). ^1H NMR spectra (C_6D_6, 500 MHz).

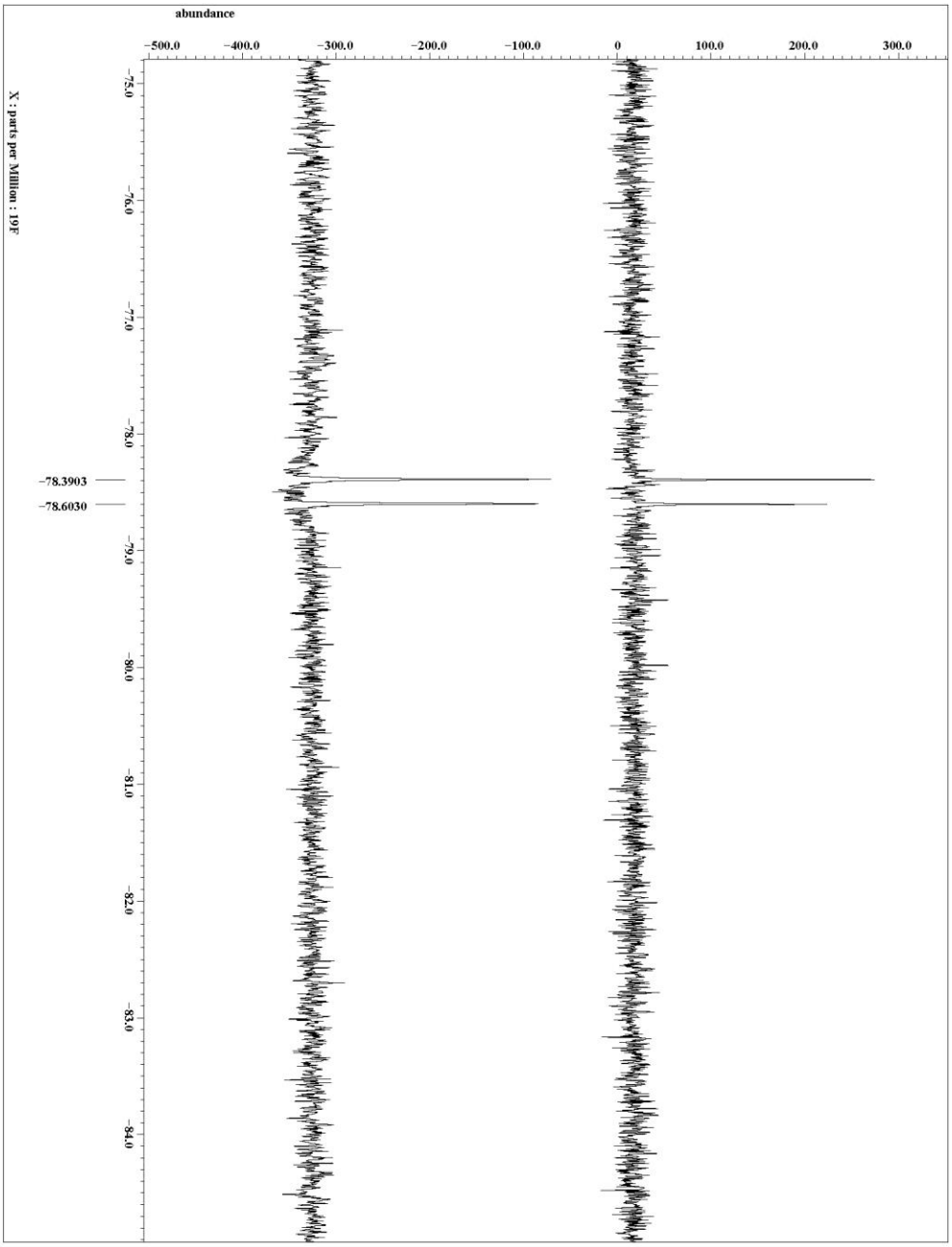

Figure 5-30. 7 with CHF_3 and 1,4-CHD at 165 °C for 0 h (bottom) and 220 h (top). ^{19}F NMR spectra (C_6D_6, 470 MHz).

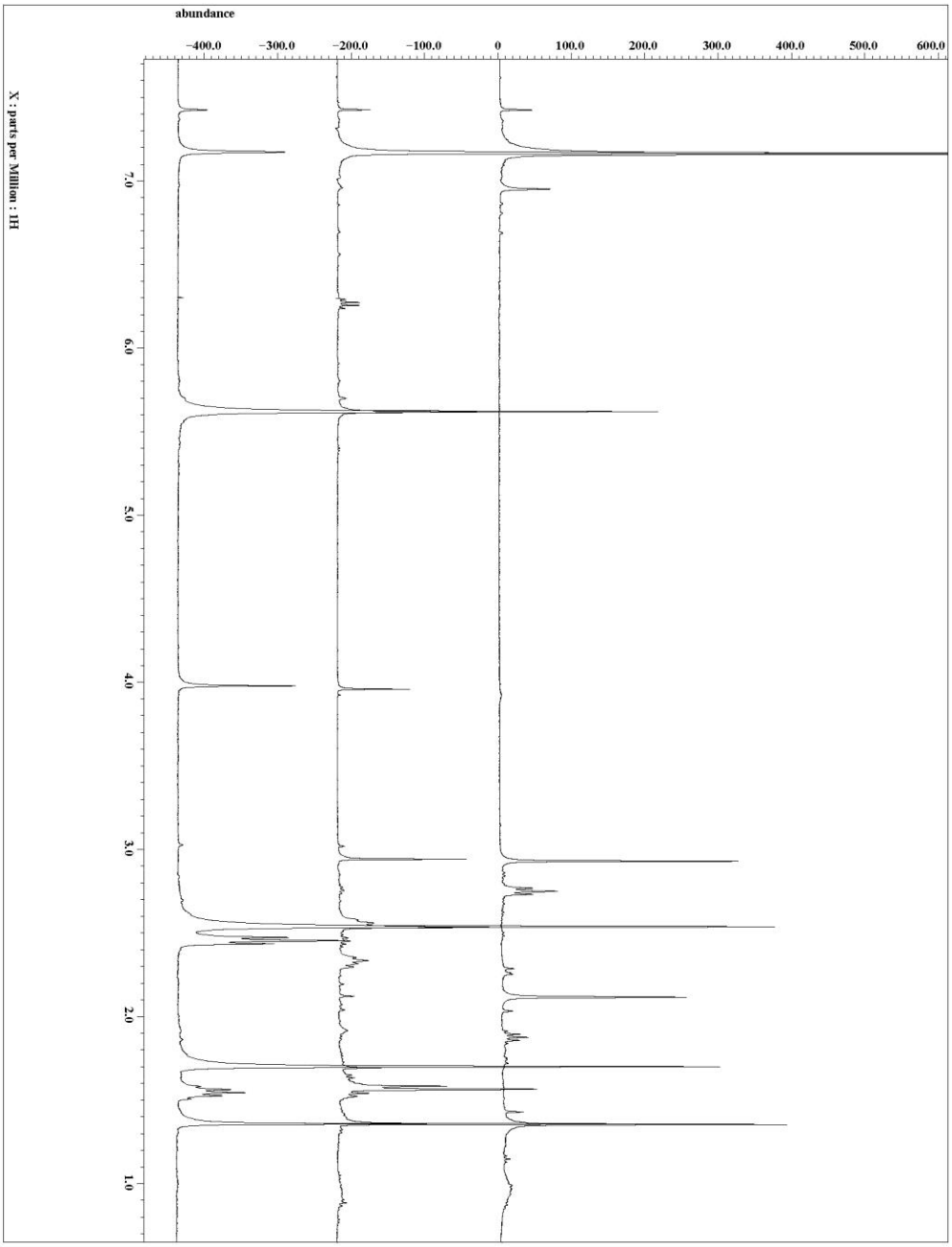

Figure 5-31. 7 with CHI_3 and 1,4-CHD. Time 0 (bottom), 100 °C for 24 h (middle), and 165 °C for 3 h (top). ^{1}H NMR spectra (C_6D_6, 500 MHz).

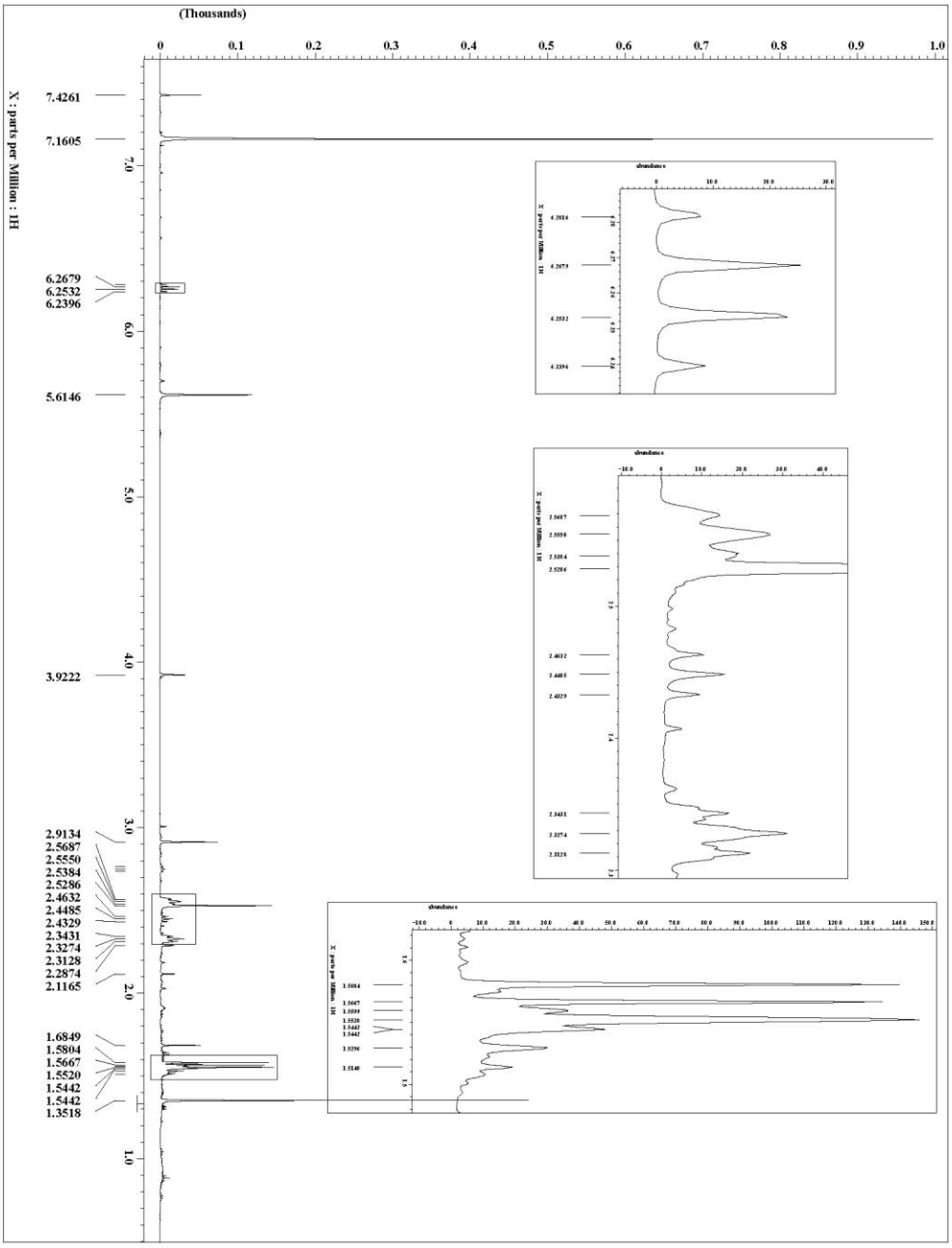

Figure 5-32. 18 ^{1}H NMR spectrum (C_6D_6, 500 MHz).

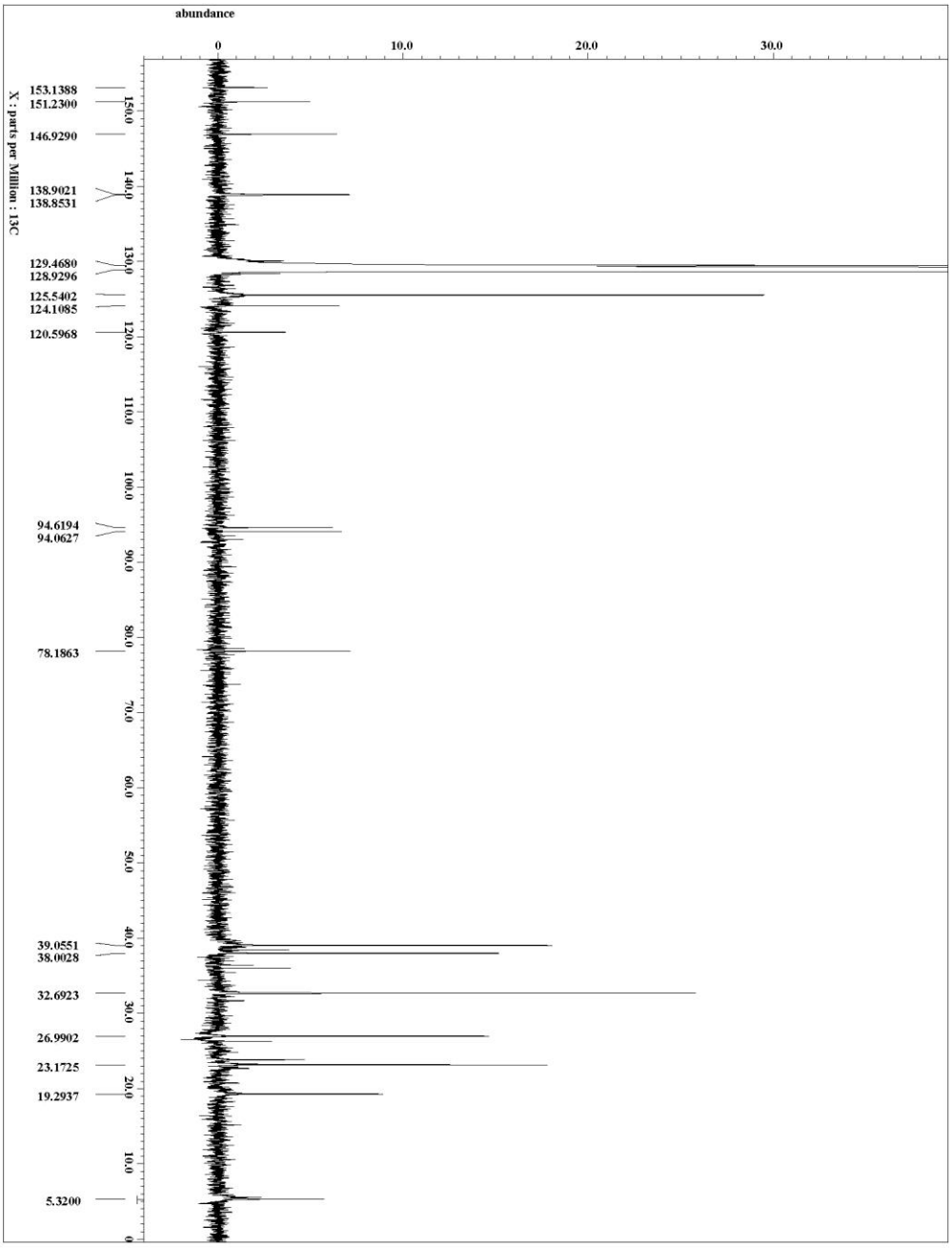

Figure 5-33. 18 ^{13}C NMR spectrum (C_6D_6, 125 MHz).

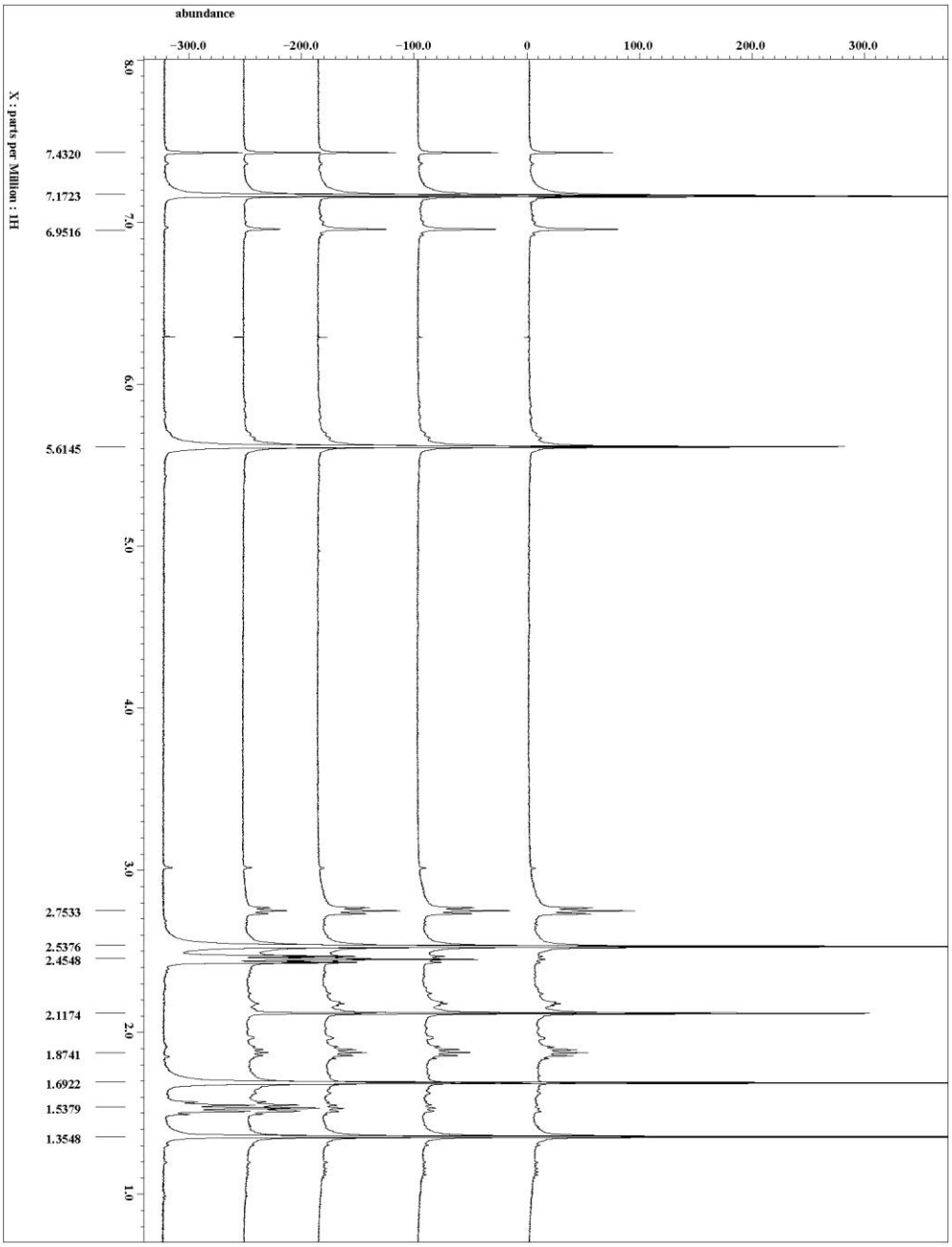

Figure 5-34. 7 in the presence of 1,4-CHD in C_6D_6 at 165 °C at time (h): 0, 48, 192, 260, 450 ^{1}H NMR spectra (C_6D_6, 400 MHz).

5-5.4 Heat of Reaction Calculation

The thermal reaction of haloforms with 1,4-cyclohexadiene generates HX *in situ*.

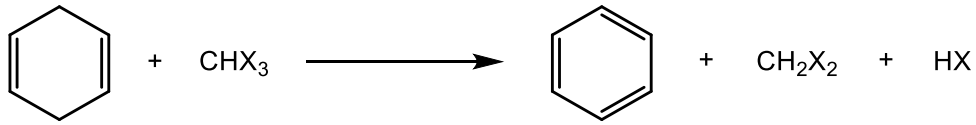

Scheme 5-30 Generation of HX by heating CHX_3 with 1,4-CHD.

The ΔH_{rxn}^{o} was calculated according to eq. 1 using standard values for the ΔH_f^{o} for all substrates and products.[8]

$$\Delta H_{rxn}^{o} = (\Delta H_f^{o}(HX) + \Delta H_f^{o}(Benzene) + \Delta H_f^{o}(CH_2X_2)) - (\Delta H_f^{o}(CHD) + \Delta H_f^{o}(CHX_3)) \quad \text{eq. 1}$$

Table 5.1 Standard Enthalpy of Formation (kJ/mol).[8]

CHF_3	-695.4	CH_2F_2	-450.7	HF	-272.6
$CHCl_3$	-134.3	CH_2Cl_2	-124.1	HCl	-92.3
$CHBr_3$	9.4	CH_2Br_2	-11.1	HBr	-36.4
CHI_3	181.1	CH_2I_2	68.5	HI	26.4
1,4-CHD	69.7	C_6H_6	48.95		

Table 5.2 Enthalpy of Reaction (kcal/mol) for the Reaction of Haloforms with 1,4-Cyclohexadiene.

F	Cl	Br	I
-11.6	-24.6	-18.6	-25.6

5-6 Acknowledgements

The material in Chapter 5, in part, is currently being prepared for submission for publication with the following authors: Cope, S.K.; O'Connor, J.M.; Hitt, D.M.; Raub, A. G. The dissertation author was the primary investigator and author of this material.

5-7 References

1. (a) O'Connor, J.M.; Friese, S.J. *Organometallics* **2008**, *27*, 4280. (b) O'Connor, J.M.; Friese, S.J.; Rodgers, B.L. *J. Am. Chem. Soc.* **2005**, *127*, 16342. (c) O'Connor, J.M.; Friese, S.J.; Tichenor, M. *J. Am. Chem. Soc.* **2002**, *124*, 3506. (d) O'Connor, J.M.; Lee, L.I.; Gantzel, P. *J. Am. Chem. Soc.* **2000**, *122*, 12057. (e) Friese, S.; PhD. Dissertation, University of California, San Diego **2004**.

2. Hitt, D.; PhD. Dissertation, University of California, San Diego **2011**.

3. Calculations performed by Kim Baldridge using BP86 density functional, Def2-TZVPP basis set, GAMESS Program.

4. Cambridge Isotope Laboratories, NMR Solvent Data Chart. http://www.isotope.com/userfiles/files/assetLibrary/NMR_solvents_data_chart_&_storage.pdf (accessed June 25, 2015).

5. Fulmer, G.R.; Miller, A.J.M.; Sherden, N.H.; Gottlieb, H.E.; Nudelman, A.; Stoltz, B.M.; Bercaw, J.E.; Goldberg, K.I. *Organometallics* **2010,** *29*, 2176.

6. Raub, A.W. UC San Diego, San Diego, CA. Unpublished work, 2012.

7. O'Connor, J.M.; Friese, S.J.; Rodgers, B.L.; Rheingold, A.L.; Zakharov, L. *J. Am. Chem. Soc.* **2005**, *127*, 9346.

8. ΔH_f^o obtained from: (a) *CRC Handbook of Chemistry and Physics*; Lide, D.R., Ed.; CRC Press: New York, 1996; 77th ed. (b) National Institute of Standards and Technology Chemistry Webbook. http://webbook.nist.gov/ (accessed August 13, 2015).

9. Baciocchi, E.; Mattioli, M.; Romano, R.; Ruzziconi, R. *J. Org. Chem.* **1991**, *56*, 7154.

10. The volume of the J.Young tube was determined by weighing the oven-dried tube and then adding de-ionized H_2O to the approximate position of the Teflon seat and then reweighing.

11. Sartori, P.; Habel, W. *J. Fluor. Chem.* **1980**, *16*, 265.

12. Darwent, B.deB. *Nat. Stand. Ref. Data Ser., Nat. Bur. Stand.* **1970**, *31*.

13. Gao, Y.; DeYonker, N.J.; Garrett III, E.C.; Wilson, A.K.; Cundari, T.R.; Marshall, P. *J. Phys. Chem. A* **2009**, *113*, 6955.

14. Fahey, R.C.; Lee, D.J. *J. Am. Chem. Soc.* **1966**, *88*, 5555.

15. Shibata, T.; Ueno, Y.; Kanda, K. *Synlett* **2006,** *3*, 411.

16. Lo, C.Y.; Kumar, M.P.; Chang, H.K.; Lush, S.F.; Liu, R.S. *J. Org. Chem.* **2005**, *70*, 10482.

17. Raamat, E.; Kaupmees, K.; Ovsjannikov, G.; Trummal, A.; Kutt, A.; Saame, J.; Koppel, I.; Kaljurand, I.; Lipping, L.; Rodima, T.; Pihl, V.; Koppel, I.A.; Leito, I. *J. Phys. Org. Chem.* **2012**, *26*, 162.

18. Jensen, F.R.; Bushweller, C.H.; Beck, B.H. *J. Am. Chem. Soc.* **1969**, *91*, 344.

19. Hansch, C.; Leo, A.; Taft, R.W. *Chem. Rev.* **1991**, *91*, 165